
Development and Understanding of Rhodium-Catalysed Conjugate Arylation for Process Chemistry Applications

PhD Thesis

Stephen Lovelock

Supervised by

Dr Alastair Roberts

GlaxoSmithKline

Professor Glenn Burley

Department of Pure and Applied Chemistry, University of Strathclyde



January 2019

Declaration

This thesis is the result of the author's original research. It has been composed by the author and has not been previously submitted for examination which has led to the award of a degree.

The copyright of this thesis belongs to GSK in accordance with the author's contract of engagement with GSK under the terms of the United Kingdom Copyright Acts. Due acknowledgement must always be made of the use of any material contained in, or derived from, this thesis.

Stephen Lovelock

January 2019

Acknowledgements

I am very grateful to my supervisors and to Katherine Wheelhouse for their ongoing supervision and willingness to find time for discussion, support and encouragement. The members of 2G121 also provided regular assistance, discussion and encouragement. As the occupant of the adjacent fume cupboard, Calvin Manning contributed to many enjoyable project-related discussions, and also provided valuable assistance with running the DoE experiments and interpreting the results. Lee Boulton was a regular source of advice, especially on practical synthetic matters. Assistance with chiral HPLC methods was provided by Graham Stevens, Adrian Bateman, and Andy Knaggs. Colin Edge provided the computational results reported in this thesis, along with helpful discussion regarding the computational work.

I am also grateful for the opportunity to have explored the chemistry detailed in this report, which I would not have had the opportunity to do outside of this collaborative programme.

Abstract

Asymmetric rhodium-catalysed conjugate arylation is an important carbon–carbon bond-forming reaction of increasing industrial relevance. The control of enantioselectivity has been explored extensively in the published literature, however the competing deboronation reaction has received little attention. This uncontrolled side-reaction often necessitates the use of up to 10 equivalents of the arylboron reagent, rendering the methodology unattractive for large scale industrial purposes.

In this thesis, a pharmaceutically-relevant rhodium-catalysed conjugate addition of an arylboronic acid pinacol ester to an unsaturated ester with heteroaryl functionality has been investigated, with significant improvements to the enantioselectivity, chemoselectivity and green metrics made compared with a previous process used on kilogram scale. The original process delivered poor enantioselectivity, required uneconomical rhodium loadings and a large excess of the arylboron reagent.

A cheaper and highly selective catalyst system was identified following extensive and informed investigations into the behaviour of different ligand and rhodium salt combinations. The optimised process utilises an inexpensive chiral ligand from a ligand class previously overlooked by industry. The new system delivers up to 97% *ee* with virtually complete selectivity for the desired conjugate arylation reaction over the competing protodeboronation reaction. Furthermore, factors that are important for the success and selectivity of the desired reaction have been efficiently identified using a statistical Design of Experiment approach. This has enabled the loading of the precious metal catalyst to be lowered by > 85% whilst maintaining 97% selectivity for the 1,4-addition reaction over protodeboronation.

An empirical investigation of the structural motifs of the substrates and the ligand that were important in enabling a high selectivity for conjugate arylation over protodeboronation to be achieved is also presented. The heteroaryl functionality of the enoate was found to contribute to the selectivity, but could prevent consumption of the arylboron reagent altogether if a suitable sterically-shielding group was not present. The structural motifs of the ligand had a significant impact on the chemoselectivity of the reaction, with electronic factors, steric factors and functionality affecting the relative amounts of conjugate arylation product and protodeboronation product.

Computational chemistry and an analysis of published crystallographic data enabled the high selectivity for conjugate arylation over protodeboronation that the optimised reaction process affords to be rationalised. Ligands expected to facilitate the exchange of a solvent molecule bound to the metal centre for the enoate electrophile delivered the highest selectivities for conjugate arylation. Conversely, ligands and arylboron reagents expected to impede the exchange of a bound solvent molecule for the enoate electrophile gave elevated levels of the protodeboronation product.

Abbreviations

*	Indicates chirality at the specified position or within the specified component, unless used in relation to a molecular orbital in which case it is used to identify an antibonding orbital
[B], [M]	Unspecified complex of boron or metal M, such as Ar[B] to denote ArBpin, ArB(OH) ₂ , etc.
°C	Degrees Celsius
{ ¹ H}	Indicates that proton decoupling has been performed (NMR)
Å	Ångström (10 ⁻¹⁰ m)
ν	Frequency (IR)
Ac	Acetyl
acac	Acetylacetonate anion
ANOVA	Analysis of Variance
API	Active Pharmaceutical Ingredient
app.	Apparent, such as app. d to denote a feature that resembles a doublet (NMR)
aq	Aqueous
Ar	Aryl
area%	Indicates a percentage measured by area (HPLC)
AU	Absorbance unit (HPLC)
bar	Bar (absolute pressure)
BINAP	2,2'-Bis(diphenylphosphino)-1,1'-binaphthyl
Bn	Benzyl
Boc	<i>tert</i> -Butyloxycarbonyl
BOD	Bicyclo[2.2.2]octa-2,5-diene
Bpin	Pinacol borane fragment, such that HBpin is pinacol borane and B ₂ pin ₂ is bis(pinacolatodiboron)
bpy	2,2'-Bipyridine
cat.	Catalyst or catalytic (amount)
COD	Cyclooctadiene
COE	Cyclooctene
corr.	Corrected, such as relating to a yield corrected for residual solvent or water
CPME	Cyclopentyl methyl ether
Cy	Cyclohexyl
<i>d.e.</i>	Diastereomeric excess
DABCO	1,4-Diazabicyclo[2.2.2]octane
DBN	1,5-Diazabicyclo[4.3.0]non-5-ene
DCM	Dichloromethane
DIAD	Di- <i>iso</i> -propyl azodicarboxylate
DIBAL	Di- <i>iso</i> -butylaluminium hydride
Dioxane	1,4-Dioxane
DIPA	Di- <i>iso</i> -propylamine
DIPEA	Di- <i>iso</i> -propylethylamine
DMAP	Dimethylamino pyridine

DME	Dimethoxyethane
DMF	<i>N,N</i> -Dimethylformamide
DMSO	Dimethyl sulfoxide
DoE	Statistical Design of Experiment
dppb	1,4-Bis(diphenylphosphino)butane
dppf	1,1'-Bis(diphenylphosphino)ferrocene
-d_x	Deuterated, such as THF- <i>d</i> ₈ to denote fully-deuterated THF
E	Denotes the stereochemistry of a substituted alkene for which the highest priority groups on each carbon are <i>trans</i> to each other
e.r.	Enantiomeric ratio
EDC	<i>N</i> -(3-dimethylaminopropyl)- <i>N'</i> -ethyl- carbodiimide hydrochloride
ee	Enantiomeric excess
eq	Molar equivalents (also Eq.)
Et	Ethyl
eV	Electron volt
FT	Fourier transform
GC	Gas Chromatography
GCMS	Gas Chromatography – Mass Spectrometry
h	Hour(s)
HMBC	Heteronuclear Multiple Bond Correlation (NMR)
HOMO	Highest Occupied Molecular Orbital
HPLC	High Performance Liquid Chromatography
HRMS	High Resolution Mass Spectrometry
HSQC	Heteronuclear Single Quantum Correlation (NMR)
IMS	Industrial Methylated Spirits
IPA	<i>iso</i> -Propyl alcohol
ⁱPr	<i>iso</i> -Propyl
IR	Infrared (spectroscopy)
<i>J</i>	Magnitude of the NMR coupling constant
<i>K</i>	Equilibrium constant
<i>k</i>	Relative response factor
KHMDS	Potassium bis(trimethylsilyl)amide
L	Ligand
LCMS	Liquid Chromatography – Mass Spectrometry
LDA	Lithium di- <i>iso</i> -propylamide
lit.	Literature data
LUMO	Lowest Unoccupied Molecular Orbital
<i>m</i>	<i>meta</i>
M	Molecule, such as [M] ⁺ denoting the molecular ion (Mass Spectrometry)
M. pt.	Melting point
M/C	Specified metal on carbon, such as Pd/C denoting a palladium on carbon heterogeneous catalyst
m/z	Mass/charge ratio (mass spectrometry)
MDAP	Mass-Directed Autopurification

Me	Methyl
MeTHF	2-Methyltetrahydrofuran
MIBK	Methyl <i>iso</i> -butyl ketone
MIDA	<i>N</i> -methyliminodiacetic acid fragment, such as that of <i>N</i> -methyliminodiacetic acid boronates
min	Minute(s)
mol%	Indicates a percentage measured by molar amount
MS	Molecular sieves
Ms	Mesyl
N/A	Not applicable
NBD	Norbornadiene
NBS	<i>N</i> -Bromosuccinimide
ⁿBu	Normal butyl
n.d.	Not determined
NMM	<i>N</i> -methylmorpholine
NMP	<i>N</i> -Methyl-2-pyrrolidone
NMR	Nuclear Magnetic Resonance
Np	2-Naphthyl
<i>o</i>	<i>ortho</i>
<i>p</i>	<i>para</i>
Ph	Phenyl
p<i>K</i>_a	$-\log_{10}K_a$ where K_a is the acid dissociate constant of the specified Brønsted acid in aqueous conditions at 25 °C and with an ionic strength approaching 0 where available
p<i>K</i>_{aH}	Denotes the p <i>K</i> _a of the conjugate acid of the specified Brønsted base
PLP	Pyridoxal phosphate (co-enzyme)
p-value	Significance level in Design of Experiment
Py	Pyridine
R	Generic substituent (may be specified)
r.t.	Room temperature
<i>rac</i>/(<i>S</i>)/(<i>R</i>)-	Racemic/(<i>S</i>)-enantiomer/(<i>R</i>)-enantiomer of a specified compound
ROESY	Rotating Frame Nuclear Overhauser Effect Spectroscopy (NMR)
rpm	Revolutions per minute
rpt	Repeat
SFC	Supercritical Fluid Chromatography
Sol	Solvent molecule (unspecified)
<i>t</i>	Time
<i>T</i>	Temperature
TBME	<i>tert</i> -Butyl methyl ether
^tBu	<i>tert</i> -Butyl
TDA-1	Tris[2-(2-methoxyethoxy)ethyl]amine
TEA	Triethylamine
Temp	Temperature
Tf	Triflyl

TFA	Trifluoroacetic acid
THF	Tetrahydrofuran
TMEDA	1,2-Bis(dimethylamino)ethane
Tol	<i>p</i> -Tolyl, unless otherwise specified
t_R	Retention time
UPLC	Ultra Performance Liquid Chromatography
vol	Process Volume, where 1 vol describes a reaction mixture for which the limiting substrate has an initial concentration of 1 g mL ⁻¹
v/v	Indicates a ratio or percentage measured by volume
wt%	Indicates a percentage measured by weight
X	Heteroatom
Z	Denotes the stereochemistry of a substituted alkene for which the highest priority groups on each carbon are <i>cis</i> to each other

Contents

Declaration.....	ii
Acknowledgements.....	iii
Abstract.....	iv
Abbreviations.....	vi
Contents	x
1 Introduction.....	1
1.1 Process Chemistry.....	2
1.2 Chirality in Active Pharmaceutical Ingredients	6
1.3 Rhodium-Catalysed Asymmetric Conjugate Arylation	11
2 Research Aims	34
3 Results and Discussion	39
3.1 Synthesis of the Pharmaceutically-Relevant Substrates.....	40
3.2 Process Development of the Pharmaceutically-Relevant Conjugate Arylation	45
3.3 Selectivity for Conjugate Arylation over Protodeboronation	114
4 Conclusions.....	160
5 Experimental.....	165
5.1 General Comments.....	166
5.2 Procedures for Section 3.1	175
5.3 Procedures for Section 3.2	184
5.4 Procedures for Section 3.3	229
6 References.....	299

1 Introduction

1.1 Process Chemistry

Process chemistry is a discipline within industrial chemical research, with the aim of developing and optimising synthetic sequences for use on large scales. The scales involved in academic and medicinal research chemistry often allow for syntheses that are not readily translated to industrial scales, where such priorities as low costs, low environmental impact, high purity and high levels of safety become of increased importance due to the scale of operation.¹ Redeveloping academic methodologies to be suitable for industrial use therefore requires significant understanding of the chemical processes and innovative approaches to solving the problems encountered with their development. A useful summary of considerations to guide the process development of a synthetic route or step towards Active Pharmaceutical Ingredient (API) manufacture is the SELECT criteria, an acronym for Safety, Environmental, Legal, Economic, Control and Throughput criteria.^{1,2}

Safety considerations particularly include the process safety of a synthetic step, considering aspects such as potential exotherms or pressure build-ups, the use of explosive gases or high-energy functional groups, and the potential exposure of operators and the public to hazardous substances, for instance to volatile carcinogenic compounds.

Environmental factors to consider include both the supply of reagents and catalysts, and the disposal of hazardous waste materials. The choice of solvent will often be a dominant component of the environmental impact, but sustainable and responsible use of natural resources also involves reconsidering the use of non-abundant materials.

Many *legal* considerations are necessary, covering all aspects of the process, both in terms of intellectual property rights of compounds or procedures, and in terms of regulations controlling the usage of certain reagents. There must be legal freedom to operate the entire process.

A consideration important to many of the SELECT criteria but perhaps more notably to the *economic* feasibility of the synthesis is the length of the synthetic route. Although clinical trials are frequently the most expensive part of the drug development process,³ this only increases the need to lower costs elsewhere. Expensive reagents and expensive or economically inefficient processes need to be avoided or minimised during process development for long-term manufacture.

The *control* requirements of a process particularly involve the reproducibility of the desired outcome and the quality of the outcome (for example yield, selectivity and purity). Many

metals that are frequently employed as catalysts, as well as solvents, are required to be controlled to strict trace levels in the API product by international guidelines,^{4,5} which are observed by the relevant US and EU regulatory bodies.^{6,7}

The *throughput* criterion regards the ability to produce sufficient API within the available time. Long synthetic schemes, reaction times and processing steps are therefore undesirable by this criterion. The use of non-abundant or unusual reagents for the long-term supply of API should also be considered against this criterion.

In reality, these criteria may sometimes work against each other. Considering a catalytic process as an example, a higher catalyst loading may offer shorter reaction times and therefore be advantageous in terms of the throughput criterion, but this may also raise concerns from environmental, economic and control perspectives. A robust understanding of a chemical process enables suitably balanced conditions for a synthetic step to be developed according to the specific requirements and priorities of the project.

Chemical catalysis is often an attractive strategy for delivering a manufacturing route that satisfies many of the SELECT criteria effectively.⁸ For example, catalysis might enable a shorter route to the API by making possible different disconnections, might decrease the quantity of a reagent required to perform a transformation, or might decrease the time and energy required for a particular step. Precious metal catalysis has become ubiquitous in drug syntheses, however the metals used are not only expensive but often carry risks associated with their supply.⁹ Table 1 summarises supply-related data for the base metal iron along with the precious metals palladium, platinum and rhodium, all of which are employed in chemical catalysis.^{9,10} Rhodium is among the least earth-abundant of all precious metals used in catalysis.

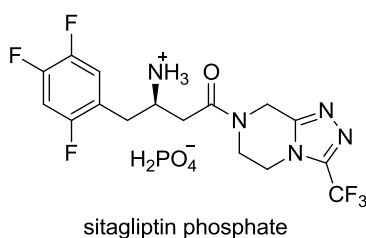
Metal	Crustal Abundance / ppm	Annual Worldwide Production / tonnes	Supply Risk
Iron	41×10^3	3.3×10^9	5.2
Palladium	6×10^{-4}	208	7.6
Platinum	1×10^{-3}	178	7.6
Rhodium	2×10^{-4}	< 30	n.d.

Table 1. Supply data for selected metals used in chemical catalysis. Crustal abundance and production data (2015) stated as compiled by Egorova et al.¹⁰ Supply risk is an index prepared by the British Geological Survey, combining multiple risk factors.⁹ The index ranges from 1 (extremely low risk) to 10 (very high risk).

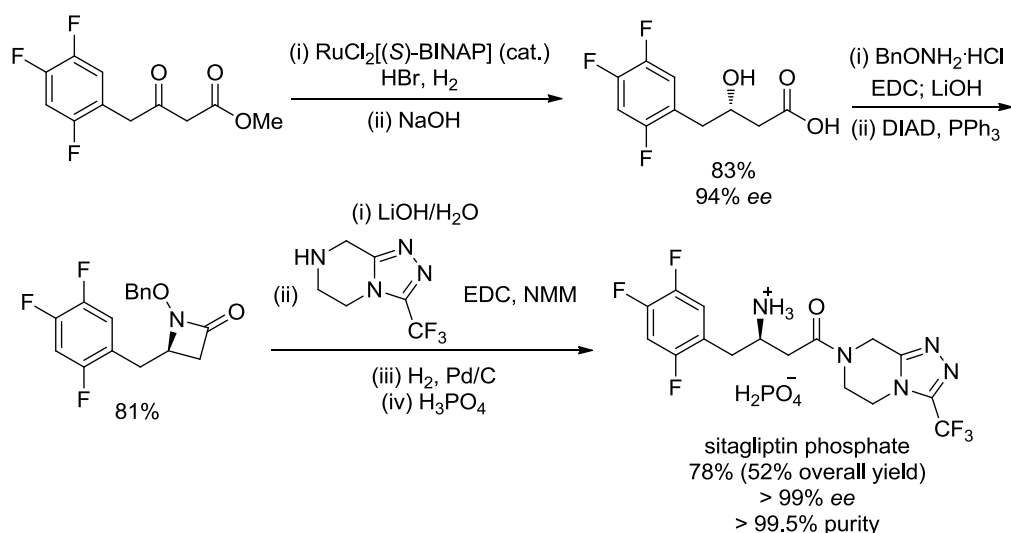
Industrial sustainability priorities drive research in two complementary directions to minimise the use of non-abundant resources.¹¹⁻¹³ The replacement of precious metal catalysts with base metal catalysts is particularly desirable but is generally met with significant

challenges to overcome, typically as a result of contrasting redox processes, the availability of the catalyst precursors, a generally lower functional group tolerance and a higher sensitivity to adventitious moisture or oxygen.^{14,15} Where base metal alternatives are not readily developable, the next most desirable goal is to identify means of utilising non-abundant metals with high efficiency so as to limit the impact of their use and the risks to the long-term supply of the metal. Examples include research to lower the catalyst loading without impacting the outcome of the reaction, and research to process the reaction waste in such a way as to recycle the metal for reuse.

The development of the manufacturing route for sitagliptin, the active ingredient in the Merck drug product, Januvia, is a particularly well-known example of process development on account of the numerous awards received by the researchers involved. Three generations of the route were developed, containing notable examples of industrial asymmetric catalysis, and with significant improvements made in relation to green chemistry and process intensification.¹⁶⁻¹⁸

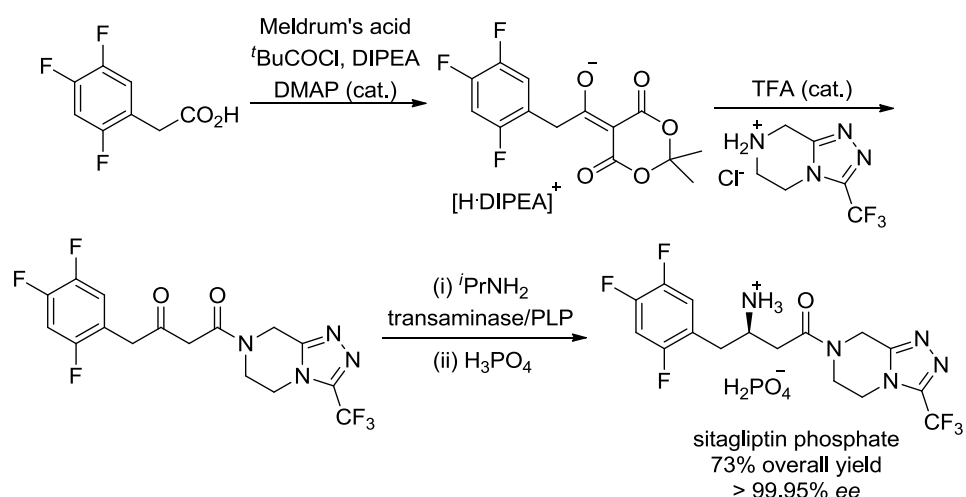


The first generation route is summarised in Scheme 1, providing the sitagliptin phosphate salt on multi-kilogram scale in 52% overall yield and excellent chemical and enantiopurity after crystallisations.¹⁹ As a means to deliver early batches of the API, the synthetic route was adequate. However, as a means for long-term manufacture, the route was unfeasibly inefficient. The most problematic aspects of the synthesis were the uses of EDC couplings and the DIAD/triphenylphosphine Mitsunobu procedure, both of which generated large amounts of waste.



Scheme 1. The first generation route to sitagliptin.

After completely redesigning the synthetic route using rhodium catalysis to give sitagliptin phosphate in 65% overall yield with a decrease of 80% in the total mass of waste and the elimination of the aqueous waste stream,²⁰ a final phase of development gave the third generation process shown in Scheme 2.²¹ Not only could the third generation synthesis afford the API salt in 73% overall yield, but additional improvements in throughput, mass of waste and cost were also achieved. This final generation synthesis required no heavy metals and no specialised manufacturing equipment, such as high pressure vessels, as a result of the enzymatic biocatalytic process employed. The transaminase enzyme was evolved to contain 27 mutations across its structure, in order to achieve the high yielding (92%) and highly enantioselective (> 99.95% ee) transformation for the API synthesis. The process has been employed on pilot plant-scale.



Scheme 2. The third generation route to sitagliptin.

1.2 Chirality in Active Pharmaceutical Ingredients

Chiral drug molecules inherently present challenges from the perspective of the SELECT criteria, with high enantiopurity being an important regulatory requirement and the asymmetric chemistry required often proving either poorly economical or under-developed. In 1993 a study of marketed drugs highlighted a significant difference in the enantiomeric form that synthetic drugs were sold in compared with those sourced naturally or semisynthetically (Figure 1).²² Natural and semisynthetic drugs (accounting for less than a third of the total number of marketed drugs) were found to exhibit chirality in 99% of cases of which 98% were marketed enantiomerically pure. Of the drugs produced synthetically, only 5% were marketed as single enantiomers, with the majority possessing no chirality (60%) and the balance being sold as racemates.

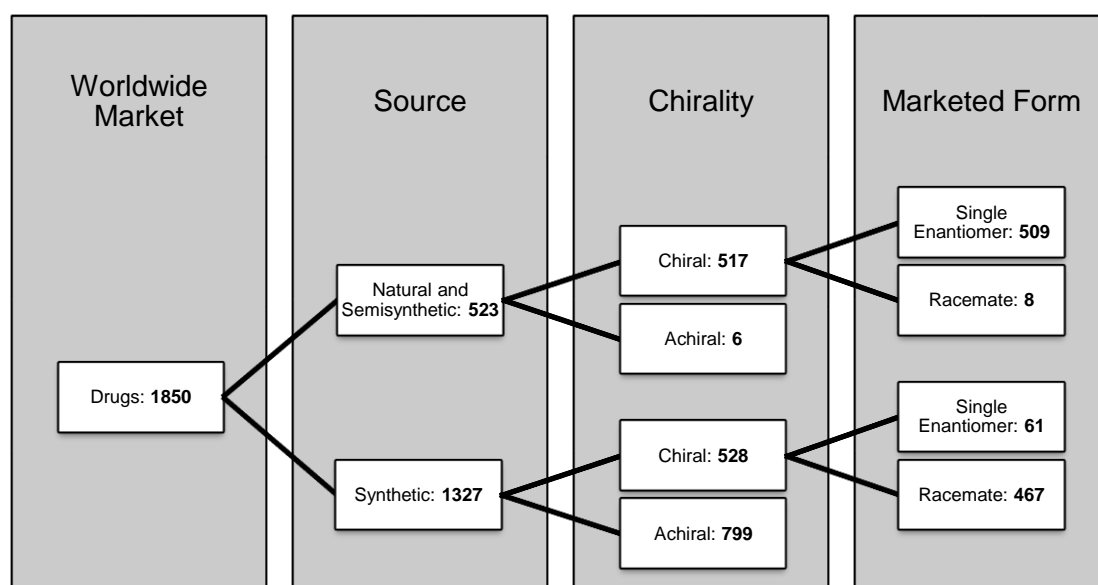


Figure 1. Summary of a 1993 study of the marketed form of drugs, adapted from *Scrip. Mag.*, 1993, Feb, 16–18.

Whilst these data are now over two decades old, more recent concern has been expressed that a continued lack in the synthesis of enantiomerically pure drug products may be hindering clinical success.²³ Biological systems are inherently chiral, with all but the simplest of the amino acid building blocks exhibiting a stereocentre, and consequently there is a general biological preference for synthetic molecules to display chirality if they are to induce a selective and potent response. The proportion of naturally-derived APIs appears only to have decreased; a survey of drug candidate molecules in 2006 observed less than 5% to have been derived from natural products.²⁴

The historic neglect of chirality in synthetic drug compounds can be attributed to insufficiently developed and precedented synthetic methodologies for asymmetric transformations that can reliably meet the high demands of the necessarily stringent regulatory requirements for drug products containing chiral centres. Significant development of sp^2 - sp^2 and related coupling reactions, which enable rapid achiral diversification along a particular vector, has no doubt served to out-compete the use of asymmetric transformations in medicinal chemistry. A 2016 publication measured the frequency of reaction types occurring at least once in a representative sample of publications from the *Journal of Medicinal Chemistry* in 2014.²⁵ The three most prevalent reactions for building up molecules (omitting functional group transformations such as deprotections and ester hydrolysis reactions) were amide formations, nucleophilic aromatic substitutions and Suzuki-Miyaura couplings, which were also the top three final step reactions. The use of asymmetric reactions was not investigated specifically by the authors (indicative of the synthetic preference within medicinal chemistry), although they estimated that only 10% of the manuscripts they examined relating to drug candidates may have employed an asymmetric transformation, in contrast with 90% of the natural product total syntheses they also reviewed for the publication.

Methods for installing chirality can be categorised into five broad categories with different advantages and disadvantages from a process chemistry perspective: chiral resolution, fine chemical and chiral pool starting materials, chiral auxiliaries, enzymatic catalysis, and chemical catalysis.²⁶

Chiral resolution of one enantiomer from another in a racemate is in most cases and by most measures the least elegant and most inefficient method for the isolation of enantiopure compounds.^{27,28} Particularly inefficient but common and often necessary forms of resolution are by preparative chiral HPLC or SFC, or by salt formation with a chiral counterion.²⁹ Enzymatic kinetic resolution is another example, whereby an enzyme reacts much more readily with one enantiomer than another, allowing the product of the resolution reaction to be isolated with high enantiopurity.³⁰ Due to the high substrate selectivity and the sensitivity to reaction conditions often observed with enzymes, enzymatic methods are generally more chemically limited forms of resolution.

A highly attractive form of chiral resolution is dynamic kinetic resolution, in which, for example, two enzymes might be used: one to epimerise or racemise a chiral centre (“dynamic”), and the other to selectively react with only one of the stereoisomers (“kinetic resolution”) to form something inert to the epimerisation conditions (Figure 2). Both

enzymatic and chemical examples have been demonstrated as well as combinations of the two.^{31–34} The primary benefit of the technique is that product of high enantiopurity can be obtained from a racemate without sacrificing half of the material as the undesired enantiomer. Related approaches based on similar principles have also been developed to transform racemates into stereomerically pure products.³⁵

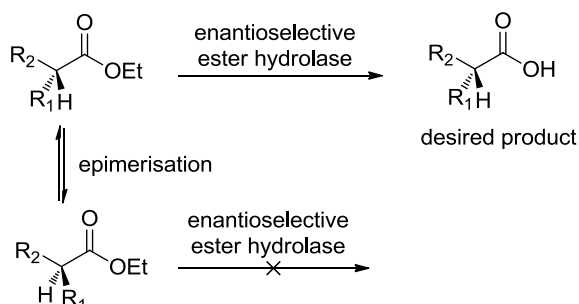


Figure 2. A general example of dynamic kinetic resolution.

Use of chiral starting materials, ideally from the chiral pool or the fine chemicals industry if not, is another common technique.^{26,36} “Purchasing in” the stereochemistry in a more simple molecule avoids the need to install it in a more complex structure, and also enables stereochemistry to be induced elsewhere in the molecule throughout the subsequent synthetic sequence.³⁷ Rather than simply passing the responsibility for inefficient chiral resolutions to a supplier, in most cases this can be a very efficient method since either both enantiomers will be sold by the supplier such that there is no overall loss in efficiency by using a chiral resolution, or there may be a well-precedented asymmetric synthesis of the material, which would be much more difficult to install on a more complex substrate. Nevertheless, diversity is limited by the supply from other industries.

Introducing chirality using chiral auxiliaries is effectively a subset of using chiral pool or fine chemicals industry materials, whereby a chiral group is temporarily installed on an intermediate (generating, for example, a chiral ester) as a means to induce stereoselectivity elsewhere, before cleaving the temporarily installed auxiliary.^{26,38,39} In general this involves two additional steps in a synthesis, and unless the auxiliary can be readily recycled it is a poorly atom economical technique. It also generally requires the labile functionality to be close to the desired stereocentre for effective stereochemical induction.

Catalysis is an attractive means of providing chirality in API syntheses, especially when the analogous racemic transformation would already require catalysis. Enzymatic catalysis has had an important role in API production for many decades and has become an area of increased utility in recent years, with high throughput platforms for enzyme evolution and

testing significantly decreasing the limitations of the high substrate specificity that enzymatic reactions often demand (Scheme 2, page 5).⁴⁰⁻⁴³ Chemical catalysis (organocatalysis or precious metal catalysis in particular) carries many of the advantages of using chiral auxiliaries and chiral starting materials without the need to employ purchased chirality in stoichiometric quantities.^{44,45} It also provides scope for the development of asymmetric variants of already precedented catalytic racemic reactions, simply by replacing achiral ligands with chiral analogues (see, for example, Section 1.3.1).

A 2006 analysis of drug candidate molecules reaching process development within GSK, AstraZeneca and Pfizer found 54% to contain at least one stereocentre, with 97% of these molecules being developed as single stereoisomers.²⁴ This renewed development of chiral APIs is reflected in the structures of recent Phase III GSK drug candidates, with more than three quarters of the small molecules exhibiting stereocentres.⁴⁶ Nevertheless these GSK structures typically lend themselves well to the use of chiral building blocks, indicating a limited scope for diversification.

The 2006 survey identified the source of the 135 chiral centres in the studied sample of molecules under process development, with more than half purchased as starting materials and more than one quarter resolved from a racemate or diastereomeric mixture (Figure 3).²⁴ Of those resolved, only around 10% employed a dynamic kinetic method, the rest presumably involving the discarding of the undesired stereoisomer. The use of such inefficient resolution methods, which often occur towards the end of a synthesis, highlights the lack of asymmetric synthetic transformations that are sufficiently robust, elegant and efficient for practical and economical utility on large scales.

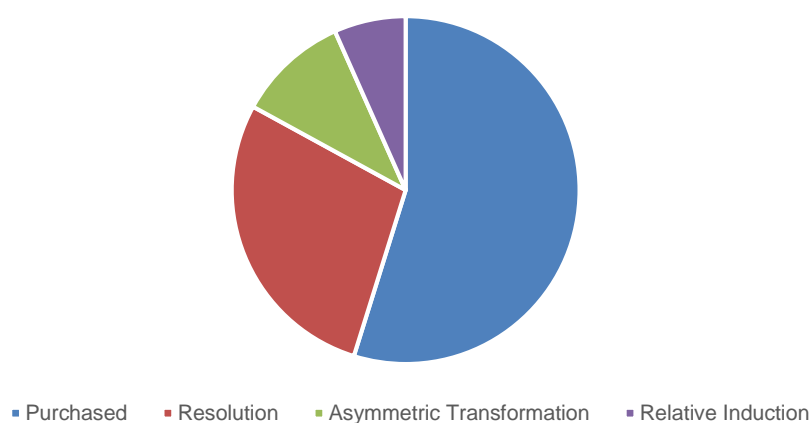
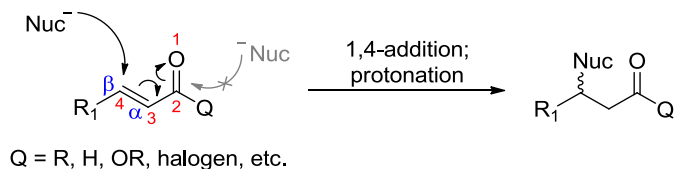


Figure 3. The source of chirality for 135 chiral centres in a 2006 study of drug candidate molecules, adapted from *Org. Biomol. Chem.*, 2006, 5, 2337.

Evidently there remains a significant need to grow a toolbox of robust asymmetric transformations suitable for large scale API manufacture. Generating new methodologies suitable for academic and medicinal chemistry laboratories paves the way for the development of new synthetic techniques that open up the chemical space to new structural motifs in biologically active compounds, but in many cases such methodologies do not translate readily to a process chemistry scale.^{1,2} One example is asymmetric conjugate arylation reactions (Section 0). To avoid this bottleneck in bringing enantio- and diastereopure drug compounds to market, research to render such transformations attractive on manufacturing scales is vital.

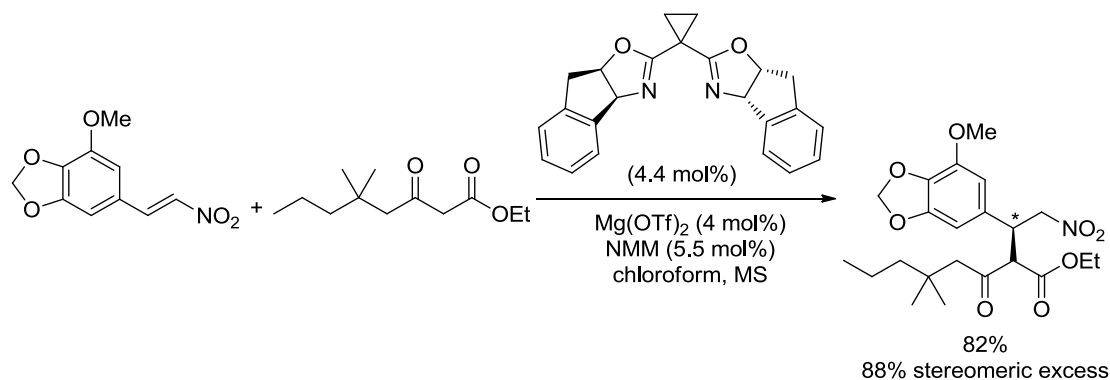
1.3 Rhodium-Catalysed Asymmetric Conjugate Arylation

Nucleophilic conjugate addition or 1,4-addition reactions have a long history in synthetic organic chemistry, beginning with Arthur Michael's seminal discovery in the late 19th century.⁴⁷ Most commonly involving the addition of a nucleophile to an α,β -unsaturated carbonyl compound, the transformation often generates at least one stereocentre and requires attack at the softer electrophilic centre (the β position) in preference to the harder centre at the carbonyl (Scheme 3).



Scheme 3. General scheme for the conjugate addition reaction of a soft nucleophile to an α,β -unsaturated carbonyl compound.

Carbon–carbon bond-forming reactions using carbon nucleophiles are extremely valuable for building up molecular structures, but significant stabilisation of the carbanion is required to enable the soft 1,4-attack for conjugate addition. An enolate is the prime example of a suitably soft carbon nucleophile, while the addition of copper salts to Grignard reagents to form organocuprates has long been known to enable sufficient “softening” of otherwise hard carbon nucleophiles.⁴⁸ An example of a catalytic asymmetric carbon–carbon bond-forming conjugate addition is given in Scheme 4, which determined the absolute stereochemistry in the synthesis of an Abbott API, previously synthesised racemically.⁴⁹



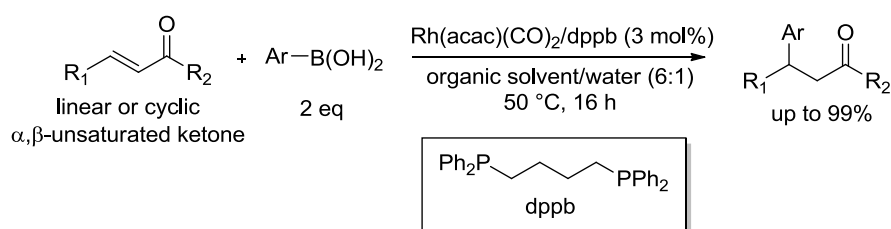
Scheme 4. An asymmetric conjugate addition employed by Abbott for the synthesis of an API.

Carbon–carbon bond-forming reactions to install aryl groups are of particular interest in the pharmaceutical and related industries. Examples exist in the academic literature using, for instance, copper catalysis to modulate the reactivity of arylmetal reagents (such as aryl Grignard and zinc reagents) and favour 1,4- over 1,2-addition to enones with ligand-directed

chiral control.⁵⁰ However, aryl Grignard reagents are challenging substrates for these procedures,^{51,52} and the advantages of using stable aryl nucleophiles increase with scale. The use of arylboron reagents has become of particular interest in the pharmaceutical industry, not least due to the familiarity of their handling and synthesis on account of the ubiquity of Suzuki-Miyaura couplings (Section 1.2). The availability, stability and functional group tolerance of arylboron reagents are significant advantages in industrial contexts, and rhodium catalysis has enabled their use as nucleophiles in conjugate addition reactions.

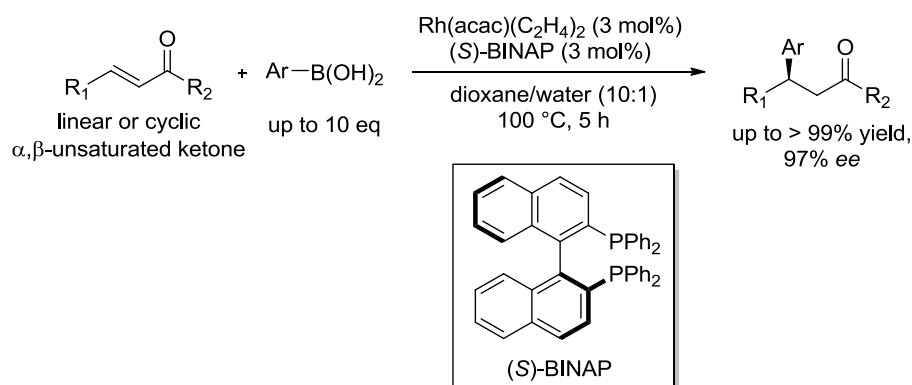
1.3.1 Seminal Reports of Rhodium-Catalysed Conjugate Addition of Arylboronic Acids to Enones

The seminal report of arylboronic acids attacking α,β -unsaturated carbonyl systems in a conjugate fashion was published by Miyaura and co-workers in 1997, who employed rhodium catalysis to couple the arylboron reagent to the electrophile (Scheme 5).⁵³ The reaction proceeded under mild, neutral, aqueous conditions, avoiding highly reactive or unstable organometallic reagents. These conditions were perceived to have been a contributing factor to no competing 1,2-addition or uncatalysed reaction being observed.



Scheme 5. The discovery of rhodium-catalysed 1,4-addition to enones employing arylboronic acid nucleophiles. The organic solvents used were DMF, toluene, cyclohexane and methanol.

This report was closely followed by an asymmetric variant by Hayashi and co-workers (Scheme 6),⁵⁴ such that the rhodium-catalysed conjugate arylation reaction using boron nucleophiles has become known as the Hayashi-Miyaura reaction. Hayashi and co-workers found that a different rhodium salt and harsher conditions than those published by Miyaura were required when using (*S*)-BINAP and other bidentate chiral phosphine ligands. NMR studies revealed the ethylene-ligated catalyst precursor to react immediately and quantitatively with the chiral ligand to form Rh(acac)[(*S*)-BINAP], which demonstrated virtually identical activity and stereoselectivity when charged as the preformed chiral complex. Unusually, although the yield fell rapidly with decreasing temperature (< 3% at 60 °C and below), the enantioselectivity was reportedly unaffected over a temperature range of 40 to 120 °C.



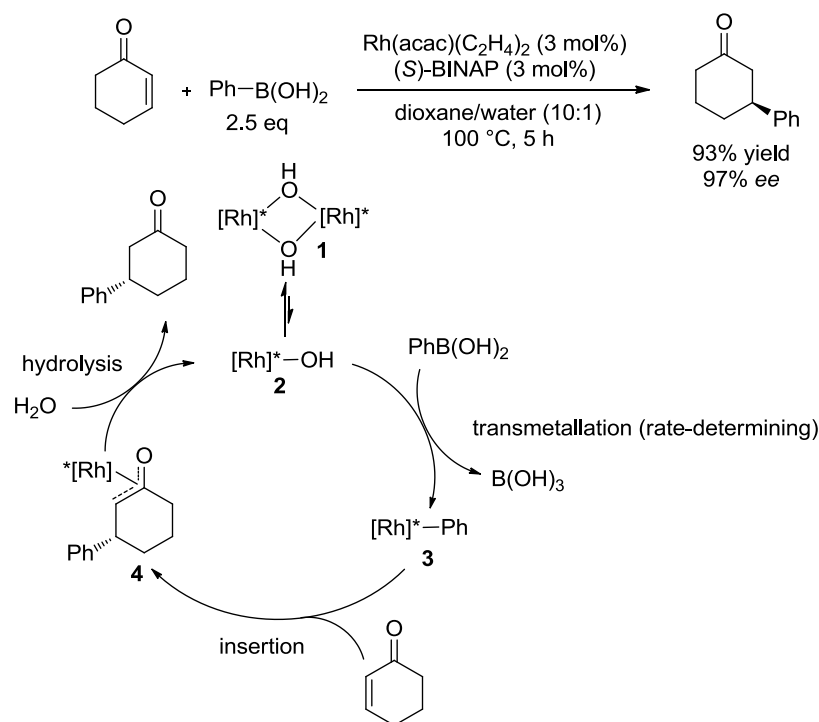
Scheme 6. The asymmetric variant of Miyaura's 1,4-addition, with minor modifications to the conditions.

Both Miyaura and Hayashi found protodeboronation of the aryl species to be a significant competing side-reaction, requiring a large excess of the arylboronic acid for the desired reaction to reliably achieve good yields. The mechanism of the deboronation is not known to have been studied specifically for rhodium-catalysed conjugate addition reactions, yet remains an important problem, particularly from a process chemistry perspective, and is discussed in more detail in Section 1.3.5.

Since the initial reports of the transformation by Miyaura and Hayashi, there has been significant interest within the academic and industrial chemistry communities to demonstrate the scope of the transformation on a diverse range of substrates and using a diverse range of ligands, rhodium salts and conditions (Sections 1.3.3 to 1.3.7).⁵⁵⁻⁶¹ The diverse range of substrates permissible in the methodology is one of its main advantages over other asymmetric conjugate addition reactions, for which there are otherwise limited examples involving the introduction of aryl groups.^{51,52,62-67} Whilst the methodology has been applied to organosilicon and various organometallic reagents, the advantages of organoboron reagents discussed in the introduction to Section 0 have resulted in these receiving the most attention.

1.3.2 General Mechanism of Rhodium-Catalysed Conjugate Arylation

Hayashi and co-workers undertook studies that provided evidence for the proposed catalytic cycle shown in Scheme 7, using 2-cyclohexenone, phenylboronic acid and Rh(acac)[(S)-BINAP] in dioxane/water (10:1) at 100 °C as one of the model systems in the investigation.⁶⁸



Scheme 7. The proposed catalytic cycle for the model system shown, based on mechanistic studies. (*) denotes chirality.

NMR studies of stoichiometric reactions beginning with the phenylrhodium species **3** (stabilised with triphenylphosphine) were performed, which demonstrated the proposed reaction steps and enabled observation of the three proposed intermediates: phenylrhodium species **3**, oxa- π -allylrhodium species **4** and the dimeric hydroxorhodium species **1**. The equilibrium between the catalytically inactive dimeric hydroxorhodium complex **1** and the active monomeric species **2** was found to lie strongly towards the dimer by kinetic analysis of a 1,4-addition reaction employing [Rh(OH)(BINAP)]₂ **2** as the rhodium salt, identifying this dimer as a catalyst resting state.⁶⁹ The same kinetic report identified transmetalation as the rate-determining step of the catalytic cycle.

Each of the three reaction steps, beginning from RhPh(BINAP)PPh₃ **3**, was found to proceed at room temperature, unlike the catalytic reaction in Scheme 6. The origin of this discrepancy was found to be that, whereas rapid transmetalation was observed with [Rh(OH)(BINAP)]₂ (complex **1**, in equilibrium with complex **2**), transmetalation using Rh(acac)(BINAP) (formed following ligand exchange in Scheme 6) was extremely slow at ambient temperatures. The acac-ligated rhodium species could be formed rapidly from the hydroxo analogue upon addition of 1 equivalent of acetylaceton, indicating that Rh(acac)(BINAP) was a resting state in the catalytic cycle, formed by the interception of [Rh(OH)(BINAP)]₂ with acetylaceton under the reaction conditions. Higher temperatures are therefore typically required for transmetalation when an acac-ligated catalyst precursor is

employed. Using $[\text{Rh}(\text{OH})(\text{BINAP})]_2$ or potassium hydroxide with $[\text{RhCl}(\text{BINAP})]_2$ instead of $\text{Rh}(\text{acac})(\text{BINAP})$ as the rhodium salt, the catalytic 1,4-addition reaction proceeded well at 35 °C. In these cases, the lower temperature also enabled a higher enantiomeric excess to be achieved and enabled the excess of phenylboronic acid to be decreased to 1.4 equivalents, due to a greater retardation of the undesired deboronation reaction than of the desired 1,4-addition reaction.

1.3.2.1 Stereocontrol in Asymmetric Rhodium-Catalysed Conjugate Arylation

A simple steric model allows the stereoselectivity of the transformation to be predicted.⁵⁴ Considering (*S*)-BINAP as an example (Figure 4), two reactive binding orientations of the enone can be envisaged. Figure 4a shows the favoured orientation of the enone, with the bulk of the enone directed away from the bulk of the phenyl ring from (*S*)-BINAP, which projects above it. Insertion into the rhodium–aryl bond in this case would give the favoured (*S*)-enantiomer. If the enone is bound to the rhodium centre with its bulk directed above the plane of the complex (Figure 4b), a destabilising steric interaction would be envisaged between it and the phenyl ring, causing the (*R*)-enantiomer to be disfavoured.

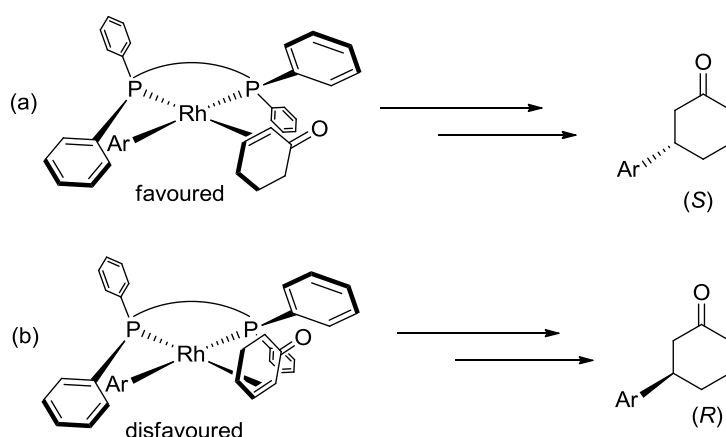


Figure 4. A simple steric model provides a predictive tool to determine the major enantiomer of the product. (a) The orientation of the enone leading to the lower energy transition state. (b) The orientation of the enone leading to the higher energy transition state. The binaphthalene backbone is represented by the curved P–P bond.

By analogy, (*S*)-BINAP would direct preferential attack to the *si* face for linear *cis*-alkenes and to the *re* face for linear *trans*-alkenes, such that the bulk of the substrate is directed away from the top right quadrant of the rhodium complex (Figure 5).

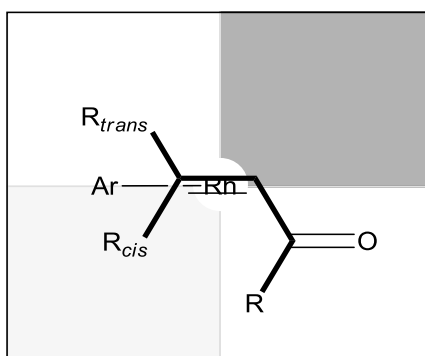
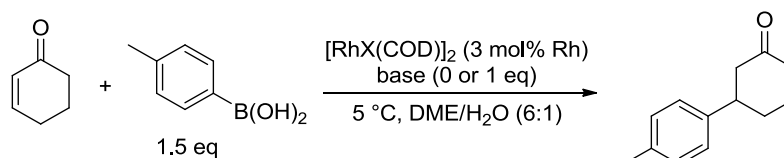


Figure 5. A schematic to show the preferred binding orientation of linear α,β -unsaturated carbonyls to $[\text{Rh}((S)\text{-BINAP})(\text{Ar})]$. Darker shading represents areas of greater steric bulk on the complex.

The same model can be used to predict the stereochemical outcome using different ligand classes such as chiral dienes (Section 1.3.4).^{70,71} However, computational studies, particularly involving chiral diene ligands, have indicated that steric differentiation alone is insufficient to account for the enantioselectivities observed and instead a more complicated description involving a stereoelectronically distorted carborhodation transition state must be invoked.^{72–74}

1.3.2.2 The Role of Base in Rhodium-Catalysed Conjugate Arylation

The role of base has been investigated by Miyaura and co-workers, revealing that its role is not solely in the generation of a hydroxorhodium species from the catalyst precursor (Section 1.3.2).⁷⁵ This primary role of the base was demonstrated by comparing the reactivity of $[\text{Rh}(\text{OH})(\text{COD})]_2$ and $[\text{RhCl}(\text{COD})]_2$ with and without potassium hydroxide (Scheme 8).



Scheme 8. Investigation of the effect of base. X = chloro- or hydroxo-ligand.

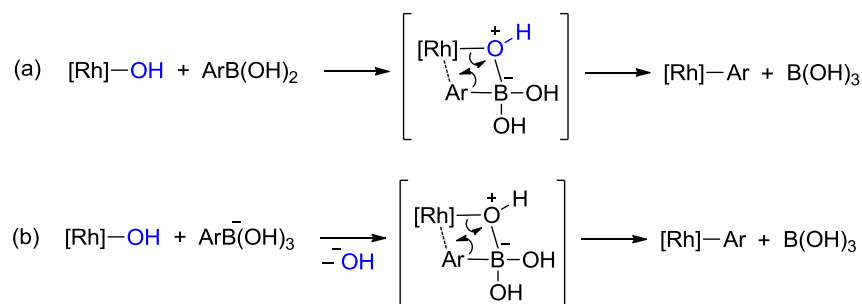
In the absence of base, $[\text{RhCl}(\text{COD})]_2$ gave no greater than trace conversion to the product, whereas use of $[\text{Rh}(\text{OH})(\text{COD})]_2$ afforded the product, albeit slowly (20% conversion within 3 hours). When the reaction was performed using $[\text{RhCl}(\text{COD})]_2$ in the presence of potassium hydroxide, conversion was near-quantitative within 1 hour. This provided support for the necessity of a hydroxorhodium or related species for facilitating transmetalation, and was consistent with observations made that $[\text{Rh}(\text{OH})(\text{COD})]_2$ (and possibly $[\text{Rh}(\text{OMe})(\text{COD})]_2$)^{75,76} provided the conjugate arylation product at room temperature without additional base, whilst $[\text{Rh}(\text{Cl})(\text{COD})]_2$ and $\text{Rh}(\text{acac})(\text{COD})$ were unsuccessful in catalysing the reaction under these conditions. Furthermore, performing the reaction in

Scheme 8 at 0 °C using $[\text{RhCl}(\text{COD})]_2$ in the presence of different inorganic bases (1 equivalent) showed conversion over 6 h to be dependent on the strength of the base: KOH (83% conversion) > K_3PO_4 (49%) > K_2CO_3 (34%) > no base (trace).

An additional role of base was indicated by the increased conversion using $[\text{RhCl}(\text{COD})]_2$ with potassium hydroxide (quantitative within 1 hour) relative to that achieved by $[\text{Rh}(\text{OH})(\text{COD})]_2$ without base (20% within 3 hours). It was also found that adding potassium hydroxide to the reaction using $[\text{Rh}(\text{OH})(\text{COD})]_2$ under the conditions in Scheme 8 gave reactivity comparable to that seen with $[\text{RhCl}(\text{COD})]_2$ under the basic conditions. This effect halved when instead triethylamine was used with $[\text{Rh}(\text{OH})(\text{COD})]_2$ (50% conversion in 1 hour). Conclusive evidence to identify this second role of base is not believed to have been found, however at the time the authors suggested that this may either be due to an accelerated hydrolysis pathway of the rhodium-enolate that results from insertion of the alkene into the rhodium–aryl bond, or may be due to the generation of a quaternary arylboronate (Scheme 9b) as has been described for a transmetalation mechanism in palladium-catalysed reactions.^{77,78}

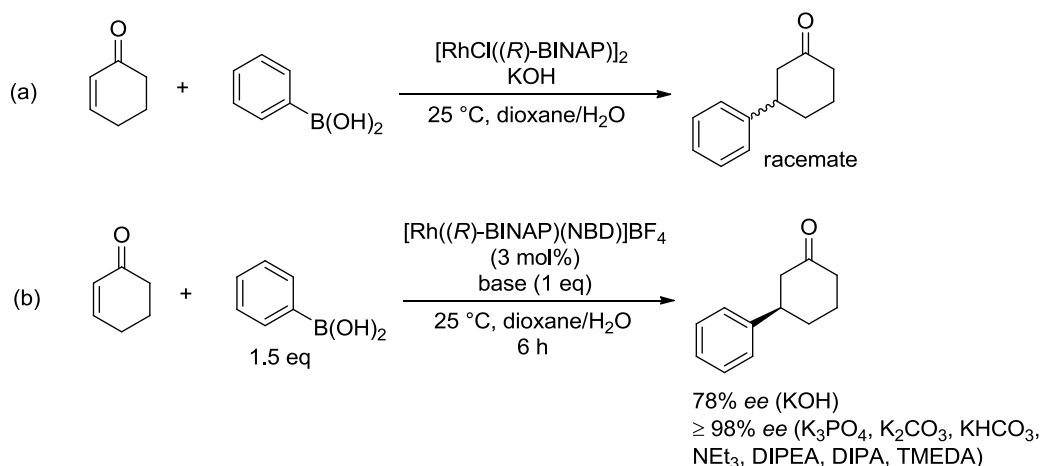
The first of these is initially compelling although it has not been supported further in the literature. The implication is that upon formation of a rhodium-enolate, the presence of base accelerates its hydrolysis, presumably via an associative mechanism. However, the fact that the rate-determining step of the cycle was found, in the absence of base, to be transmetalation indicates that this cannot be the cause of the significant rate acceleration (Section 1.3.2).^{69,79}

The second suggested reason appears to be the most widely accepted, and the implication is therefore that two transmetalation mechanisms can operate: mechanisms (a) and (b), shown in Scheme 9.⁸⁰ That mechanism (a) operates is evidenced by the activity of $[\text{Rh}(\text{OH})(\text{COD})]_2$ in the absence of base. However, acceleration in the presence of aqueous base even when using $[\text{Rh}(\text{OH})(\text{COD})]_2$ suggests that mechanism (b) can also occur, and faster than mechanism (a) when sufficient base is present for quaternisation of the organoboron species. A number of model systems have also been used to study possible transmetalation pathways both practically and computationally.^{81,82}



Scheme 9. Proposed mechanisms of transmetalation to $[\text{Rh}]-\text{OH}$ and related species (a) from arylboronic acids (b) from quaternary arylboronates.

Miyaura and co-workers also found the base to have an impact on stereoselectivity.⁷⁵ Addition of potassium hydroxide to $[\text{RhCl}((R)\text{-BINAP})]_2$ under the conditions shown in Scheme 10a afforded racemic product. The cationic rhodium complex used in Scheme 10b showed moderately good stereoselectivity with potassium hydroxide, but this was improved significantly using weaker bases. The origin of this difference has not been established and similar observations are not known to have been reported elsewhere.



Scheme 10. Reported effects of base on the stereoselectivity of 1,4-additions. (a) Formation of the racemic addition product despite the use of enantiopure ligand. (b) Poor enantioselectivity only when using KOH.

1.3.3 Rhodium Salts used as Catalyst Precursors in Conjugate Arylation

The rhodium salts commonly available as catalyst precursors for use in 1,4-addition chemistry can be broadly grouped into three classes: monomeric rhodium complexes, dimeric rhodium complexes and cationic rhodium complexes. Often these are achiral complexes, from which the chiral complexes can be preformed or formed in situ. Monomeric rhodium complexes employ a bidentate anionic ligand to stabilise the rhodium (I) centre, such as in the case of $\text{Rh}(\text{acac})\text{L}_2$ complexes (e.g. $\text{Rh}(\text{acac})(\text{CO})_2$). The dimeric complexes consist of two rhodium (I) centres, often with coordinated alkene ligands, and two bridging

counterions such as chloro- or hydroxo-ligands. A common example is $[\text{RhCl}(\text{COD})]_2$, however the cyclooctadiene ligands are themselves excellent ligands for the 1,4-addition reaction and exchange slowly with BINAP.⁶⁸ Compared to $[\text{Rh}(\text{OH})(\text{BINAP})]_2$, $[\text{Rh}(\text{OH})(\text{COD})]_2$ was found to undergo the rate-determining transmetalation step of the catalytic cycle with a larger rate constant, and the equilibrium between the inactive dimer and active monomer was found to lie further towards the monomer.⁷⁹ COD-ligated rhodium complexes are therefore an unusual choice of catalyst precursor when asymmetric product is required, since the activity of any residual COD-ligated rhodium can significantly limit the overall enantiopurity. To avoid this problem, successful asymmetric examples employing COD-ligated catalyst precursors tend to involve premixing the rhodium complex with a chiral phosphine ligand.⁸³ A popular analogue of the COD complex is $[\text{RhCl}(\text{C}_2\text{H}_4)_2]_2$, as its dominance in a recent review highlights,⁵⁷ since the ethylene ligands are rapidly and irreversibly exchanged in the reaction mixture (see Section 1.3.1).⁵⁴

Cationic rhodium complexes contain a non-coordinating counterion in place of the bidentate anionic ligands used in other monomeric complexes. Common examples include $\text{Rh}(\text{NBD})_2\text{BF}_4$ and $\text{Rh}(\text{COD})_2\text{BF}_4$. A key attraction of the norbornadiene complex is that it has been found to undergo good ligand exchange with BINAP whilst being poorly active in the arylation reaction on its own, unlike cyclooctadiene-ligated complexes. Additionally, the 1,4-addition has been found to proceed well using triethylamine instead of potassium hydroxide (cf. Section 1.3.2).^{84,85} Use of a weaker base broadens the substrate scope of the reaction to include compounds with more base-sensitive functionality.

A number of reports coupling arylboron reagents to unsaturated electrophiles have now been published using alternative metal catalysts, such as palladium,^{86–89} ruthenium,⁹⁰ copper⁹¹ and nickel,⁹² and using organocatalysis,^{93–95} however none is yet at a state to compete with the rhodium-catalysed process, some demonstrating only a limited substrate scope or not having been successfully demonstrated for asymmetric synthesis.

1.3.4 Ligand Classes Demonstrated in Rhodium-Catalysed Conjugate Arylation

Many different ligands have been developed and/or demonstrated for the rhodium-catalysed conjugate arylation reaction, which tend to fall within the classes shown in Figure 6: phosphorus ligands, bissulfoxide ligands and diene ligands.^{55,57,59} Electronic and steric modifications to the active catalyst via the ligand enable fine-tuning of the reactivity and selectivity of the reaction according to the requirements of the application, whether the

priority is for aqueous solubility,^{96,97} enantioselectivity, catalyst turnover, or for particular efficiency with a specific substrate or substrate class.^{98,99} Hybrid ligands, for example those combining olefin motifs with sulfoxide motifs, have further expanded the opportunity for fine-tuning and ligand diversification.^{55,57,59} Many of the more exotic ligands are not readily prepared or commercially available and so are not discussed in detail in this thesis, which focusses on industrially-applicable systems.

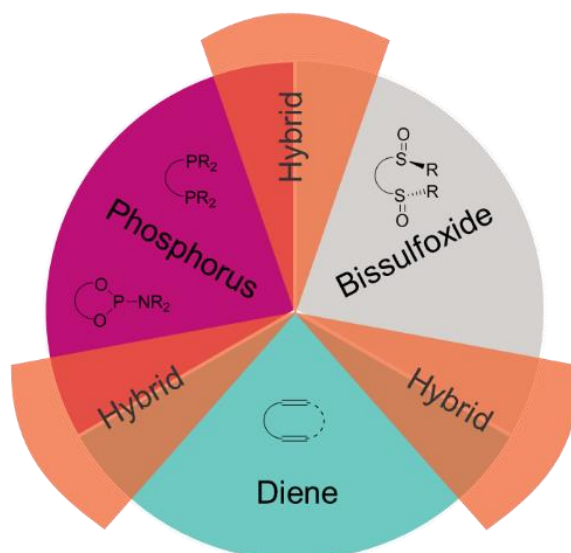
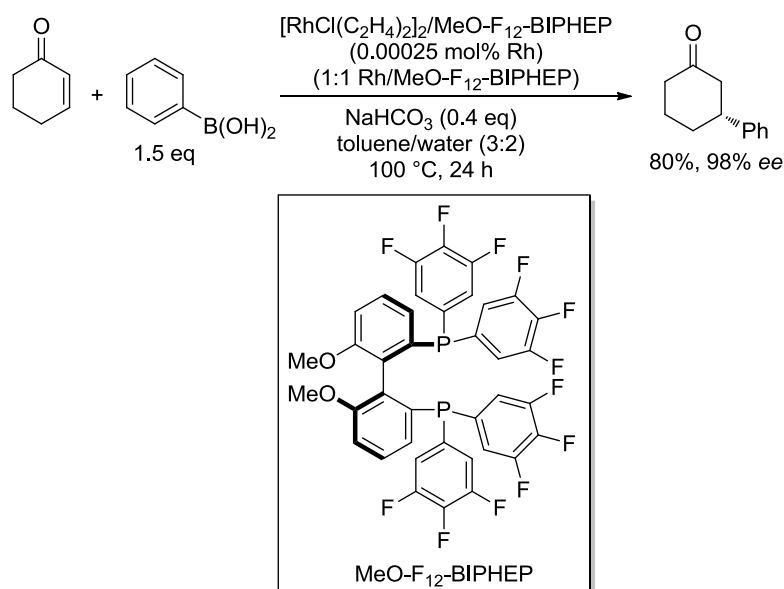


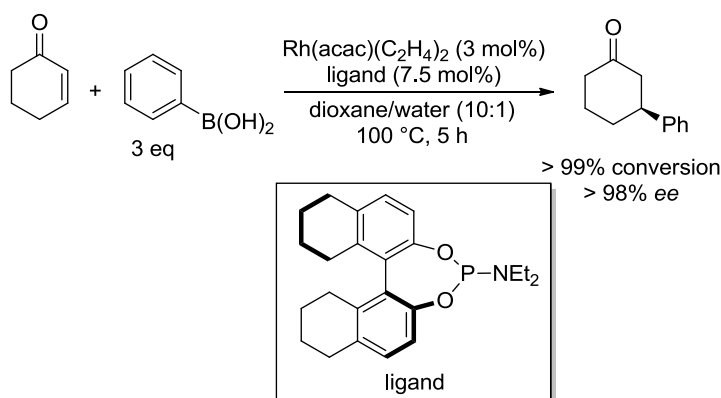
Figure 6. The main ligand classes that have been demonstrated in rhodium-catalysed 1,4-addition reactions.

Chiral bisphosphine ligands, especially axially chiral biaryl ligands, are the most well-known. The catalytic activity and turnover number achieved when using BINAP-derived ligands has been shown to correspond to the π -accepting ability of the ligand, as measured via the carbonyl stretching frequency of the corresponding $\text{RhCl}(\text{CO})(\text{bisphosphine})$ complexes.¹⁰⁰ Ligands with a greater π -accepting character provide improved stabilisation of the transition state and product of the rate-determining transmetalation step. A particularly excellent example is the strongly π -accepting ligand MeO-F₁₂-BIPHEP (Scheme 11).¹⁰⁰ The use of this ligand enabled a catalyst turnover frequency of 54,000 h⁻¹ and turnover number of 320,000. A rhodium loading of just 0.00025 mol% therefore gave good activity for asymmetric conjugate arylation. Electron-poor phosphines, such as MeO-F₁₂-BIPHEP, have also been employed to enable conjugate arylations to proceed efficiently at room temperature.^{101,102}



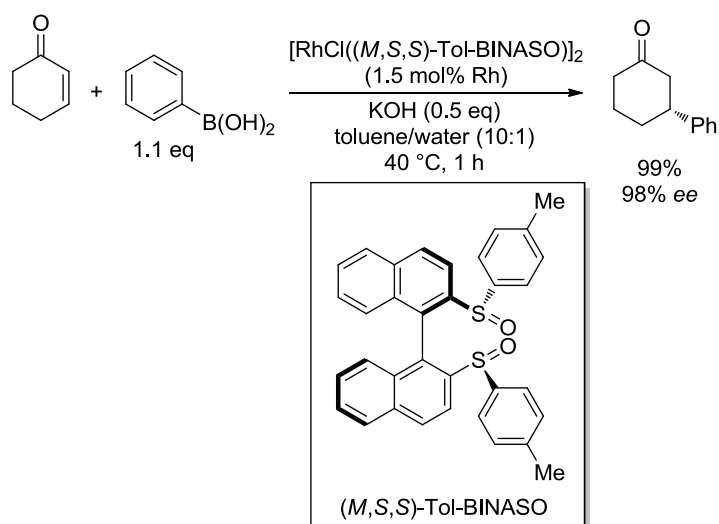
Scheme 11. MeO-F₁₂-BIPHEP was demonstrated to enable a catalyst turnover number of 320,000 in the system shown.

Chiral monophosphine ligands have also been employed in rhodium-catalysed conjugate arylations, with a 1:2 rhodium/ligand stoichiometry generally required. Phosphoramidites with axial chirality in a biaryl backbone are an example of these (Scheme 12),¹⁰³ and a direct comparison of the phosphoramidite in Scheme 12 with BINAP showed the phosphoramidite to give a significantly more active catalyst system. Using the phosphoramidite ligand (1 mol% rhodium, 1:2.5 rhodium/ligand) in aqueous dioxane at 100 °C achieved almost full conversion of cyclohexenone within 5 minutes, compared with approximately 10% conversion using BINAP. Their simple structures, combined with an increased π -accepting character relative to the classic BINAP-derived ligands on account of the lower energy phosphorus–nitrogen and phosphorus–oxygen σ^* orbitals, render phosphoramidites and related monophosphines an attractive subset of ligands.



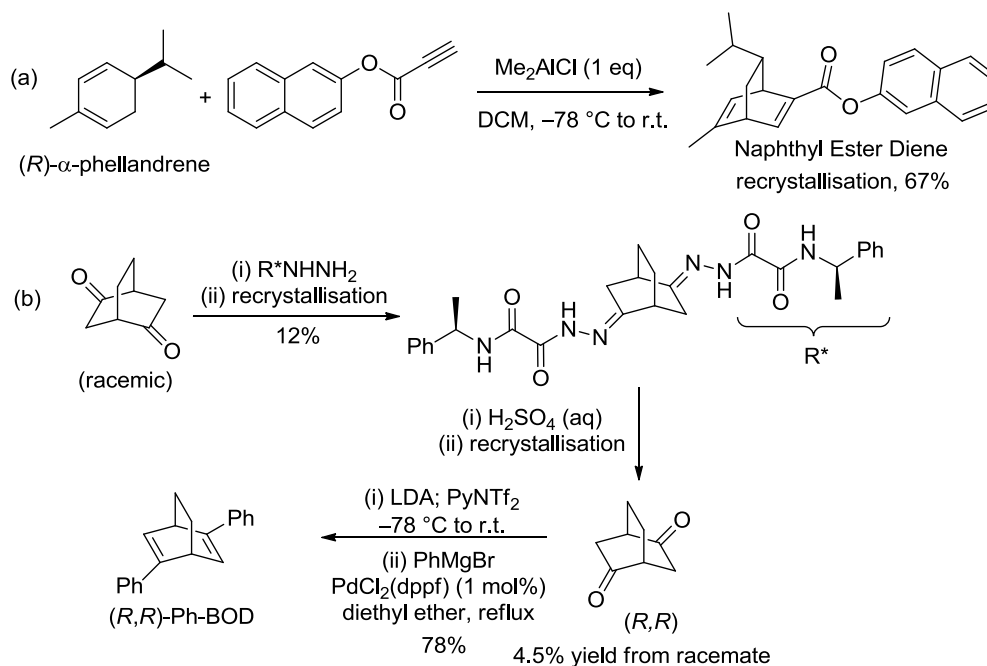
Scheme 12. Phosphoramidite ligands have been shown to perform with high activity and enantioselectivity.

Chiral sulfoxides have only recently emerged as a ligand class that can be applied to an increasingly wide range of transformations employing transition metal catalysis.¹⁰⁴ Bissulfoxide ligands have now been extensively demonstrated for use in rhodium-catalysed conjugate arylation, and can typically be prepared in reasonably short syntheses.¹⁰⁵ The first example catalysed the addition of phenylboronic acid to cyclohexenone with remarkable selectivity and efficiency, enabling the use of just 1.1 equivalents of the arylboron reagent (Scheme 13).⁹⁹



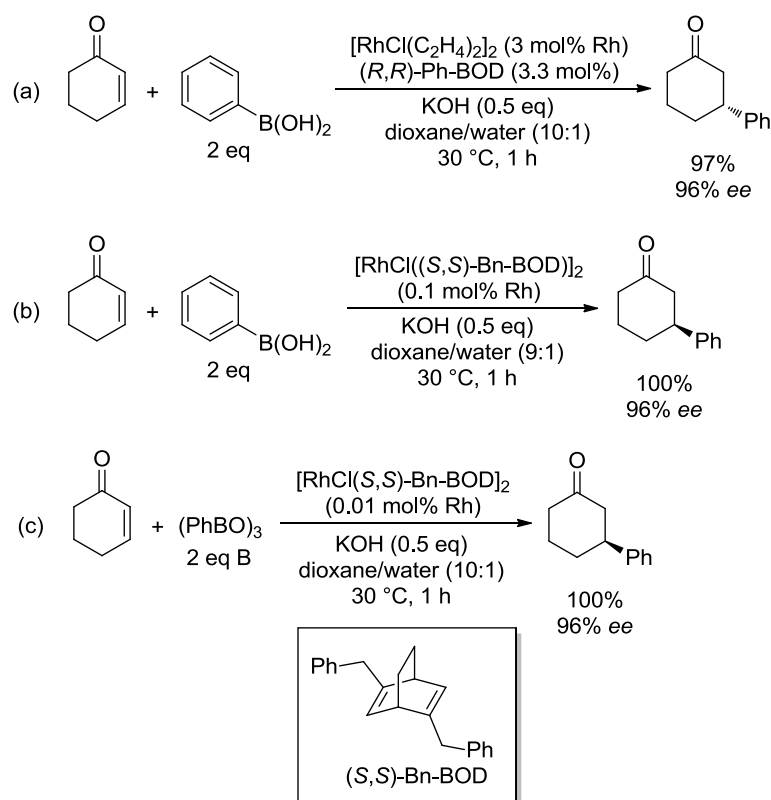
Scheme 13. The first example of a bissulfoxide employed for rhodium-catalysed 1,4-addition.

Dienes have an inherently strong π -accepting character, and their excellent performance in rhodium-catalysed 1,4-addition chemistry and other areas has led to extensive work in the diversification of this ligand class.^{70,71,106–119} Unfortunately, relatively few are commercially available and no examples of their use exist in the process chemistry literature on rhodium catalysed conjugate addition (Section 1.3.7). Two commercially available examples are the naphthyl ester diene ligand (Scheme 14a) and (*S,S*)- or (*R,R*)-Ph-BOD (Scheme 14b). The naphthyl ester diene ligand is readily prepared from the [4+2] cycloaddition of diene (*R*)- α -phellandrene to dienophile 2-naphthyl propiolate, giving the ligand in high chemical and enantiomeric purity after recrystallisation of the crude reaction mixture (Scheme 14a).¹¹² However, the synthesis of (*R,R*)-Ph-BOD is more challenging, particularly since it does not employ a chiral pool starting material (Scheme 14b);¹⁰⁷ fractional recrystallisation of the diastereomeric dihydrazone is very low yielding.¹¹³ An alternative synthesis of (*R,R*)-Ph-BOD has also been reported from 2-cyclohexenone and phenylacetaldehyde, involving an asymmetric organocatalytic Michael-aldol reaction.¹²⁰ This preparation remains low yielding (11% overall) and requires a similar number of synthetic steps, with the Michael-aldol reaction requiring up to 4 days.



Scheme 14. Reported syntheses of chiral diene ligands (a) Naphthyl Ester Diene and (b) (*R,R*)-Ph-BOD.

An example of the use of C_2 -symmetric Ph-BOD for conjugate arylation is given in Scheme 15a.⁷¹ As noted in Section 1.3.2.2, the high activity of $[\text{RhOH}(\text{COD})]_2$ can be detrimental to the overall enantioselectivity of a process when the COD-ligated rhodium salt is used in conjunction with a chiral ligand. However, when the diene ligand itself is chiral, the high activity achieved with diene ligands enables highly efficient processes to be developed, with low catalyst loadings affording products in high yield and enantiopurity (Scheme 15b and Scheme 15c).¹¹¹



Scheme 15. Use of (a) Ph-BOD and (b, c) Bn-BOD for the conjugate arylation of phenylboronic acid to cyclohexenone. In Schemes (b) and (c) in particular, the high activity of the active catalyst is demonstrated.

1.3.5 Organoboron Nucleophiles Employed in Rhodium-Catalysed Conjugate Arylation

Arylboronic acids remain the most commonly reported organoboron nucleophiles for rhodium-catalysed asymmetric conjugate arylations, however various analogues (Figure 7) have also been successfully utilised, under motives including their relative ease of purification or the stability of the alternative arylboron reagent either in storage or under the reaction conditions.^{55–61}

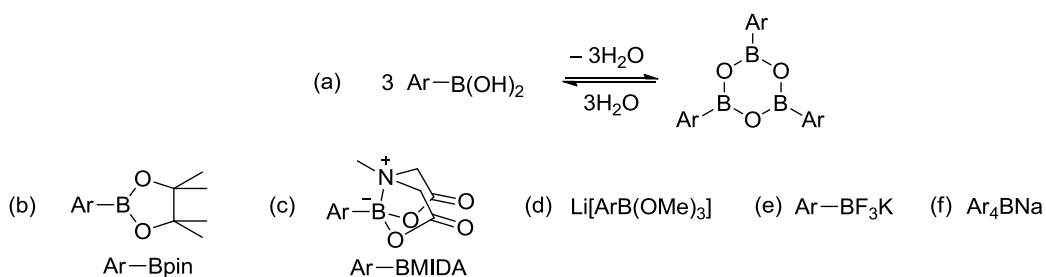


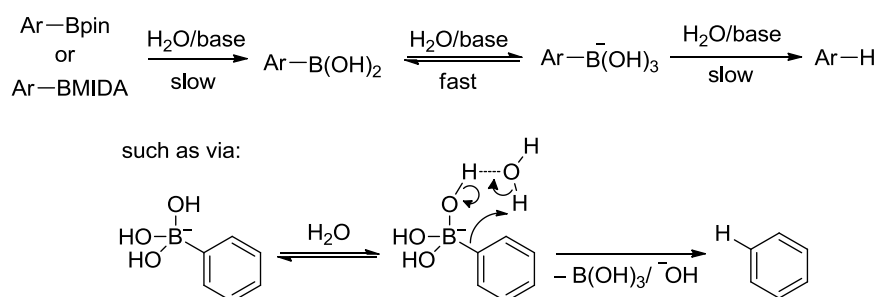
Figure 7. (a)–(f) Seven arylboron reagents utilised in rhodium-catalysed 1,4-addition reactions.

Arylboronic acids generally demonstrate good thermal, oxygen and aqueous stability, although dehydration of the acids generates the corresponding boroxines ((ArBO)₃, Figure 7a), which can be difficult to prevent in storage.⁹¹ Therefore, sources of boronic acid often

contain varying levels of the corresponding boroxine, whereas sources of boroxine can be more easily prevented from containing the boronic acid.¹²¹ As such, use of boroxines has become an attractive alternative to the use of arylboronic acids, since their use enables greater certainty in the species and stoichiometry being charged to a reaction.

Arylboronic acid pinacol esters (ArBpin, Figure 7b) are common products of palladium-catalysed Miyaura borylation¹²² and iridium-catalysed C–H borylation.¹²³ Generally more easily prepared, purified and handled than the corresponding boronic acids, these are an attractive, although much less extensively demonstrated, alternative to the boronic acids in 1,4-addition reactions.¹²⁴ It has been assumed that the arylboronic esters hydrolyse under the reaction conditions to give the corresponding arylboronic acids, which subsequently undergo transmetalation to rhodium (Section 1.3.2.2).⁵⁹

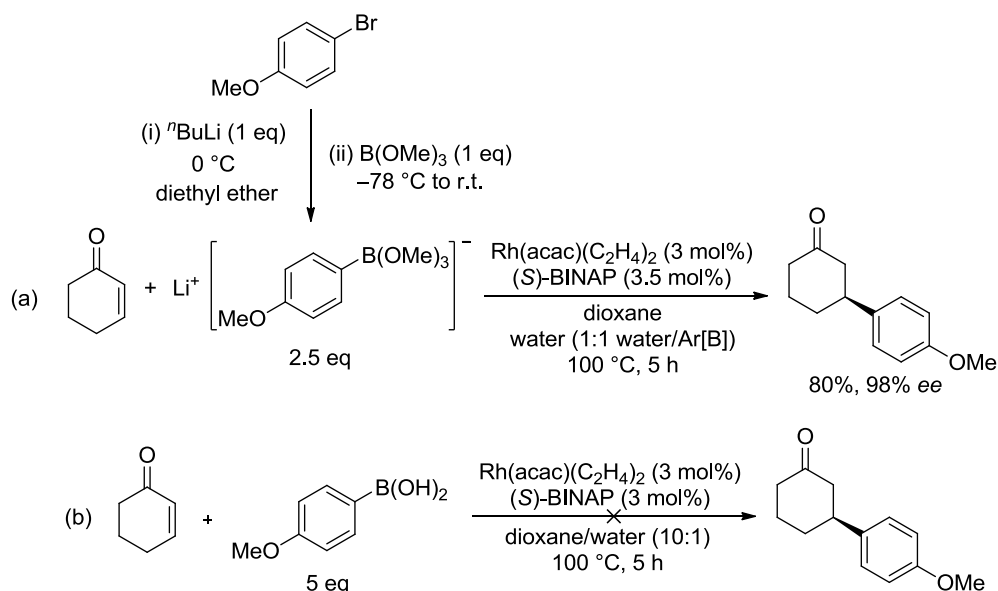
Arylboronic acids can show instability with respect to protodeboration at high temperatures and under basic conditions (Scheme 16). As a result of the ubiquity of arylboronic acids in numerous cross-coupling reactions such as the Suzuki-Miyaura coupling, many of which require high temperatures and basic conditions, significant interest has been directed towards understanding this competitive deboration pathway.^{125–129} One of the most successful means of suppressing the side-reaction has been the so-called “slow-release” strategy, in which an alternative arylboron reagent is charged to the reaction mixture.^{130,131} Under the reaction conditions, the alternative arylboron reagent then hydrolyses slowly to the parent arylboronic acid, thereby ensuring that only a minimal amount of the less stable arylboronic acid is present at any one time.



Scheme 16. Base-mediated protodeboration of arylboronic acids and related arylboron reagents.

With typical conditions employing temperatures of 100 °C and aqueous base, this can be an important consideration for rhodium-catalysed 1,4-additions. Alternative arylboron reagents have therefore been employed with the slow-release strategy in mind, leading to reports of the use of boroxines (Figure 7a),¹²¹ *N*-methyliminodiacetic acid (MIDA) boronates (Figure 7c),¹³² trimethoxyborates (Figure 7d),^{133,134} trifluoroborates (Figure 7e)^{135,136} and tetraarylborates (Figure 7f) in rhodium-catalysed conjugate addition reactions.¹³⁷ Some

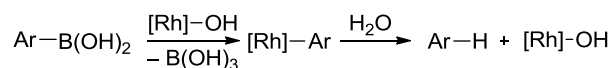
arylboron reagents are believed to transmetalate via an alternative mechanism altogether.⁵⁹ One of the first examples of the successful implementation of the slow-release approach is given in Scheme 17, which enabled isolation of the conjugate arylation product in good yield (Scheme 17a) whilst use of the parent arylboronic acid had afforded only anisole without formation of the conjugate arylation product in detectable yield (Scheme 17b).¹³³



Scheme 17. One of the first demonstrations of the use of alternative arylboron reagents in conjugate arylation. (a) Successful conjugate arylation employing a trimethoxy arylboronate generated in situ. (b) Unsuccessful conjugate arylation employing the parent boronic acid, which afforded only anisole.

In cases where particularly unstable arylboronic acids would be required, such as heteroarylboronic acids, the use of more stable alternative reagents is an important strategy for decreasing the extent of protodeboronation.¹³⁸ However, rhodium-catalysed conjugate arylations can be performed under much milder conditions than those originally reported, and yet in these cases protodeboronation often remains a significant side-reaction. In contrast to palladium chemistry, in which competitive metal-mediated consumption of the arylboron reagent is generally not a necessary consideration,¹³¹ the arylrhodium intermediate is typically more susceptible to protonolysis than the parent arylboron reagent.⁶¹

Two different mechanisms for the competing protodeboronation must therefore be considered in the case of rhodium-catalysed 1,4-addition reactions: a base-mediated pathway, and a metal-mediated pathway. Whilst the direct base-mediated protodeboronation pathway has been extensively studied, there have been no significant research efforts made in the context of rhodium-catalysed conjugate arylation to understand the rhodium-mediated pathway, involving interception of the arylrhodium intermediate in the catalytic cycle by a protic species before insertion of the alkene electrophile can occur (Scheme 18).



Scheme 18. Rhodium-mediated protodeboronation of an arylboronic acid.

1.3.6 Linear Enoates as Electrophiles in Rhodium-Catalysed Conjugate Arylation

Since the initial reports, rhodium-catalysed asymmetric conjugate arylations have been demonstrated on a large range of unsaturated electrophiles with multiple minor variations to the reaction conditions, examples of which can be found in review articles.^{55–61} Although esters have a weaker electron-withdrawing effect than their corresponding ketones, both Hayashi¹³⁴ and Miyaura¹²⁴ successfully demonstrated the reactivity of linear enoates in the reaction with arylboronic acids (2–5 equivalents) and with lithium arylborates (LiArB(OMe)₃, 2.5 equivalents, generated in situ), Miyaura finding BINAP to be the best performing ligand out of a small set of chiral phosphine ligands. Miyaura also provided one example of the conjugate arylation using phenylboronic acid pinacol ester as the arylboron reagent, with only a slight decrease in yield and no difference in enantioselectivity observed compared with the parent boronic acid.

The steric bulk of the ester moiety had a significant impact both on the rate and yield of the reaction, and the enantioselectivity of the product (Table 2).¹³⁴ The greater the bulk of the ester, the slower the reaction and the greater the extent of competing deboronation. However, an increase in steric bulk also led to an increase in the enantiomeric excess achieved (cf. Section 1.3.2.1).

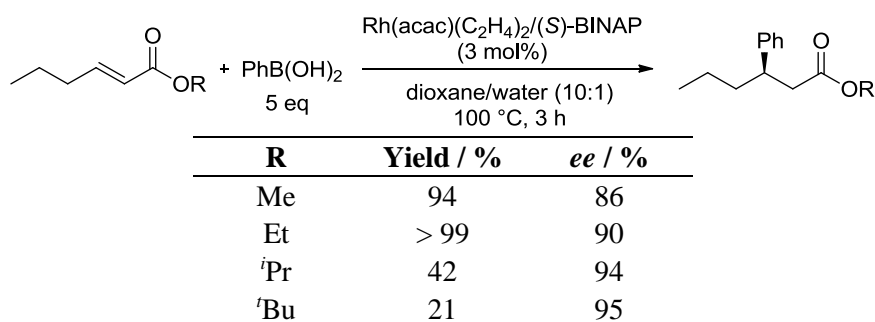
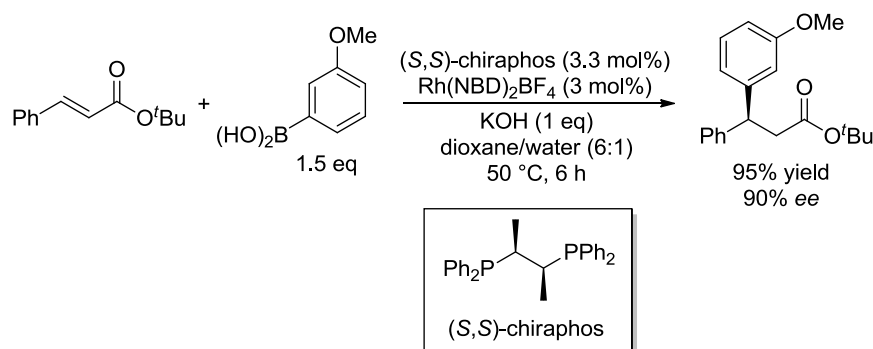


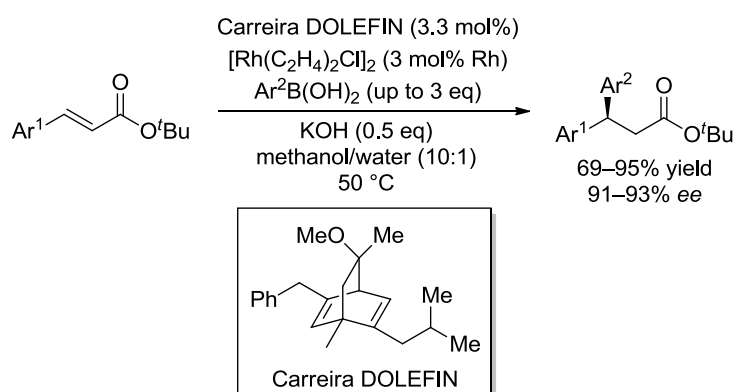
Table 2. The effect of ester bulk on the outcome of the reaction.

Rhodium-catalysed conjugate arylations to linear α,β -unsaturated esters have subsequently been demonstrated using a wide variety of different conditions.^{55,56,59,60} For example, Miyaura later contributed to research towards the synthesis of a class of biologically active compounds, which involved exploring a variety of conjugate arylation reactions including the one shown in Scheme 19.¹³⁹ In this case, the bisaryl product was afforded in high yield with high enantioselectivity.



Scheme 19. Conjugate arylation of an arylboronic acid to an enoate to generate a bisaryl product, employing chiraphos as the ligand.

The transformation is not limited to using phosphine ligands; for example, diene ligands have been effectively employed in the transformation. The conditions in Scheme 20, employing the Carreira DOLEFIN ligand, were found to be effective for a small set of simple substrates containing aromatic groups, again affording bisaryl products.¹⁴⁰ A small number of enoates with simple heteroaromatic functionality were also demonstrated, with the yields generally slightly lower (lowest 62%) and use of 1,4-dioxane as the organic solvent often improving the performance.



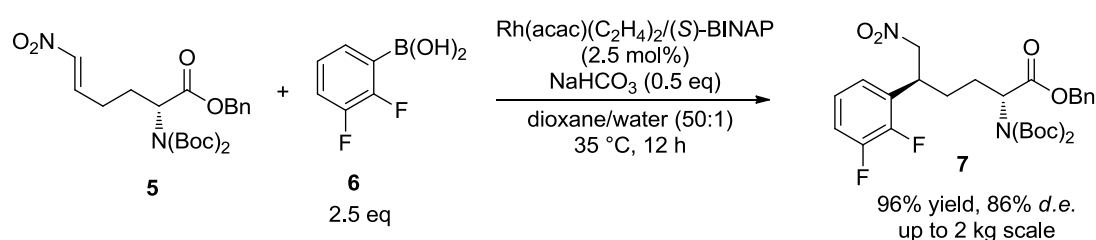
Scheme 20. Ar^1 and Ar^2 = unfunctionalised or mono-functionalised phenyl groups. For heteroaromatic examples, typically employing modified conditions, Ar^1 = furyl, thiophenyl, pyridyl and protected indolyl.

1.3.7 Process Chemistry Literature Examples of Rhodium-Catalysed Conjugate Arylation

As discussed in Section 1.1, the priorities in translating an academic or medicinal chemistry scale reaction to one that is attractive and feasible to perform on kilogram scale are often different to those required on smaller scales. The SELECT criteria (Section 1.1) summarise the underlying principles that guide these priorities: Safety, Environment, Legality, Economy, Control, Throughput. There are a small number of demonstrations in the literature

of rhodium-catalysed 1,4-addition reactions on industrially-relevant scales that have been developed in such a way as to improve the satisfaction of these criteria.²

An example published by Merck in 2008 (final conditions in Scheme 21) drew attention to some of the key challenges for scaling this chemistry.¹⁴¹ In particular, the researchers found that performing the reaction at 100 °C and in the absence of additional base caused significant protodeboronation of the arylboronic acid **6**. A decrease in the reaction temperature to 45 °C decreased the rate of this side-reaction sufficiently for their initial purposes, although further additions of boronic acid, rhodium salt and BINAP were required to achieve full consumption of the electrophile, such that the total rhodium loading used was up to 20 mol%.

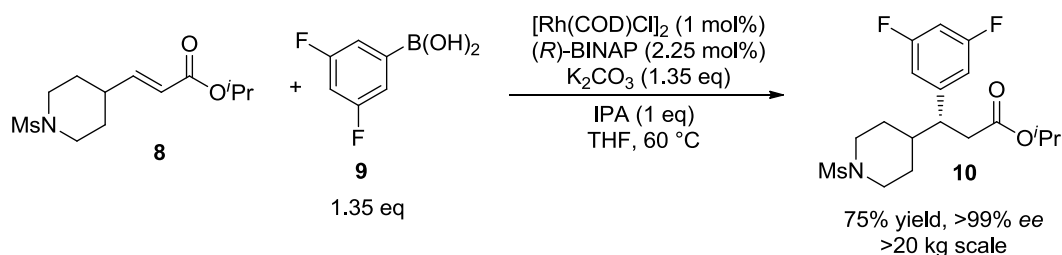


Scheme 21. An example developed by Merck that was used on 2 kg scale.

The rate-acceleration offered by the addition of inorganic base (Section 1.3.2.2) was found highly effective in this case, enabling a further temperature decrease and improved competition over the undesired protodeboronation reaction. The development work also resulted in a process with increased robustness, such that the reaction in Scheme 21 was reproducible and did not stall. However, two key aspects in particular remained insufficiently addressed from a SELECT perspective. Additional improvements would have been the replacement of dioxane with a less toxic solvent,¹⁴² and a further decrease in the equivalents of arylboronic acid **6**, since 2.5 equivalents remains very high.

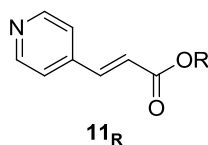
Around the same time, AstraZeneca published a 20 kg scale coupling of another electron-deficient boronic acid **9** to the linear enoate **8** (final conditions in Scheme 22).⁸³ The process underwent a number of stages of development before reaching the final conditions. Firstly, they replaced an expensive neopentyl boronic ester with the corresponding boronic acid (**9**) motivated by the decrease in cost, with the only disadvantage being that a greater amount of base was required (1 equivalent relative to the boronic acid rather than a substoichiometric amount when using the boronic ester). The selection of the inorganic base was in part directed by improving the dispersion of the solids in the reaction mixture, and these physical properties were found to improve further when the aqueous co-solvent was replaced with an alcohol as the proton source. Conveniently, protodeboronation decreased by a factor of four

upon the replacement of water with alcohol, which enabled the loading of boronic acid to be lowered from 3.5 equivalents to 1.35 equivalents. The *iso*-propyl ester of the electrophile (compound **8**) was selected based on a balance of enantioselectivity and reaction time. Concordant with the results discussed in Section 1.3.6, a trend in *ee* from 37% (ethyl ester) to 90% (*iso*-propyl ester) and 92% (*tert*-butyl ester) was seen under unoptimised conditions, but a significant increase in reaction time was also seen (< 4 h for *iso*-propyl and > 24 h for *tert*-butyl). By premixing the rhodium salt and chiral ligand sufficiently before charging the substrates, the enantiomeric excess achieved with the *iso*-propyl ester could be increased to > 99%. There was no discussion of using other catalyst precursors to try to avoid this requirement.



Scheme 22. An example by AstraZeneca employed IPA instead of water, which was found to significantly decrease protodeboronation.⁸³

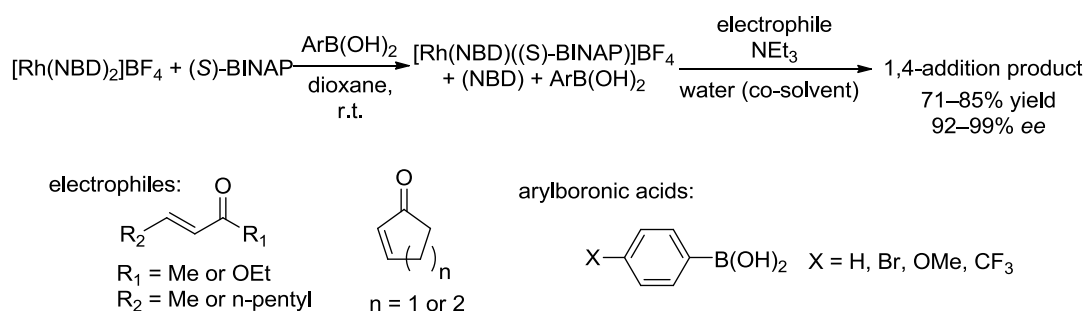
Interestingly, the 1,4-addition was found to be unsuccessful when using substrates **11_R** as the electrophiles.ⁱ The authors proposed that the pyridine nitrogen atom may have served to deactivate the rhodium catalyst by coordinating to it, and found piperidine contamination to also inhibit the 1,4-addition reaction in Scheme 22.



Work published by Abbott in 2009 focussed on developing an in situ preparation of a chiral rhodium catalyst, such that highly stereoselective, reproducible results could be obtained, ultimately on 100 g scale.^{85,143} The researchers had found that the active chiral catalysts were not readily available in sufficient quantities and with sufficient diversity (for example, only one enantiomer), and that their in-house preparation and isolation on reasonable scales would be troublesome due to the air-sensitivity of the phosphine-ligated complexes. Their investigations revealed that in situ preparation of $[\text{Rh}((S)\text{-BINAP})\text{OH}]_2$ from the corresponding COD complex was ineffective as a means to provide a highly enantioselective process, with only 55% *ee* rather than 96% *ee* (using pre-formed chiral complex) being

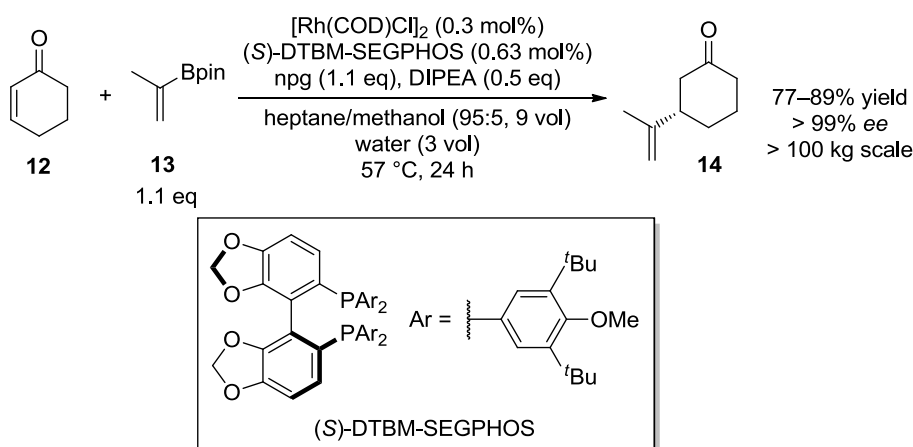
ⁱ The R group is unspecified in the publication.

achieved in the conjugate addition of *p*-bromophenylboronic acid to cyclopentenone. The authors suggested this was due to residual COD-ligated rhodium catalyst present in the reaction mixture, with its superior reactivity sufficient to significantly decrease the stereoselectivity of the reaction. Instead, they found that using Rh(NBD)₂BF₄ as the achiral precursor enabled stereoselectivities and yields comparable to those obtained using the pre-formed chiral complex to be obtained. The final procedure in Scheme 23 also gave significant process improvements in terms of arylboronic acid and catalyst loadings.



Scheme 23. The procedure employed by Abbott to prepare the active chiral catalyst in situ without either a significant competing racemic reaction or protodeboronation. The conjugate arylation used 1.05 eq ArB(OH)₂ and 1.5 mol% Rh relative to the electrophiles, at 23–27 °C.

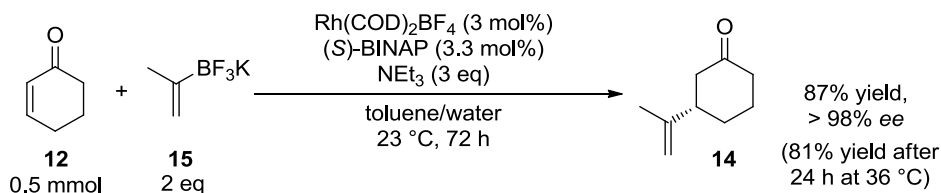
A final example was published in 2017 by Bristol-Myers Squibb (BMS), in which high-throughput ligand screening and further optimisation studies were used to develop the scalable process for the reaction shown in Scheme 24. The process was demonstrated on 1 kg scale using 0.6 mol% rhodium to give 82% yield and > 99% ee before being scaled up to 100 kg at an outsourcing partner.¹⁴⁴ In this example, an isopropenyl nucleophile rather than an aryl nucleophile was used, but their approach remains valuable for discussion here.



Scheme 24. 100 kg scale reaction developed by BMS and run five times. npg = neopentylglycol.

Although a rhodium-catalysed conjugate addition using a commercially available organoboron nucleophile under mild conditions to deliver compound **14** had already been

published (Scheme 25),¹⁴⁵ the BMS researchers considered its catalyst loading and reaction time to be unsuitable for scale up. Using this literature report as a starting point, they made sequential modifications to the system until they settled on the conditions in Scheme 24.



Scheme 25. The literature precedent for the reaction that was developed for large scale suitability by BMS and used as the basis for their initial investigations.

Using both *iso*-propenyl-Bpin **13** and *iso*-propenyl-BF₃K **15** with Rh(COD)₂BF₄, the researchers screened 16 chiral phosphine ligands and compared the GC area percent of the desired product in the reaction mixtures and the enantiomeric excess that the reactions afforded after 16 hours at 60 °C (**13**) or 42 hours at 40 °C (**15**). Using *iso*-propenyl-BF₃K **15** the reaction was limited to low enantiomeric excesses (< 75%), and although this may have simply been due to the rate of chiral catalyst formation (which was eventually pre-formed for Scheme 24) they preferred the results attained using *iso*-propenyl-Bpin **13**. At this point their most successful ligand, (*S*)-DTBM-SEGPHOS, gave approximately 60 area% product and 90% *ee*.

During subsequent optimisation of the reaction using *iso*-propenyl-Bpin **13** and (*S*)-DTBM-SEGPHOS, modifications were made to the conditions and the procedure that enabled the use of just 1.1 equivalents of *iso*-propenyl-Bpin **13** and a catalyst loading of 0.6 mol% rhodium whilst still achieving good yields, and an increase in enantiomeric excess to more than 99%. The authors reported that pinacol by-product inhibited the reaction, but that addition of neopentylglycol (npg) avoided this problem. It was this diol additive that enabled them to lower the catalyst loading to less than 1 mol%. Significant inertion of the reaction vessels was critical for delivering the high enantiomeric excess, as was pre-forming the chiral rhodium-phosphine complex.

1.3.8 Current Limitations of Rhodium-Catalysed Conjugate Arylation Methodology

The rhodium-catalysed conjugate arylation methodology has been applied to a wide range of substrate combinations, employing a wide range of ligands and rhodium salts and under wide-ranging conditions in academic and medicinal chemistry contexts.^{55–61} However, many of the ligands applied in the literature are not suitable for consideration in process chemistry

contexts on account of their commercial availability. Also, although there has been some work to understand key features of the catalytic cycle and the stereochemical induction (Section 1.3.2), a predictive tool for selecting an optimal rhodium salt, ligand, arylboron reagent and conditions is not available from the published literature, and there is no obvious starting point for developing challenging conjugate arylation reactions. The competing protodeboronation reaction in particular has received inadequate attention.

Even within process chemistry, there has been a diverse range of approaches to developing efficient reactions, sometimes involving unusual solvent mixtures, additional processing steps and additives; the only significant commonality has been the choice of ligand. Only traditional bisaryl-phosphine ligands have been applied to published examples in the process chemistry literature, with a SEGPHOS-derivative being the most adventurous choice (Section 1.3.7). The academic literature suggests that other ligand classes could be both accessible and beneficial, but perhaps the vast numbers of structurally-modified ligands in the literature, the familiarity of BINAP and uncertainties over the ease of synthesis or availability of other ligands have been deterrents to those working in this context.

2 Research Aims

2.1 Background: 1,4-Arylations for Biologically Active Compounds

A series of potential drug molecules of interest to GSK use or could use rhodium-catalysed asymmetric conjugate arylation reactions to install their bisaryl chiral centres (Figure 8). In one example, the 1,4-addition reaction has been performed on kilogram scale (Scheme 26).

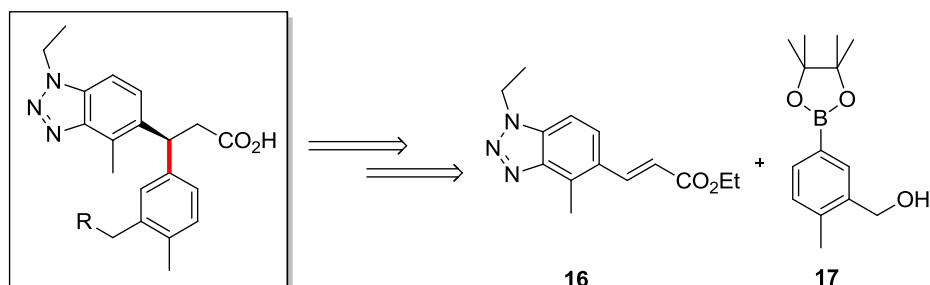
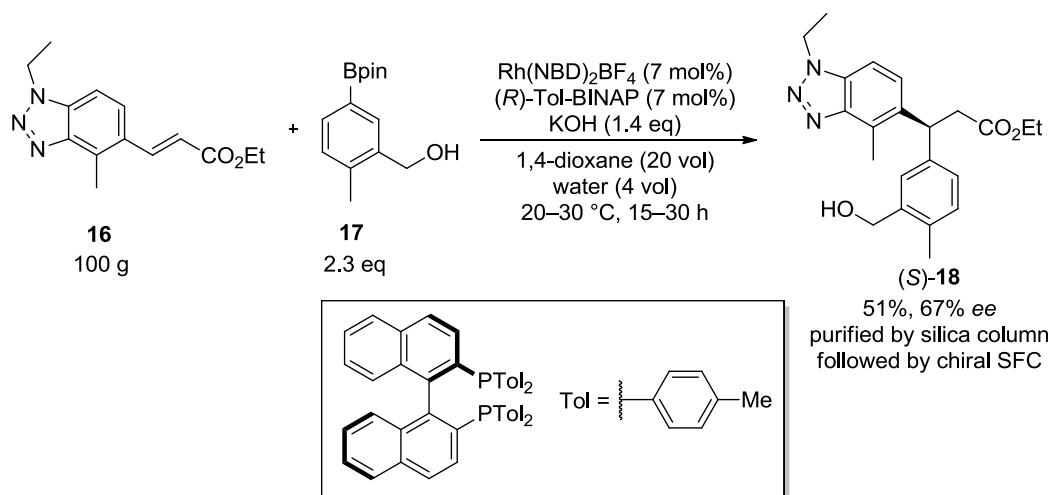


Figure 8. An example from a family of molecules of interest to GSK, where R contains varied heterocyclic functionality. The key 1,4-addition disconnection is highlighted.

The process used for the 1,4-addition in Scheme 26 is highly inadequate from a process chemistry perspective and required significant improvements in order to be suitable for long-term manufacture. Due to the competing protodeboronation reaction, the process employed a large excess of the arylboronic ester nucleophile **17** (2.3 equivalents), made in two steps from 5-bromo-2-methylbenzoic acid (40–80% yield). Despite the large excess, full conversion to the conjugate arylation product was still not observed. It is striking that this protodeboronation occurred so significantly at ambient temperatures. Similarly, the catalyst/ligand loading was extremely high whilst the enantioselectivity that it delivered was extremely poor in the context of process chemistry. Prior to charging the rhodium complex and ligand, the reaction solution was sparged with argon for two to three hours, increasing yet further the costs and time required for this process. Due to the inadequate selectivity and efficiency of the process, the product was purified by column chromatography. Chiral supercritical fluid chromatography (SFC) was then required to purify the desired enantiomer from the enantiomeric mixture, ultimately giving a low yield of the product.



Scheme 26. The process used by industrial chemists to prepare chiral bisaryl intermediate (*S*)-**18** on up to kilogram scale. A further catalyst charge of 1 mol% Rh was sometimes made after 15–20 h.

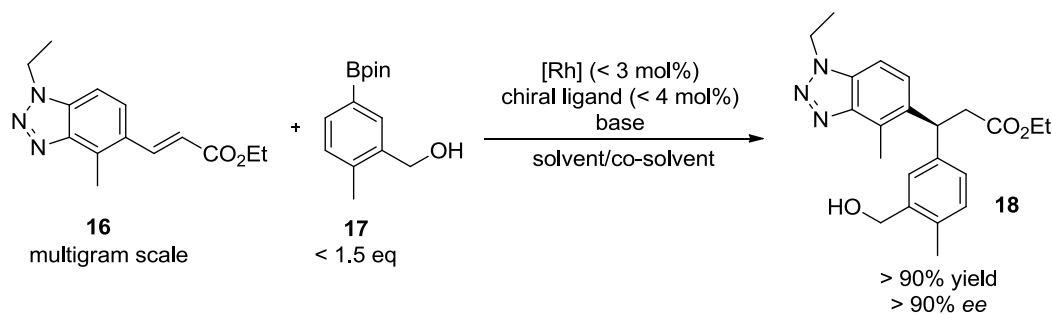
Process development and an improved understanding of the 1,4-addition reaction to give the chiral bisaryl **18** was considered to be highly beneficial for the production of the biologically active compounds. From a wider perspective, the reaction is distinct in a number of ways from the industrially-relevant 1,4-addition processes already published (Section 1.3.7), not least in terms of the functionality and the poor performance of the catalyst system in this transformation. Its development was therefore also considered to be of value to the wider process chemistry community.

As far as is known from the literature and from internal reports, there are no published rhodium-catalysed 1,4-addition reactions developed with process chemistry priorities to give bisaryl products. Furthermore, a greater and more holistic understanding of the factors affecting the competing deboronation reaction and the enantioselectivity was anticipated to provide significant value to a yet wider community of scientists. The scope of the research aims was therefore intended to bridge in both directions between advances from academic research laboratories and the development of academic methodologies for use on scale.

2.2 Process Development and Understanding of the Pharmaceutically-Relevant Conjugate Arylation

2.2.1 Objectives

The first priority of this research was the process development of the 1,4-addition reaction used to construct the chiral bisaryl core of compound **18**, with targets for the most important areas of development shown in Scheme 27.



Scheme 27. Targets for the process development of the rhodium-catalysed 1,4-addition reaction.

The most pressing improvement required was for a higher enantioselectivity to be achieved through the selection of a better performing rhodium salt, ligand and set of conditions. The next aim was to be able to lower the equivalents of the arylboron reagent and of the rhodium and ligand, decreasing the cost of the process and increasing its efficiency. Seeking to control the deboronation reaction was crucial for this, and so was studied in tandem with finding a highly active and enantioselective catalyst system for the conjugate addition. Finally, work was required to identify a more attractive solvent system from environmental, safety, conversion and enantioselectivity perspectives where relevant, and similarly to identify an optimal base for the reaction.

As well as the development of an industrially-suitable reaction, the second priority of the research was to build on the current knowledge of rhodium-catalysed conjugate arylations. As part of this, an empirical understanding of the process was required, along with an assessment of the generality of the conditions identified for the industrially-suitable reaction through a substrate- and ligand-scope. The focus of these investigations was on the competition between the conjugate arylation and protodeboronation reactions.

2.2.2 Approach

High-throughput experimentation combined with parallel reaction time-coursing was used to identify a suitable catalyst precursor and ligand combination, using conditions based on

those already employed for the reaction (Scheme 26, Section 2.1), and limiting the scope of the investigation to commercially available ligands and rhodium complexes. Cost and availability of the ligands and rhodium complexes was a factor in assessing the combinations, along with the enantioselectivity, conversion and the extent of deboration that they delivered. A similar approach was taken towards identifying suitable solvents and bases to use for the reaction.

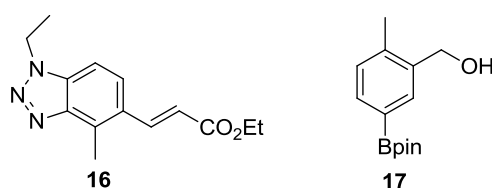
Once a suitable set of discrete variables to control had been identified, a statistical Design of Experiment approach was used to understand the continuous variables that could significantly impact the reaction, with a view to lowering both the catalyst loading and the arylboronic ester equivalents whilst maintaining good conversion and enantioselectivity. With the process understanding that this delivered, an example set of optimised conditions was then demonstrated on multigram scale.

The substrates and ligand used in the optimised process developed for the pharmaceutically-relevant system were then truncated and modulated to provide an understanding of the generality of the process, and which motifs were necessary to maintain its selectivity for conjugate arylation over protodeboration. This unusual approach could be thought of as a “reverse substrate scope”, with conditions for the reactions developed on the most complex substrate before being demonstrated on more simple substrates. By considering possible conjugate arylation and protodeboration pathways, a rationalisation for the selectivity differences was explored.

3 Results and Discussion

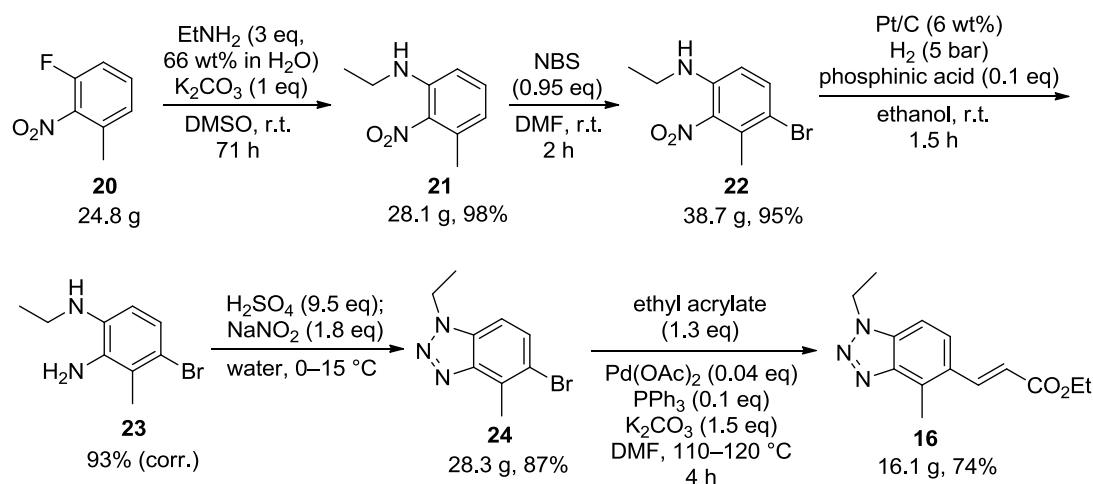
3.1 Synthesis of the Pharmaceutically-Relevant Substrates

In order to develop the process for the 1,4-addition of interest to GSK (Section 0), the key substrates employed in the rhodium-catalysed conjugate addition (compounds **16** and **17**) were synthesised based on procedures that had already been used to deliver material for early investigations, with minor modifications made where necessary. Subsequent availability of the aryl bromide precursor to enoate **16** and of the arylboronic ester **17** provided additional sources of material for the development work. In each case, the final compound was purified by column chromatography before being used in the conjugate addition reaction.



3.1.1 Synthesis of the Pharmaceutically-Relevant Enoate

The intermediate steps in the synthesis of enoate **16** (Scheme 28) required no column chromatography, with the products separated, crystallised or precipitated from the reaction mixtures in high purity. The reactions and work up procedures were performed in Controlled Laboratory Reactors, which mimic plant vessels and enable a high level of control over temperature and stirring.



Scheme 28. Synthesis of enoate **16**. Yield of compound **23** is corrected for water content, measured by Karl Fischer analysis.

The nucleophilic aromatic substitution reaction on the starting material, arylfluoride **20**, gave complete conversion to the aniline product **21**, with 78% conversion within the first 7 hours

by HPLC peak area (220 nm). This enabled isolation of the product in excellent yield (Scheme 28).

Anticipating a potential risk of dibromination in the electrophilic substitution of aniline **21** to give compound **22** (Figure 9), the reaction was first performed on 100 mg scale with an additional 0.2 equivalents of *N*-bromosuccinimide added 3 hours after the initial portionwise charge of 0.95 equivalents of the brominating agent, to give some understanding of this risk. Before the second addition, LCMS analysis revealed a 5:95 ratio of the starting material **21** to the mono-brominated product **22**. 30 minutes after the second addition, the analysis revealed dibromination had occurred with an 86:14 ratio of monobromination to dibromination products. The dibromination product was not isolated, however ¹H NMR was consistent with dibromination on the aromatic ring presumably giving compound **22-Br₂**.

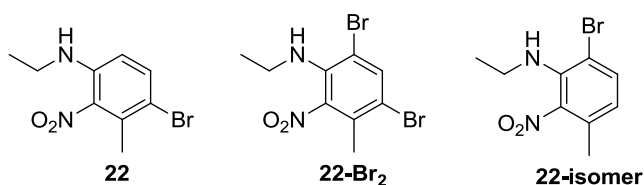


Figure 9. Three potential products from the electrophilic substitution reaction of aniline **21** with NBS.

Performing the bromination on 28 g scale (Scheme 28), HPLC analysis of the reaction mixture 2 hours after portionwise NBS addition (0.95 equivalents) revealed > 90% conversion to the desired compound **22**, with an additional 2% dibromination product **22-Br₂** (220 nm). Therefore the reaction was worked up at this point, rather than employing any subsequent charges of NBS to complete the conversion.

Remarkably, no evidence for the regioisomer **22-isomer** was detected in the isolated product. The structure of compound **22** was established by HMBC and ROESY NMR experiments (Figure 10). In particular, the ROESY experiment revealed a correlation between the methylene protons and an aromatic proton, which would not be readily explained by compound **22-isomer**. Additionally, the hydrogen atoms of the methyl substituent showed correlations only to three quaternary aromatic carbon nuclei by HMBC. This is much more readily accounted for by compound **22** than by **22-isomer**. Presumably the steric difference between the ethylaniline and the methyl groups provides sufficient differentiation to deliver compound **22** with high regioselectivity.

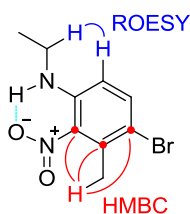
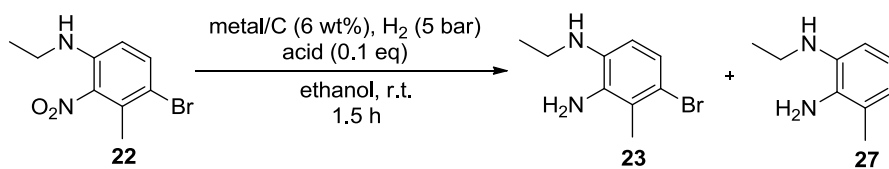


Figure 10. Key correlations in 2D NMR to establish the structure of the bromination product isolated as compound 22.

With functionalisation of the aromatic ring by nucleophilic and electrophilic substitution reactions completed with the necessary regioselectivity, the nitro group could be reduced to give the aniline **23** required for construction of the triazole. Reduction of nitro groups in the presence of halogen substituents is known to be a challenge in synthetic chemistry, due to the propensity of common reduction conditions and catalysts to afford protodehalogenated products. Various speciality catalysts have been developed and demonstrated to give improved selectivities in this reaction class.¹⁴⁶

One poorly known method to improve the chemoselectivity of nitroarene reductions in the presence of halides is to employ phosphinic acid (H_3PO_2 , hypophosphorous acid) as a substoichiometric additive, which modifies the reactivity of common heterogeneous platinum catalysts.^{147,148} A number of variations of this technique using modified platinum catalysts are also known,^{149,150} and other additives have also been demonstrated with varying levels of effectiveness.^{151–153} It should be specified that these methods employ hydrogen gas as the hydrogen source, rather than phosphinic acid itself as is the case in some methodologies.^{154–156} The mode of action of phosphinic acid in enhancing chemoselectivity has not been well established, although suggestions have included reversible modification of the catalyst active sites or even decomposition of the modifier on the catalyst surface to modulate the electronic properties. This approach, using a substoichiometric amount of phosphinic acid, had been used to deliver material for the early investigations and was also found to deliver the desired material **23** in excellent yield and purity in this work (Scheme 28).

To confirm the role of phosphinic acid in enabling the reaction to proceed with virtually complete chemoselectivity, a series of experiments were performed using the same platinum on carbon catalyst, comparing the selectivity of the reductions in the presence of phosphinic acid, phosphoric acid, acetic acid and no additive (Table 3). The reaction was also performed using a palladium on carbon catalyst with and without phosphinic acid.



Entry	Metal/C	Acid	23 (Area%)	27 (Area%)
1	Pt/C	H ₃ PO ₂	99.8	0.2
2	Pt/C	None	59.5	40.5
3	Pt/C	H ₃ PO ₄	60.7	39.3
4	Pt/C	AcOH	61.0	39.0
5	Pd/C	H ₃ PO ₂	81.8	2.9 ⁱⁱ
6	Pd/C	None	4.1	95.9

Table 3. Results showing the chemoselectivity afforded exclusively by phosphinic acid in avoiding dehalogenation during nitro-reductions. The product distribution is given as the HPLC area percent of the starting material **22 and the two products **23** and **27** at 220 nm. The catalysts were commercially available unmodified heterogeneous catalysts.**

The results in Table 3 demonstrate clearly the unique role that phosphinic acid plays in suppressing the undesired protodehalogenation reaction. Notably, phosphoric acid and acetic acid (Entries 3 and 4) show no selectivity improvement compared with the additive-free system (Entry 2). The selectivity improvement is even more impressive using a palladium catalyst, although it appears to have a negative effect on the rate of the reaction (Entry 5). Few examples of the use of this technique have been found in the recent literature,¹⁵⁷ and a thorough demonstration and substrate scope of its application to current synthetic challenges is not known to have been published. This may explain the lack of awareness within the chemistry community that this simple method offers for addressing a common problem. Since performing this work, the method has been adopted successfully for a number of challenging transformations within GSK.

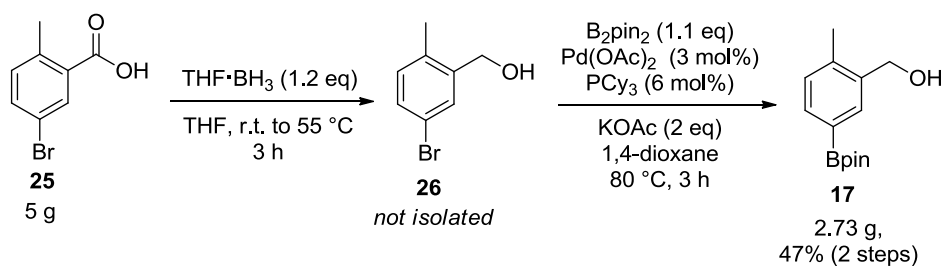
Conversion of the aniline **23** to the benzotriazole **24** proceeded smoothly, with the penultimate product isolated in 87% yield (Scheme 28). The final step was then a Heck reaction, which twice performed well, apart from the isolation. In the first instance, isolation of the product **16** was expected to be achieved by precipitation on addition of water to the reaction mixture, however this was not observed. The aqueous solution was left standing overnight, during which time brown needles grew along with dark amorphous solids. The needles were found to be the enoate **16**, in high purity by NMR and HPLC, with the amorphous solids 85% pure by HPLC peak area at 220 nm, the balance being predominantly triphenylphosphine and triphenylphosphine oxide. Further additions of water to the mother liquors caused precipitation of a further crop of the product.

ⁱⁱ 15.3 area% unreacted substrate.

In a second preparation and isolation of enoate **16**, the water was added dropwise to the reaction mixture with stirring at room temperature overnight. On this occasion, filtration gave a light orange cake with additional dark amorphous solids, and purification of the solids by column chromatography gave the material in 74% yield, as shown in Scheme 28. Subsequent crystallisation from ethyl acetate/heptane was used to provide the highest purity enoate as a colourless solid. This isolation has consistently been found to perform poorly, leading to further development work being carried out by chemists at GSK.

3.1.2 Synthesis of the Pharmaceutically-Relevant Arylboron Reagent

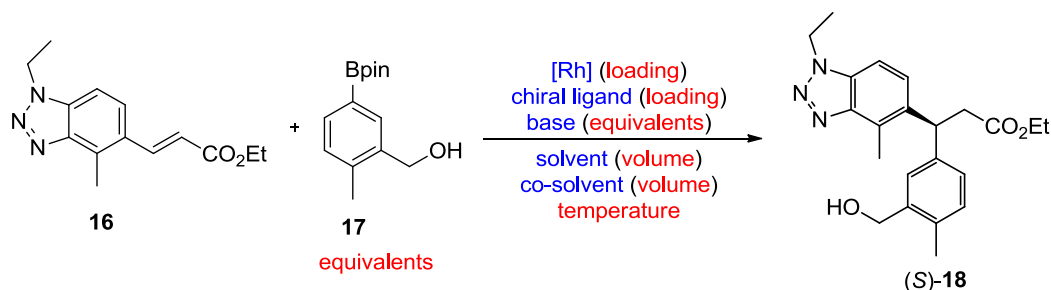
The synthesis of arylboron reagent **17** is summarised in Scheme 29. The benzylalcohol **26** was prepared by reduction of the corresponding acid **25**, based on a literature procedure.¹⁵⁸ Dropwise addition of the borane solution to a THF solution of the acid gave gas evolution with a small exotherm. The reaction was then found to require heating to 55 °C for 3 hours to generate the reduction product, before the mixture was quenched and worked up. The material was charged as a crude oil (> 96% pure by HPLC at 220 nm) in the second step, although was later resynthesised at 35–40 °C and purified by column chromatography to give a colourless crystalline solid in 96% yield. The Miyaura borylation of the arylbromide **26** to give the arylboronic acid pinacol ester **17** was complete within 3 hours at 80 °C. Precipitation from ethyl acetate/heptane was low yielding, however provided sufficient material for the initial process investigations.



Scheme 29. Synthesis of arylboron reagent **17**.

3.2 Process Development of the Pharmaceutically-Relevant Conjugate Arylation

As laid out in the approach towards the research aims (Section 2.2.2), the approach used to develop the conjugate arylation reaction from a process chemistry perspective separated the variables into the discrete variables (the identities of the catalyst precursor, ligand, solvent, co-solvent, and base) and the continuous variables (the catalyst loading, equivalents of arylboronic ester, dilution, amount of co-solvent, equivalents of base, and temperature) (Scheme 30). The discrete variables were explored predominantly using a combination of high-throughput techniques and more focussed competition and time-coursing experiments, whilst the continuous variables were investigated using a statistical Design of Experiment approach.



Scheme 30. The scope of the process development of the 1,4-addition reaction. The discrete variables investigated are highlighted in blue and the continuous variables investigated are highlighted in red.

3.2.1 Selection of Catalyst Precursor/Ligand System for Rhodium-Catalysed Asymmetric Arylation

The initial approach towards selecting a catalyst system for the desired 1,4-addition reaction involved making minimal changes to the previously used reaction conditions. Once a system had been identified, the other variables would be explored. As a result, the reactions presented in this section were performed in aqueous 1,4-dioxane with potassium hydroxide as the base. Due to the small scale that these reactions were performed on (15 mg of enone **16** for each reaction), the rhodium and ligand loadings were increased to 10 mol% to enable the materials to be handled and weighed with sufficient accuracy.

3.2.1.1 Comparative Analysis of Ligands for Asymmetric Arylation

For the first set of reactions, two of the most popular rhodium salts for asymmetric conjugate arylation were chosen from two different classes (cationic $\text{Rh}(\text{NBD})_2\text{BF}_4$ and dimeric $[\text{RhCl}(\text{C}_2\text{H}_4)_2]_2$), primarily as a way to assess 23 different commercial ligands spanning the three most common chiral ligand classes for the reaction as broadly as possible (Section

1.3.4):⁵⁹ phosphorus ligands (further divided into bisaryl-phosphines (Figure 11), phosphoramidites (Figure 15) and other diphosphines (Figure 14)), diene ligands (Figure 13) and bissulfoxide ligands (Figure 12). Only commercially available ligands were investigated, since the focus of the research was to develop a process that could be readily implemented in an industrial setting. Bespoke ligands may function very well in rhodium-catalysed 1,4-addition reactions,⁵⁹ but the requirement to firstly undertake potentially lengthy and arduous syntheses of these ligands renders them far less appealing if suitable commercial ligands exist, not least because the syntheses of the bespoke ligands are unlikely to have been developed for industrially-relevant scales. This restriction limited the extent to which the ligand classes could be explored, with the phosphine ligands unsurprisingly the most abundantly available from commercial sources, the dienes much less available and only one bissulfoxide found. No suitable hybrid ligands were commercially available.

The bisaryl-phosphine ligands (Figure 11) were selected to demonstrate a diverse spread of steric and electronic properties. (*R*)-BINAP **L7** and (*R*)-Tol-BINAP **L8** were included as benchmark ligands, with **L7** being one of the most generally well-known chiral ligands and the first ligand reported for the asymmetric rhodium-catalysed conjugate addition (Section 1.3.1), and **L8** being the ligand used in the previous GSK process (Section 2.2.1). (*R*)-H8-BINAP **L2** is an analogue of (*R*)-BINAP, with the primary difference being an increase in bulk due to the saturation and non-planarity of the cyclohexenyl rings resulting in a larger dihedral angle.¹⁵⁹ (*R*)-MeO-BIPHEP **L1** has a smaller dihedral angle than (*R*)-BINAP and is more electron-rich.¹⁶⁰ The addition of chlorine substituents in (*R*)-Cl-MeO-BIPHEP **L3** and the pyridyl rings in (*R*)-P-Phos **L4** modulate the electronic properties of this scaffold. (*R*)-SEGPHOS **L5** has a smaller calculated dihedral angle than both (*R*)-BINAP **L7** and (*R*)-MeO-BIPHEP **L1**, and was developed since a positive relationship was observed between smaller dihedral angles and higher enantioselectivities for an asymmetric hydrogenation reaction.¹⁶¹ (*R*)-DTBM-SEGPHOS **L6** is a more sterically-encumbered and electron-rich analogue of **L5**.

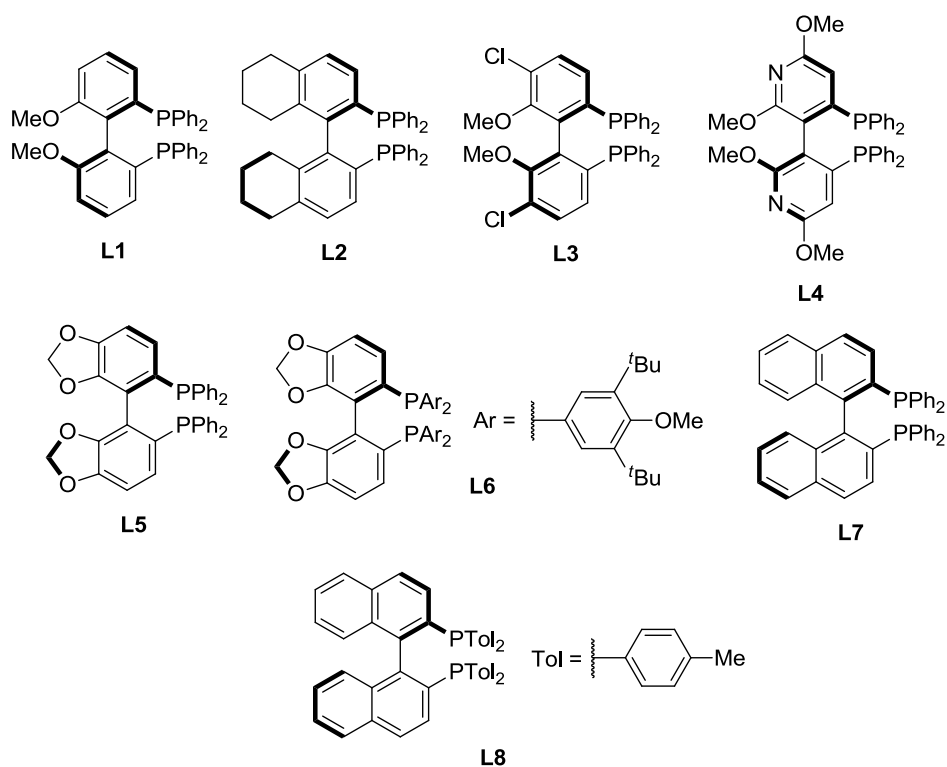


Figure 11. Bisaryl-phosphine ligands.

The chiral bissulfoxide (*M,S,S*)-Tol-BINASO **L9** was the only commercially available ligand in its class that could be sourced (Figure 12). The ligand was demonstrated to perform well in rhodium-catalysed asymmetric conjugate arylations (up to 99% yield, 99% *ee*) when its synthesis was first reported (Scheme 13, page 22).⁹⁹ High yields and enantioselectivities for the conjugate addition of simple arylboronic acids to cyclic enoates have been demonstrated under mild conditions using this ligand class.⁹⁸

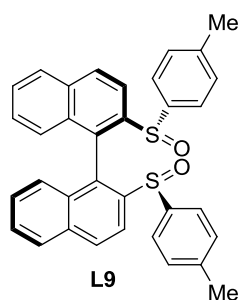


Figure 12. Bissulfoxide ligand.

Four commercially available chiral diene ligands could be sourced (Figure 13). The syntheses of the naphthyl ester diene **L11** and the enantiomer of (*S,S*)-Ph-BOD **L12** were discussed in Section 1.3.4, and **L10** is readily prepared by treatment of **L11** with methylolithium.¹¹² Ligands **L10** and **L11** present a contrast, with the latter exhibiting a more electron-poor enoate motif and aromatic functionality. **L13** (the Carreira DOLEFIN ligand)

is derived from the chiral pool reagent (*R*)-carvone.¹⁰⁸ Each of the ligands uses a bicyclo[2.2.2]octadiene (BOD) framework. Ligand **L12** is the only C_2 -symmetric diene, with the others projecting different groups from each side of the scaffold.

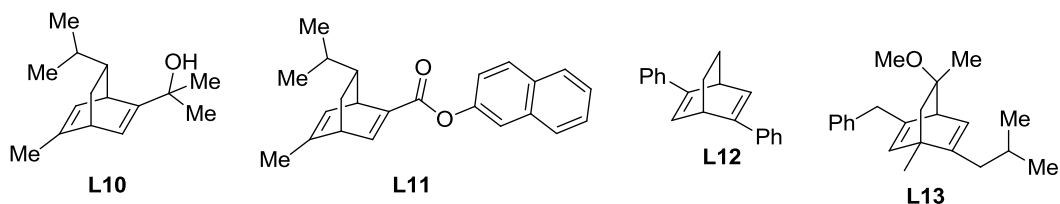


Figure 13. Chiral diene ligands.

Among the non-bisaryl diphosphines (Figure 14), (*R*)-Me-DuPhos **L14** and (*R*)-QuinoxP **L17** project the ligating phosphorus atoms at similar angles, but the electron-withdrawing nature of the quinoxaline heterocycle of **L17** provides an electronic contrast. The ligand catASium M(*R*) **L18** also has electron-poor architecture, and the increased angle between the projected phosphine ligands provides a further variation from **L14**. (*R,R*)-Diop **L15** and (*S,S*)-chiraphos **L16** are contrasted by the fixed backbone structure of **L15** and the increased ring size that would form with the rhodium centre using **L15**. (*R*)-Xylyl-PHANEphos **L19** and Walphos SL-W005-1 **L20** have very different structures to the other diphosphines and were included to maximise the variety of ligands explored.

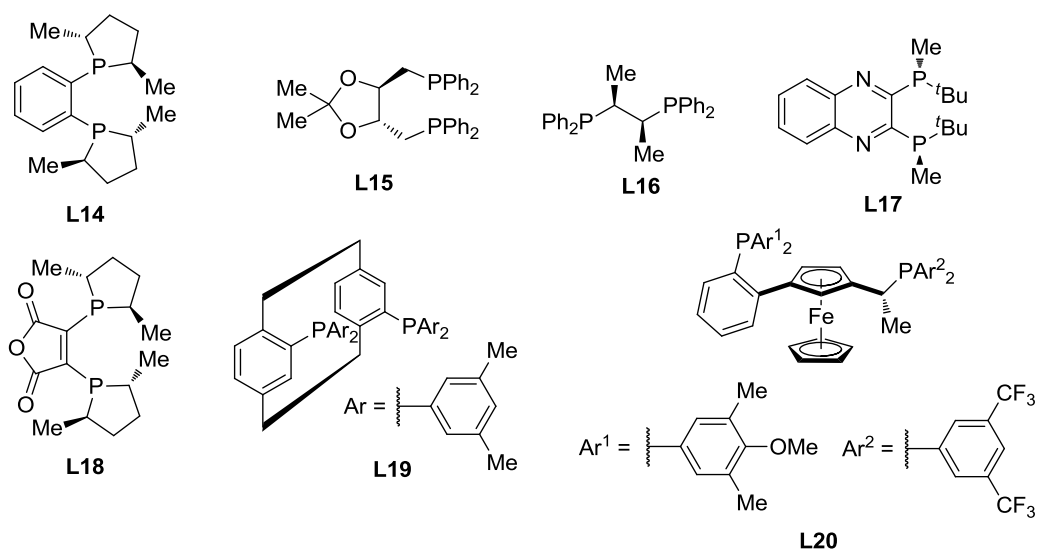


Figure 14. Other diphosphine ligands.

Three monodentate phosphoramidites were selected (Figure 15). (*R*)-MonoPhos **L21** exhibits only axial chirality, whereas **L23** combines an axially chiral BINOL-structure with chiral amine motifs. BIPOL-A1(*S*) **L22** retains the chiral amine motif but does not have fixed axial chirality, and has a less sterically-demanding biphenyl rather than binaphthyl scaffold. MonoPhos has been employed in conjugate arylation reactions of phenylboronic

acid to simple cyclic enoates under conditions based on the seminal works (Section 1.3.1); whilst the published conversions were high, the enantioselectivities achieved were very low (29–38% *ee*).¹⁶²

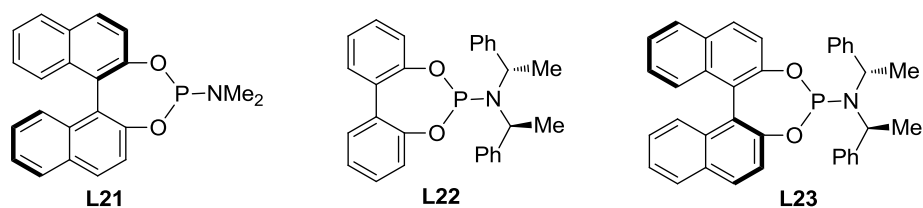
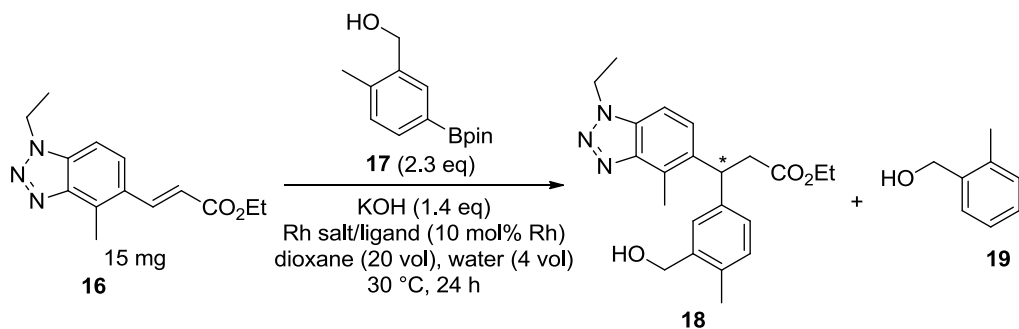


Figure 15. Phosphoramidite ligands.

The conditions used for the reactions to assess this set of ligands are shown in Scheme 31, and were based on those used in the previous GSK process (Section 2.1). The reactions were assessed by HPLC, which provided sufficient information to distinguish the performance of the rhodium salt and ligand combinations. At this phase of development, raw peak area percent data was suitable for the analysis, without translation of the data into the molar amounts of the substances using relative HPLC response factors. Molar analysis was performed for later development work (e.g. Section 3.2.3). For each of the two rhodium complexes used, one reaction was also performed in the absence of chiral ligand to show the performance of the rhodium salt on its own and therefore to give an indication of the potential racemic background reaction if the achiral ligands are not fully replaced by the chiral ligands. One reaction mixture was also prepared in the absence of rhodium salt or ligand, to assess the extent of any non-metal-mediated deboronation.



Scheme 31. Conditions used to compare ligands. Note that for monodentate ligands (phosphoramidites) 20 mol% loading was used, and for dimeric rhodium salts 5 mol% loading was used.

The reaction mixtures were prepared under inert atmosphere conditions in a nitrogen-flushed glove bag, and the results from HPLC analysis after 24 hours at 30 °C are shown in Table 4, with a visualisation of some of the data provided in Figure 16. Conversion data are the HPLC peak area percent conversions at 210 nm of the enoate **16** to the product (*R*)- and (*S*)-**18**. The “Remnant Deboronation” data provide a measure of the extent of deboronation to

o-tolylmethanol **19** by any arylboronic ester **17** that did not react with enoate **16** to give the conjugate arylation product **18**. The data were again calculated by peak area percent at 210 nm:

$$\text{Remnant Deboronation} = \frac{\text{Area}\%_{19}}{\text{Area}\%_{19} + \text{Area}\%_{17}}$$

Equation 1

In cases where there is complete conversion of the enoate **16** to the conjugate arylation product **18** and complete deboration of the remaining arylboronic ester **17** to *o*-tolylmethanol **19** (100% remnant deboration), little can be inferred about the selectivity of the reaction. In cases of complete conversion and less than 100% remnant deboration, or incomplete conversion but high remnant deboration, then a difference in reactivity between the desired reaction and the undesired protodeboration reaction can be deduced. A level of caution is required particularly in interpreting cases of complete conversion and less than 100% remnant deboration, since this could be due to slow reactivity both for the desired 1,4-addition and the undesired protodeboration rather than good selectivity for the desired reaction over the undesired reaction.

Entry	Chiral Ligand	[Rh(Cl)(C ₂ H ₄) ₂] ₂			Rh(NBD) ₂ BF ₄			
		<i>ee</i> / %	Conversion / %	Remnant Deboronation / %	<i>ee</i> / %	Conversion / %	Remnant Deboronation / %	
1	No Ligand	4	91	69	3	74	100	
2	Bisaryl-Phosphines	L1	51	93	84	56	93	100
3		L2	67	95	98	82	95	100
4		L3	69	95	94	67	92	100
5		L4	64	89	35	66	98	100
6		L5	55	94	91	64	92	100
7		L6	44	30	68	59	37	100
8		L7	64	96	96	64	93	100
9		L8	63	96	96	65	94	99
10	Bissulfoxide	L9	72	34	76	2	74	100
11	Dienes	L10	46	87	100	16	67	100
12		L11	92	97	99	77	95	100
13		L12	87	100	99	72	100	100
14		L13	66	100	99	24	80	100
15	Diphosphines	L14	5	100	79	5	100	100
16		L15	34	100	89	36	100	83
17		L16	62	100	82	74	100	99
18		L17	37	100	95	34	100	100
19		L18	6	82	77	1	84	100
20		L19	56	93	84	52	93	94
21		L20	48	99	100	52	98	100
22		L21	43	100	61	40	100	93
23	Phosphoramidites	L22	n.d.	25	66	n.d.	0	28
24		L23	n.d.	11	46	n.d.	0	42

Table 4. Summary of results from first reaction set, prioritising a broad range of ligands. Data calculated from HPLC Method D1. Note that magnitude only of *ee* values is given. The colouring is such that green indicates a more desirable result and red a less desirable result. Where conversion is very low, *ee* results have been omitted. The *ee* values for the chiral ligand-free reactions provide an idea of the precision of the *ee* values for the rest of the table.



Figure 16. A visualisation of data from Table 4.

Comparing firstly the two racemic reactions without any chiral ligand, there are clear reactivity differences between the two complexes (Entry 1). Literature reports state that $\text{Rh}(\text{NBD})_2\text{BF}_4$ is less active than other catalyst precursors such $[\text{Rh}(\text{COD})\text{Cl}]_2$ (see, for example, Section 1.3.2.2) and whilst this may be reflected in the conversion data for these results it is also certainly the case that $\text{Rh}(\text{NBD})_2\text{BF}_4$ provides a far more active catalyst for the competing deboration reaction than $[\text{Rh}(\text{Cl})(\text{C}_2\text{H}_4)_2]_2$ does. The difference between the relative rates of deboration and conjugate arylation that the active species from $\text{Rh}(\text{NBD})_2\text{BF}_4$ catalyses is emphasised by the results throughout the rest of the table. Despite the high levels of deboration still occurring when the chiral ligands were added, there was generally little difference between the enantioselectivities achieved using the two different rhodium salts when phosphine ligands were employed. This highlights the fact that the achiral background reactivity of $\text{Rh}(\text{NBD})_2\text{BF}_4$ is low with respect to conjugate arylation, but high with respect to protodeboration.

The role of the rhodium complex in the deboration mechanism was confirmed by the reaction mixture prepared without a rhodium salt or ligand (not shown in the table). In this case, a value for Remnant Deboration of no greater than 11% was measured. The results confirm that the protodeboration side-reaction can occur by at least two mechanisms, with the identity of the rhodium species in the reaction mixture playing an important role.

The enantioselectivity of the reaction showed some interesting differences between the two achiral rhodium precursors with chiral ligands. The phosphines (bisaryls, diphosphines and phosphoramidites) gave in general very little enantioselectivity differences between the two rhodium precursors whilst varying significantly between ligands. In contrast, the bissulfoxide and the chiral dienes gave consistently better enantioselectivities when used with $[\text{RhCl}(\text{C}_2\text{H}_4)_2]_2$. This is likely to be due either to differences in the ligand exchange rates or to binding strength differences between the phosphines and the dienes and bissulfoxide,^{163,164} such that for the phosphines, the equilibrium between the achiral complex and the chiral complex lies so far towards the chiral complex that its formation is essentially irreversible, whereas for the dienes and bissulfoxide, this irreversibility is achieved only by the off-gassing of ethylene.

In the case of the bissulfoxide and $\text{Rh}(\text{NBD})_2\text{BF}_4$, this exchange of the achiral ligand for the chiral bissulfoxide appeared to be so incomplete that, combined with the low activity of the bissulfoxide-ligated complex, the results for this reaction were essentially identical to the achiral, chiral-ligand-free reaction (Entry 1). The result using $[\text{RhCl}(\text{C}_2\text{H}_4)_2]_2$ as the catalyst

precursor showed that, whilst giving moderately good enantioselectivity, the bissulfoxide exhibited very poor selectivity for the desired reaction over deboronation.

Interestingly, a small number of phosphine ligands gave better enantioselectivities using the norbornadiene rhodium precursor than they did with the ethylene precursor, in contrast to that which was observed with the dienes and bissulfoxide. The bisaryls (*R*)-H8-BINAP **L2** (Entry 3) and (*R*)-SEGPPOS **L5** (Entry 6) are particularly clear examples of this. This might be explained by the literature reports discussed previously (Section 1.3.3),^{59,85} which describe Rh(NBD)₂BF₄ as being a relatively poor complex itself for the reaction but giving rapid ligand exchange to produce the more active chiral complex.

Of the phosphines, those in the bisaryl class generally gave the better enantioselectivities. (*R*)-H8-BINAP **L2** with Rh(NBD)₂BF₄ was by far the best performing combination, with high conversion also observed (Entry 3). Better conversions were seen in general using the other diphosphines but the enantioselectivities varied from very poor to moderate at best, with most generating the conjugate arylation product in less than 70% *ee*. The phosphoramidites were a particularly disappointing set of ligands, giving rhodium complexes that were poorly active both in the desired reaction and in the undesired deboronation. (*R*)-MONOPHOS **L21** (Entry 22) was the only phosphoramidite that gave good conversion, but the enantioselectivity it induced was low. The chiral dienes were the most highly performing ligand class overall in terms of stereoselectivity and conversion, with ligands **L11** and **L12** delivering particularly excellent results (92% *ee* and 87% *ee*, > 95% conversion, Entries 12 and 13 respectively).

After sampling the reaction mixtures under inert atmosphere conditions, the reaction vials were heated at 60 °C for a further 65 hours. For the reaction mixtures in which neither starting material had shown full consumption after the first 24 hours at 30 °C, the results are summarised in Table 5, except for the bissulfoxide ligand **L9** which showed no change from the 30 °C result, including with regard to deboronation. In most cases, the results in Table 5 are for ligands which have significant bulk close to the coordinating atom (for example, (*R*)-DTBM-SEGPPOS **L6** rather than (*R*)-SEGPPOS **L5**). It is presumably the case that the bulk caused slow transmetalation of the aryl group to these complexes at 30 °C rather than only slow coordination of the enoate **16**, since otherwise complete deboronation of arylboronic ester **17** after 24 hours at 30 °C might have been expected. In general, no clear positive or negative effect on the enantioselectivity was observed after heating at 60 °C, but conversion was improved. The most notable result was seen perhaps for the bulkiest phosphoramidite **L23** with [Rh(Cl)(C₂H₄)₂]₂, which was found to induce chirality with

reasonable enantioselectivity (Entry 2). However, with > 98% deboronation of the residual arylboronic ester also observed in each case, none of the results was sufficiently compelling to pursue further.

Entry	Ligand	Catalyst Precursor	24 h at 30 °C		24 h at 30 °C; 65 h at 60 °C	
			ee / %	Conversion / %	ee / %	Conversion / %
1	L22	[Rh(Cl)(C ₂ H ₄) ₂] ₂	2	25	6	43
2	L23	[Rh(Cl)(C ₂ H ₄) ₂] ₂	n.d.	11	67	32
3	L18	[Rh(Cl)(C ₂ H ₄) ₂] ₂	6	82	7	90
4	L6	[Rh(Cl)(C ₂ H ₄) ₂] ₂	44	30	44	47
5	L22	Rh(NBD) ₂ BF ₄	n.d.	0	6	61
6	L23	Rh(NBD) ₂ BF ₄	n.d.	0	16	22
7	L6	Rh(NBD) ₂ BF ₄	59	37	54	45

Table 5. The results after heating at 60 °C for a further 65 h, with data shown as a comparison with the data after 24 h at 30 °C and only for reaction vials where full consumption of either of the starting materials had not already occurred after the 24 h at 30 °C. Data analysis and calculations performed in the same manner as for Table 4.

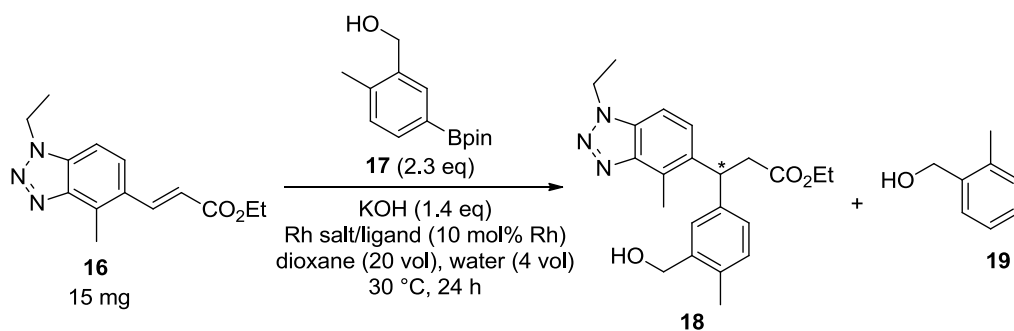
3.2.1.2 Comparative Analysis of Rhodium Salts for Asymmetric Arylation

From the large range of ligands compared in Section 3.2.1.1, a smaller subset was taken on to enable a more extensive comparison of different rhodium precursors. The ligands selected had shown either good conversion and enantioselectivity in the conjugate arylation reaction, or had performed differently in combination with the two different rhodium complexes initially studied. (*R*)-BINAP was included due to its prevalence in the literature (Section 0), and at least one ligand from each of the main ligand classes was included.

Catalyst precursors across the different classes were selected (Section 1.3.2.2). Three cyclooctadiene-ligated rhodium complexes were compared: cationic Rh(COD)BF₄, the dimeric chloro-complex [RhCl(COD)]₂ and its hydroxo-ligated analogue [Rh(OH)(COD)]₂. Use of Rh(COD)BF₄ enabled comparisons with its norbornadiene-ligated analogue Rh(NBD)BF₄, used in Section 3.2.1.1. To observe any differences between bidentate cyclooctadiene (COD) and monodentate cyclooctene (COE), [RhCl(COE)₂]₂ was selected, supplementing the results already acquired using [RhCl(C₂H₄)₂]₂ in Section 3.2.1.1. Rh(acac)(C₂H₄)₂ provided a contrast with [RhCl(C₂H₄)₂]₂ on account of its monomeric structure, and also allowed a comparison between ethylene ligands and the carbonyl ligands of Rh(acac)(CO)₂. Rh(acac)(CO)₂ and Rh(acac)(C₂H₄)₂ were the complexes employed in the first reported rhodium-catalysed 1,4-arylations with arylboron reagents (Section 1.3.1).

The results are summarised in Table 6, with the relevant results from Section 3.2.1.1 also included. The reactions were performed in the same way as for the ligand comparisons, and

the data was analysed using the same calculations as in Section 3.2.1.1. A visualisation of some of the data is provided as Figure 17.



Ligand	$[\text{Rh}(\text{Cl})(\text{COD})]_2$			$\text{Rh}(\text{COD})_2\text{BF}_4$			$[\text{RhCl}(\text{COE})_2]_2$			$\text{Rh}(\text{acac})(\text{C}_2\text{H}_4)_2$		
	Rem.			Rem.			Rem.			Rem.		
	<i>ee</i> /%	Conv./%	Deb./%	<i>ee</i> /%	Conv./%	Deb./%	<i>ee</i> /%	Conv./%	Deb./%	<i>ee</i> /%	Conv./%	Deb./%
(<i>R</i>)-H8-BINAP L2	11	100	98	32	98	99	81	94	89	53	68	28
(<i>R</i>)-SEGPPOS L5	9	100	84	29	97	91	65	93	79	56	59	28
(<i>R</i>)-BINAP L7	6	100	81	33	97	88	66	95	93	68	51	25
Bissulfoxide L9	0	99	100	1	100	100	9	25	56	41	64	47
Naphth. Diene L11	1	99	100	2	99	100	91	98	100	91	96	83
Ph-BOD L12	3	99	100	4	100	100	91	100	99	92	100	67
(<i>S,S</i>)-Chiraphos L16	4	100	100	50	100	100	55	100	46	52	86	28
No Ligand	1	100	100	0	100	100	5	95	54	8	92	52

Ligand	$\text{Rh}(\text{acac})(\text{CO})_2$			$[\text{Rh}(\text{OH})(\text{COD})]_2$			$[\text{Rh}(\text{Cl})(\text{C}_2\text{H}_4)_2]_2$			$\text{Rh}(\text{NBD})_2\text{BF}_4$		
	Rem.			Rem.			Rem.			Rem.		
	<i>ee</i> /%	Conv./%	Deb./%	<i>ee</i> /%	Conv./%	Deb./%	<i>ee</i> /%	Conv./%	Deb./%	<i>ee</i> /%	Conv./%	Deb./%
(<i>R</i>)-H8-BINAP L2	n.d.	0	7	12	100	99	67	95	98	82	95	100
(<i>R</i>)-SEGPPOS L5	n.d.	1	5	1	100	82	55	94	91	64	92	100
(<i>R</i>)-BINAP L7	n.d.	0	5	7	100	80	64	96	96	64	93	100
Bissulfoxide L9	3	79	52	1	99	100	72	34	76	2	74	100
Naphth. Diene L11	50	33	12	1	99	100	92	97	99	77	95	100
Ph-BOD L12	4	77	21	2	100	100	87	100	99	72	100	100
(<i>S,S</i>)-Chiraphos L16	n.d.	0	6	5	100	99	62	100	82	74	100	99
No Ligand	1	84	29	0	98	100	4	91	69	3	74	100

Table 6. Summary of results from reactions primarily comparing rhodium precursors. The results were analysed in the same manner as for Section 3.2.1.1, after 24 h at 30 °C. "Conv." is the peak area conversion of the enoate **16** to the product (*S*)- and (*R*)-**18**, and "Rem. Deb." is the peak area deboronation to *o*-tolylmethanol **19** of the arylboronic ester **17** not consumed by the conjugate arylation reaction.

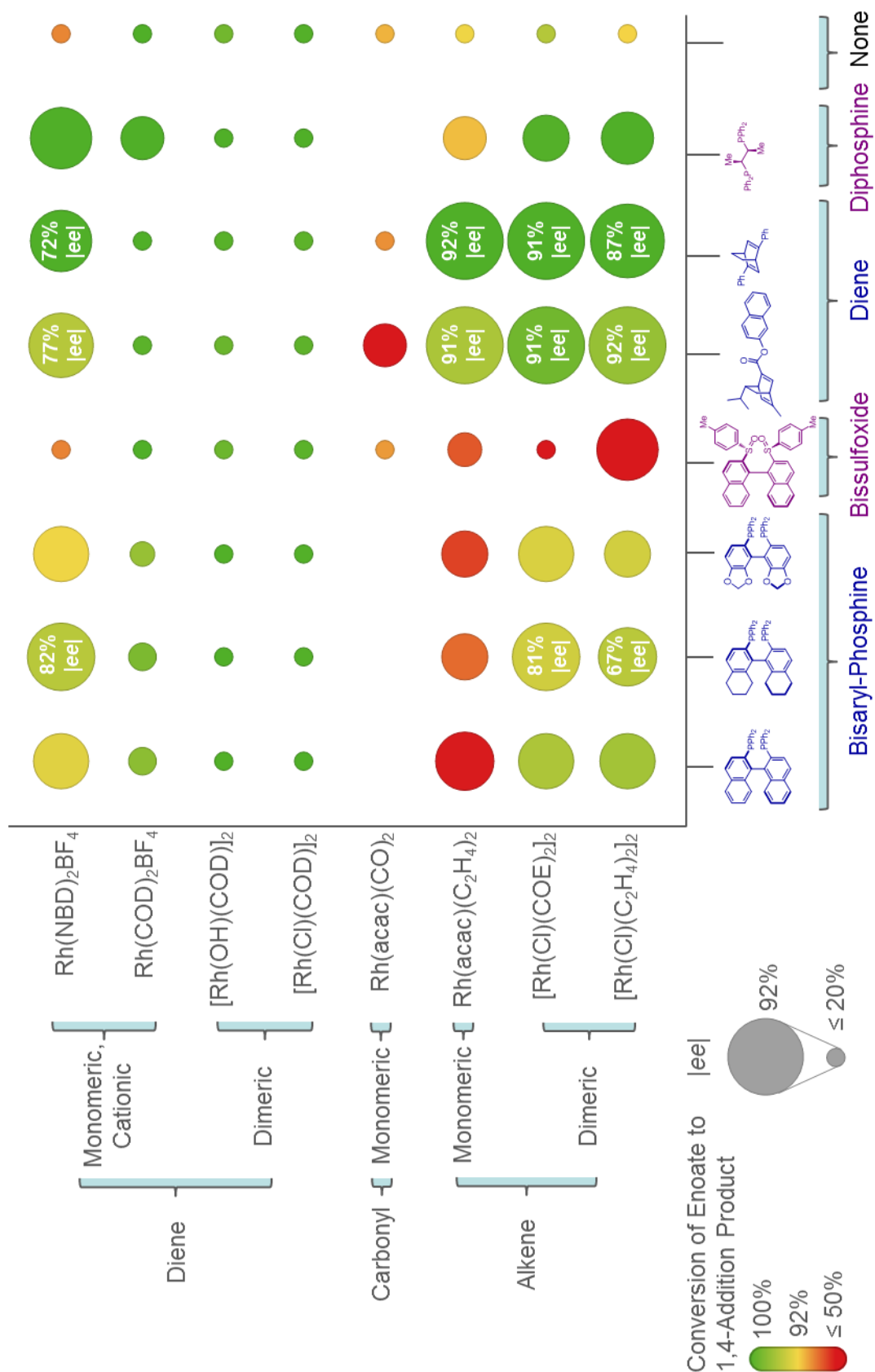


Figure 17. A visual display of the results summarised in Table 6. The vertical axis groups the rhodium salts by their class, as the horizontal axis does for the ligands.

Concordant with reports of cyclooctadiene being a very effective ligand for achiral 1,4-addition reactions (Section 1.3.3),^{68,79} Table 6 and Figure 17 show the presence of COD in the rhodium catalyst precursor complex to have resulted in consistently poor enantioselectivity with high conversion in every case. No notable differences in performance were observed between the two COD-ligated dimeric rhodium precursors, including in terms of the extent of deboronation, in agreement with the literature precedent for rapid formation of the active hydroxo-rhodium complex from the chloro-rhodium complex in the presence of potassium hydroxide.⁷⁵

In the case of the COD-ligated cationic catalyst precursor $\text{Rh}(\text{COD})_2\text{BF}_4$, the reported fast ligand exchange for cationic complexes (Section 1.3.3) was evidenced by the higher stereoselectivity achieved using phosphine ligands compared with the dimeric COD-ligated complexes, but this difference in stereoselectivity was not observed using the bissulfoxide or chiral diene ligands **L9**, **L11** or **L12**, which remained unable to compete with the achiral COD ligands. Even using the phosphine ligands, the ligand exchange was certainly not adequate for use of a COD-ligated rhodium precursor to be pursued in this work, despite reported successes in the literature (Section 1.3.7). When the chiral COD-containing catalyst precursor $\text{Rh}((R)\text{-BINAP})(\text{COD})\text{BF}_4$ was used (not shown in the table), still only 36% *ee* was achieved compared with 33% *ee* when (*R*)-BINAP was used with $\text{Rh}(\text{COD})_2\text{BF}_4$. In this case, 82% remnant deboronation was measured, with full conversion of the enoate **16** to the 1,4-addition product **18**.

Although both dienes, the difference in performance between the norbornadiene-ligated cationic precursor and the COD-ligated cationic precursor is significant, with $\text{Rh}(\text{NBD})_2\text{BF}_4$ giving vastly superior enantioselectivity. When using the bisaryl phosphine ligands, the difference in the extent of remnant deboronation is also noteworthy, with more deboronation occurring when used in combination with $\text{Rh}(\text{NBD})_2\text{BF}_4$ than with $\text{Rh}(\text{COD})_2\text{BF}_4$ (compare, for example, the results for (*R*)-BINAP **L7**). Considered with the chiral-ligand-free results, it seems that whilst $\text{Rh}(\text{NBD})_2\text{BF}_4$ may provide a less active achiral complex for 1,4-addition compared with $\text{Rh}(\text{COD})_2\text{BF}_4$, this decreased activity does not appear to be reflected to the same extent for the undesired deboronation reaction.

The monodentate cyclooctene-ligated complex $[\text{RhCl}(\text{COE})_2]_2$ universally gave significant enantioselectivity improvements across all ligand classes compared with the bidentate cyclooctadiene-ligated complex $[\text{RhCl}(\text{COD})]_2$. This improvement was similarly seen for the analogous ethylene-ligated complex $[\text{RhCl}(\text{C}_2\text{H}_4)]_2$. It would have seemed reasonable to predict that any difference between the two complexes would have been for even better

enantioselectivity to have been observed using the ethylene complex rather than the cyclooctene complex, on account of ethylene off-gassing. However, both (*R*)-H8-BINAP **L2** and (*R*)-SEGPHOS **L5** gave higher enantioselectivities for the conjugate arylation product when used with the COE-ligated precatalyst. They also gave less deboronation of the arylboronic ester. By comparison with the corresponding chiral-ligand-free results, this is likely to indicate faster ligand exchange when using $[\text{RhCl}(\text{COE})_2]_2$ compared with using $[\text{RhCl}(\text{C}_2\text{H}_4)_2]_2$.

The monoalkene-ligated precursors (COE, ethylene) resulted in less deboronation in the chiral ligand-free reactions than the diene-ligated precursors (COD, NBD) did. Compared with the COD-ligated precursors, this may simply be because the monoalkene-ligated precursors produced less active catalysts, however compared with the norbornadiene-ligated precursor this difference seems to reveal a greater selectivity for the desired 1,4-addition reaction over the deboronation side-reaction with cyclooctadiene than with norbornadiene.

The use of the monomeric complex $\text{Rh}(\text{acac})(\text{C}_2\text{H}_4)_2$ gave comparable conversions and enantioselectivities with the chiral diene ligands to the dimeric complex $[\text{Rh}(\text{Cl})(\text{C}_2\text{H}_4)_2]_2$. With the other ligands, $\text{Rh}(\text{acac})(\text{C}_2\text{H}_4)_2$ universally gave both lower conversions (except with the bissulfoxide) and lower deboronation. In the cases of the chiral dienes **L11** and **L12**, conversion was complete or nearly complete using both rhodium salts, but deboronation was much lower for the acac-ligated complex. Particularly in these cases, whether the lower deboronation was simply an effect of a less active catalyst (or the presence of fewer active catalytic species) or whether it was due to a more selective catalyst system would need to be confirmed by taking samples at earlier timepoints (Section 3.2.1.4). The chiral ligand-free results appear to suggest that $\text{Rh}(\text{acac})(\text{C}_2\text{H}_4)_2$ gives better selectivity for the desired reaction over the deboronation reaction without additional ligand added.

It is interesting that the bissulfoxide **L9** appears to have inhibited both the conjugate arylation and protodeboronation reactions by comparison with the chiral ligand-free reaction mixtures using the complexes $[\text{Rh}(\text{Cl})(\text{COE})_2]_2$, $\text{Rh}(\text{acac})(\text{C}_2\text{H}_4)_2$ and $[\text{Rh}(\text{Cl})(\text{C}_2\text{H}_4)_2]_2$, whereas with the other precatalysts it simply seemed not to bind. These other precatalysts either have strongly bound carbonyl ligands or bidentate ligands, which presumably reflects the binding strength of ligand **L9**.

$\text{Rh}(\text{acac})(\text{CO})_2$ appears to have formed new complexes with the phosphine ligands which were inactive to the 1,4-addition reaction at 30 °C. The fact that deboronation did not occur to a greater extent than that observed in the rhodium- and ligand-free reaction (Section

3.2.1.1) suggests that transmetalation is not occurring in these cases. Ph-BOD **L12** and the bissulfoxide **L9** showed little evidence of binding to the rhodium, whereas a partial extent of binding seems to have been possible with the naphthyl ester diene **L11**.

After sampling all of the reaction mixtures under an inert atmosphere, they were returned to the reaction and heated to 60 °C for 65 hours. Table 7 displays these results for the reactions involving the catalyst precursors $[\text{RhCl}(\text{COE})_2]_2$, $\text{Rh}(\text{acac})(\text{C}_2\text{H}_4)_2$ and $\text{Rh}(\text{acac})(\text{CO})_2$. The results provide complementary information that corroborates the suggestions made regarding the ligand exchanges and the activity of the catalyst systems (Table 7).

The final column in Table 7 provides a crude estimate of the enantioselectivity that would be expected to have been seen if the reaction vials were held at 60 °C without firstly being held at 30 °C. The calculation assumes consistent sampling after heating the reaction mixtures at both 30 °C and 60 °C:

$$ee_{60^\circ\text{C}} = \frac{A - a}{(A - a) + (B - b)} - \frac{B - b}{(A - a) + (B - b)} = \frac{(A - B) - (a - b)}{(A + B) - (a + b)}$$

Equation 2

where A and B are the HPLC peak areas of (*S*)- and (*R*)-**18** respectively after 24 hours at 30 °C and 65 hours at 60 °C, and where a and b are the peak areas of (*S*)- and (*R*)-**18** respectively after 24 hours at 30 °C only.

Ligand	Catalyst Precursor	Rem.			Rem.			ee _{60°C} / %
		ee / %	Conv. / %	Deb. / %	ee / %	Conv. / %	Deb. / %	
(<i>R</i>)-H8-BINAP L2	[RhCl(COE) ₂] ₂	81	94	89	80	94	100	n.d.
(<i>R</i>)-SEGPPOS L5	[RhCl(COE) ₂] ₂	65	93	79	65	95	93	n.d.
(<i>R</i>)-BINAP L7	[RhCl(COE) ₂] ₂	66	95	93	66	96	90	n.d.
Bissulfoxide L9	[RhCl(COE) ₂] ₂	9	25	56	28	40	90	47
Naphth. Diene L11	[RhCl(COE) ₂] ₂	91	98	100	91	97	100	n.d.
Ph-BOD L12	[RhCl(COE) ₂] ₂	91	100	99	90	100	99	n.d.
(<i>S,S</i>)-Chiraphos L16	[RhCl(COE) ₂] ₂	55	100	46	53	100	100	n.d.
No Ligand	[RhCl(COE) ₂] ₂	5	95	54	4	99	100	n.d.
(<i>R</i>)-H8-BINAP L2	Rh(acac)(C ₂ H ₄) ₂	53	68	28	47	86	99	42
(<i>R</i>)-SEGPPOS L5	Rh(acac)(C ₂ H ₄) ₂	56	59	28	36	80	95	22
(<i>R</i>)-BINAP L7	Rh(acac)(C ₂ H ₄) ₂	68	51	25	59	72	100	52
Bissulfoxide L9	Rh(acac)(C ₂ H ₄) ₂	41	64	47	39	70	66	n.d.
Naphth. Diene L11	Rh(acac)(C ₂ H ₄) ₂	91	96	83	91	97	100	n.d.
Ph-BOD L12	Rh(acac)(C ₂ H ₄) ₂	92	100	67	92	100	97	n.d.
(<i>S,S</i>)-Chiraphos L16	Rh(acac)(C ₂ H ₄) ₂	52	86	28	56	99	99	60
No Ligand	Rh(acac)(C ₂ H ₄) ₂	8	92	52	8	97	100	n.d.
(<i>R</i>)-H8-BINAP L2	Rh(acac)(CO) ₂	n.d.	0	7	13	49	90	13
(<i>R</i>)-SEGPPOS L5	Rh(acac)(CO) ₂	n.d.	1	5	59	70	85	61
(<i>R</i>)-BINAP L7	Rh(acac)(CO) ₂	n.d.	0	5	23	58	100	23
Bissulfoxide L9	Rh(acac)(CO) ₂	3	79	52	6	83	68	n.d.
Naphth. Diene L11	Rh(acac)(CO) ₂	50	33	12	76	82	70	83
Ph-BOD L12	Rh(acac)(CO) ₂	4	77	21	43	98	45	70
(<i>S,S</i>)-Chiraphos L16	Rh(acac)(CO) ₂	n.d.	0	6	49	67	60	49
No Ligand	Rh(acac)(CO) ₂	1	84	29	4	90	50	n.d.

Table 7. Comparison of selected results after heating for a subsequent 65 h at 60 °C.

In all cases using Rh(acac)(CO)₂, except perhaps with the bissulfoxide **L9**, the reactions were now found to progress, and the enantioselectivities improved when using the chiral diene ligands **L11** and **L12**. This supports the hypothesis that ligand exchange had not fully occurred at 30 °C when using Rh(acac)(CO)₂ with the chiral dienes. Heating to 60 °C enabled the ligand exchange to occur and the reactions to proceed with the newly formed chiral complexes. Therefore at 60 °C, the calculated enantiomeric excesses were 83% (**L11**) and 70% (**L12**), rather than the low (50% *ee*, **L11**) or negligible (**L12**) enantioselectivities afforded at 30 °C.

In contrast, the overall enantioselectivities observed in the conjugate arylation product decreased upon heating for the reactions using bisaryl-phosphine ligands with Rh(acac)(C₂H₄)₂. This is concordant with the expectation that when the chiral ligands were

already bound to rhodium at 30 °C to give active metal centres, subsequent heating served only to decrease the efficiency of the transfer of chirality, both by decreasing the energy difference between the diastereomeric transition states and by enabling a higher proportion of reactions to proceed via the higher energy pathway. This is reflected in the lower calculated enantiomeric excesses for if the reactions using bisaryl-phosphine ligands with Rh(acac)(C₂H₄)₂ had been performed only at 60 °C.

This effect was similarly observed using the bissulfoxide ligand. If a bissulfoxide **L9**-rhodium complex is considered to be able to deliver an enantioselectivity of 72% *ee* at 30 °C (as in the reaction using [RhCl(C₂H₄)₂]₂, Table 6), then the calculated enantiomeric excess for a bissulfoxide **L9**-rhodium complex at 60 °C is notably lower (47% *ee* using [RhCl(COE)₂]₂, Table 7). Likewise, the chiral dienes **L11** and **L12** were found to transfer chirality with up to 92% *ee* at 30 °C, whereas at 60 °C enantiomeric excesses of 83% (**L11**) and 70% (**L12**) were calculated when using Rh(acac)(CO)₂.

The role of temperature in increasing the extent of deboronation is also highlighted by the results in Table 7. Increasing the temperature from 30 °C to 60 °C appears to have increased the rate of deboronation more than the rate of the 1,4-addition with good generality. A catalyst system that performs well at lower temperatures is therefore a more attractive choice.

3.2.1.3 Competition Experiments to Determine Relative Extents of Conjugate Arylation and Protodeboronation

A large excess of arylboronic ester **17** (2.3 equivalents) was used to compare the broad spread of ligands and rhodium salts in Sections 3.2.1.1 and 3.2.1.2, enabling conditions to be used that closely resembled those of the previous process (Section 2.1). It also provided an opportunity for good conversions to bisaryl **18** to be attained, even if the extent of deboronation was high, so that enantiomeric excesses could be measured with good confidence. The excess of arylboron reagent **17** was small enough to enable legitimate inferences to be drawn based on the extent of remnant deboronation measured, however the measure was limited by only having two timepoints. For many of the best performing catalyst systems, the selectivity of the systems for the desired 1,4-addition reaction over the competing deboronation reaction could not be deduced from the data.

Therefore, a smaller set of reactions were performed with one-to-one stoichiometry of the enoate **16** and the arylboronic ester **17** to directly compare the selectivity of the catalyst systems for the desired reaction over the competing protodeboronation reaction. The dienes

L11 and **L12** were used due to the excellent conversions and enantioselectivities previously achieved using them, along with (*R*)-H8-BINAP **L2**, since this was the phosphine ligand that delivered the highest enantioselectivities. The four rhodium salts which had enabled the highest enantioselectivities to be achieved were also used: [Rh(Cl)(C₂H₄)₂]₂, [RhCl(COE)₂]₂, Rh(acac)(C₂H₄)₂ and Rh(NBD)₂BF₄. Conversion was calculated as the peak area conversion of the enoate **16** to the 1,4-addition product **18** in the same manner as for Sections 3.2.1.1 and 3.2.1.2. Deboronation was calculated as the HPLC peak area conversion to *o*-tolylmethanol **19** according to:

$$\text{Deboronation} = \frac{\text{Area}\%_{19}}{\text{Area}\%_{19} + \text{Area}\%_{17} + \text{Area}\%_{18}}$$

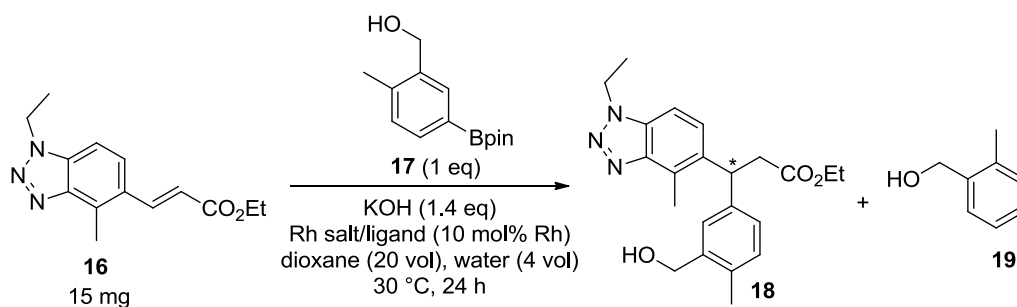
Equation 3

A measure of the residual arylboronic ester **17** was also made, calculated as:

$$\text{Residual } 17 = \frac{\text{Area}\%_{17}}{\text{Area}\%_{17} + \text{Area}\%_{18} + \text{Area}\%_{19}}$$

Equation 4

The results are summarised in Table 8.



Ligand	[RhCl(COE) ₂] ₂				Rh(acac)(C ₂ H ₄) ₂			
	ee / %	Conv. / %	Deb. / %	Residual 17 / %	ee / %	Conv. / %	Deb. / %	Residual 17 / %
(<i>R</i>)-H8-BINAP L2	77	86	27	0	72	61	23	39
Naphth. Diene L11	91	90	17	0	92	98	8	1
Ph-BOD L12	88	100	5	0	85	100	3	2
No Ligand	2	82	22	10	4	83	30	1

Ligand	[Rh(Cl)(C ₂ H ₄) ₂] ₂				Rh(NBD) ₂ BF ₄											
	ee / %	Conv. / %	Deb. / %	Residual 17 / %	ee / %	Conv. / %	Deb. / %	Residual 17 / %								
(<i>R</i>)-H8-BINAP L2	73	85	26	2	82	84	32	0								
Naphth. Diene L11	93	95	9	0	85	80	88	87	15	10	0	0				
Ph-BOD L12	90	90	100	100	4	2	1	0	45	23	64	63	57	44	0	0
No Ligand	3	71	33	1	2	3	60	55	55	51	0	0				

Table 8. Summary of results from competition experiments, employing just one equivalent of arylboronic ester **17**. The results have been calculated in the same way as for previous sections, by HPLC area% ratios at 210 nm using HPLC Method D1. "Conv." is the peak area conversion of **16** to **18**. "Deb." is a measure of deboronation. The results in blue are from repeated reactions.

In general, the identity of the ligand was found to have the greatest effect on the selectivity of the catalyst system for the desired 1,4-addition reaction over the protodeboronation reaction. Remarkably and surprisingly, the chiral diene ligands **L11** and **L12** gave exceptionally high conversions of the enoate to the desired product when used with all of the catalyst precursors containing monodentate alkene ligands, despite no excess of the arylboronic ester being used. This selectivity was particularly high with the ethylene-ligated catalyst precursors.

The high selectivity observed for the conjugate arylation reaction when using ligands **L11** and **L12** does not seem to be generally true of alkene or even diene ligands. The reactions in which no additional ligand was charged enable comparisons to be made between this and the reaction selectivities achieved using each of the monoalkene-ligated complexes ([RhCl(COE)₂]₂, [RhCl(C₂H₄)₂]₂ and Rh(acac)(C₂H₄)₂) and with another diene-ligated complex (Rh(NBD)₂BF₄). None of these displayed good selectivity for the desired reaction, suggesting something uniquely advantageous about the structure of ligands **L11** and **L12**.

over that of norbornadiene or the two mono-alkenes (Figure 18). This is explored further in Section 3.3.2.

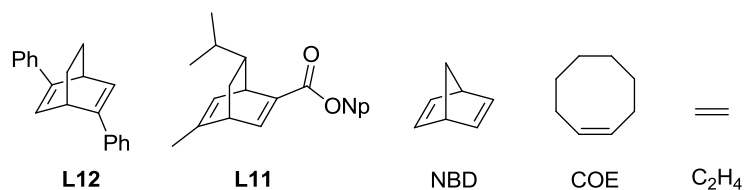


Figure 18. Comparison of the alkene ligands used in the competition experiments.

$\text{Rh}(\text{NBD})_2\text{BF}_4$ was particularly poor in its selectivity for the conjugate arylation reaction over deboronation, and this was reflected in the performance of the chiral dienes **L11** and **L12** when used with $\text{Rh}(\text{NBD})_2\text{BF}_4$, especially for Ph-BOD **L12**. The repeated reactions verified these results (the variability when used with Ph-BOD **L12** was also reflected in later time-coursing experiments, Section 3.2.1.4), with the chiral diene ligands delivering significantly decreased selectivity for both the transfer of chirality and the desired reaction when used in combination with $\text{Rh}(\text{NBD})_2\text{BF}_4$. Comparison of these results with the chiral ligand-free reaction indicates either an equilibrium between the achiral and chiral complexes that lies further towards the achiral complex than in other cases, or that ligand exchange is unusually slow relative to the activity of the achiral complex in this case, despite use of a cationic catalyst precursor. When 2.3 equivalents of arylboronic ester **17** was used (Table 4, Section 3.2.1.1), the enantiomeric excess finally achieved was higher than in these cases, suggesting that it may be a slow ligand exchange rather than the position of the equilibrium. Further evidence of this was found in time-coursing experiments (Section 3.2.1.4). These experiments, which are discussed later, also support the implication seen from the consistently high enantioselectivities of ligands **L11** and **L12** with the monoalkene-ligated catalyst precursors in Table 8 that efficient and fast replacement of the achiral ligands with the chiral dienes occurs in these cases.

(*R*)-H8-BINAP **L2** was far less selective for the desired 1,4-addition over deboronation than the chiral dienes were, although was more selective than the achiral catalyst precursors in some cases. When (*R*)-H8-BINAP was used in combination with $\text{Rh}(\text{acac})(\text{C}_2\text{H}_4)_2$, the total consumption of arylboron reagent **17** was found to be lower than when $\text{Rh}(\text{acac})(\text{C}_2\text{H}_4)_2$ was used without additional ligand. It could perhaps be the case that $\text{Rh}(\text{acac})(\text{H8-BINAP})$ forms within a reasonably short time-frame, and that the subsequent exchange of acac for hydroxide, or transmetalation to the acac-ligated complexes, is slower for this complex than for the ethylene-ligated precursor. An acac-bound anionic ligand would be expected to result in a slower reaction rate (Section 1.3.2).

(*R*)-H8-BINAP was again found to deliver its highest enantioselectivity when used with the cationic Rh(NBD)₂BF₄ catalyst precursor, which may reflect a rapid ligand exchange in this case, and a less active achiral rhodium complex. The order of catalyst precursors for enantioselectivity achieved from (*R*)-H8-BINAP was Rh(NBD)₂BF₄ > [Rh(Cl)(COE)₂]₂ > [RhCl(C₂H₄)₂]₂ ≈ Rh(acac)(C₂H₄)₂, which may be rationalised as follows. Ligand exchange of H8-BINAP with Rh(NBD)₂BF₄ is particularly rapid and the achiral background reaction is reasonably slow for the 1,4-addition. Ligand exchange with the remaining three complexes is good but the enantiomeric excess is decreased by the background achiral reaction. This is slowest for [RhCl(COE)₂]₂ as suggested by the residual arylboronic ester in the case with no chiral ligands, which therefore enables the second highest enantiomeric excess to be achieved in this case. Note that the two cases showing residual arylboronic ester in Table 8 (Rh(acac)(C₂H₄)₂ with H8-BINAP and [RhCl(COE)₂]₂ without additional ligand) are consistent with previous observations (Table 7, Section 3.2.1.2).

3.2.1.4 Time-Coursing Experiments with Conjugate Arylation Catalyst Systems

Time-coursing experiments were performed in parallel for a selection of catalyst precursors and ligand combinations, in order to provide comparisons of the reaction rates. Each of the ligands from the competition experiments were used, along with all of catalyst precursors except for [RhCl(COE)₂]₂ (Section 3.2.1.3). The reactions used one equivalent of arylboronic ester **17**, and unstandardised HPLC peak area data at 210 nm was sufficient for comparisons to be made between the different systems. Samples were taken over 7 hours before a final sample at 70 hours. Each of the reaction mixtures was kept under nitrogen, however due to the sampling requirements the reactions could not be performed in the sealed nitrogen-filled reactor that had been used for the previous experiments. Within reasonable error, most of the reactions reached conversions comparable to those observed in the competition experiments within the 70 hours, with the exception of the experiments using (*R*)-H8-BINAP, for which the conversions were decreased slightly. An overview of the conversion data from the first set of reactions is provided in Figure 19. In general, the rates of reaction were high.

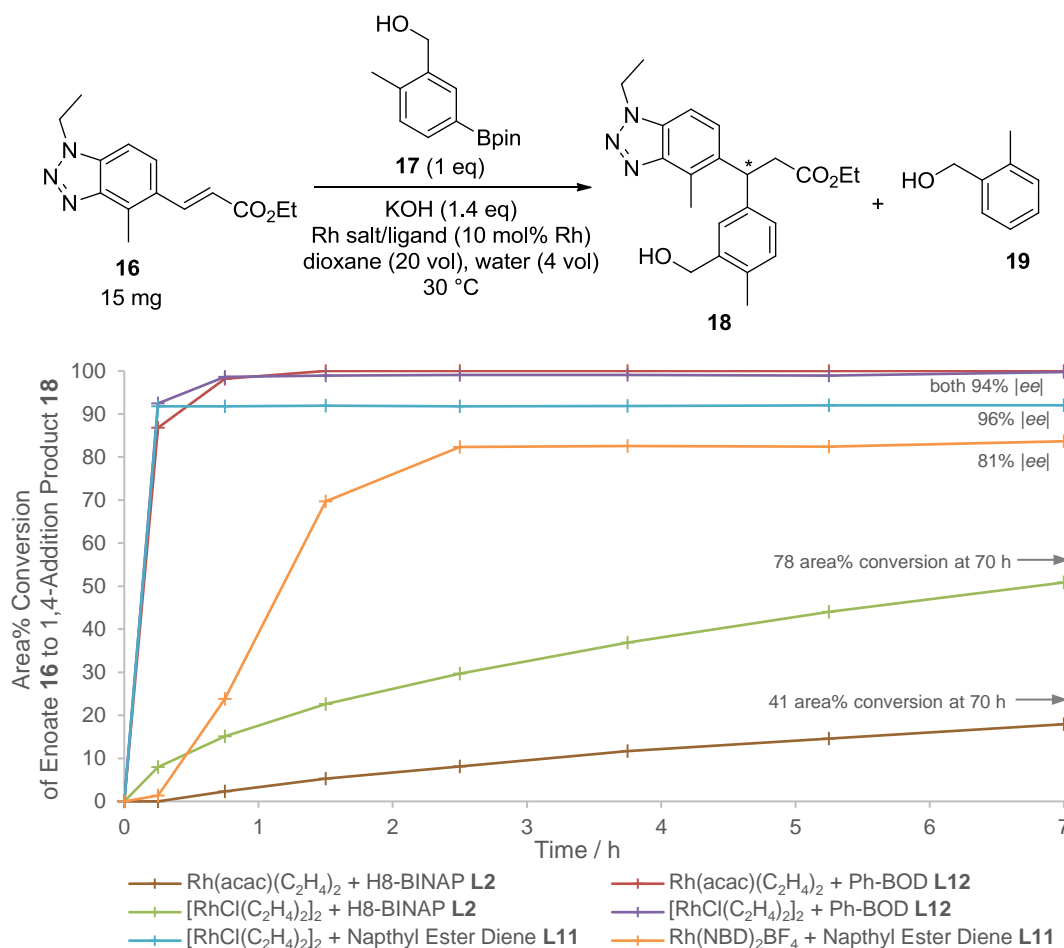


Figure 19. An overview of the conversion data for the first set of timepoint experiments. Enantiomeric excess data was not considered sufficiently reliable for the cases with (*R*)-H8-BINAP due to low peak areas of either or both enantiomers combined with less clean chromatograms in these cases.

The combinations of Ph-BOD **L12** both with $\text{Rh}(\text{acac})(\text{C}_2\text{H}_4)_2$ and with $[\text{RhCl}(\text{C}_2\text{H}_4)_2]_2$ were selected for time-coursing due to the difference in deboronation observed between them in Table 6 (page 56). It had been postulated that the lower level of deboronation seen with $\text{Rh}(\text{acac})(\text{C}_2\text{H}_4)_2$ may have been due to both the desired and undesired reactions proceeding more slowly when using this catalyst precursor, but this was only found to be marginally the case during the time-coursing experiments (Figure 19). Both complexes achieved near-quantitative conversions to 1,4-addition product **18** in less than one hour. However, $\text{Rh}(\text{acac})(\text{C}_2\text{H}_4)_2$ gave *o*-tolylmethanol **19** with only 1.0 and 1.3 HPLC area% at 15 and 45 minutes respectively, whilst $[\text{RhCl}(\text{C}_2\text{H}_4)_2]_2$ gave *o*-tolylmethanol **19** with 1.8 and 2.1 HPLC area% at the same timepoints. At such low peak area percentages caution should be observed, however the combination of this result with the results in Table 6 could suggest that the two catalyst systems exhibit different propensities for deboronation after transmetalation of the arylboronic ester to the active catalyst. It may also be that the catalyst

system employing $\text{Rh}(\text{acac})(\text{C}_2\text{H}_4)_2$ can achieve fewer catalyst turnovers, which could also account for the difference observed in Table 6.

(*R*)-H8-BINAP **L2** was investigated with the same two rhodium complexes because Table 8 (page 64) had suggested a much slower reaction rate for this ligand with $\text{Rh}(\text{acac})(\text{C}_2\text{H}_4)_2$. Although neither reaction proceeded to the same extent as it had done in the competition experiment, the difference between the two complexes was evident, with both deboronation and the desired reaction proceeding much more slowly with $\text{Rh}(\text{acac})(\text{C}_2\text{H}_4)_2$. Interestingly, selectivity for the desired 1,4-addition over the deboronation reaction was worse when using (*R*)-H8-BINAP with $\text{Rh}(\text{acac})(\text{C}_2\text{H}_4)_2$ (57:43 HPLC peak area ratio of compounds **18:19** at 7 h) than with $[\text{RhCl}(\text{C}_2\text{H}_4)_2]_2$ (70:30 HPLC peak area ratio of compounds **18:19** at 7 h).

The comparison of the naphthyl ester diene **L11** with $[\text{RhCl}(\text{C}_2\text{H}_4)_2]_2$ and with $\text{Rh}(\text{NBD})_2\text{BF}_4$ provided an increased level of understanding regarding the formation of the chiral catalysts. Used with $[\text{RhCl}(\text{C}_2\text{H}_4)_2]_2$, the reaction was complete within 15 minutes, matching the overall reaction rate for the first 15 minutes observed using $[\text{RhCl}(\text{C}_2\text{H}_4)_2]_2$ with Ph-BOD **L12**. However, unlike for **L12**, no further reaction was observed, due to complete consumption of the remaining arylboronic ester to give the deboronation product within that time also. A plot of the peak areas for the reaction using the naphthyl ester diene **L11** with $[\text{RhCl}(\text{C}_2\text{H}_4)_2]_2$ is shown in Figure 20.

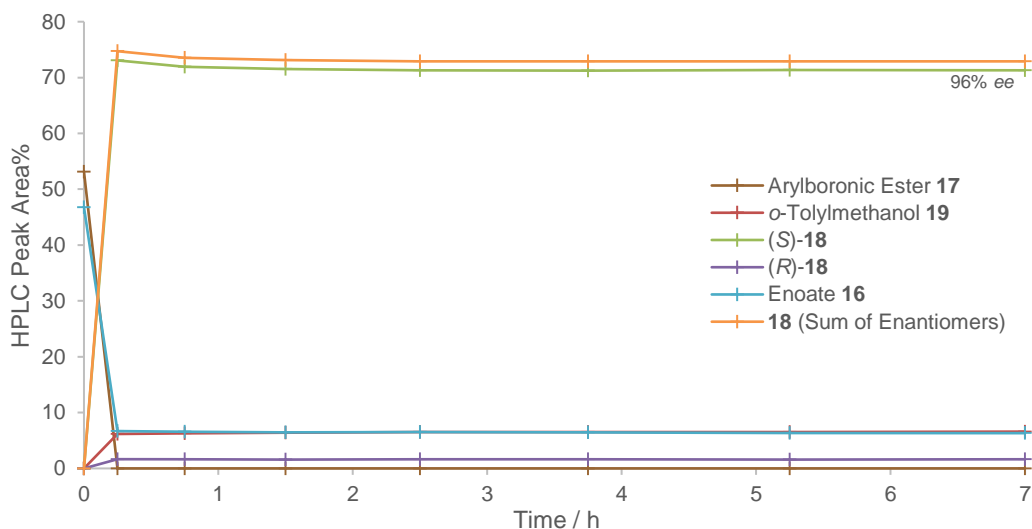


Figure 20. Area percent data for the combination of $[\text{RhCl}(\text{C}_2\text{H}_4)_2]_2$ and the naphthyl ester ligand **L11** at 210 nm.

In comparison, the reaction using the naphthyl ester diene **L11** with $\text{Rh}(\text{NBD})_2\text{BF}_4$ proceeded much more slowly, occurring over 3 hours and displaying a characteristic S-shape in the conversion as a more active catalyst gradually formed (Figure 21). The gradual ligand

exchange was confirmed by the enantioselectivities observed at the different timepoints; the enantiomeric excess increased from no more than 74% *ee* at 24% peak area conversion (45 minutes) to 82% *ee* by 82% peak area conversion (2 hours 30 minutes), when the reaction was virtually complete. This also implies that an active achiral complex is formed more quickly than the ligand exchange can take place.

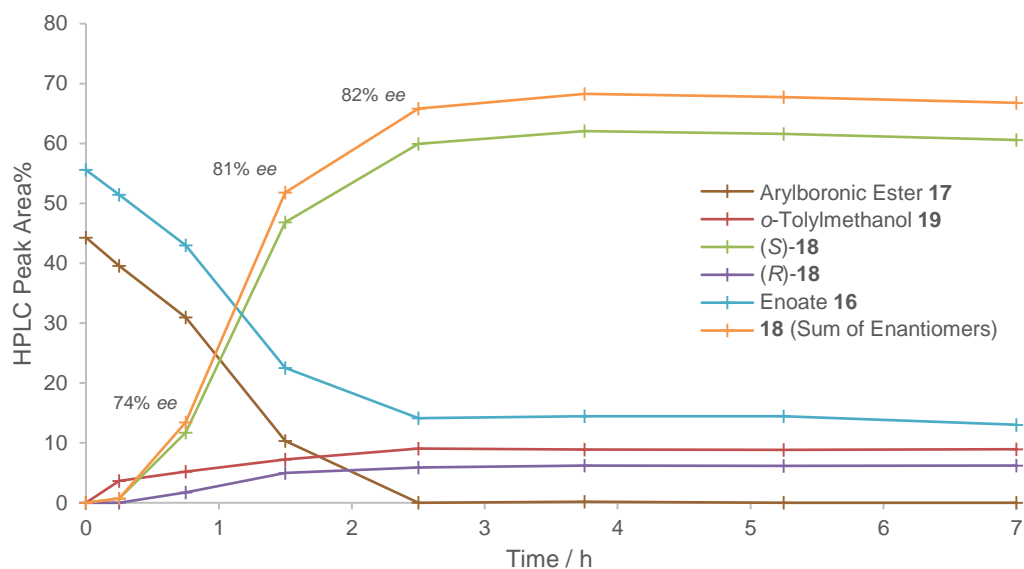


Figure 21. Area percent data for the combination of $\text{Rh}(\text{NBD})_2\text{BF}_4$ and the naphthyl ester diene ligand **L11**.

A second collection of time-coursing experiments was then performed, focussing on the $\text{Rh}(\text{NBD})_2\text{BF}_4$ catalyst precursor. In this set of reactions, Ph-BOD **L12** and (*R*)-H8-BINAP **L2** were used, both with and without premixed with the catalyst precursor in dioxane for 17 hours, and the arylboronic ester was used both in excess (2.3 equivalents) and stoichiometrically (1 equivalent). The results, including one repeated experiment, are summarised in Figure 22. Only the first four hours of data are shown, since further changes in conversion and enantiomeric excess were not observed after this period of time.

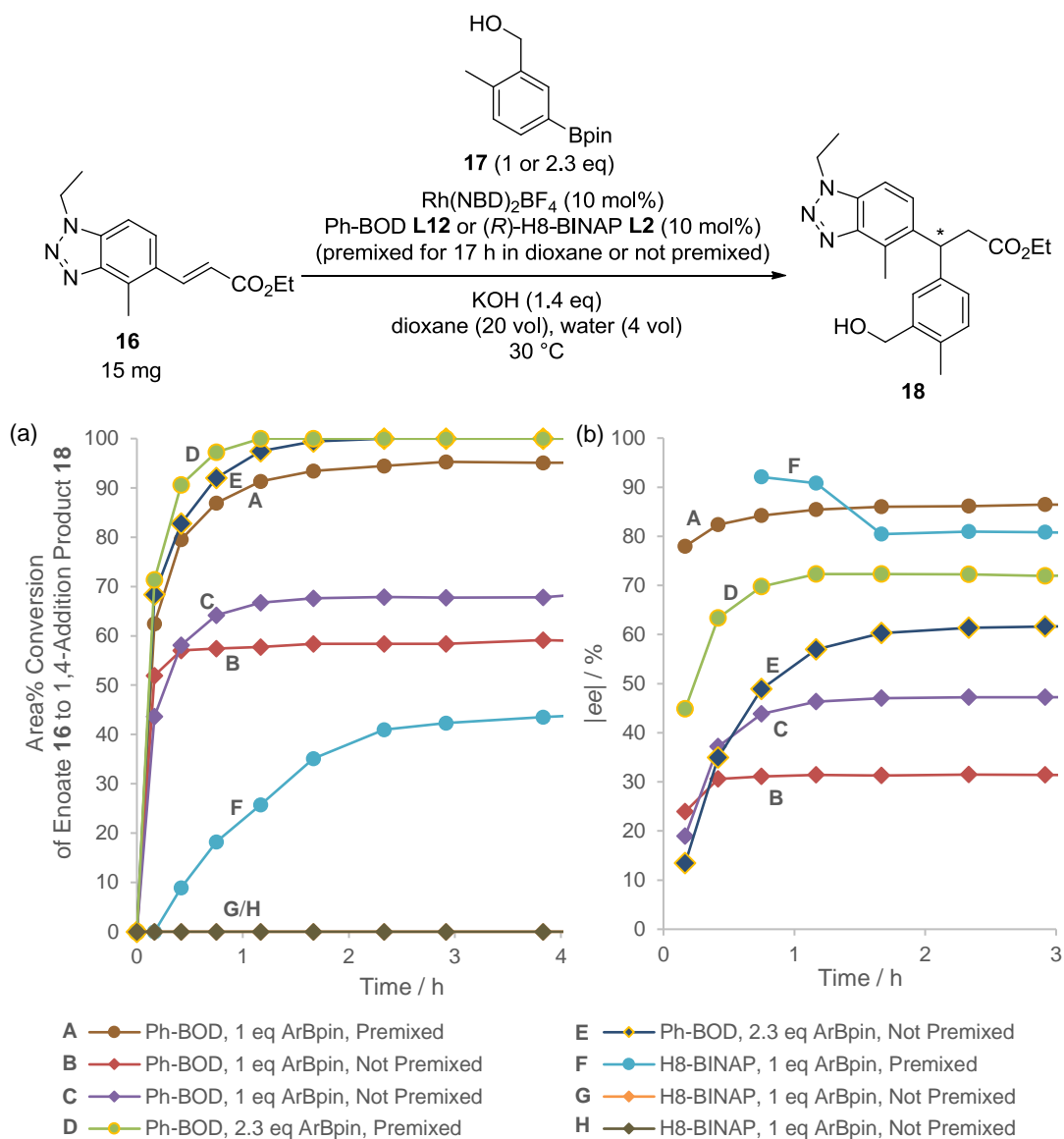
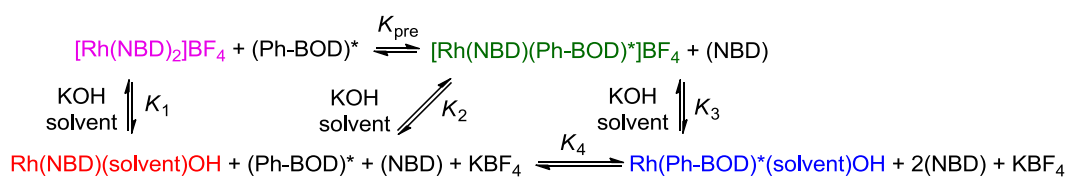


Figure 22. (a) Peak area conversion of the enoate **16** to the 1,4-addition product **18** over 4 h and (b) the enantiomeric excess of (*R*)- or (*S*)-**18** over 3 h. No further changes observed after these timepoints.

Considering firstly Ph-BOD **L12** and the effect of premixing the chiral ligand with the rhodium precatalyst in dioxane at the reaction temperature overnight (Plot A, cf. Plots B and C, Figure 22a), it is clear that premixing led to the desired reaction proceeding more rapidly and with decreased deboronation. Premixing also decreased the extent to which the enantiomeric excess increased over the first 1–2 hours of the reaction, however it is striking that an improvement in enantioselectivity was still observed when premixing had been performed. This cannot simply be explained by suggesting that premixing occurred for an insufficient amount of time or at an insufficiently high temperature, since when using 2.3 equivalents of arylboronic ester (Plots D and E), the enantiomeric excess achieved by the case with no premixing was rapidly comparable to that of the case with premixing, even

exceeding the enantioselectivity observed at the earliest timepoint for the reaction mixture containing premixed rhodium salt and ligand. The presence of hydroxide therefore appears to be important for either the rate of ligand exchange or the equilibrium position of that exchange. For example, as illustrated in Scheme 32, it could be the case that the equilibrium in the absence of hydroxide (K_{pre}) either lies a little further towards an achiral complex or takes a long time to reach the equilibrium position, whereas the equilibrium in the presence of hydroxide lies further towards the chiral side and/or reaches that equilibrium position more quickly (K_4). Therefore, the initial addition of hydroxide to a premixed solution of chiral ligand and achiral precatalyst would give a higher proportion of achiral active catalyst than would be present at equilibrium in the presence of hydroxide.



Scheme 32. A simplified example of the complexes and equilibria that could be involved when mixing $\text{Rh(NBD)}_2\text{BF}_4$ with Ph-BOD L12, with and without potassium hydroxide. The catalyst precursors are shown in purple (achiral) and green (chiral). The active complexes are shown in red (achiral) and blue (chiral).

Curiously, after premixing Ph-BOD with the precatalyst, a higher enantiomeric excess was achieved when only one equivalent of arylboronic ester was used (86% *ee*, Plot A, Figure 22b) than when 2.3 equivalents was used (72% *ee*, Plot D, Figure 22b). Although this may at first appear surprising, the difference corroborates what has been proposed above (Scheme 32). Since transmetalation (usually considered to be the rate-determining step) will be slowed when only one equivalent of the arylboronic ester is present, there is more time for ligand exchange to occur. This would give a higher proportion of chiral active catalyst before the reaction has proceeded to a significant extent.

When the $\text{Rh(NBD)}_2\text{BF}_4$ and Ph-BOD were not premixed, the reaction mixture using the greater excess of arylboronic ester resulted in the higher enantioselectivity of the conjugate arylation product at the end of the reaction (62% *ee* rather than 31–47% *ee*, Plots E, B and C, Figure 22b). In this case, the greater excess of arylboronic ester simply allows a higher enantiomeric excess to be ultimately achieved, since the reaction continues to progress while more chiral active catalyst forms.

The discrepancy between the two repeated runs using Ph-BOD with one equivalent of arylboronic ester and no premixing (Plots B and C) might be accounted for by a small discrepancy in the length of time that it took for the aqueous hydroxide to be added to their

reaction mixtures. The hydroxide was always the last component of the reaction mixtures to be added. Regardless of the cause, the variation seen in this case reflects the variation observed specifically for this combination in the competition experiments (Section 3.2.1.3).

The results of the reactions using (*R*)-H8-BINAP **L2** were unexpected (Plots F, G and H, Figure 22a). No conversion to the product was seen in the two repeated cases for which no premixing was performed, in contrast to the results in Section 3.2.1.3. This was due to complete catalyst inactivity rather than due to a vastly increased extent of deboronation. The repeated reaction was performed on a different occasion and in both of these instances, deboronation reached levels comparable only to the background base-mediated levels (Section 3.2.1.1). Having confirmed by NMR that the batch of ligand used had not oxidised in storage, the explanation remaining seemed to be that, in the case of (*R*)-H8-BINAP, ligand exchange is very fast but the resulting complex is very sensitive to air and therefore to the sampling method; even achiral reactivity was not observed. The sensitivity must be significant, since every reasonable precaution was made to keep the reaction mixtures air-free and to avoid cross-contamination from the sampling needle.

When (*R*)-H8-BINAP was premixed with the catalyst precursor, some conversion was seen, however this remained much lower than had been achieved in Section 3.2.1.3. Curiously, the enantioselectivity appeared to decrease from 92% *ee* to 81% *ee* over the first few timepoints in this case (Plot F, Figure 22b). 81% *ee* is similar to that previously observed, such as in Section 3.2.1.3. The observed decrease in enantioselectivity may simply have been due to the low levels of product in the early samples resulting in misleading analysis, however it could also be explained by a similar argument to that proposed above to explain the gradual increase in enantiomeric excess for the reactions using Ph-BOD **L12** (Scheme 32). In this case, the equilibrium position between the achiral and chiral active catalysts would have to be further towards the achiral catalyst than the equilibrium position between the achiral and chiral catalyst precursors.

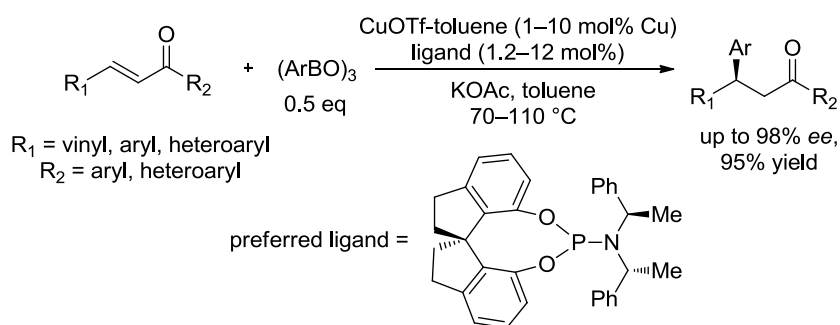
Attempts to repeat this time-coursing experiment with (*R*)-H8-BINAP, alongside one that was not sampled until the end of the time period, indicated again the very high air-sensitivity of this combination. The time-coursing experiment gave no conversion, and the reaction mixture sampled only at the end of the time period gave 74% peak area conversion of the enoate to the product with 71% *ee*. These data are both approximately 10 percentage points lower than the equivalent results from the earlier competition experiment (Section 3.2.1.4); in this later case, the reaction was not prepared in a glove bag or carried out in a sealed reactor. Similar observations regarding the air-sensitivity of a rhodium/(*R*)-BINAP complex

have been made externally, also leading to capricious reactivity resulting in poor reproducibility.¹⁶⁵

3.2.1.5 Assessment of Alternative Metal Systems for the Pharmaceutically-Relevant Conjugate Arylation

In Section 1.1, the motivation within industry to substitute precious metal-catalysed processes for base metal-catalysed processes was discussed. Therefore, literature reports of non-rhodium-catalysed conjugate arylations of arylboron reagents to electron deficient alkenes were investigated before any further investigations of a rhodium-catalysed process were undertaken.

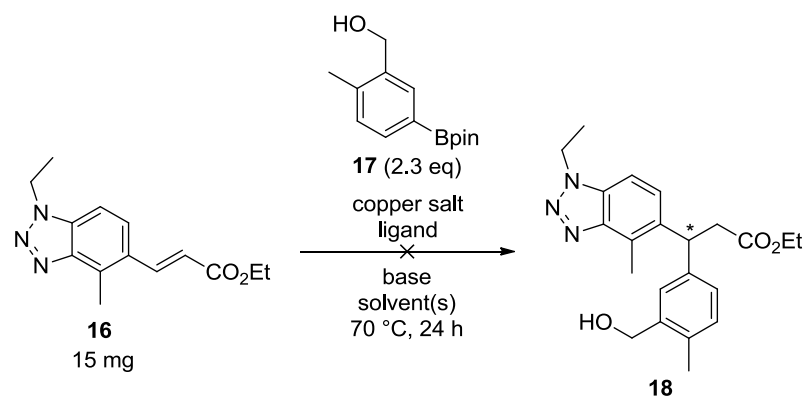
A 2016 report demonstrated asymmetric conjugate addition of boroxines to enones using a copper (I) salt with phosphoramidite ligands (Scheme 33).⁹¹ Copper/phosphoramidite systems had already been demonstrated to catalyse conjugate additions of dialkylzinc reagents to enones.¹⁶⁶



Scheme 33. The first reported copper-catalysed 1,4-addition reaction utilising an arylboron reagent and chiral ligand.

The authors found that weakly basic acetates promoted the reaction while stronger bases inhibited the reaction. No obvious proton source is explicitly present in their reported reaction conditions. The publication stated that the reaction was not possible with pinacol boronic ester reagents or with enoates as electrophiles.

Despite significantly expanding the set of conditions reported in the literature, this statement was found to hold true for the substrates of interest in this research. A diverse set of reaction mixtures was trialled for the 1,4-addition of arylboronic ester **17** to enoate **16**, broadening the range of copper salts, ligands and conditions employed (Table 9). No conversion to the 1,4-addition product was observed using any of the conditions used, although deboration occurred to varying extents.

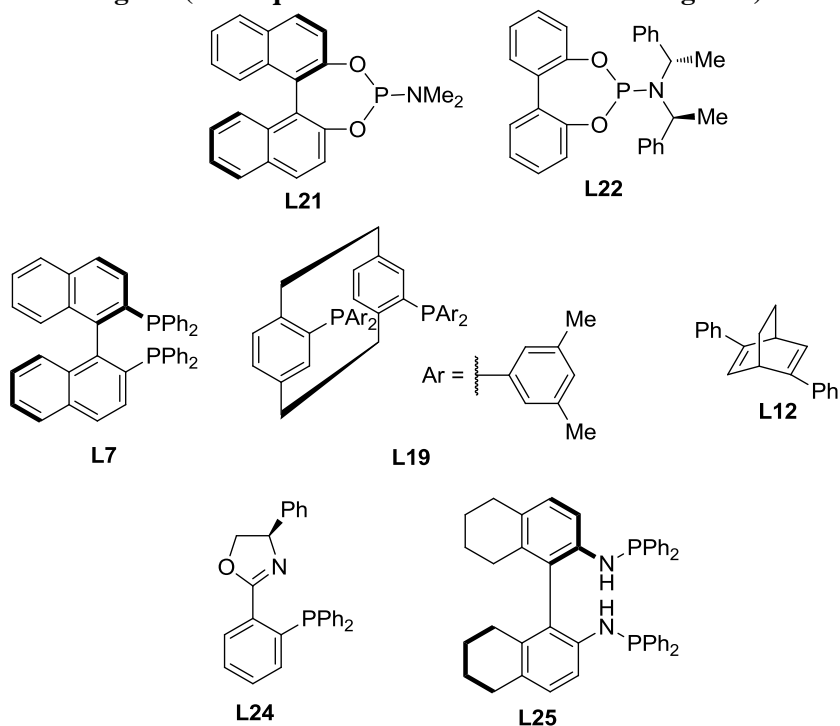


Reaction Components

Copper Salt (10 mol% Cu)

$(\text{CuOTf})_2 \cdot \text{C}_6\text{H}_5\text{CH}_3$
 CuOAc
 $\text{Cu}(\text{OTf})_2$
 CuCl

Ligand (0.12 eq for both mono- and bidentate ligands)



Solvent(s)

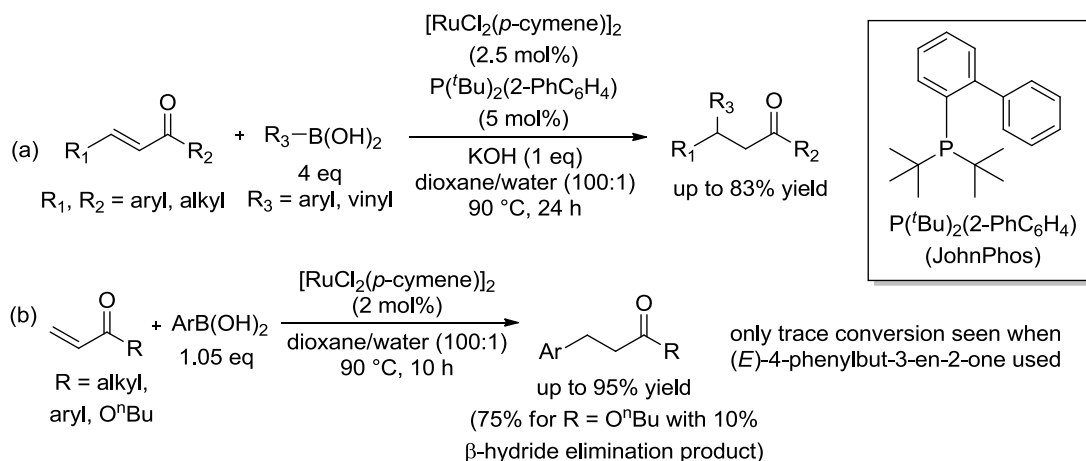
Toluene (20 vol)
 Dioxane (20 vol)
 Water (co-solvent) (4 vol)

Base

KOAc (2 eq)
 KOH (1.4 eq)

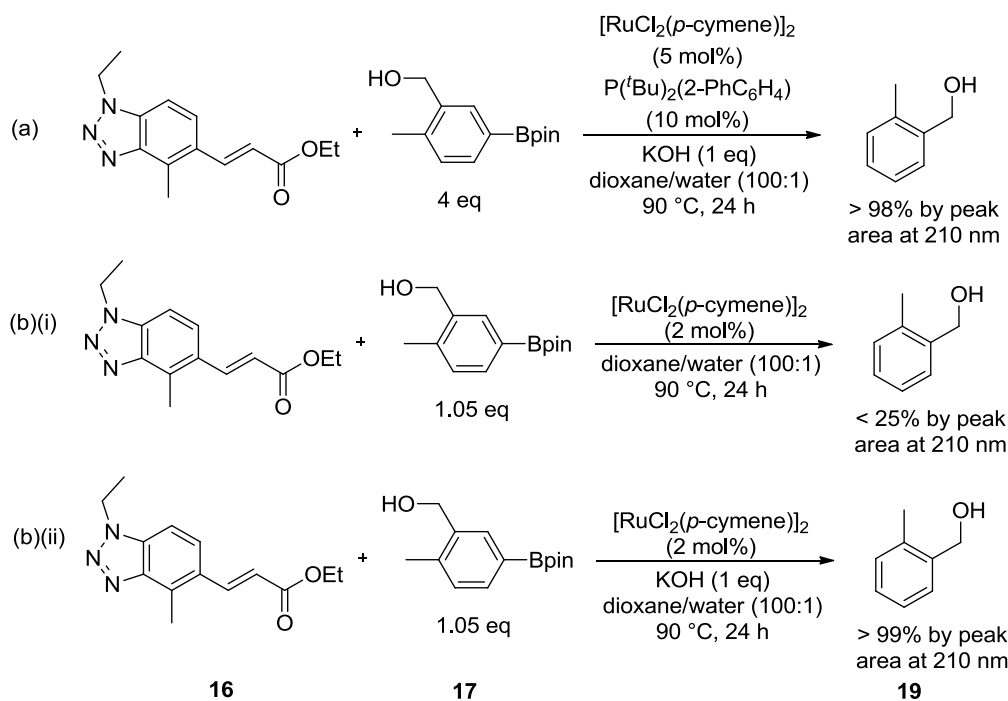
Table 9. 48 different combinations of copper salt, ligand, base and solvents were attempted in speculative reactions, attempting to give 1,4-addition product 18.

The reaction was also attempted using ruthenium, which is another base metal that has been applied to 1,4-addition reactions. Again, the literature does not show examples using enoates, and the racemic literature examples use boronic acids rather than boronic esters (Scheme 34).^{90,167} No asymmetric reports were known to have been published, and so the achiral conditions were used as a starting point in this work.



Scheme 34. The two literature reports of racemic reactions that were the basis of investigations trialling ruthenium catalysis for the desired 1,4-addition reaction (a) using the JohnPhos ligand under basic conditions, and (b) without JohnPhos or base.

In the first instance, a reaction was trialled based on Scheme 34a,⁹⁰ with the only modifications being that 10 mol% of the ligand (JohnPhos) and 5 mol% of the ruthenium dimer were charged, and that an arylboronic ester (**17**) was used rather than a boronic acid (Scheme 35a). After 24 hours, the reaction mixture was analysed by HPLC at 210 nm, which revealed < 1 area% of the desired 1,4-addition product, with neither the corresponding mass ion of this product nor of the analogous compound that would result from a β -hydride elimination to give a tertiary alkene detected by LCMS. Instead, almost quantitative protodeboronation of the arylboronic ester was observed. Assuming that this deboronation was ruthenium-mediated, it appears that transmetalation successfully occurred to the ruthenium centre but that insertion of the enoate could not compete with hydrolysis of the arylruthenium species. The enoate appeared largely, if not completely, untouched.

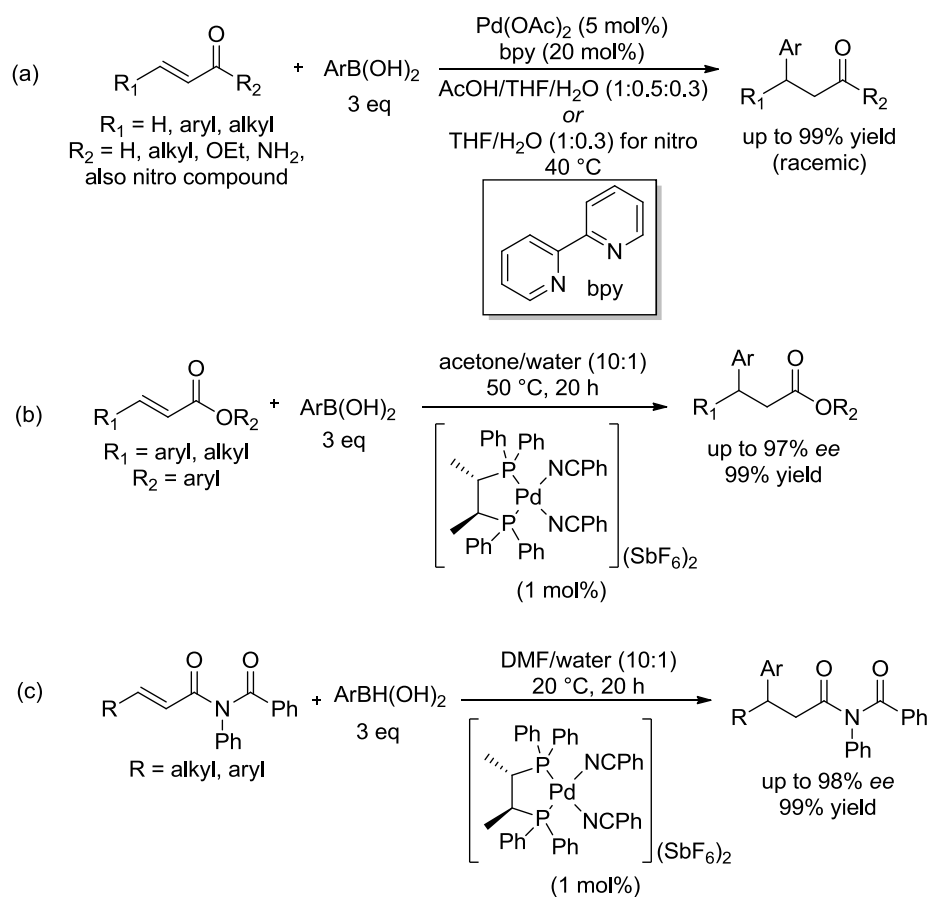


Scheme 35. (a)–(c) The results of the attempted reactions using ruthenium catalysis.

Additional attempts were made based on Scheme 34b,¹⁶⁷ which is similar to the reaction in Scheme 34a but which does not employ additional ligand or base. Prochiral substrates were not employed in the literature report, which demonstrated the process only for arylboronic acids with simple α,β -unsaturated ketones. The conditions reportedly minimised the protodeboronation of the arylboronic acids, allowing their loadings to be significantly decreased. Since an arylboronic ester was employed in the work described here, two attempts were made: one without base, as is the case for the literature report, and one with base (Scheme 35b(i) and Scheme 35b(ii)). None of the desired 1,4-addition product could be detected even in trace amounts by either HPLC or LCMS analysis and in neither reaction mixture was there evidence of any conversion of the enoate. No evidence of the β -hydride elimination product was seen in either case. Deboronation proceeded so cleanly and quantitatively in the case of Scheme 35b(ii), that these conditions have since been employed to prepare analytical markers of various deboronated substrates for a number of projects at GSK.

A final attempt to avoid the need for rhodium catalysis was made with palladium. The β -hydride elimination side-reaction is a particular problem for palladium-catalysed 1,4-addition reactions, which is perhaps unsurprising given the success of the Heck coupling reaction.⁸⁹ Three literature reports (Scheme 36) inspired both racemic and asymmetric

attempts to apply palladium catalysis to the 1,4-addition of interest in this research,^{86–88} since even palladium is more earth-abundant than rhodium (Table 1, page 3).¹⁰



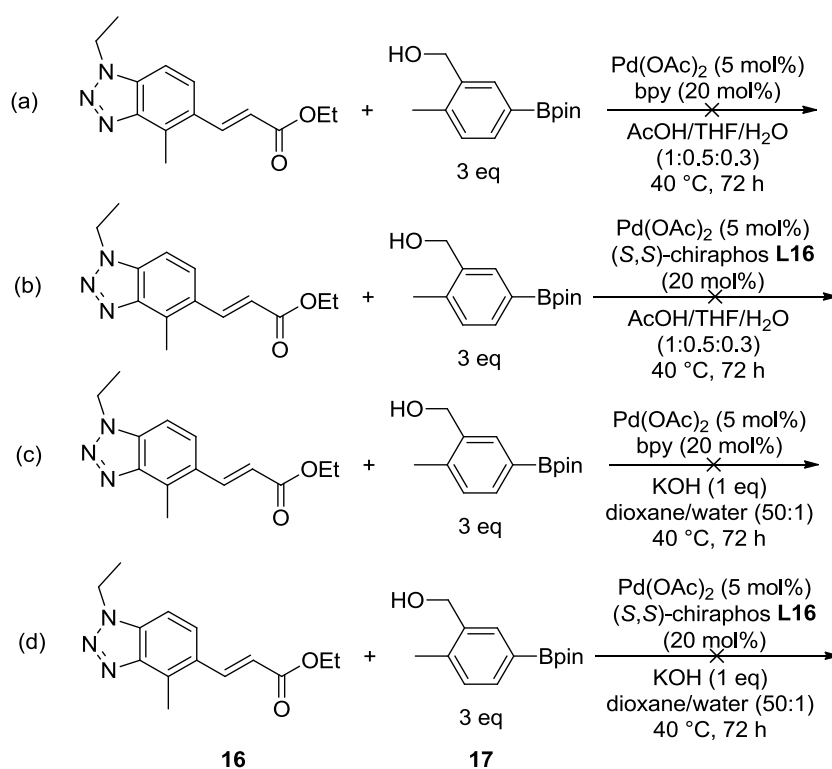
Scheme 36. (a)–(c) The literature reports of palladium-catalysed 1,4-addition reactions that inspired attempts for the 1,4-addition of interest in this research.

The use of a bidentate nitrogen ligand (2,2'-bipyridine, bpy) as the ligand in the racemic example (Scheme 36a) was reported to be crucial for the inhibition of the β -hydride elimination giving the Heck-type product.⁸⁶ A selection of chiral nitrogen ligands was trialled for the reaction in the report, however each gave a very poor yield of the desired product. In the literature example in Scheme 36b, the authors reported that it was essential for R_2 to be an aryl group; if alkyl esters were used, the Heck product was formed instead.⁸⁷ The authors who discovered the transformation in Scheme 36c found that the conditions used avoided formation of the Heck-type products.⁸⁸

Four attempts were made to achieve the 1,4-addition of arylboronic ester **17** to enoate **16** using palladium catalysis (Scheme 37), none of which proved fruitful. For each of the mixtures under acidic conditions (Scheme 37a and b), HPLC analysis at 210 nm after 72 hours revealed almost exclusively the starting materials, with deboronation also very low (< 3 area%). Both showed one to two additional unidentified peaks, which did not appear to

be ligand-related and accounted for < 20 area%, however no suitable mass ions were observed either for the 1,4-addition product or the β -hydride elimination product by LCMS.

Supposing that transmetalation did not occur to the palladium complex, the mixtures were prepared under basic conditions (Scheme 37c and d). Under these conditions, the additional HPLC peaks seen for the mixtures under acidic conditions were no longer present, and deboronation remained very low (< 15 area% and < 1 area% respectively). In three of the four cases, a peak with retention time suitable for the 1,4-addition product was observed, but only at trace levels ((a) 2.1 area%, (c) 2.2 area%, (d) 1.3 area%) and no suitable mass ion was detected in any case by LCMS. Attempts to avoid the use of rhodium were therefore not pursued any further.



Scheme 37. (a)–(d) Attempts to use palladium-catalysis for the desired 1,4-addition.

3.2.1.6 Final Selection of Rhodium Salt and Chiral Ligand for the Pharmaceutically-Relevant Conjugate Arylation

The sections above describe an extensive exploration of catalyst precursors and ligands for performing the 1,4-addition reaction of the arylboronic ester **17** to the enoate **16** of particular interest in this work. Alternatives to rhodium can be comfortably dismissed as not being sufficiently developed for the requirements of this research, and an understanding of the effects of different rhodium precursors, chiral ligands, boronic ester equivalents, and the

premixing of rhodium salts and chiral ligands had been achieved in good detail. This work provided a sufficient basis to select $[\text{RhCl}(\text{C}_2\text{H}_4)_2]_2$ as the rhodium precursor and the chiral naphthyl ester diene ligand **L11** for further investigation and process development. As far as is known, this combination is unprecedented for industrial use.

A number of additional factors confirmed this combination to be the most appropriate choice for further development. Firstly, cost considerations present this as an attractive catalyst system. Table 10 shows the prices of rhodium precursors scaled by the rhodium content and the prices of the naphthyl ester diene **L11** and (*R*)-Tol-BINAP **L7** (used in the original process, Section 0), based on the largest pack sizes advertised on the website of SigmaAldrich.ⁱⁱⁱ Pleasingly, both $[\text{RhCl}(\text{C}_2\text{H}_4)_2]_2$ and the naphthyl ester diene **L11** were cheaper than the rhodium precursor and ligand used to date.

Catalyst Precursor / Ligand	Price
$\text{Rh}(\text{NBD})_2\text{BF}_4$	£78/mmol Rh (£317.50/2g)
$[\text{RhCl}(\text{COE})_2]_2$	£103/mmol Rh (£286.50/1g)
$\text{Rh}(\text{acac})(\text{C}_2\text{H}_4)_2$	(£107/mmol Rh (£413/1g)
$[\text{RhCl}(\text{C}_2\text{H}_4)_2]_2$	£76/mmol Rh (389.50/1g)
(<i>R</i>)-Tol-BINAP L7	£68/mmol (£99.60/1g)
Naphthyl Ester Diene L11	£21/mmol (£63.50/1g)

Table 10. Prices of catalyst precursors and ligands as advertised by SigmaAldrich, stated to the nearest £/mmol. £/mmol Rh denotes the molar price with respect to the molar amount of rhodium.

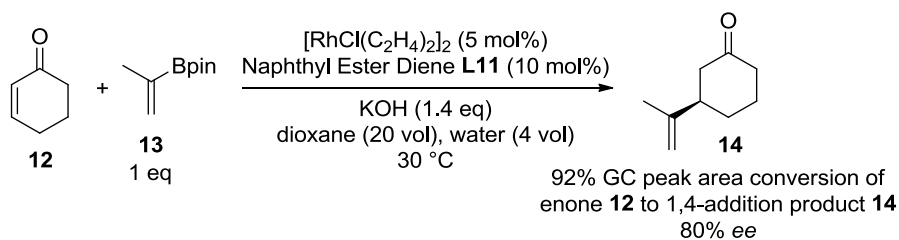
The low cost of ligand **L11** is believed to be largely due to its ease of synthesis (Section 1.3.4).¹¹² Fortuitously the stereochemistry of the commercial ligand gave the desired absolute stereochemistry required in the 1,4-addition product **18**. The opposite enantiomer of the ligand is not readily available or readily prepared, since the phellandrene chiral pool starting material only occurs naturally as the (*R*)-enantiomer. Ph-BOD **L12** also performed very well, but is far more expensive ($\text{£}222 \text{ mmol}^{-1}$)^{iv} due its more elaborate and low yielding preparation and the lack of a chiral pool starting material (cf. Section 1.3.4).¹¹³ The ligand **L12** was therefore not pursued further in the development of the pharmaceutically-relevant conjugate arylation reaction for suitability in a large-scale production context.

The high activity of dienes in rhodium-catalysed 1,4-addition reactions has been known since early on in the development of the methodology (Section 1.3.2.2). No evidence for the use of chiral diene ligands in rhodium-catalysed asymmetric conjugate addition reactions has

ⁱⁱⁱ <https://www.sigmaaldrich.com/united-kingdom.html>, prices based on those shown when accessed on 01 Sep 2017.

^{iv} SigmaAldrich price for (*S,S*)-enantiomer (ligand **L12**) as advertised on 25 Nov 2017.

been found in an industrial context, despite their exceptional performance in the system studied here. In a recent report in *Organic Process Research and Development*, chiral dienes were overlooked even in a high-throughput chiral ligand screen; only phosphine ligands were investigated.¹⁴⁴ To compare the performance of the unoptimised system selected here with those in the literature report, the reported transformation was performed using the conditions shown in Scheme 38. The enantiomeric excess achieved (80% *ee*) was superior to all but one of the catalyst systems used for the high throughput screen in the literature report (c. 90% *ee* using (*R*)-DTBM-SEGPHOS, the remaining ligands delivering < 70% *ee*), and the conversion (92%) was comparable to the highest conversion in the literature report (c. 85%, which gave virtually no stereoselectivity).

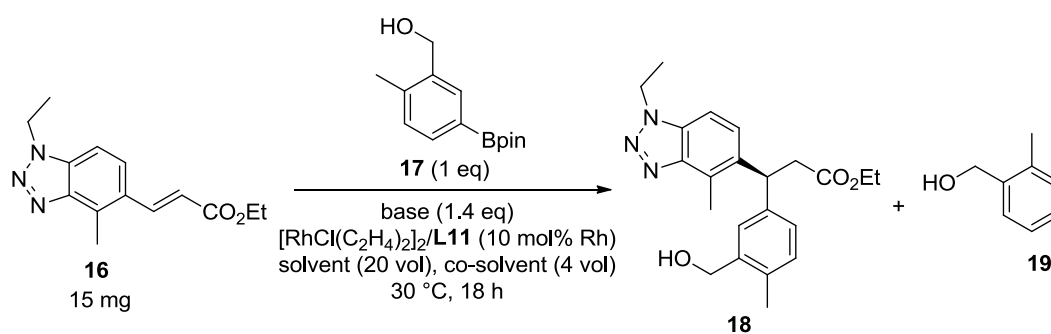


Scheme 38. A transformation of interest in a recent literature report, using the unoptimised system selected in this work.

3.2.2 Solvent and Base Selection for Pharmaceutically-Relevant Conjugate Arylation

1,4-Dioxane is an undesirable solvent for industrial use due to its suspected carcinogenicity towards humans, incurring regulatory issues.¹⁴² Since the original process for the pharmaceutically-relevant conjugate arylation employed dioxane, replacing the reaction solvent with an alternative was to be an important aspect of the process development. Therefore, before considering the continuous variables that might affect the reaction, the 1,4-addition reaction was trialled using a number of different solvents and solvent systems, selected either due to literature precedent or due to their acceptance as preferred solvents for large scale use (Section 1.1).¹⁴² A broad coverage of chemical space was surveyed, with principal component analysis of solvent properties used to ensure that good breadth was achieved. Simultaneously, a broad selection of bases was also trialled for the reaction, with considerations made for environmental, health and safety factors,¹⁶⁸ whilst ensuring a variety of inorganic and organic bases were incorporated with diverse basicities. The carboxylate presumed to have formed from hydrolysis of the enoate **16** under the reaction conditions had been regularly seen as a trace (< 2.5 area%) impurity in the work to identify a suitable catalyst system.

The results from the first set of reactions are given in Table 11. As in Section 3.2.1, conversion is stated as the HPLC peak area conversion of the enoate **16** to the 1,4-addition product **18**, calculated using an achiral HPLC method at 210 nm. Similarly, deboronation is the HPLC peak area conversion of the arylboronic ester **17^v** to *o*-tolylmethanol **19**, measured using the achiral HPLC method and calculated analogously to that in Section 3.2.1.3. The proportion of the total peak area of the chromatogram accounted for by enoate **16**, arylboronic ester **17** and 1,4-addition product **18** was also calculated to provide a measure of the extent to which any undesired processes also occurred under the conditions. The measure, Area%_{16,17,18}, was calculated as the sum of the peak area percent for compounds **16**, **17** and **18**, with the total peak area having been corrected for solvents with chromophores at 210 nm.



Entry	Base (1.4 eq)	Solvent (300 μL) ^{vi}	Co-Solvent (60 μL)	ee / %	Conv. / %	Deb. / %	Area% _{16,17,18}
1	KOH	Dioxane	Water	94	92	9.1	71
2	-	Dioxane	Water	92	7	0.8	90
3	NaHCO ₃	Dioxane	Water	95	92	7.9	82
4	K ₂ CO ₃	Dioxane	Water	92	90	9.6	76
5	KHCO ₃	Dioxane	Water	95	82	16.1	78
6	K ₃ PO ₄	Dioxane	Water	95	93	6.3	77
7	NEt ₃	Dioxane	Water	95	96	2.6	87
8	DIPEA	Dioxane	Water	95	97	2.2	87
9	DIPA	Dioxane	Water	95	96	2.5	86
10	NEt ₃	Dioxane	Ethanol	98	35	5.2	85
11	NaOEt	Dioxane	Ethanol	93	98	4.9	72
12	KOEt	Dioxane	Ethanol	93	98	6.3	69
13	-	Dioxane	Ethanol	n.d.	1	0.4	90
14	NEt ₃	Dioxane	Trifluoroethanol	97	49	2.7	87
15	KOMe	Dioxane	Methanol	95	94	10.2	42

^v Arylboronic ester **17** gives two peaks in the HPLC method used (Method C): the arylboronic ester itself and the corresponding boronic acid. The peaks areas were summed where relevant to give a total peak area corresponding to compound **17**.

^{vi} 360 μL when no additional co-solvent is specified.

Entry	Base (1.4 eq)	Solvent (300 μ L) ^{vi}	Co-Solvent (60 μ L)	ee / %	Conv. / %	Deb. / %	Area% _{16,17,18}
16	KOH	Toluene	Water	91	64	35.3	65
17	K ₃ PO ₄	Toluene	Water	93	85	12.3	82
18	K ₂ CO ₃	Toluene	Water	92	87	11.3	80
19	NEt ₃	Toluene	Water	94	91	8.6	86
20	NaHCO ₃	Toluene	Water	94	87	12.3	84
21	KOH	THF	Water	95	88	8.3	76
22	K ₂ CO ₃	THF	IPA	95	95	3.9	81
23	K ₂ CO ₃	THF	Ethanol	95	94	5.7	81
24	KOH	MeTHF	Water	95	46	2.1	89
25	NEt ₃	IPA	-	97	85	14.7	75
26	NEt ₃	Ethanol	-	94	97	1.5	90
27	NEt ₃	Methanol	-	93	97	2.0	91
28	KOH	Methanol	Water	92	93	8.9	53
29	-	AcOH	-	n.d.	0.7	2.8	89
30	KOAc	AcOH	-	n.d.	0.6	12.9	85
31	-	AcOH/Water ^{vii}	-	n.d.	0.6	6.9	88
32	KOAc	AcOH/Water	-	n.d.	0.6	15.5	86
33	DIPEA	Heptane	Methanol	92	94	1.4	88
34	DIPEA	Heptane ^{viii}	Methanol	92	96	2.0	88
35	DIPEA	Heptane/MeOH/Water ^{ix}	-	89	98	0.8	90
36	KOH	ⁱ PrOAc	Water	95	93	6.4	85
37	KOH	EtOAc	Water	95	87	11.8	81
38	KOH	Anisole	Water	95	64	36.2	62
39	KOH	DMSO	Water	87	73	22.0	56
40	KOH	1-Butanol	Water	91	93	9.9	68
41	KOH	Acetone	Water	94	93	7.0	76
42	KOH	CPME	Water	95	84	15.0	76
43	KOH	Cyclopentanone	Water	94	88	11.0	73
44	KOH	Dimethyl Carbonate	Water	95	90	8.8	81
45	KOH	Propylene Carbonate	Water	96	56	43.9	62
46	KOH	Ethylene Glycol	Water	67	94	7.7	50
47	KOH	Acetonitrile	Water	92	90	8.2	78
48	KOH	MIBK	Water	94	76	22.9	72

Table 11. Comparison of different solvent and base systems. “Conv.” is peak area conversion and “Deb.” is peak area deboronation. Note that the enantiomers of the product eluted particularly closely in the chiral HPLC system (Method D1) used here, such that small *ee* variations should be interpreted cautiously.

The dioxane/water system used in Section 3.2.1 was the basis of a small base screen (Entries 1–9).⁷⁵ The enantiomeric excesses achieved were reasonably consistent, but the conversions

^{vii} 1:1 by volume for this entry and the entry below (Entries 31 and 32).

^{viii} 2-methyl-1,3-propanediol (1 eq) as an additive for this entry and the entry below (Entries 34 and 35).

^{ix} (Heptane/MeOH)/Water ratio 3(95:5):1 by volume.

of enoate **16** to the bisaryl product **18** were affected dramatically by the identity of the base. In the case where no base was added (Entry 2), conversion to the product was extremely low (7%), and very little change to the substrates was otherwise evidenced by HPLC. In general, some correlation to the pK_{aH} of the base was observed, with $KHCO_3$ (pK_{aH} 6 in water) giving 82% peak area conversion (Entry 5), K_2CO_3 (pK_{aH} 9) giving 90% conversion (Entry 4), the organic bases (pK_{aH} 11) giving greater than 95% conversion (Entries 7–9) and KOH (pK_{aH} 16) giving 92% conversion (Entry 1).¹⁶⁸ In these cases, lower conversion appeared to correspond to greater amounts of deboronation product, with the organic bases giving the lowest extents of the undesired side-reaction. Base strength also correlated with the extent to which side-reactions appeared to occur. In general, the organic bases gave the highest values for Area%_{16,17,18}.

Inspired by the report described in Section 1.3.7, in which the replacement of water with alcohol was found to be advantageous for decreasing deboronation,⁸³ a number of reactions were trialled with water replaced by ethanol or trifluoroethanol (Entries 10–14). Although small differences in the enantiomeric excesses shown in Table 11 should be interpreted cautiously, it appears to be the case that this substitution served to increase the enantiomeric excess measured when triethylamine was used as the base (98% *ee* and 97% *ee*, Entries 10 and 14 respectively, cf. 95% *ee* using an aqueous co-solvent, Entry 7); however the conversions decreased significantly from 96% to less than 50% and there was no decrease in deboronation. This effect on conversion is discussed in more detail in Section 3.2.3. When using the strong ethoxide bases, high conversions were observed and some decrease in deboronation was evidenced compared with using aqueous inorganic bases, but this did not come with the benefit of increased enantioselectivity (Entries 11 and 12). Again, the values for Area%_{16,17,18} were found to decrease with the use of strong base. Attempting an analogous reaction with methanol as the co-solvent gave significant levels of transesterification, which accounts for the low value for Area%_{16,17,18} shown in Entry 15. This was similarly seen in the methanol/water/KOH solvent/base system (Entry 28).

The solvent systems most resembling those used successfully in the report in which alcohol was substituted for water are those with THF as the major solvent (Entries 21–23). Compared with the case using water as the co-solvent (Entry 21), replacement with alcohol did increase conversion and decrease deboronation (Entry 22 and 23) however the effects were reasonably small (< 8 percentage points difference for conversion, < 5 percentage points difference for deboronation) and different bases were used in these reactions. Curiously, replacement of THF with MeTHF gave very low conversion of the enoate to the

bisaryl product, and incomplete consumption of the arylboron reagent was observed. This suggests that transmetalation was slowed significantly in this case (Entry 24). Assuming that the transmetalation occurs to a rhodium species with one solvent molecule ligated to it, it could be speculated that the methyl group of MeTHF serves to block the site for transmetalation (see also Section 3.3.3.1).

The reactions using toluene as the solvent were based on literature precedent,¹⁶⁹ and generally performed unremarkably (Entries 16–20). Use of potassium hydroxide as the base gave significant levels of deboronation (Entry 16), which was also seen when the reactions were performed in anisole (Entry 38). This propensity of aromatic solvent towards increased levels of deboronation was reflected in the weaker bases also used with toluene, although to a lesser extent. A comparison of the performance of ethanol, toluene and dioxane is given in Figure 23, with the data displayed as an average of reactions using tripotassium phosphate and sodium hydrogen carbonate.

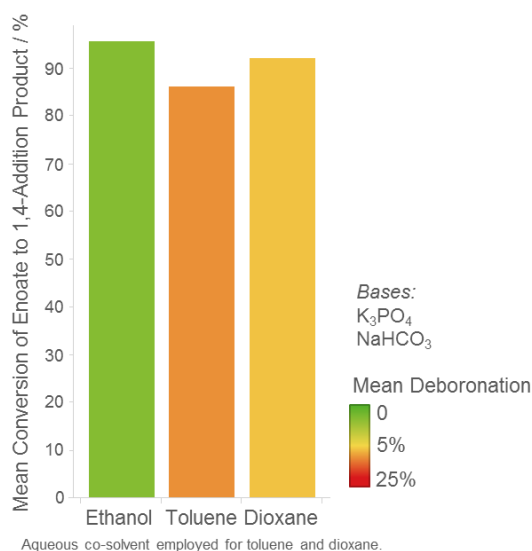


Figure 23. A display of data from Table 11 and Table 12 (below), comparing the peak area percent conversion and deboronation when performing the reaction in ethanol, toluene and dioxane, averaged over the reactions using tripotassium phosphate and sodium bicarbonate as the base.

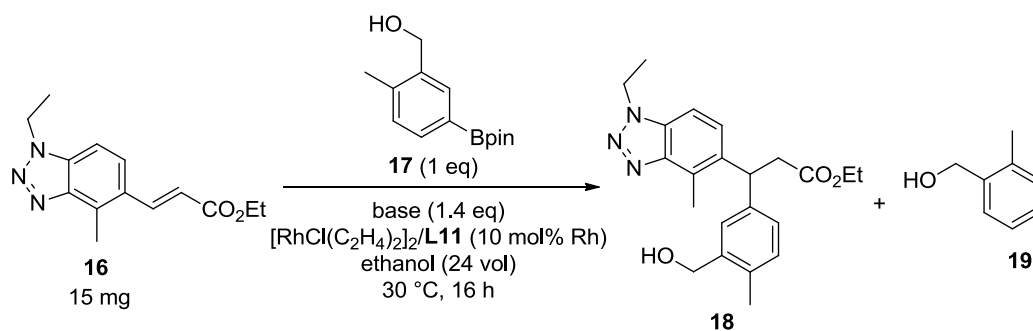
The three reactions including heptane as a solvent were inspired by a report which found the combination of heptane, methanol and water with the diol additive (2-methyl-1,3-propanediol) to give improved conversion and ultimately to allow lower catalyst loading (Entries 33–35).¹⁴⁴ The entries show improved conversion with the stoichiometric additive (Entry 34, cf. Entry 33) and improved conversion again with the precise solvent system used in the literature report (Entry 35). The enantioselectivity delivered in these cases was lower than other more compelling solvent and base systems in this investigation however.

The last thirteen entries were selected as a broad range of greener solvents across a number of solvent families (Entries 36–48). Isopropyl acetate performed well, although none of the solvents stood out as particularly attractive for further investigation. Anisole, DMSO, MIBK and especially propylene carbonate gave particularly poor selectivity for the desired reaction over deboration.

Four reactions were attempted under acidic conditions, using acetic acid in the solvent system (Entries 29–32). In agreement with the literature precedent for the rhodium-catalysed 1,4-addition reactions being successful under basic conditions, no more than trace conversion to the product was seen under these conditions. Interestingly, the deboration reaction proceeded in all cases, particularly in the presence of potassium acetate. It is unclear whether or not this was via a rhodium-mediated mechanism.

The most compelling solvent systems identified by this set of reactions were those employing alcohol as the solvent, without any other co-solvent (Entries 25–27). Generally, a protic co-solvent is required to provide a proton for the catalytic cycle to complete (Section 1.3.2), but if the major solvent can be protic whilst still enabling adequate catalyst turnover and good conversion to the desired enantiomer of the conjugate arylation product, then the solvent system can be simplified significantly. Using IPA gave excellent enantioselectivity, but the conversion was limited by significant deboration (Entry 25). Methanol and ethanol gave both good enantiomeric excesses and conversions of the enoate **16** to the bisaryl product **18**. Combined with the green chemistry credentials associated with ethanol,¹⁴² the use of ethanol was also attractive with respect to avoiding any risk of transesterification of the enoate or the bisaryl product. Furthermore, the API synthesis used before this work involved storing the 1,4-addition product (*S*)-**18** as a solution in ethanol. Using ethanol as the reaction solvent for the new 1,4-addition reaction process would therefore minimise the further work required for adoption on scale.

To further investigate the use of ethanol as a solvent in combination with a variety of bases, a second set of reactions was performed (Table 12). A visual display of the data comparing Entries 6–21 is provided in Figure 24 (page 88).



Entry	$\text{p}K_{\text{aH}}$	Base (1.4 eq)	Ethanol (360 μL)	Conversion / %	Deboronation / %	Area% _{16,17,18}
1	10.77	NEt_3	Ethanol (anhydrous)	87	1.6	89
2	10.77	NEt_3	IMS	94	1.7	92
3	10.77	NEt_3	Ethanol (not degassed)	88	1.7	93
4	10.77	NEt_3	Ethanol/Water ^x	98	2.9	91
5	10.77	NEt_3	Ethanol (air-sparged) ^{xi}	80	1.9	93
6	10.77	NEt_3	Ethanol	91	1.7	92
7	10.75	DIPEA	Ethanol	96	1.0	92
8	11.05	${}^i\text{Pr}_2\text{NH}$	Ethanol	98	1.0	88
9	5.17	Pyridine	Ethanol	0	0.0	88
10	8.4	DABCO	Ethanol	34	25.3	80
11	5.97	2-Picoline	Ethanol	1	0.0	98
12	6.02	4-Picoline	Ethanol	0	0.0	88
13	10.98	NHEt_2	Ethanol	70	2.7	91
14	7.3	TDA-1	Ethanol	54	1.2	95
15	13.5	DBN	Ethanol	3	9.1	76
16	4.76	KOAc	Ethanol	68	19.2	80
17	5.95	NaHCO_3	Ethanol	94	1.0	91
18	9.1	K_2CO_3	Ethanol	96	4.1	83
19	5.95	KHCO_3	Ethanol	96	1.4	90
20	11.74	K_3PO_4	Ethanol	97	2.2	85
21	9.1	Na_2CO_3	Ethanol	96	1.2	90

Table 12. A comparison of solvent and base effects with ethanol as the primary solvent of interest. Data is as described for Table 11. $\text{p}K_{\text{aH}}$ values are given according to literature data.¹⁶⁸

The first six entries compare different solvents or differently prepared solvents. Entries 1, 4 and 6 were intended to give an indication of the importance of water in the reaction, since the literature investigations have highlighted the importance of forming a hydroxorhodium species (Section 1.3.2). The first entry used commercially anhydrous ethanol, the sixth used standard-grade ethanol and the fourth used a 50/50 mixture of ethanol/water. An increase in conversion of enoate **16** to bisaryl **18** was seen in this order, however it was subsequently discovered by Karl Fischer analysis that both the anhydrous ethanol and the standard-grade

^x 1:1 by volume.

^{xi} Ethanol was sparged with compressed air before dissolution of solid reagents.

ethanol contained similar levels of water. Although the nitrogen line used to sparge the solvents contained in-line silica to remove water vapour from the nitrogen source, the anhydrous ethanol was found to increase from 0.015 wt% water to 0.4 wt% water after employing this degassing technique. The standard-grade ethanol was measured to have 0.3 wt% water after sparging with nitrogen. Nevertheless, a difference was certainly seen between the two reactions run using ethanol (Entries 1 and 6), and the reaction using 1:1 ethanol/water (Entry 4). The industrial methylated spirits (IMS, 1.7 wt% water, Entry 2) also gave greater conversion than the ethanol with a lower water content.

The third and fifth entries used the same ethanol as Entry 6, but these were either not degassed (Entry 3) or were sparged with compressed air (Entry 5), with a view to gaining an appreciation for the air-sensitivity of the system. A decrease in conversion was seen from degassed ethanol (Entry 6), to non-degassed ethanol (Entry 3), to air-sparged ethanol (Entry 5), however the reaction was not significantly inhibited even in this latter case. It was also considered possible that the non-degassed ethanol may have performed less well than the degassed ethanol in part due to having a slightly lower water content, since it was not sparged with wet nitrogen.

The remaining entries, displayed visually in Figure 24, compare different bases with degassed standard-grade ethanol as the solvent. Both inorganic and organic bases were selected across a wide range of pK_{aH} values with consideration for their green chemistry attributes.¹⁶⁸ In general, no clear trend was observed between pK_{aH} and Area%_{16,17,18}, conversion or deboration. Nevertheless, significant differences were found. Perhaps most strikingly, the pyridine bases (pyridine, 2-picoline and 4-picoline) did not enable any conversion above trace levels, and similarly no deboration occurred (Entries 9, 11, 12). The implication is that transmetalation was inhibited, potentially by poisoning the catalyst. It has been suggested in the literature that a substrate bearing pyridine-functionality has prevented a 1,4-addition reaction from occurring (Section 1.3.7).⁸³ If this is the case here, it is interesting that the triazole of the enoate **16** does not similarly prevent the desired reaction. This is explored in Section 3.3.1.3.

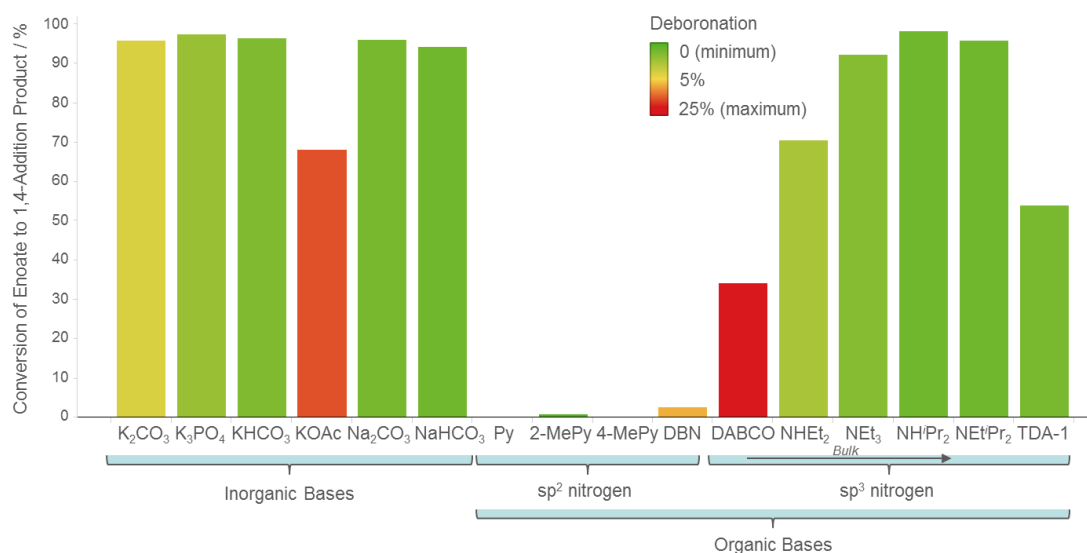
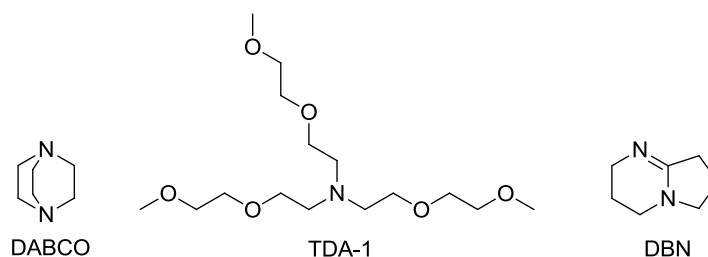


Figure 24. A visual display of the data from Entries 6–21 of Table 12 (above).

Trace conversion and very low conversion were also seen with DBN and DABCO, however in these cases significant levels of deboronation were also observed (Entries 15 and 10). As with the pyridine bases, DBN possesses an sp²-hybridised nitrogen in a ring. DABCO has sp³-hybridised nitrogens, however its tethered structure leaves the nitrogen lone pairs largely unhindered, such that it could be an excellent ligand for coordination to rhodium. TDA-1 (tris[2-(2-methoxyethoxy)ethyl]amine) consists of a tertiary amine with six ether groups, and whilst predominantly used as a phase-transfer catalyst, it has also found utility in complexing to Grignard reagents.¹⁷⁰ It would not be implausible to suggest that it chelates to rhodium (I), and that this is the cause of the low conversion observed here (Entry 14). In general, it appears that nitrogen-containing bases with a good ability to ligate to the rhodium centre act to prevent or significantly inhibit the desired 1,4-addition reaction.



The remaining organic bases enabled vastly improved reactivity, with a rough correlation observed between bulk and conversion. Triethylamine (TEA, NEt₃), di-*iso*-propylethylamine (DIPEA, NEtⁱPr₂), di-*iso*-propylamine (DIPA, ⁱPr₂NH) and diethylamine (NHEt₂) all have pK_{aH} values around 11, but the peak area conversions observed to the desired 1,4-addition product increased from diethylamine (70%, Entry 13) to triethylamine (91%, Entry 6) to di-*iso*-propylamine and di-*iso*-propylethylamine (> 95%, Entries 8 and 7). The origin of this

trend may also be found in the decreasing ability of the bases to ligate the rhodium complex with increasing bulk.

The inorganic bases performed universally well with the exception of potassium acetate, which was the weakest base employed in these reactions (Entries 16–21). In general they afforded the desired product in high conversions, although the reactions gave lower values for Area%_{16,17,18} than the better organic bases. Additionally, there are notable disadvantages for increasing the scale of a heterogeneous reaction rather than a homogeneous reaction, since the nature of the stirring is far more important in the former. This can lead to difficulties when the scale of a heterogeneous reaction is increased and performed in different reactor vessels, due to mass transfer effects. From this perspective, the inorganic bases were therefore less attractive for use in the developed process than the organic bases were.

The rates of the rhodium-catalysed reactions using a selection of the bases were compared using the conditions shown in Figure 25, with relative HPLC response factors used to determine the reaction compositions as for the later Section 3.3.2.2. Di-*iso*-propylethylamine and triethylamine were compared with the inorganic potassium salts, potassium hydroxide, potassium carbonate, and potassium hydrogen carbonate.

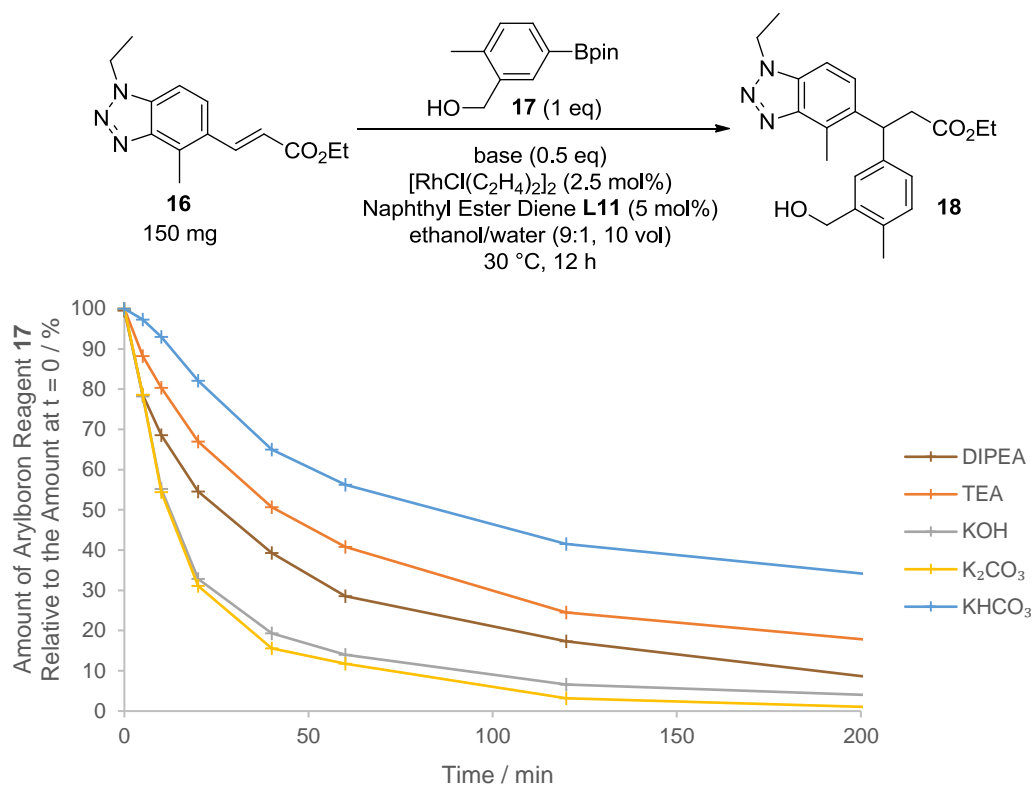
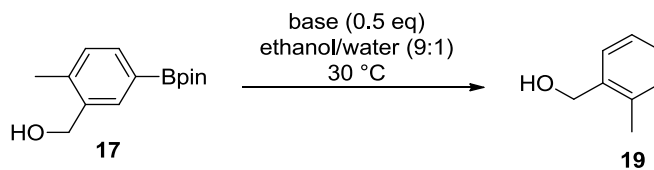


Figure 25. Consumption of arylboron reagent 17 over time for a selection of bases. The profile for the consumption of enoate is very similar.

As anticipated from Section 1.3.2.2, the inorganic bases resulted in the fastest reactions, except potassium hydrogen carbonate, which, with the lowest pK_{aH} , gave the slowest reaction. Aside from this, no significant trend was observed based on the strength of the base in contrast to that discussed in Section 1.3.2.2. Both di-*iso*-propylethylamine (DIPEA) and triethylamine (TEA) gave slower reactions than the inorganic bases (excluding potassium hydrogen carbonate), with the less bulky base (triethylamine) being the slower of the two. This is consistent with the data displayed in Table 12 and Figure 24, and with the suggestion that the less bulky amine bases can coordinate more readily to the rhodium centre to give a catalytically inactive species.

The selectivity of the systems for conjugate arylation over protodeboronation was generally very good. The organic bases gave the highest selectivities (both 97:3 molar ratio of conjugate arylation product to protodeboronation product), with potassium hydroxide and potassium hydrogen carbonate also performing reasonably well (92:8 and 90:10 respectively). Curiously, potassium carbonate gave the lowest selectivity (83:17), which is also consistent with the data in Table 12 and Figure 24. To probe whether or not these differences could be explained by a purely base-mediated protodeboronation, arylboron reagent **17** was treated with di-*iso*-propylethylamine, potassium hydroxide and potassium

carbonate (0.5 equivalents) in the same volume of ethanol/water as for Figure 25 (Scheme 39).



Scheme 39. Experiments to observe the relative extents of any base-mediated protodeboronation using DIPEA, KOH and K₂CO₃. The total reaction volume here is the same as for Figure 25.

Di-*iso*-propylethylamine gave undetectable levels of *o*-tolylmethanol over 72 hours, whereas the deboronation product was evident within 24 hours using the inorganic bases. Quantitative analysis of the experiment was limited by an unknown species generated in the reactions with the inorganic bases, but the results nevertheless showed that a purely base-mediated deboronation mechanism was insufficient to account for the differences observed in Figure 25 either between di-*iso*-propylethylamine and potassium hydroxide or between potassium hydroxide and potassium carbonate. Whereas the experiments using rhodium gave 1%, 6% and 14% conversions to *o*-tolylmethanol within 1 hour using di-*iso*-propylethylamine, potassium hydroxide and potassium carbonate respectively (Figure 25), in the absence of rhodium there were no detectable levels of the protodeboronation product using any of the bases at this timepoint (Scheme 39). Neither can a difference in the turnover frequencies of the catalyst with the different bases account for the different levels of deboronation, since 34%, 24% and 29% residual enoate **16** was observed at 1 hour for each of di-*iso*-propylethylamine, potassium hydroxide and potassium carbonate respectively in the rhodium-catalysed reactions. It must be that a more complex mechanism is responsible for the difference between potassium carbonate and potassium hydroxide, which does not depend only on the identity of the base.

Considering the advantages of a homogeneous reaction mixture combined with the conversion of enoate **16** to bisaryl **18** and the extent of protodeboronation, di-*iso*-propylethylamine was selected as the base to be used for further investigations, along with ethanol as the primary solvent.

3.2.3 Analysis of Continuous Variables for the Pharmaceutically-Relevant Conjugate Arylation

With the discrete variables for the reaction selected, the continuous variables were firstly explored using a statistical Design of Experiment (DoE) approach. This enabled an understand to be built of which variables required controlling to maximise a desirable effect

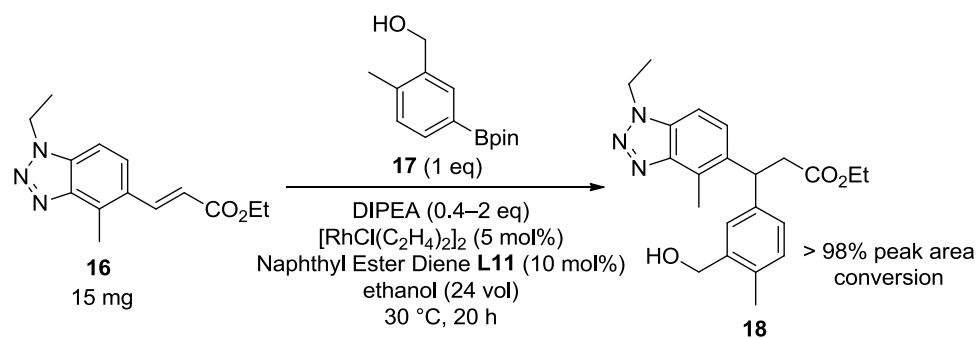
or minimise an undesirable effect, and which did not affect the reaction.^{171,172} Based on observations from Sections 3.2.1 and 3.2.2, six factors were selected for investigation over ranges decided with consideration for what would be acceptable on scale: solvent volumes (10–50 volumes), precatalyst/ligand loading (1–8 mol%), temperature (10–50 °C), added water content (0–20% of total solvent volumes), equivalents of arylboronic ester (1–1.5 equivalents) and equivalents of DIPEA (0.5–2.5 equivalents). Three responses were to be measured to assess these factors: conversion of enoate **16** to 1,4-addition product **18**, selectivity for the 1,4-addition over deboronation, and the enantiopurity of the product **18**.

The form of Design of Experiment used was designed for factor-screening rather than optimisation. The value of a factor-screening DoE is that the significant factors affecting a particular response can be identified efficiently, but its key limitation is its inability to model significant curvature within a response. For example, it could be that a lower limit of 10 °C gives 30% conversion for a particular reaction, a centre-point of 30 °C gives 100% conversion and an upper limit of 50 °C gives 80% conversion. The statistical analysis would be able to correctly identify increasing temperature from 10 °C to 50 °C as having a positive effect on conversion, but it would not be able to sufficiently account for the centre-point giving 100% conversion in the model that it creates. This method is adequate for the purposes here, where identification of the key factors affecting the three responses over the ranges studied is required rather than an accurate model of the process space.

3.2.3.1 Preliminary Experiments for a Design of Experiment Analysis

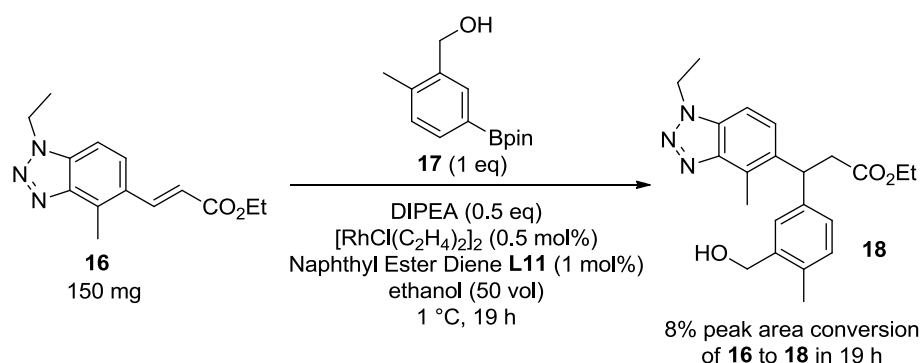
Before the DoE could be performed, it was important to ensure that the combined upper and lower limits selected for each factor would both give conversion and to varying extents. It was also important that there was no sudden discrete change at a certain level of any factor, such as might be observed if, for example, some of the reaction mixtures are not in solution under the combination of conditions or if the conversion falls suddenly below one equivalent of base. Therefore, a number of preliminary experiments were performed to confirm the suitability of the ranges chosen for the DoE experiments.

Firstly, experiments were performed with varying equivalents of DIPEA (Scheme 40), using 0.4, 0.7, 1.0, 1.4 and 2.0 equivalents of base relative to enoate **16**. The HPLC traces showed no significant variation across this range of conditions at all, with a peak area conversion of > 98% (enoate **16** to 1,4-addition product **18**, 210 nm) observed in each case. Furthermore, very little difference was seen when ethanol was replaced with 1:1 ethanol/water.



Scheme 40. Reactions to observe any differences in peak area conversion over a range of equivalents of DIPEA.

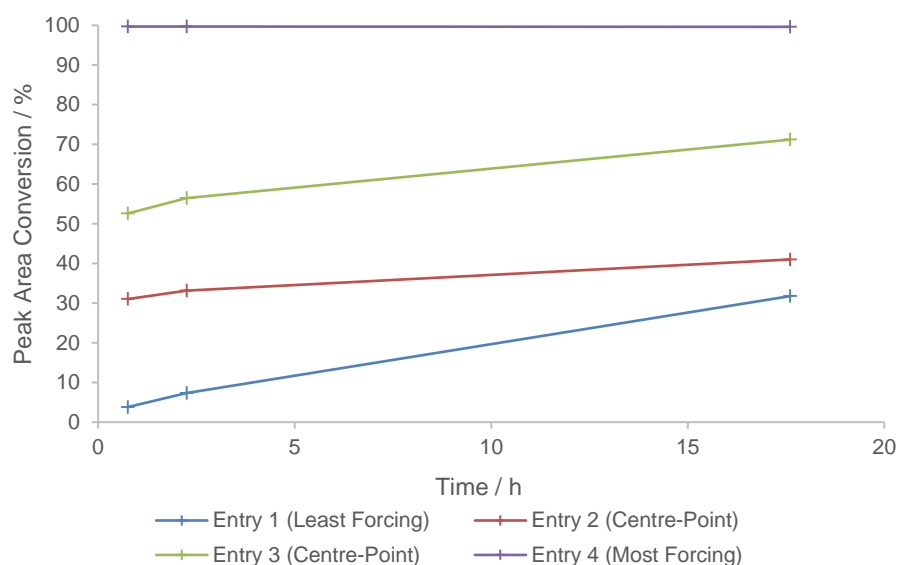
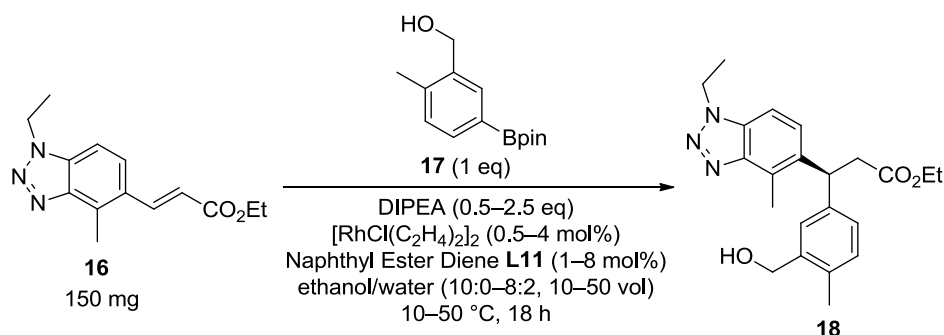
The lower limits originally planned for the DoE were then tested, specifically the combination of one equivalent of arylboronic ester, 1 mol% rhodium and ligand, 0.5 equivalents of DIPEA, 50 volumes of ethanol with no water, and a temperature of 1 °C. This reaction proceeded adequately, with around 8% peak area conversion (210 nm) of enoate to 1,4-addition product observed in 19 hours (Scheme 41). However, it was subsequently noticed that complete solubility was not achieved when the low temperature condition was combined with the high concentration (4 volumes) originally intended to be the upper limit. As such, the low temperature was revised to 10 °C and the most concentrated condition revised to 10 volumes, which enabled complete dissolution with up to 20% of the total solvent volumes being water.



Scheme 41. Trial reaction to determine the suitability of potential lower limits of the reaction for the Design of Experiment.

The combined lower and upper limits of the DoE (the “least forcing” and “most forcing” conditions respectively) were then tested along with two centre-point experiments in the STEM Integrity 10 Reaction Station to be used in the DoE and prepared in the manner intended for the DoE (Table 13). The enantiopurity was determined after achiral purification of the product, since transfer of the chiral HPLC method to a different instrument had enabled baseline separation of the enantiomers of the product to be achieved at the expense

of baseline separation between the later-running minor enantiomer, the enoate and the ligand.



Entry	Catalyst Loading / mol% Rh	ArBpin 17 Equivalents	DIPEA Equivalents	Total Volumes / vol	Water Content / % of Total Volumes	Temp. / °C	ee / %
1	1.0	1.0	0.5	50	0	10	n.d.
2	4.5	1.25	1.5	30	10	30	n.d.
3	4.5	1.25	1.5	30	10	30	97
4	8.0	1.5	2.5	10	20	50	96

Table 13. Testing of the lower and upper limits of the planned DoE with two centre-points. Note that the catalyst precursor and ligand were added in 1:1 Rh/ligand stoichiometry. Peak area conversions determined as for Table 12. Enantiomeric excesses determined using the same chiral method as used previously, but installed on a different instrument. Time = 0 when reaction mixtures placed in Integrity 10 Reaction Station.

The results showed that the planned ranges were suitable for the DoE, although significant variability was indicated by the large discrepancy between the conversions of enoate **16** to bisaryl **18** in the two centre-point reactions. A number of possible aspects of the preparation may have contributed to this. Firstly, all of the solids, including the small amounts of the rhodium complex, were weighed directly into the much heavier and awkwardly shaped reaction tubes, potentially giving errors in the masses dispensed. Secondly, after dispensing the solids into the tubes, the tubes were sparged with a nitrogen flow before addition of

solvent to try to ensure an inert atmosphere; however there would have been a risk that the solids may have been displaced from the volume of the tubes in which the reaction would occur. Thirdly, DIPEA was added before the tubes were either brought to temperature or degassed by nitrogen/vacuum cycles.

Each of these aspects of the preparation was revised for the DoE: (1) all of the solids were weighed into appropriate weighing boats and the boats re-weighed after transferring the contents to the reaction vessels, (2) the tubes were not sparged with nitrogen when containing solids and instead the tubes were cycled through three nitrogen/vacuum cycles on the Integrity 10 Reaction Station immediately after addition of the degassed solvent(s), (3) DIPEA was added after the mixtures had been allowed to reach temperature for 40 minutes, and addition of DIPEA marked the start of the reaction time. To ensure that this last aspect of the preparation would be suitable, the conditions from Entry 4 (Table 13) were repeated, but with the base added after the rest of the reaction mixture had been at 50 °C for 1 hour. Sampling the mixture after 1 hour at 50 °C and before addition of base revealed no conversion to the product and no observable deterioration of the substrates. Within 5 minutes of adding the base, the reaction was virtually complete.

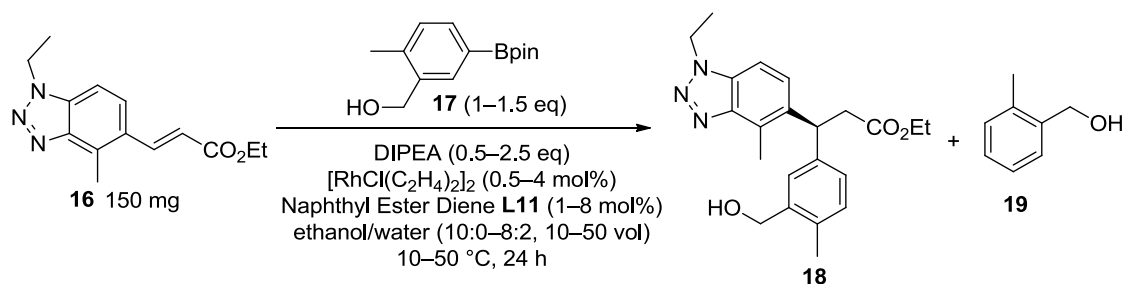
3.2.3.2 Factorial Design of Experiment

One of the main attractions of a Design of Experiment approach to understanding important factors in a reaction is that the statistical analysis enables far fewer experiments to be performed than every combination would require.^{173,174} In the case of varying six factors in a factor-screening DoE, the complete set of experiments (the full factorial “white design”) would be 2^6 , i.e. 64 experiments not including centre-points to validate the data. In principle however, the statistical analysis could enable this number to be decreased to as few as 8 experiments (a “red design”). The danger of decreasing to such a low number is that factors can be aliased with each other when the analysis deconvolutes the results to identify which factors are significant in contributing to a certain response. In this case, factors can be aliased with two-factor interactions, which are not uncommon. For example, it could be that either temperature or a combination of equivalents of arylboronic ester with percentage of water has a significant effect on the rate of the reaction, but which of these it is would not be able to be definitively extracted from the data. In certain circumstances, it might be that the two-factor interaction aliased with a single-factor can be ruled out either on chemical grounds or if the factors contained in the two-factor interaction do not show an influence on their own.

Since it was intended to use an Integrity 10 Reaction Station for this DoE, the maximum number of experiments able to be run in one “block” would be 10. Correspondingly, performing a red design would also require 10 experiments: eight combinations of the upper and lower limits of the six factors with two centre-point experiments. The next fewest number of experiments for a factor-screening DoE with seven factors would constitute a “yellow design” involving 16 experiments. The advantage of the yellow design is that single-factor interactions are only aliased with multi-factor interactions involving no fewer than three factors each, which are much more readily disregarded than two-factor interactions are. However, since the yellow design would need to be run in two blocks due to the number of wells in an Integrity 10 Reaction Station, each block containing two centre-points, there was no advantage to starting with a yellow design. Instead, a red design was used with the knowledge that this could be augmented into a yellow design (“foldover”) if aliasing was found to be a problem and a greater bank of data was required. Therefore, just 10 reactions were performed initially for this investigation. Analysis of the results revealed that a foldover to a yellow design was required, and so an additional ten experiments were subsequently performed. The results of the DoE, showing analysis from both the red and the yellow designs for comparison, are presented in Section 3.2.3.3.

3.2.3.3 Results and Analysis of the Factorial Design of Experiment

Table 14 summarises the conditions for the reactions run in the initial red design and in the foldover, and Table 15 presents an overview of the results. The reactions were run as two blocks in an Integrity 10 Reaction Station, with the reaction-well temperatures set in advance to those shown in Table 14. The reactions were prepared as described in Section 3.2.3.1, and sampled at 1 hour, 3 hours and 19 hours. For each reaction mixture, the volume sampled was such that it would contain 1 mg of enoate **16** for a scenario in which no reaction had occurred, and this sample was diluted with 1 mL of a 1.02 mg mL⁻¹ solution of mesitylene in ethanol. The relative absorbances at 215 nm had been calculated for the enoate **16**, the desired 1,4-addition product **18** and the deboronated side product **19** with respect to mesitylene.



Run	A:	B:	C:	D:	E:	F:
	Total Volumes / vol 10–50	Water / %v/v of Solvent 0–20	Temp. / °C 10–50	ArBpin Equivalents 1–1.5	Base Equivalents 0.5–2.5	Rhodium Loading / mol% 1–8
1	10	0	50	1.5	0.5	1
2	30	10	30	1.25	1.5	4.5
3	10	20	50	1	0.5	8
4	10	0	10	1.5	2.5	8
5	50	20	50	1.5	2.5	8
6	50	20	10	1.5	0.5	1
7	30	10	30	1.25	1.5	4.5
8	50	0	10	1	0.5	8
9	50	0	50	1	2.5	1
10	10	20	10	1	2.5	1
11	50	20	50	1	0.5	1
12	10	0	10	1	0.5	1
13	10	20	10	1.5	0.5	8
14	50	20	10	1	2.5	8
15	50	0	50	1.5	0.5	8
16	10	20	50	1.5	2.5	1
17	30	10	30	1.25	1.5	4.5
18	50	0	10	1.5	2.5	1
19	10	0	50	1	2.5	8
20	30	10	30	1.25	1.5	4.5

Table 14. The conditions of the reaction mixtures run for the DoE experiment. The conditions are shown such that the lower limits are highlighted blue, the upper limits are highlighted red, and centre-points are highlighted green.

To avoid errors caused by sampling and diluent volumes with the use of an external standard, the molar conversion of the enoate **16** to the desired 1,4-addition product **18** was calculated in each case, rather than the apparent solution yield. To provide a measure for the selectivity of the reaction, the relative molar amounts of undesired deboronated product **19** and desired 1,4-addition product **18** were compared, and the data is presented in Table 15 as the percentage of these two products accounted for by the desired product. The relative molar amounts of species **16**, **18** and **19** were determined using HPLC response factors (Equation 8, page 220).

The enantiopurity of the desired product was measured after 24 hours using a chiral HPLC that gave excellent baseline separation between the two enantiomers and very low noise, allowing the enantiomeric excesses to be determined to high precision. Before chiral analysis, a portion of each reaction mixture was purified by column chromatography.

Run	Conversion / %			Selectivity of Reaction / %			ee / %
	1 h	3 h	19 h	1 h	3 h	19 h	
1	49.3	79.7	97.5	98.2	97.9	84.4	93.4
2	98.5	100	100	90.7	83.4	82.8	94.4
3	90.7	90.3	90.5	92.2	92.0	92.1	93.1
4	11.2	29.6	74.3	89.1	94.9	97.7	96.6
5	96.6	96.7	98.5	67.6	67.4	67.8	93.2
6	2.9	6.2	13.4	77.4	79.6	85.8	95.1
7	97.8	99.4	100	91.2	84.4	84.1	94.5
8	11.9	24.7	50.4	90.1	93.0	94.4	96.4
9	33.3	52.3	68.2	96.0	95.7	93.3	92.8
10	7.2	18.4	70.1	85.7	91.2	94.3	94.7
11	90.9	92.2	92.6	94.1	93.7	93.6	92.3
12	2.6	6.4	18.6	100	87.0	95.2	96.3
13	41.5	77.5	100	95.8	94.9	86.0	95.6
14	56.1	87.5	88.5	92.0	91.9	91.3	95.2
15	99.0	100	100	88.2	77.9	71.2	93.5
16	98.3	98.6	98.6	85.8	77.4	70.1	92.3
17	98.1	100	100	90.5	84.6	83.2	94.4
18	2.3	4.7	14.8	62.3	74.7	89.8	96.1
19	83.7	93.8	94.6	96.7	95.9	95.8	94.9
20	98.5	100	100	90.1	83.4	82.2	94.3

Table 15. Summary of results for the reaction mixtures used in the DoE experiment. The results are shown such that large values are highlighted green and low values are highlighted red.

The data was analysed in Design-Expert 10 software. Where appropriate, mathematical transformations were applied to the responses, and half-normal plots were used to assess the significance of factors to include in the model. In general, terms with p-values < 0.05 in the analysis of variance (ANOVA) tables for the statistical models were considered statistically significant and included in the models.

3.2.3.3.1 Conversion of the Pharmaceutically-Relevant Enoate to the Bisaryl Product

Takings samples of the reactions at 1 hour, 3 hours and 19 hours provided an understanding of factors that affect the rate of the reaction as well as those that affect the overall outcome. Table 16 presents an overview of the significant factors extracted by the statistical analysis used in Design-Expert 10.

	Timepoint	Response Range	Significant Factors (p-value)
Red	1 h	2.9–98.5%	{Temp <i>or</i> Water + Catalyst Loading} ↑ (< 0.0001) > {Catalyst Loading <i>or</i> Temp + Water} ↑ (0.0007) > {Water <i>or</i> Temp + Catalyst Loading} ↑ (0.0021)
	3 h	6.2–100%	Temp ↑ (0.0001) > Catalyst Loading ↑ (0.0215)
	19 h	13.4–100%	Temp ↑ (0.0387)
Yellow	1 h	2.3–99.0%	Temp ↑ (< 0.0001) > Catalyst Loading ↑ (< 0.0001) > Water ↑ (< 0.0001)
	3 h	4.7–100%	Temp ↑ (< 0.0001) > Catalyst Loading ↑ (< 0.0001) > Water ↑ (0.0007) > Temp + Catalyst Loading ↓ (0.0075)
	19 h	13.4–100%	Temp ↑ (0.0001) > Catalyst Loading ↑ (0.0046) > Water ↑ (0.0296) > Temp + Catalyst Loading ↓ (0.0500)

Table 16. Significant factors affecting conversion as determined by statistical analysis. The conclusions from both the red and yellow designs are included for comparison. ↑ indicates a positive effect on the response, whilst ↓ indicates a negative effect.

These results demonstrate clearly the different quality of analysis enabled by the red and yellow DoE designs. Particularly looking at the red design at the 1-hour timepoint, the significant factors could either be temperature, catalyst loading and an interaction between temperature and catalyst loading, or they could be temperature, an interaction between temperature and water content, and water content, or they could be an interaction between water content and catalyst loading, catalyst loading and water content, or they could be temperature, catalyst loading and water. The yellow design enables the last of these options to be identified unambiguously as the list of significant factors. The half-normal plot is shown in Figure 26, in which factors further to the right had a more significant effect.

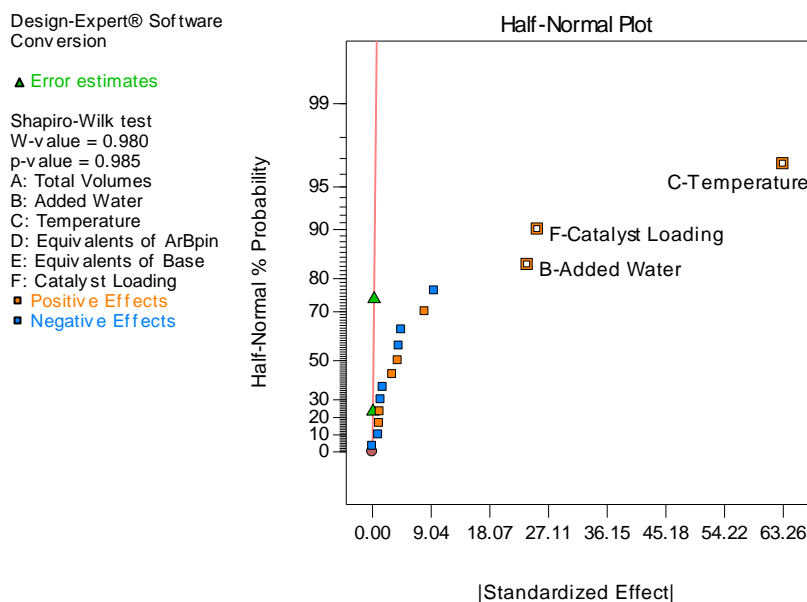


Figure 26. Half-normal plot for the 1-hour conversion data.

A further advantage of the yellow design is drawn out at the 19-hour timepoint, where there is an insufficient data set to extract the significant factors in the red design. On its own this could at first appear to be an encouraging result since it seems to indicate that none of the factors ultimately affect conversion significantly over the ranges studied. However, looking at the raw conversion data shows otherwise, and this is reflected in the data from the yellow design.

From a sustainability perspective, looking to decrease the loading of the expensive and scarce resource, rhodium, it is encouraging that temperature plays a more significant role in conversion than the catalyst loading does over the ranges studied in the DoE experiments, showing that a low rhodium loading can be readily offset by a higher temperature. This is demonstrated in Runs 1, 11 and 16, and the offset is reflected by the third most significant factor being a negative interaction between temperature and catalyst loading whereby higher temperature results in catalyst loading having less of an effect on conversion and vice versa.

The importance of water both in the initial (1 hour-averaged) rate and the overall conversion is exemplified by comparing Runs 9 and 11, with the former (0% water) progressing slowly from 33% to 68% conversion between 1 hour and 19 hours, and the latter (20% water) virtually complete after 1 hour. This may reflect a requirement to form a hydroxorhodium species for generating an effective active catalyst. A published study of the importance of water in systems using alcohol solvent has not been found.

It is interesting and encouraging that the arylboronic ester loading and the equivalents of base do not seem to have a significant effect on the conversion or even on the initial rate. This is not to say that the other factors definitely do not have any effect. For example, comparing Runs 1 and 9 suggests that solvent volumes or arylboronic ester equivalents could have some effect. Nevertheless, it provides a useful means to identify the factors that are most critical to control in designing a successful process, and it provides confidence that the arylboronic ester loading and even catalyst loading will be able to be lowered by control of the more significant factors.

3.2.3.3.2 Selectivity for the Conjugate Arylation over Deboronation

To probe any effects on the selectivity for the desired conjugate arylation reaction over the competing deboronation reaction, the amount of 1,4-addition product **18** as a percentage of the total amount of the two known products (i.e. the desired 1,4-addition product **18** and the undesired deboronation product **19**) was calculated. In this case, the analysis had to be interpreted carefully, since the equivalents of arylboronic ester was one of the factors in the DoE. If an excess of arylboronic ester is used and deboronation does not occur until after the enoate is fully consumed, the actual selectivity for the desired reaction is 100% in principle. However, the calculation used here will decrease the apparent selectivity, affecting the interpretation of the results. The true selectivity at the 1-hour timepoint should be reasonably well reflected in the calculation, but it should be anticipated that this will be much less the case for the later timepoints.

The significant factors extracted by the statistical analysis are presented in Table 17. The identification of the arylboronic ester equivalents as a significant factor at each timepoint should be largely ignored since this is an artefact of the calculation used to prepare the data. Also, for the 19-hour data, the limitations of the calculation are too significant since many of the reactions had reached completion by this point. This is evidenced by temperature and added water not being significant factors at the 1-hour timepoint but becoming significant at 19 hours. These same factors were found to increase conversion of the enoate **16** to the desired product **18**; temperature at least would increase the rates both of transmetalation and of any non-rhodium mediated deboronation. The fact that they become significant at 19 hours only reflects the fact that in many cases the enoate has been fully or nearly fully consumed by this point. This timepoint is therefore not discussed here.

Timepoint	Response Range	Significant Factors (p-value)
1 h	62.3–100%	ArBpin eq ↓ (0.0004) > Total Volumes ↓ (0.0008) > Volumes + ArBpin ↓ (0.0014) > Base eq ↓ (0.0041) > Base + ArBpin ↓ (0.0159)
3 h	67.4–97.9%	ArBpin eq ↓ (0.0030) > Volumes + ArBpin ↓ (0.0036) > Total Volumes ↓ (0.0173)
19 h	67.8–97.7%	ArBpin eq ↓ (< 0.0001) > Temp ↓ (0.0004) > Temp + ArBpin ↓ (0.0004) > Added Water ↓ (0.0114) ^{xii}

Table 17. Significant factors affecting the calculated selectivity for the desired reaction over deboronation (yellow design only).

The most informative results are provided by the 1-hour timepoint, when the limitations of the calculation have their smallest effect. Interestingly, the total solvent volumes and the base were identified as significant factors, along with their interactions with the equivalents of arylboronic ester. The half-normal plot is shown in Figure 27. Added water is ranked as the seventh factor, and is statistically insignificant.

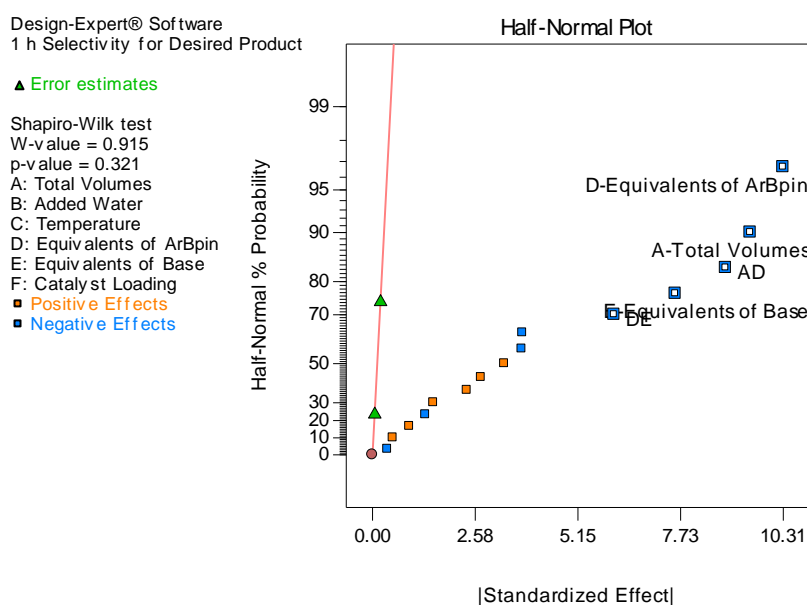


Figure 27. Half-normal plot for the 1-hour selectivity data.

The negative effect of solvent volumes on the selectivity of the reaction is readily rationalised by the fact that protodeboronation is dependent on just one non-solvent species (either the arylboron species or an arylrhodium species) whereas the desired reaction is dependent on two non-solvent species (an arylrhodium species and the enoate). Decreasing the concentration of the reaction mixture therefore slows the desired reaction by more than

^{xii} Additional factors can also be found to have $p < 0.05$ at 19 h however they were much less significant than those tabulated. If they are all included, the factor list would be: ArBpin eq ↓ (< 0.0001) > Temp ↓ (< 0.0001) > Temp + ArBpin ↓ (< 0.0001) > Added Water ↓ (< 0.0001) > Total Volumes ↓ (0.0006) > Added Water + ArBpin ↓ (0.0012) > Volumes + Water ↑ (0.0049) > Volumes + ArBpin ↓ (0.0073).

protodeboronation is slowed. The negative effect of base is interesting, not least because it was not a significant factor for conversion of the enoate to the 1,4-addition product.

The two negative interactions of each of these factors with arylboronic ester equivalents point to the inherently good selectivity of this reaction. These interactions indicate that at lower equivalents of arylboronic ester, the negative effects of both the solvent volumes and the equivalents of base on the selectivity of the reaction are of little significance. Figure 28 compares surface plots for the modelled effects of these factors on selectivity at the two extremes of arylboronic ester equivalents: (a) at 1 equivalent and (b) at 1.5 equivalents.

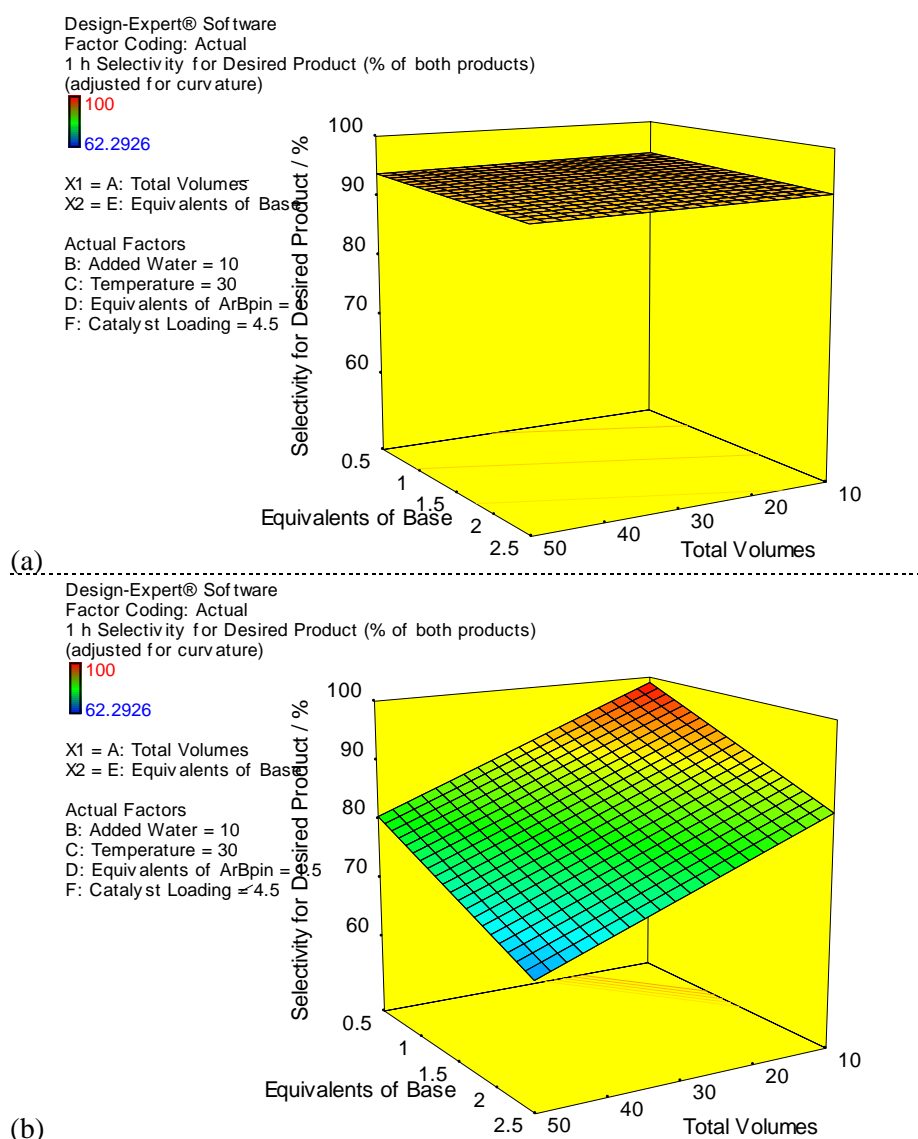


Figure 28. A surface plot of the model predictions for the selectivity of the desired reaction over the deboronation at 1 h as total volumes and base equivalents vary at (a) 1 eq, (b) 1.5 eq ArBpin.

With 1.5 equivalents of arylboronic ester the effects of both base and solvent volumes are large, with selectivity varying from around 60% selectivity to nearly 100% selectivity

(Figure 28b). However, at the far more desirable operating condition of just 1 equivalent of arylboronic ester, the variation in selectivity is less than 2 percentage points (Figure 28a). It is likely that the low selectivity predicted to be achievable under the conditions in Figure 28b arises only because the limitations of the assumption begin to have an effect on the 1-hour data when an excess of arylboron reagent is employed. This affirms the notion that the discrete variables selected for the conjugate arylation reaction ensure a high actual selectivity for 1,4-addition over protodeboronation. Indeed, the statistical analysis of the 1-hour selectivity data was indicative of a data set that was reasonably normally-distributed.

If the amount of deboronated substrate **19** at 1 hour is considered on its own, calculated using only the external mesitylene standard and therefore reliant on accurate sampling volumes, then temperature, added water, catalyst loading and then total volumes are the most significant factors, all having a positive effect on increasing the amount of deboronation product **19**. In particular, the fact that a model can be built in which the catalyst loading has a significant and positive effect on the extent of deboronation supports a rhodium-mediated deboronation mechanism dominating in this system. This is reinforced by the observation that the arylboron loading itself does not have a significant effect on the amount of deboronation product formed. The half-normal plot for this response is shown in Figure 29.

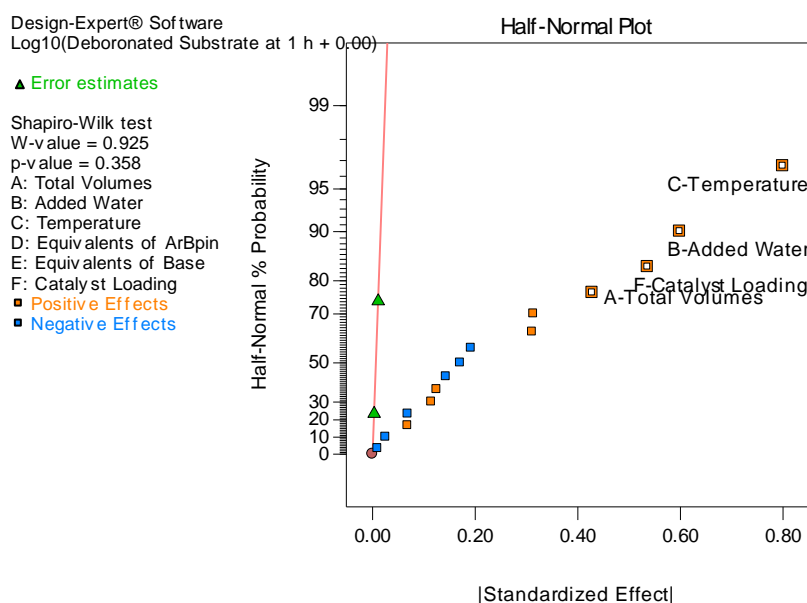


Figure 29. Half-normal plot for the factors affecting the amount of deboronated product at 1 h, calculated using the external standard.

3.2.3.3.3 Enantiopurity of the Pharmaceutically-Relevant Bisaryl Product

Temperature and water content had a negative effect on the enantiomeric excess achieved by the reaction (Table 18). Catalyst loading was found to have a positive effect, although this was a much less significant factor. The half-normal plot of the statistical analysis is given in Figure 30.

Response Range	Significant Factors (p-value)
92.3–96.6%	Temp ↓ (< 0.0001) > Water ↓ (< 0.0001) > Catalyst Loading ↑ (0.0011)

Table 18. Significant factors affecting the enantiopurity of the desired product (yellow DoE design).

The effect of temperature on enantiomeric excess is readily explained, both by higher temperatures providing more thermal energy such that higher energy barriers (i.e. to form the disfavoured enantiomer) can be more easily overcome, and by the bond lengths in the rhodium species being elongated such that the transfer of chirality is less effective as a result of lower energy differences between the two diastereomeric transition states.

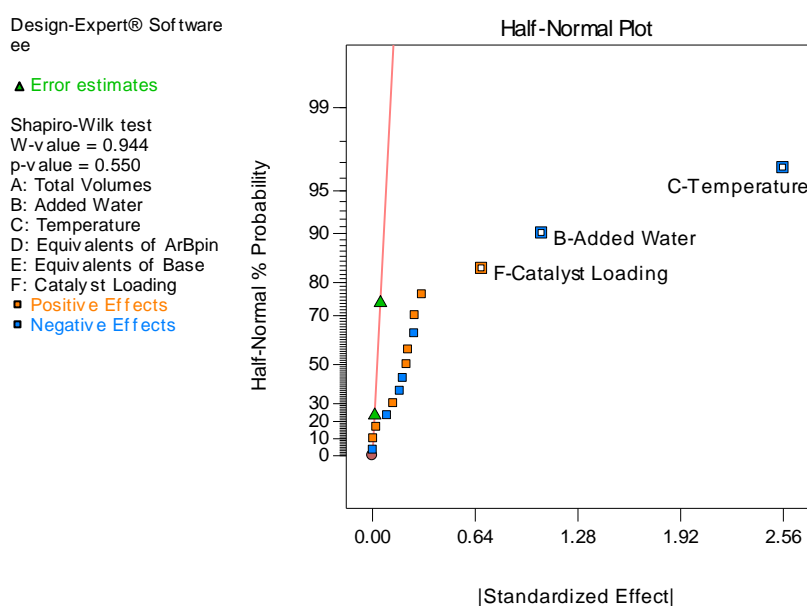


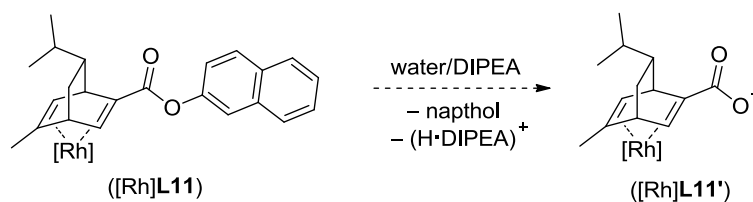
Figure 30. Half-normal plot of enantiomeric excess analysis for the yellow DoE design.

The role of water is less obvious, but its effect has been reported in the literature. A report from 2002 using a water-soluble chiral BINAP-derived ligand found water to have a negative impact on the enantioselectivity of reactions between phenylboronic acid and cyclohexenone using $\text{Rh}(\text{acac})(\text{C}_2\text{H}_4)_2$ as the achiral catalyst precursor (61% *ee* in dioxane/water 1:10, 84% *ee* in dioxane/water 10:1).⁹⁶ The negative effect was even more significant using the COD-ligated precursor $\text{Rh}(\text{COD})_2\text{PF}_6$ (4% *ee* and 66% *ee* respectively). Although the authors do not discuss the reasons for the effect, in their case it could be

reasonable for the differences in enantiomeric excess to be related to the rate of formation of an active catalyst over the rate of formation of an active chiral catalyst. The water content also had a large accelerating effect on the rate of the reaction, but they found that replacing water with ethylene glycol enabled the reaction to proceed at a good rate whilst maintaining a high enantiomeric excess.

Another report in 2009 found a decrease in the water content of a dioxane/water solvent system to give both higher conversions and chiral purities for reactions involving substrates with large lipophilic groups, although they do not show the extent of the improvement or whether or not the improvement in conversion was due to competing deboronation.⁸⁵ In this case, the chiral rhodium species was formed in situ from $\text{Rh}(\text{NBD})_2\text{BF}_4$ and (*S*)-BINAP before addition of reagents or water. Again, the reasons for the effect of water were not discussed.

One possibility in the pharmaceutically-relevant 1,4-addition reaction could be that the naphthyl ester ligand **L11** is slowly hydrolysed under the reaction conditions, resulting in a much less sterically directing ligand (Scheme 42). This could explain both the negative effect of water on enantiomeric excess and the positive effect of increasing catalyst loading. The rate of conversion to the desired product would be higher relative to ligand hydrolysis in the case of higher catalyst loading than it would be in the case of lower catalyst loading. However, it should be noted that no two-factor interaction between the water content of the solvent and the catalyst loading was found to be significant in the statistical analysis.



Scheme 42. A possible explanation for the effect of catalyst loading and water content on enantioselectivity.

The statistical model predicted that adding no water to the reaction whilst keeping the reaction at 10 °C would enable enantiomeric excesses of up to 96.6% to be achieved, whilst increasing the water content to 20% with a temperature of 50 °C would decrease the enantiomeric excess to 92.3% (Figure 31). This is admittedly not an enormous variation (98.3:1.7 and 96.15:3.85 *e.r.* respectively), but is nevertheless something worth controlling and can make a large difference to the amount of drug product deliverable in large scale synthesis and to the ease with which the API can be delivered in high enantiopurity.

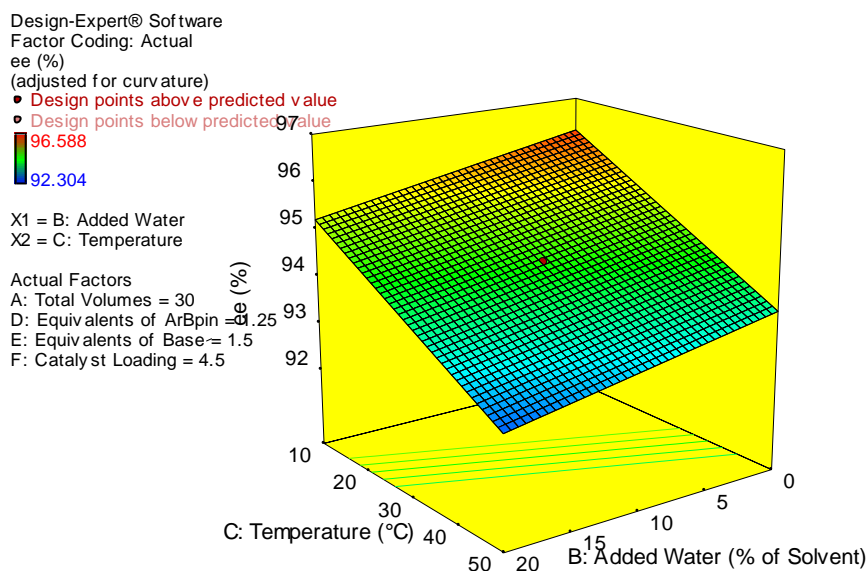
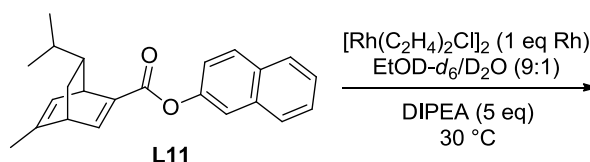


Figure 31. The predictions of the statistical model for the relationship between *ee* and temperature and water content. The red dots are the data from the centre-point experiments.

To explore the potential for transesterification or ester hydrolysis of ligand **L11** to occur under the reaction conditions (Scheme 42), the ligand was treated according to Scheme 43. It had been hoped that any changes would be able to be monitored by ¹H NMR, however solubility proved to be insufficient at the concentration required for certain stages of the experiment. Firstly, a ¹H NMR experiment of the ligand itself in the deuterated ethanol/water mixture was performed before addition of the rhodium salt. Full dissolution was not achieved following addition of the rhodium salt, either overnight in ethanol only, or in the ethanol/water mixture over 24 hours. For this reason, an adequate NMR spectrum of the ligand ligated to rhodium could not be acquired. Addition of DIPEA gave full dissolution of the mixture within 72 hours and so a ¹H NMR spectrum was recorded. The only protons which could be confidently assigned as relating to ligand **L11**, without overlapping with signals from other species, were those in the aromatic region. These had shifted significantly from those of the unligated diene and instead matched the chemical shifts and multiplicities of free naphthol. The only other signals in the aromatic region were trace amounts of the unligated ligand. HPLC analysis also provided evidence for the presence of naphthol, although the possibility of this occurring under the HPLC conditions was not discounted.



Scheme 43. Subjection of ligand **L11** to conditions similar to those of the conjugate arylation conditions in this DoE, to observe any changes by NMR or HPLC.

The only distinction from naphthol by ^1H NMR was that the signals for the two aromatic protons *ortho* to the oxygen decreased in intensity over time. After the initial 72 hours, these signals were at approximately 70% and 90% of the expected intensity, and after a further 3 days at 30 °C the signals had decreased to approximately 50% and 90%. Another 19 days at room temperature saw the integrations decrease to 30% and 90%. Suspecting hydrogen/deuterium exchange to be occurring (Figure 32), LCMS analysis was performed and compared with an authentic sample of naphthol. The mass spectrum acquired was consistent with mono-deuterium incorporation, and the relative mass ion intensities were in reasonable agreement with the ^1H NMR spectrum. Whilst hydrogen/deuterium exchange with rhodium (I) complexes is known,^{175,176} the mechanism and active species in this case remain undetermined.

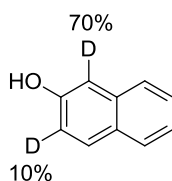


Figure 32. The final levels of deuterium incorporation believed to have occurred from treating diene L11 to the conditions in Scheme 43.

3.2.3.4 Evaluation of the DoE Results

Curvature was significant in each of the yellow models for conversion data, but since this was a factor-screening DoE the curvature could not be adequately modelled. As a result, although the models generated for conversion were significant, the lack of fit of the model was also significant since the centre-point experiments were not well modelled (Figure 33). The centre-points were generally in excellent agreement with each other, giving the models very low noise. In this case therefore, the identification of significant factors is valid but caution should be applied with any attempts to design a specific set of conditions from this model.

Design-Expert® Software
Factor Coding: Actual
Conversion (adj%)
(adjusted for curvature)
● Design Points

X1 = B: Added Water

Actual Factors

A: Total Volumes = 30
C: Temperature = 30
D: Equivalents of ArBpin = 1.5
E: Equivalents of Base = 1.5
F: Catalyst Loading = 4.5

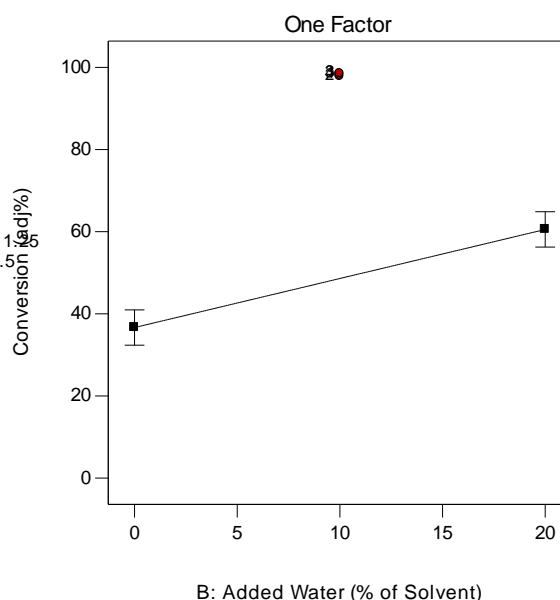
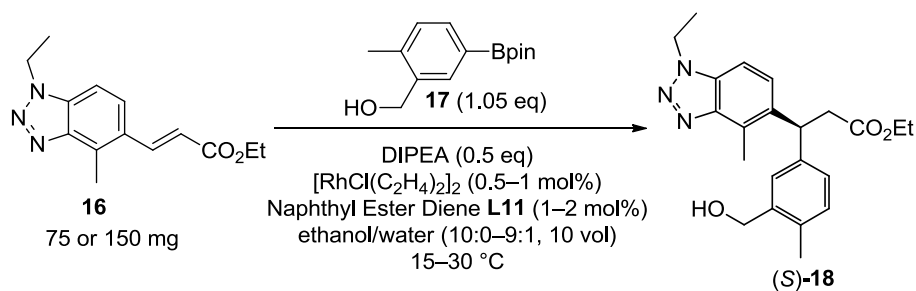


Figure 33. An example model graph for conversion data at 1 h, showing the centre-points lying far from the line predicted by the model.

In the case of the model for enantioselectivity, both curvature and lack of fit were not found to be significant, which is demonstrated in the good agreement between the model surface and the centre-points marked as red dots in Figure 31 (page 107).

3.2.3.5 Trial Conditions for the Conjugate Arylation Reaction

A series of trial experiments were then conducted to try to select appropriate and attractive conditions to demonstrate the reaction on a larger scale, considering the information extracted from the DoE study and remaining within its extremes. The centre-point experiments (Runs 2, 7, 17 and 20, Table 15, page 98) gave extremely good results and already represented a significant improvement on the original process in terms of catalyst loading, solvent, enantiopurity, reaction time and arylboronic ester equivalents. Nevertheless, desiring to increase further the enantiopurity whilst minimising the catalyst loading and arylboronic ester equivalents and maintaining the high conversion, further reactions were performed in the same manner as they had been for the DoE experiment. The results are presented in Table 19.



Entry	Water / Catalyst loading / Temperature / Time / Conversion / ee / %	%	mol% Rh	°C	h	%	%
1	0	1	ambient	21	34	n.d.	
2	0	2	ambient	21	52	94.7	
3	0	2	30	20.5	60	94.9	
4	10	2	30	20.5	95	93.7	
5	10	1	30	21.75	94	93.8	

Table 19. Trial reactions performed to seek an attractive set of successful conditions to demonstrate the process on multigram scale. Ambient temperature was between 15 and 20 °C.

To avoid the negative effect of water and temperature on enantioselectivity, Entries 1 and 2 in Table 19 and Figure 34 were performed with catalyst loadings of 1 mol% and 2 mol% at ambient temperature (15–20 °C), however the conversion in each case was very low over 21 hours. Repeating this at 30 °C gave only a slight improvement in conversion (Entry 3), although it was encouraging that there was no particular change in the enantiopurity. Using ethanol/water as the solvent system with 10% water provided a large increase in conversion (Entry 4) and it was found that adequate activity was possible with a catalyst loading of just 1 mol% in this case (Entry 5). The addition of water did decrease the enantiopurity of the product, but only by approximately one percentage point. The improvement to the conversion that this afforded more than outweighed this disadvantage.

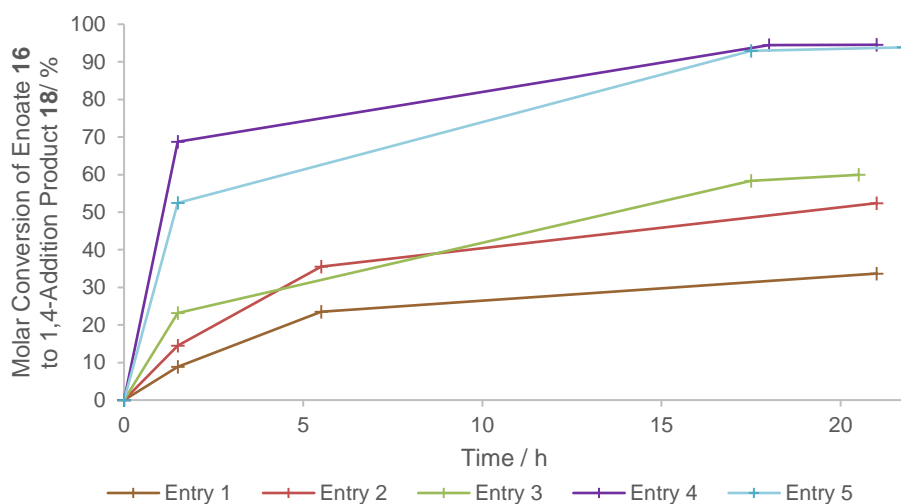


Figure 34. Conversion over time for the reactions shown in Table 19, measured using HPLC response factors.

The low conversions observed for Entries 1 and 2 were reflected reasonably well in the DoE model, despite the high curvature evident in the model and not adequately accounted for by a factor-screening DoE. Using the conditions from Table 19 with a catalyst loading of 2 mol%, the model predicts a particularly steep drop in conversion as the water content approaches 0% and the temperature approaches 0 °C (Figure 35).

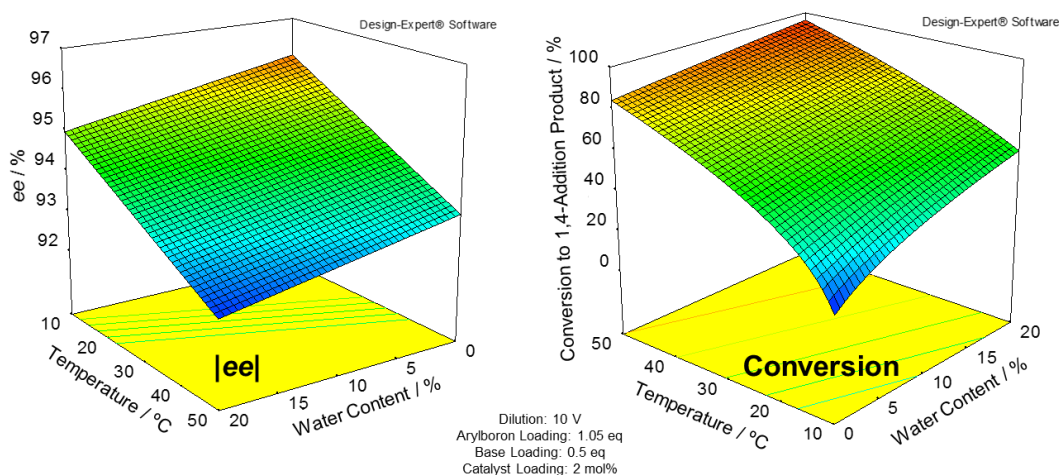
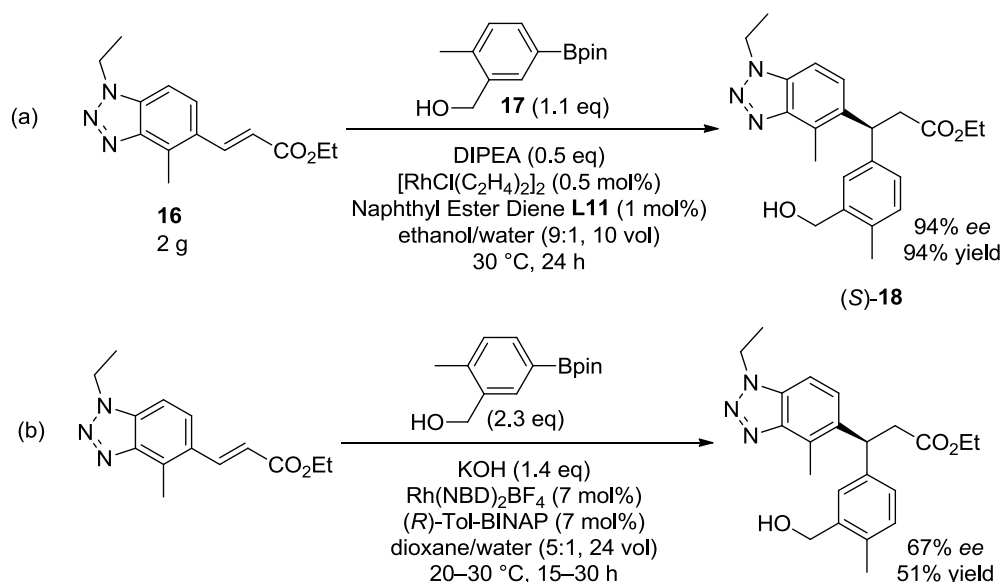


Figure 35. Surface plots predicted by the DoE model at 19 h, with conditions set to the levels used in Table 19, with catalyst loading at 2 mol% Rh. The rapid drop in conversion towards 0% added water and 10 °C is not predicted at higher catalyst loadings.

The necessity of water for good conversion at low catalyst loadings was not identified in the report published by AstraZeneca, in which the replacement of aqueous co-solvent with an alcohol gave decreased levels of deboronation (Section 1.3.7).⁸³ The success of their reaction may have been as a result of using elevated temperatures; if the effects in Figure 35 are generally true of other conjugate arylation reactions, then a higher temperature can compensate for a lack of water. In the reaction to form bisaryl **19**, as explored by this Design of Experiment, water was not found to be a significant factor in determining the selectivity for conjugate arylation over protodeboronation, and higher temperatures had a more significant negative impact on enantioselectivity than water did over the ranges studied. In this case, addition of water to the reaction mixture was preferable to increasing the temperature further.

3.2.4 Multigram-Scale Process Demonstration of the Conjugate Arylation using the Optimised Reaction Conditions

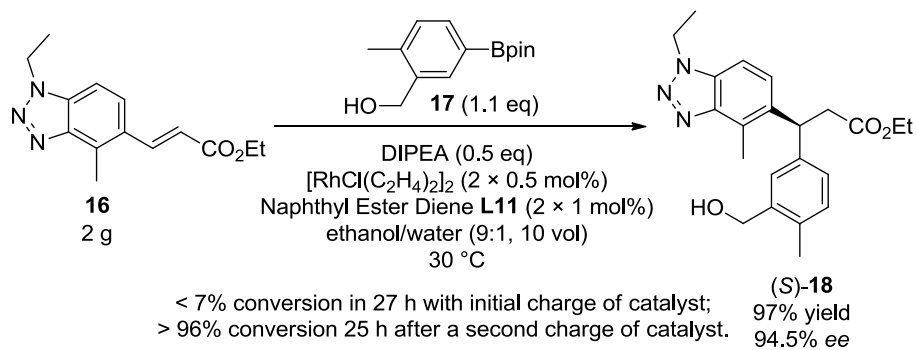
To demonstrate the developed process on multigram scale, conditions based on Entry 5 of Table 19 (page 110) were applied to two grams of the enoate **16** (Scheme 44a). The reaction reached > 98% molar conversion within 24 hours and the product was purified by column chromatography in 94% isolated yield. Chiral HPLC revealed an enantiomeric excess of 93.9% of the desired enantiomer (*S*)-**18**, consistent with the 150 mg scale result in Table 19. By comparison with the original process (Scheme 44b), the optimised reaction provides the required bisaryl product **18** in significantly higher enantioselectivity and yield, whilst employing a much smaller excess of the arylboron reagent **17** and a much lower loading of the rhodium catalyst. This is achieved in an ethanolic solvent system, using the inexpensive chiral diene ligand **L11** derived from the chiral pool.



Scheme 44. (a) A 2 g scale demonstration of the optimised conditions. (b) The original process used to prepare (*S*)-**18**.

A previous attempt performed on the same scale and in the same manner had shown < 7% molar conversion of the enoate **16** to the desired 1,4-addition product **18** in 27 hours (Scheme 45). Notably, the reaction mixture had reddened upon addition of base but after 27 hours the colour had reverted to its original appearance. Encouragingly, a second charge of rhodium salt and ligand was able to restart the reaction and within 25 hours of this second charge, 96% conversion had been achieved. 40 hours after the second charge, full consumption of the arylboronic ester had occurred, with > 97% conversion of the enoate to the 1,4-addition product. In this case, the product was isolated in 97% yield by column chromatography with an enantiopurity of 94.5% *ee*. At low catalyst loadings, the risk of

catastrophic catalyst poisoning increases, and so the fact that the reaction could be restarted to give a similar outcome to the reaction which proceeded without issue is an important observation.



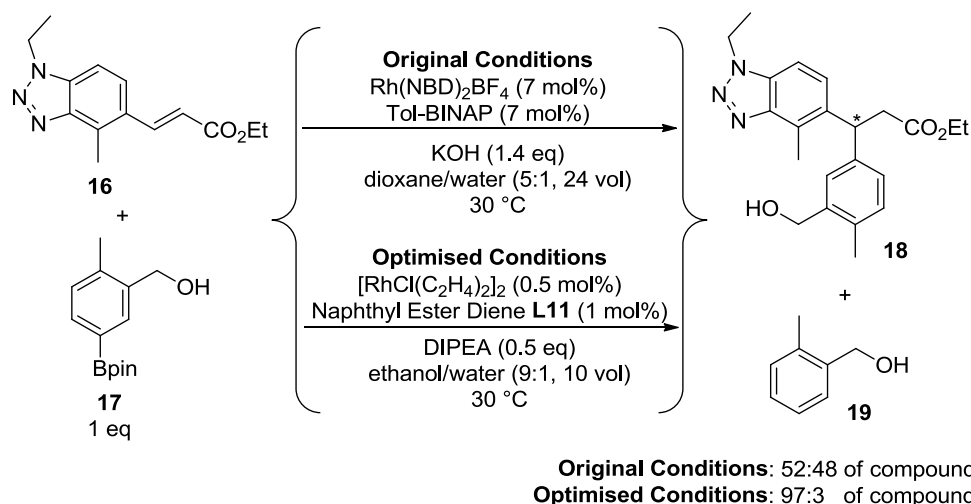
Scheme 45. A previous 2 g scale reaction, which could be restarted with an additional catalyst charge after stalling.

It is possible that the stalling of the reaction resulted from adventitious oxygen entering the vessel. Performing the reaction on 150 mg scale with no degassing of the solvents and with the headspace open to air gave no more than negligible conversion of either starting material.

3.3 Selectivity for Conjugate Arylation over Protodeboronation

Many different ligands and ligand classes have been explored from the perspective of the enantiocontrol that they induce in rhodium-catalysed conjugate arylation reactions.⁵⁹ In contrast, the effect that the ligands have on the product ratio of conjugate arylation product to protodeboronation product has been much less explored. One reason for this may be a perceived lack of interest or demand, given that on smaller scales using a large excess of arylboron reagent is rarely problematic. However, this reaction selectivity becomes very important on large scales, especially when high value materials are being used and when the product is required in high purity. Use of excess reagents results not only in inefficient processes, but typically results in more difficult purifications and increases the amount of waste that must be appropriately disposed of.

A comparison of the previously-employed process with the optimised process developed in Section 3.2 shows a striking selectivity difference when both are performed using 1:1 stoichiometry of enoate **16** to arylboron reagent **17** (Scheme 46). The original conditions gave almost no selectivity in favour of either the desired or undesired product, whereas the optimised conditions showed virtually complete selectivity for the desired product.



Scheme 46. Comparison of the product ratios afforded by the starting point conditions for this work, and the final developed conditions. Molar ratios calculated using HPLC response factors as for Section 3.2.3.3.

This section details investigations performed to give an empirical understanding of structural features of the substrates and the diene ligand that are important in enabling the high selectivity afforded by the developed process. Where appropriate, possible reasons for the importance of any structural motifs are discussed. Effects on the stereochemistry of the conjugate arylation are not the focus of this work, and as such enantiomeric excesses are generally not stated and not discussed in detailed.

The mechanisms involved in rhodium-catalysed conjugate arylation are not known to have been explored in significantly more depth than that laid out in Section 1.3.2 (Figure 36)⁶⁸. In particular a detailed understanding of the individual processes involved in the catalytic cycle has not been established, despite this being of great importance for the rational design of ligands and processes. It has already been established in this work that base-mediated protodeboronation is negligible under the optimised conditions (page 91), and there has also been little evidence that the arylboronic acid pinacol ester **17** must first be hydrolysed to the boronic acid before transmetalation can occur. These findings question some assumptions made in the literature, perhaps due to analogies drawn from the Suzuki-Miyaura coupling reaction (Section 1.3.5). The question under primary consideration in this section is therefore what affects the relative extents of the two possible transformations that the arylrhodium intermediate undergoes (species **3** in Figure 36): protoderhodation and migratory insertion of the electrophile.

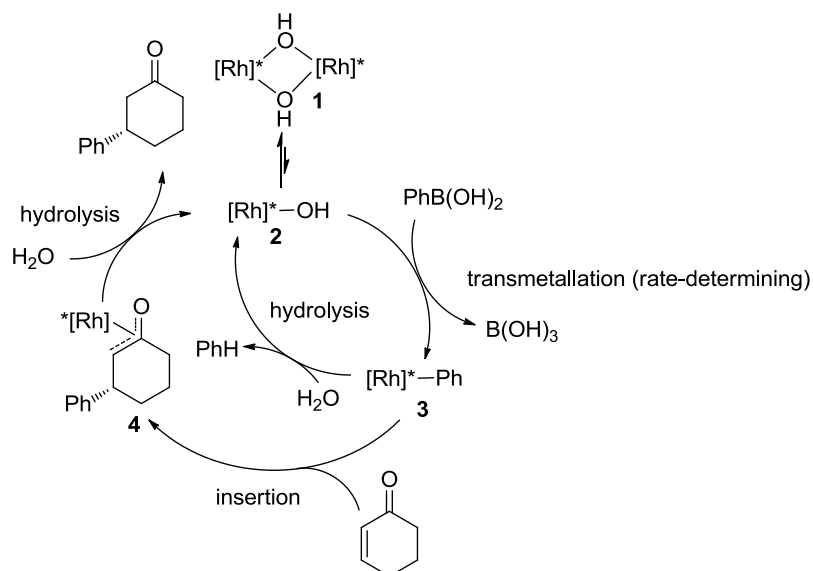


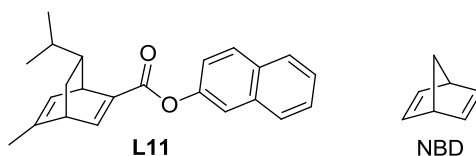
Figure 36. The general mechanism accepted for rhodium-catalysed conjugate arylation, adapted from that shown in Section 1.3.2 to include a competitive protoderhodation process by hydrolysis of the arylrhodium intermediate **3**.

3.3.1 Influence of Structural Motifs of the Substrates on Selectivity for Conjugate Arylation over Protodeboronation

In order to understand the structural origins of the remarkable selectivity for the 1,4-addition product over the protodeboronation product in the optimised process, as opposed to the selectivity originating from the reaction conditions, a scoping exercise was performed using substrates with truncated and modulated functionality relative to that of the pharmaceutically-relevant substrates **16** and **17**. The focus of the substrate scope was to

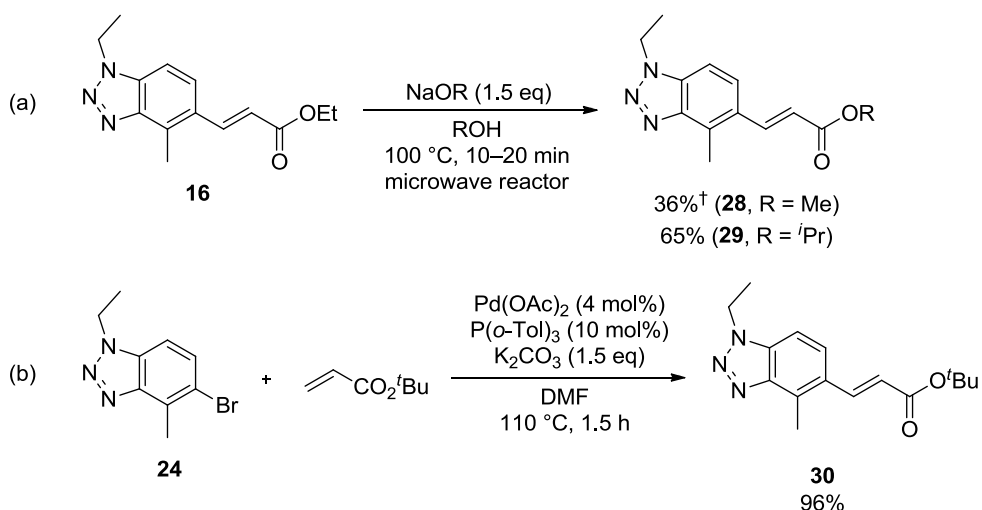
observe the importance of any structural motifs of the pharmaceutically-relevant substrates on the selectivity for conjugate arylation over protodeboronation. The role of structural motifs of the ligand are explored in Section 3.3.2.

Most of the substrates were subjected to two sets of conditions: one employing $[\text{Rh}(\text{C}_2\text{H}_4)_2\text{Cl}]_2$ with the naphthyl ester ligand **L11** (Conditions A) and one employing $[\text{Rh}(\text{NBD})\text{Cl}]_2$ with no additional ligand added (Conditions B), since a significant difference between ligand **L11** and norbornadiene had already been observed (see, for example, Table 8, page 64). The selectivity of the systems for 1,4-addition over deboronation was determined by measuring the consumption of the enoate at full consumption of the arylboron reagent by solution assay. This approach assumed that the arylboron reagent was consumed either in the formation of the 1,4-addition product or the protodeboronation product and that the enoate was consumed only in the formation of the 1,4-addition product. Inspection of the HPLC traces of the reaction mixtures defended this assumption within reasonable expectations.



3.3.1.1 Effect of the Steric Bulk of the Ester Group on Reaction Selectivity for Conjugate Arylation over Protodeboronation

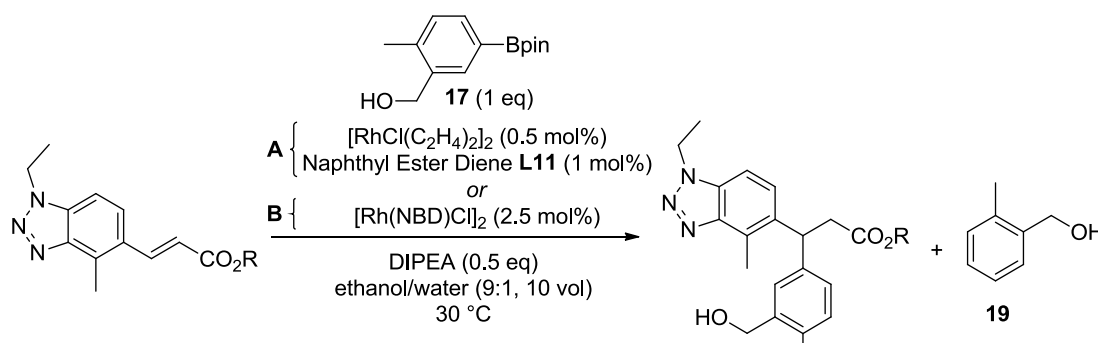
The steric bulk of the ester group in an enoate is known to have an effect on the relative amounts of conjugate addition product and protodeboronation product in rhodium-catalysed arylations (Table 2, page 27).¹³⁴ Presumably this is due to the increased bulk leading to a higher energy rhodium-enoate complex and a higher energy transition state towards that complex, resulting in a decreased ability of the enoate to intercept the arylrhodium complex before protoderhodation occurs. The methyl, *iso*-propyl and *tert*-butyl analogues of ethyl ester **16** were prepared according to Scheme 47, and their consumptions in the rhodium-catalysed reactions are detailed in Table 20.



Scheme 47. Synthesis of (a) methyl, *iso*-propyl and (b) *tert*-butyl enoate analogues of enoate **16. [†]Yield after crystallisation following column chromatography.**

Synthesis of the three enoates **28** (Me), **29** (*i*Pr) and **30** (*t*Bu) proceeded smoothly, and the products were readily purified by column chromatography in good to excellent yield except for the methyl ester, a portion of which was purified by crystallisation following chromatography. The Heck reaction (Scheme 47b) employed tri(*o*-tolyl)phosphine as the ligand rather than triphenylphosphine as for synthesis of enoate **16** (Scheme 28, page 40), anticipating that the increased steric demand of the *o*-tolyl groups would ensure high *E/Z* selectivity in the Heck reactions.

The results in Table 20 demonstrate the expected relationship between the steric bulk of the ester motif and the selectivity of the reaction for 1,4-addition over protodeboronation, however the differences are much smaller than those implied for the system investigated by Hayashi (Section 1.3.6, page 27).¹³⁴ In particular, there is no noticeable difference between the performance of the *iso*-propyl ester **29** and the *tert*-butyl ester **30** in the reaction conditions optimised for the ethyl ester **16**. Impressively, the selectivity of the system remains high (9:1 1,4-addition/protodeboronation) even for the *tert*-butyl ester. Similarly, whilst the protodeboronation trend is still present using the norbornadiene ligand, the differences are barely noticeable with this catalyst system. This may be as a result of additional functionality of the enoates contributing to delivering high reaction selectivity, and also as a result of the ligands (especially norbornadiene) being relatively sterically undemanding.



Entry	Enoate	Arylboron Reagent	Consumption of Enoate	
			Conditions A	Conditions B
1	 28	 17	> 96% ⁱ (87%) [†]	n.d.
2	 16	 17	97% ⁱⁱ (83%)	24% (25%)
3	 29	 17	90% ⁱⁱⁱ (88%)	23% (21%)
4	 30	 17	90% (78%)	21% (25%)

Table 20. Consumption of enoate at full consumption of arylboron reagent, determined by solution assay. Isolated yield of 1,4-addition product given in parentheses. [†]Isolated by MDAP rather than by column chromatography.

The structure of **L11** is such that it projects much less steric bulk than the BINAP ligand employed by Hayashi, which may account for the results using **L11** being less affected by the bulk of the ester substrate (Figure 37). This draws attention to the importance of creating and using chiral ligands that do not just project large steric bulk, but which differentiate well

ⁱ 96% consumption of enoate with c. 96% consumption of aryl boron reagent.

ⁱⁱ Selectivity for conjugate arylation product over protodeboronation product, taken from Scheme 46, in which the reaction was sampled at 87% consumption of enoate with incomplete consumption of aryl boron reagent.

ⁱⁱⁱ Additional catalyst charge was required to give full consumption of aryl boron reagent.

between the spatially distinct directions. As long as there is a significant difference between the more sterically encumbered direction and the less sterically encumbered direction, large sterically directing groups should not be necessary.

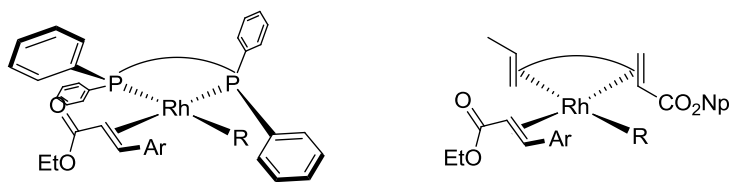
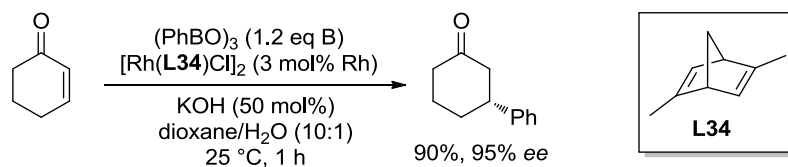


Figure 37. A schematic to demonstrate the different extent to which BINAP and L11 are sterically demanding.

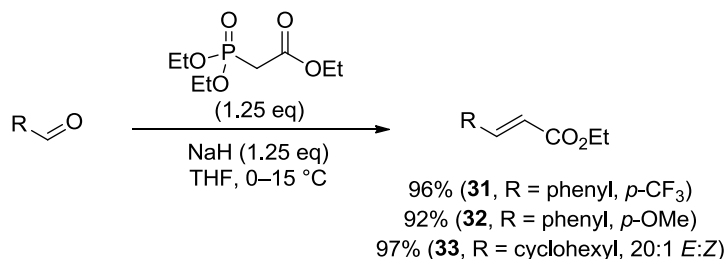
In a later publication, Hayashi noted that even the chiral dimethyl-substituted norbornadiene scaffold **L34** provided sufficient steric differentiation to afford an enantiomeric excess of 95% in the conjugate arylation of 2-cyclohexenone with phenylboroxine (Scheme 48).¹¹⁷



Scheme 48. Conjugate arylation published by Berthon-Gelloz et al. (2006), employing the sterically undemanding chiral ligand **L34** but nevertheless delivering high enantioselectivity.

3.3.1.2 Effect of the Electronics of the Enoate on Reaction Selectivity for Conjugate Arylation over Protodeboronation

The kinetics and thermodynamics of the enoate binding to the arylrhodium species must be an important factor in determining the selectivity for 1,4-addition over protoderhodation. As well as the bulk of the enoate, the electronics of the carbon–carbon double bond would be expected to affect this. To observe any effect of the electronics of the enoate in the optimised system, the *p*-trifluoromethyl- and *p*-methoxy-substituted ethyl cinnamate derivatives were prepared along with the cyclohexyl analogue according to Scheme 49, and studied under the conjugate arylation conditions.



Scheme 49. Synthesis of electronically varied enoates using the Horner-Wadsworth-Emmons reaction.

The Horner-Wadsworth-Emmons reactions performed very well in each case, giving good selectivity for the *E*-alkenes. The worst performing reaction was for the synthesis of the cyclohexyl enoate **33**, with separation of the stereoisomers also proving difficult. Nevertheless, a sufficient amount of the *E*-isomer was isolated without contamination by the *Z*-isomer for investigation under the rhodium-catalysed reaction conditions (Table 21).

Entry	Enoate	Arylboron Reagent	Consumption of Enoate	
			Conditions A	Conditions B
1			95% (89%)	25% (21%)
2			92% (71%)	9% (5%)
3			89% (86%)	2% (< 5%)
4			92% ^{iv} (77%)	18% ^v (6%)

Table 21. Consumption of enoate at full consumption of aryl boron reagent, determined by solution assay. Isolated yield of 1,4-addition product given in parentheses.

The selectivity trend for the cinnamate derivatives was most obvious using norbornadiene, but the same trend remained evident under the optimised conditions using ligand **L11**. With norbornadiene, the consumption of the enoates fell from 25% for the electron-poor enoate **31**

^{iv} Experiment performed in duplicate, with the same consumption of enoate observed in both cases.

^v Average of two experiments.

to just 2% for the electron-rich enoate **32**. A comparison of the HOMO and LUMO energies for the enoates calculated using a restricted Hartree-Fock method is given in Table 22, along with the energies for enoate **16**.

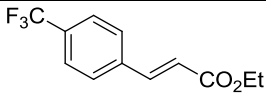
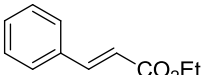
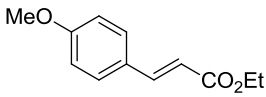
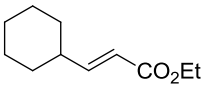
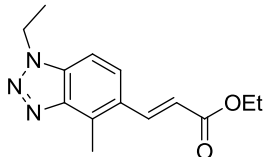
Entry	Enoate	Orbital Energy / eV	
		HOMO	LUMO
1		-9.345	1.181
2		-8.789	1.666
3		-8.609	1.775
4		-10.194	3.037
5		-8.456	1.820

Table 22. HOMO and LUMO energies for enoates **31–34** and **16**, calculated using a restricted Hartree-Fock method.

Entries 1–3 show a trend in HOMO and LUMO energies across the ethyl cinnamate derivatives, with the trifluoromethyl-substituted enoate **31** possessing the lowest energy orbitals and delivering the highest selectivity for conjugate arylation. Alkenes are understood to bind to transition metals both by donating electron density towards the metal from the alkene π -orbital (HOMO) and by accepting electron density from the metal into the alkene π^* -orbital (LUMO) (see Section 3.3.3.1). Whilst the ability of the enoate to donate electron density decreases from the methoxy-substituted substrate **32** to the trifluoromethyl-substituted substrate **31**, the ability of the enoate to accept electron density increases. The lower LUMO energies are also likely to correspond to a more activated substrate for insertion into the rhodium–aryl bond. A correlation between the reactivity of enoates and the stability of the resulting rhodium–enoate complex or the insertion rate, both of which would correlate with the enoate LUMO energies, was noticed by Miyaura in early work using $\text{Rh}(\text{COD})(\text{MeCN})_2\text{BF}_4$ to catalyse the addition of phenylboronic acid to unsaturated esters.¹²⁴

The cyclohexyl substrate **33** does not fit this trend (Entry 4), with its selectivity for conjugate arylation using both **L11** and norbornadiene much better than the HOMO and LUMO energies would predict. With the lowest energy HOMO and the highest energy LUMO, it would have the poorest energy match for both electron-donating and -accepting bonding modes with the rhodium centre. In this case, the lack of conjugation may provide an explanation. Whilst conjugation with the aromatic system lowers the orbital energies for the aromatic enoates, it also results in much more diffuse orbitals with the orbitals spread more evenly across the molecule (Figure 38). The less diffuse LUMO of cyclohexyl ethyl acrylate **33** and its more narrowly defined dipole may enable a greater propensity for the migration of the aryl group into the enoate.

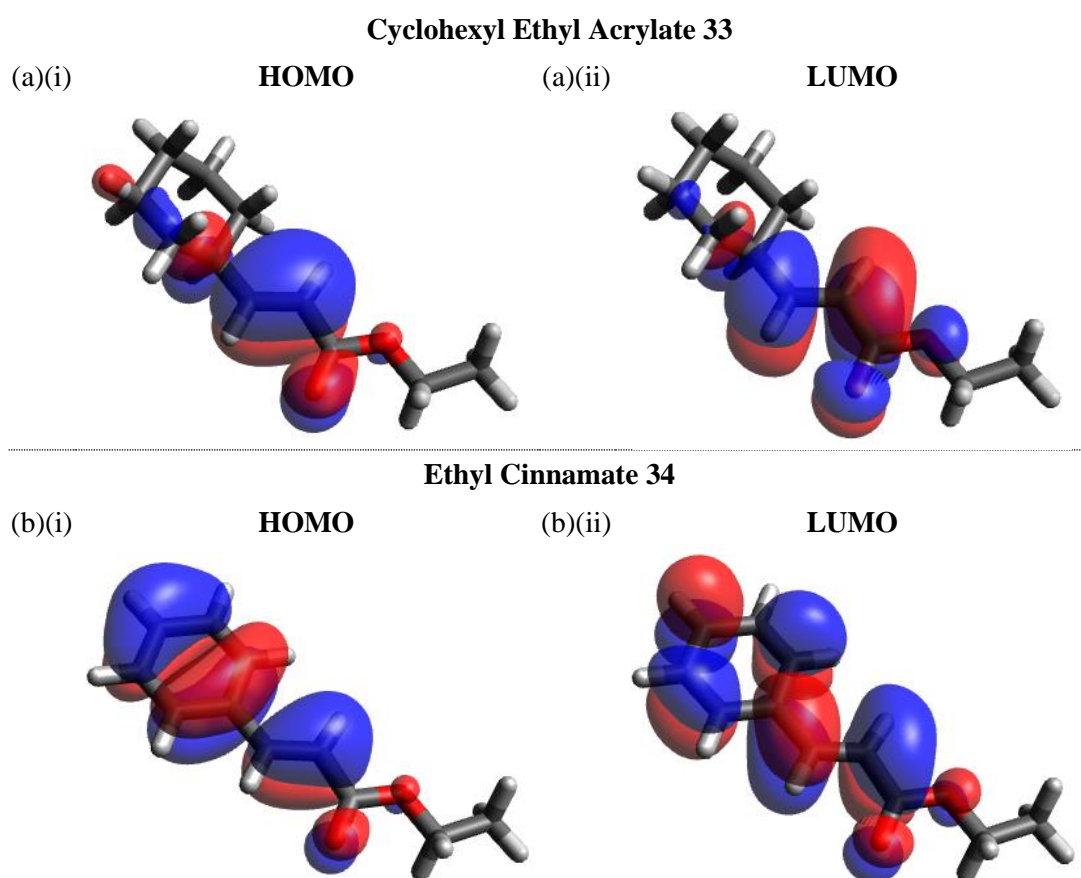


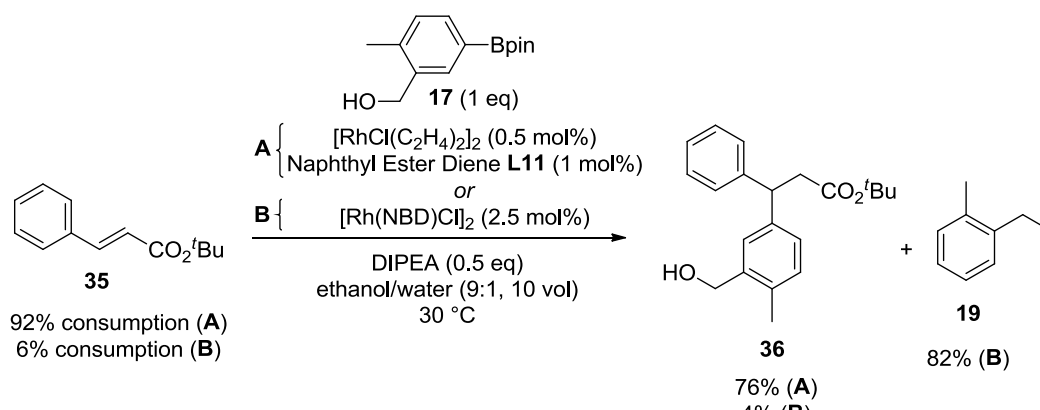
Figure 38. A comparison of the calculated (i) HOMOs and (ii) LUMOs of (a) cyclohexyl ethyl acrylate **33** and (b) ethyl cinnamate **34**.

The fact that the cyclohexyl substrate **33** performs well demonstrates that aromaticity is not an important component of the enoate for high reaction selectivity to be achieved. In Section 3.2.2 (page 84) it was noticed that aromatic solvents performed particularly badly in the 1,4-addition reaction. One possible explanation could have been that a π -stacking interaction between the **L11**-ligated arylrhodium complex and the enoate helped to ensure good selectivity, but the high selectivity afforded by the cyclohexyl ethyl acrylate eliminates that

explanation. Instead, it may be that aromatic solvents disrupt an important π -stacking interaction between the aryl group of the arylrhodium complex and the naphthyl group of **L11**, unless more complex solvent effects are responsible for the drop in selectivity (see also Figure 52, page 153).

The similarity between the selectivity results for the *p*-trifluoromethyl-substituted ethyl cinnamate derivative **31** and for the pharmaceutically-relevant enoate **16** seems surprising (Table 21). Computation suggests that the energies of the filled and unfilled orbitals at the alkene of enoate **16** are much more similar to the *p*-methoxy-substituted ethyl cinnamate derivative **32**, suggesting that the net effect of the triazole is to donate electron density into the alkene (Table 22). Evidently the high selectivity observed with enoate **16** cannot be explained by the electronics of the enoate alone (see Section 3.3.1.3).

The consumption of *tert*-butyl cinnamate **35** was also measured under the 1,4-addition reaction conditions (Scheme 50). Curiously, little difference was observed compared with ethyl cinnamate **34** (Table 21). In contrast, changing from the triazole-containing pharmaceutically-relevant enoate **16** to ethyl cinnamate saw the extent of deboronation triple using **L11**. The lack of difference between ethyl and *tert*-butyl cinnamate compared with that between triazole-containing **16** and ethyl cinnamate suggests that the increase in sterics from ethyl to *tert*-butyl has an insignificant impact on the selectivity relative to the loss of the triazole motif.

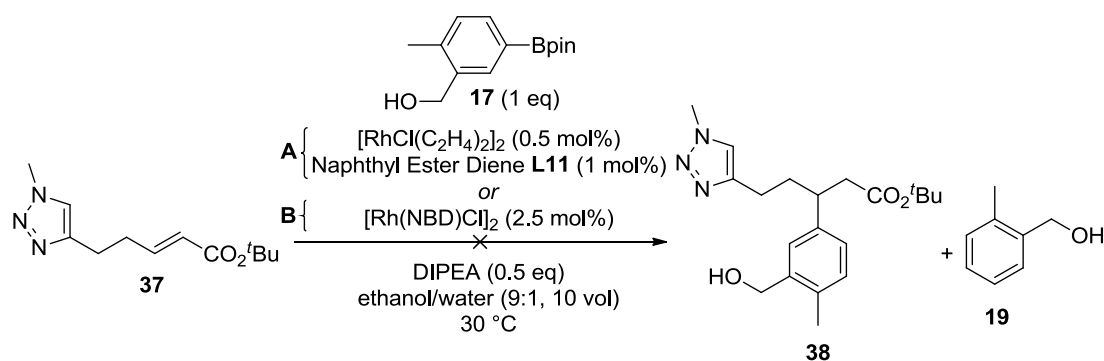


Scheme 50. Consumption of *tert*-butyl cinnamate in the 1,4-addition reaction conditions.

3.3.1.3 Effect of the Triazole on Conjugate Arylation and Deboronation

As noted in the previous section, the triazole motif appears to have a positive impact on the selectivity of the rhodium-catalysed process for 1,4-addition over protodeboronation using both **L11** and norbornadiene, which is not accounted for by the electronics of the enoate.

With an alkyltriazole analogue **37** of benzotriazole **30** (Scheme 47b, page 117) available, the effect of deleting only the phenyl portion of the enoate was explored (Scheme 51).



Scheme 51. Alkyltriazole enoate **37** was found to prevent formation of both the 1,4-addition product **38** and the protodeboronation product, with no consumption of enoate **37** or arylboron reagent **17** observed over 94 h.

Using neither norbornadiene nor **L11** as the ligand gave any consumption of either the enoate **37** or the arylboron reagent **17**. Organic bases containing sp^2 -hybridised nitrogen atoms had been found to shut down the reactivity of the system in Section 3.2.2 (page 88), and so it was already surprising that enoate **16**, for which the reaction was developed, was tolerated. To determine whether it was the triazole alone which shut down the reactivity in Scheme 51 or whether a more specific explanation needed to be invoked, such as the bidentate binding mode of enoate **37** suggested in Figure 39, a spiking experiment was performed (Scheme 52).

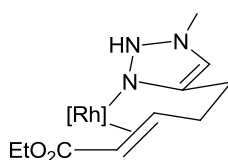
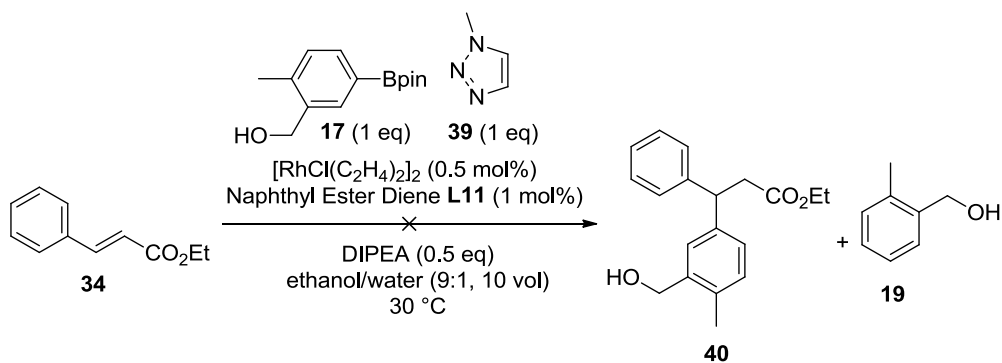


Figure 39. A suggested bidentate binding mode of the enoate **37** to rhodium in a pseudo 6-membered ring.

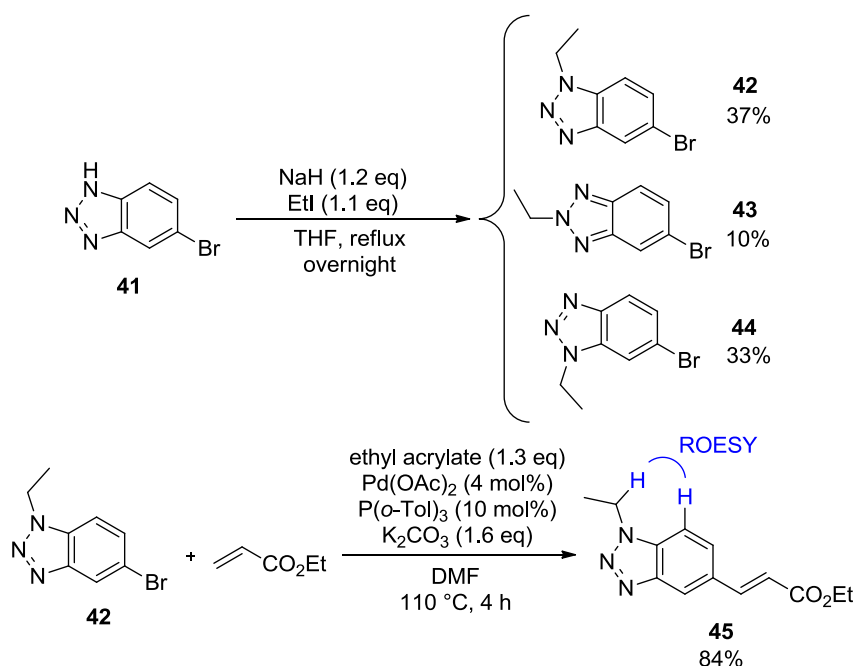
The spiking experiment involved addition of one equivalent of methyl triazole **39** to the ethyl cinnamate reaction using the optimised reaction conditions. As for the alkyltriazole enoate substrate **37**, no reactivity was observed, demonstrating that a binding mode specific to the alkyltriazole substrate did not need to be invoked. Instead, a more general means of catalyst poisoning by the triazole appeared to be operating.



Scheme 52. A spiking experiment, which demonstrated that triazole functionality could shut down the reactivity of the 1,4-addition system.

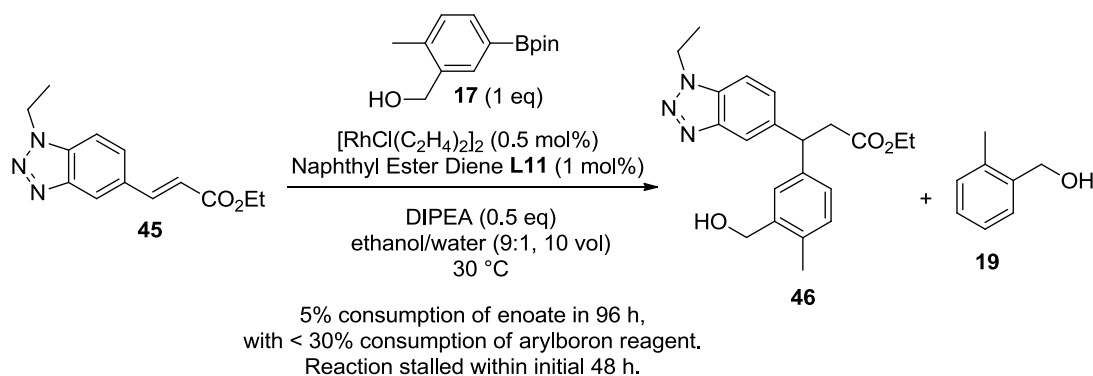
If both methyl triazole **39** and the alkyltriazole substrate **37** shut down the reactivity of the system by coordination to the metal centre whilst the benzotriazole substrates **16** and **30** (Section 3.3.1.1) did not, then it had to be concluded that some property of the benzotriazole substrates decreased their propensity to coordinate to the metal centre via the triazole. The differences in reactivity could in principle arise either due to the electronics of a benzotriazole being sufficiently different from an alkyltriazole, or due to the methyl group positioned *ortho* to the most electron-rich nitrogen lone pair, only in the case of enoate **16** and related substrates, acting to destabilise any binding of the triazole to the metal. The electronic difference was expected to be insignificant, and so an analogue of compound **16** with a methyl deletion was prepared to test its steric effect (Scheme 53).

N-Alkylation of benzotriazole **41** proceeded as expected, to give a mixture of three regioisomers in a ratio determined primarily by the HOMO distribution of the anion (Scheme 53a). Attempts to maximise the proportion of alkylation product **42** by avoiding high temperatures were impeded by very low conversions below reflux, however sufficient material was nevertheless afforded by the refluxed reaction. The Heck reaction of **42** with ethyl acrylate performed well (Scheme 53b), as it had for similar substrates. A ROESY NMR experiment confirmed that the material corresponded to the desired isomer, with a correlation observed between the methylene of the *N*-ethyl group and an aromatic proton assigned as shown below on account of its appearance as a doublet with $J = 8.6$ Hz by ^1H NMR spectroscopy.



Scheme 53. Synthesis of the benzotriazole enoate **45**, with no methyl substitution on the phenyl ring.

Under the optimised conjugate arylation reaction conditions, only 5% consumption of enoate **45** was observed after 48 and 96 hours, with > 70% residual arylboron reagent **17** (Scheme 54). Attempts to purify the small amount of 1,4-addition product **46** away from the enoate **45** were unsuccessful, however the key structural features of the product were observable by NMR (see Section 5.4.2.2.3).



Scheme 54. Reactivity of the developed system with benzotriazole substrate **45**.

The experiment demonstrated how enoate **16** was tolerated well by the catalyst system whilst sp^2 -containing organic bases were not. The presence of a methyl group *ortho* to the most electron-rich nitrogen lone pair of the benzotriazole is essential for transmetalation of the arylboron reagent. Presumably the methyl substituent provides a sufficiently sterically destabilising interaction in any hypothetical [Rh–N] species for such species either not to form, or to form with sufficient reversibility. Whether or not this is true both of the enoate

and of the 1,4-addition product has not been definitively determined, but is largely unimportant given that one is formed by the other. Furthermore the electronic distinction between the highest energy lone pair of the enoate and of the 1,4-addition product is not expected to be significant. It is interesting that the central nitrogen atom of the triazole does not prevent the reactivity of the catalyst. This would either be due to its lone pair being less electron-rich, or due to the steric effect of the adjacent *N*-alkyl group (Figure 40). Since the *N*-alkyl group projects out in a different direction from the triazole to the primary direction of the lone pair, it may be that the electronic differences between the lone pairs of the nitrogen atoms is sufficient to account for this. A combination of these effects may be responsible.

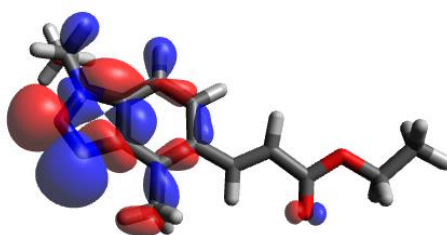


Figure 40. The calculated highest energy occupied orbital involving the sp^2 -nitrogen lone pairs for enoate **16** (-11.850 eV).

The triazole motif of the enoate **16** plays an interesting role in the 1,4-addition reaction. On the one hand, it has been shown to be advantageous in enhancing the selectivity of the reaction for conjugate arylation over protodeboronation. An explanation based on the electronics of the alkene is insufficient to account for this (Section 3.3.1.2), but some extent of reversible binding to the rhodium complex (rather than a solvent molecule) may play a role (Figure 41). On the other hand, its ability to bind to rhodium via the most electron-rich nitrogen atom must be tempered for reactivity to be possible at all, such as by a sterically blocking methyl group *ortho* to the nitrogen atom.

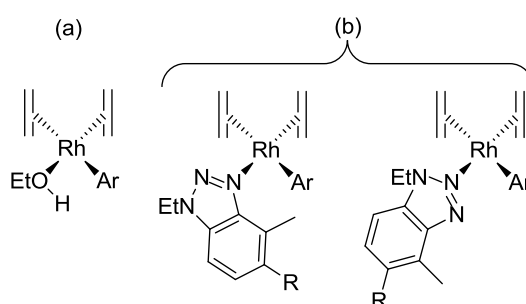


Figure 41. (a) Possible resting state of the arylrhodium species, with the vacant site occupied by a solvent molecule potentially set up for intramolecular protoderhodation. (b) Suggested resting states with the vacant site occupied by the benzotriazole. The representations of diene ligands coordinated to rhodium omit the full structures of the scaffolds for clarity.

The rate of consumption of arylboron reagent **17** under the 1,4-addition reaction conditions at 5 mol% rhodium was compared with and without the benzotriazole-containing enoate **16** present (Figure 42). The fact that the arylboron reagent is consumed more slowly in the presence of the enoate is compatible with the suggestion in Figure 41, suggesting that the enoate (or the bisaryl product) has an inhibitory effect on the consumption of arylboron reagent (see also Figure 48, page 147).

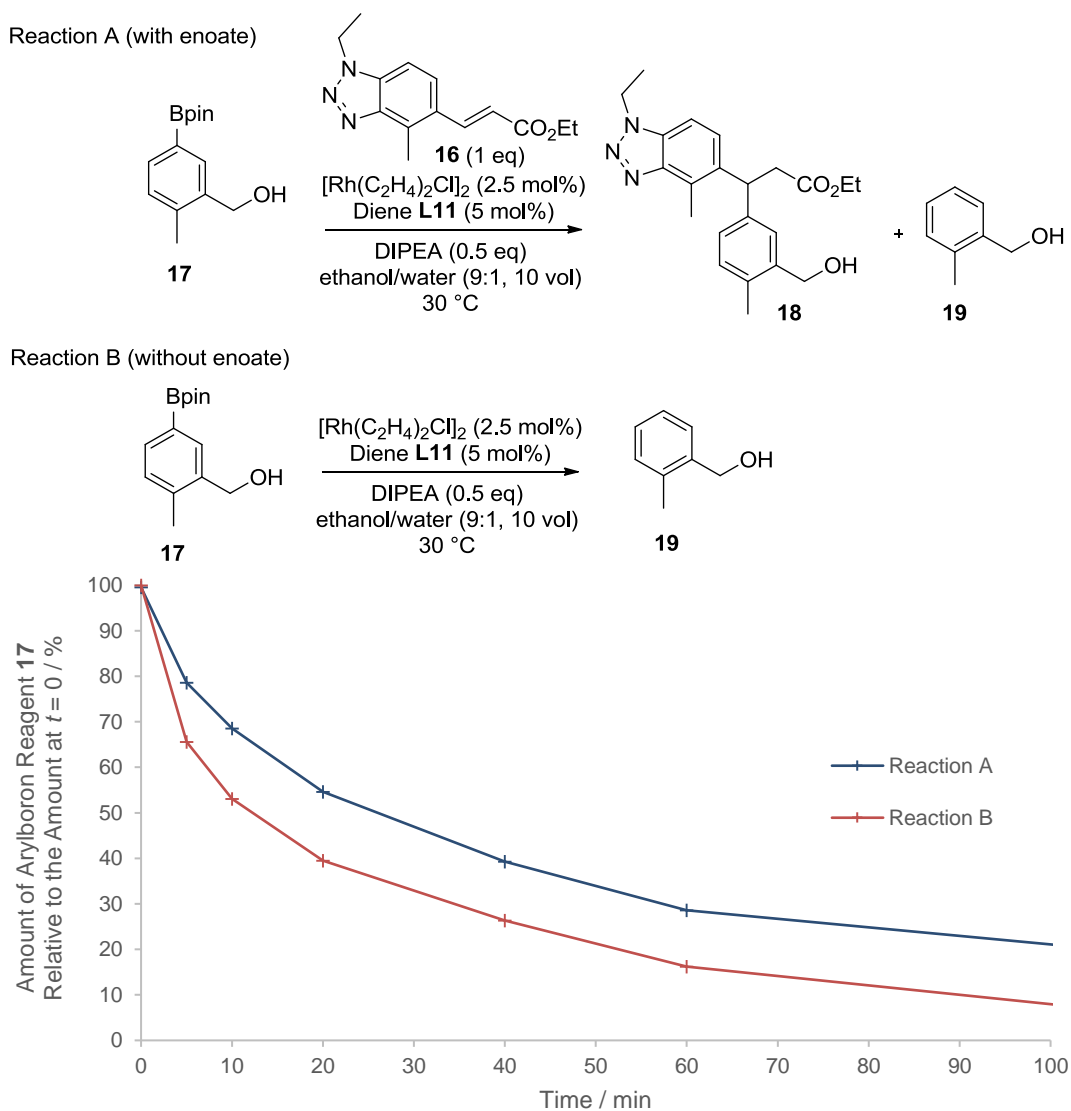


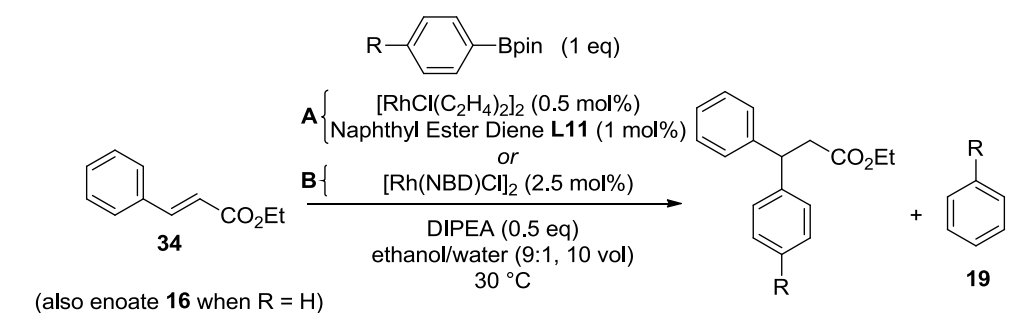
Figure 42. The amount of arylboron reagent **17** over time with and without enoate **16** present, assuming no reactions occurred other than conjugate arylation and protodeboronation. Relative amounts determined by HPLC response factors.

3.3.1.4 Effect of the Arylboron Reagent on Reaction Selectivity for Conjugate Arylation over Protodeboronation

The importance of the structure of the arylboron reagent on the reaction selectivity was probed in two ways. Firstly, modulations of the aryl portion were explored with a view to

examining electronic effects, and secondly the boron moiety was modulated to compare the results using the pinacol boronic ester with the boronic acid.

The effect of modulating the aryl group could be determined using commercially available boronic esters (Table 23). The intention was to observe any electronic effects, however the steric effect of the *para*-substituents appeared to outweigh any electronic effect in the optimised system using **L11**. This was presumably because substitution on the phenyl ring of the arylrhodium complex disfavoured the approach or binding of the enoate. Removing substitution altogether (arylboron reagent **48**) gave excellent selectivity using ethyl cinnamate (Entry 2) and no evidence of any protodeboronation using enoate **16** (Entry 4). The results with enoate **16** are consistent with the observations already made regarding the positive effect of the triazole motif on the reaction selectivity. The substrates in Entry 4 delivered the highest selectivity for conjugate arylation observed throughout the investigations in Section 3.3.1 for the optimised conditions, with no protodeboronation product observed throughout the experiment in this case. The electronic effects were noticeable using the less sterically demanding norbornadiene catalyst system, with higher levels of conjugate arylation correlating with a more electron-poor aryl group.



Entry	Enoate	Arylboron Reagent	Consumption of Enoate	
			Conditions A	Conditions B
1			n.d. ^{vi} (82%)	n.d. (10%)
2			95% (86%)	11% (12%)
3			86% (79%)	1% (2%)

^{vi} Trifluorotoluene co-eluted with ethyl cinnamate.

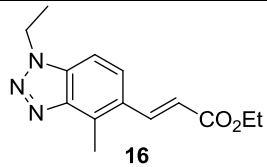
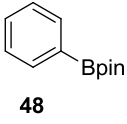
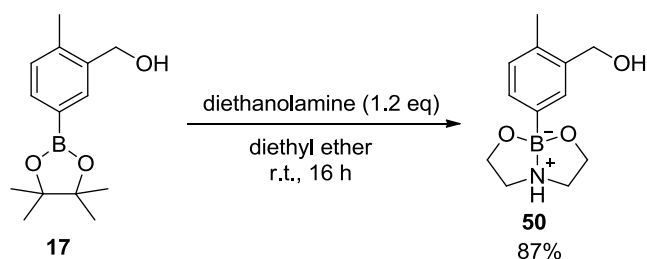
Entry	Enoate	Arylboron Reagent	Consumption of Enoate	
			Conditions A	Conditions B
4			96% ^{vii} (76%) [†]	37% (28%) [†]

Table 23. Consumption of enoate at full consumption of aryl boron reagent, determined by solution assay. Isolated yield of 1,4-addition product given in parentheses. [†]Isolated by MDAP rather than by column chromatography.

To compare the selectivity for conjugate arylation over protodeboronation afforded when using the arylboronic acid pinacol ester **17** with that of the parent boronic acid, the acid was first generated from the ester. Direct hydrolysis of the ester was not successful due to its stability, and so the acid was generated instead via the diethanolamine boronate (**50**, Scheme 55 and Scheme 56) based on a published procedure.¹⁷⁷

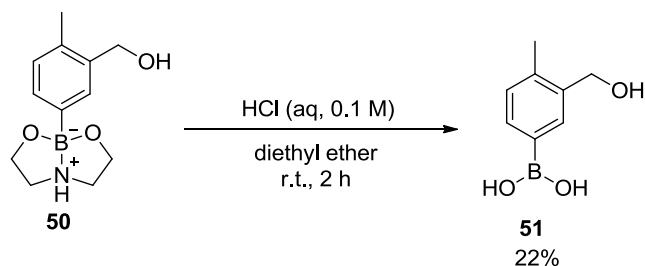


Scheme 55. Synthesis of diethanolamine boronate analogue of the boronic ester **17**.

Diethanolamine boronates have themselves been applied to palladium-catalysed cross-coupling reactions,¹⁷⁸ and could be considered to be activated for transmetalation on account of the elongated carbon–boron bond relative to that of the parent boronic acid.^{127,179} Subjection of arylboronate **50** to the 1,4-addition reaction conditions using both **L11** and norbornadiene with enoate **16** showed extremely poor reactivity (< 10% consumption of both reagents in 66 hours using ligand **L11**, and < 33% consumption of the arylboron reagent with negligible consumption of enoate **16** using norbornadiene), most likely as a result of coordination of diethanolamine to rhodium, analogously to that proposed for the base TDA-1 (Section 3.2.2, page 88). It was not determined whether or not this occurred as a result of impurities with the arylboron reagent or due to the generation of diethanolamine via some amount of hydrolysis of the boronate under the reaction conditions.

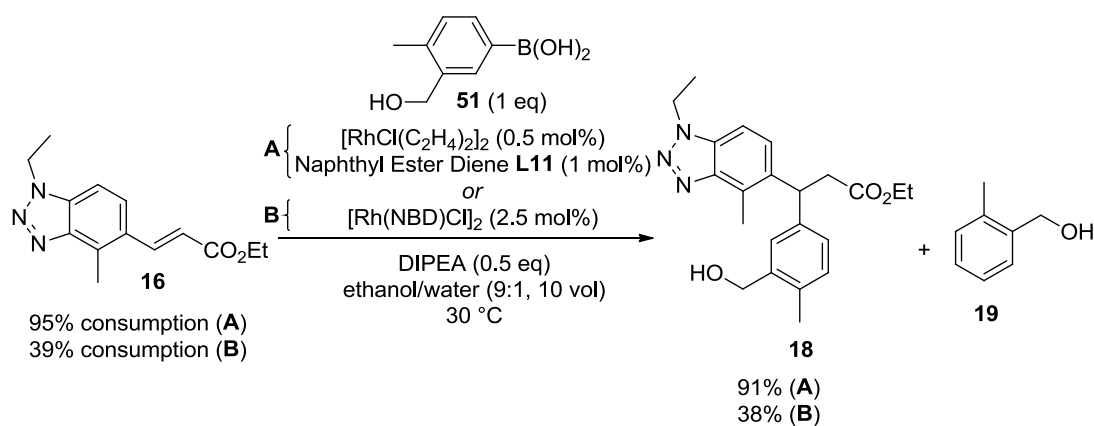
^{vii} Reaction stalled at 91% consumption of enoate **16**. An additional catalyst charge gave 96% consumption of the enoate. No deboronation product was detectable throughout the experiment.

The boronate **50** readily hydrolysed in the presence of aqueous hydrochloric acid (Scheme 56) to generate the corresponding boronic acid, however extraction of the acid from the aqueous phase proved difficult, resulting in the low yield shown.



Scheme 56. Hydrolysis of the diethanolamine boronate to give the boronic acid **51**.

The arylboronic acid **51** performed very well in the 1,4-addition reactions, giving good selectivity for arylation (Scheme 57). The selectivity was very similar to that observed using arylboronic ester **17**, and provides further evidence that a slow-release strategy of the sort commonly employed for Suzuki couplings is not important for limiting protodeboronation in this system.¹³¹ In particular, 38% consumption of the enoate was the highest observed in this work for the norbornadiene-ligated system. As expected, use of arylboronic acid **51** rather than arylboronic acid pinacol ester **17** had no noticeable effect on enantioselectivity (94% *ee* in both cases).

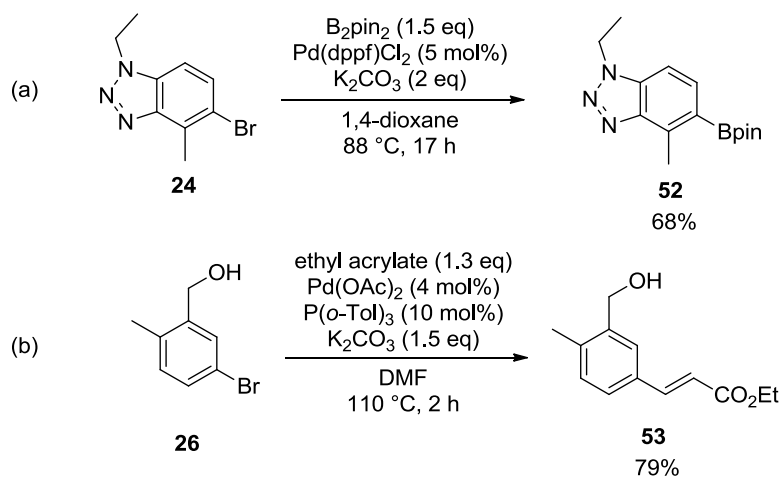


Scheme 57. Use of arylboronic acid **51** in the 1,4-addition reaction with enoate **16**.

3.3.1.5 Effect of Reversing the Coupling Partners on Reaction Selectivity for Conjugate Arylation over Protodeboronation

The final investigation of the substrates was to determine the effect on the reaction selectivity of swapping the coupling partners, such that the benzotriazole was introduced as the arylboron reagent and the benzylalcohol as the enoate. Since this work seeks to explore the utility of the chiral pool-derived ligand **L11** for industrial applications, its common availability as only the (*R*)-enantiomer demands an alternative means of generating the

opposite enantiomer of a conjugate arylation product. Since both the enoate **16** and the arylboron reagent **17** were prepared from the corresponding arylbromides (Section 3.1), swapping the direction of the coupling carries no additional synthetic demands in terms of substrate synthesis, as shown by the facile preparations of arylboron reagent **52** and enoate **53** (Scheme 58). Performing the conjugate arylation reaction with these would be expected to deliver material with the opposite absolute stereochemistry ((*R*)-**18** rather than (*S*)-**18**). In contrast, preparing the (*S*)-enantiomer of the ligand from (*R*)-carvone to deliver the opposite enantiomer of the conjugate arylation product would require a number of additional steps.¹¹⁹



Scheme 58. (a) Preparation of the benzotriazole boronic ester **51** from the corresponding bromide **24**. (b) Preparation of the benzylalcohol enoate **52** from the corresponding bromide **26**.

Under the optimised rhodium-catalysed conjugate arylation reaction conditions using **L11**, bisaryl **18** was afforded in low yield using the enoate and arylboron reagent shown in Scheme 58, with only 45% consumption of the enoate **53** observed (Table 24). Conversely, the system delivered excellent enantioselectivity, achieving an enantiomeric excess of 98% for the (*R*)-enantiomer. Running the reaction using ethyl cinnamate as the enoate showed almost identical selectivity (Entry 2), identifying the arylboron substrate **52** as being responsible for the origin of the poor selectivity. Performing the reaction with *o*-tolylboronic acid pinacol ester (Entry 3) showed the high levels of protodeboronation product to result primarily from the *ortho*-methyl group (Entry 3, cf. Entry 4). The fact that *ortho* substitution on the arylboronic ester is particularly harmful to the selectivity for the 1,4-addition may result from hindering the binding of the enoate to the resulting arylrhodium complex (see Section 3.3.3.1).

$$\text{Ar}^2\text{Bpin (1 eq)}$$

$$\text{A} \left\{ \begin{array}{l} [\text{RhCl}(\text{C}_2\text{H}_4)_2]_2 \text{ (0.5 mol\%)} \\ \text{Naphthyl Ester Diene L11 (1 mol\%)} \end{array} \right.$$

$$\text{or}$$

$$\text{B} \left\{ \begin{array}{l} [\text{Rh}(\text{NBD})\text{Cl}]_2 \text{ (2.5 mol\%)} \end{array} \right.$$

$$\xrightarrow[\text{DIPEA (0.5 eq)}]{\text{ethanol/water (9:1, 10 vol)}} \text{Ar}^1\text{CH}(\text{Ar}^2)\text{CH}_2\text{CO}_2\text{Et} + \text{Ar}^2\text{-H}$$

$$30^\circ\text{C}$$

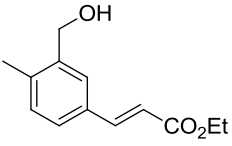
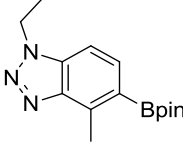
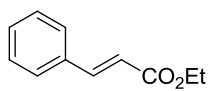
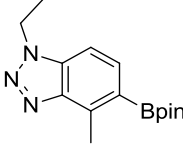
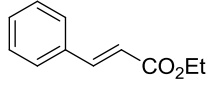
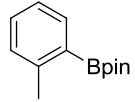
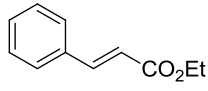
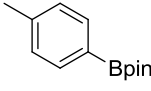
Entry	Enoate	Arylboron Reagent	Consumption of Enoate	
			Conditions A	Conditions B
1	 53	 52	45% ^{viii} (43%)	6% (4%)
2	 34	 52	46% (29%) [†]	n.d.
3	 34	 54	75% [‡]	13% [‡]
4	 34	 55	93% (75%) [†]	6% (7%) [†]

Table 24. Consumption of enoate at full consumption of aryl boron reagent, determined by solution assay. Isolated yield of 1,4-addition product given in parentheses. The protodeboronation product for Entry 1 was isolated in 75% yield from the reaction using norbornadiene. [‡]Determined by ¹H NMR with a high number of scans. [†]Isolated by MDAP rather than by column chromatography.

It is notable that the features essential for the success of the optimised reaction for the developed system using enoate **16** and arylboron reagent **17** are detrimental to the reaction when the coupling partners are reversed as in Entry 1. The *ortho*-methyl group of the benzotriazole is indispensable for reactivity when the benzotriazole is introduced as the enoate (enoate **16**, Section 3.3.1.3), whereas it significantly decreases the selectivity for conjugate arylation when the benzotriazole is present as the arylboron reagent (arylboron species **52**, Entries 1 and 2). Similarly, the triazole functionality provides an enhancement to the reaction selectivity when present as part of the enoate (enoate **16**, Sections 3.3.1.2 and 3.3.1.3), whereas it has an additional negative impact on the selectivity when it is present as part of the arylboron reagent (arylboron species **52**, Entry 2 cf. Entry 3). This additional

^{viii} Additional catalyst charge was required to give full consumption of the arylboron reagent.

negative effect of the triazole might be sufficiently explained by the much larger size of the aryl group in this case compared with arylboron species **17**, with steric effects appearing to outweigh electronic effects for the arylboron reagents when using ligand **L11** (Section 3.3.1.4). A reversal of the pharmaceutically-relevant coupling partners would therefore not be attractive for industrial applications in this case.

3.3.2 Influence of the Diene Ligand Structure on Selectivity for Conjugate Arylation over Protodeboronation

The specific substrates used in the pharmaceutically-relevant transformation have been shown to affect the selectivity observed for conjugate arylation over protodeboronation, with the benzotriazole in particular enhancing the selectivity (Section 3.3.1). However, the most significant control over the selectivity came from the choice of diene ligand, with norbornadiene consistently shown to give much worse selectivity for the desired reaction than the naphthyl ester diene **L11** gives. To probe the structural features of ligand **L11** that are important in delivering high selectivity, and those of norbornadiene that give a strong preference for the protodeboronation product, a series of diene ligands were sourced or prepared so that their performance in the reaction could be compared (Figure 43).

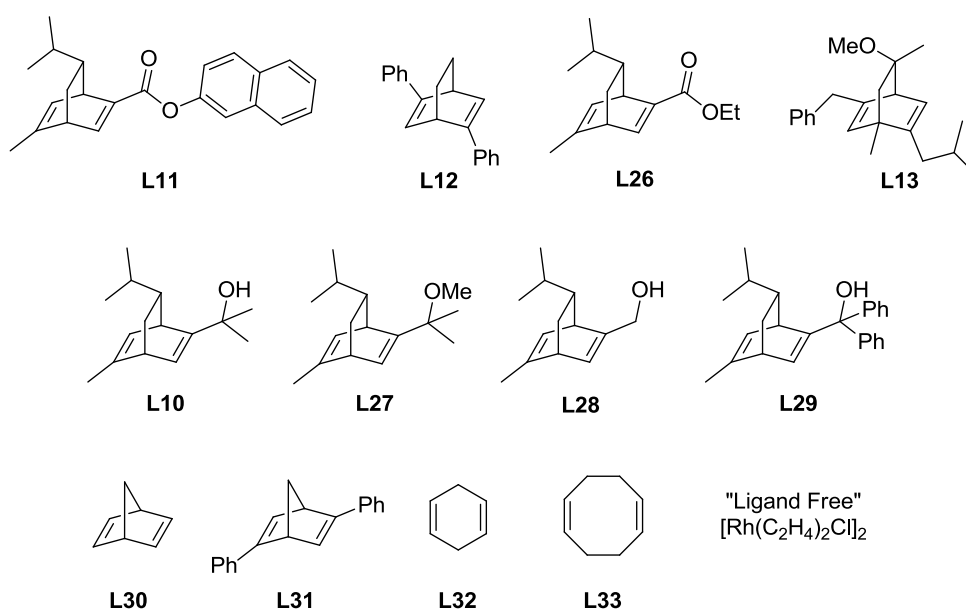


Figure 43. Diene ligands compared under rhodium-catalysed conjugate arylation conditions.

The dienes in the top two rows of Figure 43 were selected to provide contrasting functionality on the bicyclo[2.2.2]octa-2,5-diene (BOD) scaffold. Ph-BOD **L12** had already been observed to perform similarly well to diene **L11** (Section 3.2.1.3). Noting that in both ligands at least one alkene could be conjugated into the pendant group, and that aromatic

groups are present in both ligands, **L26** and **L13** were selected to probe the importance of these features. In the case of the ethyl ester **L26**, there are no aromatic groups present such that any stabilising π -stacking interaction between the arylrhodium intermediate and aromaticity on the ligand is prevented whilst still allowing conjugation into an electron-withdrawing group and any interactions that are not dependant on aromaticity, and the additional methylene linker between the phenyl group and the alkene in **L13** prevents conjugation of aromatic functionality with the alkene.

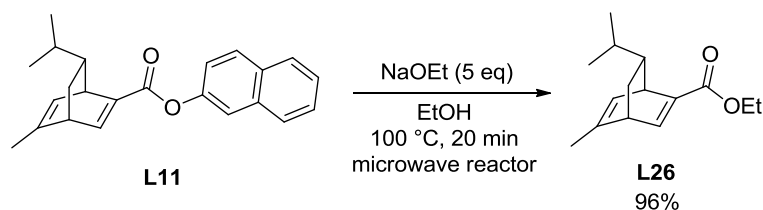
The hydroxy-containing ligand **L10** had already been shown to perform worse than other diene ligands in the initial ligand investigations (Section 3.2.1.1). Whilst ligand **L13** provides a comparison with the dienes **L11** and **L12** to indicate if the lack of alkene conjugation is important in this, **L29** contains unconjugated phenyl functionality to provide an indication of whether or not the lack of any aromatic groups causes the lower selectivity. The ligand **L29** is extremely bulky at the tertiary alcohol sp^3 -carbon, which could itself influence reactivity. The two ligands **L27** and **L28** were therefore prepared to observe to what extent it is simply the bulk of the diene **L10** or the hydroxy-functionality that lowers the selectivity of the ligand for conjugate arylation.

Ph-NBD **L31** was selected as a means of bridging between the norbornadiene ligand **L30**, with a strong preference for protodeboronation, and Ph-BOD **L12**, with a strong preference for conjugate arylation. The result given by **L31** was expected to give an indication of the extent to which the norbornadiene scaffold or the lack of functionality were responsible for the poor activity of norbornadiene for conjugate arylation. Simple dienes **L32** and **L33** were selected with the intent of further exploring the role of the structure of the scaffold, although use of **L32** as a sacrificial source of hydrogen in transfer hydrogenation^{180,181} and a reported failed attempt to isolate $[\text{RhCl}(\text{L32})]_2$ (possibly as a result of the planarity of the diene)¹⁸² tempered expectations for the use of 1,4-cyclohexadiene as a ligand. Finally, the ethylene-complexed rhodium source was selected to be used in the absence of any diene ligands, to determine whether the poor performance of norbornadiene could be explained by it being readily exchanged for solvent or substrate.

3.3.2.1 Diene Ligand Syntheses

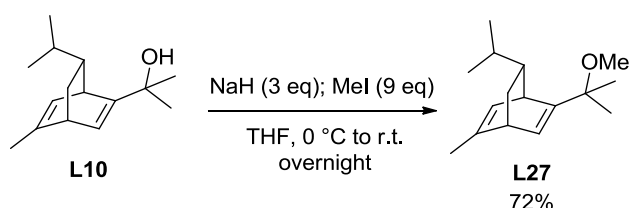
The ethyl ester ligand **L26** was prepared by transesterification of the naphthyl ester **L11** under basic conditions, with full consumption of the starting material important on account of the difficulty of separating **L26** from **L11** by column chromatography. The procedure in

Scheme 59 delivered the desired material in high yield and purity, with none of the naphthyl ester detectable by NMR or HPLC.



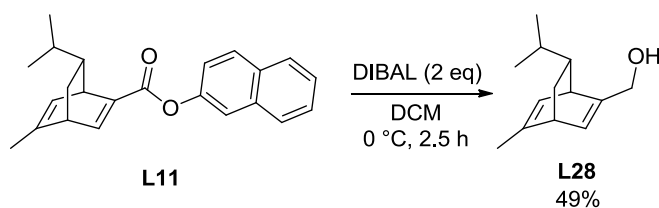
Scheme 59. Transesterification of L11 to give the ethyl ester analogue L26.

The preparation of the methoxy-ether diene **L27** from the tertiary hydroxy-substituted diene **L10** was based on a literature procedure (Scheme 60) and afforded the required diene in adequate yield.¹¹⁵



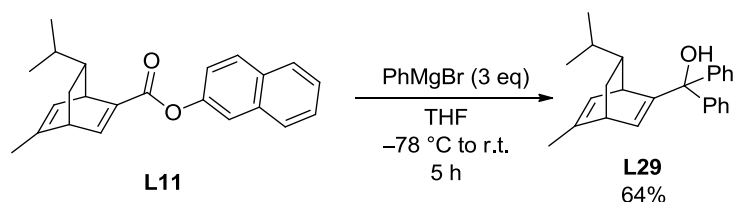
Scheme 60. Esterification of the hydroxy-containing diene L10.

The same literature report detailed a synthesis of diene **L28** from the methyl ester analogue of **L11**, and this was adapted here for its preparation from the naphthyl ester **L11** (Scheme 61). Since the product **L28** was found to co-elute with naphthol on silica in heptane/ethyl acetate solvent systems, a basic wash with aqueous K_3PO_4 was added to the work up. Unfortunately this appeared to draw out as much of the desired product as it did naphthol from the organic phase, impacting the isolated yield. Use of DIBAL enabled a clean reaction, in contrast to an attempt employing LiAlH_4 .



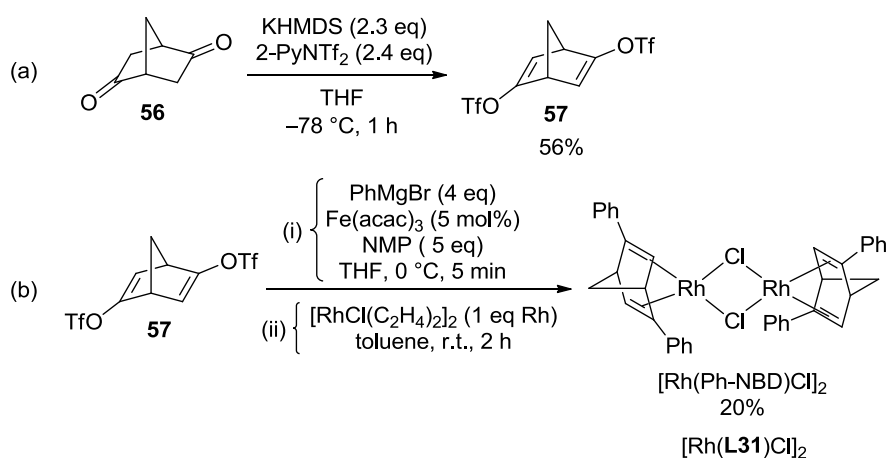
Scheme 61. Reduction of the naphthyl ester L11 to the primary alcohol using DIBAL.

Preparation of the previously unreported bisphenyl tertiary alcohol **L29** by treatment of the naphthyl ester **L11** with phenylmagnesium bromide (Scheme 62) proceeded smoothly once the temperature was allowed to warm above -78 °C, giving the product in excellent purity and good yield after column chromatography.



Scheme 62. Reduction of the naphthyl ester **L11** with an excess of phenylmagnesium bromide to give the tertiary alcohol **L29**.

The most challenging ligand to prepare was Ph-NBD **L31** (Scheme 63). Its synthesis and isolation as the rhodium salt $[\text{Rh}(\text{Ph-NBD})\text{Cl}]_2$ is detailed in the literature,¹¹⁷ and its synthesis in this work was based closely on that report. Preparation of the bistriflate **57** from diketone **56** (Scheme 63a) was performed with careful control of the temperature to give an adequate yield of the acid-sensitive product.



Scheme 63. Preparation of ligand **L31**, isolated as the rhodium chloride salt $[\text{Rh}(\text{Ph-NBD})\text{Cl}]_2$.

The Ph-NBD ligand itself could be produced consistently in the iron-catalysed Kumada coupling shown in Scheme 63b(i), along with significant quantities of the biphenyl side-product. However, significant difficulty was encountered in its isolation and subsequent complexation with rhodium. The authors of the literature report warn that **L31** is poorly stable with respect to decomposition until it is complexed to the rhodium, although the dominant mechanisms and causes of this are not well understood. The literature procedure involves isolating the crude ligand (with biphenyl) from the Kumada reaction mixture before its dissolution in toluene and addition of the rhodium salt. The rhodium complex $[\text{Rh}(\text{Ph-NBD})\text{Cl}]_2$ exhibits good stability.

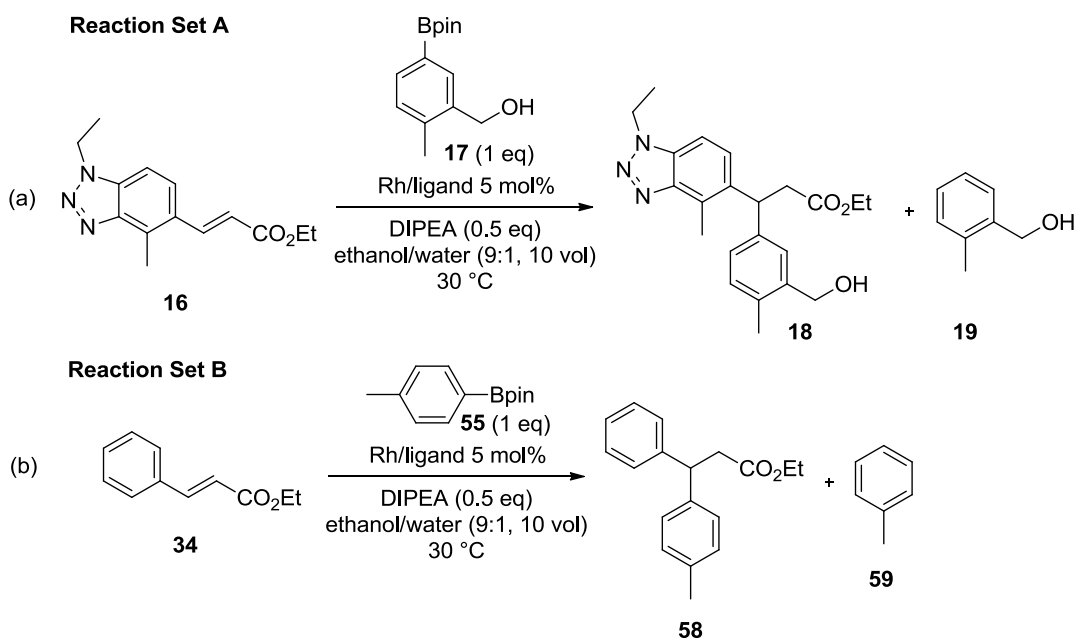
Multiple attempts to prepare the complex failed, and careful monitoring throughout the procedures from setting up the Kumada reaction through to the work up of the crude ligand and complexation to rhodium gave confidence in the conclusion that the ligand was successfully formed and survived throughout the work up (with biphenyl a convenient

internal HPLC standard), but began to decompose more rapidly upon removal of the volatiles (mainly heptane) from the washed, dried and filtered (silica plug) organic phase. Performing the work up with pentane rather than heptane enabled *in vacuo* removal of the volatiles to be avoided altogether; toluene and $[\text{Rh}(\text{C}_2\text{H}_4)_2\text{Cl}]_2$ were instead added directly to the crude pentane solution, which was blown down under a nitrogen flow. Despite the use of pentane seeming to result in poorer separation during the work up of the Kumada coupling, with precipitation of unknown solids, successful isolation of the red-orange complex by column chromatography was achieved in low, but sufficient, yield (Scheme 63b).

It seems plausible that addition of a stoichiometric rather than substoichiometric quantity of rhodium to the crude ligand relative to the bistriflate **57** contributed to the low yield. When a substoichiometric quantity of rhodium was added to the crude ligand, the only coloured band that eluted through the silica column corresponded to the desired complex. However, when a stoichiometric quantity was added, an earlier eluting coloured band was collected, which decomposed on standing. A similar coloured band was collected in the failed attempts to prepare the complex, and it seems reasonable to propose that the addition of too much rhodium to the ligand resulted in a proportion of the rhodium chloride dimers only ligating one molecule of diene **L31** rather than the required two.

3.3.2.2 Comparative Analysis of the Selectivity for Conjugate Arylation over Protodeboronation Afforded by Diene Ligands

The performance of the diene ligands for rhodium-catalysed conjugate arylation was compared using both the pharmaceutically-relevant substrate set (substrates **16** and **17**, Reaction Set A) and ethyl cinnamate **34** with *p*-tolylboronic acid pinacol ester **55** (Reaction Set B), in 1:1 stoichiometry (Scheme 64). In each case, a catalyst loading of 5 mol% was employed, and the reaction mixtures were held at 30 °C for 30 minutes before addition of DIPEA. Where available, the pre-ligated rhodium chloride salts were used (such as $[\text{Rh}(\text{COD})\text{Cl}]_2$), but otherwise $[\text{Rh}(\text{C}_2\text{H}_4)_2\text{Cl}]_2$ was used as the rhodium source with the ligand and rhodium charged in 1:1 stoichiometry.



Scheme 64. (a) The pharmaceutically-relevant substrate set (Set A) reaction and (b) the simple substrate set (Set B) reaction used to compare the selectivity of different diene ligands for conjugate arylation over protodeboronation.

The reaction mixtures were sampled over a 12-hour period, and the molar amount of each of the species being monitored was calculated using relative response factors determined from purified standards, assuming that the enoate either reacted to give the bisaryl product or underwent no reaction at all. The results confirmed that this assumption was valid to within a small percentage error. The molar ratios of conjugate arylation product to deboronation product are summarised in Table 25, averaged over appropriate timepoints, and were corroborated by ^1H NMR spectroscopy in the case of Reaction Set A. Due to their poor reactivity, the reactions using ligands **L29**, **L32** and using the ethylene-ligated rhodium salt without diene present are omitted from the table and discussed separately.

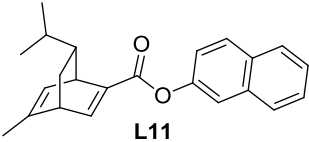
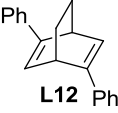
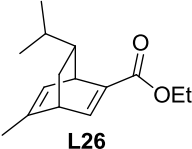
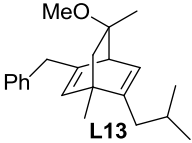
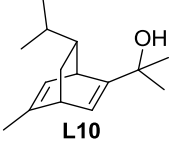
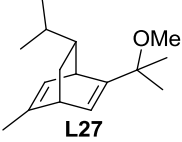
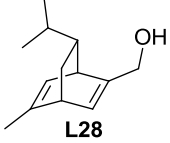
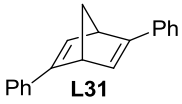

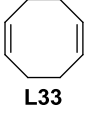
Entry	Ligand	Reaction Set A Arylation/Deboronation Product Ratios	Reaction Set B Arylation/Deboronation Product Ratios
1	 L11	97:3	90:10
2	 L12	98:2	97:3
3	 L26	98:2	92:8
4	 L13	90:10	84:16
5	 L10	44:56	54:46
6	 L27	88:12	75:25
7	 L28	53:47	81:19
8	 L31	97:3	97:3
9	 L30	28:72	10:90
10	 L33	91:9	77:23

Table 25. Summary of molar product ratios under rhodium-catalysed conjugate arylation conditions using 10 different diene ligands. Set A (enoate 16, arylboron reagent 17) and Set B (ethyl cinnamate 34, *p*-tolylboronic acid pinacol ester 55) refer to Scheme 64. Ratios determined by HPLC using relative response factors and summed to 100, and averaged over appropriate timepoints.

Each of the ligands in Table 25 enabled clear molar ratios of the bisaryl conjugate arylation products **18** and **58** to the protodeboronation products *o*-tolylmethanol **19** and toluene **59** respectively to be determined, with little variation observed as the reactions progressed. The results show a spread of ratios, enabling a number of general observations to be extracted about the important features of ligand **L11** for delivering high selectivity for the conjugate arylation product. It is also worth noting that the ratios here are consistent with the results in Section 3.3.1.

The first general observation to make is that the shape of the diene scaffold appears to hold significance in determining the selectivity of the reaction. The difference noticed in Section 3.3.1 between ligands **L11** and norbornadiene **L30** could have been speculated either to have been caused by a lack of pendant functionality on the norbornadiene scaffold or by the different shapes of the scaffolds themselves. Comparing the results for norbornadiene (**L30**, Entry 9) with COD (**L33**, Entry 10) and also with the BOD-scaffolded ligand **L27** (Entry 6) clearly demonstrates that a lack of functionalisation on a diene ligand cannot be responsible alone for a selectivity for protodeboronation rather than conjugate arylation. Interestingly, COD and ligand **L27** displayed similar product ratios with both substrate sets.

The second observation to make is that conjugation with the alkenes has a positive effect on the selectivity for conjugate arylation over protodeboronation. Most strikingly, whilst virtually all of the ligands show a notable drop in selectivity for the arylation product when moving from the pharmaceutically-relevant substrate set (Set A) to the ethyl cinnamate/*p*-tolylboronic acid pinacol ester substrate set (Set B), the two bisphenyl ligands Ph-BOD (**L12**, Entry 2) and Ph-NBD (**L31**, Entry 8) show nearly identical selectivity with both systems. Impressively, the functionalisation of norbornadiene with two phenyl groups more than compensates for any disadvantage that the norbornadiene scaffold may give.

Substrate Set B suggests that losing conjugation with one of the alkenes causes a drop in selectivity (**L11**, Entry 1 and **L26**, Entry 3 cf. **L12**, Entry 2), and a further drop is seen with both substrate sets on taking the phenyl ring out of conjugation with the alkene in the Carreira DOLEFIN ligand (**L13**, Entry 4). There is some evidence that losing the phenyl altogether has still a further impact on selectivity (for example Entry 6, Set B) although there may be alternative explanations for this (Figure 54, page 154).

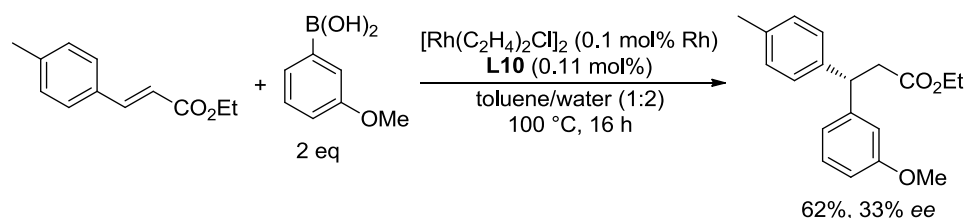
The similarity between the performance of esters **L11** and **L26** demonstrates that there is no advantage in selectivity for arylation over protodeboronation as a result of using the naphthyl ester rather than an alkyl ester. If any secondary interactions are important in stabilising the

arylrhodium intermediate, the naphthyl group appears to be perfunctory. Further comparison between the performance of the esters (**L11**, **L26**) and the bisphenyl dienes (**L12**, **L31**) with Substrate Set B suggests that the alkenes do not have to be conjugated to specifically electron-withdrawing groups, or at least it appears to show that some conjugation with both alkenes is more beneficial than conjugation of just one alkene to an electron-withdrawing motif.

One final general observation regards hydroxy functionality and steric bulk. As already noted, nearly all of the ligands show a drop in selectivity for Substrate Set B compared to Substrate Set A. Uniquely, the ligands containing hydroxy functionality (**L10** and **L28**) show the reverse selectivity order, with the higher reaction selectivities for conjugate arylation achieved using Substrate Set B. As anticipated from previous results, **L10** (Entry 5) showed unusually poor selectivity for conjugate arylation in both cases, especially with the pharmaceutically-relevant substrate set (Set A). Ligands **L27** (Entry 6) and **L28** (Entry 7) were intended to give an indication of the extent to which the hydroxy motif and the vinylic steric bulk were each responsible for this. Curiously, it appears that whilst both factors contributed to the poor selectivity for both substrate sets in an almost summative fashion, Set A was more negatively affected by the presence of a hydroxy group while Set B was more negatively affected the vinylic bulk.

Although not the focus of this discussion, the asymmetric induction delivered by **L10** requires comment. Enantiomeric excesses were measured for Reaction Set A, and three ligands were found to favour (*R*)-**18** rather than (*S*)-**18** (as favoured by **L11**): (*S,S*)-**L12** (–88% *ee*), (*S,S,S*)-**L13** (–72% *ee*) and (*R,R,R*)-**L10** (–48% *ee*). The results using ligands **L12** and **L13** are readily accounted for by the stereochemical model described in Section 1.3.2.1, along with the results for the remainder of the chiral dienes, all of which favoured (*S*)-**18**. However, the model cannot account for the stereochemistry induced by ligand **L10**, which is the opposite to that delivered by either **L27** (63% *ee*) or by **L28** (75% *ee*).

Although the unusual asymmetric induction of ligand **L10** was not reported in early literature either for a 1,2-addition reaction to a nosylimine¹¹² or for a 1,4-addition reaction to enones,¹¹⁵ the result is concordant with the previous experiments performed in Section 3.2.1.1 and was also acknowledged in a 2015 report using an enoate substrate (Scheme 65).¹⁸³ It is curious that both the free hydroxy (cf. **L27**) and the methyl groups (cf. **L28**) are required for the stereochemical preference to reverse.



Scheme 65. A literature report of conjugate arylation to an enoate using diene **L10**, giving concordant stereochemical induction to that observed in this work.

The necessary orientations of an enoate to deliver the observed enantioselectivities using ligands **L27** and **L10** are shown in Figure 44a and Figure 44b respectively. Figure 44a shows the stereochemical model, with the bulky pendant diene substituents dictating the preferred reactive orientation of the enoate for the carboration step. In Figure 44b, a hydrogen-bonding interaction has been invoked to account for the reversal of the orientation of the enoate. It may be that the methyl groups are preferentially directed away from any steric congestion around the metal centre, causing the hydroxy group to be oriented correspondingly towards the enoate. This orientation of the hydroxy group would not be necessary using ligand **L28**, without the dimethyl groups.

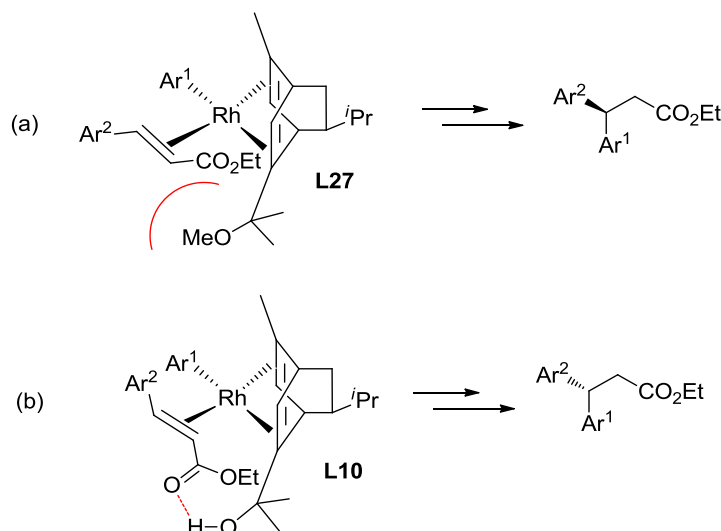
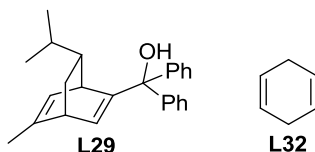


Figure 44. Proposed model to account for the stereochemical preference induced by ligand **L10**. (a) The standard steric model, which successfully predicts the stereochemical preference induced by ligand **L27**. (b) A hydrogen-bonding model, proposed here to account for selectivity delivered by ligand **L10**.

The diphenyl analogue of **L10** (**L29**, below) was intended to probe whether or not unconjugated phenyl motifs would contribute to any improvement in selectivity relative to **L10**, however the results suggested that the bulk of the ligand was too great for an active conjugate arylation catalyst to form, perhaps with the steric bulk being so significant as to prevent coordination of the diene itself to metal centre. Using both substrate sets, < 2% conversion of the enoate to the 1,4-addition product was observed over the time course, and < 5% conversion of the arylboron reagent to the protodeboronation product occurred in

4 hours. A similar lack of reactivity was observed using 1,4-cyclohexadiene (**L32**, below), presumably as a result of cyclohexadiene either not coordinating to the rhodium, or being reduced upon coordination.



In both cases, these reactions were set up using the unligated dienes with $[\text{RhCl}(\text{C}_2\text{H}_4)_2]_2$ as the rhodium source, and the reaction profiles that they generated were not dissimilar from those using $[\text{RhCl}(\text{C}_2\text{H}_4)_2]_2$ with no diene ligand added (Figure 45). Notably, the results of these reactions were distinctly different from those observed during the initial experiments to select a catalyst system in Section 3.2.1.1 (see Table 4, Entry 1, page 51). Figure 45 shows that the amount of arylboron reagent consumed without concomitant generation of either the bisaryl or protodeboronation products increased to 10% over the first hour before plateauing. Similar observations were made using Substrate Set B during the first five minutes. This observation would be compatible with an oxidative homocoupling of the arylboron reagent to give a catalytically inactive rhodium species. Evidence of the homocoupled products was not clearly observed, but the non-catalytic activity of the rhodium in an unexpected reaction pathway is nevertheless demonstrated here.

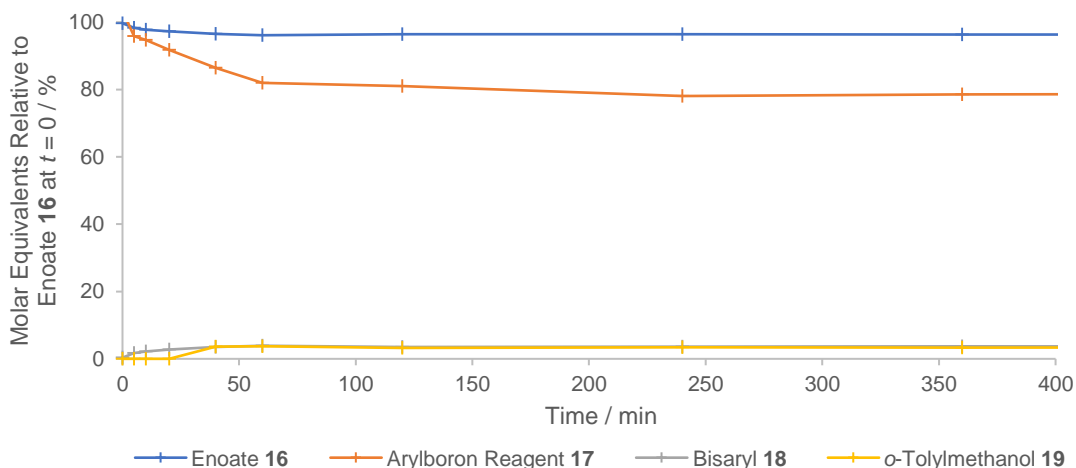


Figure 45. Reaction profile for Substrate Set A with $[\text{RhCl}(\text{C}_2\text{H}_4)_2]_2$ and no diene ligand.

Importantly, the results using $[\text{RhCl}(\text{C}_2\text{H}_4)_2]_2$ with no diene ligand added rule out any significant activity for either conjugate arylation or protodeboronation without a diene ligand coordinated to the rhodium. The inactivity of $[\text{RhCl}(\text{C}_2\text{H}_4)_2]_2$ for conjugate arylation under these conditions is an advantage, since it ensures that no significant achiral reaction can occur when the ethylene-ligated rhodium salt is used as the rhodium salt in combination with

a chiral diene ligand, as in the optimised process. It also demonstrates that the poor selectivity of norbornadiene for conjugate arylation is unlikely to be a result of the diene being exchanged for either solvent or substrate.

An example of the reaction profile over time generated for the successful reactions is shown in Figure 46, for the naphthyl ester diene **L11** with Substrate Set A. In this case, *o*-tolylmethanol **19** is undetectable until 40 minutes into the reaction, with the product ratio changing very slightly from 98:2 (**18:19**) at this point to 97:3 (**18:19**) by the end of the reaction.

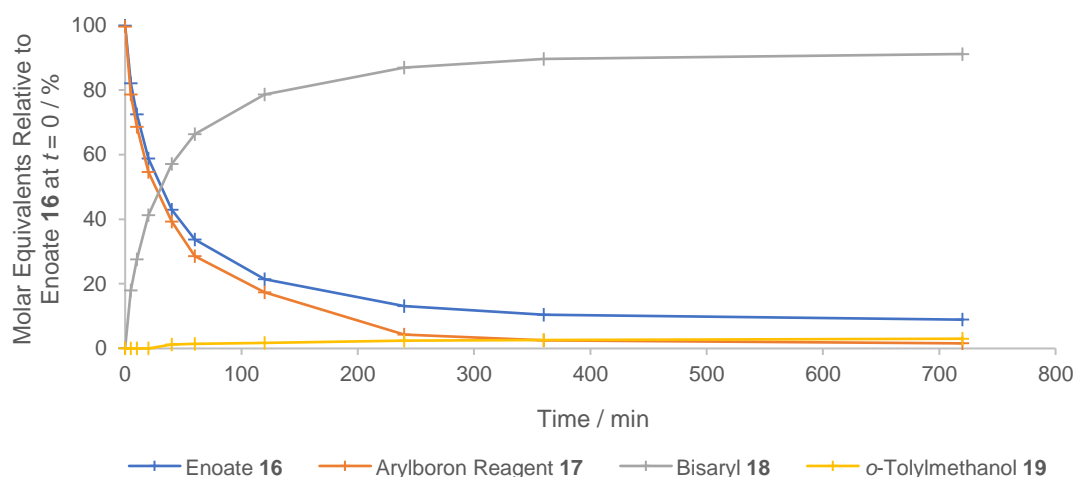


Figure 46. Reaction composition over time for the naphthyl ester ligand **L11 with Substrate Set A.**

In general, the product ratios either remained reasonably stable throughout the duration of the experiment or the proportion of bisaryl product decreased slightly as might be expected due to the dependence of forming the bisaryl product on the concentration of enoate. The only exceptions to this were the reactions that employed the DOLEFIN ligand **L13**. In these cases, the proportion of bisaryl product relative to the protodeboronation product increased from 87:13 (bisaryl/desboron products) at 9% consumption of enoate **16** to 92:8 (bisaryl/desboron products) within 27% consumption of enoate **16** in the case of Substrate Set A, and from 77:23 (bisaryl/desboron products) at 7% consumption of enoate **34** to 88:12 (bisaryl/desboron products) within 35% consumption of enoate **34** in the case of Substrate Set B. In both cases, the proportion then decreased again for the remainder of the reaction with final product ratios of 82:18 for Substrate Set A and 85:15 for Substrate Set B.

The COD ligand also behaved unusually, but only with Substrate Set A (Figure 47, lower reaction profile over time). After an initial formation of *o*-tolylmethanol **19** in approximately 5% in situ yield with a product ratio of 85:15 (products **18:19**) within the first 5 minutes

following addition of DIPEA, no further formation of the deboronation product was observed within the subsequent 2 hours, such that the product ratio improved to 93:7 as the bisaryl **18** continued to be produced with remarkable selectivity. In contrast, the reaction using COD with Substrate Set B proceeded similarly to those using other ligands. This may relate to the activation of the catalyst and the possible role of the benzotriazole in moderating the extent of deboronation, but a sufficiently satisfying rationale for this behaviour has not been identified.

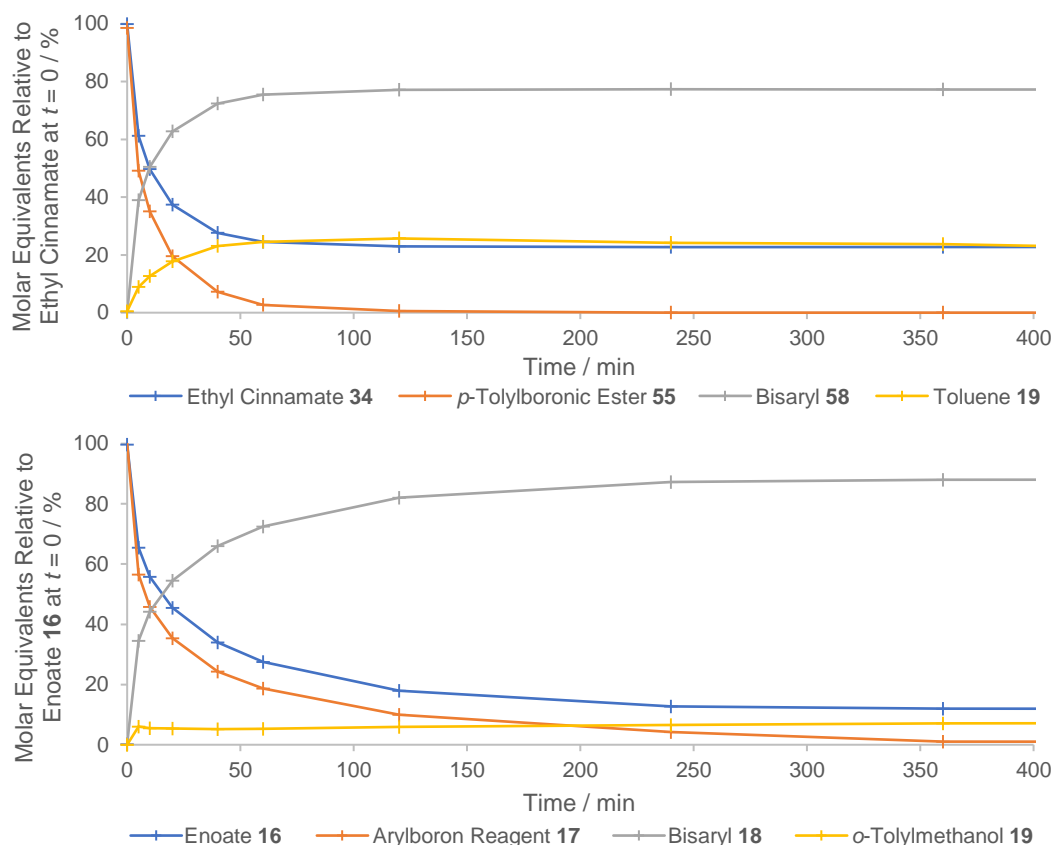


Figure 47. Top: The reaction composition over time for the COD ligand with Reaction Set B. Bottom: The reaction composition over time for the COD ligand with Reaction Set A.

A comparison of the rates of consumption of the arylboron reagents in both substrate sets for a selection of ligands is displayed in Figure 48. In almost all cases, the reactions between ethyl cinnamate and *p*-tolylboronic acid pinacol ester (Substrate Set B) gave faster consumption of the arylboron reagent than those between the pharmaceutically-relevant substrates (Substrate Set A). The result shown in Figure 42 (page 128) for the use of the naphthyl ester diene **L11** with only the arylboron reagent **17** and no enoate **16** present is reproduced here, with the initial rate of arylboron consumption similar to the reaction using ethyl cinnamate and *p*-tolylboronic acid pinacol ester and faster than the rate using arylboron reagent **17** with the benzotriazole-containing enoate **16**. The suggestion that the

benzotriazole may act to inhibit the protoderhodation pathway (as discussed in Section 3.3.1.3) is consistent with these results. The one exception to this was with the Ph-NBD ligand **L31**, which proceeded extremely slowly and with remarkably high selectivity for the conjugate arylation product in both cases.

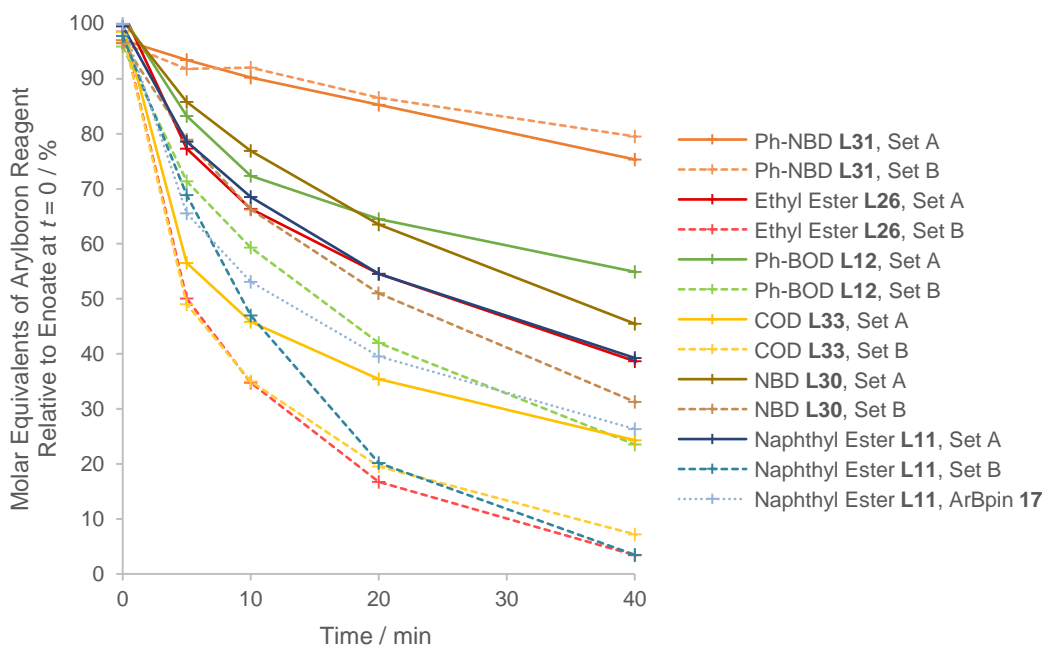


Figure 48. Rates of arylboron consumption for selected ligands, comparing across Substrate Sets A and B.

Looking across certain groups of ligands a relationship between the rate of arylboron consumption and the overall selectivity of the reaction seems to be present. For example, for both substrate sets in Figure 48 the consumption of arylboron reagent using Ph-NBD **L31** proceeds much more slowly than when using the naphthyl ester **L11** which in turn proceeds more slowly than COD **L33**, correlating with the increased proportion of protodeboronation product in this order. However, using Substrate Set A the selectivity difference between ligands **L31** and **L11** was not as significant as the rate difference might suggest, and the rates of consumption using norbornadiene **L30** at least show that the relationship is not true across all of the ligands, demonstrating that caution is required in comparing rates. Such caution is necessary not only because deactivation pathways for the rhodium catalysis have not been established, but also because the selectivity between protoderhodation and conjugate arylation would depend on the relative rates of the protoderhodation and 1,4-addition pathways from the arylrhodium intermediate, and because transmetalation may be rate-limiting if these systems behave similarly to the systems discussed in Section 1.3.2.

3.3.3 Mechanistic Considerations for Reaction Selectivity for Conjugate Arylation over Protodeboronation

The mechanistic details of the operative conjugate arylation and protoderhodation pathways of the arylrhodium intermediates under conjugate addition conditions are not known to have been probed in any depth, with interest generally directed towards a detailed understanding of the asymmetric induction of the conjugate arylation,^{72–74,184–187} and some attention also given to the transmetalation step.^{81,82} Nevertheless, a first principles consideration of the properties of the dienes and the factors that would impact possible pathways can account for many of the selectivity differences observed in the previous two sections.

The binding of an alkene to a transition metal is classically described by the Dewar-Chatt-Duncanson model, whereby an alkene donates electron density towards the metal centre from its π HOMO via a σ -type electron donation and accepts electron density from the metal centre into its π^* LUMO via a π -type electron-accepting interaction (Figure 49).^{188,189}

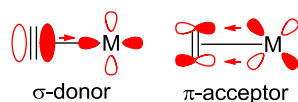


Figure 49. Schematic of the Dewar-Chatt-Duncanson model of the bonding between an alkene and a transition metal.

The donation of electron density from an alkene π orbital towards a metal centre and especially the back-donation of electron density from the metal centre into the alkene π^* orbital cause a weakening of the carbon–carbon double bond. As a result, the carbon–carbon bond length can be used as a measure of the extent of bonding between the metal and the alkene. With this in mind, available crystal structures of relevant $[\text{RhCl}(\text{diene})]_2$ complexes were extracted from the literature and the bond lengths measured. Rhodium chloride complexes with Ph-BOD **L12**, Ph-NBD **L31**, the ethyl ester **L26**, COD **L33** and norbornadiene **L30** ligands were studied (Table 26).

Entry	Ligand	Complex	C–C Double Bond Mean Length / Å	Reaction Set B Arylation/Deboronation Product Ratio
1	L12	$[\text{Rh}(\text{Ph-BOD})\text{Cl}]_2$	1.413 ⁷¹	97:3
2	L31	$[\text{Rh}(\text{Ph-NBD})\text{Cl}]_2$	1.411 ¹¹⁷	97:3
3	L26	$[\text{Rh}(\text{L26})\text{Cl}]_2$	1.410; 1.394 ¹⁹⁰	92:8
4	L33	$[\text{Rh}(\text{COD})\text{Cl}]_2$	1.399 ¹⁹¹	77:23
5	L30	$[\text{Rh}(\text{NBD})\text{Cl}]_2$	1.396 ¹⁹²	10:90

Table 26. Comparison of the average alkene bond lengths in literature crystal structures. The final column is reproduced from Table 25.

In each case the carbon–carbon double bond is elongated relative to free ethylene (1.330 Å),¹⁹³ approaching the carbon–carbon single bond length of ethane (1.522 Å) to differing extents.¹⁹⁴ The trend in the carbon–carbon bond lengths broadly correlates with the trend in product ratios observed for these ligands (Table 25, page 140), such that ligands exhibiting the longest bond lengths gave the highest ratios of conjugate arylation product to protodeboronation product whilst those exhibiting the shortest bond lengths gave the lowest ratios of conjugate arylation product to protodeboronation product. Equivalently, complexes in which there is a stronger bonding interaction between the diene and the rhodium gave higher selectivities for conjugate arylation over protoderhodation.

Additionally, the bonding and antibonding orbitals of a set of unligated dienes were calculated by a restricted Hartree-Fock method, as for the enoates in Section 3.3.1.2. The orbital energies are given in Table 27, along with the calculated energies for the unsubstituted BOD scaffold (Entry 7). Whilst the orbital energies of the unligated ligands are not the sole factors in determining the ability of the dienes to bind to the rhodium centre, a similar trend can broadly be identified, particularly with the dienes calculated to have lower LUMO energies giving the highest selectivities for conjugate arylation.

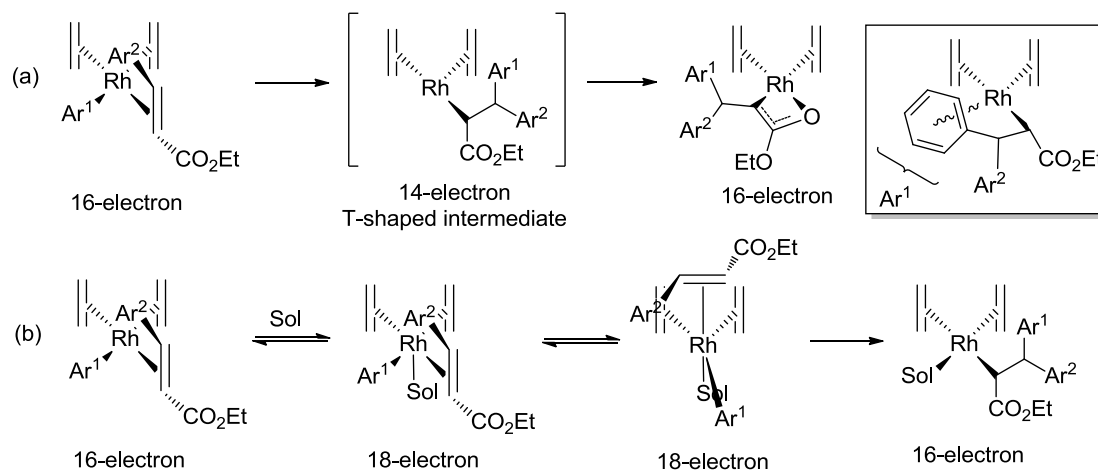
Entry	Ligand	Orbital Energy / eV		Reaction Set B Arylation/Deboronation Product Ratio
		Alkene HOMO	Alkene LUMO	
1	L12	-8.124	2.686	97:3
2	L31	-7.961	2.328	97:3
3	L26	-9.061; -9.922	2.874; 4.819	92:8
4	L11	-9.173; -10.065	2.671; 4.725	90:10
5	L33	-9.357	4.417	77:23
6	L30	-8.798	3.488	10:90
7	BOD	-9.071	3.767	n.d.

Table 27. HOMO and LUMO energies calculated for a selection of dienes by a restricted Hartree-Fock method. The final column is reproduced from Table 25.

The observation that alkene ligands enable faster rates of transmetalation than phosphine ligands (Section 1.3.4) has often been attributed to the π -accepting character of the dienes. Since transmetalation has been identified as the rate-determining step of the systems used in kinetic studies (Section 1.3.2), diene ligands have been recognised to enable conjugate arylations to proceed with decreased protodeboronation as a result of the lower temperatures required by these typically more active catalyst systems.⁵⁵ The reactions comparing the reaction selectivity using different diene ligands in Section 3.3.2.2 were all performed at the same temperature, and so there must be additional ways in which the properties of the ligands affect the relative proportions of conjugate arylation and protodeboronation products.

3.3.3.1 Effects of Diene Ligands and Substrates on Ligand Substitution Reactions

Whilst mechanistic understanding of the protoderhodation and conjugate arylation pathways is limited, the relationship between ligand properties and reaction selectivity may be partly explained by considering the classic ligand exchange mechanism for a square planar 16-electron complex.¹⁹⁵ Regardless of the mechanisms by which protoderhodation of the aryl group might occur, it is certainly the case that a solvent ligand must be exchanged for the enoate in order for conjugate arylation to proceed. The more readily this exchange can take place, the higher the ratio of conjugate arylation product to protodeboronation product can be expected to be. By analogy with the accepted mechanisms for carbonylation,¹⁹⁶ two possible pathways by which the conjugate arylation could subsequently occur are given in Scheme 66.^{ix}



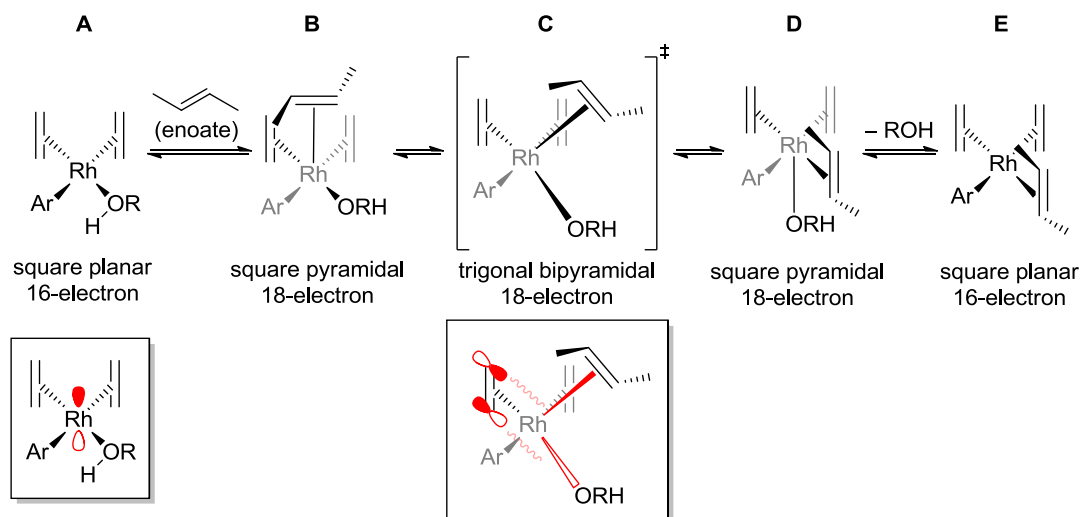
Scheme 66. Suggested pathways for conjugate arylation to occur from the rhodium-aryl-enoate intermediate, by analogy with carbonylation mechanisms. Unspecified solvent is represented by Sol.

The published computational studies to explore the transfer of chirality to the conjugate arylation product in the carborhodation step have assumed the pathway in Scheme 66a,^{72–74,184,186} and certainly this scheme accounts most readily for the asymmetric induction typically observed (cf. Section 1.3.2.1). The T-shaped intermediate could be envisaged to be stabilised initially by the migrated aryl group (insert), and would then collapse to the oxa- π -allylrhodium complex observed in the original mechanistic studies (Section 1.3.2).⁶⁸

The classic ligand exchange mechanism for a square planar 16-electron complex is shown in Scheme 67, in which the starting point is the rhodium complex resulting from transmetalation of the aryl group from boron to rhodium (Complex A), and the end point is

^{ix} Throughout this section the representations of diene ligands coordinated to rhodium typically omit the full structures of the scaffolds for clarity.

the rhodium complex with the enoate bound instead of a solvent molecule (Complex **E**, the starting point in Scheme 66).¹⁹⁵ Given that little is understood of the protoderhodation mechanism, it is important to note that whilst it might be the case that either Complex **A** or Complex **E** could interact with a solvent molecule to protolytically cleave the rhodium–aryl bond, only Complex **E** is set up for subsequent insertion of the aryl group into the enoate to give the conjugate arylation product. Therefore, it is reasonable to expect that more facile ligand exchange to transform Complex **A** into Complex **E** will result in a higher proportion of conjugate arylation product forming.



Scheme 67. The classic ligand exchange mechanism for a square planar 16-electron complex, showing exchange of a solvent ligand ($R = \text{Et}$ or H , i.e. EtOH or H_2O) for the enoate electrophile represented as an *E*-alkene.

It should firstly be noted that the accepted mechanism for ligand exchange on a square planar rhodium (I) complex is associative, with the incoming ligand initially interacting with the empty rhodium p_z orbital lying perpendicular to the xy -plane defined by the already-bound ligands to give a square pyramidal 18-electron complex (Complex **B**).^{197,x} In order for exchange to take place, this new ligand must transfer onto the xy -plane with the outgoing ligand now sat along the z -axis (Complex **D**), from which position dissociation can occur to give the exchange product (Complex **E**). The transition state for this rearrangement involves the incoming, outgoing and the *trans*-positioned ligands defining the trigonal plane of a temporary trigonal bipyramidal structure (Transition State **C**, shown with the ligands defining the temporary xy -plane in black).

The rate of this ligand substitution is significantly affected by the ligand *trans* to the leaving group in Complex **A**. This effect is known as the “*trans* effect”, and can consist of two

^x Throughout this section the axes are defined with no regard for the identity of the ligands such that, in the case of a square planar complex, the z -axis is always defined perpendicular to the plane.

different contributions:^{195,197,198} a ground state contribution referred to as the “*trans* influence” and a transition state contribution referred to by the same term as the overall effect. The less significant of the two is the ground state contribution, which acts to destabilise the bond between the outgoing ligand and the metal as a result of the electronic synergy in the bonding between the two ligands (Figure 50). In particular it is the shared interaction with metal p_x or p_y orbitals that gives rise to the effect. If the *trans* ligand (T) is a good σ -donor into the reasonably high energy p orbital, then correspondingly the bonding effect between the metal and the outgoing ligand (X) will be weakened.

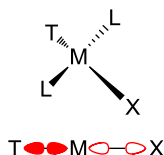


Figure 50. Schematic of the “*trans* influence”.

Alkenes are reasonably good σ -donor ligands,¹¹³ with the electrons in the more diffuse π -orbital a better energy match than an oxygen lone pair. However, conjugation of the alkene would be expected to lower the energy of the π -orbital, and so the *trans* influence would be expected to be more significant for norbornadiene **L30** than Ph-NBD **L31**. Curiously, the calculated HOMO energies for the unligated dienes in Table 27 (Entries 2 and 6) show the opposite, however a comparison of the Rh–Cl bond lengths for the two corresponding rhodium chloride complexes shows the bond to be longer in the case of $[\text{Rh}(\text{NBD})\text{Cl}]_2$.^{117,192}

The transition state contribution is generally the dominant effect and is relevant when the *trans* ligand is a good π -acceptor. In this case, the electron-rich trigonal bipyramidal transition state can be stabilised by donation of the increased electron density into the π -accepting orbitals of the *trans* ligand (Figure 51). Due to the extent of their π -accepting character resulting from the electronically accessible π^* orbital, alkenes have a particularly strong *trans* effect. As conjugation of the alkene increases, the π^* orbital becomes increasingly accessible and so the stabilising effect on the trigonal bipyramidal transition state would increase accordingly, accelerating the ligand substitution process. Correspondingly, the alkene bond length would be expected to increase in line with its ability to accept electron density.

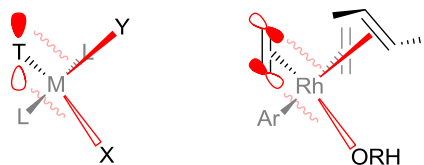


Figure 51. Schematic of the "trans effect" (transition state contribution), where Y and X are the incoming and outgoing ligands respectively. Right: Transition State C reproduced from Scheme 67.

In the case of rhodium-catalysed conjugate arylation, it therefore seems reasonable to suggest that the product ratio is at least partially determined by the ability of the diene ligand to stabilise the electron-rich transition state invoked for the exchange of a solvent ligand for the enoate (Scheme 67 and Figure 51), since this will be a contributing factor to the rate of the exchange. The bond length data in Table 26 and the HOMO/LUMO energies of the substituted diene scaffolds in Table 27 are consistent with this.

It may even be possible to account for the solvent effects which showed a lower selectivity for conjugate arylation when aromatic solvents were employed using ligand **L11** (Figure 52 below, cf. Figure 23 on page 84). A higher proportion of isomer **B** could be envisaged to exist following transmetalation in the case of using a non-aromatic solvent, with favourable secondary orbital interactions between the aryl group and the naphthyl ester stabilising the complex. If the complex were instead solubilised in an aromatic solvent, this stabilising interaction would be less significant and the proportion of isomer **B** might decrease. Isomer **B** would be expected to react faster than isomer **A** in a ligand exchange reaction involving substitution of the solvent ligand for the enoate, since the solvent ligand is *trans* to the more electron-accepting double bond in isomer **B**.

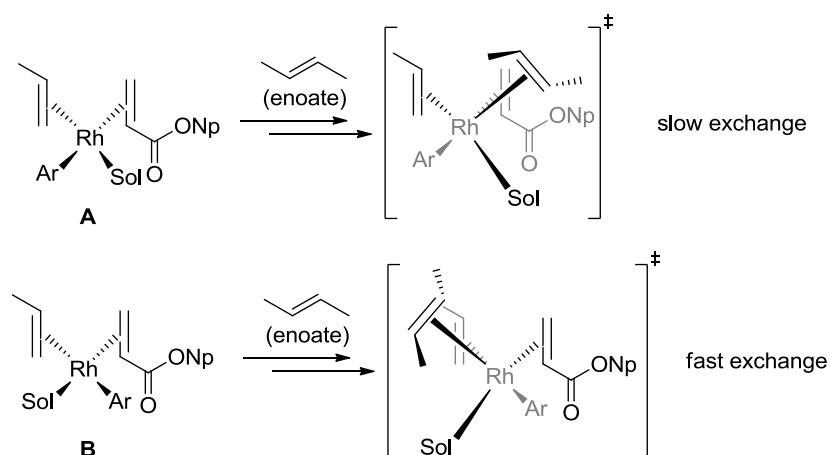


Figure 52. Comparison of ligand exchange transition states resulting from isomers A and B of arylrhodium intermediates with ligand **L11**.

The bond lengths of the ligated diene **L26** and the HOMO/LUMO energies of the unligated dienes **L11** and **L26** could account for the rate difference proposed in Figure 52. Table 26

shows a notable difference between the lengths of the two alkene bonds in the rhodium chloride salt with the ethyl ester **L26** (Entry 3), with the methyl-substituted alkene predictably displaying the shorter bond length. The calculated HOMO/LUMO energies of the two ester-substituted dienes **L11** and **L26** similarly show notable differences between the two alkenes (Table 27, Entries 3 and 4, also Figure 53).

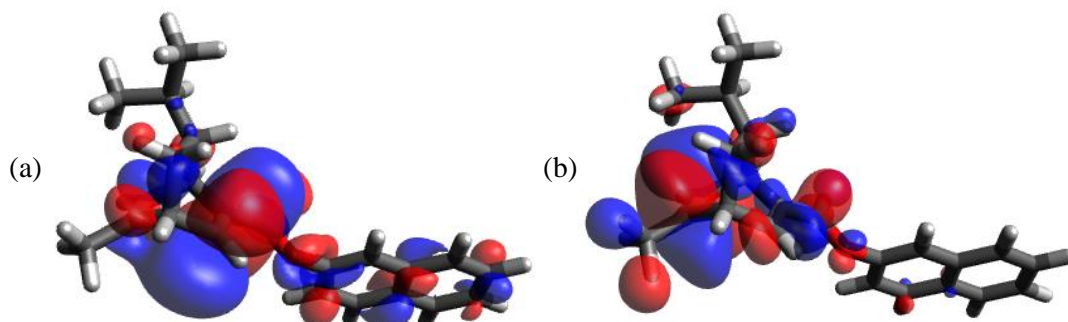


Figure 53. The two antibonding alkene orbitals calculated for **L11** at (a) 2.671 eV and (b) 4.725 eV.

Steric effects are also a factor in relevant ligand substitution reactions, with steric bulk slowing the rate of ligand exchange for associative mechanisms. This may explain the lower selectivities observed when using dienes with bulky substituents (Table 25, page 140) as well as when more substituted arylboron reagents were used (Sections 3.3.1.4 and 3.3.1.5). Figure 54 shows two examples, one in which the ligand **L27** projects bulk in the z -direction and another in which bulk is projected by an *ortho*-methyl substituent on the aryl group, both decreasing the ability of the enoate to approach the p_z orbital and therefore hindering the substitution of a solvent ligand for the enoate.

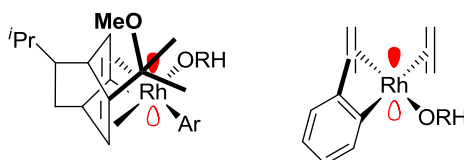
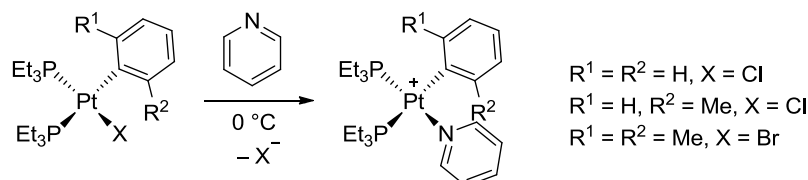


Figure 54. Schematic to demonstrate the sterics effects on an associative ligand substitution reaction.

In 1961, Pearson demonstrated the extent of this effect with the ligand substitution reactions shown in Scheme 68.¹⁹⁹ The relative rates of the substitution reaction for aryl = phenyl, *o*-tolyl, and mesityl were 90,000:200:1.



Scheme 68. Experiments performed by Pearson and co-workers to observe the steric effect of a *cis*-aryl group on the substitution of a halide ligand for pyridine.

3.3.3.2 Effects of Diene Ligands and Substrates on Protoderhodation

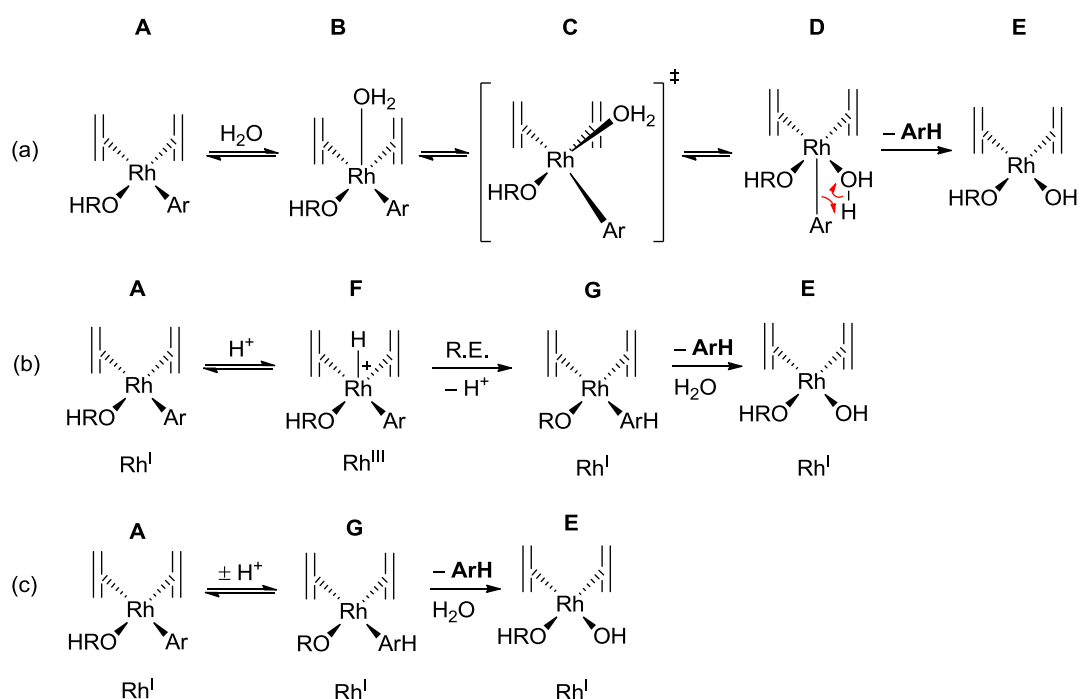
The difference between the product ratios when using COD or norbornadiene as the diene ligand is difficult to adequately account for in what has been discussed. The data in Table 26 (page 148) showed some difference in carbon–carbon alkene bond length between the two corresponding rhodium chloride dimers, but this difference is very small and older crystal structures of $[\text{Rh}(\text{COD})\text{Cl}]_2$ even suggest that COD might have the shorter bond lengths.^{200,201} The LUMO energies in Table 27 (page 149) similarly cannot account for the selectivity difference using COD and norbornadiene, and neither do the LUMO energies for the unsubstituted BOD scaffold (Entry 7) account for the selectivities that this framework appears to contribute to. It seems likely that there is an additional factor impacting the selectivity, which ligand exchange rates cannot account for.

Complexity is introduced by the fact that a slow ligand exchange pathway may not lead to elevated levels of protoderhodation as long as the protoderhodation pathway also proceeds slowly. Similarly, it could be the case that some diene ligands enable rapid and reversible exchange of a solvent ligand for the enoate, but that the energy barrier for the carboration insertion step is insurmountable whilst that for protoderhodation is not. Since solvent/enoate exchange rates cannot adequately account for differences in product ratios delivered by the different diene scaffolds themselves, consideration of the rates of potential protoderhodation pathways is necessary.

Three postulated pathways are shown in Scheme 69.^{xi} In Scheme 69a, a 5-coordinate 18-electron complex is invoked with the aryl group sitting along the *z*-axis, before protoderhodation can occur (Complex **D**).^{xii} This pathway essentially involves simultaneous ligand exchange and protonolysis between the aryl group and an incoming alcohol or water molecule.

^{xi} As for Section 3.3.3.1, the representations of diene ligands coordinated to rhodium omit the full structures of the scaffolds for clarity.

^{xii} As for Section 3.3.3.1, the axes are defined with no regard for the identity of the ligands such that, in the case of a square pyramidal complex, the *z*-axis is always defined perpendicular to the square plane.



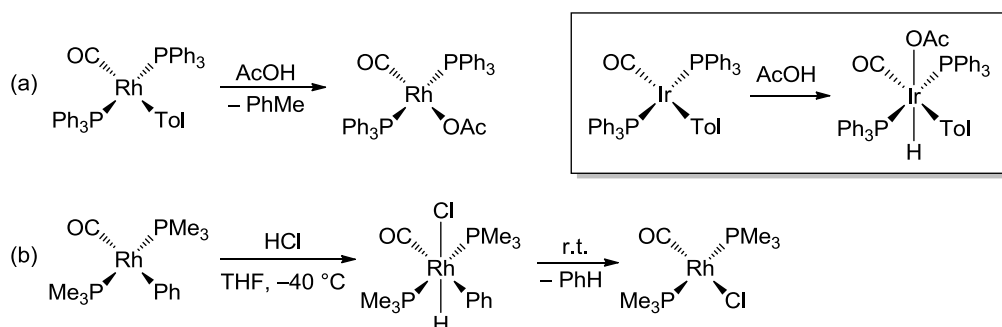
Scheme 69. Three suggested pathways for protoderhodation of an arylrhodium complex.

In Scheme 69b and Scheme 69c, pathways based on precedent from metal alkyl systems are suggested, involving either (b) initial protonation of the metal centre or (c) direct protonation of the rhodium–aryl bond.²⁰² The first of these requires formal oxidation of the rhodium (I) species to rhodium (III) (Complex **F**) before reductive elimination to generate the rhodium arene complex (Complex **G**). Evidence of this type of protonolysis pathway has been presented for CpFe(CO)₂–alkyl complexes treated with trifluoroacetic acid,²⁰³ and it is also believed to be active in the cleavage of the metal–alkyl bond in *trans*-HPt[(CH₂)_nCN](PPh₃)₂ (*n* = 1 or 3) with hydrochloric acid.²⁰⁴

Pathways involving direct protonation of metal–carbon bonds are less common, but notably this does not require formal oxidation of the metal centre. In particular, strong *trans*-donor ligands have been suggested to encourage direct protonation, and in the case of Scheme 69c this could even be envisaged to occur via an intramolecular protonation from the solvent ligand (Complex **A**),^{205,206} although some of the evidence for this rather than oxidative protonation of the metal as in Scheme 69b has been under discussion more recently.^{207,208} A study combining experimental kinetic data with computational work has defended both mechanisms as operable for benzylplatinum (II) complexes depending on the reaction conditions.²⁰⁹

A number of studies published involving phenylrhodium species provide additional evidence for the protonation pathways (Scheme 70). Scheme 70a summarises observations published

in 1984.²¹⁰ Treatment of the tolylrhodium complex with acetic acid liberated toluene and allowed characterisation of the rhodium acetate. In the case of performing the analogous transformation with a tolyliridium complex, the iridium (III) complex shown in the insert could be identified. By 1993, the intermediate octahedral rhodium (III) complex in Scheme 70b had been observed at low temperatures by NMR.²¹¹ Warming to room temperature liberated benzene and gave the square planar rhodium-chloride complex.



Scheme 70. Published reports detailing the protolytic cleavage of rhodium–aryl bonds.

The pathway involving ligand exchange in Scheme 69a is the least compelling on the grounds that the propensity of the diene to facilitate ligand exchange processes has been found to correlate with an increased proportion of conjugate arylation product rather than protodeboronation product. It is also the least precedented. However, the pathways in Scheme 69b and Scheme 69c may begin to account for some of the observed selectivity differences. For example, in Section 3.3.1.4 a trend was observed using the norbornadiene-ligated rhodium complex, in which more electron-rich arylboron reagents were shown to have a greater propensity to undergo protodeboronation. This can be rationalised by the pathways in Scheme 69b and Scheme 69c, which are favoured by more electron-rich metal centres.

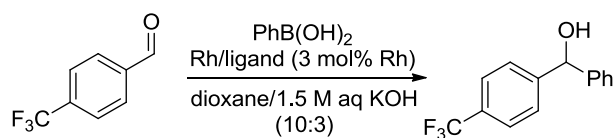
Considering a similar explanation for the differences observed between the diene scaffolds, and particularly the high levels of deboronation product using norbornadiene, the trend in product ratios (Table 25, page 140) was compared with the calculated HOMO energies of the unligated alkenes (Table 27, page 149, Entries 5–7). A correlation between the two was observed, with norbornadiene having the highest energy HOMO (–8.798 eV) and COD having the lowest energy HOMO (–9.357 eV). Mulliken population analysis also calculated a slightly higher charge density on the alkene carbons in norbornadiene (–0.24 C) compared with those of BOD (–0.22 C). Considered alone, these data could defend the notion that the ligation of norbornadiene to rhodium can result in a more electron-rich metal centre than the ligation of either COD or BOD.

The same trend is observed for the relative binding strengths of the unsubstituted scaffolds as determined by equilibrium experiments (Figure 55),¹⁸² however the situation is complicated by entropic factors and furthermore the authors of the cited report suggest that both norbornadiene and BOD have a stronger π -accepting character than that of COD. The calculated LUMO energies are compatible with that statement. Indeed, much of the binding strength of norbornadiene is attributed to the strain relief that occurs upon pyramidalisation of the ligating carbon atoms, which in turn is related to an increased propensity for the diene to accept electron density from the metal.^{113,114} The interplay between the electron-donating and -accepting capabilities of diene ligands and the difficulty of estimating their relative importance necessitate caution in drawing conclusions.¹¹³

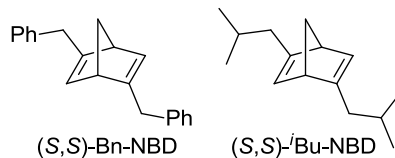


Figure 55. Relative stabilities of rhodium chloride complexes of the diene scaffolds.

The unique propensity of the unsubstituted norbornadiene ligand to facilitate the protodeboronation reaction is evident from a publication reporting the 1,2-addition of phenylboronic acids to aryl aldehydes using substituted norbornadiene ligands (Scheme 71).²¹² Seeking to optimise their reaction using $[\text{Rh}(\text{NBD})\text{Cl}]_2$ rather than the chiral dienes that they had prepared themselves, the authors found 6 equivalents of phenylboronic acid were required to achieve full conversion of the aldehyde. In contrast, Bn-NBD required only two equivalents of the arylboronic acid. This was also the case using $^i\text{Bu-NBD}$, although with this ligand the reaction was performed at a much lower temperature. These observations cannot be accounted for by the hypothesis that more electron-rich diene ligands result in higher levels of protoderhodation, unless the increased steric bulk of the substituted norbornadiene scaffolds is sufficient to significantly decrease the donation of electron density from the dienes to the metal centre by increasing the rhodium–alkene bond lengths in the arylrhodium intermediates.



Rh/ligand = [Rh(NBD)Cl]₂; PhB(OH)₂ (6 eq); 78% (6 h, 50 °C)
 Rh/ligand = [Rh(C₂H₄)₂Cl]₂/Bn-nbd; PhB(OH)₂ (2 eq); 96% (1 h, 50 °C)
 Rh/ligand = [Rh(C₂H₄)₂Cl]₂/Bu-nbd; PhB(OH)₂ (2 eq); 99% (1 h, 0 °C)



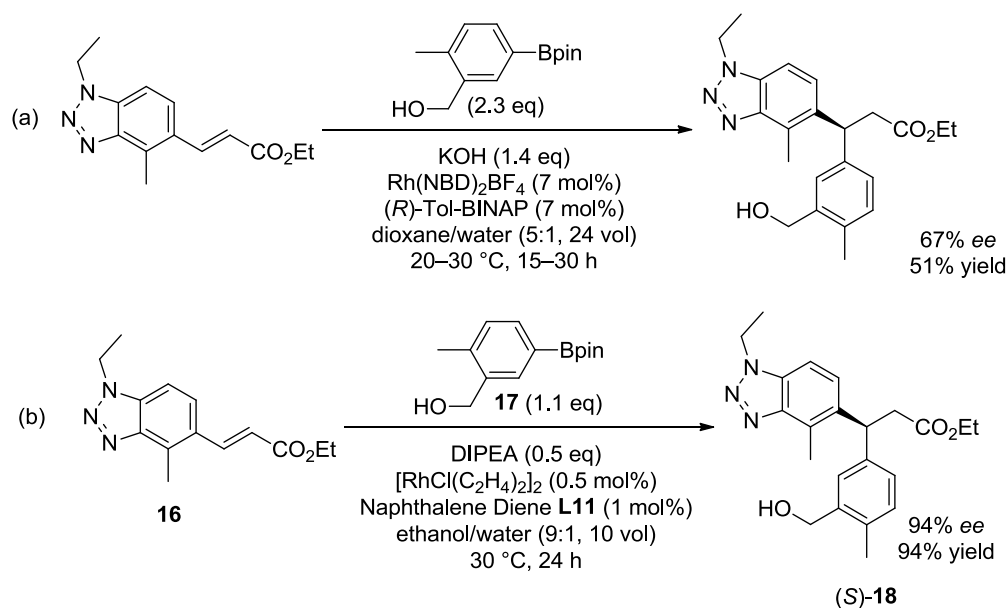
Scheme 71. Reported use of the norbornadiene-ligated rhodium complex and its substituted analogues in the 1,2-addition of phenylboronic acid to *p*-trifluoromethylbenzaldehyde.

Whilst it seems plausible that the electron-donating capability of diene ligands could in principle contribute to the extent of protoderhodation that occurs under conjugate arylation conditions, other unidentified factors must play a significant role.

4 Conclusions

4.1 Conclusions

The work presented in Section 3.2 has enabled significant improvements to be made to an industrially-relevant conjugate arylation reaction (Scheme 72).



Scheme 72. (a) Original conditions for the 1,4-addition reaction. (b) Optimised conditions from the process development of the 1,4-addition.

In particular the improvements include:

- Increase in isolated yield from 51% to 94%.
- Increase in enantioselectivity from 67% to 94% *ee*.
- Increase in selectivity of the reaction system for conjugate arylation over protodeboronation, from 52:48 to 97:3 conjugate arylation/protodeboronation.
- Decrease in the required equivalents of the arylboron reagent from 2.3 equivalents to 1.1 equivalents.
- Decrease in catalyst loading by more than 85%; from 7 mol% to 1 mol%.

Additionally, the new process employs a vastly preferable solvent system from a SELECT perspective and the reaction proceeds in greater concentration. The precatalyst and ligand are both cheaper than those used in the original process. The ligand selected for the optimised process had been previously overlooked by industry despite its excellent activity, selectivity, and facile preparation from the chiral pool reagent (*R*)- α -phellandrene.¹¹²

The continuous factors affecting the outcome of the reaction were efficiently probed by a statistical Design of Experiment approach, which demonstrated the scope to tune the reaction

conditions depending on the requirements of the process. It was found that an aqueous solvent system enabled good conversions to be achieved whilst maintaining low catalyst loadings and temperatures, and without significantly impacting the extent of protodeboronation. This protodeboronation reaction was found to occur almost exclusively via a rhodium-mediated pathway under the optimised conditions, contrary to the established modes of protodeboronation in Suzuki-Miyaura couplings.¹³¹ Solutions to the issue of protodeboronation are therefore required not only in the selection of arylboron reagents (Section 1.3.5), but even more in catalyst design. An investigation into the application of different bases revealed that nitrogen-containing bases can inhibit or prevent reactivity for both conjugate arylation and protodeboronation, with sp^2 -hybridised and sterically unencumbered nitrogen atoms being particularly detrimental.

Subsequent research to understand the features of the substrates and diene ligand that were important in enabling a high selectivity for conjugate arylation over protodeboronation in the optimised process delivered insights that can be more generally applied (Section 3.3).

From the substrate investigations:

- The triazole motif of the pharmaceutically-relevant enoate **16** contributed to the high selectivity of the reaction for conjugate arylation over protodeboronation, but some steric shielding of the most electron-rich nitrogen lone pair was essential for reactivity.
- The reaction selectivity of the optimised system was less negatively affected by the steric demand of the ester than published investigations employing a BINAP ligand.
- The reaction selectivity was found to correlate with the electronics of the enoate, such that a more electron-poor enoate delivered higher selectivity for conjugate arylation than a more electron-rich enoate.
- The electronics of the arylboron reagent were less important than the steric demand of the arylboron reagent.

From the ligand investigations:

- The structure of the diene backbone had a significant effect on the selectivity of the reaction for conjugate arylation over protodeboronation: BOD \approx COD \gg NBD.
- Conjugation of the alkenes with aromatic or electron-withdrawing functionality improved the selectivity for conjugate arylation, sufficiently to outweigh the negative effects of the scaffold in the case of Ph-NBD **L31**.

- Sterically demanding vinylic groups and allylic hydroxy functionality on the diene ligands increased the proportion of protodeboronation product. The combination of these groups in ligand **L10** reversed the enantiomeric preference of the conjugate arylation product delivered by the system.

The effect of the dienes and substrates on the rates of ligand exchange has been postulated to account for many of the significant effects on the selectivity of the reaction for conjugate arylation over protodeboronation. Systems that would be expected to enable the highest rates of exchange between a solvent molecule and the enoate delivered the highest selectivities for conjugate arylation. There is some evidence that diene structures and arylboron reagents delivering the lowest proportions of conjugate arylation product over protodeboronation product may give more electron-rich metal centres and therefore facilitate protonolysis of the arylrhodium intermediate. Other unidentified factors must also be important in determining the reaction selectivity in some cases, particularly in the case of the unsubstituted norbornadiene ligand.

4.1.1 General Considerations for the Process Development of Rhodium-Catalysed Asymmetric Conjugate Additions

A number of important considerations can be drawn from the work described in this thesis for the optimisation of related conjugate addition reactions. Firstly, the work has demonstrated the importance of assessing rhodium salts and ligands from as wide a set of classes as possible, and in particular has demonstrated the detrimental behaviour of $\text{Rh}(\text{NBD})_2\text{BF}_4$ with respect to the undesired protodeboronation reaction and the excellent activity of a commercially available and readily-prepared diene ligand **L11**. Previous reports in the process chemistry literature (Section 1.3.7) have completely overlooked this ligand class. For one of the reported transformations, the unoptimised application of **L11** was shown to give both excellent conversion and high enantioselectivity (Section 3.2.1.6).

The work has also demonstrated the effectiveness of seeking a solution to protodeboronation based primarily on the catalyst precursor and ligand, rather than relying on subsequent modifications of the conditions or use of additives. Sections 3.3.1 and 3.3.2 suggested that, although the specific substrates employed in the pharmaceutically-relevant transformation had some beneficial impact on the selectivity for conjugate arylation over protodeboronation, the structure of the ligand had the most dramatic impact. It may be that the ligand **L11** is more generally applicable to challenging conjugate arylations within process chemistry.

Finally, this work has exemplified the benefit of using statistical Design of Experiment at an early stage in process development, as an efficient means of identifying important factors to control and of enabling more economical processes to be developed. Whilst some forms of DoE are justifiably considered too resource-intensive for early process development, the factor-screening DoE used in this work provided an important contribution to developing the optimised conditions without excessive use of resources. For example, Section 3.2.3.5 showed that the factor-screening DoE was adequate to reveal the importance of water at low catalyst loadings and moderate temperatures. Without this, a process with unnecessarily high catalyst loadings or temperatures could have been progressed.

4.2 Future Work

The empirical investigations of a pharmaceutically-relevant conjugate arylation described in this thesis have uncovered challenges in rhodium-catalysed conjugate arylation methodology that are insufficiently understood and studied in the published literature. In particular, the competing protodeboronation reaction has received inadequate attention and the high propensity of norbornadiene to deliver the protodeboronation product remains insufficiently rationalised. A detailed understanding of the operative conjugate arylation and protoderhodation pathways of the arylrhodium intermediate has not been well established in the literature, despite its importance for the design and development of ligands for efficient conjugate arylation processes. Mechanistic and computational work is therefore required to assess the veracity of the postulated origins of the reaction selectivity in Section 3.3.3 and especially the suggested protoderhodation pathways in Section 3.3.3.2. A detailed understanding of the effects of different ligands on the carborhodation step could also prove valuable.

5 Experimental

5.1 General Comments

All reagents and solvents were used as obtained from commercial sources, and glassware was used without drying by heat treatment unless specified otherwise. Reactions were typically performed under nitrogen, as specified. Specialised reactors were used where appropriate: controlled laboratory reactors (CLRs, typically Reactor-Ready CLRs marketed by Radleys) were used for reactions on > 5 g scale, CAT96 reactors developed by HEL Group were used where specified, STEM Integrity 10 Reaction Stations developed by Electrothermal (Cole-Parmer) were used where specified and were used in combination with an Amigo Workstation developed by Amigo Chem where specified. Reactions employing microwave heating were performed in a Biotage microwave reactor. Column chromatography was performed using Biotage Isolera Prime systems with pre-packed silica cartridges. Where appropriate, such as when the product of a reaction was a highly viscous oil, yields have been corrected for residual solvent following NMR analysis.

Nuclear magnetic resonance spectra were acquired using a Bruker AV400 Spectrometer and processed using ACDLABS 12.0, with spectra recorded at 26–28 °C. Chemical shifts (δ) are quoted in parts per million (ppm) relative to the accepted shifts of the residual solvent protons or carbons relative to tetramethylsilane in the cases of ^1H and ^{13}C data.²¹³ Coupling constants (J) are quoted in Hertz, with multiplicity reported as s = singlet, d = doublet, t = triplet, q = quartet, quin = quintet, spt = septet, m = multiplet (unspecified), br = broad. Data are reported in the form: [chemical shift / ppm] ([multiplicity], [integral], [coupling constant]). ^{13}C spectra were acquired with broadband proton decoupling.

Infrared spectra were recorded over 4000–650 cm^{-1} using a Perkin Elmer Spectrum One FT-IR spectrophotometer fitted with a Perkin Elmer Universal Attenuated Total Reflectance sampling accessory. Solid samples were compressed as powers or formed as a film from an evaporated solution and liquid samples were used neat. Absorptions are reported in wavenumber (cm^{-1}) for distinctive bands.

Melting points have been measured using an OptiMelt Automated Melting Point system.

Karl Fischer analysis was performed using solid- or liquid-analysis systems where appropriate. Solid analysis used a Metrohm 774 Oven Sample Processor with 756 Coulometer. Liquid-analysis used a Mettler Toledo V10S Volumetric Karl Fischer Titrator.

Low resolution mass spectra were recorded using a Waters ZQ mass spectrometer, running in positive and negative electrospray ionisation mode with a quadrupole detector. The mass spectrometer was coupled to the following UPLC methods:

Method	LCMS Method A				
Column	Acquity UPLC CSH C18 (50 mm × 2.1 mm × 1.7 μm)				
Mobile Phase	A	0.1% v/v Solution of formic acid in water			
	B	0.1% v/v Solution of formic acid in acetonitrile			
Flow Rate	1 mL min ⁻¹				
Gradient Profile	Time / min	0	1.5	1.9	2.0
	% A	97	5	5	97
	% B	3	95	95	3
Column Temperature	40 °C				
UV Detection	Summation over 210–350 nm unless otherwise specified				
Injection Volume	0.5 μL				

Method	LCMS Method B				
Column	Acquity UPLC CSH C18 (50 mm × 2.1 mm × 1.7 μm)				
Mobile Phase	A	Aqueous ammonium bicarbonate (10 mM) adjusted to pH 10 with ammonia solution			
	B	Acetonitrile			
Flow Rate	1 mL min ⁻¹				
Gradient Profile	Time / min	0	1.5	1.9	2.0
	% A	0	3	3	100
	% B	100	97	97	0
Column Temperature	40 °C				
UV Detection	Summation over 210–350 nm unless otherwise specified				
Injection Volume	0.3 μL				

HPLC data were obtained according to the following tables, and where relevant absolute HPLC peak area data is reported in the form [Peak Area / mAU min]:

Method	HPLC Method A			
Instrument	Agilent 1100 Series HPLC			
Column	Agilent Zorbax SB-C18			
Mobile Phase	A	0.05% v/v Trifluoroacetic acid in water		
	B	0.05% v/v Trifluoroacetic acid in acetonitrile		
Flow Rate	1.5 mL min ⁻¹			
Gradient Profile	Time / min	0	2.5	3
	% A	100	5	5
	% B	0	95	95
Column Temperature	60 °C			
UV Detection	220 nm unless specified otherwise			
Injection Volume	1 µL			

Method	HPLC Method B			
Instrument	Agilent 1100 Series HPLC			
Column	Phenomenex Luna C18 (50 mm × 2 mm × 3 µm)			
Mobile Phase	A	0.05% v/v Trifluoroacetic acid in water		
	B	0.05% v/v Trifluoroacetic acid in acetonitrile		
Flow Rate	1 mL min ⁻¹			
Gradient Profile	Time / min	0	8	8.01
	% A	100	5	100
	% B	0	95	0
Column Temperature	40 °C			
UV Detection	220 nm unless specified otherwise			
Injection Volume	1 µL			

Method	HPLC Method C				
Column	X-Select CSH (4.6 mm × 150 mm × 2.5 μm)				
Mobile Phase	A	0.05% v/v Trifluoroacetic acid in water			
	B	0.05% v/v Trifluoroacetic acid in acetonitrile			
Flow Rate	1.0 mL min ⁻¹				
Gradient Profile	Time / min	0	30.00	30.01	37.00
	% A	100	5	100	100
	% B	0	95	0	0
Column Temperature	40 °C				
UV Detection	Specified for each instance				
Injection Volume	10 μL				

Method	HPLC Methods D1, D2, D3				
Column	Chiralpak OJ-H (250 mm × 4.6 mm × 5.0 μm)				
Mobile Phase	Ethanol/n-hexane 25:75 (v/v)				
Flow Rate	1.0 mL min ⁻¹				
Column Temperature	40 °C				
UV Detection	210 nm				
Injection Volume	0.5–25 μL				

HPLC Method D1 was installed on a different system to Methods D2 and D3. Method D3 had an improved baseline compared with Method D2.

Method	HPLC Method E				
Column	Chiralpak AD (250 mm × 4.6 mm × 5.0 μm)				
Mobile Phase	Ethanol/heptane/ <i>iso</i> -propylamine 30:70:0.1 (v/v)				
Flow Rate	1.0 mL min ⁻¹				
Column Temperature	25 °C				
UV Detection	210 nm				
Injection Volume	1 μL				

Method	HPLC Method F
Column	Chiralpak IG5 (250 mm × 4.6 mm × 5.0 μm)
Mobile Phase	Ethanol/heptane/ <i>iso</i> -propylamine 50:50:0.1 (v/v)
Flow Rate	1.0 mL min ⁻¹
Column Temperature	25 °C
UV Detection	250 nm
Injection Volume	5–25 μL

Method	HPLC Method G
Column	Chiralpak IG5 (250 mm × 4.6 mm × 5.0 μm)
Mobile Phase	Ethanol/heptane/ <i>iso</i> -propylamine 70:30:0.1 (v/v)
Flow Rate	1.0 mL min ⁻¹
Column Temperature	25 °C
UV Detection	250 nm
Injection Volume	5–25 μL

Method	HPLC Method H
Column	Chiralpak OJ-H (250 mm × 4.6 mm × 5.0 μm)
Mobile Phase	Ethanol/heptane/ <i>iso</i> -propylamine 70:30:0.1 (v/v)
Flow Rate	1.0 mL min ⁻¹
Column Temperature	25 °C
UV Detection	250 nm
Injection Volume	5–25 μL

Method	HPLC Method I
Column	Chiralpak IG5 (250 mm × 4.6 mm × 5.0 μm)
Mobile Phase	Ethanol/heptane/ <i>iso</i> -propylamine 75:25:0.1 (v/v)
Flow Rate	1.0 mL min ⁻¹
Column Temperature	25 °C
UV Detection	250 nm
Injection Volume	5–25 μL

Method	HPLC Method J
Column	Chiralpak IG5 (250 mm × 4.6 mm × 5.0 μm)
Mobile Phase	<i>iso</i> -Propanol/heptane/ <i>iso</i> -propylamine 95:5:0.1 (v/v)
Flow Rate	1.0 mL min ⁻¹
Column Temperature	25 °C
UV Detection	250 nm
Injection Volume	5–25 μL

Achiral GC data were acquired according to the following method:

Instrument	Agilent 6890 Series GC			
Column	Agilent DB5-HT (15 m × 0.25 mm × 0.10 μm)			
Carrier Gas	Helium			
Gas Pressure	1.7 bar			
Injection Split	Split (100:1)			
Oven Program	Ramp Rate / °C min ⁻¹	Final Temperature / °C	Hold Time / min	Elapsed Time / min
	-	50	0.5	0.50
	75	320	2.5	6.60
Temperatures / °C	Injector	Detector	Oven	
	275	320	275	
Injection Volume	1 μL			

Chiral GC data were acquired according to the following method:

Column	Alpha DEX 120 (30 m × 0.25 mm × 0.25 μm)		
Carrier Gas	Helium		
Gas Flow	2.0 mL min ⁻¹		
Injection Split	Split (30:1)		
Oven Program	Ramp Rate / °C min⁻¹	Final Temperature / °C	Elapsed Time / min
	-	80	0
	2	110	15.0
	20	220	5.5
Temperatures / °C	Injector		Detector
	200 °C		300 °C
Injection Volume	1 μL		

MDAP was performed with a Water ZQ mass spectrometer in positive and negative ionisation modes, attached to the following LC methods:

Method	MDAP Method A					
Column	Xselect CSH C18 (150 mm × 30 mm × 5 μm)					
Mobile Phase	A	Ammonium bicarbonate (10 mM aqueous solution, adjusted to pH 10 with ammonia solution)				
	B	Acetonitrile				
Flow Rate	40 mL min ⁻¹					
Gradient Profile	Time / min	0	1	10	10.5	15
	% A	70	70	15	1	1
	% B	30	30	85	99	99
Column Temperature	Ambient					
UV Detection	210–250 nm					
Injection Volume	1.0 mL					

Method	MDAP Method B					
Column	Xselect CSH C18 (150 mm × 30 mm × 5 μm)					
Mobile Phase	A	Ammonium bicarbonate (10 mM aqueous solution, adjusted to pH 10 with ammonia solution)				
	B	Acetonitrile				
Flow Rate	40 mL min ⁻¹					
Gradient Profile	Time / min	0	1	20	20.5	25
	% A	70	70	15	1	1
	% B	30	30	85	99	99
Column Temperature	Ambient					
UV Detection	210–350 nm					
Injection Volume	1.0 mL					

Method	MDAP Method C					
Column	Xselect CSH C18 (150 mm × 30 mm × 5 μm)					
Mobile Phase	A	Ammonium bicarbonate (10 mM aqueous solution, adjusted to pH 10 with ammonia solution)				
	B	Acetonitrile				
Flow Rate	40 mL min ⁻¹					
Gradient Profile	Time / min	0	1	20	20.5	25
	% A	50	50	1	1	1
	% B	50	50	99	99	99
Column Temperature	Ambient					
UV Detection	210–350 nm					
Injection Volume	1.0 mL					

HRMS data were acquired according to the following method unless specified otherwise:

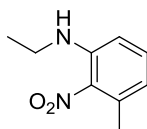
Instrument	Agilent HP1100 HPLC / Thermofinnigan Exactive Mass Spectrometer			
Column	Luna C18 (50 mm × 2.1 mm × 3 μm)			
Mobile Phase	A	0.05% v/v Trifluoroacetic acid in water		
	B	0.05% v/v Trifluoroacetic acid in acetonitrile		
Flow Rate	1 mL min ⁻¹			
Gradient Profile	Time / min	0	8	10
	% A	95	5	5
	% B	5	95	95
Column Temperature	40 °C			
Injection Volume	2.0 μL			

Where available, literature references are given for the analytical data of known compounds. Unless stated otherwise, reported data is in agreement with literature data.

5.2 Procedures for Section 3.1: Synthesis of Pharmaceutically-Relevant Substrates

5.2.1 Synthesis of (*E*)-Ethyl 3-(1-ethyl-4-methyl-1*H*-benzo[*d*][1,2,3]triazol-5-yl)acrylate 16 (Procedures for Section 3.1.1)

5.2.1.1 *N*-Ethyl-3-methyl-2-nitroaniline 21



1-Fluoro-3-methyl-2-nitrobenzene (**20**, 24.8 g, 160 mmol) was dissolved in dimethyl sulfoxide (DMSO, 115 mL) and potassium carbonate (22.1 g, 160 mmol) was added. Ethanamine (40.4 mL of 66–72 wt% solution in water, 479 mmol) solution was added dropwise and the resulting orange mixture was stirred for 71 h under nitrogen. HPLC analysis confirmed reaction completion (> 99 area% product) before water (125 mL, dropwise addition) and *tert*-butyl methyl ether (TBME, 135 mL) were added and the biphasic mixture was stirred for 30 min. The phases were allowed to settle (15 min) and the organic phase was separated. The aqueous phase was extracted once more with TBME (135 mL). The combined organic phases were washed once with water (75 mL) before removal of the volatiles to give *N*-ethyl-3-methyl-2-nitroaniline (28.1 g, 156 mmol, 98%).

Appearance: Orange oil.

ν (neat): 3403 (br.), 2970, 2931, 2872, 1600, 1502, 1345, 1273, 1148 cm^{-1} .

^1H NMR (400 MHz, CDCl_3): δ 7.21 (dd, 1H, $J = 7.4, 8.5$ Hz), 6.65 (d, 1H, $J = 8.5$ Hz), 6.50 (d, 1H, $J = 7.4$ Hz), 6.45 (br. s, 1H), 3.24 (dq, 2H, $J = 4.9, 7.2$ Hz), 2.46 (s, 3H), 1.30 (t, 3H, $J = 7.2$ Hz).

^{13}C NMR (101 MHz, CDCl_3): δ 144.0, 135.7, 135.6, 133.2, 119.1, 111.1, 38.0, 21.4, 14.5.

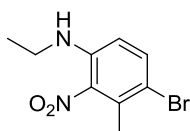
LCMS (Method A): $t_R = 1.18$ min, $[\text{M}+\text{H}]^+$ 181.0, > 97%.

HPLC (Method A): $t_R = 2.51$ min, > 99%.

HRMS: ($\text{C}_9\text{H}_{12}\text{N}_2\text{O}_2$) $[\text{M}+\text{H}]^+$ requires 181.0977, found $[\text{M}+\text{H}]^+$ 181.0971.

^1H NMR literature data concordant.²¹⁴

5.2.1.2 4-Bromo-*N*-ethyl-3-methyl-2-nitroaniline **22**



N-Ethyl-3-methyl-2-nitroaniline (**21**, 28.1 g, 156 mmol) was dissolved in *N,N*-dimethyl formamide (DMF, 240 mL) at room temperature. *N*-Bromosuccinimide (26.4 g, 148 mmol) was charged portionwise and the mixture was stirred for 2 h under nitrogen. HPLC analysis revealed < 5 area% residual starting material and up to 2 area% dibromination product (220 nm). Water (11.7 vol, 330 mL) was added dropwise and the mixture stirred for a further 1.5 h. The orange solids were filtered, washed with water (1 vol) and dried at 40–50 °C under reduced pressure overnight, to give 4-bromo-*N*-ethyl-3-methyl-2-nitroaniline (38.7 g, 149 mmol, 96%).

Appearance: Orange solid.

Melting point: 102.5–103.5 °C.

Karl Fisher: 0.37 wt% water.

ν (neat): 3416, 2974, 2922, 2870, 1603, 1517, 1491, 1384, 1348, 1266, 1205, 1157, 1089, 798 cm^{-1} .

^1H NMR (400 MHz, CDCl_3): δ 7.47 (d, 1H, $J = 9.0$ Hz), 6.55 (d, 1H, $J = 9.1$ Hz), 5.59 (br. s., 1H), 3.20 (dq, 2H, $J = 4.9, 7.2$ Hz), 2.43 (s, 3H), 1.29 (t, 3H, $J = 7.2$ Hz).

^{13}C NMR (101 MHz, CDCl_3): δ 141.6, 137.9, 136.4, 133.2, 112.0, 111.7, 38.1, 20.3, 14.4.

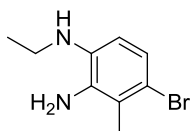
LCMS (Method A, 254 nm): $t_R = 1.33$ min, $[\text{M}+\text{H}]^+$ 258.9 and 260.9, > 99%.

HPLC (Method A): $t_R = 2.64$ min, > 97%.

HRMS: ($\text{C}_9\text{H}_{11}\text{BrN}_2\text{O}_2$) $[\text{M}+\text{H}]^+$ requires 259.0077, found $[\text{M}+\text{H}]^+$ 259.0070.

Structure confirmed by HMBC and ROESY 2D NMR.

5.2.1.3 4-Bromo-*N*¹-ethyl-3-methylbenzene-1,2-diamine **23**



Pt/C (2.28 g, 11.0 mmol) and 4-bromo-*N*-ethyl-3-methyl-2-nitroaniline (**22**, 37.7 g, 145 mmol) were charged to a hydrogenation vessel previously purged with nitrogen, and ethanol (430 mL) and phosphinic acid solution in water (50 wt% solution, 1.14 g, 8.64 mmol) were then added. The vessel was purged with nitrogen again ($3 \times \text{N}_2/\text{vent}$) and then with hydrogen ($3 \times \text{H}_2/\text{vent}$). The mixture was stirred under H_2 (5 bar) at ambient

temperature. After 1.5 h, HPLC and LCMS confirmed < 1% residual starting material relative to the aniline product. The mixture was filtered through a small pad of celite which was then washed twice with ethanol (2 × 40 mL). The filtrate was concentrated under reduced pressure (3–4 vol, 120 mL). Water (115 mL) was added dropwise and the mixture was concentrated again (3–4 vol) before cooling to 0–10 °C. Additional water (420 mL) was added dropwise and the cold mixture stirred for 1 h before filtration. The wet cake was washed with water (40 mL) and stored at –18 °C (37.8 g with 17.4 wt% water, 135 mmol, 93%).

Appearance: Brown solid.

Melting point: 86–88 °C.

Karl Fisher: 17.4 wt% water.

ν (neat): 3403, 3325 (br.), 2972, 2926, 2873, 1594, 1571, 1503, 1455, 1435, 1377, 1333, 1290, 1233, 1186, 1152 cm^{-1} .

^1H NMR (400 MHz, CDCl_3): δ 7.04 (d, 1H, $J = 8.5$ Hz), 6.48 (d, 1H, $J = 8.5$ Hz), 3.34 (br. s, 3H), 3.14 (q, 2H, $J = 7.1$ Hz), 2.35 (s, 3H), 1.33 (t, 3H, $J = 7.1$ Hz).

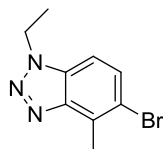
^{13}C NMR (101 MHz, CDCl_3): δ 136.4, 134.2, 123.1, 121.9, 114.7, 111.4, 39.1, 17.2, 15.0.

LCMS (Method A, 254 nm): $t_R = 0.68$ min, $[\text{M}+\text{H}]^+$ 229.0 and 231.0, > 99%.

HPLC (Method A): $t_R = 1.75$ min, > 98%.

HRMS: ($\text{C}_9\text{H}_{13}\text{BrN}_2$) $[\text{M}+\text{H}]^+$ requires 229.0335, found $[\text{M}+\text{H}]^+$ 229.0333.

5.2.1.4 5-Bromo-1-ethyl-4-methyl-1*H*-benzo[*d*][1,2,3]triazole 24



Sulfuric acid (69.0 mL, 1.30 mol) was added dropwise to water (68 mL), maintaining a temperature below 50 °C. Wet 4-bromo-*N*¹-ethyl-3-methylbenzene-1,2-diamine (**23**, 83 wt%, 37.5 g, 136 mmol) was charged portionwise to the reaction vessel at 0–15 °C. The mixture was stirred within this temperature range for 2 h under nitrogen, before the dropwise addition of sodium nitrite (17.1 g, 248 mmol) in water (515 mL), maintaining the same temperature range. Having confirmed < 1% residual starting material (LCMS, HPLC), additional water (120 mL) was charged dropwise to the reaction mixture at 0–10 °C. The mixture was filtered and the cake washed with water (190 mL). The solids were dried at 40–50 °C for > 12 h to give 5-bromo-1-ethyl-4-methyl-1*H*-benzo[*d*][1,2,3]triazole (28.3 g, 118 mmol, 87%).

Appearance: Purple solid.

Melting point: 78.5–79.5 °C.

Karl Fisher: 0.06 wt% water.

ν (neat): 3065, 2986, 2940, 1590, 1483, 1449, 1417, 1376, 1350, 1309, 1264, 1237, 1202, 1165, 1127, 1088, 1042, 989, 967, 870, 802, 764, 747 cm^{-1} .

^1H NMR (400 MHz, CDCl_3): δ 7.59 (d, 1H, $J = 8.6$ Hz), 7.23 (d, 1H, $J = 8.6$ Hz), 4.66 (q, 2H, $J = 7.4$ Hz), 2.83 (s, 3H), 1.62 (t, 3H, $J = 7.3$ Hz).

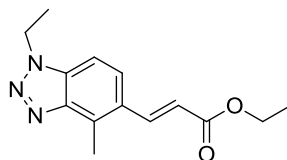
^{13}C NMR (101 MHz, CDCl_3): δ 147.0, 131.5, 131.2, 130.9, 118.8, 107.6, 43.4, 17.0, 15.0.

LCMS (Method A, 254 nm): $t_R = 1.05$ min, $[\text{M}+\text{H}]^+$ 240.0 and 242.0, > 99%.

HPLC (Method A): $t_R = 2.33$ min, > 99%.

HRMS: ($\text{C}_9\text{H}_{10}\text{BrN}_3$) $[\text{M}+\text{H}]^+$ requires 240.0131, found $[\text{M}+\text{H}]^+$ 240.0123.

5.2.1.5 (*E*)-Ethyl 3-(1-ethyl-4-methyl-1*H*-benzo[*d*][1,2,3]triazol-5-yl)acrylate **16**



Degassed DMF (160 mL) was charged to a vessel containing 5-bromo-1-ethyl-4-methyl-1*H*-benzo[*d*][1,2,3]triazole (**24**, 20 g, 83 mmol), potassium carbonate (17.2 g, 124 mmol), palladium (II) acetate (756 mg, 3.37 mmol) and triphenylphosphine (2.21 g, 8.41 mmol) under nitrogen. Ethyl acrylate (11.7 mL, 107 mmol) was added and the reaction mixture was stirred for 4 h at 110–120 °C. The mixture was cooled to 20–30 °C and sampled to confirm < 1% residual starting material (HPLC, LCMS) before it was filtered through celite. The cake was washed with DMF (40 mL) before water (300 mL) was added dropwise to the filtrate at room temperature. The resulting mixture was stirred overnight and the solids formed in that time were collected by filtration and washed with water (40 mL).^{xiii} The solids were of varying quality and were purified by column chromatography (10–60% ethyl acetate in heptane). Later fractions were contaminated with a highly coloured impurity and the product could be crystallised away from this in heptane/ethyl acetate. The resulting batches of (*E*)-ethyl 3-(1-ethyl-4-methyl-1*H*-benzo[*d*][1,2,3]triazol-5-yl)acrylate were dried in a vacuum oven at 40 °C for > 12 h (16.1 g, 61.9 mmol, 74%).

^{xiii} Isolation of the product by crystallisation or precipitation from water/DMF proved troublesome. A previous preparation on the same scale had collected 16.7 g solids (brown needles (12.2 g) with dark amorphous solids) after the DMF/water mixture was allowed to stand overnight. In this case, 3.7 g of the product was estimated to be remaining in the liquors by HPLC analysis and a further 400 mg was estimated to be contained in oily residues. In total, a further 2.7 g was precipitated from the liquors by further additions of water with cooling in an ice bath.

Appearance: Colourless solid.

Melting point: 75.5–76.0 °C.

ν (neat): 2988, 2902, 1696, 1626, 1606, 1492, 1448, 1389, 1382, 1364, 1307, 1265, 1252, 1180, 1159, 1035, 977, 858, 797, 680 cm^{-1} .

^1H NMR (400 MHz, CDCl_3): δ 8.14 (d, 1H, $J = 15.8$ Hz), 7.71 (d, 1H, $J = 8.9$ Hz), 7.36 (d, 1H, $J = 8.9$ Hz), 6.42 (d, 1H, $J = 15.9$ Hz), 4.68 (q, 2H, $J = 7.4$ Hz), 4.30 (q, 2H, $J = 7.1$ Hz), 2.92 (s, 3H), 1.63 (t, 3H, $J = 7.4$ Hz), 1.36 (t, 3H, $J = 7.1$ Hz).

^{13}C NMR (101 MHz, CDCl_3): δ 167.0, 145.0, 141.1, 133.0, 131.6, 128.2, 125.8, 119.2, 107.1, 60.6, 43.4, 15.1, 14.4, 13.4.

LCMS (Method A, 254 nm): $t_R = 1.05$ min, $[\text{M}+\text{H}]^+ 260.1$.

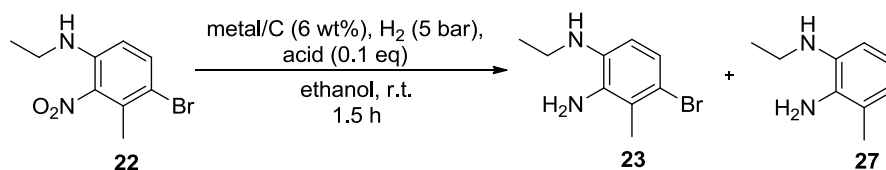
HPLC (Method A): $t_R = 2.33$ min, > 98%.

HPLC (Method B): $t_R = 5.38$ min.

HPLC (Method C): $t_R = 19.97$ min.

HRMS: ($\text{C}_{14}\text{H}_{17}\text{N}_3\text{O}_2$) $[\text{M}+\text{H}]^+$ requires 260.1394, found $[\text{M}+\text{H}]^+ 260.1385$.

5.2.1.6 Selectivity Afforded by Phosphinic Acid in the Nitro Reduction of 21



Pt/C (3 mg, Johnson Matthey type 128M, 5wt%Pt) and 4-bromo-*N*-ethyl-3-methyl-2-nitroaniline (50 mg, 0.19 mmol) were charged to a vial, and ethanol (0.55 mL) and phosphinic acid solution in water (50 wt% solution, 1.25 μL , 0.011 mmol) were then added. The capped, pierced vial was transferred to a CAT96 reactor, which was purged with nitrogen ($3 \times \text{N}_2/\text{vent}$) and then with hydrogen ($3 \times \text{H}_2/\text{vent}$). The mixture was stirred under H₂ (5 bar) at 30 °C and sampled after 5 h (LCMS, HPLC).

This was repeated in parallel using Pd/C (3 mg, Johnson Matthey type 39, 5 wt%Pd) instead of Pt/C, and both of these were repeated in parallel omitting phosphinic acid. Additionally, two further reactions were prepared with Pt/C as described above, replacing aqueous phosphinic acid with phosphoric acid (0.78 μL , 0.011 mmol, with additional 0.75 μL water) and with acetic acid (0.65 μL , 0.011 mmol, with additional 0.75 μL water). The HPLC results are presented in Section 3.1.1.

The debrominated compound, *N*¹-ethyl-3-methylbenzene-1,2-diamine, was isolated by MDAP Method A as a red solid from the reaction which had employed Pd/C without phosphinic acid (22 mg, 0.15 mmol, 76%).

***N*¹-ethyl-3-methylbenzene-1,2-diamine 27**

Appearance: Red solid.

Melting point: 64.8–66.4 °C.

ν (neat): 3403, 3392, 3322, 3281, 3200, 3039, 2971, 2932, 2852, 1603, 1586, 1519, 1476, 1460, 1375, 1341, 1298, 1258, 1227, 1187, 1159, 1137 cm^{-1} .

¹H NMR (400 MHz, CDCl₃): δ 6.76 (t, 1H, $J = 7.7$ Hz), 6.64 (d, 1H, $J = 7.7$ Hz), 6.61 (d, 1H, $J = 7.7$ Hz), 3.29 (br. s, 3H), 3.16 (q, 2H, $J = 7.1$ Hz), 2.23 (s, 3H), 1.32 (t, 3H, $J = 7.1$ Hz).

¹³C NMR (101 MHz, CDCl₃): δ 137.4, 132.7, 122.8, 120.7, 119.6, 110.3, 39.1, 17.6, 15.2.

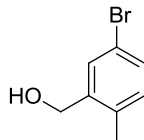
LCMS (Method A, 254 nm): $t_R = 0.35$ min, [M+H]⁺ 151.0, > 95%.

HPLC (Method A): $t_R = 1.47$ min, > 99%.

HRMS: (C₉H₁₄N₂) [M+H]⁺ requires 151.1230, found [M+H]⁺ 151.1225.

5.2.2 Synthesis of (2-Methyl-5-(4,4,5,5-tetramethyl-1,3,2-dioxaborolan-2-yl)phenyl)methanol **17** (Procedures for Section 3.1.2)

5.2.2.1 (5-Bromo-2-methylphenyl)methanol **26**



A solution of borane tetrahydrofuran complex (28 mL, 1.0 M in THF, 28 mmol) was added dropwise to a solution of 5-bromo-2-methylbenzoic acid (**26**, 5.00 g, 23.3 mmol) in tetrahydrofuran (THF, 20 mL) under nitrogen, giving a small exotherm to below 30 °C with gas evolution before the exotherm increased to 50 °C. After stirring for 1 h at ambient temperature, and to ensure conversion to the desired product, the reaction mixture was heated to 55 °C for 5.5 h before being allowed to cool to room temperature. Methanol (5 mL) was added dropwise with gas evolution observed, followed by acidification of the mixture with ammonium chloride (4.5 g, 84 mmol) in water (15 mL). Additional water (20 mL) was added, and the organic phase was separated. The aqueous phase was extracted with ethyl acetate (2 × 20 mL), and the combined organic portions were washed with water (2 × 20 mL) and brine (1 × 10 mL) before being dried over magnesium sulfate. The volatiles were removed and the crude oil was analysed by HPLC and NMR before being used directly in the next step.

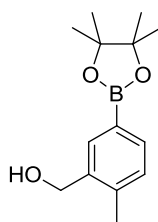
¹H NMR (400 MHz, CDCl₃): δ 7.53 (s, 1H), 7.32 (d, 1H, *J* = 7.9 Hz), 7.03 (d, 1H, *J* = 8.0 Hz), 4.66 (br. s., 2H), 2.27 (s, 3H).

HPLC (Method A): *t_R* = 2.09 min, > 96%.

¹H NMR literature data concordant.²¹⁵

See Section 5.4.2.1.12 for a procedure including isolation of compound **26**.

5.2.2.2 (2-Methyl-5-(4,4,5,5-tetramethyl-1,3,2-dioxaborolan-2-yl)phenyl)methanol **17**



Potassium acetate (4.56 g, 46.5 mmol), bis(pinacolato)diboron (6.49 g, 25.6 mmol), tricyclohexylphosphine (0.391 g, 1.395 mmol) and palladium(II) acetate (0.157 g, 0.698 mmol) were charged to a vessel which was then purged with nitrogen ($3 \times$ vacuum/ N_2). 1,4-Dioxane (45 mL) was then added with the crude oil of (5-bromo-2-methylphenyl)methanol **26**. The mixture was degassed ($3 \times$ vacuum/ N_2) before stirring at 70–80 °C. Within 3 h, full consumption of the starting material was evidenced by HPLC and LCMS. The mixture was cooled to room temperature and filtered through celite, which was washed with ethyl acetate (10 mL). The filtrate was concentrated (1 vol) before dissolution in ethyl acetate (25 mL). This organic solution was washed with saturated aqueous sodium bicarbonate (25 mL) and brine (25 mL), dried over magnesium sulfate, and concentrated again (1 vol) below 45 °C after filtering again through celite.

The concentrated organic phase was heated to 50–60 °C with stirring before being allowed to cool slowly to room temperature and then to 0 °C. Heptane (45 mL) was then added dropwise, and the resulting mixture was stirred for 15 h at 0–25 °C. Pale grey solids were afforded, which were filtered. The wet cake was slurried in heptane (15 mL), refiltered and then washed with heptane (10 mL). After drying in a vacuum oven at 40–50 °C for 18 h, a low yield of the product **17** was afforded (1.64 g, 6.61 mmol, 28% over two steps). The combined filtrate and heptane washes were stirred at –4 to –10 °C for 2.5 h, which gave a further crop of solids. The solids were collected, washed with heptane (10 mL) and dried in a vacuum oven as above to give an additional batch of product **17** (1.09 g, 4.39 mmol, 19%, combined yield 47% over two steps).

Appearance: Colourless solid.

Melting point: 64.8–65.2 °C.

ν (neat): 3301 (br.), 2967, 2927, 1611, 1374, 1351, 1309, 1281, 1217, 1153, 1128, 1089, 1026, 966, 906, 855, 823 cm^{-1} .

1H NMR (400 MHz, $CDCl_3$): δ 7.76 (s, 1H), 7.66 (d, 1H, $J = 7.4$ Hz), 7.20 (d, 1H, $J = 7.5$ Hz), 4.71 (s, 2H), 2.40 (s, 3H), 1.34 (s, 12H).

^{13}C NMR (101 MHz, CDCl_3): δ 140.1, 138.1, 134.5, 134.3, 130.0, 83.8, 63.8, 24.9, 19.0.*

LCMS (Method A, 254 nm): $t_R = 1.05$ min, $[(\text{M}-\text{H}_2\text{O})+\text{H}]^+$ 231.0.

HPLC (Method A): $t_R = 2.35$ min, 1.46 min (arylboronic acid), > 99%.

HPLC (Method C): $t_R = 20.20$ min, 9.27 min (arylboronic acid).

HRMS (positive mode ASAP^{xiv}): ($\text{C}_{14}\text{H}_{21}\text{BO}_3$) $[(\text{M}-\text{H}_2\text{O})+\text{H}]^+$ requires 231.1551, found 231.1541 (major); $[(\text{M}-\text{H}_2)+\text{H}]^+$ requires 247.1500, found 247.1491 (minor).

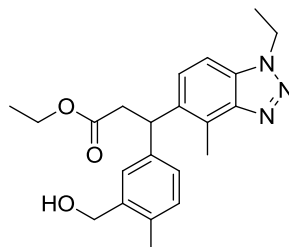
*One quaternary carbon could not be observed by ^{13}C NMR. Boron is known to suppress adjacent ^{13}C resonances.²¹⁶

The product was purified by column chromatography (15–80% ethyl acetate in heptane, 97% recovery) before use in subsequent reactions.

^{xiv} Atmospheric Solids Analysis Probe

5.3 Procedures for Section 3.2: Process Development of the Pharmaceutically-Relevant Conjugate Arylation

5.3.1 *rac*-Ethyl 3-(1-ethyl-4-methyl-1*H*-benzo[*d*][1,2,3]triazol-5-yl)-3-(3-(hydroxymethyl)-4-methylphenyl)propanoate **18**



(*E*)-Ethyl 3-(1-ethyl-4-methyl-1*H*-benzo[*d*][1,2,3]triazol-5-yl)acrylate (**16**, 100 mg, 0.386 mmol) was charged to a vessel and (2-methyl-5-(4,4,5,5-tetramethyl-1,3,2-dioxaborolan-2-yl)phenyl)methanol (**17**, 220 mg, 0.887 mmol) added as a solution in 1,4-dioxane (2 mL). The atmosphere was inerted and the solution was sparged with nitrogen. *rac*-2,2'-Bis(di-*p*-tolylphosphanyl)-1,1'-binaphthalene (**L8**, 18.3 mg, 0.027 mmol) was charged followed by Rh(NBD)₂BF₄ (10 mg, 0.027 mmol), and potassium hydroxide (30.3 mg, 0.540 mmol) in degassed water (0.4 mL), and the mixture was again degassed (3 × vacuum/N₂) before stirring at room temperature for three days. The reaction mixture was concentrated and ethyl acetate (1 mL) was added before filtering the mixture through cotton wool. The filtrate was washed with water (2 × 0.5 mL) and brine (0.5 mL) and dried over magnesium sulfate. The solution was concentrated to an oil and purified by column chromatography (20–70% ethyl acetate in heptane) to give the desired compound *rac*-**18** as a viscous yellow oil (97.3 mg, 0.255 mmol, 66%).

Appearance: viscous yellow oil.^{xv}

ν (neat): 3391, 2986, 2940, 2870, 1732, 1500, 1449, 1372, 1263, 1240, 1156, 1039 cm⁻¹.

¹H NMR (400 MHz, CDCl₃): δ 7.37 (d, 1H, *J* = 8.7 Hz), 7.30 (d, 1H, *J* = 8.7 Hz), 7.23 (s, 1H), 7.12–7.04 (app. s, 2H), 4.99 (t, 1H, *J* = 8.0 Hz), 4.65 (s, 2H), 4.64 (q, 2H, *J* = 7.3 Hz), 4.02 (q, 2H, *J* = 7.1 Hz), 3.15 (dd, 1H, *J* = 7.5, 15.4 Hz), 3.05 (dd, 1H, *J* = 8.6, 15.4 Hz), 2.86 (s, 3H), 2.29 (s, 3H), 1.63 (br. s, 1H), 1.60 (t, 3H, *J* = 7.4 Hz), 1.11 (t, 3H, *J* = 7.1 Hz).

¹³C NMR (101 MHz, CDCl₃): δ 171.6, 147.0, 140.9, 138.9, 136.2, 134.2, 131.2, 130.5, 128.2, 126.8, 126.7, 126.6, 106.6, 63.5, 60.5, 43.1, 41.6, 41.0, 18.2, 15.0, 14.1, 13.3.

^{xv} During process development work, the product was found to be a colourless viscous oil with a closely eluting yellow impurity that has not been observed or identified. Later preparations enabled its isolation as a colourless oil.

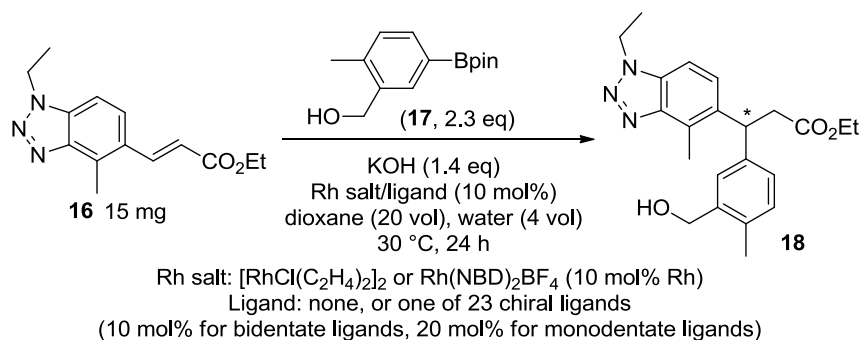
HPLC (Method C): $t_R = 19.45$ min, > 99%.

HRMS: (C₂₂H₂₇N₃O₃) [M+H]⁺ requires 382.2125, found [M+H]⁺ 382.2116.

rac-**18** could also be prepared using [RhCl(COD)]₂ under analogous conditions to those above with no additional ligand.

5.3.2 Selection of Catalyst Precursor and Ligand for the Pharmaceutically-Relevant Conjugate Arylation (Procedures for Section 3.2.1)

5.3.2.1 Comparative Analysis of Ligands for Asymmetric Arylation (Procedure for Section 3.2.1.1)



Ligands were weighed into reaction vials followed by rhodium salts according to Table 28 (page 187). The vials were stored under air overnight before the vials were placed inside a nitrogen-filled glove bag. The two substrates **16** (15.0 mg, 57.8 μmol) and **17** (33.0 mg, 133 μmol) were added volumetrically as a nitrogen-sparged solution in dioxane (48 \times 300 μL), inside the glove bag. Potassium hydroxide (4.5 mg, 81 μmol) was added as a nitrogen-sparged aqueous solution (48 \times 60 μL), and the vials were then capped and pierced (2 \times blunt needle) inside the glove bag before being transferred to a CAT96 reactor. The reactor was purged with nitrogen (3 \times N_2 /vent) before the reaction vials were stirred at 30 $^\circ\text{C}$ for 24 h under nitrogen.

Additionally, a vial (Vial 49) was prepared in the same manner without ligand or rhodium salt. This was stirred under nitrogen at 30 $^\circ\text{C}$ for 24 h on a hotplate/stirrer.

The vials were sampled after 24 h (23 μL into ethanol (977 μL)) inside a nitrogen-filled glove bag, and the reaction vials were then resealed, pierced (2 \times blunt needle) and transferred again to the CAT96 reactor. The reactor was purged with nitrogen and the vials were stirred at 60 $^\circ\text{C}$ for 65 h before sampling again in the same manner.

The samples were analysed by HPLC (Method D1), and the results are summarised in Table 29 (page 188) and Table 30 (page 189).

Vial	Rhodium Salt			Ligand				
	Identity	Amount Mass / μmol / mg		Identifier	CAS Number	Amount Mass / μmol / mg		
1	[Rh(Cl)(C ₂ H ₄) ₂] ₂	2.78	1.08	L10	IPA Diene	1063949-39-2	5.8	1.3
2	[Rh(Cl)(C ₂ H ₄) ₂] ₂	3.22	1.25	L11	Naphthyl Diene	1188966-75-7	5.8	1.9
3	[Rh(Cl)(C ₂ H ₄) ₂] ₂	3.06	1.19	L1	(<i>R</i>)-MeO-BIPHEP	133545-16-1	5.8	3.4
4	[Rh(Cl)(C ₂ H ₄) ₂] ₂	2.82	1.10	L2	(<i>R</i>)-H8-BINAP	139139-86-9	5.8	3.6
5	[Rh(Cl)(C ₂ H ₄) ₂] ₂	2.85	1.11	L14	(<i>R,R</i>)-Me-DuPhos	147253-67-6	5.8	1.8
6	[Rh(Cl)(C ₂ H ₄) ₂] ₂	3.12	1.21	L21	(<i>R</i>)-MonoPhos	157488-65-8	11.6	4.2
7	[Rh(Cl)(C ₂ H ₄) ₂] ₂	3.04	1.18	L3	(<i>R</i>)-Cl-BIPHEP	185913-97-7	5.8	3.8
8	[Rh(Cl)(C ₂ H ₄) ₂] ₂	3.00	1.17	L4	(<i>R</i>)-P-Phos	221012-82-4	5.8	3.7
9	[Rh(Cl)(C ₂ H ₄) ₂] ₂	3.18	1.24	L5	(<i>R</i>)-SEGPPOS	244261-66-3	5.8	3.5
10	[Rh(Cl)(C ₂ H ₄) ₂] ₂	2.93	1.14	L15	(<i>R,R</i>)-Diop	32305-98-9	5.8	2.9
11	[Rh(Cl)(C ₂ H ₄) ₂] ₂	2.94	1.14	L19	(<i>R</i>)-Xylyl-PHANePhos	325168-89-6	5.8	4.0
12	[Rh(Cl)(C ₂ H ₄) ₂] ₂	3.10	1.21	L22	Bipol-A1(<i>S</i>)	376355-58-7	11.6	5.1
13	[Rh(Cl)(C ₂ H ₄) ₂] ₂	2.96	1.15	L23	Phosphoramidite	380230-02-4	11.6	6.2
14	[Rh(Cl)(C ₂ H ₄) ₂] ₂	3.01	1.17	L20	Walphos SL-W005-1	494227-30-4	5.8	6.1
15	[Rh(Cl)(C ₂ H ₄) ₂] ₂	2.91	1.13	L18	catASium M(<i>R</i>)	505092-86-4	5.8	1.9
16	[Rh(Cl)(C ₂ H ₄) ₂] ₂	3.03	1.18	L6	(<i>R</i>)-DTBM-SEGPPOS	566940-03-2	5.8	6.8
17	[Rh(Cl)(C ₂ H ₄) ₂] ₂	2.92	1.14	L16	(<i>S,S</i>)-Chiraphos	64896-28-2	5.8	2.5
18	[Rh(Cl)(C ₂ H ₄) ₂] ₂	3.12	1.21	L9	(<i>M,M,S</i>)-Tol-BINASO	722455-72-3	5.8	3.1
19	[Rh(Cl)(C ₂ H ₄) ₂] ₂	2.99	1.16	L7	(<i>R</i>)-BINAP	76189-55-4	5.8	3.6
20	[Rh(Cl)(C ₂ H ₄) ₂] ₂	2.93	1.14	L12	Ph-BOD	850409-83-5	5.8	1.5
21	[Rh(Cl)(C ₂ H ₄) ₂] ₂	2.88	1.12	L13	Carreira DOLEFIN	862499-50-1	5.8	1.8
22	[Rh(Cl)(C ₂ H ₄) ₂] ₂	3.11	1.21	L17	(<i>R</i>)-QuinoxP	866081-62-1	5.8	1.9
23	[Rh(Cl)(C ₂ H ₄) ₂] ₂	3.10	1.20	L8	(<i>R</i>)-Tol-BINAP	99646-28-3	5.8	3.9
24	[Rh(Cl)(C ₂ H ₄) ₂] ₂	2.99	1.16	N/A	No Ligand	N/A	N/A	N/A
25	Rh(NBD) ₂ BF ₄	5.69	2.13	L10	IPA Diene	1063949-39-2	5.8	1.3
26	Rh(NBD) ₂ BF ₄	5.70	2.13	L11	Naphthyl Diene	1188966-75-7	5.8	1.9
27	Rh(NBD) ₂ BF ₄	5.77	2.16	L1	(<i>R</i>)-MeO-BIPHEP	133545-16-1	5.8	3.4
28	Rh(NBD) ₂ BF ₄	5.67	2.12	L2	(<i>R</i>)-H8-BINAP	139139-86-9	5.8	3.6
29	Rh(NBD) ₂ BF ₄	5.82	2.18	L14	(<i>R,R</i>)-Me-DuPhos	147253-67-6	5.8	1.8
30	Rh(NBD) ₂ BF ₄	5.74	2.15	L21	(<i>R</i>)-MonoPhos	157488-65-8	11.6	4.2
31	Rh(NBD) ₂ BF ₄	5.91	2.21	L3	(<i>R</i>)-Cl-BIPHEP	185913-97-7	5.8	3.8
32	Rh(NBD) ₂ BF ₄	5.72	2.14	L4	(<i>R</i>)-P-Phos	221012-82-4	5.8	3.7
33	Rh(NBD) ₂ BF ₄	5.89	2.20	L5	(<i>R</i>)-SEGPPOS	244261-66-3	5.8	3.5
34	Rh(NBD) ₂ BF ₄	5.85	2.19	L15	(<i>R,R</i>)-Diop	32305-98-9	5.8	2.9
35	Rh(NBD) ₂ BF ₄	5.78	2.16	L19	(<i>R</i>)-Xylyl-PHANePhos	325168-89-6	5.8	4.0
36	Rh(NBD) ₂ BF ₄	5.75	2.15	L22	Bipol-A1(<i>S</i>)	376355-58-7	11.6	5.1
37	Rh(NBD) ₂ BF ₄	5.92	2.21	L23	Phosphoramidite	380230-02-4	11.6	6.2
38	Rh(NBD) ₂ BF ₄	5.74	2.15	L20	Walphos SL-W005-1	494227-30-4	5.8	6.1
39	Rh(NBD) ₂ BF ₄	5.76	2.16	L18	catASium M(<i>R</i>)	505092-86-4	5.8	1.9
40	Rh(NBD) ₂ BF ₄	5.84	2.19	L6	(<i>R</i>)-DTBM-SEGPPOS	566940-03-2	5.8	6.8
41	Rh(NBD) ₂ BF ₄	5.86	2.19	L16	(<i>S,S</i>)-Chiraphos	64896-28-2	5.8	2.5
42	Rh(NBD) ₂ BF ₄	5.89	2.20	L9	(<i>M,M,S</i>)-Tol-BINASO	722455-72-3	5.8	3.1
43	Rh(NBD) ₂ BF ₄	5.80	2.17	L7	(<i>R</i>)-BINAP	76189-55-4	5.8	3.6
44	Rh(NBD) ₂ BF ₄	5.79	2.17	L12	Ph-BOD	850409-83-5	5.8	1.5
45	Rh(NBD) ₂ BF ₄	5.80	2.17	L13	Carreira DOLEFIN	862499-50-1	5.8	1.8
46	Rh(NBD) ₂ BF ₄	5.88	2.20	L17	(<i>R</i>)-QuinoxP	866081-62-1	5.8	1.9
47	Rh(NBD) ₂ BF ₄	5.86	2.19	L8	(<i>R</i>)-Tol-BINAP	99646-28-3	5.8	3.9
48	Rh(NBD) ₂ BF ₄	5.90	2.21	N/A	No Ligand	N/A	N/A	N/A

Table 28. Rhodium salts and ligands dispensed to reaction vials for ligand comparisons.

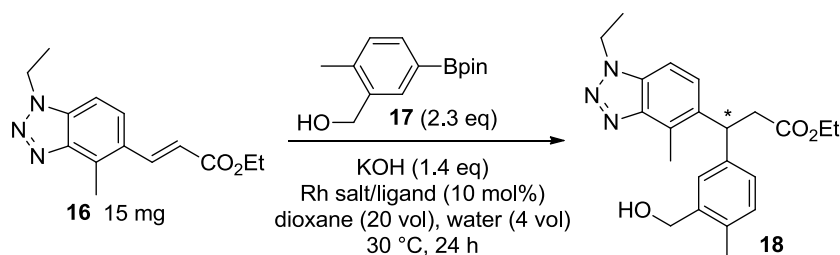
Vial	Rhodium Salt	Ligand	HPLC Area%				
			16	17	(S)-18	(R)-18	19
1	[Rh(Cl)(C ₂ H ₄) ₂] ₂	L10 IPA Diene	7.94		14.02	38.03	32.94
2	[Rh(Cl)(C ₂ H ₄) ₂] ₂	L11 Naphthyl Diene	2.26	0.14	61.81	2.55	17.57
3	[Rh(Cl)(C ₂ H ₄) ₂] ₂	L1 (<i>R</i>)-MeO-BIPHEP	3.54	4.23	37.49	12.17	22.33
4	[Rh(Cl)(C ₂ H ₄) ₂] ₂	L2 (<i>R</i>)-H8-BINAP	3.03	0.56	47.11	9.18	23.09
5	[Rh(Cl)(C ₂ H ₄) ₂] ₂	L14 (<i>R,R</i>)-Me-DuPhos	0.24	4.33	31.39	34.56	16.62
6	[Rh(Cl)(C ₂ H ₄) ₂] ₂	L21 (<i>R</i>)-MonoPhos		6.54	17.07	42.54	10.16
7	[Rh(Cl)(C ₂ H ₄) ₂] ₂	L3 (<i>R</i>)-Cl-BIPHEP	2.48	1.56	7.62	41.08	22.52
8	[Rh(Cl)(C ₂ H ₄) ₂] ₂	L4 (<i>R</i>)-P-Phos	5.32	19.07	35.48	7.71	10.22
9	[Rh(Cl)(C ₂ H ₄) ₂] ₂	L5 (<i>R</i>)-SEGPPOS	3.66	2.30	41.97	12.33	23.88
10	[Rh(Cl)(C ₂ H ₄) ₂] ₂	L15 (<i>R,R</i>)-Diop		2.24	19.63	39.50	18.87
11	[Rh(Cl)(C ₂ H ₄) ₂] ₂	L19 (<i>R</i>)-Xylyl-PHANEphos	2.87	3.93	32.23	9.06	20.17
12	[Rh(Cl)(C ₂ H ₄) ₂] ₂	L22 Bipol-A1(<i>S</i>)	15.21	16.32	2.43	2.54	32.01
13	[Rh(Cl)(C ₂ H ₄) ₂] ₂	L23 Phosphoramidite	15.07	21.48	1.80		18.51
14	[Rh(Cl)(C ₂ H ₄) ₂] ₂	L20 Walphos SL-W005-1	0.67	0.07	14.77	42.14	20.99
15	[Rh(Cl)(C ₂ H ₄) ₂] ₂	L18 catASium M(<i>R</i>)	6.80	8.29	16.80	14.83	28.39
16	[Rh(Cl)(C ₂ H ₄) ₂] ₂	L6 (<i>R</i>)-DTBM-SEGPPOS	12.90	11.49	3.96	1.53	24.07
17	[Rh(Cl)(C ₂ H ₄) ₂] ₂	L16 (<i>S,S</i>)-Chiraphos		3.85	11.94	51.27	17.14
18	[Rh(Cl)(C ₂ H ₄) ₂] ₂	L9 (<i>M,M,S</i>)-Tol-BINASO	15.82	9.99	7.12	1.14	31.13
19	[Rh(Cl)(C ₂ H ₄) ₂] ₂	L7 (<i>R</i>)-BINAP	2.31	1.01	45.06	9.88	21.46
20	[Rh(Cl)(C ₂ H ₄) ₂] ₂	L12 Ph-BOD		0.22	4.25	63.72	18.91
21	[Rh(Cl)(C ₂ H ₄) ₂] ₂	L13 Carreira DOLEFIN		0.20	12.18	59.04	18.32
22	[Rh(Cl)(C ₂ H ₄) ₂] ₂	L17 (<i>R</i>)-QuinoxP		0.94	21.54	47.19	19.30
23	[Rh(Cl)(C ₂ H ₄) ₂] ₂	L8 (<i>R</i>)-Tol-BINAP	2.13	0.98	47.70	10.82	24.04
24	[Rh(Cl)(C ₂ H ₄) ₂] ₂	N/A No Ligand	3.60	8.16	19.93	18.41	17.87
25	Rh(NBD) ₂ BF ₄	L10 IPA Diene	15.70		13.06	18.16	49.06
26	Rh(NBD) ₂ BF ₄	L11 Naphthyl Diene	3.69		62.67	8.01	19.70
27	Rh(NBD) ₂ BF ₄	L1 (<i>R</i>)-MeO-BIPHEP	4.80		47.56	13.61	27.66
28	Rh(NBD) ₂ BF ₄	L2 (<i>R</i>)-H8-BINAP	3.24		55.05	5.57	24.91
29	Rh(NBD) ₂ BF ₄	L14 (<i>R,R</i>)-Me-DuPhos			36.20	39.87	20.30
30	Rh(NBD) ₂ BF ₄	L21 (<i>R</i>)-MonoPhos		1.27	20.25	47.33	15.69
31	Rh(NBD) ₂ BF ₄	L3 (<i>R</i>)-Cl-BIPHEP	4.88		9.40	47.76	27.32
32	Rh(NBD) ₂ BF ₄	L4 (<i>R</i>)-P-Phos	1.37		59.69	12.10	21.69
33	Rh(NBD) ₂ BF ₄	L5 (<i>R</i>)-SEGPPOS	5.09		49.71	11.03	28.51
34	Rh(NBD) ₂ BF ₄	L15 (<i>R,R</i>)-Diop		3.35	23.97	50.59	16.41
35	Rh(NBD) ₂ BF ₄	L19 (<i>R</i>)-Xylyl-PHANEphos	4.13	1.55	38.98	12.35	24.64
36	Rh(NBD) ₂ BF ₄	L22 Bipol-A1(<i>S</i>)	16.82	23.34			9.21
37	Rh(NBD) ₂ BF ₄	L23 Phosphoramidite	15.65	21.18			15.48
38	Rh(NBD) ₂ BF ₄	L20 Walphos SL-W005-1	1.20		15.19	47.72	20.67
39	Rh(NBD) ₂ BF ₄	L18 catASium M(<i>R</i>)	9.59		24.96	25.21	37.81
40	Rh(NBD) ₂ BF ₄	L6 (<i>R</i>)-DTBM-SEGPPOS	13.91		6.35	1.66	37.22
41	Rh(NBD) ₂ BF ₄	L16 (<i>S,S</i>)-Chiraphos		0.11	9.84	66.97	19.59
42	Rh(NBD) ₂ BF ₄	L9 (<i>M,M,S</i>)-Tol-BINASO	11.72		16.06	16.57	54.97
43	Rh(NBD) ₂ BF ₄	L7 (<i>R</i>)-BINAP	4.59		49.89	10.79	26.94
44	Rh(NBD) ₂ BF ₄	L12 Ph-BOD			10.57	64.47	20.24
45	Rh(NBD) ₂ BF ₄	L13 Carreira DOLEFIN	11.32		17.19	28.28	40.42
46	Rh(NBD) ₂ BF ₄	L17 (<i>R</i>)-QuinoxP	0.20		25.48	51.92	19.34
47	Rh(NBD) ₂ BF ₄	L8 (<i>R</i>)-Tol-BINAP	4.09	0.16	52.99	11.05	25.45
48	Rh(NBD) ₂ BF ₄	N/A No Ligand	13.86		19.55	20.60	45.30
49	No rhodium salt	N/A No Ligand	20.17	26.00			3.10

Table 29. HPLC analysis (Method D1) for reactions at 30 °C. Enolate 16 at 9.6 min, arylboron reagent 17 at 3.9 min, bisaryl (S)-18 at 8.0 min, (R)-18 at 8.7 min, *o*-tolylmethanol 19 at 4.4 min.

Vial	Rhodium Salt	Ligand	HPLC Area%				
			16	17	(S)-18	(R)-18	19
12	[Rh(Cl)(C ₂ H ₄) ₂] ₂	L22 Bipol-A1(S)	13.67	0.37	5.39	4.81	45.24
13	[Rh(Cl)(C ₂ H ₄) ₂] ₂	L23 Phosphoramidite	14.92		5.92	1.19	40.73
15	[Rh(Cl)(C ₂ H ₄) ₂] ₂	L18 catASium M(R)	4.08	0.41	20.17	17.46	24.22
16	[Rh(Cl)(C ₂ H ₄) ₂] ₂	L6 (R)-DTBM-SEGPHOS	12.56	0.40	8.00	3.15	30.70
36	Rh(NBD) ₂ BF ₄	L22 Bipol-A1(S)	9.74		8.15	7.17	35.90
37	Rh(NBD) ₂ BF ₄	L23 Phosphoramidite	14.87		2.48	1.79	41.25
40	Rh(NBD) ₂ BF ₄	L6 (R)-DTBM-SEGPHOS	13.90		8.71	2.60	32.13

Table 30. HPLC analysis (Method D1) for reactions after additional heating at 60 °C. Enoate **16** at 9.6 min, arylboron reagent **17** at 3.9 min, bisaryl (S)-**18** at 8.0 min, (R)-**18** at 8.7 min, *o*-tolylmethanol **19** at 4.4 min.

5.3.2.2 Comparative Analysis of Rhodium Salts for Asymmetric Arylation (Procedure for Section 3.2.1.2)



Rh salt: one of six catalyst precursors (10 mol% Rh)
Ligand: none, or one of seven chiral ligands (10 mol%)

Ligands were weighed into reaction vials followed by rhodium salts according to Table 31 (page 190). The vials were stored under air overnight before being placed inside a nitrogen-filled glove bag. The two substrates **16** (15.0 mg, 57.8 μmol) and **17** (33.0 mg, 133 μmol) were added volumetrically as a nitrogen-sparged solution in dioxane (48 × 300 μL), inside the glove bag. Potassium hydroxide (4.5 mg, 81 μmol) was added as a nitrogen-sparged aqueous solution (48 × 60 μL), and the vials were then capped and pierced (2 × blunt needle) inside the glove bag before being transferred to a CAT96 reactor. The reactor was purged with nitrogen (3 × N₂/vent) before the reaction vials were stirred at 30 °C for 24 h under nitrogen.

The vials were sampled after 24 h (23 μL into ethanol (977 μL)) inside a nitrogen-filled glove bag, and the reaction vials were then resealed, pierced (2 × blunt needle) and transferred again to the CAT96 reactor. The reactor was purged with nitrogen and the vials were stirred at 60 °C for 65 h before sampling again in the same manner.

An additional reaction (Vial 49) was prepared and sampled in the same manner but stirred at 30 °C under nitrogen on a hotplate/stirrer, using a chiral rhodium precatalyst with no additional ligand: [Rh((R)-BINAP)(COD)]BF₄ (5.3 mg, 5.8 μmol). The samples were analysed by HPLC (Method D1), and the results are summarised in Table 32 (page 191) and Table 33 (page 192).

Vial	Rhodium Salt			Ligand				
	Identity	Amount / μmol	Mass / mg	Identifier	CAS Number	Amount / μmol	Mass / mg	
1	[RhCl(COD)] ₂	2.9	1.4	L11	Naphthyl Ester Diene	1188966-75-7	5.8	1.9
2	[RhCl(COD)] ₂	2.9	1.4	L2	(<i>R</i>)-H8-BINAP	139139-86-9	5.8	3.6
3	[RhCl(COD)] ₂	2.9	1.4	L5	(<i>R</i>)-SEGPPOS	244261-66-3	5.8	3.5
4	[RhCl(COD)] ₂	2.9	1.4	L16	(<i>S,S</i>)-Chiraphos	64896-28-2	5.8	2.5
5	[RhCl(COD)] ₂	2.9	1.4	L9	(<i>M,M,S</i>)-Tol-BINASO	722455-72-3	5.8	3.1
6	[RhCl(COD)] ₂	2.9	1.4	L7	(<i>R</i>)-BINAP	76189-55-4	5.8	3.6
7	[RhCl(COD)] ₂	2.9	1.4	L12	Ph-BOD	850409-83-5	5.8	1.5
8	[RhCl(COD)] ₂	2.9	1.4	N/A	No Ligand	N/A	N/A	N/A
9	Rh(COD) ₂ BF ₄	5.8	2.3	L11	Naphthyl Ester Diene	1188966-75-7	5.8	1.9
10	Rh(COD) ₂ BF ₄	5.8	2.3	L2	(<i>R</i>)-H8-BINAP	139139-86-9	5.8	3.6
11	Rh(COD) ₂ BF ₄	5.8	2.3	L5	(<i>R</i>)-SEGPPOS	244261-66-3	5.8	3.5
12	Rh(COD) ₂ BF ₄	5.8	2.3	L16	(<i>S,S</i>)-Chiraphos	64896-28-2	5.8	2.5
13	Rh(COD) ₂ BF ₄	5.8	2.3	L9	(<i>M,M,S</i>)-Tol-BINASO	722455-72-3	5.8	3.1
14	Rh(COD) ₂ BF ₄	5.8	2.3	L7	(<i>R</i>)-BINAP	76189-55-4	5.8	3.6
15	Rh(COD) ₂ BF ₄	5.8	2.3	L12	Ph-BOD	850409-83-5	5.8	1.5
16	Rh(COD) ₂ BF ₄	5.8	2.3	N/A	No Ligand	N/A	N/A	N/A
17	[RhCl(COE)] ₂	2.9	2.1	L11	Naphthyl Ester Diene	1188966-75-7	5.8	1.9
18	[RhCl(COE)] ₂	2.9	2.1	L2	(<i>R</i>)-H8-BINAP	139139-86-9	5.8	3.6
19	[RhCl(COE)] ₂	2.9	2.1	L5	(<i>R</i>)-SEGPPOS	244261-66-3	5.8	3.5
20	[RhCl(COE)] ₂	2.9	2.1	L16	(<i>S,S</i>)-Chiraphos	64896-28-2	5.8	2.5
21	[RhCl(COE)] ₂	2.9	2.1	L9	(<i>M,M,S</i>)-Tol-BINASO	722455-72-3	5.8	3.1
22	[RhCl(COE)] ₂	2.9	2.1	L7	(<i>R</i>)-BINAP	76189-55-4	5.8	3.6
23	[RhCl(COE)] ₂	2.9	2.1	L12	Ph-BOD	850409-83-5	5.8	1.5
24	[RhCl(COE)] ₂	2.9	2.1	N/A	No Ligand	N/A	N/A	N/A
25	Rh(acac)(C ₂ H ₄) ₂	5.8	1.5	L11	Naphthyl Ester Diene	1188966-75-7	5.8	1.9
26	Rh(acac)(C ₂ H ₄) ₂	5.8	1.5	L2	(<i>R</i>)-H8-BINAP	139139-86-9	5.8	3.6
27	Rh(acac)(C ₂ H ₄) ₂	5.8	1.5	L5	(<i>R</i>)-SEGPPOS	244261-66-3	5.8	3.5
28	Rh(acac)(C ₂ H ₄) ₂	5.8	1.5	L16	(<i>S,S</i>)-Chiraphos	64896-28-2	5.8	2.5
29	Rh(acac)(C ₂ H ₄) ₂	5.8	1.5	L9	(<i>M,M,S</i>)-Tol-BINASO	722455-72-3	5.8	3.1
30	Rh(acac)(C ₂ H ₄) ₂	5.8	1.5	L7	(<i>R</i>)-BINAP	76189-55-4	5.8	3.6
31	Rh(acac)(C ₂ H ₄) ₂	5.8	1.5	L12	Ph-BOD	850409-83-5	5.8	1.5
32	Rh(acac)(C ₂ H ₄) ₂	5.8	1.5	N/A	No Ligand	N/A	N/A	N/A
33	Rh(acac)(CO) ₂	5.8	1.5	L11	Naphthyl Ester Diene	1188966-75-7	5.8	1.9
34	Rh(acac)(CO) ₂	5.8	1.5	L2	(<i>R</i>)-H8-BINAP	139139-86-9	5.8	3.6
35	Rh(acac)(CO) ₂	5.8	1.5	L5	(<i>R</i>)-SEGPPOS	244261-66-3	5.8	3.5
36	Rh(acac)(CO) ₂	5.8	1.5	L16	(<i>S,S</i>)-Chiraphos	64896-28-2	5.8	2.5
37	Rh(acac)(CO) ₂	5.8	1.5	L9	(<i>M,M,S</i>)-Tol-BINASO	722455-72-3	5.8	3.1
38	Rh(acac)(CO) ₂	5.8	1.5	L7	(<i>R</i>)-BINAP	76189-55-4	5.8	3.6
39	Rh(acac)(CO) ₂	5.8	1.5	L12	Ph-BOD	850409-83-5	5.8	1.5
40	Rh(acac)(CO) ₂	5.8	1.5	N/A	No Ligand	N/A	N/A	N/A
41	[Rh(OH)(COD)] ₂	2.9	1.3	L11	Naphthyl Ester Diene	1188966-75-7	5.8	1.9
42	[Rh(OH)(COD)] ₂	2.9	1.3	L2	(<i>R</i>)-H8-BINAP	139139-86-9	5.8	3.6
43	[Rh(OH)(COD)] ₂	2.9	1.3	L5	(<i>R</i>)-SEGPPOS	244261-66-3	5.8	3.5
44	[Rh(OH)(COD)] ₂	2.9	1.3	L16	(<i>S,S</i>)-Chiraphos	64896-28-2	5.8	2.5
45	[Rh(OH)(COD)] ₂	2.9	1.3	L9	(<i>M,M,S</i>)-Tol-BINASO	722455-72-3	5.8	3.1
46	[Rh(OH)(COD)] ₂	2.9	1.3	L7	(<i>R</i>)-BINAP	76189-55-4	5.8	3.6
47	[Rh(OH)(COD)] ₂	2.9	1.3	L12	Ph-BOD	850409-83-5	5.8	1.5
48	[Rh(OH)(COD)] ₂	2.9	1.3	N/A	No Ligand	N/A	N/A	N/A

Table 31. Rhodium salts and ligands dispensed to reaction vials for rhodium salt comparisons.

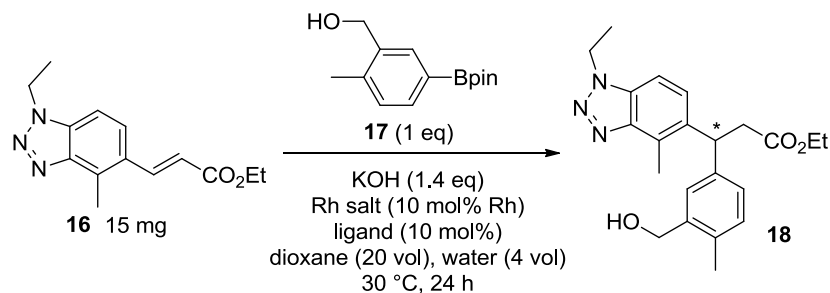
Vial	Rhodium Salt	Ligand	HPLC Area%				
			16	17	(S)-18	(R)-18	19
1	[RhCl(COD)] ₂	L11 Naphthyl Ester Diene	0.50		35.95	35.40	17.00
2	[RhCl(COD)] ₂	L2 (R)-H8-BINAP	0.15	0.30	40.74	32.65	18.57
3	[RhCl(COD)] ₂	L5 (R)-SEGPLHOS	0.12	3.75	41.37	34.80	19.44
4	[RhCl(COD)] ₂	L16 (S,S)-Chiraphos		0.07	37.45	40.88	18.99
5	[RhCl(COD)] ₂	L9 (M,M,S)-Tol-BINASO	0.37		34.14	34.11	30.14
6	[RhCl(COD)] ₂	L7 (R)-BINAP		4.34	38.94	34.72	18.73
7	[RhCl(COD)] ₂	L12 Ph-BOD	0.46		36.16	38.24	18.43
8	[RhCl(COD)] ₂	N/A No Ligand	0.17		39.65	39.18	19.44
9	Rh(COD) ₂ BF ₄	L11 Naphthyl Ester Diene	0.40		37.11	35.69	16.17
10	Rh(COD) ₂ BF ₄	L2 (R)-H8-BINAP	1.47	0.13	44.61	22.78	20.47
11	Rh(COD) ₂ BF ₄	L5 (R)-SEGPLHOS	2.52	2.30	45.54	24.89	23.67
12	Rh(COD) ₂ BF ₄	L16 (S,S)-Chiraphos			19.22	58.31	19.12
13	Rh(COD) ₂ BF ₄	L9 (M,M,S)-Tol-BINASO			35.59	34.61	28.74
14	Rh(COD) ₂ BF ₄	L7 (R)-BINAP	2.09	3.04	46.11	23.44	21.72
15	Rh(COD) ₂ BF ₄	L12 Ph-BOD			36.88	39.99	18.07
16	Rh(COD) ₂ BF ₄	N/A No Ligand			39.86	39.85	19.83
17	[RhCl(COE)] ₂	L11 Naphthyl Ester Diene	1.17		68.60	3.36	18.02
18	[RhCl(COE)] ₂	L2 (R)-H8-BINAP	3.80	2.50	51.82	5.58	21.16
19	[RhCl(COE)] ₂	L5 (R)-SEGPLHOS	4.54	6.25	52.20	10.97	22.93
20	[RhCl(COE)] ₂	L16 (S,S)-Chiraphos	0.13	11.78	17.40	59.30	10.15
21	[RhCl(COE)] ₂	L9 (M,M,S)-Tol-BINASO	18.78	30.58	3.33	2.80	38.32
22	[RhCl(COE)] ₂	L7 (R)-BINAP	3.14	1.90	54.64	11.20	24.88
23	[RhCl(COE)] ₂	L12 Ph-BOD		0.29	3.36	71.54	18.95
24	[RhCl(COE)] ₂	N/A No Ligand	2.88	14.00	29.53	26.82	16.15
25	Rh(acac)(C ₂ H ₄) ₂	L11 Naphthyl Ester Diene	2.77	3.34	57.19	2.78	16.04
26	Rh(acac)(C ₂ H ₄) ₂	L2 (R)-H8-BINAP	11.61	30.46	19.16	5.88	11.57
27	Rh(acac)(C ₂ H ₄) ₂	L5 (R)-SEGPLHOS	13.91	34.07	15.84	4.47	13.18
28	Rh(acac)(C ₂ H ₄) ₂	L16 (S,S)-Chiraphos	7.29	26.60	11.21	35.32	10.14
29	Rh(acac)(C ₂ H ₄) ₂	L9 (M,M,S)-Tol-BINASO	12.24	26.81	15.52	6.47	24.06
30	Rh(acac)(C ₂ H ₄) ₂	L7 (R)-BINAP	14.03	36.45	12.13	2.32	11.86
31	Rh(acac)(C ₂ H ₄) ₂	L12 Ph-BOD		5.05	2.82	67.91	10.46
32	Rh(acac)(C ₂ H ₄) ₂	N/A No Ligand	4.74	13.62	30.63	25.85	14.89
33	Rh(acac)(CO) ₂	L11 Naphthyl Ester Diene	28.30	44.44	10.57	3.52	5.90
34	Rh(acac)(CO) ₂	L2 (R)-H8-BINAP	20.76	47.72			3.44
35	Rh(acac)(CO) ₂	L5 (R)-SEGPLHOS	22.41	62.10		0.33	3.27
36	Rh(acac)(CO) ₂	L16 (S,S)-Chiraphos	25.19	63.98			3.87
37	Rh(acac)(CO) ₂	L9 (M,M,S)-Tol-BINASO	9.34	23.43	17.87	16.71	25.26
38	Rh(acac)(CO) ₂	L7 (R)-BINAP	20.46	60.28			3.34
39	Rh(acac)(CO) ₂	L12 Ph-BOD	11.33	30.31	17.84	19.27	7.88
40	Rh(acac)(CO) ₂	N/A No Ligand	8.88	25.42	24.13	23.54	10.63
41	[Rh(OH)(COD)] ₂	L11 Naphthyl Ester Diene	0.92		35.75	35.07	17.62
42	[Rh(OH)(COD)] ₂	L2 (R)-H8-BINAP		0.20	40.00	31.74	19.39
43	[Rh(OH)(COD)] ₂	L5 (R)-SEGPLHOS	0.09	4.49	37.86	36.84	20.73
44	[Rh(OH)(COD)] ₂	L16 (S,S)-Chiraphos		0.19	36.20	40.23	21.09
45	[Rh(OH)(COD)] ₂	L9 (M,M,S)-Tol-BINASO	0.90		32.62	33.08	32.86
46	[Rh(OH)(COD)] ₂	L7 (R)-BINAP	0.08	4.67	38.98	33.73	19.08
47	[Rh(OH)(COD)] ₂	L12 Ph-BOD	0.27		36.04	37.81	19.73
48	[Rh(OH)(COD)] ₂	N/A No Ligand	1.30		38.43	38.72	20.70
49	Rh((R)-BINAP)(COD)BF ₄	N/A No ligand	0.25	4.35	47.44	22.44	20.13

Table 32. HPLC analysis (Method D1) for reactions at 30 °C. Enoate 16 at 9.6 min, arylboron reagent 17 at 3.9 min, bisaryl (S)-18 at 8.0 min, (R)-18 at 8.7 min, *o*-tolylmethanol 19 at 4.4 min.

Vial	Rhodium Salt	Ligand	HPLC Area%				
			16	17	(S)-18	(R)-18	19
17	[RhCl(COE) ₂] ₂	L11 Naphthyl Ester Diene	1.98	0.02	68.53	3.40	18.36
18	[RhCl(COE) ₂] ₂	L2 (R)-H8-BINAP	3.73	0.05	53.99	6.03	22.07
19	[RhCl(COE) ₂] ₂	L5 (R)-SEGPHOS	3.83	2.02	54.56	11.75	25.81
20	[RhCl(COE) ₂] ₂	L16 (S,S)-Chiraphos			18.36	60.30	19.02
21	[RhCl(COE) ₂] ₂	L9 (M,M,S)-Tol-BINASO	16.59	5.83	7.19	4.05	53.25
22	[RhCl(COE) ₂] ₂	L2 (R)-BINAP	2.91	2.61	55.94	11.39	24.23
23	[RhCl(COE) ₂] ₂	L12 Ph-BOD		0.19	3.90	71.60	19.30
24	[RhCl(COE) ₂] ₂	N/A No Ligand	0.59		33.57	30.74	22.91
25	Rh(acac)(C ₂ H ₄) ₂	L11 Naphthyl Ester Diene	1.98	0.04	59.08	2.83	18.93
26	Rh(acac)(C ₂ H ₄) ₂	L2 (R)-H8-BINAP	6.83	0.33	30.05	10.74	31.14
27	Rh(acac)(C ₂ H ₄) ₂	L5 (R)-SEGPHOS	9.38	1.94	25.99	12.12	35.30
28	Rh(acac)(C ₂ H ₄) ₂	L16 (S,S)-Chiraphos	0.36	0.19	15.03	53.33	21.87
29	Rh(acac)(C ₂ H ₄) ₂	L9 (M,M,S)-Tol-BINASO	8.45	18.69	13.79	6.06	36.84
30	Rh(acac)(C ₂ H ₄) ₂	L7 (R)-BINAP	11.22		22.84	5.85	35.37
31	Rh(acac)(C ₂ H ₄) ₂	L12 Ph-BOD		0.52	2.82	63.72	18.31
32	Rh(acac)(C ₂ H ₄) ₂	N/A No Ligand	1.92		35.55	30.56	23.00
33	Rh(acac)(CO) ₂	L11 Naphthyl Ester Diene	9.28	9.72	37.82	5.21	22.92
34	Rh(acac)(CO) ₂	L2 (R)-H8-BINAP	17.70	5.12	9.40	7.27	44.13
35	Rh(acac)(CO) ₂	L5 (R)-SEGPHOS	10.14	8.41	18.55	4.76	49.38
36	Rh(acac)(CO) ₂	L16 (S,S)-Chiraphos	13.16	21.99	6.87	19.94	32.48
37	Rh(acac)(CO) ₂	L9 (M,M,S)-Tol-BINASO	6.52	15.53	16.53	14.68	33.58
38	Rh(acac)(CO) ₂	L7 (R)-BINAP	15.32		12.99	8.09	51.65
39	Rh(acac)(CO) ₂	L12 Ph-BOD	1.04	13.66	15.07	38.11	11.00
40	Rh(acac)(CO) ₂	N/A No Ligand	4.95	16.71	22.96	21.00	16.48

Table 33. HPLC analysis (Method D1) for reactions after additional heating at 60 °C. Enoate **16** at 9.6 min, arylboron reagent **17** at 3.9 min, bisaryl (S)-**18** at 8.0 min, (R)-**18** at 8.7 min, *o*-tolylmethanol **19** at 4.4 min.

5.3.2.3 Competition Experiments to Determine Relative Extents of Conjugate Arylation and Protodeboronation (Procedure for Section 3.2.1.3)



Ligands and rhodium salts were weighed into vials according to Table 34 (page 193), and the vials were placed inside a nitrogen-filled glove bag. The two substrates **16** (15.0 mg, 57.8 μmol) and **17** (14.4 mg, 57.8 μmol) were added volumetrically as a nitrogen-sparged solution in dioxane (16 × 300 μL), inside the glove bag. Potassium hydroxide (4.5 mg, 81 μmol) was added as a nitrogen-sparged aqueous solution (16 × 60 μL), and the vials were then capped and pierced (2 × blunt needle) inside the glove bag before being transferred to a

CAT96 reactor. The reactor was purged with nitrogen ($> 3 \times N_2/\text{vent}$) before the reaction vials were stirred at 30 °C for 24 h under nitrogen. The vials were sampled after 24 h (23 μL into ethanol (977 μL)).

To confirm the results, four reactions were repeated (Vials 17 to 20, see Section 3.2.1.3). The reaction vials were prepared in the same manner except that Schlenk line techniques were used rather than a glove bag. The vials were transferred to a CAT96 reactor after preparation and the rest of the experiment performed in the same manner.

The samples were analysed by HPLC (Method D1), and the results are summarised in Table 35 (page 194).

Vial	Rhodium Salt		Ligand			
	Identity	Amount / Mass μmol / mg	Identifier	CAS Number	Amount μmol	Mass / mg
1	$[\text{RhCl}(\text{COE})_2]_2$	2.9 2.1	L11 Naphthyl Ester Diene	1188966-75-7	5.8	1.9
2	$[\text{RhCl}(\text{COE})_2]_2$	2.9 2.1	L2 (<i>R</i>)-H8-BINAP	139139-86-9	5.8	3.6
3	$[[\text{RhCl}(\text{COE})_2]_2]$	2.9 2.1	L12 Ph-BOD	850409-83-5	5.8	1.5
4	$[[\text{RhCl}(\text{COE})_2]_2]$	2.9 2.1	N/A No Ligand	N/A	N/A	N/A
5	$\text{Rh}(\text{acac})(\text{C}_2\text{H}_4)_2$	5.8 1.5	L11 Naphthyl Ester Diene	1188966-75-7	5.8	1.9
6	$\text{Rh}(\text{acac})(\text{C}_2\text{H}_4)_2$	5.8 1.5	L2 (<i>R</i>)-H8-BINAP	139139-86-9	5.8	3.6
7	$\text{Rh}(\text{acac})(\text{C}_2\text{H}_4)_2$	5.8 1.5	L12 Ph-BOD	850409-83-5	5.8	1.5
8	$\text{Rh}(\text{acac})(\text{C}_2\text{H}_4)_2$	5.8 1.5	N/A No Ligand	N/A	N/A	N/A
9	$[\text{Rh}(\text{Cl})(\text{C}_2\text{H}_4)_2]_2$	2.9 1.1	L11 Naphthyl Ester Diene	1188966-75-7	5.8	1.9
10	$[\text{Rh}(\text{Cl})(\text{C}_2\text{H}_4)_2]_2$	2.9 1.1	L2 (<i>R</i>)-H8-BINAP	139139-86-9	5.8	3.6
11	$[\text{Rh}(\text{Cl})(\text{C}_2\text{H}_4)_2]_2$	2.9 1.1	L12 Ph-BOD	850409-83-5	5.8	1.5
12	$[\text{Rh}(\text{Cl})(\text{C}_2\text{H}_4)_2]_2$	2.9 1.1	N/A No Ligand	N/A	N/A	N/A
13	$\text{Rh}(\text{NBD})_2\text{BF}_4$	5.8 2.2	L11 Naphthyl Ester Diene	1188966-75-7	5.8	1.9
14	$\text{Rh}(\text{NBD})_2\text{BF}_4$	5.8 2.2	L2 (<i>R</i>)-H8-BINAP	139139-86-9	5.8	3.6
15	$\text{Rh}(\text{NBD})_2\text{BF}_4$	5.8 2.2	L12 Ph-BOD	850409-83-5	5.8	1.5
16	$\text{Rh}(\text{NBD})_2\text{BF}_4$	5.8 2.2	N/A No Ligand	N/A	N/A	N/A
17	$[\text{Rh}(\text{Cl})(\text{C}_2\text{H}_4)_2]_2$	2.9 1.1	L12 Ph-BOD	850409-83-5	5.8	1.5
18	$\text{Rh}(\text{NBD})_2\text{BF}_4$	5.8 2.2	L11 Naphthyl Ester Diene	1188966-75-7	5.8	1.9
19	$\text{Rh}(\text{NBD})_2\text{BF}_4$	5.8 2.2	L12 Ph-BOD	850409-83-5	5.8	1.5
20	$\text{Rh}(\text{NBD})_2\text{BF}_4$	5.8 2.2	N/A No Ligand	N/A	N/A	N/A

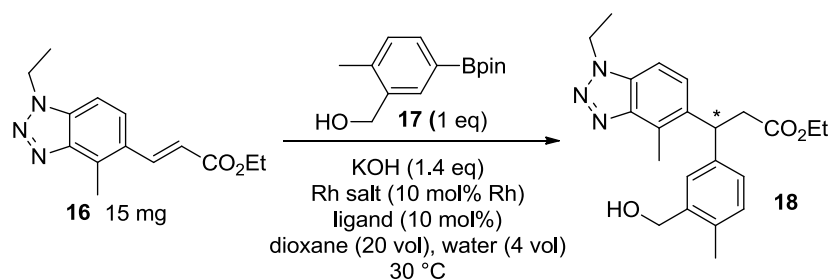
Table 34. Rhodium salts and ligands dispensed to reaction vials for competition experiments.

Vial	Rhodium Salt	Ligand	HPLC Area%				
			16	17	(S)-18	(R)-18	19
1	[RhCl(COE) ₂] ₂	L11 Naphthyl Diene	7.45		62.43	3.10	13.13
2	[RhCl(COE) ₂] ₂	L2 (R)-H8-BINAP	7.93		43.58	5.53	18.20
3	[[RhCl(COE) ₂] ₂	L12 Ph-BOD			5.15	80.39	4.60
4	[[RhCl(COE) ₂] ₂	N/A No Ligand	11.73	7.42	26.87	25.68	16.70
5	Rh(acac)(C ₂ H ₄) ₂	L11 Naphthyl Diene	1.52	0.73	62.75	2.58	5.72
6	Rh(acac)(C ₂ H ₄) ₂	L2 (R)-H8-BINAP	14.93	23.69	20.04	3.21	14.40
7	Rh(acac)(C ₂ H ₄) ₂	L12 Ph-BOD		1.34	5.92	71.00	2.54
8	Rh(acac)(C ₂ H ₄) ₂	N/A No Ligand	10.03	0.37	25.04	23.28	20.70
9	[Rh(Cl)(C ₂ H ₄) ₂] ₂	L11 Naphthyl Diene	3.23	0.35	64.14	2.18	6.90
10	[Rh(Cl)(C ₂ H ₄) ₂] ₂	L2 (R)-H8-BINAP	7.29	1.11	34.72	5.41	14.72
11	[Rh(Cl)(C ₂ H ₄) ₂] ₂	L12 Ph-BOD		0.88	4.11	77.33	3.25
12	[Rh(Cl)(C ₂ H ₄) ₂] ₂	N/A No Ligand	15.58	0.72	19.96	18.73	19.52
13	Rh(NBD) ₂ BF ₄	L11 Naphthyl Diene	8.70		61.32	4.82	11.56
14	Rh(NBD) ₂ BF ₄	L2 (R)-H8-BINAP	8.37		40.13	3.87	20.28
15	Rh(NBD) ₂ BF ₄	L12 Ph-BOD	14.92		7.35	19.15	34.62
16	Rh(NBD) ₂ BF ₄	N/A No Ligand	20.16		14.87	15.34	37.34
17	[Rh(Cl)(C ₂ H ₄) ₂] ₂	L12 Ph-BOD	0.27		4.28	81.69	1.95
18	Rh(NBD) ₂ BF ₄	L11 Naphthyl Diene	10.87		63.88	7.21	8.25
19	Rh(NBD) ₂ BF ₄	L12 Ph-BOD	20.62		13.85	21.90	27.87
20	Rh(NBD) ₂ BF ₄	N/A No Ligand	27.87		16.68	17.86	35.63

Table 35. HPLC analysis (Method D1) for reactions at 30 °C. Enoate 16 at 9.6 min, arylboron reagent 17 at 3.9 min, bisaryl (S)-18 at 8.0 min, (R)-18 at 8.7 min, *o*-tolylmethanol 19 at 4.4 min.

5.3.2.4 Time-Coursing Experiments with Conjugate Arylation Catalyst Systems (Procedures for Section 3.2.1.4)

5.3.2.4.1 First Set of Time-Coursing Experiments (Figure 19, page 67)



Ligands and rhodium salts were weighed into vials according to Table 36 (page 195), and the vials were capped and inerted (N₂-sparge). The two substrates **16** (15.0 mg, 57.8 μmol) and **17** (14.4 mg, 57.8 μmol) were added volumetrically as a nitrogen-sparged solution in dioxane (6 × 300 μL), inside the glove bag. Potassium hydroxide (4.5 mg, 81 μmol) was added as a nitrogen-sparged aqueous solution (6 × 60 μL), before stirring at 30 °C on a hotplate/stirrer under a positive pressure of nitrogen. Samples were taken at *t* = 15 min, 45 min, 1.5 h, 2.5 h, 3.75 h, 5.25 h, 7 h and 70 h. Sampling was performed by diluting a 5 μL sample of the mixtures into 200 μL of ethanol. The sampling-syringe was washed in ethanol and then in dioxane (3 × successive wash vials) between samples.

The samples were analysed by HPLC (Method D1), and the results are summarised in Table 37 (page 196).

Vial	Rhodium Salt			Ligand				
	Identity	Amount / μmol	Mass / mg	Identifier	CAS Number	Amount / μmol	Mass / mg	
1	Rh(acac)(C ₂ H ₄) ₂	5.8	1.5	L2	(R)-H8-BINAP	139139-86-9	5.8	3.6
2	Rh(acac)(C ₂ H ₄) ₂	5.8	1.5	L12	Ph-BOD	850409-83-5	5.8	1.5
3	[RhCl(C ₂ H ₄) ₂] ₂	2.9	1.1	L2	(R)-H8-BINAP	139139-86-9	5.8	3.6
4	[RhCl(C ₂ H ₄) ₂] ₂	2.9	1.1	L12	Ph-BOD	850409-83-5	5.8	1.5
5	[RhCl(C ₂ H ₄) ₂] ₂	2.9	1.1	L11	Naphthyl Ester Diene	1188966-75-7	5.8	1.9
6	Rh(NBD) ₂ BF ₄	5.8	2.2	L11	Naphthyl Ester Diene	1188966-75-7	5.8	1.9

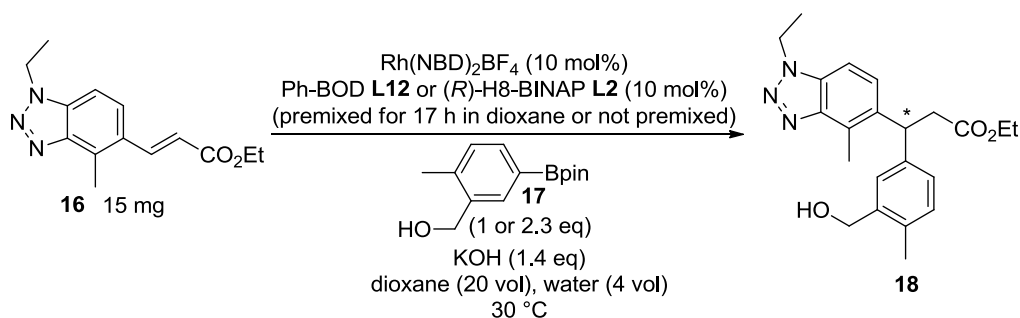
Table 36. Rhodium salts and ligands dispensed for the first set of time-coursing experiments.

Vial	Rhodium Salt / Ligand	Timepoint	HPLC Area%				
			16	17	(S)-18	(R)-18	19
1	Rh(acac)(C ₂ H ₄) ₂ / (R)-H8-BINAP	0	35.58	49.74			
		15 min	34.05	46.60			0.99
		45 min	28.13	39.97	0.66		0.79
		1 h 30 min	25.34	35.59	1.41		1.06
		2 h 30 min	23.73	33.27	2.10		1.40
		3 h 45 min	23.22	31.62	2.84	0.24	1.84
		5 h 15 min	20.34	30.07	3.23	0.24	4.64
		7 h	21.69	27.41	4.41	0.33	3.49
	70 h	16.18	8.01	10.35	0.75	16.61	
2	Rh(acac)(C ₂ H ₄) ₂ / Ph-BOD	0	35.898	43.41			
		15 min	10.186	9.92	2.11	64.94	0.98
		45 min	1.52	0.83	2.55	78.55	1.29
		1 h 30 min		3.21	2.47	74.69	1.93
		2 h 30 min		5.18	2.28	69.41	5.25
		3 h 45 min		6.03	2.26	67.73	5.92
		5 h 15 min		6.99	2.12	64.70	6.66
		7 h		8.28	2.31	69.54	2.92
	70 h		13.76	1.69	52.95	6.65	
3	[RhCl(C ₂ H ₄) ₂] ₂ / (R)-H8-BINAP	0	40.09	49.97			0.42
		15 min	29.41	38.18	2.56		1.96
		45 min	25.50	34.41	4.20	0.34	2.64
		1 h 30 min	22.81	31.76	6.07	0.60	3.29
		2 h 30 min	20.71	28.73	7.94	0.81	3.98
		3 h 45 min	19.20	25.18	10.22	1.02	4.45
		5 h 15 min	17.49	21.16	12.43	1.32	5.59
		7 h	16.36	16.67	15.43	1.50	7.25
	70 h	10.70	0.02	32.60	4.62	20.34	
4	[RhCl(C ₂ H ₄) ₂] ₂ / Ph-BOD	0	40.46	52.12			
		15 min	6.35	2.16	2.54	75.57	1.58
		45 min	1.17		2.76	82.64	2.05
		1 h 30 min	0.87	1.21	2.67	79.57	3.39
		2 h 30 min	0.76	1.82	2.62	78.81	3.94
		3 h 45 min	0.73	3.00	2.54	76.15	4.91
		5 h 15 min	0.86	2.89	2.36	77.56	4.78
		7 h	0.21	3.20	2.23	77.78	4.99
	70 h	0.16	7.48	1.94	68.32	7.20	

Vial	Rhodium Salt / Ligand	Timepoint	HPLC Area%				
			16	17	(S)-18	(R)-18	19
5	[RhCl(C ₂ H ₄) ₂] ₂ / Naphthyl Ester Diene	0	46.74	53.12			
		15 min	6.71		73.07	1.65	6.15
		45 min	6.57		71.95	1.61	6.28
		1 h 30 min	6.44		71.54	1.60	6.40
		2 h 30 min	6.51		71.28	1.62	6.49
		3 h 45 min	6.44		71.26	1.65	6.51
		5 h 15 min	6.36		71.34	1.59	6.53
		7 h	6.31		71.31	1.61	6.59
		70 h	6.86	2.62	65.17	1.64	8.49
6	Rh(NBD) ₂ BF ₄ / Naphthyl Ester Diene	0	55.59	44.29			
		15 min	51.47	39.56	0.72		3.68
		45 min	42.99	30.98	11.72	1.72	5.22
		1 h 30 min	22.55	10.36	46.82	4.99	7.24
		2 h 30 min	14.13		59.93	5.91	9.06
		3 h 45 min	14.44	0.16	62.07	6.21	8.90
		5 h 15 min	14.46		61.59	6.17	8.85
		7 h	13.04		60.58	6.21	8.94
		70 h	14.37	2.91	56.49	6.16	9.64

Table 37. HPLC analysis (Method D1) for time-coursing experiments. Enoate **16** at 9.6 min, arylboron reagent **17** at 3.9 min, bisaryl (S)-**18** at 8.0 min, (R)-**18** at 8.7 min, *o*-tolylmethanol **19** at 4.4 min.

5.3.2.4.2 Second Set of Time-Coursing Experiments (Figure 22, page 70)



Ph-BOD **L12** (5 × 1.5 mg, 5.8 μmol) or (R)-H8-BINAP **L2** (3 × 3.6 mg, 5.8 μmol) and Rh(NBD)₂BF₄ (8 × 2.2 mg, 5.8 μmol) were weighed into vials according to Table 38. The reaction vials for which premixing of the ligand and catalyst precursor were to be performed in (Table 38) were capped and inerted (N₂-sparge) before addition of nitrogen-sparged dioxane (3 × 150 μL). These vials were stirred under nitrogen at 30 °C for 17 h, and the remaining vials were left under air for that time before they were capped and sparged with nitrogen. The two substrates **16** (8 × 15.0 mg, 57.8 μmol) and **17** (6 × 14.4 mg, 57.8 μmol; 2 × 33.0 mg, 133 μmol) were added volumetrically as nitrogen-sparged solutions in dioxane (3 × 150 μL, 5 × 300 μL) to each vial (Table 38). The solutions were therefore prepared according to the required concentration to reach the intended substrate loading with the intended total volumes of dioxane (20 vol). The *t* = 0 timepoint was then taken before potassium hydroxide (4.5 mg, 81 μmol) was added as a nitrogen-sparged aqueous solution

(8 × 60 μL). The reaction vials were stirred at 30 °C on a hotplate/stirrer under a positive pressure of nitrogen. Samples were taken at $t = 10$ min, 25 min, 45 min, 1 h 10 min, 1 h 40 min, 2 h 15 min, 2 h 55 min, 3 h 40 min, 4 h 30 min, 5 h 25 min, 24 h, prepared as in Section 5.3.2.4.1.

Vial	Dioxane (Premixing) / μL	Dioxane (Substrates) / μL	Equivalents of ArBpin 17	Ligand
1	150	150	1.0	L12 Ph-BOD
2	-	300	1.0	L12 Ph-BOD
3	150	150	2.3	L12 Ph-BOD
4	-	300	1.0	L12 Ph-BOD
5	150	150	1.0	L2 (R)-H8-BINAP
6	-	300	1.0	L2 (R)-H8-BINAP
7	-	300	2.3	L12 Ph-BOD
8	-	300	1.0	L2 (R)-H8-BINAP

Table 38. Reaction vial preparation for the second set of time-coursing experiments.

The samples were analysed by HPLC (Method D1), and the results are summarised in Table 39.

Vial	Ligand (Premix Y/N)	Equivalents of ArBpin 17	Timepoint	HPLC Area%				
				16	17	(S)-18	(R)-18	19
1	Ph-BOD (Y)	1.0	0	36.44	47.91			
			10 min	21.80	16.99	3.99	32.28	9.72
			25 min	13.40	8.45	4.59	47.53	10.03
			45 min	9.13	4.35	4.78	55.81	9.92
			1 h 10 min	6.42	0.31	4.94	63.00	9.14
			1 h 40 min	4.45		4.43	58.93	10.66
			2 h 15 min	3.70		4.35	58.52	10.58
			2 h 55 min	3.17		4.37	60.04	10.39
			3 h 40 min	3.08		4.08	55.69	10.50
			4 h 30 min	3.02		4.07	55.22	11.12
			5 h 25 min	2.92		3.98	54.03	11.28
24 h	2.00		3.40	47.71	12.38			
2	Ph-BOD (N)	1.0	0	37.68	48.33			
			10 min	27.46	2.42	11.29	18.39	26.75
			25 min	24.70		11.38	21.42	28.89
			45 min	24.20		11.26	21.40	29.56
			1 h 10 min	23.78		11.14	21.33	29.84
			1 h 40 min	23.08		11.13	21.25	29.43
			2 h 15 min	22.86		10.97	21.05	29.65
			2 h 55 min	22.54		10.85	20.79	29.40
			3 h 40 min	21.70		10.79	20.62	30.00
			4 h 30 min	22.13		10.81	20.73	29.42
			5 h 25 min	21.99		10.67	20.65	29.89
24 h	19.86		9.87	20.96	30.49			
3	Ph-BOD (Y)	2.3	0	24.64	65.24			
			10 min	13.34	20.69	9.16	24.09	16.70
			25 min	5.89	9.71	10.44	46.54	16.03
			45 min	1.97	5.24	10.52	59.08	14.84

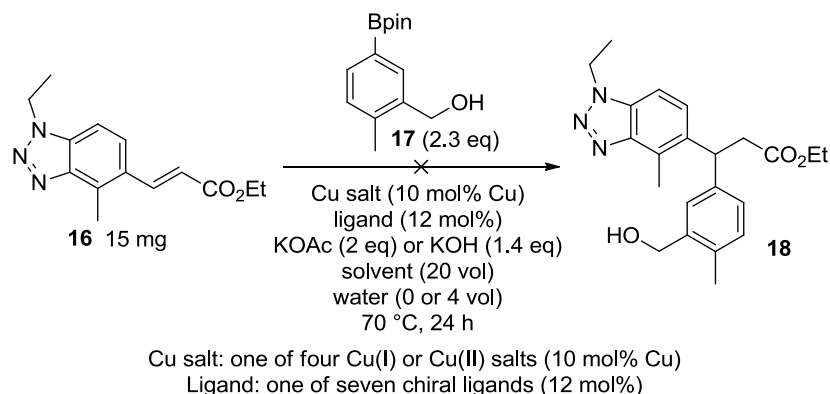
Vial	Ligand (Premix Y/N)	Equivalents of ArBpin 17	Timepoint	HPLC Area%				
				16	17	(S)-18	(R)-18	19
			1 h 10 min		2.23	10.58	65.83	14.53
			1 h 40 min		1.01	10.70	66.66	15.85
			2 h 15 min		0.22	10.75	66.68	16.77
			2 h 55 min		0.05	10.88	66.67	16.94
			3 h 40 min			10.69	66.79	17.23
			4 h 30 min		0.23	10.77	65.51	17.13
			5 h 25 min		0.10	10.78	66.30	17.33
			24 h			10.76	65.39	17.53
4	Ph-BOD (N)	1.0	0	37.56	49.45			
			10 min	30.57	10.67	9.61	14.10	21.79
			25 min	25.88	2.68	11.28	24.61	23.28
			45 min	23.32	0.60	11.73	30.04	23.01
			1 h 10 min	22.12		11.90	32.45	23.00
			1 h 40 min	21.69		11.98	33.28	22.71
			2 h 15 min	21.50		11.98	33.41	22.85
			2 h 55 min	21.60		11.96	33.39	22.64
			3 h 40 min	21.50		11.93	33.41	22.75
			4 h 30 min	21.02		11.55	35.16	21.85
			5 h 25 min	21.42		11.93	33.37	22.61
			24 h	20.57		11.41	33.71	22.99
5	(R)-H8-BINAP (Y)	1.0	0	41.37	48.32			1.00
			10 min	34.55	37.70			1.37
			25 min	31.06	34.84	3.04		2.45
			45 min	28.68	31.03	6.13	0.25	3.34
			1 h 10 min	27.19	27.93	8.99	0.43	4.20
			1 h 40 min	25.53	25.25	12.47	1.35	5.10
			2 h 15 min	24.43	23.01	15.34	1.62	5.85
			2 h 55 min	24.72	20.12	16.38	1.73	5.61
			3 h 40 min	24.47	19.54	17.01	1.86	5.97
			4 h 30 min	25.84	15.36	18.44	2.04	6.15
			5 h 25 min	24.33	19.24	17.05	1.85	6.21
			24 h	22.49	19.56	16.81	1.82	6.81
6	(R)-H8-BINAP (N)	1.0	0	30.57	37.24			2.46
			10 min	26.97	34.34			0.95
			25 min	24.45	33.28			1.49
			45 min	23.12	32.62			1.85
			1 h 10 min	22.40	31.64			2.25
			1 h 40 min	21.84	31.39			2.51
			2 h 15 min	21.16	30.98			2.56
			2 h 55 min	22.42	30.34			2.68
			3 h 40 min	21.34	29.92			2.85
			4 h 30 min	20.41	30.09			2.47
			5 h 25 min	20.12	29.37			2.71
			24 h	18.76	27.06			3.31
7	Ph-BOD (N)	2.3	0	23.20	47.80			0.72
			10 min	14.32	21.81	13.39	17.55	16.49
			25 min	9.53	14.35	14.88	30.88	16.65
			45 min	5.14	8.56	15.16	44.14	16.09
			1 h 10 min	1.81	3.94	15.04	54.84	15.47
			1 h 40 min	0.42	3.76	14.87	60.03	14.87

Vial	Ligand (Premix Y/N)	Equivalents of ArBpin 17	Timepoint	HPLC Area%				
				16	17	(S)-18	(R)-18	19
			2 h 15 min		2.26	14.81	61.93	15.15
			2 h 55 min		1.82	14.76	62.16	15.30
			3 h 40 min		1.71	14.66	62.26	15.28
			4 h 30 min		1.55	14.84	62.06	15.41
			24 h		1.70	14.84	61.20	15.67
8	(R)-H8-BINAP (N)	1.0	0	33.77	37.55			5.65
			10 min	24.73	33.27			1.03
			25 min	23.11	33.10			1.14
			45 min	19.34	32.72			1.32
			1 h 10 min	18.33	31.55			1.78
			1 h 40 min	18.13	30.26			2.47
			2 h 15 min	18.23	28.89			3.08
			2 h 55 min	18.59	29.56			3.24
			3 h 40 min	18.25	29.94			3.26
			4 h 30 min	18.34	29.32			3.41
			24 h	17.09	20.87			4.32

Table 39. HPLC analysis (Method D1) for time-coursing experiments. Enoate 16 at 9.6 min, arylboron reagent 17 at 3.9 min, bisaryl (S)-18 at 8.0 min, (R)-18 at 8.7 min, *o*-tolylmethanol 19 at 4.4 min.

5.3.2.5 Assessment of Alternative Metal Systems for the Pharmaceutically-Relevant Conjugate Arylation (Procedures for Section 3.2.1.5)

5.3.2.5.1 Copper Catalysis (Table 9, page 74)



Copper salts and ligands were weighed into reaction vials according to Table 40 (page 201) along with potassium acetate (42×11.4 mg, $116 \mu\text{mol}$, Vials 1 to 42 only). The vials were left under air overnight before being placed inside a nitrogen-filled glove bag. The two substrates **16** (48×15.0 mg, $57.8 \mu\text{mol}$) and **17** (48×33.0 mg, $133 \mu\text{mol}$) were added volumetrically as nitrogen-sparged solutions in dioxane ($20 \times 300 \mu\text{L}$, Vials 29 to 48) or toluene ($28 \times 300 \mu\text{L}$, Vials 1 to 28), inside the glove bag. Potassium hydroxide (4.5 mg, $81 \mu\text{mol}$) was added as a nitrogen-sparged aqueous solution ($6 \times 60 \mu\text{L}$, Vials 43 to 48), and the vials were then capped and pierced ($2 \times$ blunt needle) inside the glove bag before being transferred to a CAT96 reactor. The reactor was purged with nitrogen ($> 3 \times \text{N}_2/\text{vent}$) before

the reaction vials were stirred at 70 °C for 24 h under nitrogen. The vials were sampled after 24 h (23 μ L into ethanol (977 μ L)) and analysed by HPLC (Method D1).

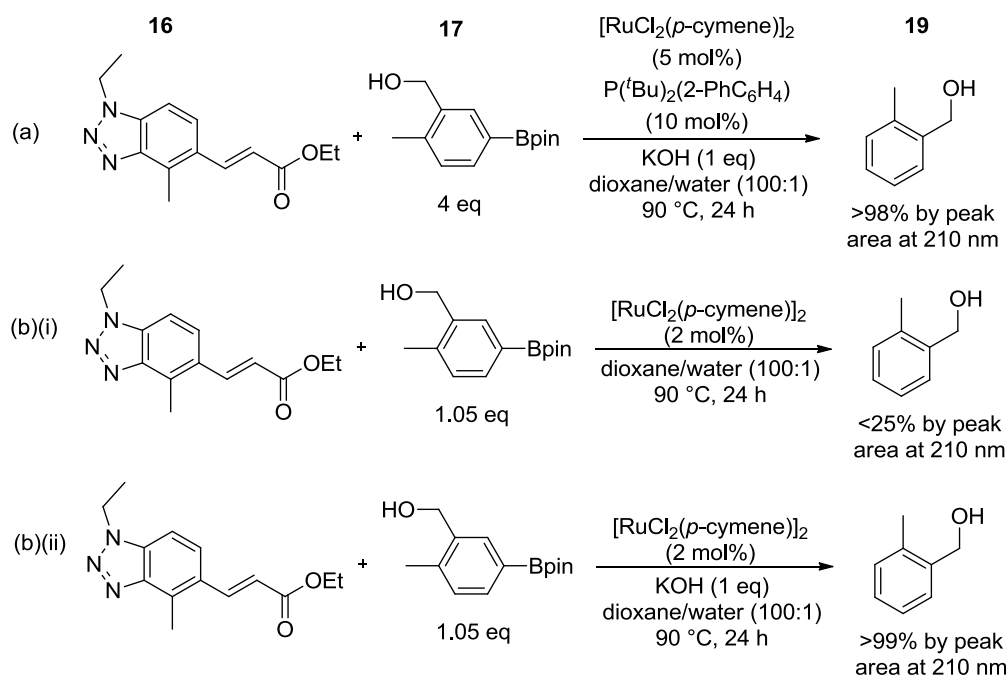
Conversion to the desired product was not observed in any reaction vial.

Vial	Copper Salt			Ligand			Amount Mass /	
	Identity	Amount / μ mol	Mass /mg	Identifier	CAS Number	Amount / μ mol	Mass /mg	
1	(CuOTf) ₂ ·Tol	2.9	1.5	L23	Phosphoramidite	380230-02-4	6.9	3.7
2	(CuOTf) ₂ ·Tol	2.9	1.5	L21	(R)-MonoPhos	157488-65-8	6.9	2.5
3	(CuOTf) ₂ ·Tol	2.9	1.5	L19	(R)-Xylyl-PHANEphos	325168-89-6	6.9	4.8
4	(CuOTf) ₂ ·Tol	2.9	1.5	L24	Oxazoline	167171-03-1	6.9	2.8
5	(CuOTf) ₂ ·Tol	2.9	1.5	L25	(R)-H8-BINAM-P	208248-67-3	6.9	4.6
6	(CuOTf) ₂ ·Tol	2.9	1.5	L7	(R)-BINAP	76189-55-4	6.9	4.3
7	(CuOTf) ₂ ·Tol	2.9	1.5	L12	Ph-BOD	850409-83-5	6.9	1.8
8	Cu(OAc)	5.8	0.7	L23	Phosphoramidite	380230-02-4	6.9	3.7
9	Cu(OAc)	5.8	0.7	L21	(R)-MonoPhos	157488-65-8	6.9	2.5
10	Cu(OAc)	5.8	0.7	L19	(R)-Xylyl-PHANEphos	325168-89-6	6.9	4.8
11	Cu(OAc)	5.8	0.7	L24	Oxazoline	167171-03-1	6.9	2.8
12	Cu(OAc)	5.8	0.7	L25	(R)-H8-BINAM-P	208248-67-3	6.9	4.6
13	Cu(OAc)	5.8	0.7	L7	(R)-BINAP	76189-55-4	6.9	4.3
14	Cu(OAc)	5.8	0.7	L12	Ph-BOD	850409-83-5	6.9	1.8
15	Cu(OTf) ₂	5.8	2.1	L23	Phosphoramidite	380230-02-4	6.9	3.7
16	Cu(OTf) ₂	5.8	2.1	L21	(R)-MonoPhos	157488-65-8	6.9	2.5
17	Cu(OTf) ₂	5.8	2.1	L19	(R)-Xylyl-PHANEphos	325168-89-6	6.9	4.8
18	Cu(OTf) ₂	5.8	2.1	L24	Oxazoline	167171-03-1	6.9	2.8
19	Cu(OTf) ₂	5.8	2.1	L25	(R)-H8-BINAM-P	208248-67-3	6.9	4.6
20	Cu(OTf) ₂	5.8	2.1	L7	(R)-BINAP	76189-55-4	6.9	4.3
21	Cu(OTf) ₂	5.8	2.1	L12	Ph-BOD	850409-83-5	6.9	1.8
22	CuCl	5.8	0.6	L23	Phosphoramidite	380230-02-4	6.9	3.7
23	CuCl	5.8	0.6	L21	(R)-MonoPhos	157488-65-8	6.9	2.5
24	CuCl	5.8	0.6	L19	(R)-Xylyl-PHANEphos	325168-89-6	6.9	4.8
25	CuCl	5.8	0.6	L24	Oxazoline	167171-03-1	6.9	2.8
26	CuCl	5.8	0.6	L25	(R)-H8-BINAM-P	208248-67-3	6.9	4.6
27	CuCl	5.8	0.6	L7	(R)-BINAP	76189-55-4	6.9	4.3
28	CuCl	5.8	0.6	L12	Ph-BOD	850409-83-5	6.9	1.8
29	(CuOTf) ₂ ·Tol	2.9	1.5	L23	Phosphoramidite	380230-02-4	6.9	3.7
30	(CuOTf) ₂ ·Tol	2.9	1.5	L21	(R)-MonoPhos	157488-65-8	6.9	2.5
31	(CuOTf) ₂ ·Tol	2.9	1.5	L19	(R)-Xylyl-PHANEphos	325168-89-6	6.9	4.8
32	(CuOTf) ₂ ·Tol	2.9	1.5	L24	Oxazoline	167171-03-1	6.9	2.8
33	(CuOTf) ₂ ·Tol	2.9	1.5	L25	(R)-H8-BINAM-P	208248-67-3	6.9	4.6
34	(CuOTf) ₂ ·Tol	2.9	1.5	L7	(R)-BINAP	76189-55-4	6.9	4.3
35	(CuOTf) ₂ ·Tol	2.9	1.5	L12	Ph-BOD	850409-83-5	6.9	1.8
36	Cu(OTf) ₂	5.8	2.1	L23	Phosphoramidite	380230-02-4	6.9	3.7
37	Cu(OTf) ₂	5.8	2.1	L21	(R)-MonoPhos	157488-65-8	6.9	2.5
38	Cu(OTf) ₂	5.8	2.1	L19	(R)-Xylyl-PHANEphos	325168-89-6	6.9	4.8
39	Cu(OTf) ₂	5.8	2.1	L24	Oxazoline	167171-03-1	6.9	2.8
40	Cu(OTf) ₂	5.8	2.1	L25	(R)-H8-BINAM-P	208248-67-3	6.9	4.6
41	Cu(OTf) ₂	5.8	2.1	L7	(R)-BINAP	76189-55-4	6.9	4.3
42	Cu(OTf) ₂	5.8	2.1	L12	Ph-BOD	850409-83-5	6.9	1.8
43	(CuOTf) ₂ ·Tol	2.9	1.5	L23	Phosphoramidite	380230-02-4	6.9	3.7

Vial	Copper Salt			Ligand				
	Identity	Amount Mass / μmol	Amount Mass / mg	Identifier	CAS Number	Amount Mass / μmol	Amount Mass / mg	
44	(CuOTf) ₂ ·Tol	2.9	1.5	L21	(<i>R</i>)-MonoPhos	157488-65-8	6.9	2.5
45	(CuOTf) ₂ ·Tol	2.9	1.5	L19	(<i>R</i>)-Xylyl-PHANEphos	325168-89-6	6.9	4.8
46	(CuOTf) ₂ ·Tol	2.9	1.5	L24	Oxazoline	167171-03-1	6.9	2.8
47	(CuOTf) ₂ ·Tol	2.9	1.5	L7	(<i>R</i>)-BINAP	76189-55-4	6.9	4.3
48	(CuOTf) ₂ ·Tol	2.9	1.5	L12	Ph-BOD	850409-83-5	6.9	1.8

Table 40. Copper salts and ligands dispensed to reaction vials to seek activity for the desired 1,4-addition.

5.3.2.5.2 Ruthenium Catalysis (Scheme 35, page 76)



(a) $[\text{Ru}(p\text{-cymene})\text{Cl}_2]_2$ (3.1 mg, 5.1 μmol), 2-(di-*tert*-butylphosphino)biphenyl (3.0 mg, 10 μmol), enoate **16** (25.9 mg, 100 μmol) and arylboronic ester **17** (99.0 mg, 400 μmol) were charged to a microwave vial, and the air was replaced with nitrogen ($3 \times \text{vacuum}/\text{N}_2$). Nitrogen-sparged dioxane (1 mL) and potassium hydroxide (5.6 mg, 0.10 mmol) as an aqueous solution (10 μL) were added and the mixture was degassed again ($3 \times \text{vacuum}/\text{N}_2$). The vial was removed from the Schlenk line and the reaction mixture was stirred at 90 °C for 24 h before sampling into acetonitrile and analysing by HPLC (Method C) and LCMS (Method A).

(b) $[\text{Ru}(p\text{-cymene})\text{Cl}_2]_2$ (2×2.5 mg, 4.1 μmol), enoate **16** (2×52.0 mg, 200 μmol) and arylboronic ester **17** (2×52.1 mg, 210 μmol) were charged to two microwave vials, and the air was replaced with nitrogen ($3 \times \text{vacuum}/\text{N}_2$). Nitrogen-sparged dioxane (2×0.6 mL) and water (6 μL , (b)(i)) or aqueous potassium hydroxide (11 mg, 0.20 mmol (KOH), 6 μL , (b)(ii)) were added and the mixtures were degassed again ($3 \times \text{vacuum}/\text{N}_2$). The vials were

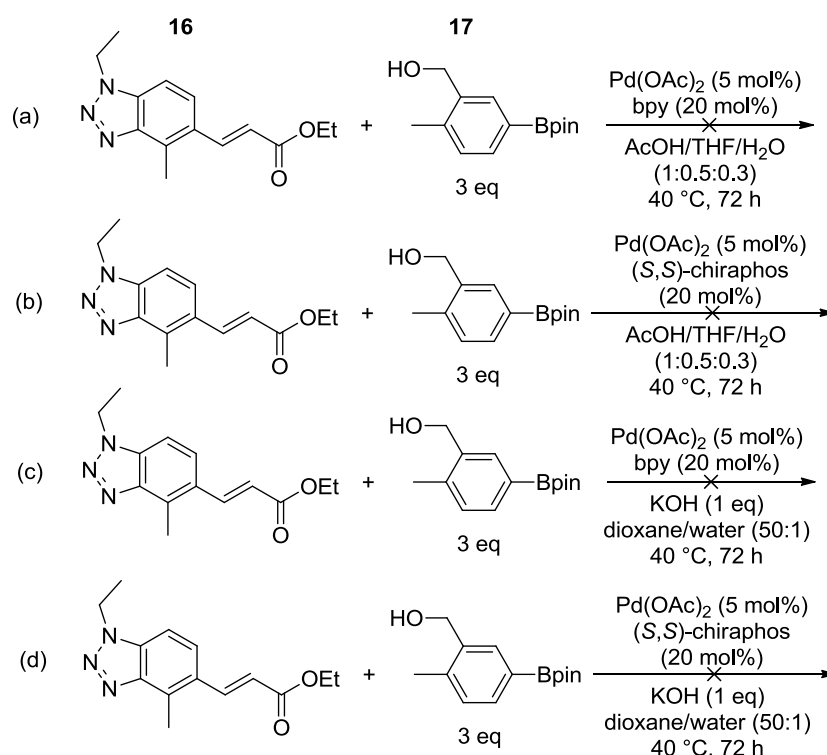
removed from the Schlenk line and the reaction mixtures were stirred at 90 °C for 24 h before sampling into acetonitrile and analysing by HPLC (Method C) and LCMS (Method A).

HPLC results are summarised in Table 41 (page 202).

Reaction	HPLC Area%				
	16	17 (9.2 min)	17 (20.2 min)	18	19
(a)	14.4	1.1	2.5	0.7	58.5
(b)(i)	37.1	17.2	25.3		5.4
(b)(ii)	32.8				35.0

Table 41. HPLC analysis (Method C, 210 nm) for attempts to employ ruthenium catalysis in the pharmaceutically-relevant conjugate arylation. Enoate **16** at 20.0 min, arylboron reagent **17** at 20.2 min (ArBpin) and 9.2 min (ArB(OH)₂), bisaryl **18** at 19.4 min, *o*-tolylmethanol **19** at 13.4 min.

5.3.2.5.3 Palladium Catalysis (Scheme 37, page 78)

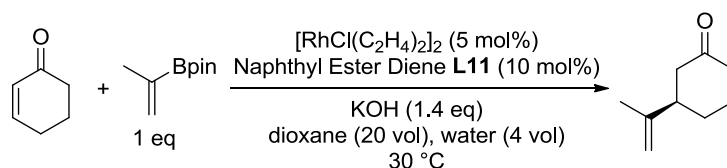


Pd(OAc)₂ (4 × 2.2 mg, 9.8 μmol), 2,2'-bipyridine (2 × 6.3 mg, 40 μmol, (a) and (c)) or (*S,S*)-chiraphos (2 × 17.1 mg, 40 μmol, (b) and (d)), enoate **16** (4 × 52 mg, 200 μmol) and arylboronic ester **17** (4 × 149 mg, 600 μmol) were charged to microwave vials, and the air was replaced with nitrogen (3 × vacuum/N₂). Nitrogen-sparged THF (2 × 0.1 mL), acetic acid (2 × 0.2 mL) and water (2 × 6 μL) were then added for (a) and (b), and nitrogen-sparged dioxane (2 × 0.3 mL) and potassium hydroxide (11.2 mg, 0.20 mmol) as a nitrogen-sparged aqueous solution (2 × 6 μL) were then added for (c) and (d). The mixtures were degassed again (3 × vacuum/N₂) and the vials removed from the Schlenk line before the reaction

mixtures were stirred at 40 °C for 72 h. The reaction mixtures were sampled into acetonitrile and analysed by HPLC (Method C, 210 nm) and LCMS (Method A).

No more than trace conversion either to the desired 1,4-addition product **18** or the deboronated substrate **19** (< 3 HPLC area% for (a), (b) and (d), < 15 area% for (c)) was observed in any case.

5.3.2.6 Demonstration of Selected Catalyst/Ligand System for a Published Process Chemistry Reaction (Procedure for Scheme 38, page 80, Section 3.2.1.6)



[RhCl(C₂H₄)₂]₂ (1.1 mg, 2.8 μmol) and the naphthyl ester diene ligand **L11** (1.9 mg, 5.7 μmol) were charged to a reaction vial, which was then purged with nitrogen. Cyclohexenone (5.6 mg, 58 μmol) and (isopropenyl)pinacolboronic ester (9.8 mg, 58 μmol) were dissolved in nitrogen-sparged dioxane (300 μL) and the solution was further degassed before transfer to the reaction vial. potassium hydroxide (4.5 mg, 81 μmol) as a nitrogen-sparged aqueous solution (60 μL) was added and the mixture was stirred at 30 °C for 19 h. GC analysis revealed complete consumption of the (isopropenyl)pinacolboronic ester and 92% peak area conversion of the cyclohexenone (6.64 peak area%) to a new species (81.40 peak area%). ¹H NMR of the crude reaction mixture was in good agreement with literature for the desired product 3-(prop-1-en-2-yl)cyclohexanone,²¹⁷ and chiral GC analysis revealed the product to have been formed in 80% *ee*. Absolute stereochemistry assigned by comparison with the literature.¹⁴⁴

The reaction was also performed racemically to validate the chiral GC method, using [RhCl(COD)]₂ with no additional ligand. The reaction was complete within 24 h.

Cyclohexenone GC: *t_R* = 0.96 min.

(Isopropenyl)pinacolboronic ester GC: *t_R* = 1.07 min.

3-(Prop-1-en-2-yl)cyclohexanone GC: *t_R* = 1.54 min.

(*R*)-3-(Prop-1-en-2-yl)cyclohexanone chiral GC: *t_R* = 14.97 min.

(*S*)-3-(Prop-1-en-2-yl)cyclohexanone chiral GC: *t_R* = 15.03 min.

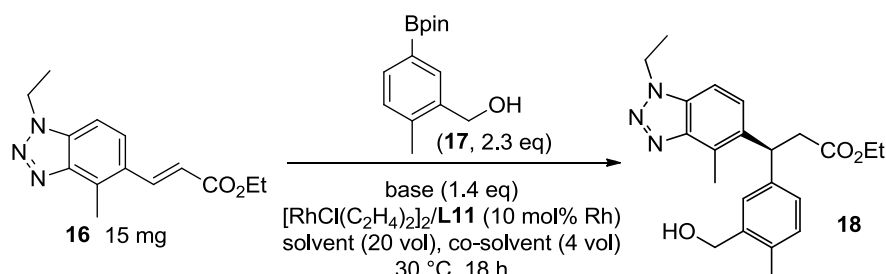
3-(Prop-1-en-2-yl)cyclohexanone ¹H NMR (from crude): δ 4.78 (m, 1H), 4.73 (m, 1H),

2.48–2.22 (m, 5H), 2.13–1.99 (m, 1H), 1.99–1.89 (m, 1H), 1.75 (s, 3H), 1.72–1.53 (m, 2H).

¹H NMR literature data concordant.²¹⁷

5.3.3 Solvent and Base Selection for the Pharmaceutically-Relevant Conjugate Arylation (Procedures for Section 3.2.2)

5.3.3.1 First Set of Comparative Reactions: Solvent and Base (Table 11, page 82)



$[\text{RhCl}(\text{C}_2\text{H}_4)_2]_2$ (48×1.1 mg, $2.9 \mu\text{mol}$), the naphthyl ester diene ligand **L11** (48×1.9 mg, $5.8 \mu\text{mol}$), enoate **16** (48×15.0 mg, $58 \mu\text{mol}$), and arylboronic ester **17** (48×14.4 mg, $58 \mu\text{mol}$) were weighed into reaction vials, with solid bases then added according to Table 42 (page 206). The vials were capped, pierced ($2 \times$ blunt needle) and transferred to a CAT96 reactor for nitrogen/vent cycles to be performed. The vials were retrieved from the reactor and nitrogen-sparged solvents (20 vol) and co-solvents (4 vol) were added by syringe followed by 2-methyl-1,3-propanediol ($5.1 \mu\text{L}$, $57 \mu\text{mol}$, Vials 34 and 35 only) and nitrogen-sparged liquid bases^{xvi} according to Table 42. The vials were returned to the CAT96 reactor and nitrogen/vent cycles were performed again before the reaction mixtures were stirred at 30 °C for 18 h under nitrogen.

The vials were sampled ($23 \mu\text{L}$ into ethanol ($977 \mu\text{L}$) and into acetonitrile ($977 \mu\text{L}$)) for chiral HPLC (Method D1) achiral HPLC (Method C) respectively.

The results are summarised in Table 43 (page 207).

^{xvi} Including alcoholic solutions of methoxide and ethoxide bases, which were not nitrogen-sparged, and an aqueous potassium hydroxide solution prepared from KOH (379 mg) in water (5 mL) such that 4.5 mg of KOH was dissolved in 60 μL of the aqueous solution. In each case of KOH being used, this was added as the co-solvent.

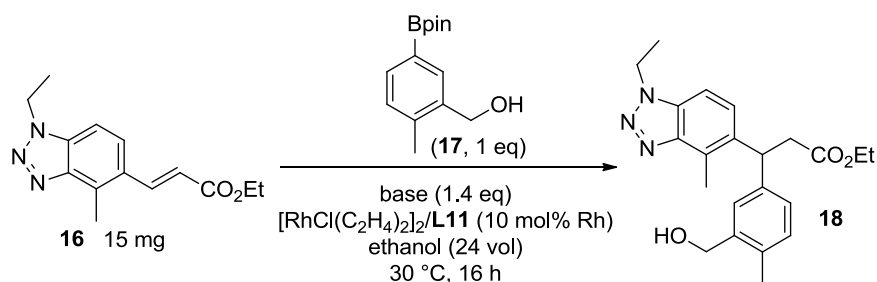
Vial	Base (1.4 eq, 81 μ mol)		Solvent (300 μ L)	Co-Solvent (60 μ L)
	Identity	Mass / mg (Volume / μ L)		
1	KOH (aq)	<i>as co-solvent</i>	Dioxane	Water
2	No Base	N/A	Dioxane	Water
3	NaHCO ₃	6.784	Dioxane	Water
4	K ₂ CO ₃	11.251	Dioxane	Water
5	KHCO ₃	8.032	Dioxane	Water
6	K ₃ PO ₄	17.231	Dioxane	Water
7	NEt ₃	(11.5)	Dioxane	Water
8	DIPEA	(14.0)	Dioxane	Water
9	DIPA	(11.5)	Dioxane	Water
10	NEt ₃	(11.5)	Dioxane	Ethanol
11	NaOEt (21wt%)	(30.0)	Dioxane	Ethanol
12	KOEt (24 wt%)	(32.0)	Dioxane	Ethanol
13	No Base	N/A	Dioxane	Ethanol
14	NEt ₃	(11.5)	Dioxane	Trifluoroethanol
15	NaOMe (25 wt%)	(19.0)	Dioxane	Methanol
16	KOH (aq)	<i>as co-solvent</i>	Toluene	Water
17	K ₃ PO ₄	17.159	Toluene	Water
18	K ₂ CO ₃	11.258	Toluene	Water
19	NEt ₃	(11.5)	Toluene	Water
20	NaHCO ₃	6.813	Toluene	Water
21	KOH (aq)	<i>as co-solvent</i>	THF	Water
22	K ₂ CO ₃	11.197	THF	IPA
23	K ₂ CO ₃	11.212	THF	Ethanol
24	KOH (aq)	<i>as co-solvent</i>	2-Methyl-THF	Water
25	NEt ₃	(11.5)	IPA	IPA
26	NEt ₃	(11.5)	Ethanol	Ethanol
27	NEt ₃	(11.5)	Methanol	Methanol
28	KOH (aq)	<i>as co-solvent</i>	Methanol	Water
29	No Base	N/A	Acetic Acid	Acetic Acid
30	KOAc	8.023	Acetic Acid	Acetic Acid
31	No Base	N/A	AcOH/Water	AcOH/Water
32	KOAc	8.138	AcOH/Water	AcOH/Water
33	DIPEA	(14.0)	Heptane	Methanol
34	DIPEA	(14.0)	Heptane	Methanol
35	DIPEA	(14.0)	Heptane/MeOH/Water	Heptane/MeOH/Water
36	KOH (aq)	<i>as co-solvent</i>	<i>iso</i> -Propyl Acetate	Water
37	KOH (aq)	<i>as co-solvent</i>	Ethyl Acetate	Water
38	KOH (aq)	<i>as co-solvent</i>	Anisole	Water
39	KOH (aq)	<i>as co-solvent</i>	DMSO	Water
40	KOH (aq)	<i>as co-solvent</i>	1-Butanol	Water
41	KOH (aq)	<i>as co-solvent</i>	Acetone	Water
42	KOH (aq)	<i>as co-solvent</i>	Cyclopropylmethylether	Water
43	KOH (aq)	<i>as co-solvent</i>	Cyclopentanone	Water
44	KOH (aq)	<i>as co-solvent</i>	Dimethyl Carbonate	Water
45	KOH (aq)	<i>as co-solvent</i>	Propylene Carbonate	Water
46	KOH (aq)	<i>as co-solvent</i>	Ethylene Glycol	Water
47	KOH (aq)	<i>as co-solvent</i>	Acetonitrile	Water
48	KOH (aq)	<i>as co-solvent</i>	Methyl <i>iso</i> -Butyl Ketone	Water

Table 42. Bases and solvents dispensed to reaction vials in the first set of reactions to observe solvent and base effects. (Heptane/MeOH)/Water is 3(95:5):1 by volume. AcOH/Water is 1:1 by volume.

Vial	HPLC Area% (Achiral)					HPLC Area% (Chiral)	
	16	17 (9.2 min)	17 (20.2 min)	18	19	(S)-18	(R)-18
1	5.46			65.54	6.53	66.42	2.04
2	39.31	24.55	23.06	2.94	0.43	2.20	0.09
3	6.73			75.55	6.48	74.00	1.87
4	7.97			68.23	7.23	65.07	2.55
5	14.09			63.59	12.17	63.63	1.60
6	5.67			71.65	4.79	70.01	1.95
7	3.80			82.70	2.25	81.78	2.05
8	2.57			84.73	1.92	80.45	1.98
9	3.18			82.41	2.09	80.54	2.07
10	32.78	15.04	20.14	17.28	2.85	16.10	0.19
11	1.28		1.00	69.55	3.65	73.46	2.66
12	1.10		0.70	67.14	4.57	70.60	2.73
13	39.38	21.73	28.11	0.45	0.23	0.42	0.19
14	28.92	12.93	17.32	28.04	1.63	27.61	0.47
15	2.33	0.14		39.53	4.49	15.49	0.38
16	23.53		0.21	41.10	22.55	15.75	0.72
17	11.86			68.36	9.62	31.54	1.15
18	10.19			70.19	8.95	29.87	1.20
19	7.97			78.48	7.37	35.52	1.12
20	10.87			72.80	10.25	31.24	0.96
21	9.14			67.03	6.07	66.24	1.62
22	3.93			76.74	3.10	73.61	2.00
23	5.13			75.78	4.54	71.37	1.85
24	30.15	13.86	19.44	25.45	1.27	63.52	1.63
25	11.23			64.17	11.08	23.83	0.33
26	2.31	0.19	0.32	87.60	1.35	80.43	2.61
27	2.87			88.09	1.77	84.64	2.92
28	3.74			49.64	4.83	33.71	1.41
29	40.44	28.63	19.26	0.27	1.36	N/A	N/A
30	41.08	25.78	17.63	0.24	6.45	N/A	N/A
31	41.75	33.13	12.64	0.25	3.39	N/A	N/A
32	42.54	31.57	11.63	0.25	7.95	N/A	N/A
33	5.34	1.44	1.97	79.06	1.21	68.93	2.91
34	3.41	0.27	0.27	84.01	1.69	74.77	3.13
35	1.96			88.29	0.68	81.11	4.73
36	6.19			79.09	5.41	72.07	2.00
37	10.96			70.27	9.43	61.68	1.60
38	21.96		0.30	39.42	22.50	12.98	0.33
39	15.49		0.11	40.86	11.54	18.87	1.27
40	4.61			63.69	6.96	64.51	2.97
41	5.21			70.64	5.31	72.07	2.24
42	11.79			64.28	11.38	63.40	1.78
43	8.46			64.56	7.98	63.27	1.79
44	7.90		0.15	72.71	7.00	72.10	1.70
45	27.45			34.55	27.03	33.76	0.62
46	2.90			47.34	3.93	40.71	7.97
47	8.09			70.25	6.24	68.63	2.71
48	17.33		0.21	54.01	16.08	53.04	1.61

Table 43. HPLC analysis for solvent/base comparisons. Enoate 16 at 20.0 min, arylboron reagent 17 at 20.2 min (ArBpin) and 9.2 min (ArB(OH)₂), bisaryl 18 at 19.4 min, *o*-tolylmethanol 19 at 13.4 min (Method C, 210 nm). (S)-18 at 8.0 min, (R)-18 at 8.7 min (Method D1).

5.3.3.2 Second Set of Comparative Reactions: Ethanolic Systems (Table 12, page 86)



[RhCl(C₂H₄)₂]₂ (21 × 1.1 mg, 2.9 μmol), the naphthyl ester diene ligand **L11** (21 × 1.9 mg, 5.8 μmol), enoate **16** (21 × 15.0 mg, 58 μmol) and arylboronic ester **17** (21 × 14.4 mg, 58 μmol) were weighed into reaction vials, with solid bases then added according to Table 45 (page 209). The vials were capped, pierced (2 × blunt needle) and transferred to a CAT96 reactor for nitrogen/vent cycles to be performed. The vials were retrieved from the reactor and solvents (24 vol, nitrogen-sparged unless otherwise specified) were added by syringe followed by liquid bases according to Table 45. The vials were returned to the CAT96 reactor and nitrogen/vent cycles were performed again before the reaction mixtures were stirred at 30 °C for 3 h under nitrogen and then left under nitrogen for a further 13 h before sampling (23 μL into ethanol (977 μL)).

The samples were analysed by achiral HPLC (Method C) and the results are summarised in Table 46 (page 209).

Karl-Fischer analysis of solvents:

Solvent	Water Content / wt%	
	Assay 1	Assay 2
Ethanol (anhydrous, N ₂ -sparged)	0.416	0.413
Ethanol (anhydrous, source bottle)	0.015	n.d.
Ethanol (standard)	0.277	n.d.
IMS	1.725	n.d.

Table 44. Karl-Fischer analysis of solvents to determine water content.

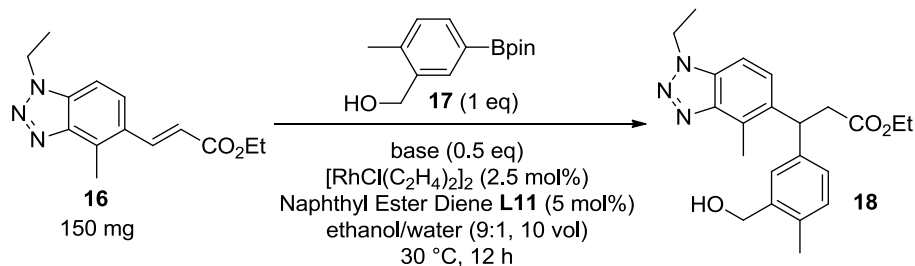
Vial	Base (1.4 eq, 81 μ mol)		Solvent (360 μ L)
	Identity	Mass / mg (Volume / μ L)	
1	NEt ₃	(11.5)	Ethanol (anhydrous)
2	NEt ₃	(11.5)	IMS
3	NEt ₃	(11.5)	Ethanol (not degassed)
4	NEt ₃	(11.5)	Ethanol/Water 1:1
5	NEt ₃	(11.5)	Ethanol (air-sparged)
6	NEt ₃	(11.5)	Ethanol
7	DIPEA	(14.0)	Ethanol
8	DIPA	(11.5)	Ethanol
9	Pyridine	(6.5)	Ethanol
10	DABCO	(27.0)	Ethanol
11	2-Methylpyridine	(8.0)	Ethanol
12	4-Methylpyridine	(8.0)	Ethanol
13	Diethylamine	(8.5)	Ethanol
14	TDA-1	(26.0)	Ethanol
15	DBN	(10.0)	Ethanol
16	KOAc	8.029	Ethanol
17	NaHCO ₃	6.789	Ethanol
18	K ₂ CO ₃	11.301	Ethanol
19	KHCO ₃	8.436	Ethanol
20	K ₃ PO ₄	19.329	Ethanol
21	Na ₂ CO ₃	9.052	Ethanol

Table 45. Bases and solvents dispensed to reaction vials in the second set of reactions to observe solvent and base effects. Unless otherwise specified, solvents were degassed by sparging with nitrogen.

Vial	Base	HPLC Area%				
		16	17 (9.2 min)	17 (20.2 min)	18	19
1	NEt ₃	10.10	3.92	5.71	69.66	1.32
2	NEt ₃	5.50	1.47	2.35	83.14	1.51
3	NEt ₃	10.38	3.99	5.85	72.89	1.39
4	NEt ₃	2.25			88.81	2.68
5	NEt ₃	15.66	6.38	9.24	61.41	1.50
6	NEt ₃	7.34	2.44	3.88	77.90	1.44
7	DIPEA	3.77	1.08	1.60	85.25	0.86
8	DIPA	1.59			86.29	0.88
9	Pyridine	38.22	22.70	27.34		
10	DABCO	35.48	12.72	12.93	18.38	14.94
11	2-Methylpyridine	42.66	24.82	29.94	0.29	
12	4-Methylpyridine	40.18	22.47	25.37		
13	Diethylamine	21.02	12.76	7.27	49.89	1.96
14	TDA-1	28.24	14.56	19.10	32.96	0.82
15	DBN	39.94	24.12	10.71	1.06	3.61
16	KOAc	22.92	4.26	4.78	48.44	13.68
17	NaHCO ₃	5.11	1.75	2.37	81.67	0.88
18	K ₂ CO ₃	3.62			79.50	3.44
19	KHCO ₃	3.29	0.29	0.40	86.04	1.26
20	K ₃ PO ₄	2.39			82.48	1.89
21	Na ₂ CO ₃	3.66	0.62	0.91	84.67	1.03

Table 46. HPLC analysis (Method C, 210 nm) for solvent/base comparisons in ethanolic solvent systems. Enoate 16 at 20.0 min, arylboron reagent 17 at 20.2 min (ArBpin) and 9.2 min (ArB(OH)₂), bisaryl 18 at 19.4 min, *o*-tolylmethanol 19 at 13.4 min.

5.3.3.3 Rate Comparison using Different Bases (Figure 25, page 90)



General Procedure

A solution of enoate **16** (150 mg, 578 μmol) and aryloboron reagent **17** (143 mg, 578 μmol) in degassed ethanol/water (1.5 mL, 9:1 ethanol/water) was charged to a reaction vial containing $[\text{RhCl}(\text{C}_2\text{H}_4)_2]_2$ (5.6 mg, 14 μmol), the naphthyl ester diene **L11** (9.6 mg, 29 μmol) and the specified inorganic base (290 μmol) where relevant. The reaction mixture was degassed ($3 \times \text{vacuum}/\text{N}_2$) and stirred under nitrogen at 30 °C in an Integrity 10 Reaction Station with Amigo Workstation. In the case of triethylamine, the base (40 μL , 290 μmol) was added at this point.

The first sample (50 μL) was taken 5 min after charging the substrate solution and then according to the results tables below over a 12 h period. Samples were quenched into 1:1 acetonitrile/water with 0.05% trifluoroacetic acid (1 mL) and washed in with ethanol (200 μL). The analytical samples were further diluted (5 fold) before analysing by HPLC Method C at 215 nm, using the response factors in Table 86, page 266 and the approach detailed in Equation 10 to Equation 15 (page 269).

The results using triethylamine, potassium hydroxide, potassium carbonate and potassium hydrogen carbonate are given below. The reaction using DIPEA was prepared according to the related procedure in Section 5.4.3.2 and the results are given in Section 5.4.3.2.1.

5.3.3.3.1 Triethylamine

Time / min	HPLC Peak Area				
	Enoate	ArBpin	ArB(OH) ₂	Bisaryl	Desboron
5	1258.860		1036.427	655.838	
10	1082.725		889.534	1169.584	
20	892.314		721.810	1988.221	
40	723.050		571.927	3199.085	
60	586.250		449.966	3763.399	12.522
120	385.521		259.203	4535.907	18.695
240	204.935		115.619	3861.909	19.518
360	227.973		111.571	5511.716	27.582
720	193.928		67.776	5937.830	35.768

Table 47. HPLC Peak Area data (Method C, 215 nm) for conjugate arylation using triethylamine as the base. Enoate 16 at 19.7 min, arylboron reagent 17 at 20.0 min (ArBpin) and 9.1 min (ArB(OH)₂), bisaryl 18 at 19.2 min, *o*-tolylmethanol 19 at 13.1 min.

Time / min	Calculated Reaction Composition				Discrepancy	Product Ratio	
	Enoate	Ar[B]	Bisaryl	Desboron		Bisaryl	Desboron
0	100	100	0	0			
5	91	88	9	0	2.8	100	0
10	83	80	17	0	2.7	100	0
20	70	67	30	0	3.4	100	0
40	54	51	46	0	3.7	100	0
60	45	41	55	1	3.3	98	2
120	31	25	69	2	4.8	98	2
240	22	15	78	2	5.0	97	3
360	18	10	82	2	5.2	97	3
720	15	6	85	3	5.6	97	3

Table 48. Interpretation of HPLC data for conjugate arylation using triethylamine as the base.

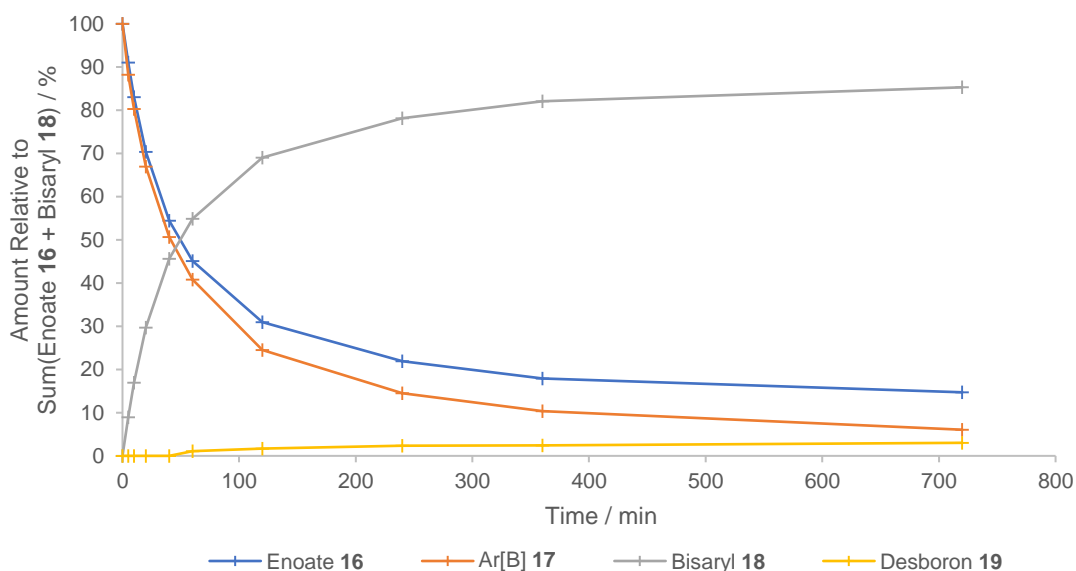


Figure 56. Calculated reaction composition over time.

5.3.3.3.2 Potassium Hydroxide

Time / min	HPLC Peak Area				
	Enoate	ArBpin	ArB(OH) ₂	Bisaryl	Desboron
5	1066.635		856.760	1176.531	23.255
10	285.799		216.551	930.063	12.999
20	282.579		198.533	2267.231	30.989
40	233.622		133.536	3059.161	44.386
60	167.719		82.431	2772.205	40.422
120	99.103		30.820	2374.259	35.889
240	69.553		11.059	2128.849	31.461
360	151.225		15.001	5103.551	75.677
720	152.473			5620.744	85.327

Table 49. HPLC Peak Area data (Method C, 215 nm) for conjugate arylation using potassium hydroxide as the base. Enoate 16 at 19.7 min, arylboron reagent 17 at 20.0 min (ArBpin) and 9.1 min (ArB(OH)₂), bisaryl 18 at 19.2 min, *o*-tolylmethanol 19 at 13.1 min.

Time / min	Calculated Reaction Composition				Discrepancy	Product Ratio	
	Enoate	Ar[B]	Bisaryl	Desboron		Bisaryl	Desboron
0	100	100	0	0			
5	83	78	17	2	2.5	90	10
10	62	55	38	3	3.5	92	8
20	40	33	60	5	2.0	93	7
40	29	19	71	6	3.3	92	8
60	24	14	76	6	3.7	92	8
120	18	7	82	7	4.2	92	8
240	15	3	85	7	4.6	92	8
360	14	2	86	8	4.4	92	8
720	13	0	87	8	4.7	92	8

Table 50. Interpretation of HPLC data for conjugate arylation using potassium hydroxide as the base.

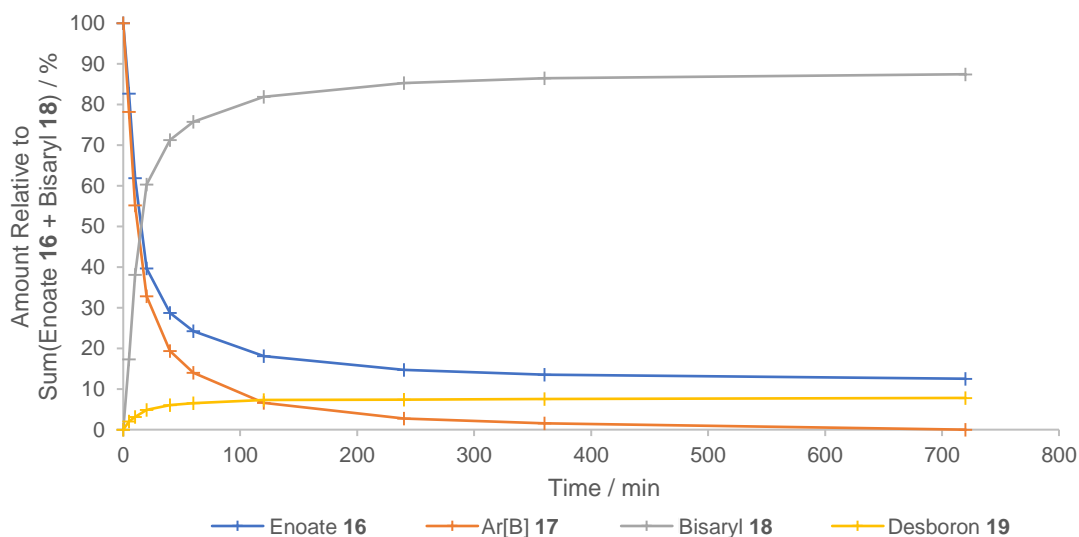


Figure 57. Calculated reaction composition over time.

5.3.3.3.3 Potassium Carbonate

Time / min	HPLC Peak Area				
	Enoate	ArBpin	ArB(OH) ₂	Bisaryl	Desboron
5	1037.390		827.658	1067.867	37.709
10	819.703		604.007	2577.247	71.740
20	343.206		210.092	2392.030	68.929
40	229.909		94.146	2550.538	83.946
60	239.017		83.937	3163.895	108.657
120	314.121		36.183	5365.817	195.872
240	236.484			4488.696	166.898
360	274.422			5325.996	197.872
720	282.815			5520.219	205.576

Table 51. HPLC Peak Area data (Method C, 215 nm) for conjugate arylation using potassium carbonate as the base. Enoate 16 at 19.7 min, arylboron reagent 17 at 20.0 min (ArBpin) and 9.1 min (ArB(OH)₂), bisaryl 18 at 19.2 min, *o*-tolylmethanol 19 at 13.1 min.

Time / min	Calculated Reaction Composition				Discrepancy	Product Ratio	
	Enoate	Ar[B]	Bisaryl	Desboron		Bisaryl	Desboron
0	100	100	0	0			
5	84	79	16	3	1.7	83	17
10	63	54	37	6	2.2	86	14
20	43	31	57	10	2.4	86	14
40	32	16	68	13	3.6	84	16
60	29	12	71	14	2.3	83	17
120	24	3	76	16	4.0	82	18
240	22	0	78	17	4.7	82	18
360	21	0	79	17	4.2	82	18
720	21	0	79	17	4.1	82	18

Table 52. Interpretation of HPLC data for conjugate arylation using potassium carbonate as the base.

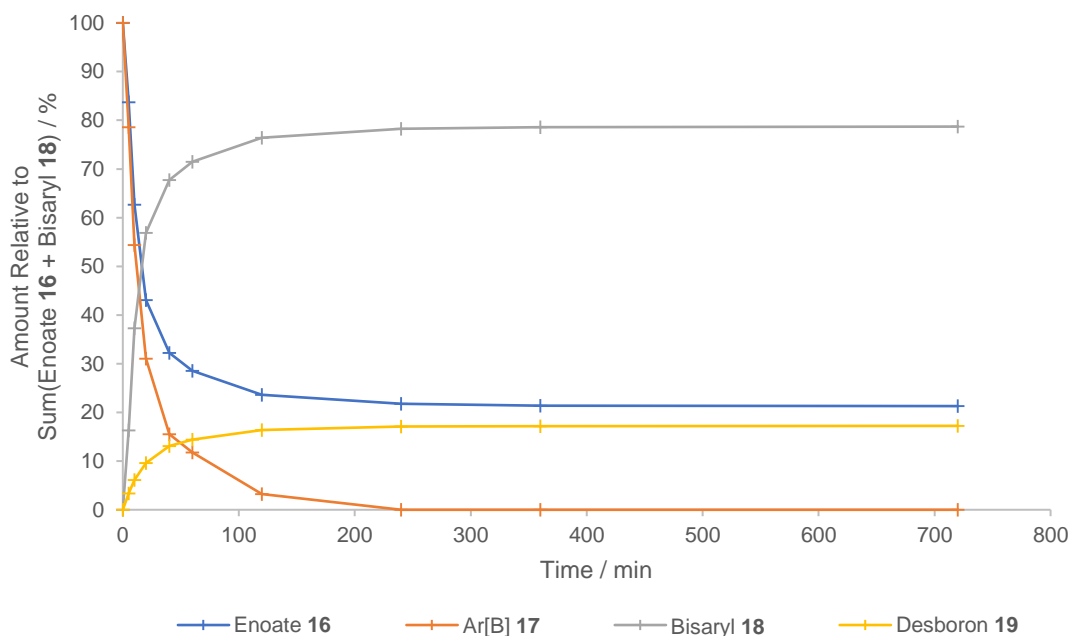


Figure 58. Calculated reaction composition over time.

5.3.3.3.4 Potassium Hydrogen Carbonate

Time / min	HPLC Peak Area				
	Enoate	ArBpin	ArB(OH) ₂	Bisaryl	Desboron
5	1250.261		1056.471	151.981	
10	1057.458		891.622	376.195	
20	909.679		750.495	878.424	16.315
40	539.431		419.729	1168.621	27.251
60	372.335		283.506	1168.813	27.186
120	244.176		172.378	1289.493	25.617
240	101.008		66.960	830.613	14.936
360	92.996		54.979	973.714	16.385
720	44.862		24.051	683.015	11.688

Table 53. HPLC Peak Area data (Method C, 215 nm) for conjugate arylation using potassium hydrogen carbonate as the base. Enoate 16 at 19.7 min, arylboron reagent 17 at 20.0 min (ArBpin) and 9.1 min (ArB(OH)₂), bisaryl 18 at 19.2 min, *o*-tolylmethanol 19 at 13.1 min.

Time / min	Calculated Reaction Composition				Discrepancy	Product Ratio	
	Enoate	Ar[B]	Bisaryl	Desboron		Bisaryl	Desboron
0	100	100	0	0			
5	98	97	2	0	0.5		
10	94	93	6	0	0.7		
20	85	82	15	2	0.7	90	10
40	71	65	29	4	2.0	88	12
60	63	56	37	5	1.4	88	12
120	50	42	50	6	2.6	90	10
240	39	31	61	6	2.1	90	10
360	34	23	66	7	3.6	91	9
720	26	16	74	7	2.0	91	9

Table 54. Interpretation of HPLC data for conjugate arylation using potassium bicarbonate as the base.

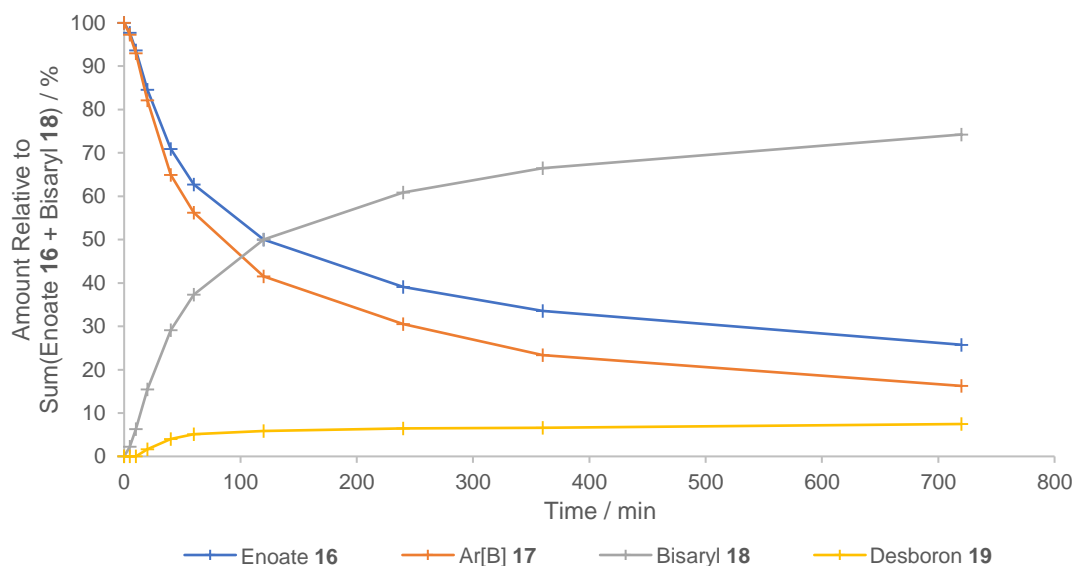
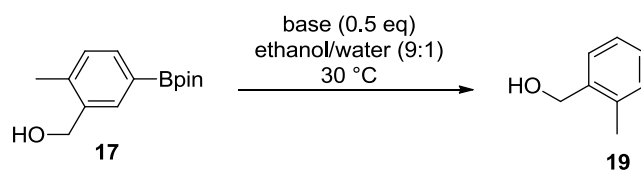


Figure 59. Calculated reaction composition over time.

5.3.3.4 Base-Mediated Protodeboronation (Scheme 39, page 91)



Arylboron reagent **17** (3×143 mg, $578 \mu\text{mol}$) was charged to three reaction vials. DIPEA ($50 \mu\text{L}$, $290 \mu\text{mol}$) was added to the first vial after dissolution of the arylboron reagent in ethanol/water (9:1 ethanol/water, 1.5 mL). KOH (16 mg, $290 \mu\text{mol}$) was added to the second vial followed by ethanol/water (9:1 ethanol/water, 1.5 mL). K_2CO_3 (40 mg, $290 \mu\text{mol}$) was added to the final vial followed by ethanol/water (9:1 ethanol/water, 1.5 mL). Each vial was degassed ($3 \times$ vacuum/ N_2) before stirring at 30°C and sampling at 1 h, 24 h, 72 h and 168 h. Samples were quenched into 1:1 acetonitrile/water with 0.05% trifluoroacetic acid (1 mL).

The samples were analysed by HPLC Method C at 215 nm, using the response factors in Table 87, p. 267.

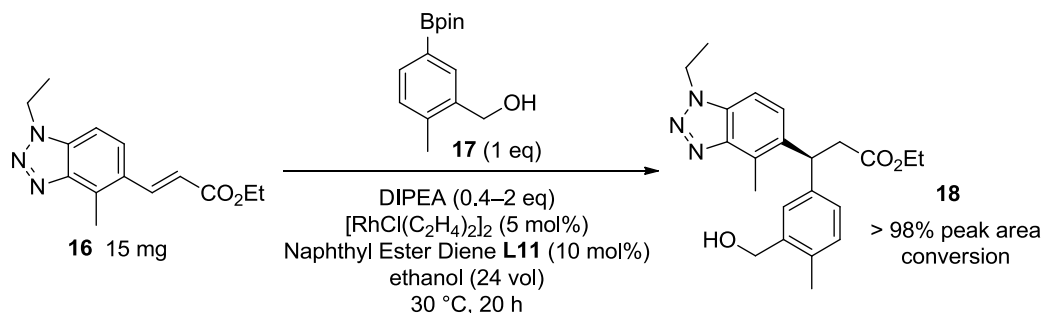
Base	Time / h	HPLC Peak Area			Discrepancy / Peak Area%	Compound Ratio	
		ArBpin	ArB(OH) ₂	Desboron		Arylboron	Desboron
DIPEA	1	250.770	1330.779		0	100	0
	24	22.557	1461.874		0	100	0
	72	135.523	1309.051	26.723	1.680	98	2
	168	60.949	1511.682	60.123	3.002	96	4
KOH	1	41.950	1554.162		0.544	100	0
	24	13.710	1378.322	43.141	0.812	97	3
	72	15.588	1166.372	236.352	5.958	82	18
	168		646.747	632.889	20.949	48	52
K_2CO_3	1	17.667	1522.142		0.522	100	0
	24	13.613	1435.994	62.297	0.744	95	5
	72		1205.547	267.059	7.510	81	19
	168		833.191	507.219	24.178	60	40

Table 55. HPLC Peak Area data (Method C, 215 nm). Arylboron reagent 17 at 20.4 min (ArBpin) and 9.3 min (ArB(OH)₂), *o*-tolymethanol 19 at 13.6 min. "Discrepancy" is the percentage of the total HPLC peak area unaccounted for by the known arylboron species and *o*-tolymethanol. This predominantly arose from one other species at 17.3 min.

5.3.4 Analysis of Continuous Variables for the Pharmaceutically-Relevant Conjugate Arylation (Procedures for Section 3.2.3)

5.3.4.1 Preliminary Experiments for Design of Experiment (Procedures for Section 3.2.3.1)

5.3.4.1.1 Base Equivalents (Scheme 40, page 93)



$[\text{RhCl}(\text{C}_2\text{H}_4)_2]_2$ (6×1.1 mg, $2.8 \mu\text{mol}$), the naphthyl ester diene ligand **L11** (6×1.9 mg, $5.7 \mu\text{mol}$), enoate **16** (6×15.0 mg, $58 \mu\text{mol}$) and arylboronic ester **17** (6×14.4 mg, $58 \mu\text{mol}$) were weighed into reaction vials. The vials were capped, pierced ($2 \times$ blunt needle) and transferred to a CAT96 reactor for nitrogen/vent cycles to be performed. The vials were retrieved from the reactor and nitrogen-sparged ethanol ($5 \times 360 \mu\text{L}$, $180 \mu\text{L}$ (Vial 6 only)) and water ($180 \mu\text{L}$ (Vial 6 only)) were added by syringe. DIPEA was then added according to Table 56. The vials were returned to the CAT96 reactor and nitrogen/vent cycles were performed again before the reaction mixtures were stirred at 30 °C for 20 h under nitrogen before sampling ($23 \mu\text{L}$ into ethanol ($977 \mu\text{L}$)).

The samples were analysed by achiral HPLC (Method C) and chiral HPLC (Method D2), and the results are summarised in Table 57 (page 217).

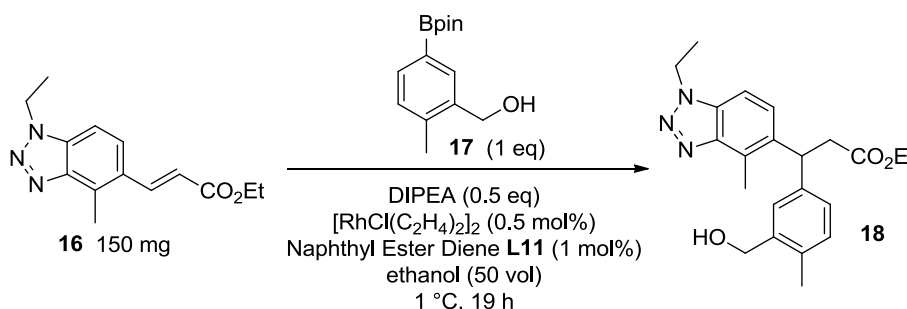
Vial	DIPEA		
	Equivalents	Amount / μmol	Volume / μL
1	0.4	23	4
2	0.7	41	7
3	1.0	58	10
4	1.4	81	14
5	2.0	116	20
6	1.4	81	14

Table 56. Amount of DIPEA charged to reaction vials to observe any effects on the amount of base over this range.

Vial	HPLC Area% (Achiral)					HPLC Area% (Chiral)	
	16	17 (9.2 min)	17 (20.2 min)	18	19	(S)-18	(R)-18
1	1.49	0.32	0.40	86.36	0.66	85.32	3.23
2	1.35			86.55	0.62	82.73	2.88
3	0.83			85.64	0.71	83.70	2.52
4	0.85			86.92	0.77	83.67	2.29
5	1.05			86.37	0.71	81.01	2.61
6	2.59			87.06	1.39	79.18	2.83

Table 57. HPLC analysis to observe effects of base equivalents. Enoate **16** at 20.0 min, arylboron reagent **17** at 20.2 min (ArBpin) and 9.2 min (ArB(OH)₂), bisaryl **18** at 19.4 min, *o*-tolylmethanol **19** at 13.4 min (Method C, 210 nm). (S)-**18** at 8.4 min, (R)-**18** at 9.2 min (Method D2). Note that in Method D2, (S)-**18** and (R)-**18** exhibited baseline separation (an improvement over Method D1) but there was not baseline separation between (R)-**18** and enoate **16** and the naphthyl ester diene **L11**.

5.3.4.1.2 Originally Intended Least Forcing Conditions (Scheme 41, page 93)



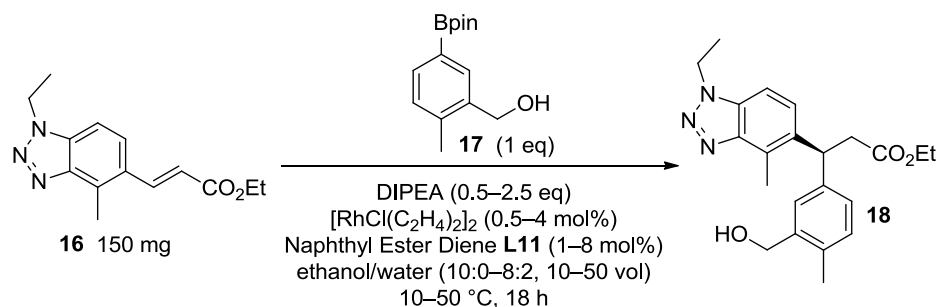
[RhCl(C₂H₄)₂]₂ (1.1 mg, 2.8 μmol), the naphthyl ester diene ligand **L11** (1.9 mg, 5.7 μmol), enoate **16** (150 mg, 578 μmol) and arylboronic ester **17** (144 mg, 578 μmol) were weighed into an Integrity 10 reaction tube. The tube was sparged with nitrogen before addition of degassed ethanol (7.5 mL) and DIPEA (51 μL, 289 μmol). The reaction mixture was degassed (3 × vacuum/N₂) and the tube was placed in an Integrity 10 reaction well set at -0.5 °C (1 °C internal reaction temperature) with the stirring set at 400 rpm. The reaction mixture was sampled after 4 h and 19 h (50 μL in 950 μL EtOH diluent) and analysed by HPLC (Method C).

The results are summarised in Table 58.

Time / h	HPLC Area%				
	16	17 (9.2 min)	17 (20.2 min)	18	19
4	43.27	21.58	29.44	1.63	0.54
19	42.54	22.98	27.87	3.49	0.29

Table 58. HPLC analysis (Method C, 210 nm) for initially-trialled least forcing conditions. Enoate **16** at 20.0 min, arylboron reagent **17** at 20.2 min (ArBpin) and 9.2 min (ArB(OH)₂), bisaryl **18** at 19.4 min, *o*-tolylmethanol **19** at 13.4 min.

5.3.4.1.3 Least Forcing, Most Forcing, and Two Centre-Point Conditions (Table 13, page 94)



$[\text{RhCl}(\text{C}_2\text{H}_4)_2]_2$, the naphthyl ester diene ligand **L11** and arylboronic ester **17** were charged to Integrity 10 reaction tubes according to Table 59 (page 219) along with enoate **16** (5×150 mg, 578 μmol). The tubes were sparged with nitrogen for 20 min before addition of degassed ethanol, water and DIPEA according to Table 59. The reaction mixtures were degassed ($3 \times$ vacuum/ N_2) and the tubes were placed in Integrity 10 reaction wells at temperatures set according to Table 59 with stirring set at 500 rpm. The reaction mixtures were sampled at 50 min, 2 h 15 min and 17 h 35 min after they were placed in the reaction wells. Samples were taken such that the volume sampled would contain 1 mg of enoate **16** for a scenario in which no reaction had occurred, and these were diluted with ethanol to give 1 mL solutions for HPLC analysis.

Reaction Tube 5 (Table 59) was prepared separately and in the same manner, except that the base was not added until the catalyst precursor/reagent solution had been allowed to reach temperature. A sample was taken when at temperature for 1 h and before addition of base (yellow solution), then 5 min after addition of base (red solution) and 45 min after addition of base. The samples were prepared in the same manner as for the other reactions.

The samples were analysed by HPLC (Method C).

The reaction mixtures from Tubes 3, 4 and 5 were purified by column chromatography (45%/70% ethyl acetate in heptane as a step gradient) to give batches of the bisaryl product **18** as colourless viscous oils. Enantiomeric excesses were determined by Chiral HPLC (Method D2).

The results are summarised in Table 60 (page 219).

Tube	[RhCl(C ₂ H ₄) ₂] ₂		Naphthyl Diene L11		Arylboronic Ester 17		Solvents / mL		DIPEA		T / °C
	Amount / μmol	Mass / mg	Amount / μmol	Mass / mg	Amount / μmol	Mass / mg	Ethanol	Water	Amount / μmol	Volume / μL	
1	2.8	1.1	5.7	1.9	578	143.5	7.50	0	289	50.5	10
2	13	5.1	26	8.7	723	179.4	4.35	0.15	867	151.5	30
3	13	5.1	26	8.7	723	179.4	4.35	0.15	867	151.5	30
4	23	9.0	46	15.4	868	215.3	1.20	0.30	1450	252.5	50
5	23	9.0	46	15.4	868	215.3	1.20	0.30	1450	252.5	50

Table 59. Variables for the least and most forcing conditions for the DoE, along with two centre-point conditions.

Vial	Timepoint	HPLC Area%					Isolated 18	
		16	17 (9.2 min)	17 (20.2 min)	18	19	Yield	ee / %
1	50 min	42.46	22.82	31.33	1.68	0.21		
	2 h 15 min	41.33	22.20	30.30	3.25	0.30	n.d.	n.d.
	17 h 35 min	35.83	19.08	26.34	16.67	0.33		
2	50 min	32.39	21.87	28.45	14.56	0.52		
	2 h 15 min	31.83	22.46	26.42	15.76	0.74	n.d.	n.d.
	17 h 35 min	30.00	22.06	22.19	20.84	1.66		
3	50 min	26.43	17.54	23.54	29.31	0.65	77 mg	97
	2 h 15 min	25.01	17.49	21.15	32.37	0.87	(35%)	
	17 h 35 min	19.03	13.64	14.83	47.01	1.81		
4	50 min	0.25			78.72	7.54	203 mg	96
	2 h 15 min	0.27			77.82	7.50	(92%)	
	17 h 35 min	0.30			77.01	7.47		
5	< 0	33.00	32.68	32.58	0.34		212 mg	92
	5 min	0.24	2.43	2.76	88.48	4.56	(96%)	
	50 min	0.10			62.47	6.04		

Table 60. Summary of results for reactions assessing the suitability of the DoE design and procedure. HPLC analysis (Method C, 210 nm): enoate 16 at 20.0 min, arylboron reagent 17 at 20.2 min (ArBpin) and 9.2 min (ArB(OH)₂), bisaryl 18 at 19.4 min, *o*-tolylmethanol 19 at 13.4 min.

5.3.4.1.4 External HPLC Calibration for Section 3.2.3.3

UV response factor ratios at 215 nm were calculated for **16**, **18** and **19** relative to mesitylene for HPLC Method C. Two acetonitrile solutions containing approximately 1 mg mL⁻¹ of each of the species were prepared according to Table 61, and two portions of each solution were analysed using HPLC Method C.

Response factor ratios were calculated according to the following equations, where k_x is the response factor ratio by mass and k_m is the response factor ratio by molar amount of substance Y relative to mesitylene, $Area\%$ is the HPLC peak area% at 215 nm, $Mass$ is the mass of the substance (e.g. in the acetonitrile solution), M is the molar mass of the substance and $Amount$ is the molar amount of the substance (e.g. in the acetonitrile solution):

$$k_x = \frac{(Area\%_{mesitylene}/Area\%_Y)}{(Mass_{mesitylene}/Mass_Y)}$$

Equation 5

$$k_m = \frac{(Area\%_{mesitylene}/Area\%_Y)}{(Mass_{mesitylene}/Mass_Y)} \times \frac{M_{mesitylene}}{M_Y}$$

Equation 6

such that in any given sample

$$Mass_Y = k_x \times Mass_{mesitylene} \times \frac{Area\%_Y}{Area\%_{mesitylene}}$$

Equation 7

and

$$Amount_Y = k_m \times Amount_{mesitylene} \times \frac{Area\%_Y}{Area\%_{mesitylene}}$$

Equation 8

The results of the HPLC analysis are summarised in Table 62 along with the calculated and averaged relative response factors.

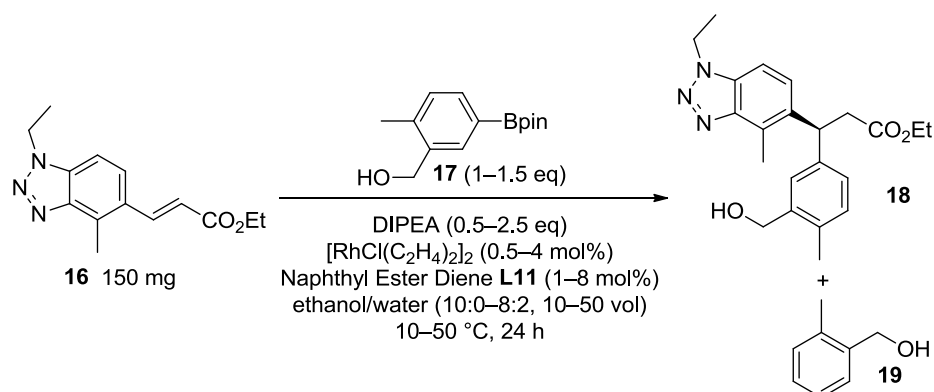
Compound	25 mL Acetonitrile Solution 1		25 mL Acetonitrile Solution 2	
	Amount / μ mol	Mass / mg	Amount / μ mol	Mass / mg
16	97.11	25.18	99.69	25.85
18	67.16	25.62	70.15	26.76
19	198.9	24.30	210.0	25.66
Mesitylene	207.5	24.94	210.1	25.25

Table 61. Acetonitrile solutions prepared in preparation for use of an external HPLC standard.

HPLC Sample	Mesitylene		16		18			19		
	Area%	Area%	k_x	k_m	Area%	k_x	k_m	Area%	k_x	k_m
Solution 1, Vial 1	24.25	10.82	2.264	1.049	35.30	0.7058	0.2224	19.12	1.236	1.216
Solution 1, Vial 2	24.18	10.77	2.267	1.051	35.14	0.7068	0.2227	19.05	1.236	1.216
Solution 2, Vial 1	23.75	10.76	2.260	1.047	35.39	0.7114	0.2241	19.37	1.246	1.226
Solution 2, Vial 2	23.70	10.76	2.256	1.045	35.38	0.7099	0.2237	19.34	1.245	1.225
Average			2.262	1.048		0.7085	0.2232		1.241	1.221

Table 62. HPLC Area% (Method C, 215 nm) and calculated response factor ratios for compounds 16, 18 and 19 relative to mesitylene.

5.3.4.2 Factor-Screening Design of Experiment Reactions (Procedure for Section 3.2.3.3)



$[\text{RhCl}(\text{C}_2\text{H}_4)_2]_2$, the naphthyl ester diene ligand **L11** and arylboronic ester **17** were charged to Integrity 10 reaction tubes according to Table 63 (page 222) along with enoate **16** (20×150 mg, 578 μmol). Each tube was then charged with degassed ethanol and water according to Table 63 (page 222) and degassed ($3 \times$ vacuum/ N_2) immediately before placing the reaction tube in an Integrity 10 reaction well at a temperature set according to Table 63 and with stirring set at 500 rpm. After a tube had been in the reaction well for 40 min, DIPEA was added ($t = 0$) according to Table 63, resulting in a reddening of the otherwise yellow solutions according to the precatalyst concentration. The reaction mixtures were sampled at $t = 1$ h, 3 h and 19 h (10 μL for reaction solutions with 1.5 mL solvent, 30 μL for those with 4.5 mL solvent and 50 μL for those with 7.5 mL solvent) and the samples diluted into 1 mL of a 1.02 mg mL^{-1} mesitylene solution in ethanol. HPLC analysis was performed using Method C (215 nm). After 24 h, a portion of each reaction mixture was purified by column chromatography (45%/70% ethyl acetate in heptane as a step gradient) and the isolated product **18** was analysed by chiral HPLC (Method D3, (*S*)-**18** at 7.3 min, (*R*)-**18** at 8.1 min).

The results are summarised in Table 64 (page 223).

Tube	[RhCl(C ₂ H ₄) ₂] ₂		Naphthyl Diene L11		Arylboronic Ester 17		Solvents / mL		DIPEA		T / °C
	Amount / μmol	Mass / mg	Amount / μmol	Mass / mg	Amount / μmol	Mass / mg	Ethanol	Water	Amount / μmol	Volume / μL	
1	2.8	1.1	5.7	1.9	868	215.3	1.50	0.00	289	50.5	50
2	13	5.1	26	8.7	723	179.4	4.05	0.45	867	151.5	30
3	23	9.0	46	15.4	578	143.5	1.20	0.30	289	50.5	50
4	23	9.0	46	15.4	868	215.3	1.50	0.00	1450	252.5	10
5	23	9.0	46	15.4	868	215.3	6.00	1.50	1450	252.5	50
6	2.8	1.1	5.7	1.9	868	215.3	6.00	1.50	289	50.5	10
7	13	5.1	26	8.7	723	179.4	4.05	0.45	867	151.5	30
8	23	9.0	46	15.4	578	143.5	7.50	0.00	289	50.5	10
9	2.8	1.1	5.7	1.9	578	143.5	7.50	0.00	1450	252.5	50
10	2.8	1.1	5.7	1.9	578	143.5	1.20	0.30	1450	252.5	10
11	2.8	1.1	5.7	1.9	578	143.5	6.00	1.50	289	50.5	50
12	2.8	1.1	5.7	1.9	578	143.5	1.50	0.00	289	50.5	10
13	23	9.0	46	15.4	868	215.3	1.20	0.30	289	50.5	10
14	23	9.0	46	15.4	578	143.5	6.00	1.50	1450	252.5	10
15	23	9.0	46	15.4	868	215.3	7.50	0.00	289	50.5	50
16	2.8	1.1	5.7	1.9	868	215.3	1.20	0.30	1450	252.5	50
17	13	5.1	26	8.7	723	179.4	4.05	0.45	867	151.5	30
18	2.8	1.1	5.7	1.9	868	215.3	7.50	0.00	1450	252.5	10
19	23	9.0	46	15.4	578	143.5	1.50	0.00	1450	252.5	50
20	13	5.1	26	8.7	723	179.4	4.05	0.45	867	151.5	30

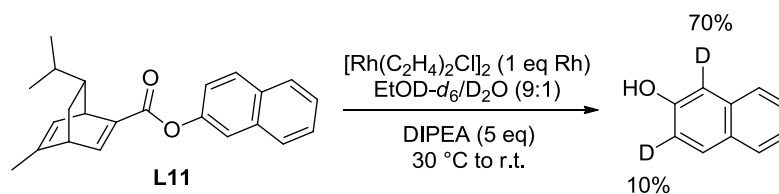
Table 63. Variables for the DoE reactions.

Tube	Timepoint	HPLC Area%					Isolated 18	ee / %
		16	17 (9.2 min)	17 (20.2 min)	18	19		
1	1 h	8.52	5.68	7.00	38.98	0.13	39.35	
	3 h	2.98	3.24	3.87	55.14	0.22	33.82	93.4
	19 h	0.34	1.22	1.48	62.02	2.10	32.18	
2	1 h	0.21	0.55	0.68	65.51	1.23	29.98	
	3 h		0.11		64.83	2.36	29.99	94.4
	19 h		0.08		64.76	2.45	29.26	
3	1 h	1.38			62.83	0.97	32.60	
	3 h	1.39	0.07		60.97	0.96	33.03	93.1
	19 h	1.35	0.05		60.61	0.96	32.33	
4	1 h	15.79	8.33	10.71	9.31	0.21	53.60	
	3 h	11.79	6.53	8.19	23.32	0.23	47.61	96.6
	19 h	3.84	3.16	3.82	52.18	0.23	34.76	
5	1 h	0.45			60.88	5.33	28.09	
	3 h	0.44	0.05		60.56	5.37	28.05	93.2
	19 h	0.20			60.82	5.27	27.41	
6	1 h	20.96	13.88	11.74	2.99	0.16	49.46	
	3 h	19.75	16.43	8.18	6.09	0.29	47.56	95.1
	19 h	17.45	15.46	6.44	12.71	0.39	45.46	
7	1 h	0.32	0.64	0.69	65.71	1.15	29.54	
	3 h	0.09	0.14		65.53	2.22	29.34	94.5
	19 h				65.04	2.26	29.46	
8	1 h	18.86	6.66	8.36	11.97	0.24	51.36	
	3 h	15.16	5.42	6.55	23.31	0.32	46.46	96.4

Tube	Timepoint	HPLC Area%					Mesitylene	Isolated 18 <i>ee</i> / %
		16	17 (9.2 min)	17 (20.2 min)	18	19		
9	19 h	8.77	2.91	3.61	41.82	0.45	39.84	92.8
	1 h	13.22	4.47	5.60	30.97	0.24	44.57	
	3 h	8.61	2.92	3.40	44.31	0.36	39.01	
10	19 h	5.18	1.48	1.79	52.26	0.68	35.18	94.7
	1 h	19.00	9.32	5.94	6.96	0.21	57.79	
	3 h	15.31	7.92	4.36	16.24	0.29	54.99	
11	19 h	4.74	2.05	0.90	52.14	0.58	38.69	92.3
	1 h	1.41	0.13		66.49	0.76	30.79	
	3 h	1.20			66.44	0.82	30.62	
12	19 h	1.13			66.24	0.84	30.58	96.3
	1 h	19.65	8.51	9.12	2.49		59.96	
	3 h	18.21	7.98	8.09	5.80	0.16	58.19	
13	19 h	16.13	6.18	6.46	17.32	0.16	52.58	95.6
	1 h	9.11	7.09	5.54	30.37	0.25	43.23	
	3 h	2.98	3.51	2.61	48.10	0.47	35.97	
14	19 h		1.22	0.99	58.04	1.72	31.60	95.2
	1 h	7.69	3.01	1.68	46.15	0.74	37.87	
	3 h	1.93			63.23	1.02	31.27	
15	19 h	1.73			62.20	1.09	31.70	93.5
	1 h	0.14	1.48	1.52	61.85	1.51	28.14	
	3 h		0.55	0.62	61.19	3.17	28.39	
16	19 h				61.24	4.54	28.23	92.3
	1 h	0.22	1.56	1.11	60.44	1.83	34.23	
	3 h	0.20	0.45	0.27	65.31	3.49	29.48	
17	19 h	0.19			61.33	4.78	32.75	94.4
	1 h	0.27	0.63	0.60	64.90	1.25	30.09	
	3 h				66.45	2.21	28.36	
18	19 h				67.45	2.49	26.22	96.1
	1 h	20.76	12.22	12.21	2.31	0.26	51.13	
	3 h	19.76	11.77	11.67	4.57	0.28	50.41	
19	19 h	17.08	10.27	10.48	13.98	0.29	46.57	94.9
	1 h	2.29	0.59	0.53	55.32	0.35	38.35	
	3 h	0.85			60.38	0.48	34.96	
20	19 h	0.75			61.02	0.48	33.55	94.3
	1 h	0.21	0.63	0.57	65.35	1.32	29.54	
	3 h				64.71	2.35	29.74	
	19 h				71.69	2.84	20.98	

Table 64. Summary of results for the DoE reactions. HPLC analysis (Method C, 215 nm): enoate 16 at 19.9 min, arylboron reagent 17 at 20.2 min (ArBpin) and 9.2 min (ArB(OH)₂), bisaryl 18 at 19.4 min, *o*-tolylmethanol 19 at 13.4 min, mesitylene at 25.7 min.

5.3.4.2.1 Ligand Stability (Scheme 43, page 107)



To the naphthyl ester diene **L11** (1.9 mg, 5.7 μmol) and $[\text{RhCl}(\text{C}_2\text{H}_4)_2]_2$ (1.1 mg, 2.9 μmol) was added nitrogen-sparged ethanol- d_6 (630 μL), and the mixture was stirred under nitrogen at 30 $^\circ\text{C}$. Within 20 minutes a cloudy yellow mixture formed, however full dissolution was not achieved within 17 h. At this point D_2O (70 μL) was added and after an additional 23 h without full dissolution, DIPEA (5 μL , 29 μmol) was added causing a clear yellow solution to be formed within 71 h. ^1H NMR was acquired (128 scans) under nitrogen, and reacquired after a further 77 h at 30 $^\circ\text{C}$ and again after 19 days at room temperature.

The aromatic regions of the NMR spectra were compared as discussed in Section 3.2.3.3.3, along with authentic samples of naphthol and the unligated naphthyl ester diene **L11** (Figure 60, below).

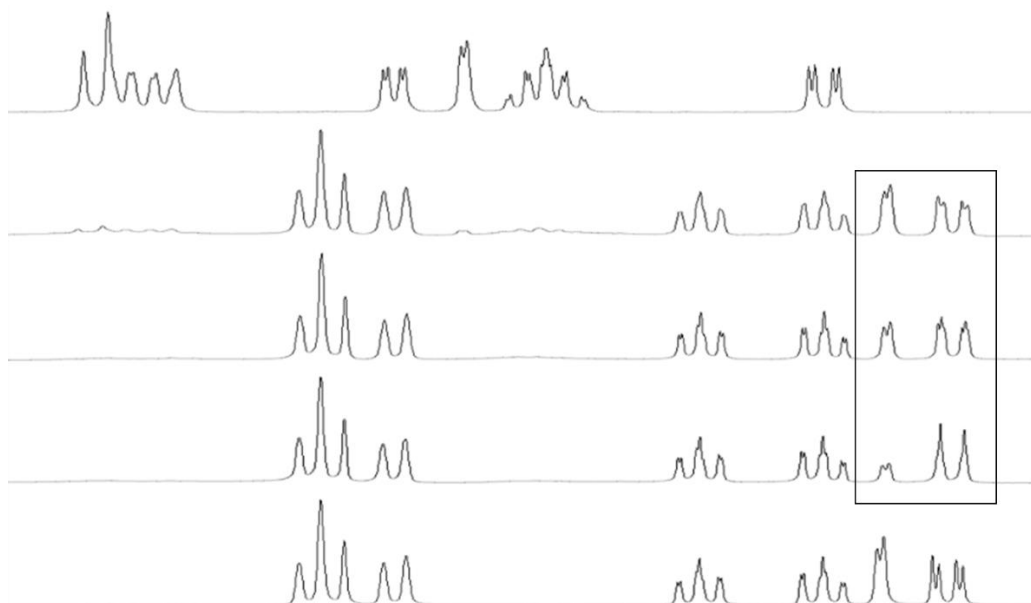


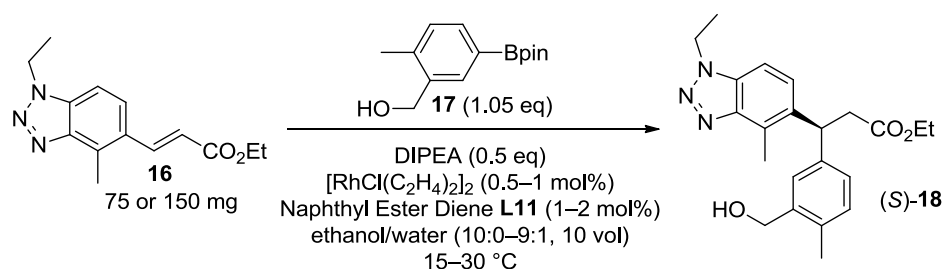
Figure 60. Spectra shown from 8.00 ppm to 7.00 ppm. From top to bottom: Unligated **L11**, reaction solution after 71 h at 30 $^\circ\text{C}$, after a further 77 h at 30 $^\circ\text{C}$, after a further 19 days at room temperature, authentic naphthol. Note the boxed resonances, which decrease in relative intensity over time to 30% and 90%.

Comparison of the final reaction solution and an authentic naphthol sample by LCMS Method B gave matching retention times (0.93 min) and the following mass spectra:

Authentic naphtholate ($C_{10}H_7O^-$) requires 143.1 (100%) and 144.1 (11%), found 143.1 (100%) and 144.1 (11%).

Naphtholate- d_1 ($C_{10}H_6DO^-$) requires 144.1 (100%) and 145.1 (11%), naphtholate- d_2 ($C_{10}H_5D_2O^-$) requires 145.1 (100%) and 146.1 (11%), found 143.1 (36%), 144.1 (100%), 145.1 (11%).

5.3.4.3 Trial Conditions for the Conjugate Arylation Reaction (Procedure for Section 3.2.3.5)



$[RhCl(C_2H_4)_2]_2$, the naphthyl ester diene **L11**, enone **16** and arylboronic ester **17** were charged to microwave vials according to Table 65. Degassed solvents were added according to Table 65 and the reaction mixtures were degassed ($3 \times$ vacuum/ N_2). The vials were transferred to a 30 °C sand bath if required by Table 65, and DIPEA was added ($3 \times 51 \mu L$, 289 μmol , Vials 1, 2, 5; $2 \times 25 \mu L$, 145 μmol , Vials 2, 3) to the stirred reaction mixtures. The vials were sampled and analysed over 22 h, analogously to samples in Section 5.3.4.2.

Portions of Vials 2–5 were purified by column chromatography (45%/70% ethyl acetate in heptane as a step gradient) and the isolated product was analysed by chiral HPLC (method D3).

The results are summarised in Table 66.

Vial	Enoate 16		ArBpin 17		$[RhCl(C_2H_4)_2]_2$		Diene L11		Ethanol / mL	Water / mL	$T / ^\circ C$
	Amount / μmol	Mass / mg	Amount / μmol	Mass / mg	Amount / μmol	Mass / mg	Amount / μmol	Mass / mg			
1	578	150	607	151	2.8	1.1	5.7	1.9	1.5	0	15–20
2	578	150	607	151	5.9	2.3	12	4.0	1.5	0	15–20
3	289	75	304	75	2.8	1.1	5.7	1.9	0.75	0	30
4	289	75	304	75	2.8	1.1	5.7	1.9	0.675	0.075	30
5	578	150	607	151	2.8	1.1	5.7	1.9	1.35	0.15	30

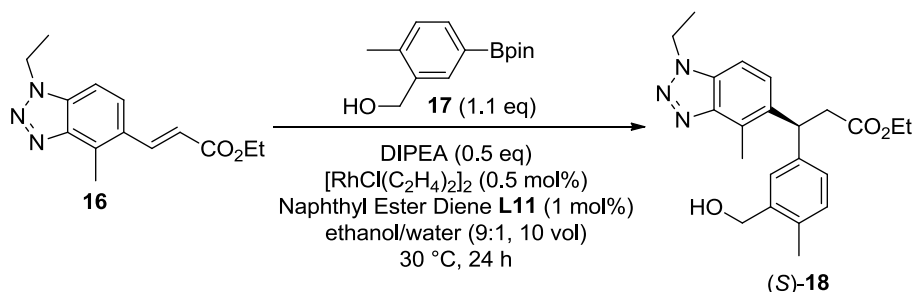
Table 65. Charges for reactions to determine suitable conditions for the 1,4-addition reaction.

Vial	Timepoint	HPLC Area%					Mesitylene	Isolated 18 <i>ee</i> / %
		16	17 (9.2 min)	17 (20.2 min)	18	19		
1	1 h 30 min	19.41	7.83	8.34	8.82		54.70	
	5 h 30 min	15.00	6.04	6.35	21.64	0.13	49.82	n.d.
	21 h	12.49	5.18	5.32	29.76	0.18	46.35	
2	1 h 30 min	17.56	6.99	7.54	13.98		52.83	
	5 h 30 min	11.87	4.78	5.00	30.67	0.14	46.27	94.7
	21 h	8.13	3.26	3.49	42.05	0.18	41.86	
3	1 h 30 min	15.51	6.23	6.46	21.97	0.13	48.47	
	17 h 30 min	7.23	1.38	4.78	47.55	0.23	37.87	94.9
	21 h 45 min	6.96	1.31	4.56	48.89	0.25	37.01	
4	1 h 30 min	5.08	2.36	1.92	52.39	0.17	37.18	
	18 h	0.82	0.29	0.21	65.26	0.32	32.10	93.7
	21 h	0.81	0.25	0.20	65.53	0.33	31.89	
5	1 h 30 min	8.30	3.90	3.00	43.05	0.17	40.50	
	17 h 30 min	1.04	0.26	0.60	64.49	0.28	32.55	93.8
	21 h 45 min	0.90	0.23	0.50	64.86	0.30	32.41	

Table 66. Summary of results for reactions to determine suitable conditions for the 1,4-addition reaction. HPLC analysis (Method C, 215 nm): enoate 16 at 19.9 min, arylboron reagent 17 at 20.2 min (ArBpin) and 9.2 min (ArB(OH)₂), bisaryl 18 at 19.4 min, *o*-tolylmethanol 19 at 13.4 min.

5.3.5 Multigram-Scale Process Demonstration of the Conjugate Arylation using the Optimised Reaction Conditions (Procedures for Section 3.2.4)

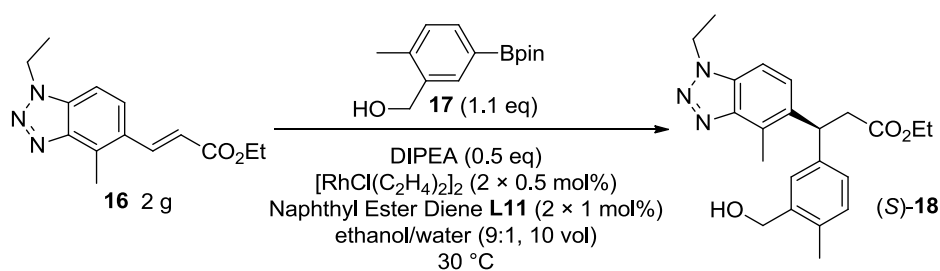
5.3.5.1 2 g Scale (Scheme 44a, page 112)



$[\text{RhCl}(\text{C}_2\text{H}_4)_2]_2$ (15.0 mg, 0.039 mmol), the naphthyl ester diene **L11** (26.0 mg, 0.078 mmol), enone **16** (2.000 g, 7.71 mmol) and arylboronic ester **17** (2.105 g, 8.48 mmol) were charged to a vessel and without any prior degassing cycles nitrogen-sparged ethanol (18 mL) and water (2 mL) were added to the solids. The mixture was then degassed ($3 \times$ vacuum/ N_2) and the temperature of the orange solution was brought to 30 °C over 30 minutes before addition of DIPEA (0.67 mL, 3.86 mmol) with a concomitant reddening of the solution. After 24 h the reaction mixture was sampled and analysis by HPLC Method C at 215 nm revealed > 98% molar conversion of the enoate **16** to the bisaryl product **18**. No further changes were observed and so the volatiles were removed. The residue was purified by column chromatography (45%/70% ethyl acetate in heptane as a step gradient) to give bisaryl **18** as a colourless oil (2.76 g, 7.24 mmol, 94%). Chiral HPLC (Method D3) revealed the product to have an enantiomeric excess of 93.9%.

Analytical data consistent with previous preparations (p. 184).

5.3.5.2 2 g Scale with stalling (Scheme 45, page 113)



< 7% conversion in 27 h with initial charge of catalyst;
> 96% conversion 25 h after a second charge of catalyst.

$[\text{RhCl}(\text{C}_2\text{H}_4)_2]_2$ (15.0 mg, 0.039 mmol), the naphthyl ester diene **L11** (26.0 mg, 0.078 mmol), enone **16** (2.000 g, 7.71 mmol) and arylboronic ester **17** (2.105 g, 8.48 mmol) were charged

to a vessel which was carefully inerted ($3 \times$ vacuum/ N_2). Nitrogen-sparged ethanol (18 mL) and water (2 mL) was added, and the vacuum/nitrogen cycles were repeated. The stirred reaction solution was heated to 30 °C. After 30 minutes, DIPEA (0.674 mL, 3.86 mmol) was added with a concomitant reddening of the reaction solution. After 27 h, 10 μ L of the reaction mixture was sampled and diluted with 1 mL of a 1.02 mg mL⁻¹ solution of mesitylene in ethanol. The reaction mixture was observed to no longer be a red colour. HPLC analysis (Method C, 215 nm) revealed poor reaction conversion, and so a second charge of $[RhCl(C_2H_4)_2]_2$ (15.0 mg, 0.039 mmol) and the naphthyl ester diene **L11** (26.0 mg, 0.078 mmol) was made to the reaction mixture. The mixture was degassed ($3 \times$ vacuum/ N_2) and sampled again in the same manner after a further 24 h 30 min and again 40 h 10 min after the second charge of catalyst, revealing complete consumption of the arylboronic ester **17**. A summary of the HPLC results is given in Table 67.

The reaction mixture was concentrated by rotary evaporation and the product purified by column chromatography (45%/70% ethyl acetate in heptane as a step gradient) to give **18** as a colourless viscous oil (2.84 g, 7.44 mmol, 97%). Chiral HPLC (Method D3) revealed the product to have an enantiomeric excess of 94.5%.

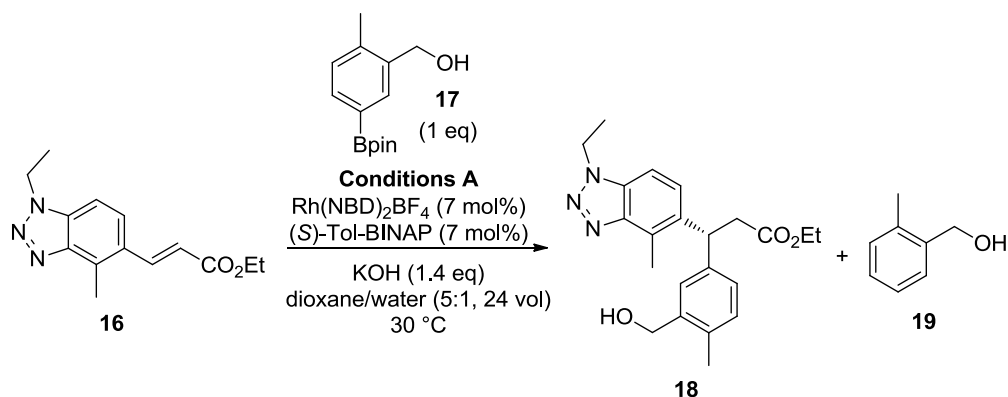
Analytical data consistent with previous preparations (p. 184).

Timepoint	HPLC Peak Area%					
	16	17 (9.2 min)	17 (20.2 min)	18	19	Mesitylene
27 h after first charge	18.88	9.18	7.08	6.34	0.48	56.50
24 h 30 min after second charge	0.53	0.22	0.19	64.93	0.65	31.97
40 h 10 min after second charge	0.30			65.28	0.73	32.05

Table 67. HPLC analysis (Method C, 215 nm) for the stalled 2 g scale 1,4-addition reaction. Enoate **16** at 19.9 min, arylboron reagent **17** at 20.2 min (ArBpin) and 9.2 min (ArB(OH)₂), bisaryl **18** at 19.4 min, *o*-tolylmethanol **19** at 13.4 min.

5.4 Procedures for Section 3.3: Selectivity for Conjugate Arylation over Protodeboronation

5.4.1 Comparison of the Original and Final Processes for the Pharmaceutically-Relevant Conjugate Arylation (Scheme 46, page 114)



Enoate **16** (100 mg, 386 μ mol), arylboron reagent **17** (96 mg, 386 μ mol), Rh(NBD)₂BF₄ (10.0 mg, 27 μ mol) and (S)-Tol-BINAP (18.3 mg, 27 μ mol)^{xviii} were charged to a reaction vial and the atmosphere was inerted before dissolution of the solids in degassed dioxane (2 mL). The solution was degassed (3 \times vacuum/N₂) and stirred under nitrogen at 30 °C for 30 minutes. Potassium hydroxide (30.3 mg, 540 μ mol) was added as a solution in degassed water (400 μ L) and the reaction mixture was degassed again. Full consumption of the arylboron reagent was observed within 89 h.

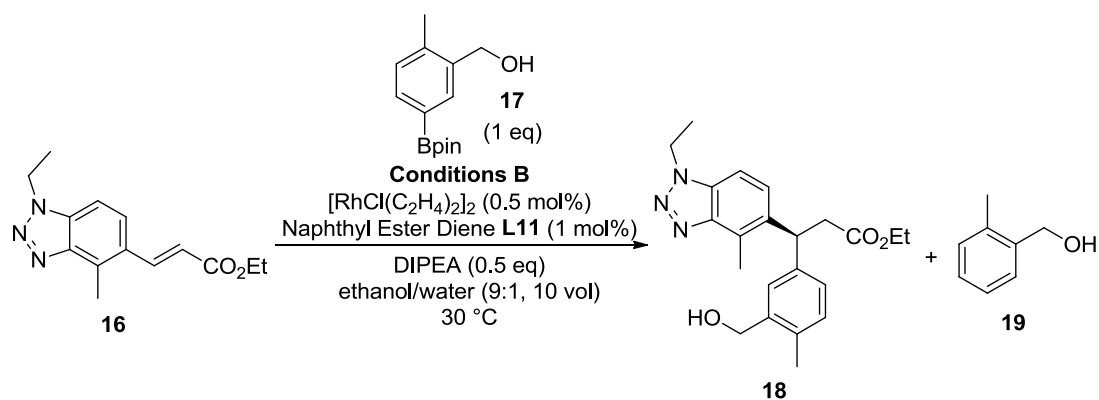
Analysis by HPLC Method C at 215 nm gave a peak area for bisaryl **18** of 1756.897 and for *o*-tolylmethanol **19** of 299.752. Use of the relative response factors (Section 5.3.4.1.4) enabled a molar ratio of 52:48 **18:19** to be determined.

The reaction mixture was filtered and partitioned between ethyl acetate and water. The aqueous phase was extracted with ethyl acetate (3 \times 20 mL) and the combined organic portions were washed with water (3 \times 20 mL) and brine (20 mL) before passing through a hydrophobic frit. The crude product was purified by column chromatography (45%/70% ethyl acetate in heptane as a step gradient) to give bisaryl **18** as a colourless oil (57 mg, 149 μ mol, 39%).

Analytical data consistent with previous preparations (p. 184).

HPLC (Method D3): 63% |*ee*|.

^{xviii} The (S)- rather than (R)-enantiomer of the BINAP ligand was employed due to availability.



Enoate **16** (150 mg, 578 μmol), arylboron reagent **17** (143 mg, 578 μmol), $[\text{RhCl}(\text{C}_2\text{H}_4)_2]_2$ (1.1 mg, 2.8 μmol) and naphthyl ester diene **L11** (1.9 mg, 5.7 μmol) were dissolved in degassed ethanol (1.35 mL) and water (150 μL) and the mixture was degassed ($3 \times \text{vacuum}/\text{N}_2$). The reaction mixture was stirred under nitrogen at 30 °C for 30 minutes before addition of DIPEA (50 μL , 290 μmol). After 42 h the reaction mixture was sampled.

Analysis by HPLC Method C at 215 nm gave a peak area for bisaryl **18** of 7847.301 and for *o*-tolylmethanol **19** of 41.919. Use of the relative response factors (Section 5.3.4.1.4) enabled a molar ratio of 97:3 **18:19** to be determined.

The volatiles were removed and the crude product was purified by column chromatography (45%/70% ethyl acetate in heptane as a step gradient) to give bisaryl **18** as a colourless oil (182 mg, 477 μmol , 83%).

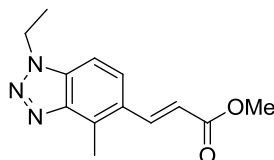
Analytical data consistent with previous preparations (p. 184).

HPLC (Method D3): 94% *ee*.

5.4.2 Influence of Structural Motifs of the Substrates on Selectivity for Conjugate Arylation over Protodeboronation (Procedures for Section 3.3.1)

5.4.2.1 Substrate Syntheses

5.4.2.1.1 (*E*)-Methyl 3-(1-ethyl-4-methyl-1*H*-benzo[*d*][1,2,3]triazol-5-yl)acrylate **28**



(*E*)-Ethyl 3-(1-ethyl-4-methyl-1*H*-benzo[*d*][1,2,3]triazol-5-yl)acrylate (**16**, 500 mg, 1.93 mmol) was charged to a microwave vial and dissolved in methanol (20 mL). Sodium methoxide (0.66 mL, 25 wt% in methanol, 2.9 mmol) was added dropwise and the vial was heated to 100 °C for 10 minutes under nitrogen in a microwave reactor. Half-saturated aqueous ammonium chloride (20 mL) was added, followed by ethyl acetate (20 mL) and the organic phase was separated. The aqueous phase was extracted with ethyl acetate (3 × 10 mL) and the combined organic portions were washed with water (3 × 10 mL) and brine (10 mL), and passed through a hydrophobic frit. The volatiles were removed and column chromatography (7–60% ethyl acetate in heptane) afforded 441 mg of the product in approximately 82% purity (¹H NMR). The material was dissolved in warm ethyl acetate and heptane was added until crystallisation was observed. The solids were filtered and washed with heptane to give the methyl ester in high purity (173 mg, 0.705 mmol, 36%).

Appearance: Colourless solid.

Melting point: 118.5–120.1 °C.

ν (neat): 2996, 2948, 1708, 1633, 1604, 1435, 1312, 1268, 1250, 1197, 1182, 1161 cm⁻¹.

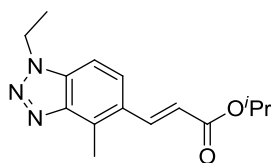
¹H NMR (400 MHz, CDCl₃): δ 8.16 (d, 1H, *J* = 15.8 Hz), 7.70 (d, 1H, *J* = 8.6 Hz), 7.36 (d, 1H, *J* = 8.9 Hz), 6.43 (d, 1H, *J* = 16.0 Hz), 4.68 (q, 2H, *J* = 7.4 Hz), 3.85 (s, 3H), 2.92 (s, 3H), 1.64 (t, 3H, *J* = 7.4 Hz).

¹³C NMR (101 MHz, CDCl₃): δ 167.3, 147.0, 141.3, 133.0, 131.6, 128.0, 125.7, 118.7, 107.1, 51.8, 43.3, 15.0, 13.3.

HPLC (Method B): *t*_R = 4.50 min, > 95%.

HRMS: (C₁₃H₁₅N₃O₂) [M+H]⁺ requires 246.1237, found [M+H]⁺ 246.1227.

5.4.2.1.2 (*E*)-*iso*-Propyl 3-(1-ethyl-4-methyl-1*H*-benzo[*d*][1,2,3]triazol-5-yl)acrylate **29**



(*E*)-Ethyl 3-(1-ethyl-4-methyl-1*H*-benzo[*d*][1,2,3]triazol-5-yl)acrylate (**16**, 500 mg, 1.93 mmol) and sodium propan-2-olate (237 mg, 2.89 mmol) were charged to a microwave vial, dissolved in *iso*-propanol (15 mL) and degassed ($3 \times$ vacuum/ N_2). The reaction mixture was heated to 100 °C for 20 minutes in a microwave reactor. Half-saturated aqueous ammonium chloride (20 mL) was added, followed by ethyl acetate (20 mL) and the organic phase was separated. The aqueous phase was extracted with ethyl acetate ($3 \times$ 10 mL) and the combined organic portions were washed with water ($3 \times$ 10 mL) and brine (10 mL), and passed through a hydrophobic frit. The volatiles were removed and column chromatography (7–60% ethyl acetate in heptane) afforded the product in high purity (343 mg, 1.26 mmol, 65%).

Appearance: Colourless solid.

Melting point: 83.1–84.0 °C.

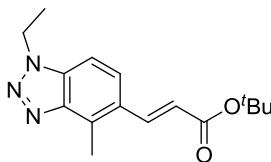
ν (neat): 2981, 2940, 2877, 1700, 1635, 1602, 1493, 1450, 1371, 1356, 1305, 1267 cm^{-1} .

1H NMR (400 MHz, $CDCl_3$): δ 8.12 (d, 1H, $J = 16.0$ Hz), 7.70 (d, 1H, $J = 8.6$ Hz), 7.35 (d, 1H, $J = 8.9$ Hz), 6.40 (d, 1H, $J = 15.8$ Hz), 5.17 (spt, 1H, $J = 6.3$ Hz), 4.67 (q, 2H, $J = 7.4$ Hz), 2.92 (s, 3H), 1.63 (t, 3H, $J = 7.4$ Hz), 1.34 (d, 6H, $J = 6.4$ Hz).

^{13}C NMR (101 MHz, $CDCl_3$): δ 166.5, 147.1, 140.8, 132.9, 131.5, 128.2, 125.8, 119.7, 107.0, 67.9, 43.3, 22.0, 15.0, 13.3.

HRMS: ($C_{15}H_{19}N_3O_2$) $[M+H]^+$ requires 274.1550, found $[M+H]^+$ 274.1546.

5.4.2.1.3 (*E*)-*tert*-Butyl 3-(1-ethyl-4-methyl-1*H*-benzo[*d*][1,2,3]triazol-5-yl)acrylate **30**



DMF (34 mL) was charged to a vessel containing 5-bromo-1-ethyl-4-methyl-1*H*-benzo[*d*][1,2,3]triazole (**24**, 2.00 g, 8.33 mmol), potassium carbonate (1.73 g, 12.5 mmol), palladium(II) acetate (75 mg, 0.33 mmol) and tri(*o*-tolyl)phosphine (254 mg, 0.833 mmol). *tert*-Butyl acrylate (1.6 mL, 11 mmol) was added and the reaction mixture was stirred at

110 °C for 1.5 h under nitrogen. The mixture was cooled to 20–30 °C, filtered through celite and diluted with ethyl acetate (100 mL). Water (200 mL) was added and the phases were separated. The aqueous phase was extracted with ethyl acetate (3 × 50 mL), and the combined organic portions were washed with water (3 × 50 mL) and brine (50 mL), and passed through a hydrophobic frit. The volatiles were removed and the product was purified by column chromatography (7–60% ethyl acetate in heptane) to give the desired compound as a yellow solid (2.3 g, 8.0 mmol, 96%).

Appearance: Yellow solid.

Melting point: 111.8–112.9 °C.

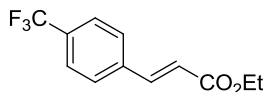
ν (neat): 2978, 2937, 2877, 1699, 1632, 1607, 1494, 1447, 1385, 1367, 1316, 1266, 1248 cm^{-1} .

^1H NMR (400 MHz, CDCl_3): δ 8.08 (d, 1H, $J = 16.0$ Hz), 7.72 (d, 1H, $J = 8.6$ Hz), 7.36 (d, 1H, $J = 8.6$ Hz), 6.38 (d, 1H, $J = 15.8$ Hz), 4.69 (q, 2H, $J = 7.4$ Hz), 2.93 (s, 3H), 1.65 (t, 3H, $J = 7.4$ Hz), 1.58 (s, 9H).

^{13}C NMR (101 MHz, CDCl_3): δ 166.3, 147.0, 140.0, 132.8, 131.2, 128.2, 125.8, 121.0, 106.9, 80.6, 43.3, 28.2, 15.0, 13.2.

HRMS: ($\text{C}_{16}\text{H}_{21}\text{N}_3\text{O}_2$) $[\text{M}+\text{H}]^+$ requires 288.1707, found $[\text{M}+\text{H}]^+$ 288.1694.

5.4.2.1.4 (*E*)-Ethyl 3-(4-(trifluoromethyl)phenyl)acrylate 31



Sodium hydride (0.366 g, 9.15 mmol, 60% mineral oil dispersion) was washed under nitrogen with heptane (3 mL), which was decanted before addition of THF (20 mL). The THF suspension was cooled to 0 °C and triethyl phosphonoacetate (1.83 mL, 9.15 mmol) was added dropwise, with the temperature kept below 10 °C. After stirring for 10 minutes, 4-(trifluoromethyl)benzaldehyde (1.00 mL, 7.32 mmol) was added with the temperature maintained below 15 °C during the addition. The reaction mixture was stirred at room temperature overnight, before addition of water (25 mL) and separation of the phases. The aqueous phase was extracted with ethyl acetate (3 × 25 mL) and the combined organic portions were washed with water (2 × 20 mL) and brine (20 mL) before passing through a hydrophobic frit. Following removal of the volatiles, the product was purified by column chromatography (8–65% dichloromethane (DCM) in heptane) to give the desired enoate as a colourless crystalline solid (1.72 g, 7.03 mmol, 96%).

Appearance: Colourless crystalline solid.

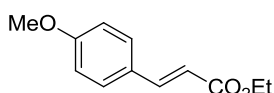
^1H NMR (400 MHz, CDCl_3): δ 7.70 (d, 1H, $J = 16.0$ Hz), 7.66 (d, 2H, $J = 9.1$ Hz), 7.63 (d, 2H, $J = 9.1$ Hz), 6.52 (d, 1H, $J = 16.0$ Hz), 4.30 (q, 2H, $J = 7.1$ Hz), 1.36 (t, 3H, $J = 7.1$ Hz).

^{13}C NMR (101 MHz, CDCl_3): δ 166.4, 142.7, 137.8, 131.7 (q, $J = 32.8$ Hz), 128.1, 125.8 (q, $J = 3.8$ Hz), 123.8 (q, $J = 272.4$ Hz), 120.9, 60.8, 14.3.

HPLC (Method A, 210 nm): $t_R = 2.60$ min, > 98%.

NMR literature data concordant.²¹⁸

5.4.2.1.5 (*E*)-Ethyl 3-(4-methoxyphenyl)acrylate 32



Sodium hydride (0.393 g, 9.82 mmol, 60% mineral oil dispersion) was washed under nitrogen with heptane (3 mL), which was decanted before addition of THF (18 mL). The THF suspension was cooled to 0 °C and triethyl phosphonoacetate (1.97 mL, 9.82 mmol) was added dropwise, with the temperature kept below 10 °C. After stirring for 30 minutes at 0 °C, 4-methoxybenzaldehyde (0.95 mL, 7.9 mmol) was added with the temperature maintained below 10 °C during the addition. An additional charge of THF (10 mL) was made to aid stirring and the reaction mixture was stirred at room temperature overnight, before addition of water (25 mL) and separation of the phases. The aqueous phase was extracted with ethyl acetate (3 × 25 mL) and the combined organic portions were washed with water (2 × 20 mL) and brine (20 mL) before passing through a hydrophobic frit. Following removal of the volatiles, the product was purified by column chromatography (3–20% ethyl acetate in heptane) to give the desired enoate as a colourless oil (1.49 g, 7.20 mmol, 92%).

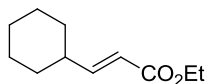
Appearance: Colourless oil.

^1H NMR (400 MHz, CDCl_3): δ 7.65 (d, 1H, $J = 16.0$ Hz), 7.48 (d, 2H, $J = 8.6$ Hz), 6.91 (d, 2H, $J = 8.9$ Hz), 6.32 (d, 1H, $J = 16.0$ Hz), 4.26 (q, 2H, $J = 7.1$ Hz), 3.85 (s, 3H), 1.34 (t, 3H, $J = 7.1$ Hz).

^{13}C NMR (101 MHz, CDCl_3): δ 167.3, 161.3, 144.2, 129.7, 127.2, 115.8, 114.3, 60.3, 55.4, 14.4.

NMR literature data concordant.²¹⁹ The literature reference does not report the most downfield ^{13}C NMR resonance (167.3 ppm).

5.4.2.1.6 (*E*)-Ethyl 3-cyclohexylacrylate 33



Sodium hydride (0.413 g, 10.3 mmol, 60% mineral oil dispersion) was washed under nitrogen with heptane (3 mL), which was decanted before addition of THF (20 mL). The THF suspension was cooled to 0–10 °C and triethyl phosphonoacetate (2.07 mL, 10.3 mmol) was added dropwise, with the temperature kept below 10 °C. After stirring for 10 minutes, cyclohexanecarboxaldehyde (1.00 mL, 8.26 mmol) was added with the temperature maintained below 15 °C. After 45 minutes the temperature was allowed to rise to room temperature and the reaction was stirred for a further 1.5 h, before addition of water (25 mL) and separation of the phases. The aqueous phase was extracted with ethyl acetate (3 × 25 mL) and the combined organic portions were washed with water (2 × 20 mL) and brine (20 mL) before passing through a hydrophobic frit. ¹H NMR of the crude product showed no evidence of cyclohexanecarboxaldehyde and a 20:1 ratio of *E/Z* product. The product was purified by column chromatography (0–5% ethyl acetate in heptane) to give colourless oils of the product mixture (1.465 g, 8.04 mmol, 97%). The fractions containing > 99% *E*-isomer amounted to 792 mg.

Appearance: Colourless oil.

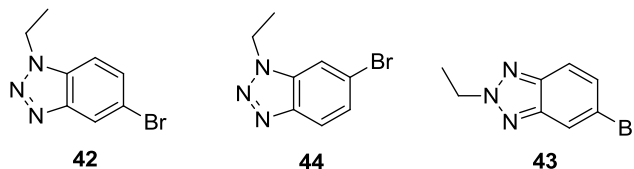
¹H NMR (400 MHz, CDCl₃): δ 6.94 (dd, 1H, *J* = 6.6, 15.8 Hz), 5.78 (dd, 1H, *J* = 1.5, 15.8 Hz), 4.21 (q, 2H, *J* = 7.1 Hz), 2.22–2.09 (m, 1H), 1.84–1.74 (m, 4H), 1.73–1.65 (m, 1H), 1.40–1.26 (m, 5H), 1.26–1.10 (m, 3H)

¹³C NMR (101 MHz, CDCl₃): δ 167.2, 154.3, 118.9, 60.1, 40.4, 31.7, 25.9, 25.7, 14.3.

HPLC (Method C, 215 nm): *t*_R = 25.8 min, > 99%.

NMR literature data concordant.^{220,221}

5.4.2.1.7 5-Bromo-1-ethyl-1*H*-benzo[*d*][1,2,3]triazole 42 and regioisomers 44 and 43



Sodium hydride (0.240 g, 6.00 mmol, 60% mineral oil dispersion) was washed under nitrogen with heptane (3 mL), which was decanted before addition of THF (10 mL) and cooling of the suspension in an ice bath. 5-Bromo-1*H*-benzo[*d*][1,2,3]triazole (1.00 g, 5.05 mmol) was added dropwise as a solution in THF (10 mL), with the temperature kept

below 20 °C. After 10 minutes the reaction mixture was allowed to warm to room temperature and iodoethane (0.45 mL, 5.5 mmol) was added with additional THF (25 mL) to aid stirring. After 2.5 h at ambient temperature, less than 10% conversion to the products was observed by LCMS analysis (254 nm). The reaction mixture was heated to reflux for 17 h before allowing to cool to room temperature. The reaction mixture was quenched with aqueous hydroxide (10 mL, 2 M) and stirred for a further 2.5 h. The phases were separated and the aqueous phase was extracted with ethyl acetate (3 × 20 mL). The combined organics were washed with water (3 × 20 mL) and brine (10 mL) before passing through a hydrophobic frit. The crude product mixture was purified by column chromatography (5-40% ethyl acetate in heptane), giving separation of the three regioisomers:

5-bromo-1-ethyl-1*H*-benzo[*d*][1,2,3]triazole **42** (417 mg, 1.85 mmol, 37%),
6-bromo-1-ethyl-1*H*-benzo[*d*][1,2,3]triazole **44** (381 mg, 1.69 mmol, 33%),
5-bromo-2-ethyl-2*H*-benzo[*d*][1,2,3]triazole **43** (114 mg, 0.504 mmol, 10%).

5-Bromo-1-ethyl-1*H*-benzo[*d*][1,2,3]triazole 42

Appearance: Colourless solid.

Melting point: 95.4–96.0 °C.

ν (neat): 3066, 2975, 2932, 1576, 1477, 1444, 1316, 1271, 1213, 1177, 1164, 1039 cm⁻¹.

¹H NMR (400 MHz, CDCl₃): δ 8.22 (d, 1H, *J* = 1.2 Hz), 7.58 (dd, 1H, *J* = 1.6, 8.7 Hz), 7.43 (d, 1H, *J* = 8.9 Hz), 4.68 (q, 2H, *J* = 7.4 Hz), 1.64 (t, 3H, *J* = 7.4 Hz).

¹³C NMR (101 MHz, CDCl₃): δ 147.3, 131.6, 130.5, 122.7, 117.1, 110.5, 43.5, 14.9.

HPLC (Method A): *t*_R = 2.13 min, > 99%.

HRMS: (C₈H₈BrN₃) [M+H]⁺ requires 225.9974, found [M+H]⁺ 225.9964.

6-Bromo-1-ethyl-1*H*-benzo[*d*][1,2,3]triazole 44

Appearance: Yellow solid.

Melting point: 67.0–68.5 °C.

ν (neat): 3061, 2970, 2932, 2879, 1605, 1446, 1318, 1265, 1235, 1177, 1134, 1089, 1042 cm⁻¹.

¹H NMR (400 MHz, CDCl₃): δ 7.93 (d, 1H, *J* = 8.9 Hz), 7.73 (d, 1H, *J* = 1.2 Hz), 7.47 (dd, 1H, *J* = 1.6, 8.7 Hz), 4.66 (q, 2H, *J* = 7.4 Hz), 1.64 (t, 3H, *J* = 7.3 Hz).

¹³C NMR (101 MHz, CDCl₃): δ 145.0, 133.7, 127.5, 121.5, 121.2, 112.2, 43.4, 14.9.

HPLC (Method A): *t*_R = 2.15 min, > 98%.

HRMS: (C₈H₈BrN₃) [M+H]⁺ requires 225.9974, found [M+H]⁺ 225.9964.

5-Bromo-2-ethyl-2H-benzo[d][1,2,3]triazole 43

Appearance: Yellow oil.

ν (neat): 3071, 2980, 2943, 1619, 1556, 1470, 1439, 1324, 1299, 1265, 1234, 1221, 1085, 1035 cm^{-1} .

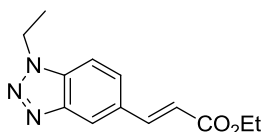
^1H NMR (400 MHz, CDCl_3): δ 8.05 (d, 1H, $J = 2.0$ Hz), 7.75 (d, 1H, $J = 9.1$ Hz), 7.46 (dd, 1H, $J = 1.7, 9.1$ Hz), 4.77 (q, 2H, $J = 7.4$ Hz), 1.72 (t, 3H, $J = 7.3$ Hz).

^{13}C NMR (101 MHz, CDCl_3): δ 145.2, 142.9, 130.0, 120.4, 119.8, 119.4, 51.8, 15.0.

HPLC (Method A): $t_R = 2.36$ min, > 98%.

HRMS: ($\text{C}_8\text{H}_8\text{BrN}_3$) $[\text{M}+\text{H}]^+$ requires 225.9974, found $[\text{M}+\text{H}]^+$ 225.9965.

5.4.2.1.8 (E)-Ethyl 3-(1-ethyl-1H-benzo[d][1,2,3]triazol-5-yl)acrylate 45



5-Bromo-1-ethyl-1H-benzo[d][1,2,3]triazole (407 mg, 1.800 mmol) was added as a solution in DMF (7 mL) to potassium carbonate (399 mg, 2.89 mmol), palladium (II) acetate (16.5 mg, 0.073 mmol) and tri(*o*-tolyl)phosphine (56 mg, 0.184 mmol). Ethyl acrylate (0.26 mL, 2.4 mmol) was added and the reaction mixture was stirred at 110 °C under nitrogen. After 4 h, the mixture was cooled to room temperature, filtered through celite and diluted with ethyl acetate to 50 mL. Water (20 mL) was added and the phases were separated. The aqueous phase was extracted with ethyl acetate (3×10 mL), and the combined organic portions were washed with water (3×20 mL) and brine (20 mL), and passed through a hydrophobic frit. The volatiles were removed and the product was purified by column chromatography (8–60% ethyl acetate in heptane) to give the desired compound as a colourless solid (371 mg, 1.51 mmol, 84%).

Appearance: Colourless solid.

Melting point: 69.8–70.2 °C.

ν (neat): 3060, 2986, 2938, 2900, 1698, 1641, 1470, 1443, 1363, 1268, 1248, 1173, 1149, 1043 cm^{-1} .

^1H NMR (400 MHz, CDCl_3): δ 8.19 (s, 1H), 7.84 (d, 1H, $J = 16.0$ Hz), 7.70 (dd, 1H, $J = 1.4, 8.7$ Hz), 7.55 (d, 1H, $J = 8.6$ Hz), 6.51 (d, 1H, $J = 16.0$ Hz), 4.71 (q, 2H, $J = 7.4$ Hz), 4.30 (q, 2H, $J = 7.1$ Hz), 1.66 (t, 3H, $J = 7.3$ Hz), 1.37 (t, 3H, $J = 7.1$ Hz).

^{13}C NMR (101 MHz, CDCl_3): δ 166.8, 146.5, 144.0, 133.5, 130.7, 126.3, 120.7, 118.7, 109.8, 60.6, 43.4, 15.0, 14.3.

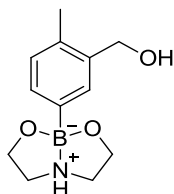
LCMS (Method A, 254 nm), $t_R = 0.98$ min, $[\text{M}+\text{H}]^+$ 246.

HPLC (Method B): $t_R = 4.65$ min, > 99%.

HRMS: (C₁₃H₁₅N₃O₂) [M+H]⁺ requires 246.1237, found [M+H]⁺ 246.1227.

Structure confirmed by ROESY 2D NMR.

5.4.2.1.9 (5-(1,3,6,2-Dioxazaborocan-2-yl)-2-methylphenyl)methanol (diethanolamine boronate) 50



(2-Methyl-5-(4,4,5,5-tetramethyl-1,3,2-dioxaborolan-2-yl)phenyl)methanol (**17**, 10 g, 40.3 mmol) was dissolved in diethyl ether (40 mL) and diethanolamine (4.64 mL, 48.4 mmol) was added. Additional volumes of diethyl ether (40 mL) were added to aid redissolution of the presumed substrate, which oiled out of the reaction mixture upon addition of the diethanolamine. Within 5 minutes, white solids coated the flask and after 2 h the vessel was transferred to a sonicator for 2 h to improve mixing before the reaction mixture was stirred overnight. The solids were collected by filtration and washed with ether (60 mL) to give the product as a white solid (8.242 g, 35.1 mmol, 87%) with no evidence of the arylboronic acid pinacol ester **17**.

NMR analysis revealed the product to contain an unknown impurity potentially related to diethanolamine and containing no aromatic protons. The level of contamination could be decreased by slurring the solids in chloroform and filtering.

Appearance: Colourless solid.

Melting point: 198.8–201.9 °C.

ν (neat): 3445 (br.), 3301 (br.), 3087 (br.), 2858, 1464, 1281, 1240, 1206, 1153, 1117, 1062, 1044, 999, 971, 870, 819, 780 cm⁻¹.

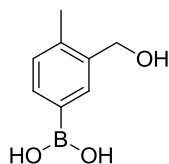
¹H NMR (400 MHz, DMSO-*d*₆): δ 7.42 (s, 1H), 7.22 (d, 1H, $J = 7.1$ Hz), 6.95 (d, 1H, $J = 7.4$ Hz), 6.76 (br. s., 1H), 4.81 (t, 1H, $J = 5.4$ Hz), 4.45 (d, 2H, $J = 5.2$ Hz), 3.92–3.83 (m, 2H), 3.82–3.74 (m, 2H), 3.07 (s, 2H), 2.87–2.79 (m, 2H), 2.22 (s, 3H).

¹³C NMR (101 MHz, DMSO-*d*₆): δ 137.8, 133.1, 132.5*, 132.0, 131.3, 128.1, 62.9, 61.9, 50.6, 18.2.

HRMS: (C₁₂H₁₈BNO₃) [M-H₂O+H]⁺ requires 218.1347, found [M-H₂O+H]⁺ 218.1347.

*Inferred from an HMBC NMR experiment.

5.4.2.1.10 (3-(Hydroxymethyl)-4-methylphenyl)boronic acid **51**



(5-(1,3,6,2-Dioxaborocan-2-yl)-2-methylphenyl)methanol (**50**, 3 g, 12.8 mmol) was suspended in diethyl ether (20 mL) and aqueous hydrochloric acid (30 mL, 0.1 M) was added, resulting in dissolution of the solids. The biphasic mixture was stirred rapidly for 2 h, by which time a precipitate had formed. This was filtered and washed with water (4×5 mL) to give the arylboronic acid as a powdery white solid (469 mg, 2.83 mmol, 22%).

Appearance: Colourless solid.

Melting point: 139.8–140.7 °C.

ν (neat): 3354, 3250 (br.), 3146, 3055, 2951, 2895, 1614, 1399, 1356, 1305, 1278, 1206, 1162 cm^{-1} .

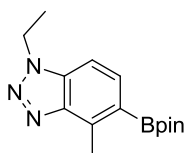
^1H NMR (400 MHz, $\text{DMSO-}d_6$): δ 7.86 (s, 2H), 7.77 (s, 1H), 7.58 (d, 1H, $J = 7.4$ Hz), 7.09 (d, 1H, $J = 7.4$ Hz), 4.96 (t, 1H, $J = 5.4$ Hz), 4.48 (d, 2H, $J = 5.4$ Hz), 2.27 (s, 3H).

^{13}C NMR (101 MHz, $\text{DMSO-}d_6$): δ 138.8, 137.4, 133.3, 132.8, 131.0*, 128.8, 61.5, 18.4.

HRMS: ($\text{C}_8\text{H}_{11}\text{BO}_3$) $[\text{M}-\text{H}_2\text{O}+\text{H}]^+$ requires 149.0768, found $[\text{M}+\text{H}]^+$ 149.0769.

*Inferred from an HMBC NMR experiment.

5.4.2.1.11 1-Ethyl-4-methyl-5-(4,4,5,5-tetramethyl-1,3,2-dioxaborolan-2-yl)-1H-benzo[d][1,2,3]triazole **52**



5-Bromo-1-ethyl-4-methyl-1H-benzo[d][1,2,3]triazole (**24**, 3.00 g, 12.5 mmol), bis(pinacolato)diboron (4.76 g, 18.7 mmol), $\text{PdCl}_2(\text{dppf})\cdot\text{DCM}$ (510 mg, 0.625 mmol) and potassium acetate (2.45 g, 25.0 mmol) were dissolved in 1,4-dioxane (60 mL) and the solution was degassed ($3 \times$ vacuum/ N_2 , N_2 -sparge). The reaction mixture was stirred at 88 °C for 17 h before being allowed to cool to room temperature.

The reaction mixture was diluted with ethyl acetate (250 mL) and filtered through celite. Water (250 mL) was added and the phases were separated. The aqueous phase was diluted with an additional portion of water (100 mL) before being extracted with ethyl acetate (100 mL). The aqueous phase was diluted again with water (100 mL) and extracted with

ethyl acetate (2 × 100 mL). The combined organic portions were washed with water (3 × 50 mL) and brine (50 mL) before being dried over magnesium sulfate.

DCM/methanol was unable to adequately separate the desired product from the desbromo side product by column chromatography, and crystallisation attempts of the purest fractions containing the boronic ester were unsuccessful. These fractions were repurified by column chromatography using a toluene/ethyl acetate solvent system (5–40% ethyl acetate in toluene), affording the product as an oil which crystallised after standing for several months (2.45 g (corr.), 8.54 mmol, 68%). To remove residual pinacol, the product was dissolved in methanol/water and the volatiles removed.²²² This procedure was repeated until the product was > 98% pure.

Appearance: White solid.

Melting point: 59.3–60.8 °C.

ν (neat): 2977, 2937, 1603, 1501, 1414, 1377, 1344, 1291, 1262, 1142, 1126, 1043, 1015, 961 cm^{-1} .

^1H NMR (400 MHz, CDCl_3): δ 7.86 (d, 1H, $J = 8.4$ Hz), 7.31 (d, 1H, $J = 8.6$ Hz), 4.68 (q, 2H, $J = 7.4$ Hz), 3.05 (s, 3H), 1.61 (t, 3H, $J = 7.3$ Hz), 1.39 (s, 12H).

^{13}C NMR (101 MHz, CDCl_3): δ 146.6, 139.7, 134.0, 133.6, 122.8*, 105.5, 83.5, 43.0, 24.8, 16.0, 14.9.

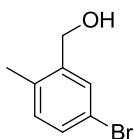
LCMS (Method A, 254 nm), $t_R = 1.23$ min, $[\text{M}+\text{H}]^+ 287.9$, > 98%.

HPLC (Method A): $t_R = 2.62$ min, 1.51 min (presumed boronic acid), > 98%.

HRMS: ($\text{C}_{15}\text{H}_{22}\text{BN}_3\text{O}_2$) $[\text{M}+\text{H}]^+$ requires 288.1878, found $[\text{M}+\text{H}]^+ 288.1869$.

*Inferred from an HMBC NMR experiment.

5.4.2.1.12 (5-Bromo-2-methylphenyl)methanol 26



5-Bromo-2-methylbenzoic acid (5.013 g, 23.31 mmol) was dissolved in THF (20 mL) and the mixture was degassed (3 × vacuum/ N_2). Borane-THF complex (28.0 mL, 28.0 mmol, 1 M) was added dropwise and after 22 h hours an addition portion was added (23.3 mL, 23.3 mmol, 1 M) before heating the solution to 40 °C. After 1 h, the reaction mixture was cooled in an ice bath and water (10 mL) was added dropwise followed by acidification with aqueous ammonium chloride to pH 5. The mixture was diluted further with water (10 mL) and the organic phase was separated. The aqueous phase was extracted with ethyl acetate

(3 × 20 mL) and the combined organic portions were washed with water (2 × 20 mL) and brine (2 × 20 mL) before being dried over magnesium sulfate. The crude product was purified by column chromatography (2–20% ethyl acetate in heptane) to give the desired compound as a colourless crystalline solid (4.497 g, 22.4 mmol, 96%).

Appearance: Colourless crystalline solid.

Melting point: 42.8–43.8 °C.

ν (neat): 3251 (br.), 2915, 2861, 1594, 1478, 1445, 1399, 1367, 1315, 1251, 1212, 1175, 1084, 1035, 994 cm^{-1} .

^1H NMR (400 MHz, CDCl_3): δ 7.54 (d, 1H, $J = 2.2$ Hz), 7.33 (dd, 1H, $J = 2.1, 8.0$ Hz), 7.04 (d, 1H, $J = 7.9$ Hz), 4.68 (d, 2H, $J = 4.9$ Hz), 2.28 (s, 3H), 1.63 (t, 1H, $J = 5.5$ Hz).

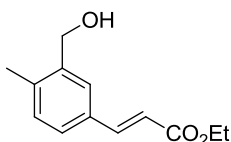
^{13}C NMR (101 MHz, CDCl_3): δ 140.8, 134.6, 131.9, 130.5, 130.0, 119.7, 62.8, 18.2.

LCMS (Method A, 254 nm), $t_R = 0.92$ min, $[\text{M}-\text{H}_2\text{O}+\text{H}]^+$ 182.8 and 184.8, > 96%.

HPLC (Method A): $t_R = 2.09$ min, > 99%.

HRMS: ($\text{C}_8\text{H}_9\text{BrO}$) $[\text{M}-\text{H}_2\text{O}+\text{H}]^+$ requires 182.9804, found $[\text{M}+\text{H}]^+$ 182.9802.

5.4.2.1.13 (*E*)-Ethyl 3-(3-(hydroxymethyl)-4-methylphenyl)acrylate **53**



DMF (8.5 mL) was added to (5-bromo-2-methylphenyl)methanol (**26**, 500 mg, 2.49 mmol), potassium carbonate (516 mg, 3.73 mmol), palladium (II) acetate (22.3 mg, 0.099 mmol) and tri(*o*-tolyl)phosphine (76 mg, 0.25 mmol) under nitrogen and the mixture was degassed (3 × vacuum/ N_2). Ethyl acrylate (0.35 mL, 3.2 mmol) was added and the reaction mixture was stirred at 110 °C for 2 h, before allowing to cool to room temperature. The cooled reaction mixture was filtered through celite and diluted with ethyl acetate to 50 mL. Water (150 mL) was added and the phases were separated. The aqueous phase was extracted with ethyl acetate (3 × 20 mL) and the combined organic portions were washed with water (3 × 20 mL) and brine (20 mL) and passed through a hydrophobic frit. The product was purified by column chromatography (7–60% ethyl acetate in heptane), affording the desired compound as a crystalline solid (432 mg, 1.96 mmol, 79%).

Appearance: Colourless solid.

Melting point: 60.2–60.4 °C.

ν (neat): 3381 (br.), 3052, 2976, 2933, 2904, 1704, 1634, 1444, 1314, 1157 cm^{-1} .

^1H NMR (400 MHz, CDCl_3): δ 7.70 (d, 1H, $J = 16.0$ Hz), 7.58 (d, 1H, $J = 1.2$ Hz), 7.39 (dd,

1H, $J = 1.5, 7.9$ Hz), 7.22 (d, 1H, $J = 7.9$ Hz), 6.45 (d, 1H, $J = 16.0$ Hz), 4.75 (d, 2H, $J = 5.7$ Hz), 4.28 (q, 2H, $J = 7.1$ Hz), 2.39 (s, 3H), 1.63 (t, 1H, $J = 5.7$ Hz), 1.36 (t, 3H, $J = 7.1$ Hz).

^{13}C NMR (101 MHz, CDCl_3): δ 167.1, 144.4, 139.3, 138.6, 132.5, 130.9, 127.4, 126.9, 117.5, 63.2, 60.4, 18.7, 14.3.

LCMS (Method A, 254 nm), $t_R = 0.95$ min, $[\text{M}+\text{H}]^+$ 221.0, > 99%.

HPLC (Method A, 215 nm): $t_R = 2.17$ min.

HRMS: ($\text{C}_{13}\text{H}_{16}\text{O}_3$) $[\text{M}+\text{H}]^+$ requires 221.1172, found $[\text{M}+\text{H}]^+$ 221.1164.

5.4.2.2 Use of Substrates in Arylation Conditions

General Procedure A (Ligand L11)

$[\text{RhCl}(\text{C}_2\text{H}_4)_2]_2$ (1.1 mg, 2.8 μmol), the naphthyl ester diene **L11** (1.9 mg, 5.7 μmol), enoate^{xviii} (578 μmol) and arylboron reagent (578 μmol) were dissolved in degassed ethanol (1.35 mL) and water (0.15 mL) before the mixture was degassed ($3 \times$ vacuum/ N_2). The reaction mixture was stirred for 30 min at 30 $^\circ\text{C}$ and sampled ($t = 0$, 10 μL of the reaction solution diluted with 1.000 mL ethanol). DIPEA (50 μL , 290 μmol) was added and the reaction mixture was stirred until stated before sampling again in the same manner. After complete consumption of the arylboron reagent, the bisaryl product was purified as stated.

General Procedure B (Ligand NBD)

$[\text{RhCl}(\text{NBD})]_2$ (6.7 mg, 15 μmol), the enoate (578 μmol) and arylboron reagent (578 μmol) were dissolved in degassed ethanol (1.35 mL) and water (0.15 mL) before the mixture was degassed ($3 \times$ vacuum/ N_2). The reaction mixture was stirred for 30 min at 30 $^\circ\text{C}$ and sampled ($t = 0$, 10 μL of the reaction solution diluted with 1.000 mL ethanol). DIPEA (50 μL , 290 μmol) was added and the reaction mixture was stirred until stated before sampling again in the same manner. After complete consumption of the arylboron reagent, the bisaryl product was purified as stated.

General Analysis (HPLC)

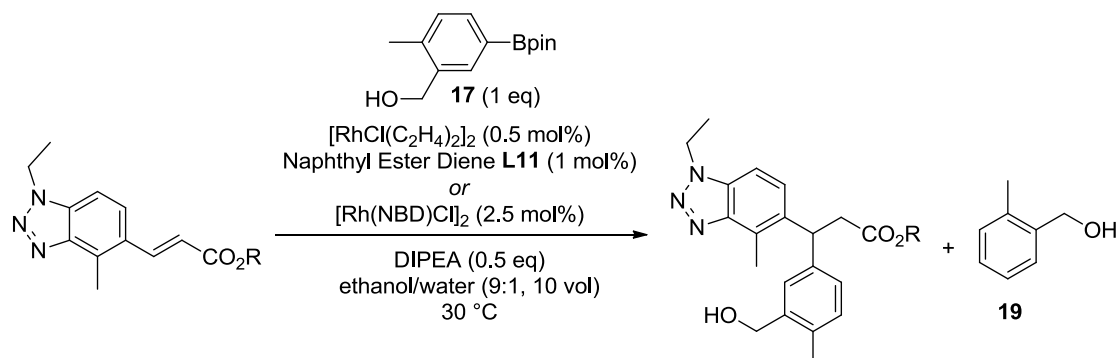
The samples taken were run consecutively on the stated HPLC systems and at a wavelength which was a stationary point in the UV spectrum of the enoate. The absolute peak area of the enoate for the sample for which the arylboron reagent had been fully consumed was divided by the absolute peak area of the enoate for the sample taken before addition of DIPEA, to

^{xviii} Liquid enoates were added as solutions in degassed ethanol in both General Procedures.

give the fraction of enoate that had not been consumed in the reaction. This value was subtracted from 1 to give the fraction of enoate that had been consumed by the reaction. Repeat sampling and analysis showed the method to be robust, with no significant variation in the calculated consumption of enoate.

Enantiomeric excesses of enantio-enriched products are stated where relevant for products isolated from Procedure A, as determined by chiral HPLC analysis.

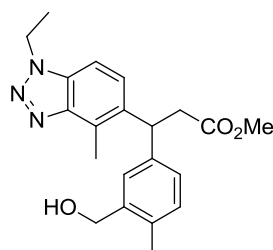
5.4.2.2.1 Effect of the Steric Bulk of the Ester Group on Reaction Selectivity (Procedures for Section 3.3.1.1)



R = Me (Table 20, page 118)

Time / h	General Procedure A		
	Enoate Peak Area	ArBpin Peak Area	ArB(OH) ₂ Peak Area
0	1240.417	964.522	356.312
64.5	55.644	34.837	16.665
0	1259.369	960.593	371.638
96	55.454	33.698	16.693

Table 68. HPLC analysis (HPLC Method B at 215 nm). Enoate at 4.42 min, ArBpin at 4.42 min, ArB(OH)₂ at 2.34 min. 96% consumption of enoate and 96% consumption of arylboron reagent.



Bisaryl product purified by MDAP Method B (185 mg, 503 μmol, 87%).

Methyl 3-(1-ethyl-4-methyl-1H-benzo[d][1,2,3]triazol-5-yl)-3-(3-(hydroxymethyl)-4-methylphenyl)propanoate

Appearance: Colourless oil.

v (neat): 3380 (br.), 2983, 2951, 2878, 1733, 1500, 1436, 1264, 1240, 1208, 1157,

1040 cm^{-1} .

^1H NMR (400 MHz, CDCl_3): δ 7.36 (d, 1H, $J = 8.6$ Hz), 7.29 (d, 1H, $J = 8.6$ Hz), 7.25 (s, 1H), 7.12–7.03 (m, 2H), 5.00 (t, 1H, $J = 8.0$ Hz), 4.68–4.58 (m, 4H), 3.58 (s, 3H), 3.17 (dd, 1H, $J = 7.6, 15.5$ Hz), 3.07 (dd, 1H, $J = 8.6, 15.5$ Hz), 2.86 (s, 3H), 2.28 (s, 3H), 2.12 (br. s., 1H), 1.59 (t, 3H, $J = 7.3$ Hz).

^{13}C NMR (101 MHz, CDCl_3): δ 172.1, 146.9, 140.7, 139.0, 136.2, 134.1, 131.1, 130.4, 128.2, 126.56, 126.53, 126.47, 106.6, 63.2, 51.7, 43.1, 41.5, 40.7, 18.1, 14.9, 13.2.

HPLC (Method B, 215 nm): $t_R = 4.58$ min, > 99%.

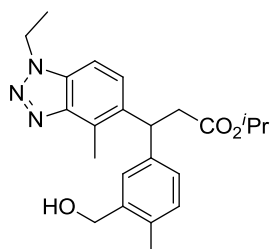
HRMS: ($\text{C}_{21}\text{H}_{25}\text{N}_3\text{O}_3$) $[\text{M}+\text{H}]^+$ requires 368.1969, found $[\text{M}+\text{H}]^+$ 368.1956.

HPLC (Method G): $t_R = 13.15$ min (major), 32.12 min (minor), 91% *ee*.

R = i Pr (Table 20, page 118)

General Procedure A				General Procedure B			
Time / h	Enoate Peak Area	ArBpin Peak Area	ArB(OH) ₂ Peak Area	Time / h	Enoate Peak Area	ArBpin Peak Area	ArB(OH) ₂ Peak Area
0	950.941	651.042	306.574	0	976.657	650.138	307.534
50.5	706.589	394.415	291.499	50.5	749.065	11.193	
0	966.517	631.191	342.515	0	983.374	616.707	348.881
118	705.276	381.284	281.592	118	765.747	11.695	1.780
126	167.073	60.715	40.859				
0	971.267	621.341	358.462				
145	99.692						

Table 69. HPLC analysis (HPLC Method A at 215 nm). Enoate at 2.45 min, ArBpin at 2.31 min, ArB(OH)₂ at 1.38 min. An additional catalyst charge was required in General Procedure A, at 120.5 h. General Procedure B was scaled to 362 μmol substrates.



Bisaryl purified by column chromatography (25–50% ethyl acetate in heptane) as a colourless oil (Procedure A: 201 mg, 508 μmol , 88%; Procedure B: 30 mg, 76 μmol , 21%).

Isopropyl 3-(1-ethyl-4-methyl-1H-benzo[*d*][1,2,3]triazol-5-yl)-3-(3-(hydroxymethyl)-4-methylphenyl)propanoate

Appearance: Colourless oil.

ν (neat): 3395 (br.), 2980, 2936, 2878, 1726, 1500, 1453, 1374, 1266, 1240, 1160, 1107, 1040 cm^{-1} .

^1H NMR (400 MHz, CDCl_3): δ 7.38 (d, 1H, $J = 8.6$ Hz), 7.30 (d, 1H, $J = 8.6$ Hz), 7.23 (s,

1H), 7.11–7.03 (m, 2H), 4.98 (t, 1H, $J = 8.1$ Hz), 4.88 (spt, 1H, $J = 6.2$ Hz), 4.69–4.58 (m, 4H), 3.11 (dd, 1H, $J = 7.4, 15.0$ Hz), 3.02 (dd, 1H, $J = 8.6, 15.0$ Hz), 2.86 (s, 3H), 2.29 (s, 3H), 1.65–1.62 (m, 1H), 1.59 (t, 3H, $J = 7.4$ Hz), 1.05 (dd, 6H, $J = 1.8, 6.3$ Hz).

^{13}C NMR (101 MHz, CDCl_3): δ 171.2, 147.0, 140.9, 138.9, 136.2, 134.2, 131.1, 130.5, 128.3, 126.8, 126.7, 126.6, 106.5, 67.8, 63.5, 43.1, 41.7, 41.3, 21.6, 18.2, 15.0, 13.3.

HPLC (Method A, 215 nm): $t_R = 2.40$ min.

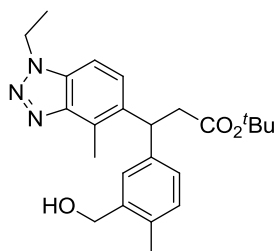
HRMS: ($\text{C}_{23}\text{H}_{29}\text{N}_3\text{O}_3$) $[\text{M}+\text{H}]^+$ requires 396.2282, found $[\text{M}+\text{H}]^+$ 396.2277.

HPLC (Method F): $t_R = 6.36$ min (major), 13.30 min (minor), 96% *ee*.

R = t Bu (Table 20, page 118)

General Procedure A				General Procedure B			
Time / h	Enoate Peak Area	ArBpin Peak Area	ArB(OH) ₂ Peak Area	Time / h	Enoate Peak Area	ArBpin Peak Area	ArB(OH) ₂ Peak Area
0	669.746	469.808	187.905	0	616.523	396.170	201.126
21.3	70.855	10.157	5.267	66	487.401		
26.3	67.160	6.103	3.549				
44	66.865						

Table 70. HPLC analysis (HPLC Method A at 215 nm). Enoate at 2.58 min, ArBpin at 2.32 min, ArB(OH)₂ at 1.39 min.



Bisaryl purified by column chromatography (30–70% ethyl acetate in heptane) followed by repeated dissolution in and removal *in vacuo* of methanol/water to decrease pinacol contamination for analysis. The product was isolated as a colourless oil (Procedure A: 184 mg, 449 μmol , 78%; Procedure B: 59 mg, 144 μmol , 25%).

***tert*-Butyl 3-(1-ethyl-4-methyl-1*H*-benzo[*d*][1,2,3]triazol-5-yl)-3-(3-(hydroxymethyl)-4-methylphenyl)propanoate**

Appearance: Colourless oil.

ν (neat): 3388 (br.), 2978, 2932, 2877, 1725, 1501, 1454, 1367, 1274, 1241, 1146, 1040 cm^{-1} .

^1H NMR (400 MHz, CDCl_3): δ 7.39 (d, 1H, $J = 8.6$ Hz), 7.30 (d, 1H, $J = 8.6$ Hz), 7.23 (s, 1H), 7.12–7.01 (m, 2H), 4.93 (t, 1H, $J = 8.2$ Hz), 4.71–4.56 (m, 4H), 3.06 (dd, 1H, $J = 7.6, 15.0$ Hz), 2.95 (dd, 1H, $J = 8.9, 15.0$ Hz), 2.85 (s, 3H), 2.29 (s, 3H), 1.67 (br. s., 1H), 1.59 (t, 3H, $J = 7.3$ Hz), 1.25 (s, 9H).

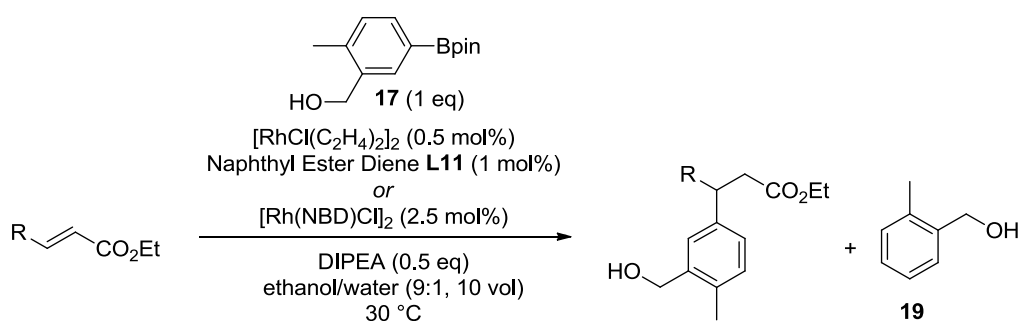
^{13}C NMR (101 MHz, CDCl_3): δ 171.0, 146.9, 141.0, 138.9, 136.4, 134.1, 131.1, 130.4, 128.2, 126.78, 126.74, 126.72, 106.4, 80.6, 63.4, 43.1, 42.3, 41.9, 27.8, 18.2, 14.9, 13.2.

HPLC (Method A): t_R = 2.492 min, > 99%.

HRMS: ($\text{C}_{24}\text{H}_{31}\text{N}_3\text{O}_3$) $[\text{M}+\text{H}]^+$ requires 410.2438, found $[\text{M}+\text{H}]^+$ 410.2420.

HPLC (Method F): t_R = 5.88 min (major), 10.75 min (minor), 94% *ee*.

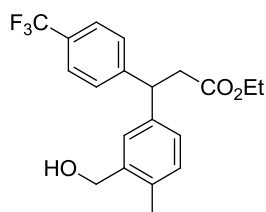
5.4.2.2.2 Effect of the Electronics of the Enoate on Reaction Selectivity (Procedures for Section 3.3.1.2)



R = phenyl, *p*-CF₃ (Table 21, page 120)

General Procedure A				General Procedure B			
Time / h	Enoate Peak Area	ArBpin Peak Area	ArB(OH) ₂ Peak Area	Time / h	Enoate Peak Area	ArBpin Peak Area	ArB(OH) ₂ Peak Area
0	955.480	524.745	237.031	0	958.882	502.398	223.074
49	44.213			49	716.628	3.105	2.752

Table 71. HPLC analysis (HPLC Method A at 210 nm). Enoate at 2.60 min, ArBpin at 2.31 min, ArB(OH)₂ at 1.36 min.



The bisaryl product was purified by column chromatography (8–60% ethyl acetate in heptane) to give a colourless oil (Procedure A: 188 mg, 513 μmol , 89%; Procedure B: 46 mg, 124 μmol , 21%).

Ethyl 3-(3-(hydroxymethyl)-4-methylphenyl)-3-(4-(trifluoromethyl)phenyl)propanoate

Appearance: Colourless oil.

ν (neat): 3427 (br.), 2982, 1732, 1619, 1325, 1162, 1112, 1069, 1018 cm^{-1} .

^1H NMR (400 MHz, CDCl_3): δ 7.54 (d, 2H, J = 8.4 Hz), 7.37 (d, 2H, J = 8.1 Hz), 7.24 (d, 1H, J = 1.5 Hz), 7.12 (d, 1H, J = 7.9 Hz), 7.07 (dd, 1H, J = 2.0, 7.9 Hz), 4.67 (d, 2H, J = 5.4 Hz), 4.60 (t, 1H, J = 8.0 Hz), 4.05 (q, 2H, J = 7.1 Hz), 3.06 (d, 2H, J = 7.9 Hz), 2.30 (s, 3H), 1.59 (t, 1H, J = 5.5 Hz), 1.14 (t, 3H, J = 7.1 Hz).

¹³C NMR (101 MHz, CDCl₃): δ 171.4, 147.7, 140.3, 139.1, 134.6, 130.7, 128.8 (q, *J* = 32.3 Hz), 128.0, 126.7, 126.6, 125.5 (q, *J* = 3.8 Hz), 124.1 (q, *J* = 271.6 Hz), 63.4, 60.6, 46.6, 40.5, 18.2, 14.1.

HPLC (Method A, 210 nm): *t_R* = 2.57 min, > 98%.

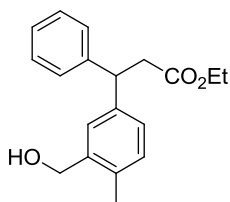
HRMS: (C₂₀H₂₁F₃O₃) [(M-H₂O)+H]⁺ requires 349.1410, found [(M-H₂O)+H]⁺ 349.1405.

HPLC (Method I): *t_R* = 5.18 min (major), 8.01 min (minor), 91% *ee*.

R = phenyl (Table 21, page 120)

General Procedure A				General Procedure B			
Time / h	Enoate Peak Area	ArBpin Peak Area	ArB(OH) ₂ Peak Area	Time / h	Enoate Peak Area	ArBpin Peak Area	ArB(OH) ₂ Peak Area
0	2653.303	2098.510	497.007	0	2525.969	1759.866	664.611
15	200.271			67	2308.743		
21	219.317						

Table 72. HPLC analysis (HPLC Method B at 210 nm). Enoate at 5.20 min, ArBpin at 4.81 min, ArB(OH)₂ at 2.34 min.



The bisaryl product was purified by column chromatography (10–40% ethyl acetate in heptane) to give a colourless oil (Procedure A: 123 mg, 412 μmol, 71%; Procedure B: 9 mg, 30 μmol, 5%).

Ethyl 3-(3-(hydroxymethyl)-4-methylphenyl)-3-phenylpropanoate

Appearance: Colourless oil.

v (neat): 3424 (br.), 2298, 1732, 1602, 1495, 1452, 1372, 1256, 1152, 1031, 893, 818, 754, 701 cm⁻¹.

¹H NMR (400 MHz, CDCl₃): δ 7.31–7.27 (m, 1H), 7.27–7.22 (m, 4H), 7.21–7.15 (m, 1H), 7.10 (app. d, 2H, *J* = 1.0 Hz), 4.65 (s, 2H), 4.54 (t, 1H, *J* = 8.0 Hz), 4.04 (q, 2H, *J* = 7.1 Hz), 3.05 (d, 2H, *J* = 8.1 Hz), 2.30 (s, 3H), 1.53 (br. s., 1H), 1.13 (t, 3H, *J* = 7.1 Hz).

¹³C NMR (101 MHz, CDCl₃): δ 171.8, 143.6, 141.3, 138.8, 134.3, 130.5, 128.6, 127.6, 127.0, 126.8, 126.5, 63.6, 60.4, 46.8, 40.8, 18.2, 14.1.

LCMS (Method A, 254 nm), *t_R* = 1.13 min, [(M-H₂O)+H]⁺ 281.0, > 96%.

HPLC (Method B, 210 nm): *t_R* = 5.29 min, > 99%.

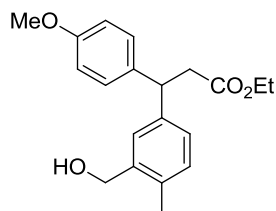
HRMS: (C₁₉H₂₂O₃) [(M-H₂O)+H]⁺ requires 281.1536, found [(M-H₂O)+H]⁺ 281.1527.

HPLC (Method E): *t_R* = 5.28 min (major), 5.70 min (minor), 92% *ee*.

R = phenyl, *p*-OMe (Table 21, page 120)

General Procedure A				General Procedure B			
Time / h	Enoate Peak Area	ArBpin Peak Area	ArB(OH) ₂ Peak Area	Time / h	Enoate Peak Area	ArBpin Peak Area	ArB(OH) ₂ Peak Area
0	2240.195	505.273	710.944	0	2192.065	466.472	679.967
76	249.918			76	2148.644		

Table 73. HPLC analysis (HPLC Method C at 215 nm). Enoate at 21.6 min, ArBpin at 20.0 min, ArB(OH)₂ at 9.2 min.



The bisaryl product was purified by column chromatography (5–47% ethyl acetate in heptane) to give a colourless oil (Procedure A: 163 mg, 496 μ mol, 86%; Procedure B: 9 mg, 27 μ mol, 5%).

Ethyl 3-(3-(hydroxymethyl)-4-methylphenyl)-3-(4-methoxyphenyl)propanoate

Appearance: Colourless oil.

ν (neat): 3447 (br.), 2932, 1732, 1610, 1512, 1463, 1372, 1249, 1179, 1035 cm^{-1} .

¹H NMR (400 MHz, CDCl₃): δ 7.22 (s, 1H), 7.16 (d, 2H, J = 8.6 Hz), 7.09 (app. s, 2H), 6.82 (d, 2H, J = 8.6 Hz), 4.65 (d, 2H, J = 4.4 Hz), 4.48 (t, 1H, J = 8.1 Hz), 4.04 (q, 2H, J = 7.1 Hz), 3.77 (s, 3H), 3.01 (d, 2H, J = 7.9 Hz), 2.30 (s, 3H), 1.59 (t, 1H, J = 5.4 Hz), 1.13 (t, 3H, J = 7.1 Hz).

¹³C NMR (101 MHz, CDCl₃): δ 171.9, 158.1, 141.7, 138.8, 135.8, 134.1, 130.5, 128.6, 126.8, 126.7, 113.9, 63.6, 60.4, 55.2, 46.0, 41.1, 18.2, 14.1.

HPLC (Method C, 215 nm): t_R = 21.12 min, > 98%.

HRMS: (C₂₀H₂₄O₄) [(M–H₂O)+H]⁺ requires 311.1642, found [(M–H₂O)+H]⁺ 311.1636.

HPLC (Method I): t_R = 6.09 min (major), 8.64 min (minor), 91% *ee*.

R = cyclohexyl (Table 21, page 120)

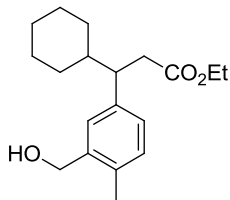
General Procedure A				General Procedure B			
Time / h	Enoate Peak Area	ArBpin Peak Area	ArB(OH) ₂ Peak Area	Time / h	Enoate Peak Area	ArBpin Peak Area	ArB(OH) ₂ Peak Area
0	2988.770	459.040	686.081	0	3117.201	453.024	710.029
67.5	241.387			67.5	2371.818		
67.5 (rpt)	237.195						

Table 74. HPLC analysis (HPLC Method C at 215 nm). Enoate at 25.8 min, ArBpin at 20.0 min, ArB(OH)₂ at 6.1 min.

The reactions were repeated:

General Procedure A				General Procedure B			
Time / h	Enoate Peak Area	ArBpin Peak Area	ArB(OH) ₂ Peak Area	Time / h	Enoate Peak Area	ArBpin Peak Area	ArB(OH) ₂ Peak Area
0	2848.513	507.098	542.841	0	2987.417	506.905	629.261
73	217.535			73	2645.005		

Table 75. HPLC analysis (HPLC Method C at 215 nm). Enoate at 25.8 min, ArBpin at 20.0 min, ArB(OH)₂ at 6.1 min. General Procedure B was scaled to 319 μ mol substrates.



The bisaryl product was purified by column chromatography (5–47% ethyl acetate in heptane) to give a colourless oil (Procedure A: 136 mg, 447 μ mol, 77%; Procedure B: 6 mg, 20 μ mol, 6%).

Ethyl 3-cyclohexyl-3-(3-(hydroxymethyl)-4-methylphenyl)propanoate

Appearance: Colourless oil.

ν (neat): 3427 (br.), 2922, 2851, 1732, 1448, 1370, 1259, 1152, 1121, 1034 cm^{-1} .

¹H NMR (400 MHz, CDCl₃): δ 7.12 (d, 1H, $J = 1.7$ Hz), 7.08 (d, 1H, $J = 7.9$ Hz), 6.98 (dd, 1H, $J = 1.7, 7.6$ Hz), 4.68 (d, 2H, $J = 5.7$ Hz), 4.04–3.90 (m, 2H), 2.90 (m, 1H), 2.78 (dd, 1H, $J = 5.7, 15.0$ Hz), 2.55 (dd, 1H, $J = 9.7, 14.9$ Hz), 2.32 (s, 3H), 1.86–1.70 (m, 2H), 1.67–1.56 (m, 3H), 1.53–1.41 (m, 2H), 1.29–1.02 (m, 3H), 1.09 (t, 3H, $J = 7.1$ Hz), 1.01–0.89 (m, 1H), 0.88–0.74 (m, 1H).

¹³C NMR (101 MHz, CDCl₃): δ 173.0, 140.8, 138.2, 133.8, 130.0, 127.6, 127.5, 63.7, 60.1, 47.8, 42.9, 38.4, 30.9, 30.8, 26.5, 26.4, 18.3, 14.1.

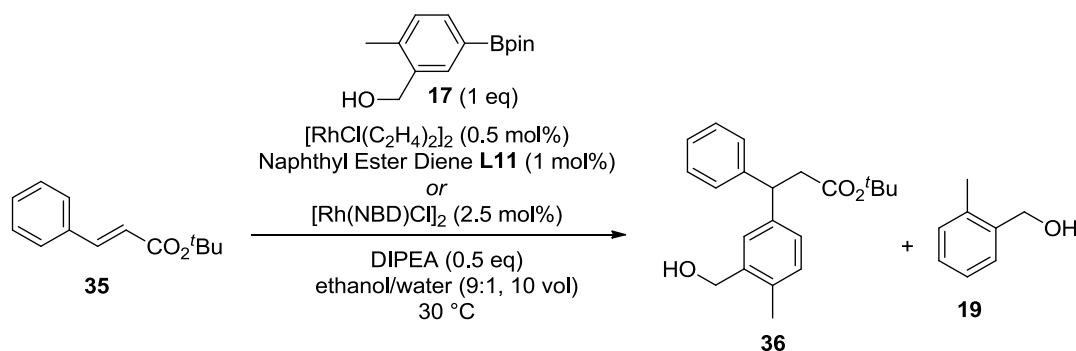
HPLC (Method C, 215 nm): $t_R = 25.1$ min, > 99%.

HRMS: (C₁₉H₂₈O₃) [(M–H₂O)+H]⁺ requires 287.2006, found [(M–H₂O)+H]⁺ 287.1999.

HPLC (Method J): $t_R = 13.35$ min (major), 16.39 min (minor), 94% *ee*.

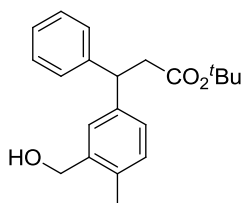
Five cyclohexyl ¹³C resonances are also reported for the related compound ethyl 3-cyclohexyl-3-phenylpropanoate,²²³ presumably resulting from restricted rotation of the cyclohexyl group.

***tert*-Butyl cinnamate with arylboron reagent 17 (Scheme 50, page 123)**



General Procedure A				General Procedure B			
Time / h	Enoate Peak Area	ArBpin Peak Area	ArB(OH) ₂ Peak Area	Time / h	Enoate Peak Area	ArBpin Peak Area	ArB(OH) ₂ Peak Area
0	2811.759	1941.770	601.365	0	2770.815	1816.911	652.944
67	220.034			67	2591.531		

Table 76. HPLC analysis (HPLC Method B at 210 nm). Enoate at 6.06 min, ArBpin at 4.81 min, ArB(OH)₂ at 2.34 min.



Bisaryl purified by column chromatography (5–50% ethyl acetate in heptane, then re-purified with 26%/31% ethyl acetate in heptane as a step gradient), however the bisaryl product was not separated from *o*-tolylmethanol under either column conditions. The yields shown are corrected for *o*-tolylmethanol, and MDAP Method C provided an analytical sample of the product (56 mg). Corrected yields of bisaryl for Procedure A: 143 mg, 438 μmol , 76%; Procedure B: 7.8 mg, 24 μmol , 4%. *o*-Tolylmethanol (58 mg, 475 μmol , 82%) was also isolated by the initial column chromatography from Procedure B.

***tert*-Butyl 3-(3-(hydroxymethyl)-4-methylphenyl)-3-phenylpropanoate**

Appearance: Colourless oil.

ν (neat): 3418 (br.), 2977, 2931, 1726, 1495, 1353, 1367, 1257, 1144 cm^{-1} .

^1H NMR (400 MHz, CDCl_3): δ 7.31–7.22 (m, 5H), 7.21–7.14 (m, 1H), 7.13–7.05 (m, 2H), 4.68–4.62 (m, 2H), 4.46 (t, 1H, $J = 8.1$ Hz), 2.96 (d, 2H, $J = 8.4$ Hz), 2.30 (s, 3H), 1.59–1.53 (m, 1H), 1.29 (s, 9H).

^{13}C NMR (101 MHz, CDCl_3): δ 171.1, 143.7, 141.5, 138.7, 134.1, 130.4, 128.4, 127.7, 127.0, 126.9, 126.4, 80.5, 63.6, 47.1, 42.1, 27.9, 18.2.

HPLC (Method B, 210 nm): $t_R = 5.93$ min, > 98%.

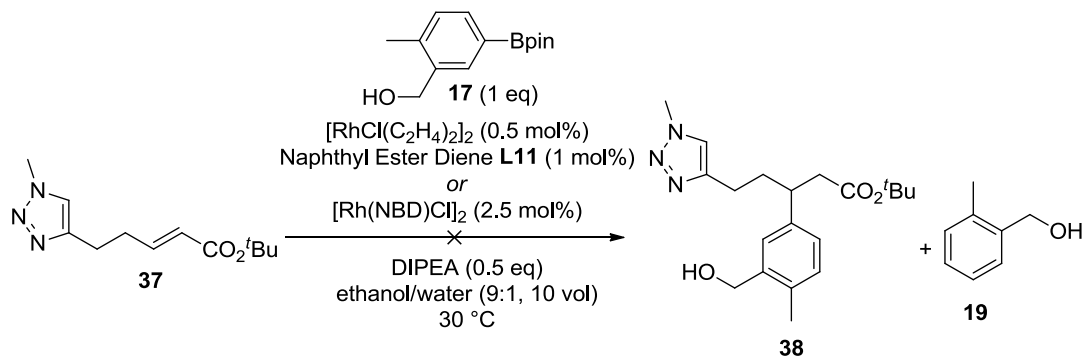
HRMS: ($\text{C}_{21}\text{H}_{26}\text{O}_3$) $[\text{M}+\text{Na}]^+$ requires 349.1774, found $[\text{M}+\text{Na}]^+$ 349.1761; $[\text{M}+\text{NH}_4]^+$

requires 344.2220, found $[M+NH_4]^+$ 344.2210.

HPLC (Method G): t_R = 5.30 min (major), 6.12 min (minor), 96% *ee*.

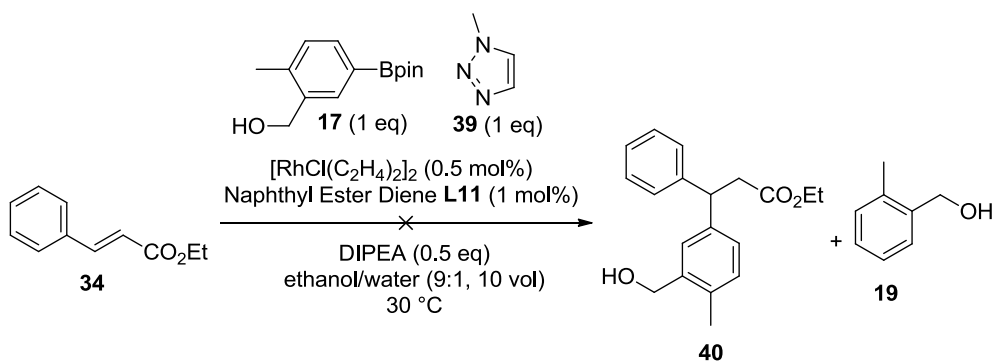
5.4.2.2.3 Effect of the Triazole on Conjugate Arylation and Deboronation (Procedures for Section 3.3.1.3)

Alkyl triazole **37** with arylboron reagent **17** (Scheme 51, page 124)



The reaction mixtures were prepared according to General Procedures A and B and both were sampled after 43 h and 94 h. Analysis by HPLC Methods A and C revealed no more than trace amounts of *o*-tolymethanol (< 2 area%) and no evidence of the conjugate arylation product **38** by comparison with an authentic sample. No notable change was observed between the reaction profiles at 43 h and 94 h and the profiles at $t = 0$.

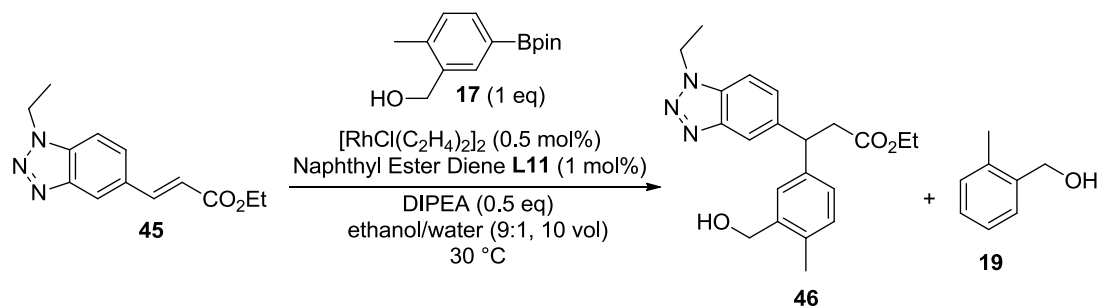
Ethyl cinnamate **34** with arylboron reagent **17** in the presence of methyl triazole **39** (Scheme 52, page 125)



The reaction mixture was prepared based on General Procedure A, modified such that 1-methyl-1*H*-1,2,3-triazole (48 mg, 578 μ mol) was added with ethyl cinnamate as a solution in degassed ethanol. The reaction mixture was sampled after 68 h and analysis by HPLC Method B revealed no evidence of the conjugate arylation product **40** and no more than a trace amount of *o*-tolymethanol (< 1 area%). No notable change was observed between the reaction profiles at 68 h and the profile at $t = 0$. Additionally, the reaction mixture was then

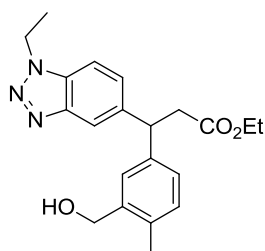
heated to 60 °C and sampled again after a further 3 h. HPLC analysis showed no notable differences compared with the earlier samples.

Analogue 45 of enoate 16, omitting *o*-methyl substitution, with arylboron reagent 17 (Scheme 54, page 126)



General Procedure A			
Time / h	Enoate Peak Area	ArBpin Peak Area	ArB(OH) ₂ Peak Area
0	1301.713	1841.429	462.308
48	1250.719	1347.377	606.009
0	1302.368	1757.770	501.401
96	1246.597	1257.462	567.798

Table 77. HPLC analysis (HPLC Method B at 210 nm). Enoate at 4.56 min, ArBpin at 4.80 min, ArB(OH)₂ at 2.33 min.



The bisaryl product, ethyl 3-(1-ethyl-1*H*-benzo[*d*][1,2,3]triazol-5-yl)-3-(3-(hydroxymethyl)-4-methylphenyl)propanoate, was partially purified from the reaction mixture by MDAP Method B, which afforded a 20:1 molar ratio of enoate substrate/conjugate arylation product. Diagnostic NMR features of the conjugate arylation product could be observed by ¹H NMR, defending its trace formation in the reaction:

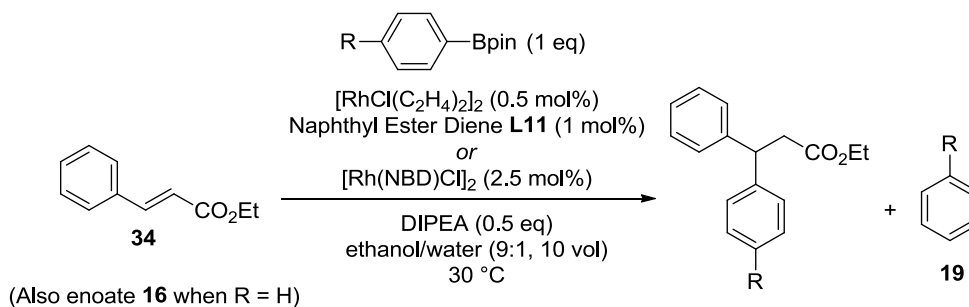
¹H NMR (400 MHz, CDCl₃): δ 7.92 (s, 1H), 7.39 (d, 1H, *J* = 8.4 Hz), 7.34 (dd, 1H, *J* = 1.5, 8.6 Hz), 7.09 (m, 2H), 4.63 (q, 2H, *J* = 7.4 Hz), 4.03 (q, 2H, *J* = 7.1 Hz), 3.14 (dd, 1H, *J* = 8.1, 15.5 Hz), 3.08 (dd, 1H, *J* = 7.6, 15.5 Hz), 2.28 (s, 3H), 2.16 (s, 1H), 1.59 (t, 3H, *J* = 7.3 Hz), 1.12 (t, 3H, *J* = 7.1 Hz).

Three proton environments could not be distinguished from the crude NMR spectrum: one proton on an aromatic ring, the proton on the tertiary alkyl carbon, and the two methylene protons of the benzylic alcohol.

Rate of consumption of arylboron reagent 17 with and without enoate 16 present (Figure 42, page 128)

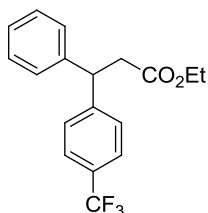
See Sections 5.4.3.2.1 and 5.4.3.2.14 for experimental procedure.

5.4.2.2.4 Effect of the Arylboron Reagent on Reaction Selectivity (Procedures for Section 3.3.1.4)



R = CF₃; enoate = ethyl cinnamate (Table 23, page 130)

Procedures A and B were followed, with > 98% consumption of the arylboron reagent achieved within 65 h in both cases. As noted in Section 3.3.1.4, trifluorotoluene and ethyl cinnamate co-eluted by HPLC.



The bisaryl product was purified by column chromatography (3–12% ethyl acetate in heptane for Procedure A, 6%/9% ethyl acetate in heptane as a step gradient for Procedure B) to give a colourless oil (Procedure A: 152 mg, 472 μmol, 82%; Procedure B: 18 mg, 56 μmol, 10%).

Ethyl 3-phenyl-3-(4-(trifluoromethyl)phenyl)propanoate

Appearance: Colourless oil.

¹H NMR (400 MHz, CDCl₃): δ 7.55 (d, 2H, *J* = 8.4 Hz), 7.37 (d, 2H, *J* = 8.1 Hz), 7.34–7.28 (m, 2H), 7.26–7.19 (m, 3H), 4.62 (t, 1H, *J* = 8.0 Hz), 4.05 (q, 2H, *J* = 7.1 Hz), 3.07 (d, 2H, *J* = 8.1 Hz), 1.13 (t, 3H, *J* = 7.1 Hz).

¹³C NMR (101 MHz, CDCl₃): δ 171.4, 147.5, 142.5, 129.0, 128.7, 128.1, 127.6, 126.9, 125.5 (q, *J* = 3.8 Hz), 122.8, 60.6, 46.9, 40.5, 14.0.

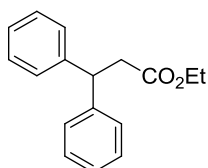
HPLC (Method H): *t_R* = 4.50 min (minor), 4.90 min (major), 89% *ee*.

NMR literature data concordant.²²⁴

R = H; enoate = ethyl cinnamate (Table 23, page 130)

General Procedure A				General Procedure B			
Time / h	Enoate Peak Area	ArBpin Peak Area	ArB(OH) ₂ Peak Area	Time / h	Enoate Peak Area	ArBpin Peak Area	ArB(OH) ₂ Peak Area
0	2878.690	939.289	383.634	0	2812.978	906.455	365.376
68.5	147.105			68.5	2506.114		

Table 78. HPLC analysis (HPLC Method B at 210 nm). Enoate at 5.19 min, ArBpin at 5.80 min, ArB(OH)₂ at 2.26 min.



The bisaryl product was purified by column chromatography (1–5% ethyl acetate in heptane) to give a colourless oil (Procedure A: 127 mg, 499 μmol, 86%; Procedure B: 18 mg, 71 μmol, 12%).

Ethyl 3,3-diphenylpropanoate

Appearance: colourless oil.

¹H NMR (400 MHz, CDCl₃): δ 7.35–7.24 (m, 8H), 7.24–7.16 (m, 2H), 4.58 (t, 1H, *J* = 8.0 Hz), 4.06 (q, 2H, *J* = 7.1 Hz), 3.08 (d, 2H, *J* = 8.1 Hz), 1.13 (t, 3H, *J* = 7.1 Hz).

¹³C NMR (101 MHz, CDCl₃): δ 171.8, 143.5, 128.5, 127.7, 126.5, 60.4, 47.1, 40.9, 14.1.

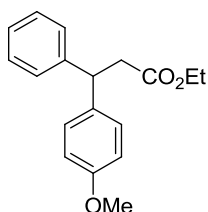
HPLC (Method B): *t_R* = 6.01 min, > 99%.

NMR literature data concordant.²²⁵

R = OMe; enoate = ethyl cinnamate (Table 23, page 130)

General Procedure A				General Procedure B			
Time / h	Enoate Peak Area	ArBpin Peak Area	ArB(OH) ₂ Peak Area	Time / h	Enoate Peak Area	ArBpin Peak Area	ArB(OH) ₂ Peak Area
0	2686.801	1777.740	158.642	0	2634.836	1751.881	159.517
43.5	362.839			43.5	2608.655	2.956	

Table 79. HPLC analysis (HPLC Method B at 210 nm). Enoate at 5.19 min, ArBpin at 5.69 min, ArB(OH)₂ at 2.56 min.



The bisaryl product was purified by column chromatography (3–20% ethyl acetate in heptane) to give a colourless oil (Procedure A: 130 mg, 457 μ mol, 79%; Procedure B: 4 mg, 14 μ mol, 2%).

Ethyl 3-(4-methoxyphenyl)-3-phenylpropanoate

Appearance: Colourless oil.

^1H NMR (400 MHz, CDCl_3): δ 7.30–7.11 (m, 7H), 6.87–6.72 (m, 2H), 4.50 (t, 1H, $J = 8.1$ Hz), 4.03 (q, 2H, $J = 7.1$ Hz), 3.76 (s, 3H), 3.01 (d, 2H, $J = 8.1$ Hz), 1.11 (t, 3H, $J = 7.1$ Hz).

^{13}C NMR (101 MHz, CDCl_3): δ 171.8, 158.1, 143.8, 135.6, 128.6, 128.5, 127.6, 126.4, 113.9, 60.4, 55.2, 46.3, 41.1, 14.1.

HPLC (Method B, 210 nm): $t_R = 5.94$ min, > 97%.

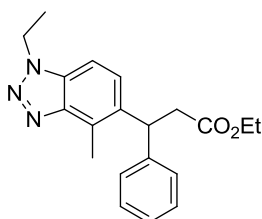
HPLC (Method G): $t_R = 5.06$ min (minor), 5.71 min (major), 92% *ee*.

NMR literature data concordant.²²⁴

R = H; enoate = pharmaceutically-relevant enoate 16 (Table 23, page 130)

General Procedure A				General Procedure B			
Time / h	Enoate Peak Area	ArBpin Peak Area	ArB(OH) ₂ Peak Area	Time / h	Enoate Peak Area	ArBpin Peak Area	ArB(OH) ₂ Peak Area
0	1542.884	1271.058	297.010	0	1510.296	1151.006	434.053
5.5	328.809	273.217	72.007	0	1532.157	1286.883	302.051
21.5	142.029	124.010	31.176	67	957.232		
46	139.449	117.366	32.905				
68.5	58.161	41.241					

Table 80. HPLC analysis (HPLC Method B at 215 nm). Enoate at 4.87 min, ArBpin at 5.80 min, ArB(OH)₂ at 2.26 min. No evidence of the deboronation product at any point in the experiment for General Procedure A. An additional catalyst charge was made in General Procedure A, at 50 h.



The bisaryl product was purified by MDAP Method B to give a colourless oil (Procedure A: 149 mg, 442 μ mol, 76%; Procedure B: 54 mg, 160 μ mol, 28%).

Ethyl 3-(1-ethyl-4-methyl-1*H*-benzo[*d*][1,2,3]triazol-5-yl)-3-phenylpropanoate

Appearance: Colourless oil.

ν (neat): 2978, 1729, 1598, 1494, 1450, 1372, 1260, 1239, 1153, 1038 cm^{-1} .

^1H NMR (400 MHz, CDCl_3): δ 7.38–7.14 (m, 7H), 5.01 (t, 1H, $J = 8.1$ Hz), 4.63 (q, 2H, $J = 7.4$ Hz), 4.02 (q, 2H, $J = 7.1$ Hz), 3.15 (dd, 1H, $J = 7.4, 15.3$ Hz), 3.05 (dd, 1H, $J = 8.6, 15.3$ Hz), 2.85 (s, 3H), 1.59 (t, 3H, $J = 7.3$ Hz), 1.09 (t, 3H, $J = 7.1$ Hz).

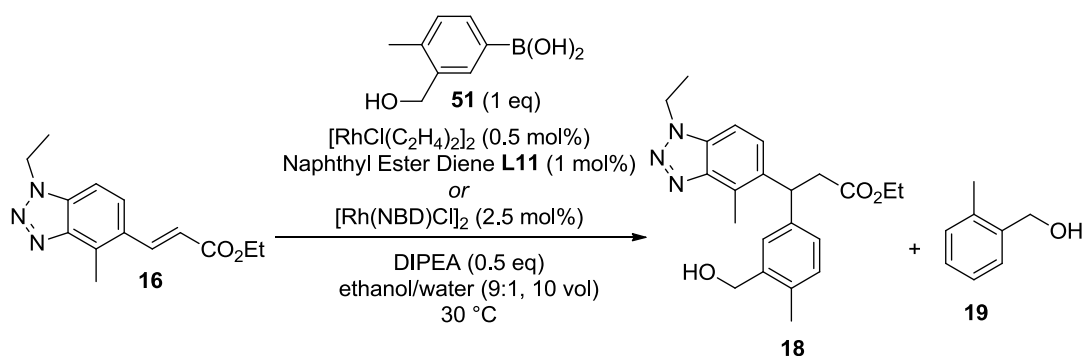
^{13}C NMR (101 MHz, CDCl_3): δ 171.6, 147.0, 143.1, 136.2, 131.2, 128.6, 128.4, 127.6, 126.6, 126.5, 106.5, 60.5, 43.2, 41.9, 41.0, 15.0, 14.1, 13.3.

HPLC (Method B, 215 nm): $t_R = 5.52$ min, > 97%.

HRMS: ($\text{C}_{20}\text{H}_{23}\text{N}_3\text{O}_2$) $[\text{M}+\text{H}]^+$ requires 338.1863, found $[\text{M}+\text{H}]^+$ 338.1853.

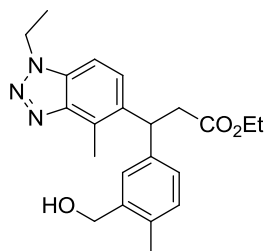
HPLC (Method F): $t_R = 6.98$ min (major), 10.49 min (minor), 94% *ee*.

Enoate **16** with arylboronic acid analogue **51** of arylboron reagent **17** (Scheme 57, 131)



General Procedure A			General Procedure B		
Time / h	Enoate Peak Area	ArB(OH) ₂ Peak Area	Time / h	Enoate Peak Area	ArB(OH) ₂ Peak Area
0	1660.470	1409.625	0	1616.613	1308.693
43	90.773		43	993.242	

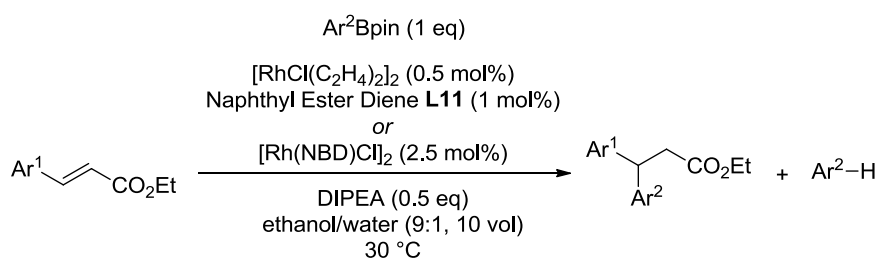
Table 81. HPLC analysis (HPLC Method C at 215 nm). Enoate at 19.8 min, ArB(OH)₂ at 9.1 min. ^1H NMR ($\text{DMSO}-d_6$) of the arylboronic acid confirmed its high purity with respect to boroxine. Crude ^1H NMR corroborated the interpretation of the HPLC results regarding the final compound distribution.



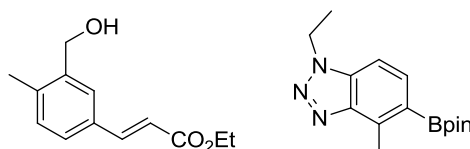
The bisaryl product **18** was isolated by column chromatography (45%/70% ethyl acetate in heptane as a step gradient) to give a colourless oil (Procedure A: 200 mg, 524 μmol , 91%, 94% *ee* (HPLC Method D3); Procedure B: 84 mg, 220 μmol , 38%).

Analytical data consistent with previous preparations (p. 184).

5.4.2.2.5 Effect of Reversing the Coupling Partners on Reaction Selectivity (Procedures for Section 3.3.1.5)

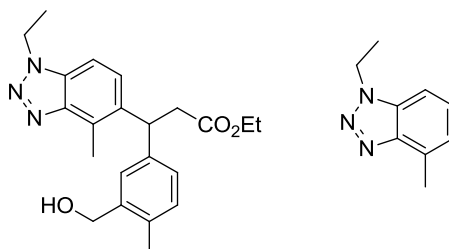


Reversal of Pharmaceutically-Relevant System (Table 24, page 133)



General Procedure A				General Procedure B			
Time / h	Enoate Peak Area	ArBpin Peak Area	ArB(OH) ₂ Peak Area	Time / h	Enoate Peak Area	ArBpin Peak Area	ArB(OH) ₂ Peak Area
0	923.767	1808.593	237.825	0	935.605	1736.481	190.810
64.5	552.971	393.121	50.686	64	876.763		1.806
72.5	548.705	385.696	52.117				
0	918.808	1779.704	244.558				
96	502.825	7.866					

Table 82. HPLC analysis (HPLC Method A at 215 nm). Enoate at 2.17 min, ArBpin at 2.60 min, ArB(OH)₂ at 1.52 min. An additional catalyst charge was made in General Procedure A, at 91.5 h. General Procedure B was scaled to 522 μmol substrates.



The bisaryl product **18** was isolated by column chromatography (Procedure A: 45%/70% ethyl acetate in heptane as a step gradient; Procedure B: 7–70% ethyl acetate in heptane) to give an oil (Procedure A: 94 mg, 247 μmol , 43%, –98% *ee* (HPLC Method D3); Procedure B: 7 mg, 18 μmol , 4%). The protodeboronation product 1-ethyl-4-methyl-1H-benzo[*d*][1,2,3]triazole was isolated from Procedure B (63 mg, 391 μmol , 75%).

Analytical data for bisaryl **18** consistent with previous preparations (p. 184).

1-Ethyl-4-methyl-1H-benzo[*d*][1,2,3]triazole

Appearance: Colourless oil.

ν (neat): 3060, 2986, 2938, 1611, 1509, 1450, 1378, 1353, 1313, 1266, 1241, 1201, 1154,

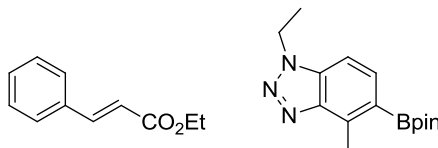
1040 cm^{-1} .

^1H NMR (400 MHz, CDCl_3): δ 7.42–7.34 (m, 2H), 7.15 (d, 1H, $J = 6.2$ Hz), 4.70 (q, 2H, $J = 7.2$ Hz), 2.83 (s, 3H), 1.64 (t, 3H, $J = 7.1$ Hz).

^{13}C NMR (101 MHz, CDCl_3): δ 146.1, 132.5, 131.0, 127.1, 123.6, 106.5, 43.2, 16.8, 15.0.

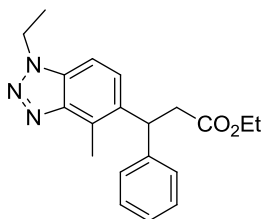
HRMS: ($\text{C}_9\text{H}_{11}\text{N}_3$) $[\text{M}+\text{H}]^+$ requires 162.1026, found $[\text{M}+\text{H}]^+$ 162.1028.

Ethyl cinnamate with benzotriazole arylboron reagent (Table 24, page 133)



General Procedure A			
Time / h	Enoate Peak Area	ArBpin Peak Area	ArB(OH) ₂ Peak Area
0	2393.598	4076.724	482.116
65	1298.977		

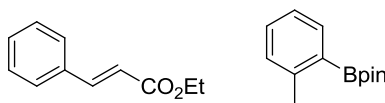
Table 83. HPLC analysis (HPLC Method B at 210 nm). Enoate at 5.18 min, ArBpin at 5.63 min, ArB(OH)₂ at 2.57 min.



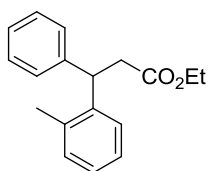
The bisaryl product was purified by MDAP Method B to give a colourless oil which contained residual ethyl cinnamate. The corrected yield of bisaryl product was 56 mg, 166 μmol , 29%, –98% *ee* (HPLC Method F).

Analytical data consistent with previous preparation (p. 255).

Ethyl cinnamate with *o*-tolylboronic acid pinacol ester (Table 24, page 133)



General Procedures A and B were followed, with HPLC analysis used to confirm consumption of the aryl boron reagent within 72 h. A portion of each reaction mixture was then concentrated and dissolved in chloroform-*d*. Quantitative ^1H NMR performed over 64 scans revealed 25:75 enoate/bisaryl for Procedure A and 87:13 enoate/bisaryl for Procedure B.



The bisaryl product, ethyl 3-phenyl-3-(*o*-tolyl)propanoate, was not isolable from the reaction mixture but could be fully accounted for from crude NMR by comparison with a literature report.²²⁴

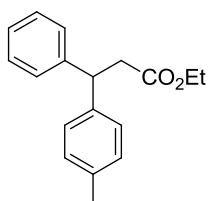
¹H NMR (400 MHz, CDCl₃): δ 7.30–7.27 (m, 1H), 7.26–7.10 (m, 8H), 4.75 (t, 1H, *J* = 8.0 Hz), 4.04 (q, 2H, *J* = 7.1 Hz), 3.03 (app. dd, 2H, *J* = 1.4, 8.0 Hz), 2.30 (s, 3H), 1.11 (t, 3H, *J* = 7.1 Hz).

Ethyl cinnamate with *p*-tolylboronic acid pinacol ester (Table 24, page 133)



General Procedure A				General Procedure B			
Time / h	Enoate Peak Area	ArBpin Peak Area	ArB(OH) ₂ Peak Area	Time / h	Enoate Peak Area	ArBpin Peak Area	ArB(OH) ₂ Peak Area
0	2592.229	799.699	212.942	0	2590.613	768.007	208.372
0	2587.849	805.505	216.276	66.5	2445.542		
66.5	183.213						
66.5	180.004						

Table 84. HPLC analysis (HPLC Method B at 210 nm). Enoate at 5.19 min, ArBpin at 6.16 min, ArB(OH)₂ at 3.02 min.



The bisaryl product was isolated by MDAP Method C to give a colourless oil (Procedure A: 117 mg, 436 μmol, 75%; Procedure B: 12 mg, 43 μmol, 7%).

Ethyl 3-phenyl-3-(*p*-tolyl)propanoate

Appearance: Colourless oil.

¹H NMR (400 MHz, CDCl₃): δ 7.32–7.02 (m, 9H), 4.51 (t, 1H, *J* = 8.0 Hz), 4.02 (q, 2H, *J* = 7.1 Hz), 3.02 (d, 2H, *J* = 8.1 Hz), 2.29 (s, 3H), 1.11 (t, 3H, *J* = 7.1 Hz).

¹³C NMR (101 MHz, CDCl₃): δ 171.8, 143.7, 140.5, 136.0, 129.2, 128.5, 127.6, 127.5, 126.4, 60.4, 46.7, 40.9, 21.0, 14.1.

HPLC (Method B, 210 nm): *t*_R = 6.35 min, > 97%.

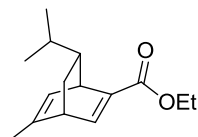
HPLC (Method H): *t*_R = 11.56 min (minor), 15.82 min (major), 92% *ee*.

NMR literature data concordant.^{86,183}

5.4.3 Influence of the Diene Ligand Structure on Selectivity for Conjugate Arylation over Protodeboronation (Procedures for Section 3.3.2)

5.4.3.1 Ligand Syntheses (Procedures for Section 3.3.2.1)

5.4.3.1.1 Ethyl 7-isopropyl-5-methylbicyclo[2.2.2]octa-2,5-diene-2-carboxylate L26



Naphthalen-2-yl 7-isopropyl-5-methylbicyclo[2.2.2]octa-2,5-diene-2-carboxylate (**L11**, 100 mg, 0.301 mmol) and sodium ethoxide (102 mg, 1.50 mmol) were dissolved in ethanol (3 mL), degassed and stirred in a microwave reactor at 100 °C for 20 min. HPLC analysis confirmed complete consumption of the naphthyl ester starting material, and so the reaction mixture was quenched with saturated ammonium chloride solution (3 mL) and partitioned between ethyl acetate and water. The aqueous phase was extracted with ethyl acetate (3 × 5 mL) and the combined organic portions were washed with water (3 × 5 mL) and brine (5 mL) and passed through a hydrophobic frit. The crude product was purified by column chromatography (0–10% ethyl acetate in heptane) to give ethyl 7-isopropyl-5-methylbicyclo[2.2.2]octa-2,5-diene-2-carboxylate as a colourless oil (68 mg, 290 μmol, 96%).

Appearance: Colourless oil.

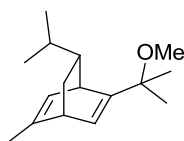
¹H NMR (400 MHz, CDCl₃): δ 7.29–7.26 (m, 1H), 5.82–5.81 (m, 1H), 4.24–4.13 (m, 2H), 4.09 (dt, 1H, *J* = 5.9, 2 Hz), 3.40–3.36 (m, 1H), 1.82 (d, 3H, *J* = 1.5 Hz), 1.60–1.54 (m, 1H), 1.29 (t, 3H, *J* = 7.1 Hz), 1.21–1.04 (m, 2H), 1.00 (d, 3H, *J* = 6.2 Hz), 1.00–0.95 (m, 1H), 0.83 (d, 3H, *J* = 6.4 Hz).

¹³C NMR (101 MHz, CDCl₃): δ 165.2, 145.6, 143.4, 141.3, 124.2, 60.1, 47.7, 44.0, 39.6, 33.8, 31.6, 21.8, 21.3, 19.0, 14.3.

HPLC (Method A): *t*_R = 2.94 min.

NMR literature data concordant.¹¹²

5.4.3.1.2 7-Isopropyl-2-(2-methoxypropan-2-yl)-5-methylbicyclo[2.2.2]octa-2,5-diene L27



The methyl ether was synthesised based on a literature procedure.¹¹⁵

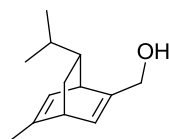
2-(7-Isopropyl-5-methylbicyclo[2.2.2]octa-2,5-dien-2-yl)propan-2-ol (**L10**, 100 mg, 0.454 mmol) was added as a solution in THF (1.5 mL) to a suspension of sodium hydride (55 mg, 60wt% dispersion in mineral oil, 1.4 mmol), which had been previously washed with heptane (2 × 1 mL), in THF (1 mL) at 0 °C. After 10 minutes, methyl iodide (0.26 mL, 4.1 mmol) was added and the reaction mixture was allowed to warm to room temperature, at which temperature it was stirred overnight before being quenched with aqueous sodium hydroxide (3 mL, 2 M). The phases were separated and the aqueous phase was extracted with diethyl ether (3 × 2 mL). The combined organic portions were washed with water (3 × 2 mL) and brine (2 mL) before drying over magnesium sulfate. The crude product was purified by column chromatography (5–20% ethyl acetate in heptane) to give a portion of 7 isopropyl-2-(2-methoxypropan-2-yl)-5-methylbicyclo[2.2.2]octa-2,5-diene in high purity (41 mg, 175 μmol, 39%) and an additional portion in approximately 90 mol% purity (total yield 77 mg, 72%).

¹H NMR (400 MHz, CDCl₃): δ 6.04 (dd, 1H, *J* = 2.0, 6.2 Hz), 5.76 (quind, 1H, *J* = 1.6, 5.9 Hz), 3.66 (td, 1H, *J* = 1.8, 6.1 Hz), 3.17 (qd, 1H, *J* = 2.3, 5.2 Hz), 2.98 (s, 3H), 1.81 (d, 3H, *J* = 1.5 Hz), 1.55 (ddd, 1H, *J* = 3.0, 8.4, 11.4 Hz), 1.28 (s, 3H), 1.26 (s, 3H), 1.16–1.02 (m, 2H), 0.97 (d, 3H, *J* = 6.1 Hz), 0.89 (ddd, 1H, *J* = 2.4, 4.5, 11.3 Hz), 0.81 (d, 3H, *J* = 5.9 Hz).

¹³C NMR (101 MHz, CDCl₃): δ 153.2, 144.9, 128.7, 124.1, 75.7, 50.8, 48.3, 43.1, 39.9, 34.0, 32.8, 26.8, 22.9, 21.9, 21.5, 19.0.

NMR literature data concordant.¹¹⁵

5.4.3.1.3 (7-Isopropyl-5-methylbicyclo[2.2.2]octa-2,5-dien-2-yl)methanol L28



Naphthalen-2-yl 7-isopropyl-5-methylbicyclo[2.2.2]octa-2,5-diene-2-carboxylate (**L11**, 500 mg, 1.50 mmol) was dissolved in dry DCM (7.5 mL) in a heat gun-dried flask and the

solution was cooled to 0 °C. DIBAL (3.0 mL, 1 M in hexanes, 3.0 mmol) was added dropwise and the mixture was stirred for 2.5 h at 0 °C before being quenched with water (10 mL). Aqueous hydrochloric acid (6 mL, 1 M) was added to disperse the solids and the phases were separated. The aqueous phase was extracted with diethyl ether (3 × 10 mL) and the combined organic portions were washed with half saturated aqueous tripotassium phosphate (3 × 10 mL), water (3 × 10 mL) and brine (10 mL) and passed through a hydrophobic frit. The crude product was purified by column chromatography (DCM) to afford (7-isopropyl-5-methylbicyclo[2.2.2]octa-2,5-dien-2-yl)methanol as a colourless oil (142 mg, 738 μmol, 49%).

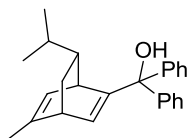
Appearance: Colourless oil.

¹H NMR (400 MHz, CDCl₃): δ 6.10 (dd, 1H, *J* = 1.6, 6.0 Hz), 5.76 (quind, 1H, *J* = 1.4, 5.9 Hz), 4.19 (d, 2H, *J* = 4.7 Hz), 3.43 (td, 1H, *J* = 1.8, 6.0 Hz), 3.21 (qd, 1H, *J* = 2.5, 5.5 Hz), 1.83 (d, 3H, *J* = 1.7 Hz), 1.58 (ddd, 1H, *J* = 3.0, 8.5, 11.2 Hz), 1.29 (t, 1H, *J* = 5.9 Hz), 1.19–1.02 (m, 2H), 0.95 (d, 3H, *J* = 6.2 Hz), 0.90 (ddd, 1H, *J* = 2.2, 4.6, 11.4 Hz), 0.82 (d, 3H, *J* = 6.4 Hz).

¹³C NMR (101 MHz, CDCl₃): δ 149.5, 145.8, 128.3, 123.4, 63.6, 48.1, 43.0, 41.6, 33.8, 32.9, 21.9, 21.5, 19.1.

NMR literature data concordant.¹¹⁵

5.4.3.1.4 (7-Isopropyl-5-methylbicyclo[2.2.2]octa-2,5-dien-2-yl) diphenylmethanol L29



Naphthalen-2-yl 7-isopropyl-5-methylbicyclo[2.2.2]octa-2,5-diene-2-carboxylate (**L11**, 400 mg, 1.20 mmol) was dissolved in THF (10 mL) in a heat gun-dried flask and the solution was cooled to -78 °C. Phenylmagnesium bromide (1.20 mL, 3 M in diethyl ether, 3.61 mmol) was added dropwise, and after 2 h the mixture was allowed to warm to room temperature. The reaction mixture was quenched with water (10 mL) after a further 3 h and extracted with ethyl acetate (3 × 10 mL). The combined organic portions were washed with water (3 × 10 mL) and brine (10 mL) and then passed through a hydrophobic frit. The crude product was purified by column chromatography (2–18% ethyl acetate in heptane) to afford (7-isopropyl-5-methylbicyclo[2.2.2]octa-2,5-dien-2-yl)diphenylmethanol as a white fluffy solid (266 mg, 772 μmol, 64%).

Appearance: Colourless solid.

Melting point: 159.9–160.9 °C.

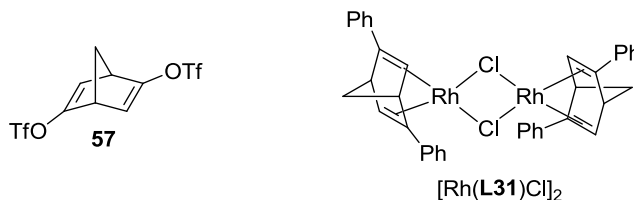
ν (neat): 3479, 3063, 2962, 2944, 2913, 2868, 1667, 1597, 1446, 1320, 1238, 1228, 1188, 1095, 1016, 1004 cm^{-1} .

^1H NMR (400 MHz, CDCl_3): δ 7.84–7.74 (m, 2H), 7.45 (s, 1H), 7.30–7.21 (m, 1H), 7.19–7.09 (m, 2H), 7.03–6.85 (m, 5H), 6.27 (d, 1H, $J = 6.9$ Hz), 3.61 (dd, 1H, $J = 2.2, 6.9$ Hz), 2.98 (d, 1H, $J = 2.0$ Hz), 2.40 (m, 1H), 2.06–1.97 (m, 1H), 1.92 (ddt, 1H, $J = 2.0, 3.8, 9.4$ Hz), 1.67 (d, 3H, $J = 1.7$ Hz), 1.31–1.21 (m, 1H), 1.12 (td, 1H, $J = 3.6, 12.6$ Hz), 1.02 (d, 3H, $J = 6.6$ Hz), 0.91 (d, 3H, $J = 6.6$ Hz)

^{13}C NMR (101 MHz, CDCl_3): δ 199.1, 140.6, 139.2, 135.3, 132.0, 129.5, 129.2, 128.0, 127.5, 126.6, 124.4, 98.8, 56.3, 45.3, 39.2, 39.1, 32.7, 32.6, 21.6, 21.3, 20.7.

UPLC (LCMS Method A): $t_R = 1.53$ min, > 95%.

5.4.3.1.5 2,5-Diphenylbicyclo[2.2.1]hepta-2,5-diene L31



The bistriflate intermediate and $[\text{Rh}(\text{Ph-NBD})\text{Cl}]_2$ were prepared based on a literature procedure.¹¹⁷

Bicyclo[2.2.1]hepta-2,5-diene-2,5-diyl bis(trifluoromethanesulfonate) 57

(*R,R*)-Bicyclo[2.2.1]heptane-2,5-dione (470 mg, 3.79 mmol) and 1,1,1-trifluoro-*N*-(pyridin-2-yl)-*N*-((trifluoromethyl)sulfonyl)methanesulfonamide (3.23 g, 9.02 mmol) were dissolved in THF (11 mL) and the solution was cooled to -78 °C. KHMDS (17.4 mL, 0.5 M in toluene, 8.71 mmol) was added very slowly, maintaining a temperature below -70 °C. The mixture was stirred for 1 h at -78 °C before being quenched with saturated aqueous sodium hydrogen carbonate (9 mL) and allowed to warm to room temperature. The layers were separated and the aqueous layer was extracted with heptane (3×10 mL). The combined organic portions were washed with aqueous sodium hydroxide (7×5 mL, 1 M), water (10 mL) and brine (10 mL) before being dried over potassium carbonate. Column chromatography (1–7% ethyl acetate in heptane) afforded bicyclo[2.2.1]hepta-2,5-diene-2,5-diyl bis(trifluoromethanesulfonate) as a colourless oil (823 mg, 2.12 mmol, 56%). The oil was stored at -18 °C.

Appearance: Colourless oil.

^1H NMR (400 MHz, CDCl_3): δ 6.53–6.51 (m, 2H), 3.55–3.53 (m, 2H), 2.64–2.63 (m, 2H).

^{13}C NMR (101 MHz, CDCl_3): δ 168.2, 123.7, 118.5 (q, $J = 321$ Hz), 73.1, 50.3.

NMR literature data concordant.¹¹⁷

2,5-Diphenylbicyclo[2.2.1]hepta-2,5-diene rhodium complex, $[\text{Rh}(\text{Ph-NBD})\text{Cl}]_2$

Bicyclo[2.2.1]hepta-2,5-diene-2,5-diyl bis(trifluoromethanesulfonate) (**57**, 200 mg, 0.515 mmol) and $\text{Fe}(\text{acac})_3$ (9.1 mg, 26 μmol) were dissolved in THF (5 mL), NMP (260 μL , 2.7 mmol) was added and the solution was cooled to 0 °C. Phenyl magnesium bromide (0.69 mL, 3 M in diethyl ether, 2.1 mmol) was added dropwise to the solution, with the temperature maintained between 0 and 1 °C throughout the addition. The mixture was stirred for an additional 5 min at 0 °C before being quenched with saturated aqueous ammonium chloride (1 mL) and diluted with water (2 mL). The phases were separated and the aqueous phase was extracted with pentane (3×2 mL). The combined organic portions were washed with water (3×2 mL) and brine (2 mL) and dried over potassium carbonate. The organics were passed through a silica plug and eluted with pentane.

The pentane solution was diluted with toluene (5 mL) and sparged with nitrogen before addition of $[\text{RhCl}(\text{C}_2\text{H}_4)_2]_2$ (100 mg, 0.258 mmol). The mixture was stirred for 2 h under a sweep of nitrogen before the complex was purified by column chromatography (10–80% DCM in heptane) to afford $[\text{Rh}(\text{Ph-NBD})\text{Cl}]_2$ as a red-orange solid (40 mg, 52 μmol , 20%).

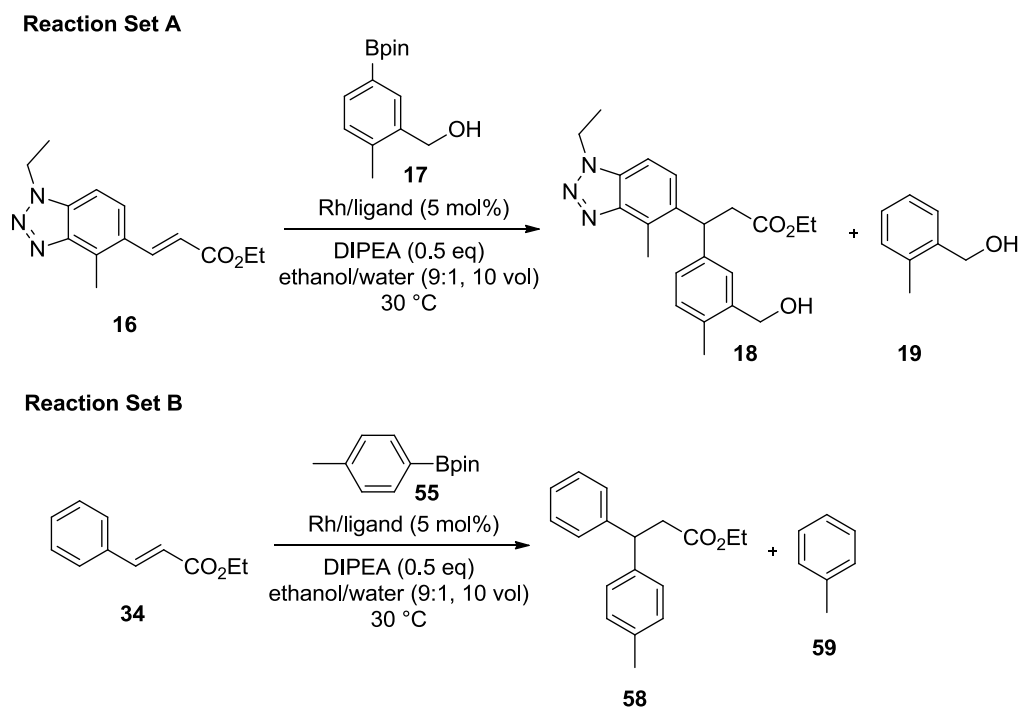
Appearance: Red solid.

^1H NMR (400 MHz, CDCl_3): δ 7.55–7.49 (m, 8H), 7.40–7.33 (m, 12H), 4.21 (m, 4H), 3.67 (m, 4H), 1.35 (s, 4H).

^{13}C NMR (101 MHz, CDCl_3): δ 138.6, 128.2, 127.8, 127.2, 65.1 (d, $J = 10.7$ Hz), 57.9 (d, $J = 6.9$ Hz), 53.0 (d, $J = 3.1$ Hz), 41.3 (d, $J = 10.7$ Hz).

NMR literature data concordant.¹¹⁷

5.4.3.2 Comparative Analysis of the Selectivity for Conjugate Arylation over Protodeboronation Afforded by Ligands (Procedures for Section 3.3.2.2)



General Procedure

A solution of enoate (578 μmol) and arylboron reagent (578 μmol) in degassed ethanol/water (1.5 mL, 9:1 ethanol/water) was charged to an Integrity 10 reaction tube containing $[\text{RhCl}(\text{diene})]_2$ (14 μmol) or $[\text{RhCl}(\text{C}_2\text{H}_4)_2]_2$ (5.6 mg, 14 μmol) and a diene (29 μmol) where required. If the diene was a liquid, it was charged with the substrate solution. The reaction mixture was degassed ($3 \times \text{vacuum}/\text{N}_2$) and stirred in an Integrity 10 Reaction Station with Amigo Workstation under nitrogen at 30 °C for 30 minutes before addition of DIPEA (50 μL , 290 μmol).

The first sample (50 μL) was taken immediately before addition of DIPEA and then according to the results tables below over a 12 h period. Samples were quenched into 1:1 acetonitrile/water with 0.05% trifluoroacetic acid (1 mL) and washed in with ethanol (200 μL). In the case of Reaction Set B (ethyl cinnamate **34** and *p*-tolylboronic acid pinacol ester **55**), the analytical samples were analysed by HPLC Method B with a 0.2 μL injection volume, recording at wavelengths 210 nm and 215 nm. In the case of Reaction Set A (pharmaceutically-relevant enoate **16** and arylboron reagent **17**), the analytical samples were further diluted (5 fold) before analysing by HPLC Method C at 215 nm. For Reaction Set A, the enantiomeric excess of the bisaryl product was determined by HPLC Method D3.

Relative Response Factors and Calculations

The relative HPLC response factors for the arylboronic acid pinacol esters and the arylboronic acids generated under the HPLC conditions could be reasonably approximated to the same value. Relative responses were determined for both starting materials and both products in each Reaction Set, relative to the enoate. Standard solutions were prepared in acetonitrile/water (1:1 v/v) with 0.05% trifluoroacetic acid to a concentration of approximately 1 mg mL⁻¹ for each compound.

The molar absorption, k_x , of compound **X** relative to the enoate was calculated as:

$$k_x = \frac{Amount_x}{Area_x} \times \frac{Area_{enoate}}{Amount_{enoate}}$$

Equation 9

where $Amount_x$ is the relative molar amount of compound **X** and $Area_x$ is the HPLC peak area arising from compound **X**.

Reaction Set A

Compound	Standard Solution 1		Standard Solution 2	
	Amount / μ mol	Mass / mg	Amount / μ mol	Mass / mg
Enoate 16	118.9	30.84	74.62	19.35
ArBpin 17	117.0	29.02	91.85	22.79
Bisaryl 18	110.1	42.00	96.37	36.76
Desboron 19	81.0	9.90	117.6	14.37

Table 85. 1:1 Standard solutions prepared in acetonitrile/water with 0.05% trifluoroacetic acid. Mass of bisaryl 18 was corrected for residual solvents using mesitylene as an NMR standard.

HPLC Sample	Enoate 16		Arylboron Reagent 17		Bisaryl 18		Desboron 19	
	19.7 min Area	20.0 min Area	9.1 min Area	k_{17}	19.2 min Area	k_{18}	13.1 min Area	k_{19}
Solution 1, Vial 1	2071.284	64.35	1671.512	1.17	10008.957	0.19	1279.435	1.10
Solution 1, Vial 2	997.862	9.382	811.859	1.19	4911.612	0.19	618.138	1.10
Solution 1, Vial 1	2076.734	32.902	1736.561	1.15	10019.288	0.19	1283.132	1.10
Solution 1, Vial 2	996.038		838.645	1.17	4906.409	0.19	620.157	1.09
Solution 2, Vial 1	1321.441	26.483	1352.651	1.18	8967.985	0.19	1828.458	1.14
Solution 2, Vial 2	660.176		687.46	1.18	4535.841	0.19	928.099	1.12
Solution 2, Vial 1	1319.851	25.648	1351.211	1.18	8954.345	0.19	1836.242	1.13
Solution 2, Vial 2	657.802		682.088	1.19	4545.555	0.19	932.206	1.11
<i>Average</i>	$k_{16} = 1$		1.18		0.19		1.11	

Table 86. HPLC Area (Method C, 215 nm) and calculated response factors for 16, 17, 18 and 19 relative to the enoate 16. Relative response factors relevant for Sections 5.4.3.2.1, 5.4.3.2.2, 5.4.3.2.3, 5.4.3.2.4, 5.4.3.2.5, 5.4.3.2.9, 5.4.3.2.10, 5.4.3.2.11.

HPLC Sample	Enoate 16	Arylboron	Reagent 17	Bisaryl 18		Desboron 19		
	20.1 min Area	20.4 min Area	9.3 min Area	k_{17}	19.6 min Area	k_{18}	13.6 min Area	k_{19}
Solution 1, Vial 1	2057.472		1992.2	1.02	10201.063	0.19	1299.789	1.08
Solution 1, Vial 2	2057.182	30.28	1996.146	1.00	10182.915	0.19	1294.308	1.08
Solution 2, Vial 1	1270.419		1570.46	1.00	8867.36	0.19	1845.089	1.09
Solution 2, Vial 2	1287.406	19.276	1603.978	0.98	8941.578	0.19	1867.514	1.09
<i>Average</i>	$k_{16} = 1$			1.00		0.19		1.08

Table 87. HPLC Area (Method C, 215 nm) and calculated response factors for 16, 17, 18 and 19 relative to the enoate 16. Relative response factors relevant for Sections 5.4.3.2.6, 5.4.3.2.7, 5.4.3.2.8, 5.4.3.2.12, 5.4.3.2.13, 5.4.3.2.14. (Servicing of HPLC Method C had resulted in different retention times and response factors.)

Reaction Set B

Compound	Standard Solution	
	Amount / μmol	Mass / mg
Enoate 34	96.47	17.00
ArBpin 55	99.49	21.70
Bisaryl 58	102.7	27.57
Desboron 59	103.6	9.55

Table 88. 1:1 Standard solutions prepared in acetonitrile/water with 0.05% trifluoroacetic acid.

HPLC Sample	Enoate 34	Arylboron Reagent 55		k_{55}	Bisaryl 58	k_{58}	Desboron 59	
	5.26 min Area	6.25 min Area	3.06 min Area		6.43 min Area		4.76 min Area	k_{59}
Vial 1	2807.644	39.882	1161.978	2.41	2842.672	1.05	1165.823	2.59
Vial 1	2851.363	39.346	1163.355	2.45	2845.396	1.07	1162.144	2.64
Vial 2	2797.905	40.606	1154.266	2.41	2833.464	1.05	1145.996	2.62
Vial 2	2793.268	39.766	1161.259	2.40	2840.97	1.05	1147.653	2.61
<i>Average</i>	$k_{34} = 1$			2.42		1.05		2.62

Table 89. HPLC Area (Method B, 210 nm and 220 nm (bisaryl)) and calculated response factors for 55, 58 and 59 relative to the enoate 34. Relative response factors relevant for Sections 5.4.3.2.1, 5.4.3.2.2, 5.4.3.2.3, 5.4.3.2.4, 5.4.3.2.5, 5.4.3.2.10, 5.4.3.2.11.

Compound	Standard Solution 1		Standard Solution 2	
	Amount / μmol	Mass / mg	Amount / μmol	Mass / mg
Enoate 34	111.7	19.68	131.0	23.08
ArBpin 55	111.0	24.21	71.62	15.62
Bisaryl 58	77.40	20.77	85.71	23.00
Desboron 59	98.22	9.05	148.4	13.67

Table 90. 1:1 Standard solutions prepared in acetonitrile/water with 0.05% trifluoroacetic acid.

HPLC Sample	Enoate 34	Arylboron Reagent 55		k_{55}	Bisaryl 58	k_{58}	Desboron 59	
	5.26 min Area	6.25 min Area	3.06 min Area		6.43 min Area		4.76 min Area	k_{59}
Solution 1, Vial 1	3595.162	789.48	670.217	2.45	2391.399	1.04	1596.613	1.98
Solution 1, Vial 2	1113.705	30.505	424.017	2.44	740.268	1.04	466.991	2.10
Solution 1, Vial 3	3570.955	163.499	1321.758	2.39	2376.71	1.04	1543.188	2.04
Solution 1, Vial 3	3506.582	160.076	1310.733	2.37	2335.236	1.04	1530.027	2.02
Solution 2, Vial 1	4095.426	475.279	452.952	2.41	2580.344	1.04	2321.818	2.00
Solution 2, Vial 2	1673.144	42.075	349.882	2.33	1051.555	1.04	898.394	2.11
Solution 2, Vial 3	4187.629	82.376	889.014	2.36	2636.246	1.04	2338.319	2.03
Solution 2, Vial 3	4169.609	82.974	893.242	2.34	2632.282	1.04	2355.893	2.00
<i>Average</i>	$k_{34} = 1$			2.39		1.04		2.03

Table 91. HPLC Area (Method B, 210 nm and 220 nm (bisaryl)) and calculated response factors for 55, 58 and 59 relative to the enoate 34. Relative response factors relevant for Sections 5.4.3.2.6, 5.4.3.2.7, 5.4.3.2.8, 5.4.3.2.9, 5.4.3.2.12, 5.4.3.2.13.

Calculations

The ratios of conjugate arylation product to protodeboronation product were calculated as:

Relative molar amount of bisaryl product =

$$100 \times \frac{k_{\text{bisaryl}} \times \text{Area}_{\text{bisaryl}}}{k_{\text{bisaryl}} \times \text{Area}_{\text{bisaryl}} + k_{\text{desboron}} \times \text{Area}_{\text{desboron}}}$$

Equation 10

Relative molar amount of protodeboronation product =

$$100 \times \frac{k_{\text{desboron}} \times \text{Area}_{\text{desboron}}}{k_{\text{bisaryl}} \times \text{Area}_{\text{bisaryl}} + k_{\text{desboron}} \times \text{Area}_{\text{desboron}}}$$

Equation 11

The reaction compositions were calculated by assuming that the enoate was either transformed into the bisaryl product or remained unchanged. The molar amounts of the four species of interest were determined relative to the enoate and then scaled relative to the sum of the enoate and the bisaryl product to give the molar equivalents of the species relative to the enoate at $t = 0$. Using the protodeboronation product as an example, where $\text{Amount}_{\text{Rel,Des}}$ is the molar amount of protodeboronation product relative to the molar amount of enoate at any given time and $\text{Amount}_{\text{Rel,Bis}}$ is the amount of bisaryl product relative to the enoate at that time, the molar equivalents of protodeboronation product relative to the enoate at $t = 0$ was calculated according to:

Molar amount of protodeboronation product relative to enoate at any given time:

$$\text{Amount}_{\text{Rel,Des}} = k_{\text{desboron}} \times \frac{\text{Area}_{\text{desboron}}}{\text{Area}_{\text{enoate}}}$$

Equation 12

Molar amount of bisaryl product relative to enoate at any given time:

$$\text{Amount}_{\text{Rel,Bis}} = k_{\text{bisaryl}} \times \frac{\text{Area}_{\text{bisaryl}}}{\text{Area}_{\text{enoate}}}$$

Equation 13

Molar equivalents of protodeboronation product at any given time relative to the enoate at $t = 0$:

$$\text{Mol}_{\text{desboron}} = \frac{\text{Amount}_{\text{Rel,Des}}}{1 + \text{Amount}_{\text{Rel,Bis}}}$$

Equation 14

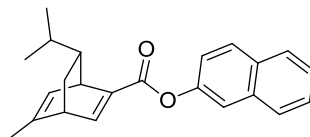
A “discrepancy” for the reaction composition was also calculated to give an indication of the precision afforded by the method, and to reveal if any other species were being formed other than the four being monitored. In the case of Reaction Set B, the discrepancy is sometimes caused as a result of the evaporation of the protodeboronation product toluene from the samples and/or reaction mixtures after extended lengths of time; when this applies, it is obvious from the calculated reaction compositions. Where Mol_Y is the molar equivalents of compound **Y** at any given time relative to the enoate at $t = 0$, the discrepancy was calculated as:

$$Discrepancy = Mol_{enoate} - (Mol_{arylboron} + Mol_{desboron})$$

Equation 15

which would equal zero for an idealised system.

5.4.3.2.1 Diene L11 (Entry 1, Table 25, page 140)



Reaction Set A

Time / min	HPLC Peak Area				
	Enoate	ArBpin	ArB(OH) ₂	Bisaryl	Desboron
0	1189.624		1007.549	10.834	
5	973.517		792.331	1127.753	
10	877.489		704.946	1760.790	
20	722.834		570.301	2678.864	
40	537.260		417.709	3778.017	14.373
60	430.182		309.605	4462.569	16.242
120	274.413		188.795	5311.334	19.733
240	172.038		48.439	6028.623	28.999
360	138.325		27.716	6241.619	31.474
720	121.474		18.293	6555.696	36.911

Table 92. HPLC Peak Area data (Method C, 215 nm) for Reaction Set A with diene L11. Enoate 16 at 19.7 min, arylboron reagent 17 at 20.0 min (ArBpin) and 9.1 min (ArB(OH)₂), bisaryl 18 at 19.2 min, *o*-tolylmethanol 19 at 13.1 min.

Time / min	Calculated Reaction Composition				Discrepancy	Product Ratio	
	Enoate	Ar[B]	Bisaryl	Desboron		Bisaryl	Desboron
0	100	100	0.2	0	0.3		
5	82	79	18	0	3.4	100	0
10	72	69	28	0	3.9	100	0
20	59	55	41	0	4.2	100	0
40	43	39	57	1	2.4	98	2
60	34	29	66	1	3.7	98	2
120	21	17	79	2	2.4	98	2
240	13	4	87	2	6.3	97	3
360	10	2	90	3	5.4	97	3
720	9	2	91	3	4.3	97	3

Table 93. Interpretation of HPLC data for Reaction Set A with diene L11.

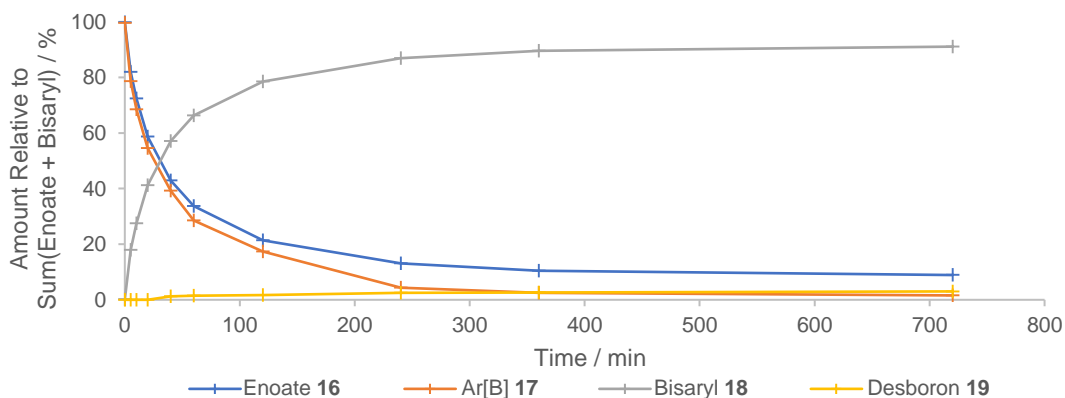
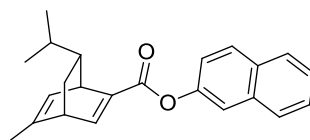


Figure 61. Calculated reaction composition over time.

Bisaryl 18: 94% *ee* (predominantly (*S*)-18).



Reaction Set B

Time / min	HPLC Peak Area				
	Enoate	ArBpin	ArB(OH) ₂	Bisaryl	Desboron
0	828.943	3.371	335.023	6.886	
5	613.588	2.267	232.147	197.983	8.149
10	498.767	2.041	181.253	420.843	15.482
20	293.198		85.242	691.829	25.475
40	148.938		14.303	796.381	30.590
60	136.296		3.916	808.964	37.610
120	119.803			797.446	43.756
240	109.071			737.423	38.455
360	112.175			743.876	32.181
720	124.804			824.789	39.316

Table 94. HPLC Peak Area data (Method B, 210 and 220 nm (bisaryl)) for Reaction Set B with diene L11. Ethyl cinnamate 34 at 5.26 min, arylboron reagent 55 at 6.25 min (ArBpin) and 3.06 min (ArB(OH)₂), bisaryl 58 at 6.43 min, toluene 59 at 4.76 min.

Time / min	Calculated Reaction Composition				Discrepancy	Product Ratio	
	Enoate	Ar[B]	Bisaryl	Desboron		Bisaryl	Desboron
0	99	98	0.9	0	1.3		
5	75	69	25	3	3.1	91	9
10	53	47	47	4	1.6	92	8
20	29	20	71	7	2.0	92	8
40	15	3	85	8	3.5	91	9
60	14	1	86	10	2.9	90	10
120	12	0	88	12	0.6	88	12
240	12	0	88	11	1.0	89	11
360	13	0	87	9	3.1	90	10
720	13	0	87	10	2.2	89	11

Table 95. Interpretation of HPLC data for Reaction Set B with diene L11.

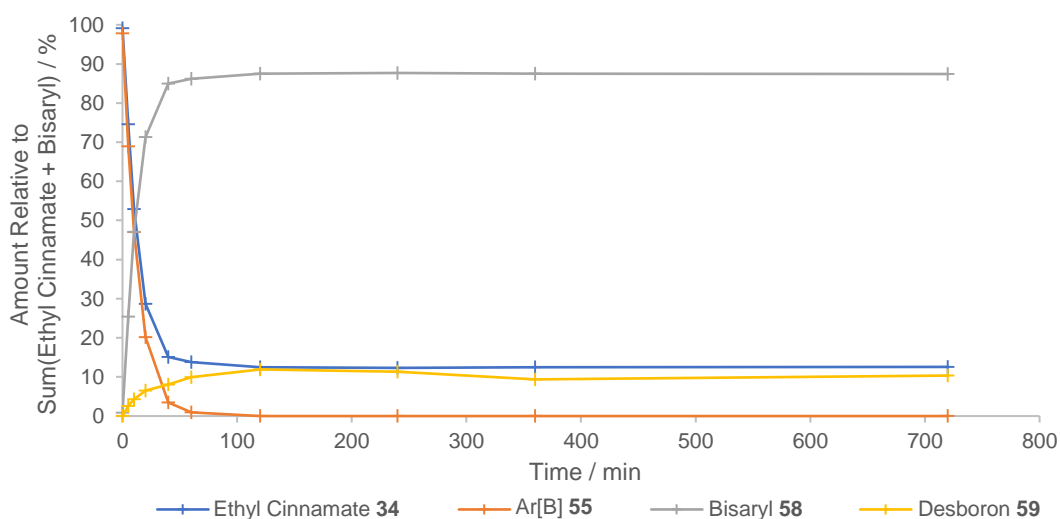
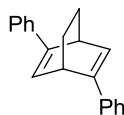


Figure 62. Calculated reaction composition over time.

5.4.3.2.2 Diene L12 (Entry 2, Table 25, page 140)



Reaction Set A

Time / min	HPLC Peak Area				
	Enoate	ArBpin	ArB(OH) ₂	Bisaryl	Desboron
0	1255.943		1084.610	22.984	
5	1025.080		875.221	1125.783	
10	934.367		762.371	1618.170	
20	832.042		688.261	2239.077	
40	701.659		585.958	2926.366	
60	635.981		523.461	3429.963	
120	507.940		408.703	4194.846	
240	385.858		269.294	4844.566	20.249
360	323.555		225.711	5028.255	19.336
720	275.388		164.779	5482.412	21.627

Table 96. HPLC Peak Area data (Method C, 215 nm) for Reaction Set A with diene L12. Enoate 16 at 19.7 min, arylboron reagent 17 at 20.0 min (ArBpin) and 9.1 min (ArB(OH)₂), bisaryl 18 at 19.2 min, *o*-tolylmethanol 19 at 13.1 min.

Time / min	Calculated Reaction Composition				Discrepancy	Product Ratio	
	Enoate	Ar[B]	Bisaryl	Desboron		Bisaryl	Desboron
0	100	101	0.3	0	-1.7		
5	83	83	17	0	-0.4	100	0
10	75	72	25	0	3.0	100	0
20	66	65	34	0	1.7	100	0
40	56	55	44	0	0.9	100	0
60	49	48	51	0	1.5	100	0
120	39	37	61	0	2.1	100	0
240	30	24	70	2	3.6	98	2
360	25	21	75	2	2.8	98	2
720	21	15	79	2	4.4	98	2

Table 97. Interpretation of HPLC data for Reaction Set A with diene L12.

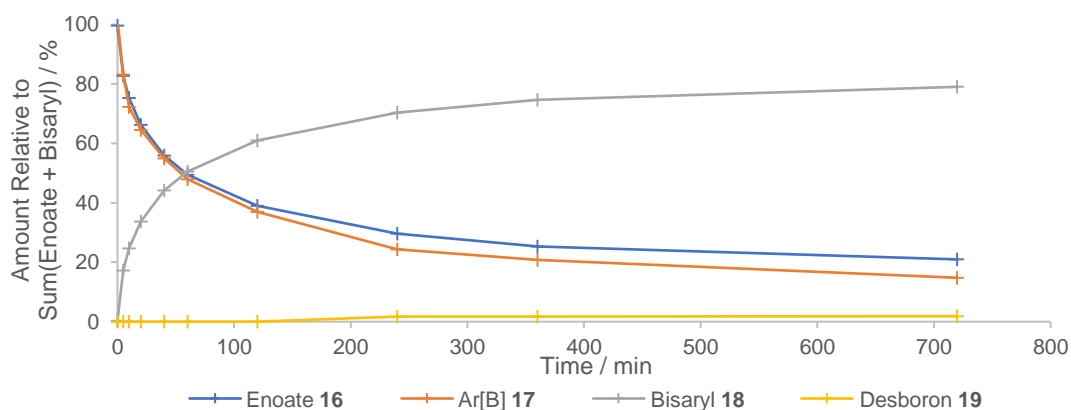
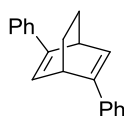


Figure 63. Calculated reaction composition over time.

Bisaryl 18: -88% *ee* (predominantly (*R*)-18 due to use of (*S,S*)-Ph-BOD).



Reaction Set B

Time / min	HPLC Peak Area				
	Enoate	ArBpin	ArB(OH) ₂	Bisaryl	Desboron
0	2310.647	327.043	590.628	2.649	2.448
5	1786.434	466.675	201.900	452.559	6.981
10	1498.297	373.817	179.473	716.468	8.346
20	1103.477	268.712	113.430	1039.962	10.143
40	711.476	164.548	61.589	1525.678	15.724
60	475.839	80.941	51.133	1755.438	21.123
120	252.994	23.721	9.887	2003.039	30.320
240	152.058	2.212		2002.498	34.810
360	133.604	2.242		2090.781	28.866
720	136.290	2.960		2151.813	32.198

Table 98. HPLC Peak Area data (Method B, 210 and 220 nm (bisaryl)) for Reaction Set B with diene L12. Ethyl cinnamate 34 at 5.26 min, arylboron reagent 55 at 6.25 min (ArBpin) and 3.06 min (ArB(OH)₂), bisaryl 58 at 6.43 min, toluene 59 at 4.76 min.

Time / min	Calculated Reaction Composition				Discrepancy	Product Ratio	
	Enoate	Ar[B]	Bisaryl	Desboron		Bisaryl	Desboron
0	100	96	0.1	0.3	3.7		
5	79	71	21	0.8	6.7	96	4
10	66	59	34	1	6.2	97	3
20	50	42	50	1	7.0	98	2
40	31	24	69	2	5.3	98	2
60	20	14	80	2	4.4	97	3
120	11	3	89	3	3.9	96	4
240	7	0	93	4	2.5	96	4
360	6	0	94	3	2.3	97	3
720	6	0	94	4	1.9	96	4

Table 99. Interpretation of HPLC data for Reaction Set B with diene L12.

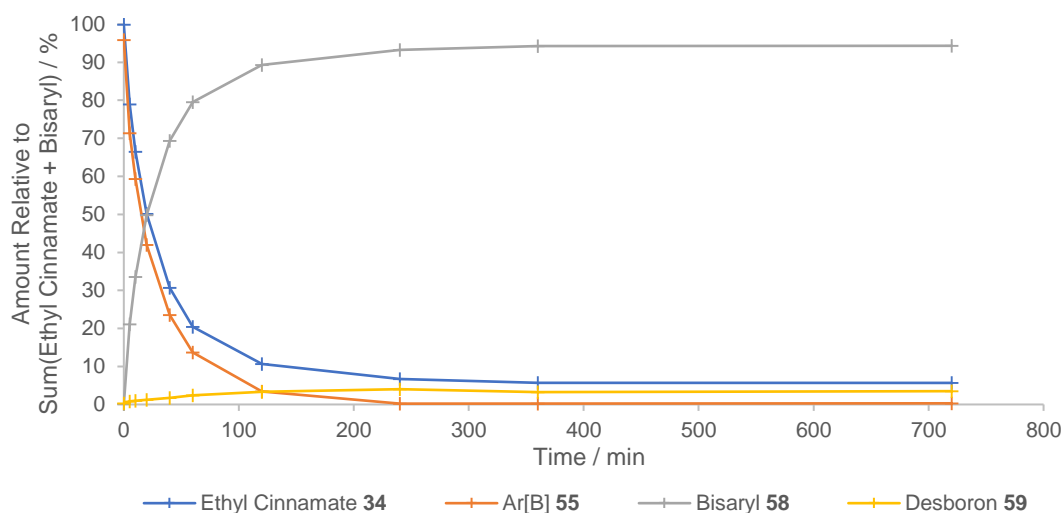
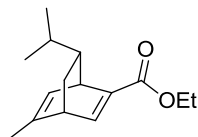


Figure 64. Calculated reaction composition over time.

5.4.3.2.3 Diene L26 (Entry 3, Table 25, page 140)



Reaction Set A

Time / min	HPLC Peak Area				
	Enoate	ArBpin	ArB(OH) ₂	Bisaryl	Desboron
0	1265.895		1102.385	14.984	
5	977.170		800.792	1280.531	
10	890.036		710.786	1959.417	
20	745.459		597.059	2870.893	
40	535.649		405.979	3694.271	
60	455.694		356.647	4343.395	12.286
120	304.687		153.036	5318.900	26.590
240	192.056		74.729	5596.682	24.447
360	165.396		41.172	5978.641	26.145
720	148.252		38.252	6270.064	29.291

Table 100. HPLC Peak Area data (Method C, 215 nm) for Reaction Set A with diene L26. Enoate 16 at 19.7 min, arylboron reagent 17 at 20.0 min (ArBpin) and 9.1 min (ArB(OH)₂), bisaryl 18 at 19.2 min, *o*-tolylmethanol 19 at 13.1 min.

Time / min	Calculated Reaction Composition				Discrepancy	Product Ratio	
	Enoate	Ar[B]	Bisaryl	Desboron		Bisaryl	Desboron
0	100	102	0.2	0	-2.5		
5	80	77	20	0	2.8	100	0
10	71	66	29	0	4.2	100	0
20	58	55	42	0	3.3	100	0
40	43	39	57	0	4.7	100	0
60	36	33	64	1	1.7	98	2
120	23	14	77	2	7.2	97	3
240	15	7	85	2	6.1	97	3
360	13	4	87	2	6.8	97	3
720	11	3	89	2	5.3	97	3

Table 101. Interpretation of HPLC data for Reaction Set A with diene L26.

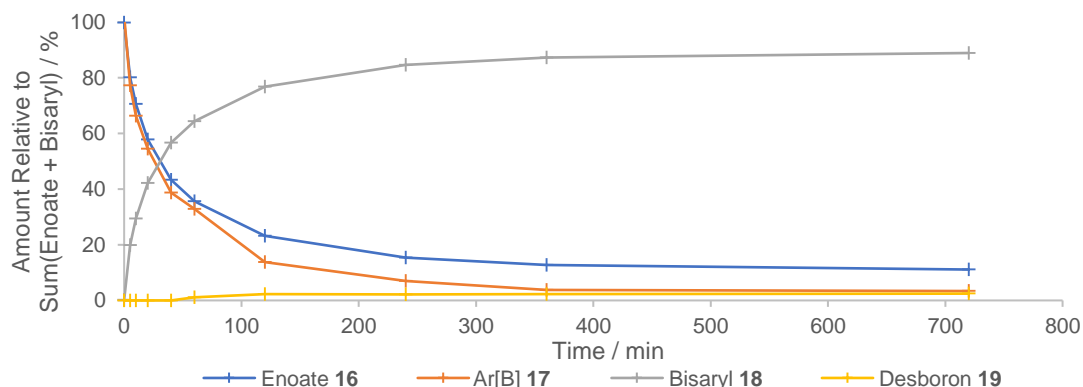
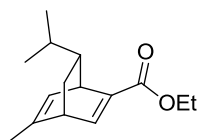


Figure 65. Calculated reaction composition over time.

Bisaryl 18: 93% *ee* (predominantly (*S*)-18).



Reaction Set B

Time / min	HPLC Peak Area				
	Enoate	ArBpin	ArB(OH) ₂	Bisaryl	Desboron
0	2292.132	188.055	752.708	12.895	4.706
5	1127.983	261.047	138.841	760.425	20.764
10	954.081	206.919	115.280	1218.094	33.648
20	533.656	96.962	53.160	1552.870	50.310
40	263.162	18.919	11.013	1777.563	69.647
60	211.336	4.338	2.193	1870.280	80.123
120	197.792			1925.064	83.771
240	210.634			2051.786	83.950
360	196.044			1904.437	75.928
720	207.271			2029.570	62.838

Table 102. HPLC Peak Area data (Method B, 210 and 220 nm (bisaryl)) for Reaction Set B with diene L26. Ethyl cinnamate 34 at 5.26 min, arylboron reagent 55 at 6.25 min (ArBpin) and 3.06 min (ArB(OH)₂), bisaryl 58 at 6.43 min, toluene 59 at 4.76 min.

Time / min	Calculated Reaction Composition				Discrepancy	Product Ratio	
	Enoate	Ar[B]	Bisaryl	Desboron		Bisaryl	Desboron
0	99	99	0.6	0.5	0.3		
5	58	50	42	3	5.6	94	6
10	43	35	57	4	3.9	94	6
20	25	17	75	6	1.8	93	7
40	12	3	88	9	0.4	91	9
60	10	0.7	90	10	-0.6	90	10
120	9	0	91	10	-1.0	90	10
240	9	0	91	9	-0.4	91	9
360	9	0	91	9	-0.1	91	9
720	9	0	91	7	1.8	93	7

Table 103. Interpretation of HPLC data for Reaction Set B with diene L26.

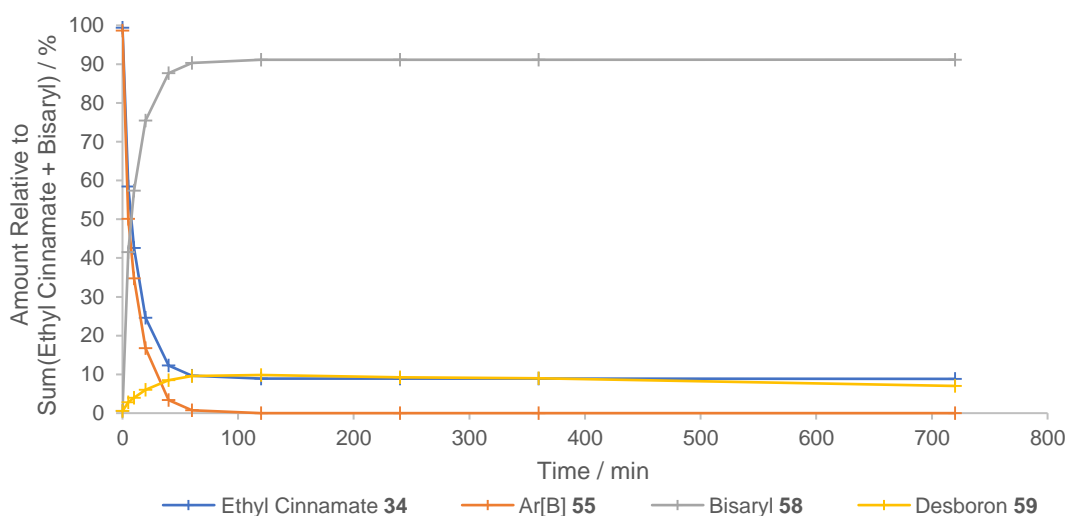
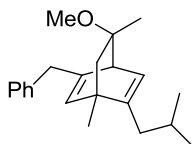


Figure 66. Calculated reaction composition over time.

5.4.3.2.4 Diene L13 (Entry 4, Table 25, page 140)



Reaction Set A

Time / min	HPLC Peak Area				
	Enoate	ArBpin	ArB(OH) ₂	Bisaryl	Desboron
0	1232.062		1066.334		
5	1107.251		930.738	413.807	
10	1068.903		886.984	688.103	16.723
20	1003.045		807.364	1129.666	18.207
40	900.746		727.763	1719.138	25.802
60	840.877		642.613	2144.767	31.324
120	712.420		513.419	2935.985	45.600
240	643.627		379.423	3981.049	81.024
360	561.297		298.550	4166.317	93.153
720	536.907		189.038	4308.610	160.680

Table 104. HPLC Peak Area data (Method C, 215 nm) for Reaction Set A with diene L13. Enoate 16 at 19.7 min, arylboron reagent 17 at 20.0 min (ArBpin) and 9.1 min (ArB(OH)₂), bisaryl 18 at 19.2 min, *o*-tolylmethanol 19 at 13.1 min.

Time / min	Calculated Reaction Composition				Discrepancy	Product Ratio	
	Enoate	Ar[B]	Bisaryl	Desboron		Bisaryl	Desboron
0	100	102	0	0	-1.9		
5	93	92	7	0	1.0		
10	89	87	11	2	0.5	87	13
20	82	78	18	2	2.6	91	9
40	73	70	27	2	1.2	92	8
60	67	61	33	3	4.0	92	8
120	56	48	44	4	4.5	92	8
240	46	32	54	6	7.6	89	11
360	42	26	58	8	7.9	88	12
720	40	16	60	13	10.0	82	18

Table 105. Interpretation of HPLC data for Reaction Set A with diene L13.

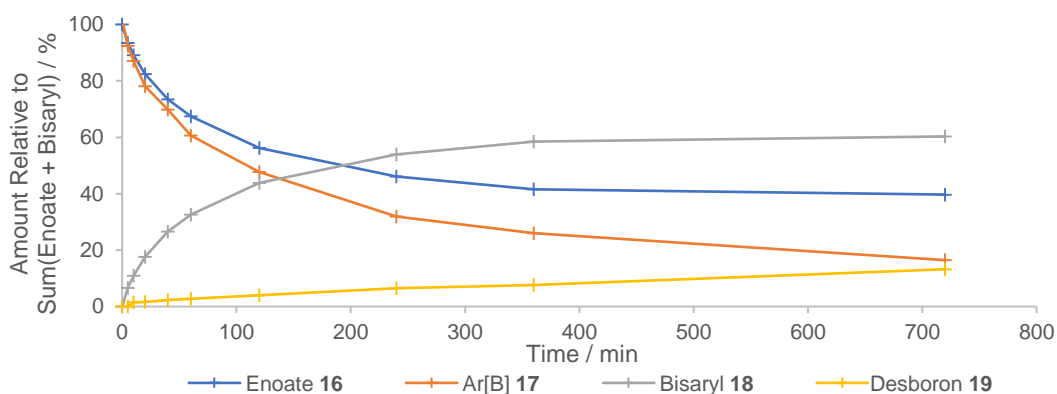
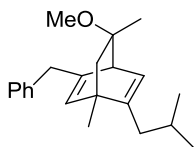


Figure 67. Calculated reaction composition over time.

Bisaryl 18: -72% *ee* (predominantly (*R*)-18).



Reaction Set B

Time / min	HPLC Peak Area				
	Enoate	ArBpin	ArB(OH) ₂	Bisaryl	Desboron
0	2210.738	115.925	768.601		6.326
5	1991.221	303.136	446.295	146.937	17.620
10	1951.112	278.195	449.541	244.387	25.762
20	1601.377	222.813	347.234	349.684	28.820
40	1498.135	209.645	306.853	567.792	45.073
60	1332.077	130.682	333.092	683.348	36.483
120	1129.484	111.289	245.747	898.052	56.405
240	1107.017	55.102	265.146	1073.153	76.009
360	1048.495	55.452	237.180	1041.749	71.438
720	1192.861	106.643	207.843	1201.768	93.713

Table 106. HPLC Peak Area data (Method B, 210 and 220 nm (bisaryl)) for Reaction Set B with diene L13. Ethyl cinnamate 34 at 5.26 min, arylboron reagent 55 at 6.25 min (ArBpin) and 3.06 min (ArB(OH)₂), bisaryl 58 at 6.43 min, toluene 59 at 4.76 min.

Time / min	Calculated Reaction Composition				Discrepancy	Product Ratio	
	Enoate	Ar[B]	Bisaryl	Desboron		Bisaryl	Desboron
0	100	97	0	0.7	2.5		
5	93	84	7	2	6.2	77	23
10	88	80	12	3	5.7	79	21
20	81	70	19	4	7.5	83	17
40	71	60	29	6	6.3	84	16
60	65	55	35	5	5.6	88	12
120	54	42	46	7	5.7	87	13
240	49	35	51	9	6.0	85	15
360	49	33	51	9	7.2	85	15
720	48	31	52	10	7.6	84	16

Table 107. Interpretation of HPLC data for Reaction Set B with diene L13.

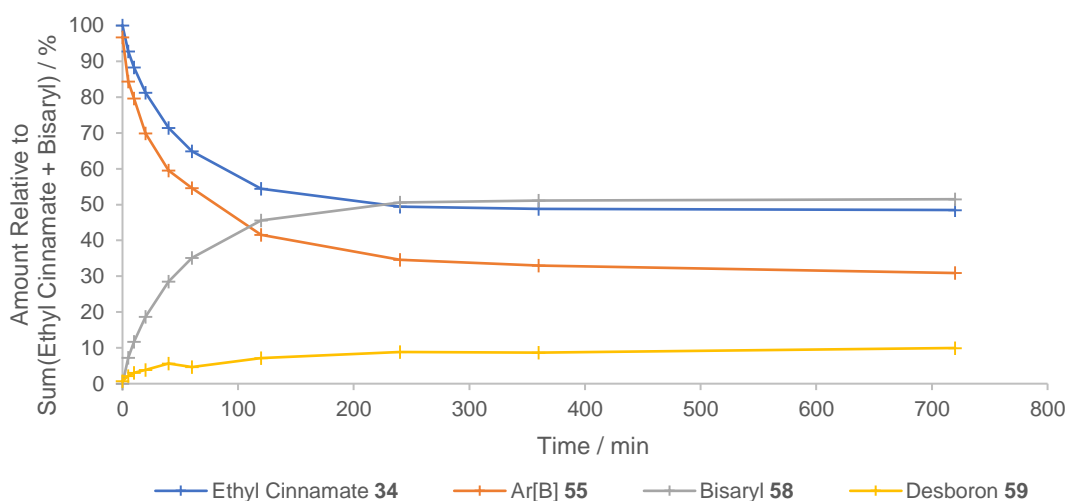
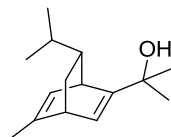


Figure 68. Calculated reaction composition over time.

5.4.3.2.5 Diene L10 (Entry 5, Table 25, page 140)



Reaction Set A

Time / min	HPLC Peak Area				
	Enoate	ArBpin	ArB(OH) ₂	Bisaryl	Desboron
0	1281.360		1091.652	11.038	
5	1132.306		792.598	604.804	133.795
10	1077.334		705.421	866.135	189.185
20	1030.184		580.681	1223.396	261.674
40	964.488		456.806	1644.718	352.402
60	927.534		363.681	1909.314	404.894
120	860.905		213.629	2356.163	500.321
240	821.039		127.571	2743.029	581.344
360	804.688		39.162	2909.524	617.849
720	792.588		19.333	2974.179	646.290

Table 108. HPLC Peak Area data (Method C, 215 nm) for Reaction Set A with diene L10. Enoate 16 at 19.7 min, arylboron reagent 17 at 20.0 min (ArBpin) and 9.1 min (ArB(OH)₂), bisaryl 18 at 19.2 min, *o*-tolylmethanol 19 at 13.1 min.

Time / min	Calculated Reaction Composition				Discrepancy	Product Ratio	
	Enoate	Ar[B]	Bisaryl	Desboron		Bisaryl	Desboron
0	100	100	0.2	0	-0.3		
5	91	75	9	12	4.0	43	57
10	87	67	13	17	2.9	44	56
20	82	54	18	23	4.4	44	56
40	76	42	24	31	2.7	44	56
60	72	33	28	35	3.8	45	55
120	66	19	34	43	4.0	44	56
240	61	11	39	48	1.8	45	55
360	59	3	41	51	5.2	44	56
720	58	2	42	53	3.7	44	56

Table 109. Interpretation of HPLC data for Reaction Set A with diene L10.

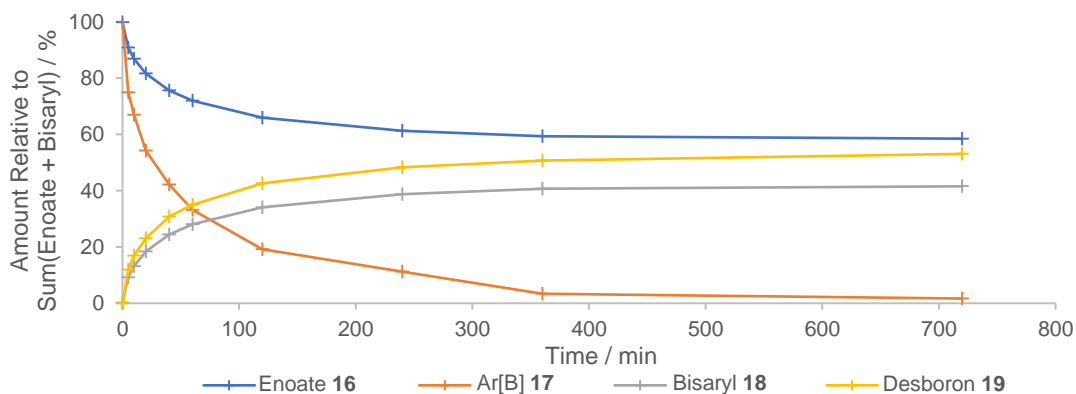
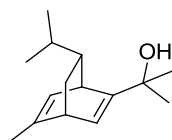


Figure 69. Calculated reaction composition over time.

Bisaryl 18: -48% *ee* (predominantly (*R*)-18).



Reaction Set B

Time / min	HPLC Peak Area				
	Enoate	ArBpin	ArB(OH) ₂	Bisaryl	Desboron
0	2294.033	148.924	795.315		2.845
5	1411.170	264.277	213.132	247.721	80.549
10	1740.944	308.817	261.406	500.360	161.649
20	1427.866	183.608	170.255	628.431	217.833
40	1312.030	130.824	119.152	803.759	284.199
60	1294.451	118.980	93.547	880.016	318.992
120	1308.944	80.742	119.091	909.360	326.373
240	1236.602	36.228	147.294	858.972	256.789
360	1221.561	39.737	139.901	844.175	224.042
720	1427.935	72.954	129.231	983.326	247.095

Table 110. HPLC Peak Area data (Method B, 210 and 220 nm (bisaryl)) for Reaction Set B with diene L10. Ethyl cinnamate 34 at 5.26 min, arylboron reagent 55 at 6.25 min (ArBpin) and 3.06 min (ArB(OH)₂), bisaryl 58 at 6.43 min, toluene 59 at 4.76 min.

Time / min	Calculated Reaction Composition				Discrepancy	Product Ratio	
	Enoate	Ar[B]	Bisaryl	Desboron		Bisaryl	Desboron
0	100	99	0	0.3	0.2		
5	84	69	16	13	2.8	55	45
10	77	61	23	19	-2.6	56	44
20	68	41	32	27	0.1	54	46
40	61	28	39	34	-1.6	53	47
60	58	23	42	38	-2.4	53	47
120	58	21	42	38	-1.2	53	47
240	58	21	42	31	5.7	57	43
360	58	21	42	28	9.5	60	40
720	58	20	42	26	11.9	62	38

Table 111. Interpretation of HPLC data for Reaction Set B with diene L10.

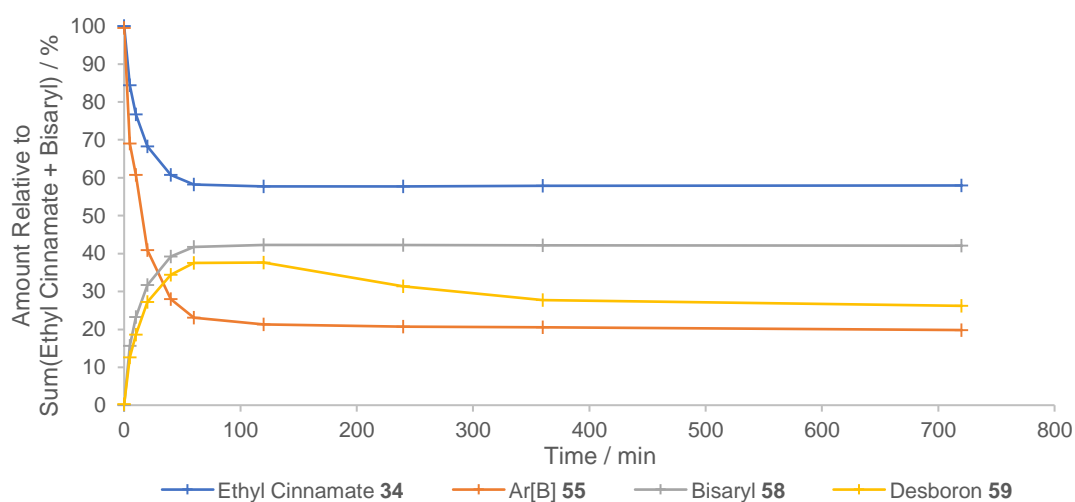
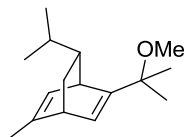


Figure 70. Calculated reaction composition over time.

5.4.3.2.6 Diene L27 (Entry 6, Table 25, page 140)



Reaction Set A

Time / min	HPLC Peak Area				
	Enoate	ArBpin	ArB(OH) ₂	Bisaryl	Desboron
0	1163.753	16.628	1163.187		
5	976.314		950.950	947.482	
10	867.464		802.073	1470.442	25.504
20	757.205		664.812	2189.970	38.421
40	664.942		538.741	3153.459	58.818
60	572.190		439.867	3546.720	71.698
120	495.207		278.646	4742.891	109.561
240	402.490		164.190	4994.340	136.382
360	384.382		86.555	5143.376	151.162
720	403.157		98.352	5359.832	162.744

Table 112. HPLC Peak Area data (Method C, 215 nm) for Reaction Set A with diene L27. Enoate 16 at 20.1 min, arylboron reagent 17 at 20.4 min (ArBpin) and 9.3 min (ArB(OH)₂), bisaryl 18 at 19.6 min, *o*-tolylmethanol 19 at 13.6 min.

Time / min	Calculated Reaction Composition				Discrepancy	Product Ratio	
	Enoate	Ar[B]	Bisaryl	Desboron		Bisaryl	Desboron
0	100	101	0	0	-1.0		
5	85	82	15	0	2.5		
10	76	70	24	2	3.6	91	9
20	65	57	35	4	4.6	91	9
40	53	43	47	5	5.1	90	10
60	46	36	54	6	4.6	89	11
120	36	20	64	9	7.2	88	12
240	30	12	70	11	6.8	86	14
360	29	6	71	12	10.0	85	15
720	29	7	71	13	9.2	85	15

Table 113. Interpretation of HPLC data for Reaction Set A with diene L27.

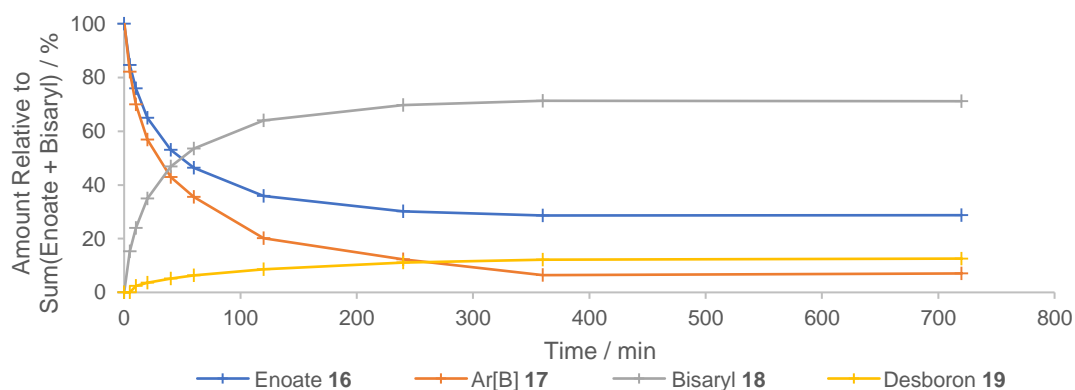
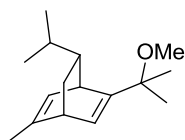


Figure 71. Calculated reaction composition over time.

Bisaryl 18: 63% *ee* (predominantly (*S*)-18).



Reaction Set B

Time / min	HPLC Peak Area				
	Enoate	ArBpin	ArB(OH) ₂	Bisaryl	Desboron
0	2349.247	475.705	471.553	3.248	3.514
5	1782.388	513.117	133.795	419.848	52.069
10	1502.991	340.629	164.663	604.566	82.109
20	1274.036	258.154	117.165	889.322	138.416
40	994.743	122.050	81.153	1120.718	204.108
60	941.613	94.572	47.409	1286.653	249.537
120	878.854	45.765	36.001	1329.386	269.446
240	897.030	49.411	24.384	1351.183	271.811
360	917.206	20.016	48.092	1377.556	232.838
720	896.567	25.558	31.909	1334.808	224.158

Table 114. HPLC Peak Area data (Method B, 210 and 220 nm (bisaryl)) for Reaction Set B with diene L27. Ethyl cinnamate 34 at 5.26 min, arylboron reagent 55 at 6.25 min (ArBpin) and 3.06 min (ArB(OH)₂), bisaryl 58 at 6.43 min, toluene 59 at 4.76 min.

Time / min	Calculated Reaction Composition				Discrepancy	Product Ratio	
	Enoate	Ar[B]	Bisaryl	Desboron		Bisaryl	Desboron
0	100	96	0.1	0.3	3.5		
5	80	70	20	5	6.0	80	20
10	71	57	29	8	6.1	79	21
20	58	41	42	13	4.4	77	23
40	46	22	54	19	4.4	74	26
60	41	15	59	22	4.2	73	27
120	39	9	61	24	6.0	72	28
240	39	8	61	24	7.3	72	28
360	39	7	61	20	12.0	75	25
720	39	6	61	20	13.3	75	25

Table 115. Interpretation of HPLC data for Reaction Set B with diene L27.

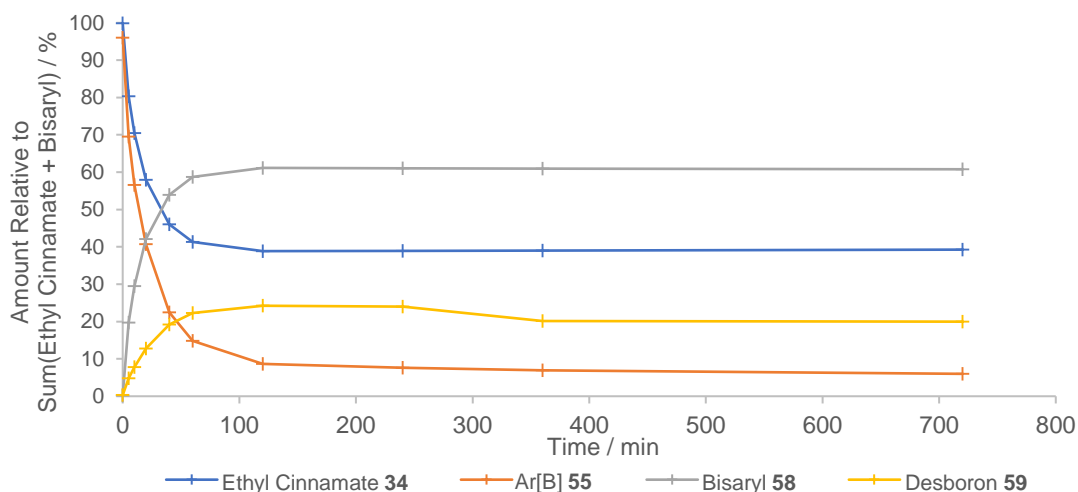
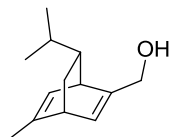


Figure 72. Calculated reaction composition over time.

5.4.3.2.7 Diene L28 (Entry 7, Table 25, page 140)



Reaction Set A

Time / min	HPLC Peak Area				
	Enoate	ArBpin	ArB(OH) ₂	Bisaryl	Desboron
0	1165.182	15.618	1141.126		
5	1060.028		957.667	642.167	86.611
10	993.394		835.228	965.187	129.770
20	938.430		696.695	1441.120	201.728
40	821.503		499.709	1889.361	278.196
60	657.810		337.217	1866.574	280.972
120	768.516		269.437	2787.097	439.804
240	696.365		153.491	2850.160	470.073
360	700.387		109.723	3007.800	494.467
720	695.210		80.749	3126.278	520.095

Table 116. HPLC Peak Area data (Method C, 215 nm) for Reaction Set A with diene L28. Enoate 16 at 20.1 min, arylboron reagent 17 at 20.4 min (ArBpin) and 9.3 min (ArB(OH)₂), bisaryl 18 at 19.6 min, *o*-tolylmethanol 19 at 13.6 min.

Time / min	Calculated Reaction Composition				Discrepancy	Product Ratio	
	Enoate	Ar[B]	Bisaryl	Desboron		Bisaryl	Desboron
0	100	99	0	0	1.1		
5	90	81	10	8	1.0	56	44
10	85	71	15	12	1.8	56	44
20	78	58	22	18	2.1	55	45
40	70	42	30	26	1.9	54	46
60	65	33	35	30	1.7	53	47
120	60	21	40	37	1.8	52	48
240	57	12	43	42	2.8	51	49
360	56	9	44	43	4.4	51	49
720	54	6	46	44	4.0	51	49

Table 117. Interpretation of HPLC data for Reaction Set A with diene L28.

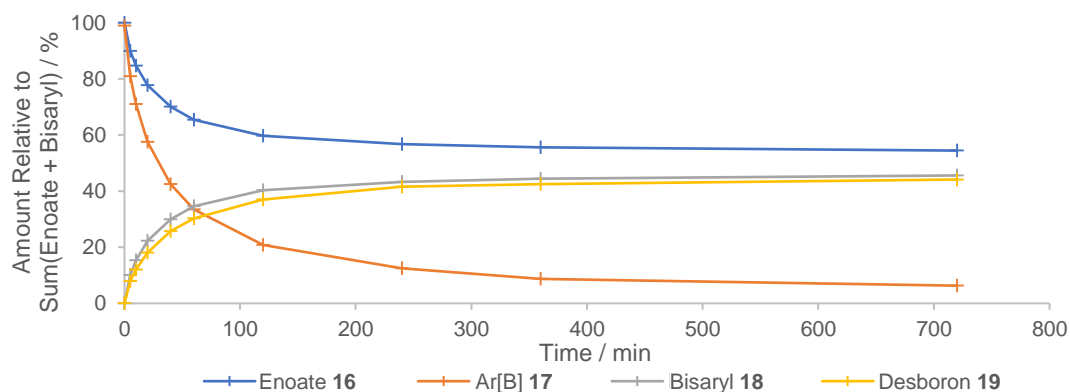
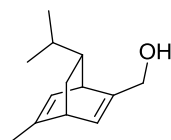


Figure 73. Calculated reaction composition over time.

Bisaryl 18: 75% *ee* (predominantly (*S*)-18).



Reaction Set B

Time / min	HPLC Peak Area				
	Enoate	ArBpin	ArB(OH) ₂	Bisaryl	Desboron
0	2208.287	333.067	563.351	2.347	
5	1437.279	367.678	132.470	620.623	56.751
10	1216.965	295.738	94.545	901.634	89.645
20	924.420	199.860	44.561	1212.227	137.042
40	701.784	73.844	34.446	1496.112	192.934
60	599.471	33.780	20.646	1541.330	203.222
120	549.928	13.088	4.968	1604.472	208.906
240	545.108	4.457	5.216	1611.167	202.168
360	556.149		5.483	1647.174	178.851
720	555.725	2.960	2.552	1645.042	157.314

Table 118. HPLC Peak Area data (Method B, 210 and 220 nm (bisaryl)) for Reaction Set B with diene L28. Ethyl cinnamate 34 at 5.26 min, arylboron reagent 55 at 6.25 min (ArBpin) and 3.06 min (ArB(OH)₂), bisaryl 58 at 6.43 min, toluene 59 at 4.76 min.

Time / min	Calculated Reaction Composition				Discrepancy	Product Ratio	
	Enoate	Ar[B]	Bisaryl	Desboron		Bisaryl	Desboron
0	100	97	0.1	0	3.2		
5	69	57	31	6	6.2	85	15
10	56	43	44	8	4.8	84	16
20	42	27	58	13	2.9	82	18
40	31	11	69	17	2.3	80	20
60	27	6	73	19	2.6	80	20
120	25	2	75	19	3.7	80	20
240	25	1	75	19	5.0	80	20
360	25	0.6	75	16	7.9	82	18
720	25	0.6	75	14	9.8	84	16

Table 119. Interpretation of HPLC data for Reaction Set B with diene L28.

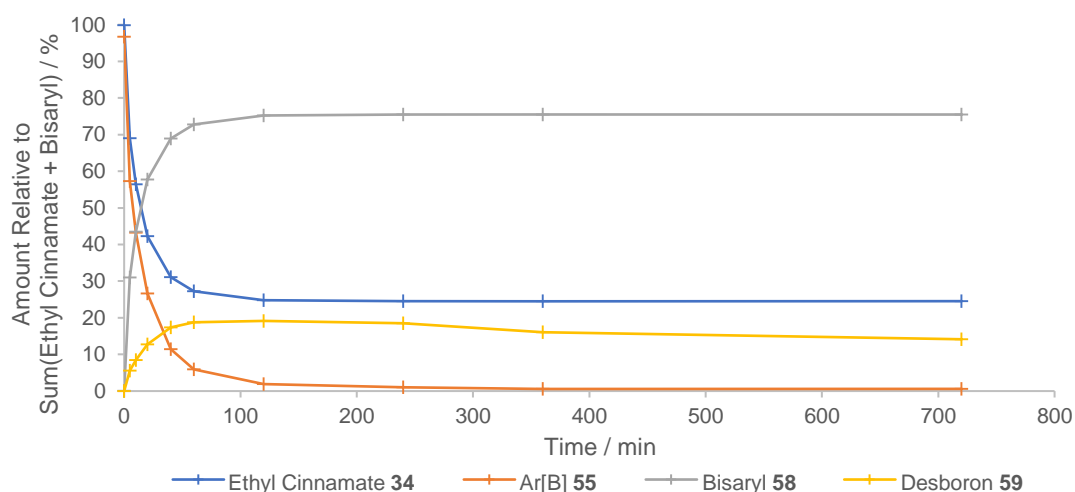
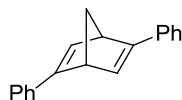


Figure 74. Calculated reaction composition over time.

5.4.3.2.8 Diene L31 (Entry 8, Table 25, page 140)



Reaction Set A

Time / min	HPLC Peak Area				
	Enoate	ArBpin	ArB(OH) ₂	Bisaryl	Desboron
0	1173.166	15.775	1141.750	81.711	
5	1053.471		1036.841	280.553	
10	1036.321		1015.365	457.755	
20	953.612		942.855	795.637	
40	902.302		888.523	1465.209	
60	825.327		808.249	1989.101	
120	637.553		615.719	3119.791	
240	429.770		333.694	4416.970	28.080
360	331.922		247.269	5219.102	31.428
720	205.991	19.952	156.609	6250.096	26.620

Table 120. HPLC Peak Area data (Method C, 215 nm) for Reaction Set A with diene L31. Enoate 16 at 20.1 min, arylboron reagent 17 at 20.4 min (ArBpin) and 9.3 min (ArB(OH)₂), bisaryl 18 at 19.6 min, *o*-tolylmethanol 19 at 13.6 min.

Time / min	Calculated Reaction Composition				Discrepancy	Product Ratio	
	Enoate	Ar[B]	Bisaryl	Desboron		Bisaryl	Desboron
0	99	97	1	0	1.7		
5	95	93	5	0	1.8	100	0
10	92	90	8	0	2.2	100	0
20	87	85	13	0	1.3	100	0
40	77	75	23	0	1.4	100	0
60	69	67	31	0	1.7	100	0
120	52	50	48	0	2.0	100	0
240	34	27	66	2	5.3	96	4
360	25	19	75	3	3.9	97	3
720	15	13	85	2	0.1	98	2

Table 121. Interpretation of HPLC data for Reaction Set A with diene L31.

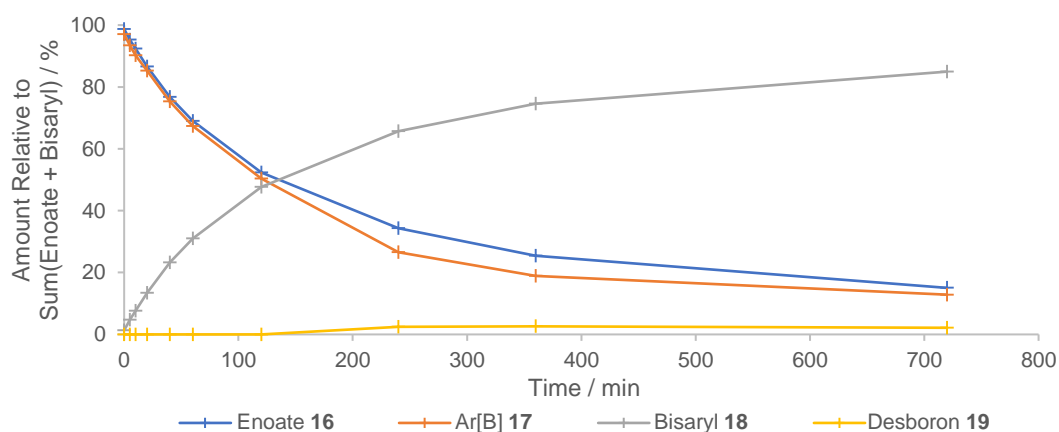
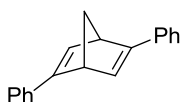


Figure 75. Calculated reaction composition over time.

Bisaryl 18: 95% *ee* (predominantly (*S*)-18).



Reaction Set B

Time / min	HPLC Peak Area				
	Enoate	ArBpin	ArB(OH) ₂	Bisaryl	Desboron
0	2380.133	449.076	513.462		
5	2173.217	661.751	195.006	51.574	2.584
10	2231.291	716.133	181.796	92.291	2.529
20	2088.384	680.300	141.238	168.390	2.577
40	1870.584	555.076	179.980	321.899	4.020
60	1801.166	429.187	283.782	492.355	6.599
120	1271.354	293.654	183.902	758.405	9.766
240	937.723	208.534	139.289	1147.840	13.987
360	707.306	179.470	68.158	1298.819	15.770
720	512.973	46.067	85.052	1791.600	28.479

Table 122. HPLC Peak Area data (Method B, 210 and 220 nm (bisaryl)) for Reaction Set B with diene L31. Ethyl cinnamate 34 at 5.26 min, arylboron reagent 55 at 6.25 min (ArBpin) and 3.06 min (ArB(OH)₂), bisaryl 58 at 6.43 min, toluene 59 at 4.76 min.

Time / min	Calculated Reaction Composition				Discrepancy	Product Ratio	
	Enoate	Ar[B]	Bisaryl	Desboron		Bisaryl	Desboron
0	100	96	0	0	3.5		
5	98	92	2	0.2	5.6		
10	96	92	4	0.2	3.6	95	5
20	92	87	8	0.2	5.5	97	3
40	85	79	15	0.4	4.9	98	2
60	78	74	22	0.6	3.8	97	3
120	62	55	38	1	5.5	98	2
240	44	39	56	1	3.7	98	2
360	34	29	66	2	4.1	98	2
720	22	13	78	2	6.0	97	3

Table 123. Interpretation of HPLC data for Reaction Set B with diene L31.

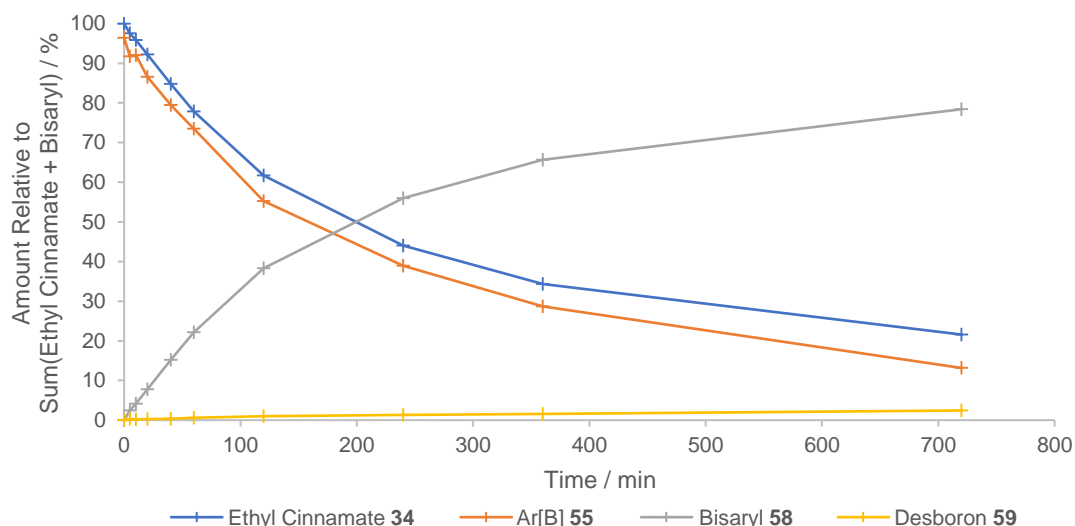


Figure 76. Calculated reaction composition over time.

5.4.3.2.9 Diene L30 (Entry 9, Table 25, page 140)



Reaction Set A

Time / min	HPLC Peak Area				
	Enoate	ArBpin	ArB(OH) ₂	Bisaryl	Desboron
0	1267.261		1084.178	9.264	
5	1200.922		908.887	245.192	112.509
10	1171.44		814.174	398.941	169.488
20	1127.846		674.185	641.550	269.495
40	1071.788		484.665	964.228	411.404
60	1059.124		404.110	1197.662	521.293
120	1007.696		204.062	1524.123	663.382
240	962.586		77.637	1706.814	754.884
360	979.967		40.318	1804.121	802.544
720	952.382		28.758	1762.016	789.949

Table 124. HPLC Peak Area data (Method C, 215 nm) for Reaction Set A with diene L30. Enoate 16 at 19.7 min, arylboron reagent 17 at 20.0 min (ArBpin) and 9.1 min (ArB(OH)₂), bisaryl 18 at 19.2 min, *o*-tolylmethanol 19 at 13.1 min.

Time / min	Calculated Reaction Composition				Discrepancy	Product Ratio	
	Enoate	Ar[B]	Bisaryl	Desboron		Bisaryl	Desboron
0	100	101	0.1	0	-0.7		
5	96	86	4	10	0.5	27	73
10	94	77	6	15	1.9	29	71
20	90	64	10	24	2.7	29	71
40	85	45	15	37	3.4	29	71
60	82	37	18	45	0.2	28	72
120	78	19	22	57	2.2	28	72
240	75	7	25	65	2.4	28	72
360	74	4	26	68	3.0	28	72
720	74	3	26	68	3.0	28	72

Table 125. Interpretation of HPLC data for Reaction Set A with diene L30.

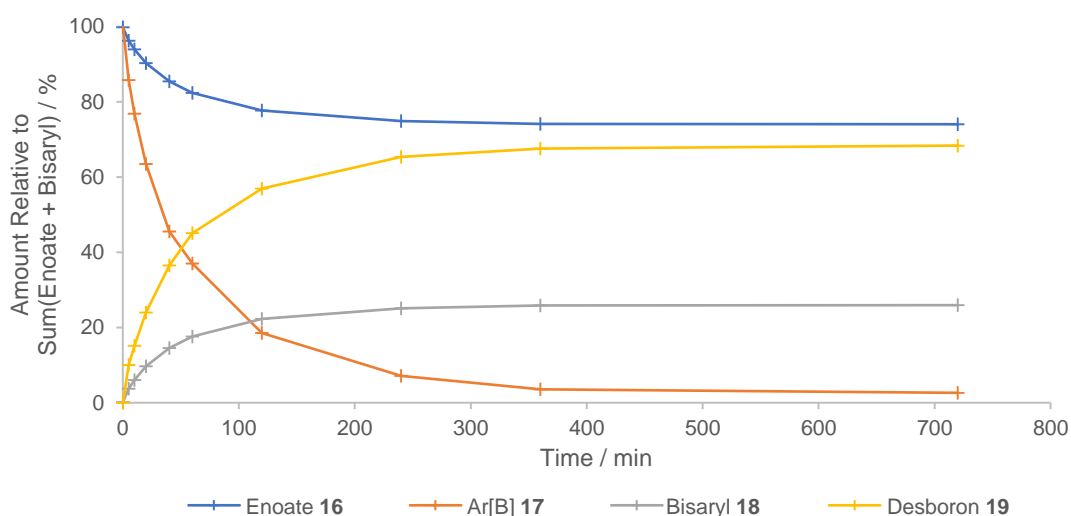


Figure 77. Calculated reaction composition over time.



Reaction Set B

Time / min	HPLC Peak Area				
	Enoate	ArBpin	ArB(OH) ₂	Bisaryl	Desboron
0	2334.255	610.002	335.257		2.943
5	2241.586	614.967	141.020	41.440	177.716
10	2168.698	449.200	172.307	65.891	285.998
20	2265.160	375.043	133.446	108.482	485.022
40	2139.379	187.644	112.892	146.909	671.685
60	2094.220	131.558	73.742	168.506	775.685
120	2096.008	55.782	43.260	199.828	879.022
240	2071.365	50.959	31.251	201.812	832.465
360	2037.048	58.639	15.724	198.962	792.921
720	2111.385	33.941	49.905	205.965	680.305

Table 126. HPLC Peak Area data (Method B, 210 and 220 nm (bisaryl)) for Reaction Set B with diene L30. Ethyl cinnamate 34 at 5.26 min, arylboron reagent 55 at 6.25 min (ArBpin) and 3.06 min (ArB(OH)₂), bisaryl 58 at 6.43 min, toluene 59 at 4.76 min.

Time / min	Calculated Reaction Composition				Discrepancy	Product Ratio	
	Enoate	Ar[B]	Bisaryl	Desboron		Bisaryl	Desboron
0	100	97	0	0.3	3.2		
5	98	79	2	16	3.4	11	89
10	97	66	3	26	4.7	11	89
20	95	51	5	41	2.8	10	90
40	93	31	7	60	2.5	10	90
60	92	22	8	70	1.2	10	90
120	91	10	9	78	3.1	10	90
240	91	9	9	74	8.0	11	89
360	91	8	9	72	11.0	11	89
720	91	9	9	59	22.7	13	87

Table 127. Interpretation of HPLC data for Reaction Set B with diene L30.

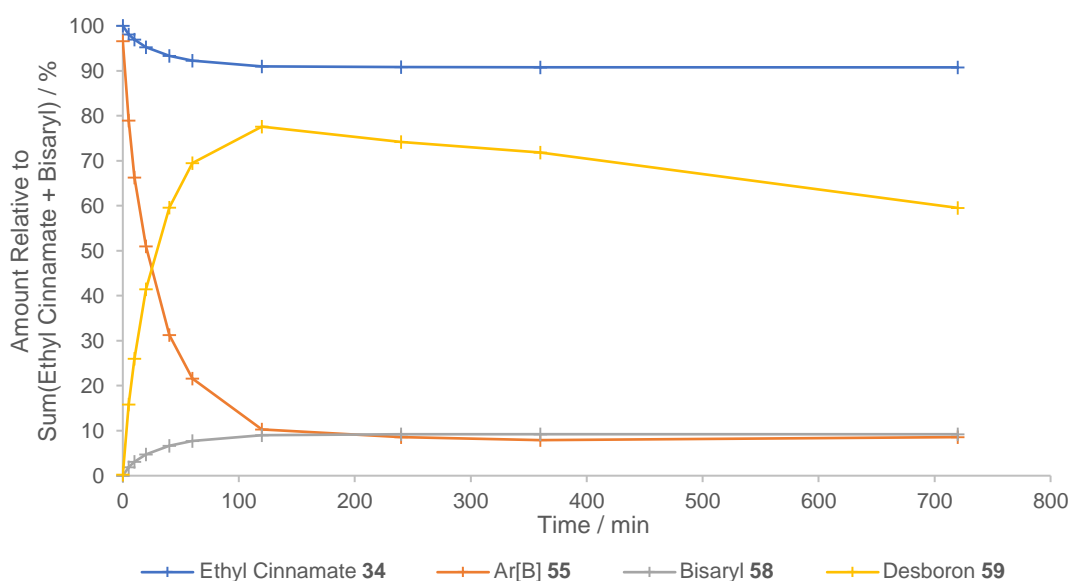


Figure 78. Calculated reaction composition over time.

5.4.3.2.10 Diene L33 (Entry 10, Table 25, page 140)



Reaction Set A

Time / min	HPLC Peak Area				
	Enoate	ArBpin	ArB(OH) ₂	Bisaryl	Desboron
0	1285.172		1096.442	21.533	
5	827.925		606.792	2304.230	68.007
10	709.459		495.505	2972.321	62.355
20	577.588		382.038	3653.217	61.464
40	436.440		264.871	4472.524	59.186
60	357.735		206.707	4977.244	62.401
120	236.112		111.515	5696.568	70.330
240	168.750		47.210	6113.597	78.740
360	156.923		11.155	6103.257	84.050
720	154.743		10.372	6096.575	86.690

Table 128. HPLC Peak Area data (Method C, 215 nm) for Reaction Set A with diene L33. Enoate 16 at 19.7 min, arylboron reagent 17 at 20.0 min (ArBpin) and 9.1 min (ArB(OH)₂), bisaryl 18 at 19.2 min, *o*-tolylmethanol 19 at 13.1 min.

Time / min	Calculated Reaction Composition				Discrepancy	Product Ratio	
	Enoate	Ar[B]	Bisaryl	Desboron		Bisaryl	Desboron
0	100	100	0.3	0	-0.4		
5	65	57	35	6	3.0	85	15
10	56	46	44	5	4.5	89	11
20	46	35	54	5	4.7	91	9
40	34	24	66	5	4.6	93	7
60	28	19	72	5	3.5	93	7
120	18	10	82	6	2.0	93	7
240	13	4	87	7	1.9	93	7
360	12	1	88	7	3.8	93	7
720	12	0.9	88	7	3.5	92	8

Table 129. Interpretation of HPLC data for Reaction Set A with diene L33.

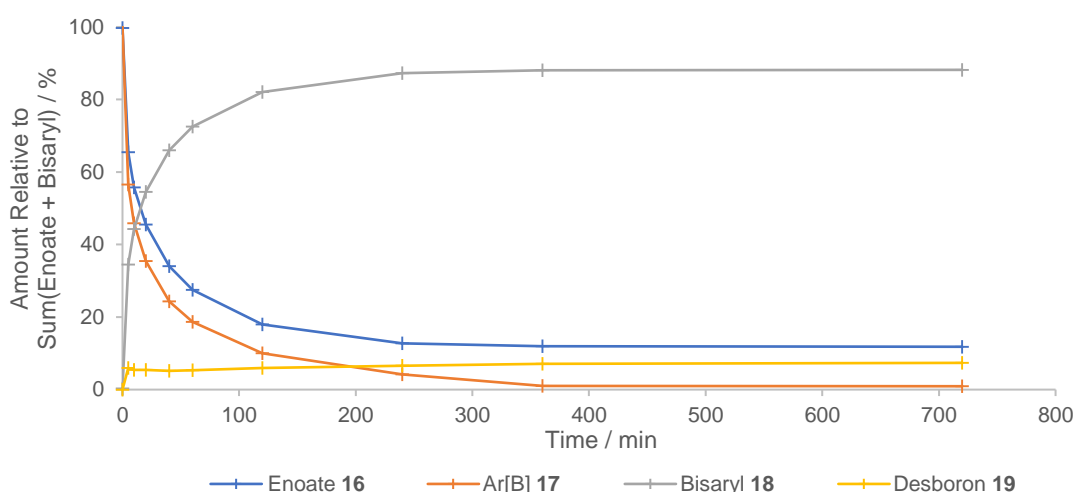


Figure 79. Calculated reaction composition over time.



Reaction Set B

Time / min	HPLC Peak Area				
	Enoate	ArBpin	ArB(OH) ₂	Bisaryl	Desboron
0	2286.849	266.227	667.500	13.167	4.260
5	1329.288	311.650	129.567	801.837	73.384
10	1088.009	211.457	106.045	1047.121	106.343
20	794.671	119.286	52.901	1266.369	144.264
40	581.139	44.125	18.281	1444.961	185.872
60	574.061	14.552	11.398	1673.873	218.820
120	496.500	2.697	2.486	1585.685	212.920
240	523.659			1692.959	213.707
360	492.394			1587.612	196.898
720	534.927			1719.192	166.164

Table 130. HPLC Peak Area data (Method B, 210 and 220 nm (bisaryl)) for Reaction Set B with diene L33. Ethyl cinnamate 34 at 5.26 min, arylboron reagent 55 at 6.25 min (ArBpin) and 3.06 min (ArB(OH)₂), bisaryl 58 at 6.43 min, toluene 59 at 4.76 min.

Time / min	Calculated Reaction Composition				Discrepancy	Product Ratio	
	Enoate	Ar[B]	Bisaryl	Desboron		Bisaryl	Desboron
0	100	98	0.6	0.5	0.8		
5	61	49	39	9	3.3	81	19
10	50	35	50	13	1.9	80	20
20	37	20	63	18	0.1	78	22
40	28	7	72	23	-2.7	76	24
60	25	3	75	24	-2.6	76	24
120	23	0.6	77	26	-3.4	75	25
240	23	0	77	24	-1.5	76	24
360	23	0	77	24	-1.0	76	24
720	23	0	77	19	4.3	81	19

Table 131. Interpretation of HPLC data for Reaction Set B with diene L33.

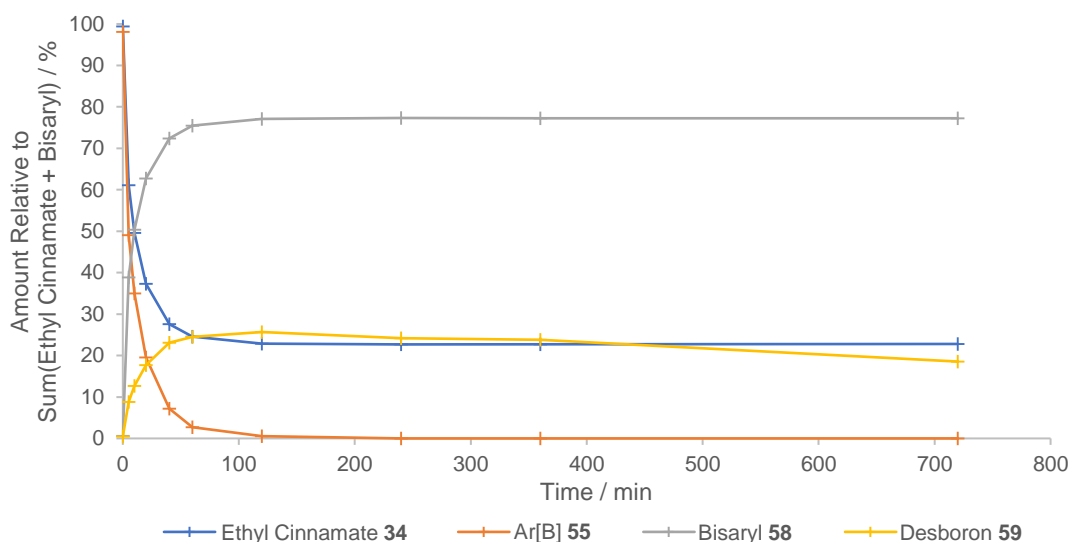


Figure 80. Calculated reaction composition over time.

5.4.3.2.11 [RhCl(C₂H₄)₂]₂ only (pages 143–144)

Reaction Set A

Time / min	HPLC Peak Area				
	Enoate	ArBpin	ArB(OH) ₂	Bisaryl	Desboron
0	1257.609		1108.309	22.543	
5	1194.761		988.838	107.136	
10	1197.161		984.543	143.874	
20	1202.969		963.996	177.685	
40	1301.307		990.655	252.048	43.713
60	1275.402		923.411	273.026	44.583
120	1255.113		895.136	244.465	38.014
240	1323.984		910.639	262.388	42.159
360	1297.686		898.525	261.177	40.877
720	1322.963		920.444	265.327	43.264

Table 132. HPLC Peak Area data (Method C, 215 nm) for Reaction Set A with ethylene only. Enoate 16 at 19.7 min, arylboron reagent 17 at 20.0 min (ArBpin) and 9.1 min (ArB(OH)₂), bisaryl 18 at 19.2 min, *o*-tolylmethanol 19 at 13.1 min.

Time / min	Calculated Reaction Composition					Product Ratio	
	Enoate	Ar[B]	Bisaryl	Desboron	Discrepancy	Bisaryl	Desboron
0	100	103	0.3	0	-3.7		
5	98	96	2	0	2.5		
10	98	95	2	0	3.1		
20	97	92	3	0	5.5		
40	96	86	4	4	6.4	50	50
60	96	82	4	4	10.4	51	49
120	96	81	4	3	12.2	52	48
240	96	78	4	3	14.9	51	49
360	96	79	4	3	14.4	52	48
720	96	79	4	4	13.9	51	49

Table 133. Interpretation of HPLC data for Reaction Set A with ethylene only.

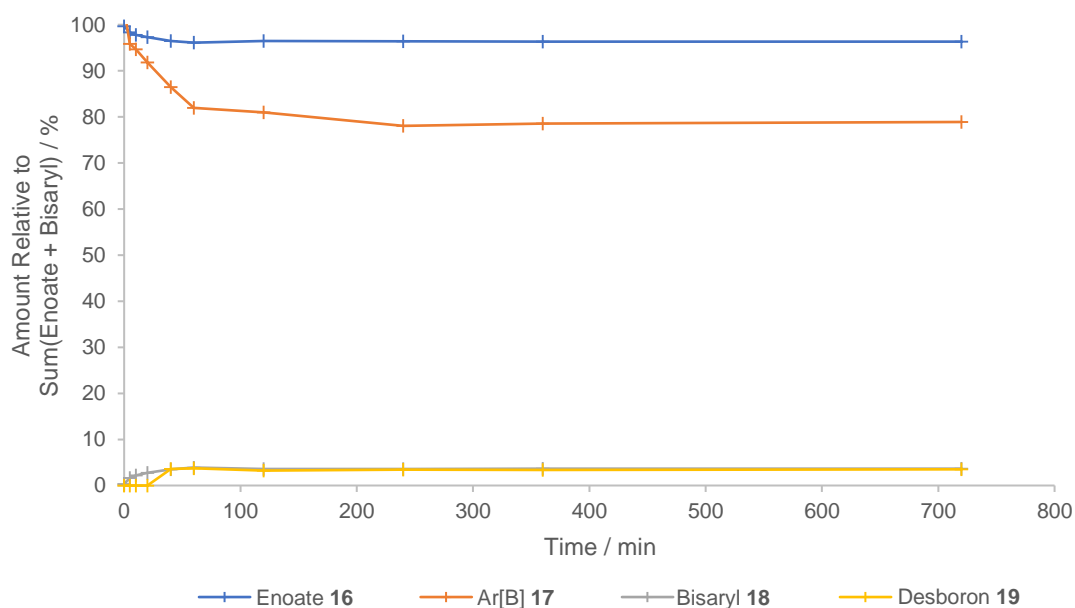


Figure 81. Calculated reaction composition over time.

[RhCl(C₂H₄)₂]₂ only

Reaction Set B

Time / min	HPLC Peak Area				
	Enoate	ArBpin	ArB(OH) ₂	Bisaryl	Desboron
0	2266.690	507.192	374.888		7.870
5	2131.034	581.942	203.941		11.926
10	2125.308	559.196	224.405		13.598
20	2187.089	558.734	246.721		15.893
40	2112.776	455.443	325.389	2.819	19.097
60	2117.878	455.898	324.605	2.957	20.978
120	2073.605	257.224	513.991	3.015	21.750
240	2012.071	308.617	432.200	2.797	22.509
360	2181.668	158.355	650.665	3.540	25.798
720	2224.977	242.426	572.416	4.244	26.167

Table 134. HPLC Peak Area data (Method B, 210 and 220 nm (bisaryl)) for Reaction Set B with ethylene only. Ethyl cinnamate 34 at 5.26 min, arylboron reagent 55 at 6.25 min (ArBpin) and 3.06 min (ArB(OH)₂), bisaryl 58 at 6.43 min, toluene 59 at 4.76 min.

Time / min	Calculated Reaction Composition				Discrepancy	Product Ratio	
	Enoate	Ar[B]	Bisaryl	Desboron		Bisaryl	Desboron
0	100	94	0	0.9	5.0		
5	100	89	0	1	9.4		
10	100	89	0	2	9.2		
20	100	89	0	2	9.1		
40	100	89	0.1	2	8.3	6	94
60	100	89	0.1	3	8.3	5	95
120	100	90	0.2	3	7.4	5	95
240	100	89	0.1	3	8.1	5	95
360	100	89	0.2	3	7.3	5	95
720	100	88	0.2	3	8.4	6	94

Table 135. Interpretation of HPLC data for Reaction Set B with ethylene only.

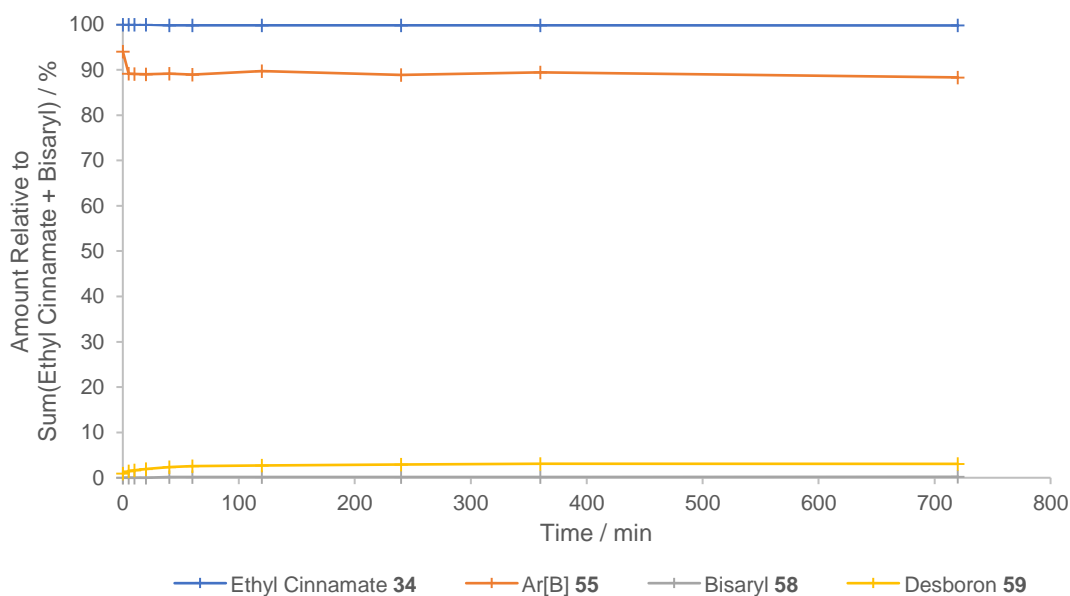
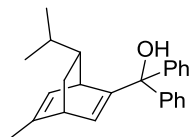


Figure 82. Calculated reaction composition over time.

5.4.3.2.12 Diene L29 (pages 143–144)



Reaction Set A

Time / min	HPLC Peak Area				
	Enoate	ArBpin	ArB(OH) ₂	Bisaryl	Desboron
0	1213.399	17.304	1200.816		
5	1132.822	14.524	1091.036	54.048	
10	1145.249	14.433	1101.894	78.810	
20	1145.207	13.900	1095.666	97.001	
40	1171.198	13.747	1072.514	111.321	
60	1177.468	13.496	1045.794	116.329	18.984
120	1223.705		1059.893	123.234	28.311
240	1331.715		1074.627	147.065	44.935
360	1296.976	16.021	1027.033	150.114	71.577
720	1367.943	17.661	1080.966	163.540	75.110

Table 136. HPLC Peak Area data (Method C, 215 nm) for Reaction Set A with diene L29. Enoate 16 at 20.1 min, arylboron reagent 17 at 20.4 min (ArBpin) and 9.3 min (ArB(OH)₂), bisaryl 18 at 19.6 min, *o*-tolylmethanol 19 at 13.6 min.

Time / min	Calculated Reaction Composition				Discrepancy	Product Ratio	
	Enoate	Ar[B]	Bisaryl	Desboron		Bisaryl	Desboron
0	100	100	0	0	0.0		
5	99	96	0.9	0	2.7		
10	99	96	1	0	2.8		
20	98	95	2	0	3.4		
40	98	91	2	0	7.4		
60	98	88	2	2	8.5	51	49
120	98	85	2	2	11.0	43	57
240	98	79	2	4	15.6	36	64
360	98	78	2	6	13.6	26	74
720	98	78	2	6	13.7	27	73

Table 137. Interpretation of HPLC data for Reaction Set A with diene L29.

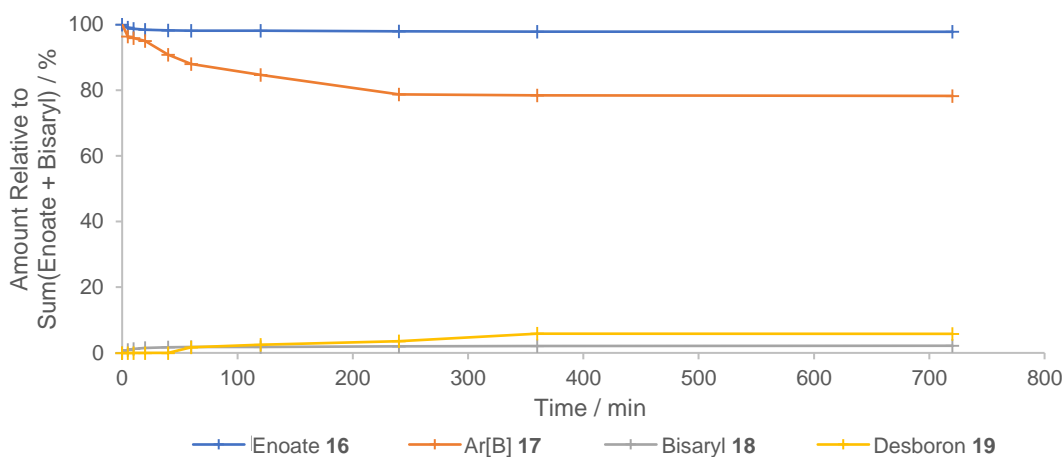
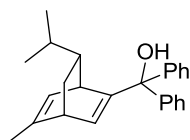


Figure 83. Calculated reaction composition over time.



Reaction Set B

Time / min	HPLC Peak Area				
	Enoate	ArBpin	ArB(OH) ₂	Bisaryl	Desboron
0	2149.008	139.260	717.403		7.344
5	2154.848	465.075	342.367		13.892
10	2139.978	442.974	357.180		15.847
20	2167.743	510.869	295.309		17.806
40	2129.438	527.370	257.199	2.733	22.999
60	2098.221	429.747	344.256	3.737	27.395
120	2116.670	435.317	334.547	5.469	36.103
240	2096.148	372.771	381.944	6.011	41.245
360	2230.384	263.178	540.392	7.579	43.188
720	2255.232	393.046	403.855	8.252	43.864

Table 138. HPLC Peak Area data (Method B, 210 and 220 nm (bisaryl)) for Reaction Set B with diene L29. Ethyl cinnamate 34 at 5.26 min, arylboron reagent 55 at 6.25 min (ArBpin) and 3.06 min (ArB(OH)₂), bisaryl 58 at 6.43 min, toluene 59 at 4.76 min.

Time / min	Calculated Reaction Composition				Discrepancy	Product Ratio	
	Enoate	Ar[B]	Bisaryl	Desboron		Bisaryl	Desboron
0	100	95	0	0.7	4.2		
5	100	89	0	1	9.3		
10	100	89	0	2	9.3		
20	100	89	0	2	9.6		
40	100	88	0.1	2	9.9	6	94
60	100	88	0.2	3	9.3	7	93
120	100	87	0.3	3	9.8	7	93
240	100	86	0.3	4	10.1	7	93
360	100	86	0.4	4	10.1	8	92
720	100	84	0.4	4	11.7	9	91

Table 139. Interpretation of HPLC data for Reaction Set B with diene L29.

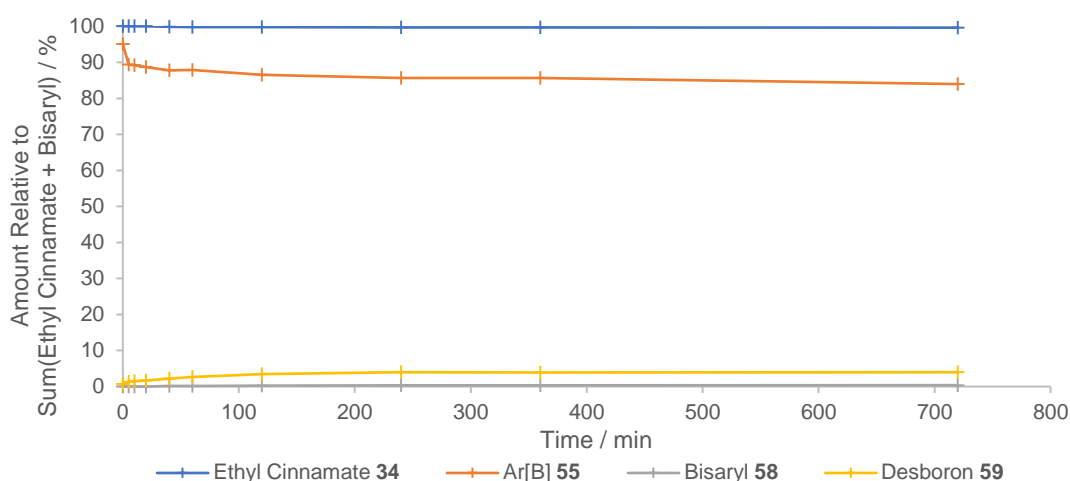


Figure 84. Calculated reaction composition over time.

5.4.3.2.13 Diene L32 (pages 143–144)



Reaction Set A

Time / min	HPLC Peak Area				
	Enoate	ArBpin	ArB(OH) ₂	Bisaryl	Desboron
0	1202.301	16.498	1203.935	24.332	
5	1166.205	14.574	1100.303	109.807	
10	999.374		922.470	139.381	
20	1216.078		1088.216	235.855	
40	1197.006		1072.487	286.056	22.241
60	1172.489		1013.206	299.742	24.330
120	1243.535		1023.234	350.470	32.435
240	1223.903		950.328	366.715	42.006
360	1287.368		998.620	389.042	45.673
720	1293.997		1001.395	395.111	48.294

Table 140. HPLC Peak Area data (Method C, 215 nm) for Reaction Set A with diene L32. Enoate 16 at 20.1 min, arylboron reagent 17 at 20.4 min (ArBpin) and 9.3 min (ArB(OH)₂), bisaryl 18 at 19.6 min, *o*-tolylmethanol 19 at 13.6 min.

Time / min	Calculated Reaction Composition				Discrepancy	Product Ratio	
	Enoate	Ar[B]	Bisaryl	Desboron		Bisaryl	Desboron
0	100	101	0	0	-1.1		
5	98	94	2	0	4.7		
10	97	90	3	0	7.8		
20	97	86	3	0	10.5		
40	96	85	4	2	8.3	69	31
60	95	82	5	2	11.1	68	32
120	95	78	5	3	14.4	65	35
240	95	73	5	4	17.9	60	40
360	95	73	5	4	17.9	59	41
720	95	73	5	4	17.8	58	42

Table 141. Interpretation of HPLC data for Reaction Set A with diene L32.

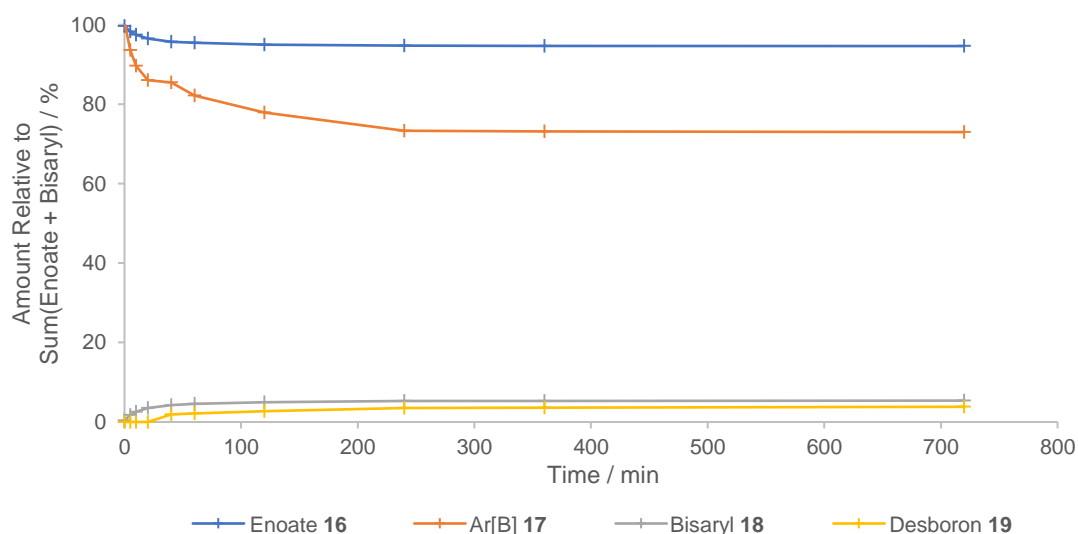


Figure 85. Calculated reaction composition over time.



Reaction Set B

Time / min	HPLC Peak Area				
	Enoate	ArBpin	ArB(OH) ₂	Bisaryl	Desboron
0	2338.579	172.837	758.446		6.491
5	2124.740	474.858	312.198		12.060
10	2172.535	500.929	300.746	2.062	14.702
20	2243.958	562.402	262.385	2.978	16.969
40	2174.763	415.832	381.999	4.548	21.721
60	2131.306	405.662	372.160	5.070	27.741
120	2260.188	315.878	508.693	5.073	34.590
240	2183.145	380.134	410.300	5.015	34.123
360	2171.311	238.259	549.589	5.155	34.442
720	2202.594	366.846	420.866	5.321	34.278

Table 142. HPLC Peak Area data (Method B, 210 and 220 nm (bisaryl)) for Reaction Set B with diene L32. Ethyl cinnamate 34 at 5.26 min, arylboron reagent 55 at 6.25 min (ArBpin) and 3.06 min (ArB(OH)₂), bisaryl 58 at 6.43 min, toluene 59 at 4.76 min.

Time / min	Calculated Reaction Composition				Discrepancy	Product Ratio	
	Enoate	Ar[B]	Bisaryl	Desboron		Bisaryl	Desboron
0	100	95	0	0.6	4.4		
5	100	88	0	1	10.5		
10	100	88	0.1	1	10.6	7	93
20	100	88	0.1	2	10.8	8	92
40	100	87	0.2	2	10.4	10	90
60	100	87	0.2	3	10.3	9	91
120	100	87	0.2	3	9.8	7	93
240	100	86	0.2	3	10.4	7	93
360	100	86	0.2	3	10.2	7	93
720	100	85	0.3	3	11.5	7	93

Table 143. Interpretation of HPLC data for Reaction Set B with diene L32.

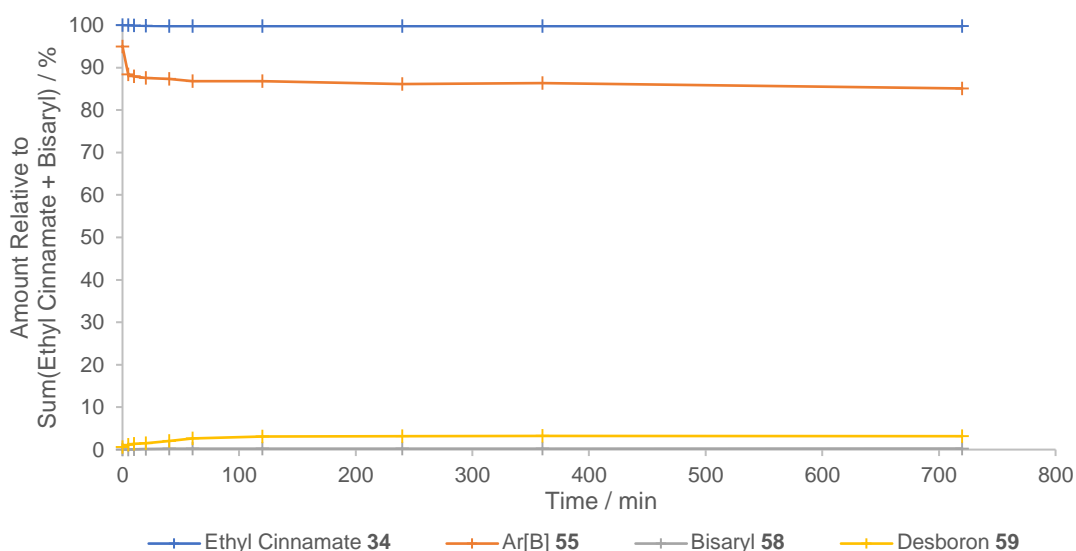
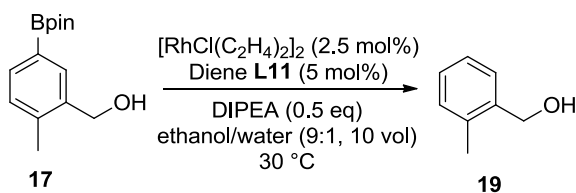


Figure 86. Calculated reaction composition over time.

5.4.3.2.14 Consumption of Arylboron Reagent 17 in the Absence of Enolate 16
(Figure 42, page 128 and Figure 48 page 147)



Time / min	HPLC Peak Area	
	ArB(OH) ₂	Desboron
0	739.659	
5	782.792	378.038
10	632.912	514.714
20	475.293	669.005
40	320.782	824.964
60	183.759	872.573
120	42.042	963.323
240	24.391	980.118
360	28.588	986.883
720	24.198	797.497

Table 144. HPLC Peak Area data (Method C, 215 nm) for the consumption of arylboron reagent 17 in the absence of enolate 16. Arylboron reagent 17 at 9.3 min (ArB(OH)₂), *o*-tolymethanol 19 at 13.6 min.

The reaction composition was calculated assuming that no other reaction occurred, and analogously to Equation 10 and Equation 11 (page 269):

Time / min	Calculated Reaction Composition	
	Ar[B]	Desboron
0	100	0
5	66	34
10	53	47
20	40	60
40	26	74
60	16	84
120	4	96
240	2	98
360	3	97
720	3	97

Table 145. Interpretation of HPLC data.

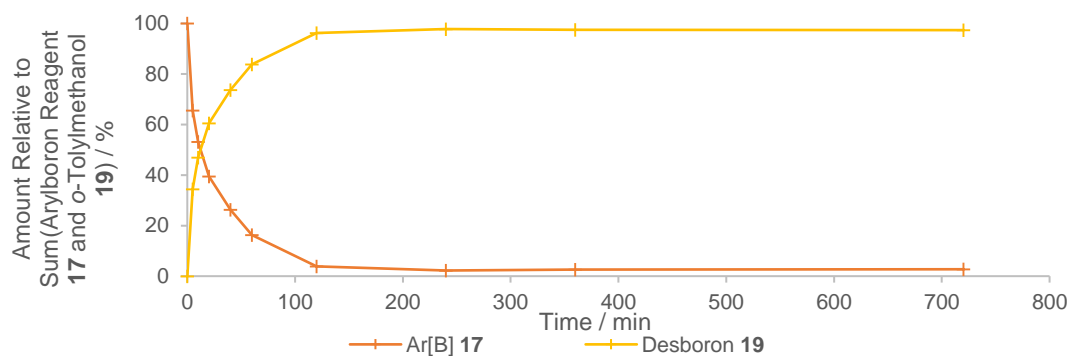


Figure 87. Calculated reaction composition over time.

5.5 Computational Chemistry in Sections 3.3.1.2 and 3.3.3 and Crystallographic Measurements in Section 3.3.3

Orbitals and orbital energies were calculated for the enoates and dienes using a restricted Hartree-Fock method with the DGDZVP basis.²²⁶ An energy minimisation was performed before calculation of the orbitals for the lowest energy conformers. Where relevant, the energies of any rotational isomers were calculated and the results from the lowest energy rotamers are those discussed. Charges on atoms were estimated from a Mulliken population analysis. Gaussian 16 (B.01) was used to run the calculations,²²⁷ and Avogadro 1.2.0 was used to visualise the results with orbital depictions rendered at an isosurface value of 0.02 atomic units.²²⁸

Published crystallographic data was found and analysed from the Cambridge Crystallographic Data Centre using ConQuest 1.23.

5.6 Miscellaneous Software

Design-Expert 10.0.3.1 (Stat-Ease, 2016) was used in the design and analysis of the factor-screening DoE (Section 3.2.3), ChemBioDraw Ultra 12.0.2d812 (CambridgeSoft, 2009) was used to prepare chemical figures and schemes, TIBCO Spotfire Analyst 7.11.1 (TIBCO Software, 2017) was used to prepare the data visualisations in Sections 3.2.1 and 3.2.2, Office 2016 (Microsoft) was used for word-processing and general data-processing.

6 References

- (1) Butters, M.; Catterick, D.; Craig, A.; Curzons, A.; Dale, D.; Gillmore, A.; Green, S. P.; Marziano, I.; Sherlock, J.-P.; White, W. *Chem. Rev.* **2006**, *106*, 3002.
- (2) Howell, G. P. *Org. Process Res. Dev.* **2012**, *16*, 1258.
- (3) Sertkaya, A.; Birkenbach, A.; Berlind, A.; Eyraund, J. *Examination of Clinical Trial Costs and Barriers for Drug Development*; Report for the US Department of Health and Human Services; Eastern Research Group: Lexington, MA, U.S.A., 2014.
- (4) ICH Guideline for Elemental Impurities (Q3D, Step 4 Version, 2014). https://www.ich.org/fileadmin/Public_Web_Site/ICH_Products/Guidelines/Quality/Q3D/Q3D_Step_4.pdf (accessed Dec 17, 2018).
- (5) ICH Guideline for Residual Solvents (Q3D(R7), Step 4 Version, 2018). https://www.ich.org/fileadmin/Public_Web_Site/ICH_Products/Guidelines/Quality/Q3C/Q3C-R7_Document_Guideline_2018_1015.pdf (accessed Dec 17, 2018).
- (6) International Conference on Harmonization (ICH) in the Office of Pharmaceutical Science (OPS). <https://www.fda.gov/AboutFDA/CentersOffices/OfficeofMedicalProductsandTobacco/CDER/ucm128047.htm> (accessed Dec 17, 2018).
- (7) International-Standard Organisations. <https://www.ema.europa.eu/en/international-standard-organisations> (accessed Dec 17, 2018).
- (8) Busacca, C. A.; Fandrick, D. R.; Song, J. J.; Senanayake, C. H. *Adv. Synth. Catal.* **2011**, *353*, 1825.
- (9) British Geological Survey Risk List 2015. <https://www.bgs.ac.uk/mineralsuk/statistics/riskList.html> (accessed Jan 7, 2019).
- (10) Egorova, K. S.; Ananikov, V. P. *Angew. Chem. Int. Ed.* **2016**, *55*, 12150.
- (11) Friedman, D.; Masciangioli, T.; Olson, S. *The Role of the Chemical Sciences in Finding Alternatives to Critical Resources: A Workshop Summary*; National Academy Press: Washington, DC, U.S.A., 2012.
- (12) *Catalysis without Precious Metals*; Bullock, R. M., Ed.; Wiley: Weinheim, Germany, 2010.
- (13) Bullock, R. M. *Science* **2013**, *342*, 1054.
- (14) Chirik, P. J.; Wieghardt, K. *Science* **2010**, *327*, 794.
- (15) Chirik, P.; Morris, R. *Acc. Chem. Res.* **2015**, *48*, 2495.
- (16) Desai, A. A. *Angew. Chem. Int. Ed.* **2011**, *50*, 1974.
- (17) Stankiewicz, A. I.; Moulijn, J. A. *Chem. Eng. Prog.* **2000**, *96*, 22.
- (18) Liu, H. Z.; Liang, X. F.; Yang, L. R.; Chen, J. Y. *Sci. China Chem.* **2010**, *53*, 1470.
- (19) Hansen, K. B.; Balsells, J.; Dreher, S.; Hsiao, Y.; Kubryk, M.; Palucki, M.; Rivera, N.; Steinhuebel, D.; Armstrong, J. D. (III); Askin, D.; Grabowski, E. J. J. *Org. Process Res. Dev.* **2005**, *9*, 634.
- (20) Hansen, K. B.; Hsiao, Y.; Xu, F.; Rivera, N.; Clausen, A.; Kubryk, M.; Krska, S.;

- Rosner, T.; Simmons, B.; Balsells, J.; Ikemoto, N.; Sun, Y.; Spindler, F.; Malan, C.; Grabowski, E. J. J.; Armstrong, J. D. (III). *J. Am. Chem. Soc.* **2009**, *131*, 8798.
- (21) Savile, C. K.; Janey, J. M.; Mundorff, E. C.; Moore, J. C.; Tam, S.; Jarvis, W. R.; Colbeck, J. C.; Krebber, A.; Fleitz, F. J.; Brands, J.; Devine, P. N.; Huisman, G. W.; Hughes, G. J. *Science* **2010**, *329*, 305.
- (22) Darbourne, A. *Scrip. Mag.* **1993**, *Feb*, 16.
- (23) Lovering, F.; Bikker, J.; Humblet, C. *J. Med. Chem.* **2009**, *52*, 6752.
- (24) Carey, J. S.; Laffan, D.; Thomson, C.; Williams, M. T. *Org. Biomol. Chem.* **2006**, *4*, 2337.
- (25) Brown, D. G.; Boström, J. *J. Med. Chem.* **2016**, *59*, 4443.
- (26) Farina, V.; Reeves, J. T.; Senanayake, C. H.; Song, J. J. *Chem. Rev.* **2006**, *106*, 2734.
- (27) Mane, S. *Anal. Methods* **2016**, *8*, 7567.
- (28) *Novel Optical Resolution Technologies*; Sakai, K., Hirayama, N., Tamura, R., Eds.; Topics in Current Chemistry; Springer: Berlin, Germany, 2007.
- (29) Nguyen, L. A.; He, H.; Pham-Huy, C. *Int. J. Biomed. Sci.* **2006**, *2*, 85.
- (30) Margolin, A. L. *Enzyme Microb. Technol.* **1993**, *15*, 266.
- (31) Pellissier, H. *Tetrahedron* **2003**, *59*, 8291.
- (32) Ward, R. S. *Tetrahedron: Asymmetry* **1995**, *6*, 1475.
- (33) El Gihani, M. T.; Williams, J. M. J. *Curr. Opin. Chem. Biol.* **1999**, *3*, 11.
- (34) Caddick, S.; Jenkins, K. *Chem. Soc. Rev.* **1996**, *25*, 447.
- (35) Faber, K. *Chem. Eur. J.* **2001**, *7*, 5004.
- (36) Paek, S.-M.; Jeong, M.; Jo, J.; Heo, Y. M.; Han, Y. T.; Yun, H. *Molecules* **2016**, *21*, 951.
- (37) Peterson, E. A.; Overman, L. E. *Proc. Natl. Acad. Sci. U.S.A.* **2004**, *101*, 11943.
- (38) Chang, S.; Halperin, S. D.; Moore, J.; Britton, R. Chiral Auxiliaries in Drug Synthesis. *Stereoselective Synthesis of Drugs and Natural Products*; Wiley: Hoboken, NJ, U.S.A., 2013; Chapter 2.
- (39) *Key Chiral Auxiliary Applications*, 2nd ed.; Roos, G., Ed.; Elsevier Academic Press: Oxford, U.K., 2014.
- (40) Wells, A. S.; Finch, G. L.; Michels, P. C.; Wong, J. W. *Org. Process Res. Dev.* **2012**, *16*, 1986.
- (41) Ogawa, J.; Shimizu, S. *Trends Biotechnol.* **1999**, *17*, 13.
- (42) Chow, J.; Streit, W. R. Screening of Enzymes: Novel Screening Technologies to Exploit Noncultivated Microbes for Biotechnology. In *Applied Biocatalysis: From Fundamental Science to Industrial Applications*; Hilterhaus, L., Liese, A., Kettling,

- U., Antranikian, G., Eds.; Wiley: Weinheim, Germany, 2016; pp 13–30.
- (43) Oue, S.; Okamoto, A.; Yano, T.; Kagamiyama, H. *J. Biol. Chem.* **1999**, *274*, 2344.
- (44) Trost, B. M. *Proc. Natl. Acad. Sci. U.S.A.* **2004**, *101*, 5348.
- (45) Hawkins, J. M.; Watson, T. J. N. *Angew. Chem. Int. Ed.* **2004**, *43*, 3224.
- (46) GlaxoSmithKline Product Pipeline. <https://www.gsk.com/en-gb/investors/product-pipeline> (accessed Nov 14, 2017).
- (47) Tokoroyama, T. *Eur. J. Org. Chem.* **2010**, 2009.
- (48) Kharasch, M. S.; Tawney, P. O. *J. Am. Chem. Soc.* **1941**, *63*, 2308.
- (49) Barnes, D. M.; Ji, J.; Fickes, M. G.; Fitzgerald, M. A.; King, S. A.; Morton, H. E.; Plagge, F. A.; Preskill, M.; Wagaw, S. H.; Wittenberger, S. J.; Zhang, J. *J. Am. Chem. Soc.* **2002**, *124*, 13097.
- (50) Burke, A. J.; Marques, C. S. M. *Conjugate Additions: Copper. Catalytic Arylation Methods: From the Academic Lab to Industrial Processes*; Wiley: Weinheim, Germany, 2015; pp 280–285.
- (51) Harutyunyan, S. R.; den Hartog, T.; Geurts, K.; Minnaard, A. J.; Feringa, B. L. *Chem. Rev.* **2008**, *108*, 2824.
- (52) López, F.; Minnaard, A. J.; Feringa, B. L. *Acc. Chem. Res.* **2007**, *40*, 179.
- (53) Sakai, M.; Hayashi, H.; Miyaura, N. *Organometallics* **1997**, *16*, 4229.
- (54) Takaya, Y.; Ogasawara, M.; Hayashi, T.; Sakai, M.; Miyaura, N. *J. Am. Chem. Soc.* **1998**, *120*, 5579.
- (55) Burns, A. R.; Lam, H. W.; Roy, I. D. Enantioselective, Rhodium-Catalysed 1,4-Addition of Organoboron Reagents to Electron-Deficient Alkenes. In *Organic Reactions*; Denmark, S. E., Ed.; Wiley: Hoboken, NJ, U.S.A., 2017; Vol. 93, pp 1–415.
- (56) Hayashi, T. *Synlett* **2001**, 879.
- (57) Heravi, M. M.; Dehghani, M.; Zadsirjan, V. *Tetrahedron: Asymmetry* **2016**, *27*, 513.
- (58) Edwards, H. J.; Hargrave, J. D.; Penrose, S. D.; Frost, C. G. *Chem. Soc. Rev.* **2010**, *39*, 2093.
- (59) Tian, P.; Dong, H.-Q.; Lin, G.-Q. *ACS Catal.* **2012**, *2*, 95.
- (60) Hayashi, T.; Yamasaki, K. *Chem. Rev.* **2003**, *103*, 2829.
- (61) Fagnou, K.; Lautens, M. *Chem. Rev.* **2003**, *103*, 169.
- (62) Breit, B.; Schmidt, Y. *Chem. Rev.* **2008**, *108*, 2928.
- (63) Rossiter, B. E.; Swingle, N. M. *Chem. Rev.* **1992**, *92*, 771.
- (64) Sibi, M. P.; Manyem, S. *Tetrahedron* **2000**, *56*, 8033.

- (65) Krause, N.; Hoffmann-Röder, A. *Synthesis* **2001**, 171.
- (66) Feringa, B. L.; Naasz, R.; Imbos, R.; Arnold, L. A. Copper-catalysed Enantioselective Conjugate Addition Reactions of Organozinc Reagents. In *Modern Organocopper Chemistry*; Krause, N., Ed.; Wiley: Weinheim, Germany, 2002; pp 224–258.
- (67) Christoffers, J.; Koripelly, G.; Rosiak, A.; Rössle, M. *Synthesis* **2007**, 1279.
- (68) Hayashi, T.; Takahashi, M.; Takaya, Y.; Ogasawara, M. *J. Am. Chem. Soc.* **2002**, *124*, 5052.
- (69) Kina, A.; Iwamura, H.; Hayashi, T. *J. Am. Chem. Soc.* **2006**, *128*, 3904.
- (70) Hayashi, T.; Ueyama, K.; Tokunaga, N.; Yoshida, K. *J. Am. Chem. Soc.* **2003**, *125*, 11508.
- (71) Otomaru, Y.; Okamoto, K.; Shintani, R.; Hayashi, T. *J. Org. Chem.* **2005**, *70*, 2503.
- (72) Kantchev, E. A. B. *Chem. Commun.* **2011**, *47*, 10969.
- (73) Gosiewska, S.; Raskatov, J. A.; Shintani, R.; Hayashi, T.; Brown, J. M. *Chem. Eur. J.* **2012**, *18*, 80.
- (74) Kantchev, E. A. B. *Chem. Sci.* **2013**, *4*, 1864.
- (75) Itooka, R.; Iguchi, Y.; Miyaura, N. *J. Org. Chem.* **2003**, *68*, 6000.
- (76) Yoshida, K.; Ogasawara, M.; Hayashi, T. *J. Org. Chem.* **2003**, *68*, 1901.
- (77) Carrow, B. P.; Hartwig, J. F. *J. Am. Chem. Soc.* **2011**, *133*, 2116.
- (78) Lennox, A. J. J.; Lloyd-Jones, G. C. *Angew. Chem. Int. Ed.* **2013**, *52*, 7362.
- (79) Kina, A.; Yasuhara, Y.; Nishimura, T.; Iwamura, H.; Hayashi, T. *Chem. Asian J.* **2006**, *1*, 707.
- (80) Miyaura, N. *Bull. Chem. Soc. Jpn.* **2008**, *81*, 1535.
- (81) Zhao, P.; Incarvito, C. D.; Hartwig, J. F. *J. Am. Chem. Soc.* **2007**, *129*, 1876.
- (82) Li, Y.-G.; He, G.; Qin, H.-L.; Kantchev, E. A. B. *Dalton Trans.* **2015**, *44*, 2737.
- (83) Brock, S.; Hose, D. R. J.; Moseley, J. D.; Parker, A. J.; Patel, I.; Williams, A. J. *Org. Process Res. Dev.* **2008**, *12*, 496.
- (84) Yamamoto, Y.; Kurihara, K.; Sugishita, N.; Oshita, K.; Piao, D.; Miyaura, N. *Chem. Lett.* **2005**, *34*, 1224.
- (85) Lukin, K.; Zhang, Q.; Leanna, M. R. *J. Org. Chem.* **2009**, *74*, 929.
- (86) Lu, X.; Lin, S. *J. Org. Chem.* **2005**, *70*, 9651.
- (87) Nishikata, T.; Kiyomura, S.; Yamamoto, Y.; Miyaura, N. *Synlett* **2008**, 2487.
- (88) Nishikata, T.; Yamamoto, Y.; Miyaura, N. *Chem. Lett.* **2007**, *36*, 1442.
- (89) Gutnov, A. *Eur. J. Org. Chem.* **2008**, 4547.

- (90) Shintani, R.; Hayashi, T. *Chem. Lett.* **2008**, *37*, 724.
- (91) Wu, C.; Yue, G.; Nielsen, C. D.-T.; Xu, K.; Hirao, H.; Zhou, J. *J. Am. Chem. Soc.* **2016**, *138*, 742.
- (92) Lin, P.-S.; Jeganmohan, M.; Cheng, C.-H. *Chem. Asian J.* **2007**, *2*, 1409.
- (93) Nguyen, T. N.; May, J. A. *Tetrahedron Lett.* **2017**, *58*, 1535.
- (94) Lee, S.; MacMillan, D. W. C. *J. Am. Chem. Soc.* **2007**, *129*, 15438.
- (95) Turner, H. M.; Patel, J.; Niljianskul, N.; Chong, J. M. *Org. Lett.* **2011**, *13*, 5796.
- (96) Amengual, R.; Michelet, V.; Genêt, J.-P. *Synlett* **2002**, 1791.
- (97) Itooka, R.; Iguchi, Y.; Miyaura, N. *Chem. Lett.* **2001**, *30*, 722.
- (98) Bürgi, J. J.; Mariz, R.; Gatti, M.; Drinkel, E.; Luan, X.; Blumentritt, S.; Linden, A.; Dorta, R. *Angew. Chem. Int. Ed.* **2009**, *48*, 2768.
- (99) Mariz, R.; Luan, X.; Gatti, M.; Linden, A.; Dorta, R. *J. Am. Chem. Soc.* **2008**, *130*, 2172.
- (100) Korenaga, T.; Maenishi, R.; Hayashi, K.; Sakai, T. *Adv. Synth. Catal.* **2010**, *352*, 3247.
- (101) Korenaga, T.; Osaki, K.; Maenishi, R.; Sakai, T. *Org. Lett.* **2009**, *11*, 2325.
- (102) Berhal, F.; Esseiva, O.; Martin, C.-H.; Tone, H.; Genet, J.-P.; Ayad, T.; Ratovelomanana-Vidal, V. *Org. Lett.* **2011**, *13*, 2806.
- (103) Boiteau, J.-G.; Minnaard, A. J.; Feringa, B. L. *J. Org. Chem.* **2003**, *68*, 9481.
- (104) Trost, B. M.; Rao, M. *Angew. Chem. Int. Ed.* **2015**, *54*, 5026.
- (105) Sipos, G.; Drinkel, E. E.; Dorta, R. *Chem. Soc. Rev.* **2015**, *44*, 3834.
- (106) Feng, C.-G.; Xu, M.-H.; Lin, G.-Q. *Synlett* **2011**, 1345.
- (107) Tokunaga, N.; Otomaru, Y.; Okamoto, K.; Ueyama, K.; Shintani, R.; Hayashi, T. *J. Am. Chem. Soc.* **2004**, *126*, 13584.
- (108) Defieber, C.; Paquin, J.-F.; Serna, S.; Carreira, E. M. *Org. Lett.* **2004**, *6*, 3873.
- (109) Hu, X.; Zhuang, M.; Cao, Z.; Du, H. *Org. Lett.* **2009**, *11*, 4744.
- (110) Cao, Z.; Du, H. *Org. Lett.* **2010**, *12*, 2602.
- (111) Chen, F.-X.; Kina, A.; Hayashi, T. *Org. Lett.* **2006**, *8*, 341.
- (112) Okamoto, K.; Hayashi, T.; Rawal, V. H. *Chem. Commun.* **2009**, 4815.
- (113) Defieber, C.; Grützmacher, H.; Carreira, E. M. *Angew. Chem. Int. Ed.* **2008**, *47*, 4482.
- (114) Johnson, J. B.; Rovis, T. *Angew. Chem. Int. Ed.* **2008**, *47*, 840.
- (115) Okamoto, K.; Hayashi, T.; Rawal, V. H. *Org. Lett.* **2008**, *10*, 4387.

- (116) Gendrineau, T.; Chuzel, O.; Eijlsberg, H.; Genet, J.-P.; Darses, S. *Angew. Chem. Int. Ed.* **2008**, *47*, 7669.
- (117) Berthon-Gelloz, G.; Hayashi, T. *J. Org. Chem.* **2006**, *71*, 8957.
- (118) Wang, Y.; Hu, X.; Du, H. *Org. Lett.* **2010**, *12*, 5482.
- (119) Li, R.; Wen, Z.; Wu, N. *Org. Biomol. Chem.* **2016**, *14*, 11080.
- (120) Abele, S.; Inauen, R.; Spielvogel, D.; Moessner, C. *J. Org. Chem.* **2012**, *77*, 4765.
- (121) Senda, T.; Ogasawara, M.; Hayashi, T. *J. Org. Chem.* **2001**, *66*, 6852.
- (122) Ishiyama, T.; Murata, M.; Miyaura, N. *J. Org. Chem.* **1995**, *60*, 7508.
- (123) Hartwig, J. F. *Acc. Chem. Res.* **2012**, *45*, 864.
- (124) Sakuma, S.; Sakai, M.; Itooka, R.; Miyaura, N. *J. Org. Chem.* **2000**, *65*, 5951.
- (125) Cox, P. A.; Leach, A. G.; Campbell, A. D.; Lloyd-Jones, G. C. *J. Am. Chem. Soc.* **2016**, *138*, 9145.
- (126) Cox, P. A.; Reid, M.; Leach, A. G.; Campbell, A. D.; King, E. J.; Lloyd-Jones, G. C. *J. Am. Chem. Soc.* **2017**, *139*, 13156.
- (127) Hall, D. G. Structure, Properties, and Preparation of Boronic Acid Derivatives. In *Boronic Acids: Preparation and Applications in Organic Synthesis, Medicine and Materials*; Hall, D. G., Ed.; Wiley: Weinheim, Germany, 2011; pp 1–133.
- (128) Kuivila, H. G.; Reuwer, J. F.; Mangravite, J. A. *Can. J. Chem.* **1963**, *41*, 3081.
- (129) Lozada, J.; Liu, Z.; Perrin, D. M. *J. Org. Chem.* **2014**, *79*, 5365.
- (130) Knapp, D. M.; Gillis, E. P.; Burke, M. D. *J. Am. Chem. Soc.* **2009**, *131*, 6961.
- (131) Lennox, A. J. J.; Lloyd-Jones, G. C. *Isr. J. Chem.* **2010**, *50*, 664.
- (132) Brak, K.; Ellman, J. A. *J. Org. Chem.* **2010**, *75*, 3147.
- (133) Takaya, Y.; Ogasawara, M.; Hayashi, T. *Tetrahedron Lett.* **1999**, *40*, 6957.
- (134) Takaya, Y.; Senda, T.; Kurushima, H.; Ogasawara, M.; Hayashi, T. *Tetrahedron: Asymmetry* **1999**, *10*, 4047.
- (135) Batey, R. A.; Thadani, A. N.; Smil, D. V. *Org. Lett.* **1999**, *1*, 1683.
- (136) Pucheault, M.; Darses, S.; Genêt, J.-P. *Eur. J. Org. Chem.* **2002**, 3552.
- (137) Shintani, R.; Tsutsumi, Y.; Nagaosa, M.; Nishimura, T.; Hayashi, T. *J. Am. Chem. Soc.* **2009**, *131*, 13588.
- (138) Albrecht, F.; Sowada, O.; Fistikci, M.; Boysen, M. M. K. *Org. Lett.* **2014**, *16*, 5212.
- (139) Itoh, T.; Mase, T.; Nishikata, T.; Iyama, T.; Tachikawa, H.; Kobayashi, Y.; Yamamoto, Y.; Miyaura, N. *Tetrahedron* **2006**, *62*, 9610.
- (140) Paquin, J.-F.; Stephenson, C. R. J.; Defieber, C.; Carreira, E. M. *Org. Lett.* **2005**, *7*, 3821.

- (141) Burgey, C. S.; Paone, D. V.; Shaw, A. W.; Deng, J. Z.; Nguyen, D. N.; Potteiger, C. M.; Graham, S. L.; Vacca, J. P.; Williams, T. M. *Org. Lett.* **2008**, *10*, 3235.
- (142) Henderson, R. K.; Jiménez-González, C.; Constable, D. J. C.; Alston, S. R.; Inglis, G. G. A.; Fisher, G.; Sherwood, J.; Binks, S. P.; Curzons, A. D. *Green Chem.* **2011**, *13*, 854.
- (143) Wallace, G. A.; Gordon, T. D.; Hayes, M. E.; Konopacki, D. B.; Fix-Stenzel, S. R.; Zhang, X.; Grongsaard, P.; Cusack, K. P.; Schaffter, L. M.; Henry, R. F.; Stoffel, R. H. *J. Org. Chem.* **2009**, *74*, 4886.
- (144) Simmons, E. M.; Mudryk, B.; Lee, A. G.; Qiu, Y.; Razler, T. M.; Hsiao, Y. *Org. Process Res. Dev.* **2017**, *21*, 1659.
- (145) Lalic, G.; Corey, E. J. *Tetrahedron Lett.* **2008**, *49*, 4894.
- (146) Blaser, H.-U.; Steiner, H.; Studer, M. *ChemCatChem* **2009**, *1*, 210.
- (147) Siegrist, U.; Baumeister, P.; Blaser, H.-U.; Studer, M. *Chem. Ind. Catal. Org. React.* **1998**, *75*, 207.
- (148) Kosak, J. R. Catalytic Reduction of Halonitroaromatic Compounds. US 4020107, 1977.
- (149) Quittman, W.; Belser, T. P.; Aufdenblatten, R. R. Process and Catalyst. US 2011/0071290, 2011.
- (150) Neumann, D.; Ritzer, J. Method for Hydrogenating Nitroaromatic Systems with Selected Platinum Catalysts. US 2014/0066658, 2014.
- (151) Kosak, J. R. *Ann. N.Y. Acad. Sci.* **1970**, *172*, 175.
- (152) Craig, W. C.; Davis, G. J.; Shull, P. O. Preparation of Chlorine Substituted Aromatic Amines. GB 1138567, 1969.
- (153) Hoogenraad, M.; Van Der Linden, J. B.; Smith, A. A.; Hughes, B.; Derrick, A. M.; Harris, L. J.; Higginson, P. D.; Pettman, A. J. *Org. Process Res. Dev.* **2004**, *8*, 469.
- (154) Popik, V. V.; Wright, A. G.; Khan, T. A.; Murphy, J. A. Hypophosphorous Acid. In *e-EROS Encyclopedia of Reagents for Organic Synthesis*; Wiley, 2004.
- (155) Baron, M.; Métay, E.; Lemaire, M.; Popowycz, F. *Green Chem.* **2013**, *15*, 1006.
- (156) Entwistle, I. D.; Jackson, A. E.; Johnstone, R. A. W.; Telford, R. P. *J. Chem. Soc., Perkin Trans. 1* **1977**, 443.
- (157) Deasy, R. E.; Slattery, C. N.; Maguire, A. R.; Kjell, D. P.; Hawk, M. K. N.; Joo, J. M.; Gu, R. L.; Moynihan, H. *J. Org. Chem.* **2014**, *79*, 3688.
- (158) Si, C.; Myers, A. G. *Angew. Chem. Int. Ed.* **2011**, *50*, 10409.
- (159) Zhang, X.; Mashima, K.; Koyano, K.; Sayo, N.; Kumobayashi, H.; Akutagawa, S.; Takaya, H. *J. Chem. Soc., Perkin. Trans. 1* **1994**, 2309.
- (160) Jeulin, S.; Duprat de Paule, S.; Ratovelomanana-Vidal, V.; Genêt, J.-P.; Champion, N.; Dellis, P. *Proc. Natl. Acad. Sci. U.S.A.* **2004**, *101*, 5799.

- (161) Shimizu, H.; Nagasaki, I.; Matsumura, K.; Sayo, N.; Saito, T. *Acc. Chem. Res.* **2007**, *40*, 1385.
- (162) Boiteau, J.-G.; Imbos, R.; Minnaard, A. J.; Feringa, B. L. *Org. Lett.* **2003**, *5*, 681.
- (163) Tsui, G. C.; Dougan, P.; Lautens, M. *Org. Lett.* **2013**, *15*, 2652.
- (164) James, B. R.; Morris, R. H. *Can. J. Chem.* **1980**, *58*, 399.
- (165) Case Study 7: The importance of factor identification.
<http://www.catalysisconsulting.co.uk/documents/Case-study-7.pdf> (accessed Nov 25, 2017).
- (166) Feringa, B. L. *Acc. Chem. Res.* **2000**, *33*, 346.
- (167) Zhang, L.; Xie, X.; Fu, L.; Zhang, Z. *J. Org. Chem.* **2013**, *78*, 3434.
- (168) Henderson, R. K.; Hill, A. P.; Redman, A. M.; Sneddon, H. F. *Green Chem.* **2015**, *17*, 945.
- (169) Zhang, Y.-F.; Chen, D.; Chen, W.-W.; Xu, M.-H. *Org. Lett.* **2016**, *18*, 2726.
- (170) Tanoury, G. J.; Senanayake, C. H. Tris[2-(2-methoxyethoxy)ethyl]amine. In *e-EROS Encyclopedia of Reagents for Organic Synthesis*; Wiley, 2003.
- (171) Owen, M. R.; Luscombe, C.; Lai, L.-W.; Godbert, S.; Crookes, D. L.; Emiabata-Smith, D. *Org. Process Res. Dev.* **2001**, *5*, 308.
- (172) Weissman, S. A.; Anderson, N. G. *Org. Process Res. Dev.* **2015**, *19*, 1605.
- (173) Barrentine, L. B. Screening Designs. *An Introduction to Design of Experiments: A Simplified Approach*; American Society for Quality: Milwaukee, WI, U.S.A., 1999; Chapter 4.
- (174) Leardi, R. *Anal. Chim. Acta* **2009**, *652*, 161.
- (175) Hanson, S. K.; Heinekey, D. M.; Goldberg, K. I. *Organometallics* **2008**, *27*, 1454.
- (176) Lockley, W. J. S.; Hesk, D. *J. Label. Compd. Radiopharm.* **2010**, *53*, 704.
- (177) Sun, J.; Perfetti, M. T.; Santos, W. L. *J. Org. Chem.* **2011**, *76*, 3571.
- (178) Bonin, H.; Delbrayelle, D.; Demonchaux, P.; Gras, E. *Chem. Commun.* **2010**, *46*, 2677.
- (179) Rettig, S. J.; Trotter, J. *Can. J. Chem.* **1975**, *53*, 1393.
- (180) Felix, A. M.; Heimer, E. P.; Lambros, T. J.; Tzougraki, C.; Meienhofer, J. *J. Org. Chem.* **1978**, *43*, 4194.
- (181) Wang, D.; Astruc, D. *Chem. Rev.* **2015**, *115*, 6621.
- (182) Volger, H. C.; Gaasbeek, M. M. P.; Hogeveen, H.; Vrieze, K. *Inorg. Chim. Acta* **1969**, *3*, 145.
- (183) Yasukawa, T.; Suzuki, A.; Miyamura, H.; Nishino, K.; Kobayashi, S. *J. Am. Chem. Soc.* **2015**, *137*, 6616.

- (184) Poater, A.; Ragone, F.; Mariz, R.; Dorta, R.; Cavallo, L. *Chem. Eur. J.* **2010**, *16*, 14348.
- (185) Luo, Y.; Berry, N. G.; Carnell, A. J. *Chem. Commun.* **2012**, *48*, 3279.
- (186) Qin, H.-L.; Chen, X.-Q.; Huang, Y.-Z.; Kantchev, E. A. B. *Chem. Eur. J.* **2014**, *20*, 12982.
- (187) Boz, E.; Haşlak, Z. P.; Tüzün, N. Ş.; Konuklar, F. A. S. *Organometallics* **2014**, *33*, 5111.
- (188) Dewar, M. J. S. *Bull. Chem. Soc. Fr.* **1951**, *18*, C71.
- (189) Chatt, J.; Duncanson, L. A. *J. Chem. Soc.* **1953**, 2939.
- (190) Zhang, Y. *CSD Commun.* **2016**, *CCDC 14495*.
- (191) Hill, T. N. *CSD Commun.* **2016**, *CCDC 14771*.
- (192) Englert, U.; Koelle, U. Z. *Krist. Cryst. Mater.* **1996**, *211*, 64.
- (193) Craig, N. C.; Groner, P.; McKean, D. C. *J. Phys. Chem. A* **2006**, *110*, 7461.
- (194) Harmony, M. D. *J. Chem. Phys.* **1990**, *93*, 7522.
- (195) Hartwig, J. F. Ligand Substitution Reactions. *Organotransition Metal Chemistry*; University Science Books: Sausalito, CA, U.S.A., 2010; pp 217–260.
- (196) Hartwig, J. F. Insertions into 16-Electron d⁸ Complexes. *Organotransition Metal Chemistry*; University Science Books: Sausalito, CA, U.S.A., 2010; pp 355–356.
- (197) Zumdahl, S. S.; Drago, R. S. *J. Am. Chem. Soc.* **1968**, *90*, 6669.
- (198) Pidcock, A.; Richards, R. E.; Venanzi, L. M. *J. Chem. Soc. A* **1966**, 1707.
- (199) Basolo, F.; Chatt, J.; Gray, H. B.; Pearson, R. G.; Shaw, B. L. *J. Chem. Soc.* **1961**, 2207.
- (200) de Ridder, D. J. A.; Imhoff, P. *Acta Crystallogr., Sect. C: Cryst. Struct. Commun.* **1994**, *50*, 1569.
- (201) Boeyens, J. C. A.; Denner, L.; Orchard, S. W.; Rencken, I.; Rose, B. G. *S. Afr. J. Chem.* **1986**, *39*, 229.
- (202) Hartwig, J. F. Electrophilic Cleavage of Metal–Carbon and Metal–Hydride σ -Bonds. *Organotransition Metal Chemistry*; University Science Books: Sausalito, CA, U.S.A., 2010; pp 454–461.
- (203) de Luca, N.; Wojcicki, A. *J. Organomet. Chem.* **1980**, *193*, 359.
- (204) Ros, R.; Michelin, R. A.; Bataillard, R.; Roulet, R. *J. Organomet. Chem.* **1978**, *161*, 75.
- (205) Romeo, R.; Minniti, D.; Lanza, S. *J. Organomet. Chem.* **1979**, *165*, C36.
- (206) Romeo, R.; D'Amico, G. *Organometallics* **2006**, *25*, 3435.

- (207) Scott, V. J.; Labinger, J. A.; Bercaw, J. E. *Organometallics* **2011**, *30*, 4374.
- (208) Mai, B. K.; Kim, Y. *Inorg. Chem.* **2016**, *55*, 9822.
- (209) Guido, E.; D'Amico, G.; Russo, N.; Sicilia, E.; Rizzato, S.; Albinati, A.; Romeo, A.; Plutino, M. R.; Romeo, R. *Inorg. Chem.* **2011**, *50*, 2224.
- (210) Arpac, E.; Mirzaei, F.; Yardimcioglu, A.; Dahlenburg, L. *Z. Anorg. Allg. Chem.* **1984**, *519*, 148.
- (211) Boyd, S. E.; Field, L. D.; Hambley, T. W.; Partridge, M. G. *Organometallics* **1993**, *12*, 1720.
- (212) Noël, T.; Vandyck, K.; Van der Eycken, J. *Tetrahedron* **2007**, *63*, 12961.
- (213) Fulmer, G. R.; Miller, A. J. M.; Sherden, N. H.; Gottlieb, H. E.; Nudelman, A.; Stoltz, B. M.; Bercaw, J. E.; Goldberg, K. I. *Organometallics* **2010**, *29*, 2176.
- (214) Piguet, C.; Bünzli, J.-C. G.; Bernardinelli, G.; Bochet, C. G.; Froidevaux, P. *J. Chem. Soc., Dalton Trans.* **1995**, 83.
- (215) Taggi, A. E.; Marcus, K. K.; McCann, S. F.; Shapiro, R.; Chen, Y. Substituted Toly Fungicide Mixtures. WO2015/157005, 2015.
- (216) Wrackmeyer, B. *Prog. Nucl. Magn. Reson. Spectrosc.* **1979**, *12*, 227.
- (217) Nakao, Y.; Chen, J.; Imanaka, H.; Hiyama, T.; Ichikawa, Y.; Duan, W.-L.; Shintani, R.; Hayashi, T. *J. Am. Chem. Soc.* **2007**, *129*, 9137.
- (218) Youn, S. W.; Kim, B. S.; Jagdale, A. R. *J. Am. Chem. Soc.* **2012**, *134*, 11308.
- (219) Jiang, T.; Livinghouse, T.; Lovick, H. M. *Chem. Commun.* **2011**, *47*, 12861.
- (220) Alhamadsheh, M. M.; Palaniappan, N.; DasChouduri, S.; Reynolds, K. A. *J. Am. Chem. Soc.* **2007**, *129*, 1910.
- (221) Onodera, G.; Hachisuka, R.; Noguchi, T.; Miura, H.; Hashimoto, T.; Takeuchi, R. *Tetrahedron Lett.* **2014**, *55*, 310.
- (222) Bagutski, V.; Ros, A.; Aggarwal, V. K. *Tetrahedron* **2009**, *65*, 9956.
- (223) Huo, H.; Harms, K.; Meggers, E. *J. Am. Chem. Soc.* **2016**, *138*, 6936.
- (224) Itoh, K.; Tsuruta, A.; Ito, J.; Yamamoto, Y.; Nishiyama, H. *J. Org. Chem.* **2012**, *77*, 10914.
- (225) Nilov, D. I.; Vasilyev, A. V. *Tetrahedron Lett.* **2015**, *56*, 5714.
- (226) Godbout, N.; Salahub, D. R.; Andzelm, J.; Wimmer, E. *Can. J. Chem.* **1992**, *70*, 560.
- (227) Frisch, M. J.; Trucks, G. W.; Schlegel, H. B.; Scuseria, G. E.; Robb, M. A.; Cheeseman, J. R.; Scalmani, G.; Barone, V.; Petersson, G. A.; Nakatsuji, H.; Li, X.; Caricato, M.; Marenich, A. V.; Bloino, J.; Janesko, B. G.; Gomperts, R.; Mennucci, B.; Hratchian, H. P.; Ortiz, J. V.; Izmaylov, A. F.; Sonnenberg, J. L.; Williams-Young, D.; Ding, F.; Lipparini, F.; Egidi, F.; Goings, J.; Peng, B.; Petrone, A.; Henderson, T.; Ranasinghe, D.; Zakrzewski, V. G.; Gao, J.; Rega, N.; Hasegawa, J.; Ishida, M.; Nakajima, T.; Honda, Y.; Kitao, O.; Nakai, H.; Vreven, T.; Throssell, K.;

Montgomery Jr., J. A.; Peralta, J. E.; Ogliaro, F.; Bearpark, M. J.; Heyd, J. J.; Brothers, E. N.; Kudin, K. N.; Staroverov, V. N.; Keith, T. A.; Kobayashi, R.; Normand, J.; Raghavachari, K.; Rendell, A. P.; Burant, J. C.; Iyengar, S. S.; Tomasi, J.; Cossi, M.; Millam, J. M.; Klene, M.; Adamo, C.; Cammi, R.; Ochterski, J. W.; Martin, R. L.; Morokuma, K.; Farkas, O.; Foresman, J. B.; Fox, D. J. *Gaussian 16, Revision B.01*; Gaussian: Wallingford, CT, U.S.A., 2016.

- (228) Hanwell, M. D.; Curtis, D. E.; Lonie, D. C.; Vandermeersch, T.; Zurek, E.; Hutchison, G. R. *J. Cheminform.* **2012**, *4*, 17.